Contributions to the theory and applications of univariate distribution-free Shewhart, CUSUM and EWMA control charts

by

Marien Alet Graham

Submitted in partial fulfilment of the requirements for the degree

Philosophiae Doctor (Mathematical Statistics)

In the Department of Statistics
In the Faculty of Natural & Agricultural Sciences

University of Pretoria

Pretoria

April 2013

Declaration

I declare that the thesis, which I hereby submit for the degree Philosophiae Doctor (Mathematical Statistics) at the University of Pretoria, is my own work and has not previously been submitted by me for a degree at this or any other tertiary institution.

Signature: _____ Date: _____

Acknowledgements

I would like to sincerely thank my supervisor, Prof. S. Chakraborti, and my co-supervisor, Dr. S.W. Human, for their extraordinary efforts throughout my tenure as a PhD student in the Department of Statistics at the University of Pretoria. Their professional knowledge, insightful observations and guidance were crucial during the entire process of doing my research. I gratefully acknowledge the collaboration with Dr. A. Mukherjee from the Indian Institute of Management Udaipur in India.

Thanks also goes to the National Research Foundation (NRF) who awarded me with a Thuthuka grant (Reference: TTK20100724000013247, Grant number: 76219), the South African Research Chairs Initiative (SARChI), STATOMET and the Department of Statistics at the University of Pretoria for supporting me financially; without their financial assistance I would not have been able to go on the study leaves and attend conferences – thank you.

I would also like to thank the Department of Information Systems, Statistics and Management Science, at the University of Alabama, USA, for allowing me to do research at their institution over three separate trips and for some financial support.

Completing this work would have been all the more difficult were it not for the support and friendship provided by the staff members at the University of Pretoria and the University of Alabama. I am indebted to them for their help.

Finally, I would like to thank my husband, Walter, for his love, support and encouragement.

Summary

Distribution-free (nonparametric) control charts can be useful to the quality practitioner when the underlying distribution is not known. The term nonparametric is not intended to imply that there are no parameters involved, in fact, quite the contrary. While the term distribution-free seems to be a better description of what we expect from these charts, that is, they remain valid for a large class of distributions, nonparametric is perhaps the term more often used. In the statistics literature there is now a rather vast collection of nonparametric tests and confidence intervals and these methods have been shown to perform well compared to their normal theory counterparts. Remarkably, even when the underlying distribution is normal, the efficiency of some nonparametric tests relative to the corresponding (optimal) normal theory methods can be as high as 0.955 (see e.g. Gibbons and Chakraborti (2010) page 218). For some other heavy-tailed and skewed distributions, the efficiency can be 1.0 or even higher. It may be argued that nonparametric methods will be 'less efficient' than their parametric counterparts when one has a complete knowledge of the process distribution for which that parametric method was specifically designed. However, the reality is that such information is seldom, if ever, available in practice. Thus it seems natural to develop and use nonparametric methods in statistical process control (SPC) and the quality practitioners will be well advised to have these techniques in their toolkits. In this thesis we only propose univariate nonparametric control charts designed to track the location of a continuous process since very few charts are available for monitoring the scale and simultaneously monitoring the location and scale of a process.

Chapter 1 gives a brief introduction to SPC and provides background information regarding the research conducted in this thesis. This will aid in familiarizing the reader with concepts and terminology that are helpful to the following chapters. Details are given regarding the three main classes of control charts, namely the Shewhart chart, the cumulative sum (CUSUM) chart and the exponentially weighted moving average (EWMA) chart.

We begin **Chapter 2** with a literature overview of Shewhart-type Phase I control charts followed by the design and implementation of these charts. A nonparametric Shewhart-type Phase I control chart for monitoring the location of a continuous variable is proposed. The chart is based on the pooled median of the available Phase I samples and the charting statistics are the counts (number of observations) in each sample that are less than the pooled median. The derivations recognize that in Phase I the signalling events are dependent and that more than one comparison is

made against the same estimated limits simultaneously; this leads to working with the joint distribution of a set of dependant random variables. An exact expression for the false alarm probability is given in terms of the multivariate hypergeometric distribution and this is used to provide tables for the control limits. Some approximations are discussed in terms of the univariate hypergeometric and the normal distributions.

In **Chapter 3** Phase II control charts are introduced and considered for the case when the underlying parameters of the process distribution are known or specified. This is referred to as the 'standard(s) known' case and is denoted Case K. Two nonparametric Phase II control charts are considered in this chapter, with the first one being a nonparametric exponentially weighted moving average (NPEWMA)-type control chart based on the sign (SN) statistic. A Markov chain approach (see e.g. Fu and Lou (2003)) is used to determine the run-length distribution of the chart and some associated performance characteristics (such as the average, standard deviation, median and other percentiles). In order to aid practical implementation, tables are provided for the chart's design parameters. An extensive simulation study shows that on the basis of minimal required assumptions, robustness of the in-control run-length distribution and out-of-control performance, the proposed NPEWMA-SN chart can be a strong contender in many applications where traditional parametric charts are currently used. Secondly, we consider the NPEWMA chart that was introduced by Amin and Searcy (1991) using the Wilcoxon signed-rank statistic (see e.g. Gibbons and Chakraborti (2010) page 195). This is called the nonparametric exponentially weighted moving average signed-rank (NPEWMA-SR) chart. In their article important questions remained unanswered regarding the practical implementation as well as the performance of this chart. In this thesis we address these issues with a more in-depth study of the NPEWMA-SR chart. A Markov chain approach is used to compute the run-length distribution and the associated performance characteristics. Detailed guidelines and recommendations for selecting the chart's design parameters for practical implementation are provided along with illustrative examples. An extensive simulation study is done on the performance of the chart including a detailed comparison with a number of existing control charts. Results show that the NPEWMA-SR chart performs just as well as and in some cases better than the competitors.

In **Chapter 4** Phase II control charts are introduced and considered for the case when the underlying parameters of the process distribution are unknown and need to be estimated. This is referred to as the 'standard(s) unknown' case and is denoted Case U. Two nonparametric Phase II control charts are proposed in this chapter. They are a Phase II NPEWMA-type control chart and a nonparametric cumulative sum (NPCUSUM)-type control chart, based on the exceedance statistics,

respectively, for detecting a shift in the location parameter of a continuous distribution. The exceedance statistics can be more efficient than rank-based methods when the underlying distribution is heavy-tailed and / or right-skewed, which may be the case in some applications, particularly with certain lifetime data. Moreover, exceedance statistics can save testing time and resources as they can be applied as soon as a certain order statistic of the reference sample is available. We also investigate the choice of the order statistics (percentile), from the reference (Phase I) sample that defines the exceedance statistic. It is observed that other choices, such as the third quartile, can play an important role in improving the performance of these exceedance charts. It is seen that these exceedance charts perform as well as and, in many cases, better than its competitors and thus can be a useful alternative chart in practice.

Chapter 5 wraps up this thesis with a summary of the research carried out and offers concluding remarks concerning unanswered questions and / or future research opportunities.

Table of Contents

Chapter 1

Introduction

1.1. Notation

The table below lists some of the abbreviations and notation that will be used frequently throughout the dissertation.

Table 1.1. Abbreviations and notation

SPC	Statistical process control
NSPC	Nonparametric statistical process control
pmf	Probability mass function
cdf	Cumulative distribution function
n	Sample size / rational subgroup size
$X_1, X_2, \ldots, X_n$	Random variables in a sample
$x_1, x_2, \ldots, x_n$	Observations in a sample
θ_0	Target value or known or specified in-control location parameter[i]
CUSUM	Cumulative sum
EWMA	Exponentially weighted moving average
ARL	Average run-length
ARL_0	In-control average run-length
ARL_δ	Out-of-control average run-length
$SDRL$	Standard deviation of the run-length
MRL	Median run-length
UCL	Upper control limit
CL	Center line
LCL	Lower control limit
FAR	False alarm rate
FAP	False alarm probability
IC	In-control
OOC	Out-of-control
TPM	Transition probability matrix
A	Absorbent
NA	Non-absorbent

[i] The location parameter could be the mean, median or some percentile of the distribution. When the underlying distribution is known to be highly skewed, the median or some percentile is preferred to the mean.

1.2. The control chart

A control chart typically is a two dimensional graphic consisting of the values of a plotting (charting) statistic plotted on the vertical axis against time or subgroup number on the horizontal axis along with the associated control limits. The charting statistic and the control limits are calculated from the data which can be individual or subgroups (samples) of observations, collected sequentially over time. A typical two-sided Shewhart-type control chart (Walter A. Shewhart developed the statistical control chart concept in 1924) is shown in Figure 1.1.

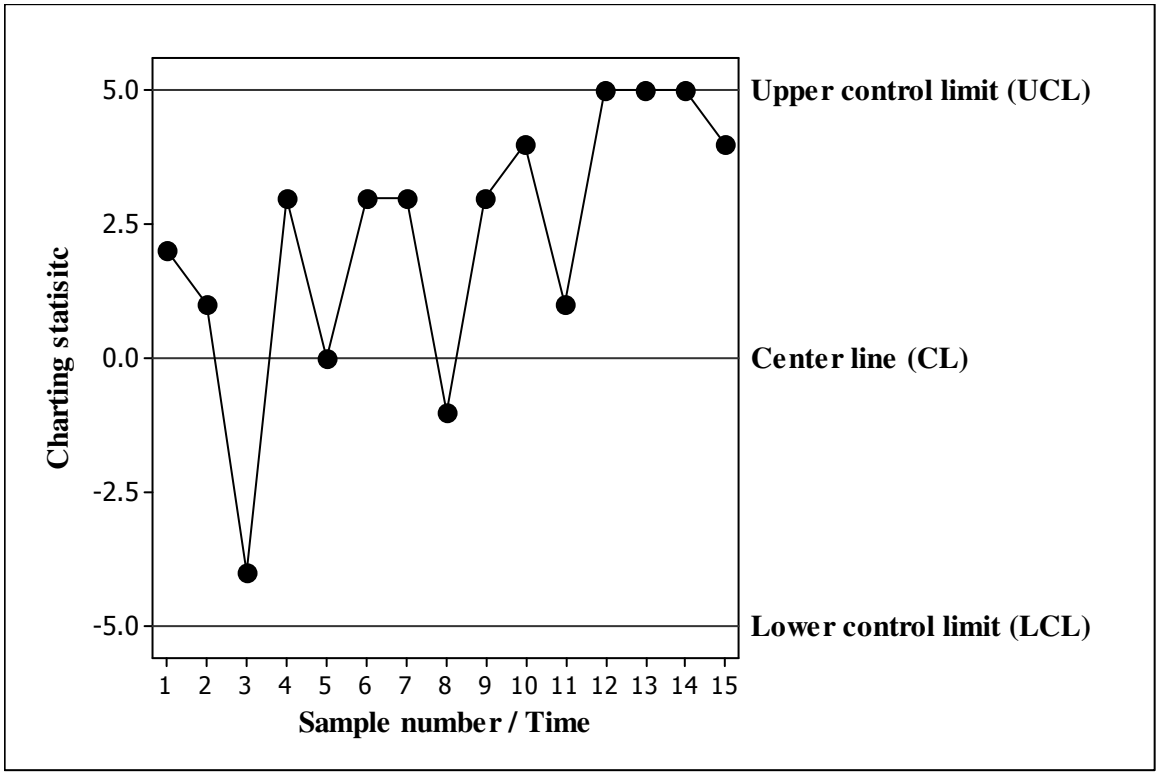

Figure 1.1. A two-sided Shewhart-type control chart

From Figure 1.1 it can be seen that a control chart usually has a center line (*CL*) and two horizontal lines, one on each side of the *CL*. The line above the *CL* is called the upper control limit (*UCL*) whereas the line below the *CL* is called the lower control limit (*LCL*). These three lines are placed on the control chart to aid the user in making an informed and objective decision whether a process is in-control (IC) or out-of-control (OOC). When a charting statistic plots on or outside either of the control limits it is said that a signal has been observed and the process is declared OOC. The event is called a signalling event. On the contrary, when the charting statistic randomly plots between the upper and the lower control limits the process is thought to be IC and hence no signal is observed on the control chart. The corresponding event is called a non-signalling event. Both one-sided and two-sided charts are considered in this thesis. The one-sided charts are more

useful when only a directional shift (higher or lower) in the location and / or scale is of interest. The two-sided charts, on the other hand, are typically used to detect a shift or change in the location and / or scale in any direction.

1.3. Distribution of chance causes

One of the main goals of statistical process control (SPC) is to distinguish between two sources of variability, namely common causes (chance causes) of variability and assignable causes (special causes) of variability (see e.g. Montgomery (2009) page 181). A common cause of variability is an inherent or natural (yet random) variability that is present in any process, whereas an assignable cause of variability may be a result of factors that are not solely random and which can be identified and eliminated. In SPC, the pattern of chance causes is usually assumed to follow some parametric distribution (such as the normal distribution). The charting statistic and the control limits depend on this assumption and as such the properties of these control charts are 'exact' only if this assumption is satisfied. However, often the chance distribution is either unknown or far from being normal in many applications and consequently the performance of standard control charts is highly affected in such situations. Thus, there is a need for some easy to use, flexible and robust control charts that do not require normality or any other specific parametric model assumption about the underlying chance distribution. Distribution-free or nonparametric control charts can serve this broader purpose. On this point see e.g. Woodall and Montgomery (1999) and Woodall (2000). These researchers and others provide ample reasons for the development of nonparametric control charts.

1.4. Nonparametric or distribution-free

The term nonparametric is not intended to imply that there are no parameters involved, in fact, quite the contrary. While the term distribution-free seems to be a better description of what we expect from distribution-free or nonparametric charts, that is, they remain valid for a large class of distributions, nonparametric is perhaps the term more often used. In the statistics literature there is now a rather vast collection of nonparametric tests and confidence intervals and these methods have been shown to perform well compared to their normal theory counterparts. Remarkably, even when the underlying distribution is normal, the efficiency of some nonparametric tests relative to the corresponding (optimal) normal theory methods can be as high as 0.955 (see e.g. Gibbons and Chakraborti (2010) page 218). For some other heavy-tailed and skewed distributions, the efficiency can be 1.0 or even higher. It may be argued that nonparametric methods will be 'less efficient' than

their parametric counterparts when one has a complete knowledge of the process distribution for which that parametric method was specifically designed. However, the reality is that such information is seldom, if ever, available in practice. Thus it seems natural to develop and use nonparametric methods in SPC and the quality practitioners will be well advised to have these techniques in their toolkits.

Nonparametric control charts also have the added advantage that they are robust. A robust statistical procedure (see e.g. Rocke et al. (1982)) is a procedure that performs well not only under ideal conditions (under which it is designed and proposed) but also under departures from the ideal. In the same spirit, a control chart is robust if its IC run-length distribution remains stable (unchanged, or nearly unchanged) when the underlying distributional assumption(s) (normality, for example) are violated (see e.g. Rocke (1989)). A nonparametric chart is robust by definition and can be more useful in situations where not much is known about the underlying process distribution. A control chart is nonparametric if its IC run-length distribution is the same for every continuous distribution (see e.g. Chakraborti et al. (2001)). Note that this definition includes the class of symmetric as well as asymmetric distributions. Thus, while the notion of robustness is somewhat vague insofar as specifying the degree of 'departure from the ideal' and the precise meaning of 'performs well', it is clear that while a robust control chart is not necessarily nonparametric, a nonparametric chart is robust.

Only univariate nonparametric control charts designed to track the location of a continuous process are considered in this body of work. The location charts continue to dominate the control charting literature, both parametric and nonparametric. An interesting and challenging problem is monitoring the scale parameter and very few charts are available for this problem. On the other hand, very recently, a few authors have considered nonparametric control charts for simultaneously monitoring the location and scale of a process. The field of multivariate control charts, particularly nonparametric charts, is interesting and the body of literature on nonparametric multivariate control charts is growing. However, that is not the focus of this work and is better postponed for the future.

1.5. Run-length distribution

"The number of rational subgroups to be collected or the number of charting statistics to be plotted on a control chart before the first OOC signal is observed is the run-length of a chart" Human and Graham (2007). The run-length is a random variable, denoted usually by N, with a mean and variance. The most widely used chart performance metric is the mean of the run-length,

referred to as the average run-length (*ARL*). However, since the run-length distribution is significantly right-skewed, researchers have advocated using other, more representative, measures for the assessment of chart performance. These include the standard deviation of the run-length (*SDRL*) and other percentiles of the run-length, more specifically, the median run-length (*MRL*), which provides additional and more meaningful information about the in-control and out-of-control performances of control charts, not given by the *ARL*. The idea of looking at percentiles, in SPC, goes back to Barnard (1959) and more recently researchers such as Gan (1994), Chakraborti (2007) and Khoo et al. (2011) have advocated the use of percentiles, such as the median, for assessment of chart performance. The run-length distribution and the characteristics of the run-length distribution can be obtained using four methods, namely

i. The exact approach (for Shewhart and some Shewhart-type charts)
ii. The Markov chain approach
iii. The integral equation approach
iv. The computer simulations (the Monte Carlo) approach

In this body of work the emphasis falls on the computer simulations (the Monte Carlo) approach and the Markov chain approach. More details on these approaches are given later on.

1.6. Nonparametric control charts

Although nonparametric statistical methods have been around since at least the 1940's in the statistical estimation and testing literature, the work of Chakraborti et al. (2001) may be viewed as the first coherent discussion of the applicability of these methods in the quality literature. Continuing this line of work, Chakraborti and Graham (2007) and most recently Chakraborti et al. (2011) provided thorough overviews of the nonparametric control charting literature. A formal definition of a nonparametric or distribution-free control chart is given in terms of its IC run-length distribution.

Definition 1.1

Distribution-free or nonparametric control chart

If the IC run-length distribution is the same for every continuous distribution, then the chart is called distribution-free.

Note that this Definition 1.1 includes the class of symmetric as well as asymmetric distributions. Chakraborti et al. (2001) summarized the advantages of nonparametric control charts as follows:

i. it is easy to implement, i.e. simplicity,

ii. no need to assume a particular parametric distribution for the underlying process,

iii. the in-control run-length distribution is the same for all continuous distributions,

iv. more robust and outlier resistant,

v. more efficiency in detecting changes when the true distribution is markedly non-normal, particularly with heavier tails, and

vi. no need to estimate the variance to set up charts for the location parameter.

It is emphasized that from a technical point of view most nonparametric procedures require the population to be continuous in order to be distribution-free and thus in a SPC context we consider the so-called 'variables control charts' (see e.g. Montgomery (2009) page 226). While the nonparametric charts offer many advantages, they are not without their critics. Some disadvantages of nonparametric control charts are as follows (see Chakraborti et al. (2001) page 306):

i. they will be 'less efficient' than their parametric counterparts when one has a complete knowledge of the process distribution for which that parametric method was specifically designed,

ii. one usually requires special tables when the sample sizes are small, and

iii. nonparametric methods are not well-known amongst all researchers and quality practitioners.

The basic point is this. If the underlying model is known or can be assumed, a parametric statistical procedure, such as a control chart, would be expected to be more efficient than a nonparametric method which does not make a model assumption. However, the reality is that in practice, such a model assumption may not often be justifiable.

1.7. Terminology and problem statement

Two important problems in usual SPC are monitoring the process mean and / or the process standard deviation. In the nonparametric setting, we consider, more generally, monitoring the center or the location (or a shift) parameter and / or a scale parameter of a process. The location parameter represents a typical value and could be the mean or some percentile, such as the median of the distribution; the latter is especially attractive when the underlying distribution is expected to be skewed. Let $F(x)$ denote the unknown cumulative distribution function (cdf) of the monitored continuous variable X. In analogy with the parametric, mainly the normal distribution case, it is assumed that F follows either

i. a location model, with a cdf $F(x-\theta)$, where $x\epsilon(-\infty,\infty)$ and $\theta\epsilon(-\infty,\infty)$ is the location parameter, or,

ii. a scale model, with a cdf $F\left(\frac{x}{\tau}\right)$, where $x\epsilon(-\infty,\infty)$ and $\tau>0$ is the scale parameter, or,

iii. a location-scale model with cdf $F\left(\frac{x-\theta}{\tau}\right)$, where $x\epsilon(-\infty,\infty)$ and $\theta\epsilon(-\infty,\infty)$ and $\tau>0$ are the location and the scale parameter, respectively.

Thus in the nonparametric setting, the problem is to track θ or τ or both, under these model assumptions, based on random samples or subgroups of data usually taken at equally spaced time points. To highlight the analogy, in the usual parametric control charting problems F is assumed to be the cdf (Φ) of the standard normal distribution whereas in the nonparametric setting, for variables data, F is some unknown continuous cdf. Although the location-scale model seems to be a natural model to consider paralleling the normal theory case with mean and variance both unknown,

most of what is currently available in the nonparametric statistical process control (NSPC) literature deals mainly with the location model. As noted earlier, this is the main focus of the present work.

1.8. Phase I and Phase II

Before going further, it is useful to note that recent work in SPC make a distinction between two phases (or stages): Phase I (also called the retrospective phase) and Phase II (also called the prospective or monitoring phase). The analysis of historical or preliminary data, in order to establish that a process is IC, generally comes under what is referred to as Phase I. A process that operates at or around a desirable level or specified target with no assignable causes of variation is said to be in statistical control, or simply in-control. In Phase I, the primary interest is assessing process stability, often trying to bring a process IC by locating and eliminating any assignable causes, estimating any unknown quantities (parameters) and setting up control charts (limits) so that effective process monitoring can begin in Phase II. Control charts play a crucial role in Phase I. They help in diagnosing source(s) of assignable causes and their removal. The process of establishing control may be iterative and the control limits in this phase are usually viewed as trial limits. Once statistical control is established, the parameters are estimated and control limits are finalized based on IC data (also called reference data). Once this is ascertained, SPC moves to the next phase, called Phase II, where the control limits and / or the estimators obtained in Phase I are used for process monitoring based on new incoming samples of data.

When the underlying parameters of the process distribution are known or specified, this is referred to as the 'standard(s) known' case and is denoted Case K. In contrast, if the distribution's parameters are unknown and need to be estimated, it is typically done in Phase I, with in-control data. This situation is referred to as the 'standard(s) unknown' case and is denoted Case U. In this text we are going to consider decision problems under both Phase I and Phase II. One of the main differences between the two phases is the fact that the false alarm rate (*FAR*) (or in-control average run-length ARL_0) is typically used to construct and evaluate Phase II control charts, whereas the false alarm probability (*FAP*) is used to construct and evaluate Phase I control charts. The *FAP* is the probability of at least one false alarm out of the comparison of all the charting statistics to the control limits simultaneously, whereas the *FAR* is the probability of a single false alarm involving only a single comparison of a charting statistic to the control limits. Various authors have studied the Phase I problem; see for example King (1954), Chou and Champ (1995), Sullivan and Woodall (1996), Jones and Champ (2002), Champ and Chou (2003), Champ and Jones (2004), Koning (2006) and Human et al. (2009). It is recognized that since not much is typically known or can be

assumed about the underlying process distribution in a Phase I setting, nonparametric Phase I control charts can be of great value.

1.9. Types of control charts

There are three main classes of control charts: the Shewhart chart, the cumulative sum (CUSUM) chart and the exponentially weighted moving average (EWMA) chart and their refinements. Relative advantages and disadvantages of these charts are well documented in the literature (see e.g. Montgomery (2009)). Analogs of these charts have been considered in the nonparametric setting. We describe some of the charts in more detail in each of the three sections that follow.

1.9.1. Shewhart-type control charts

Shewhart-type charts are the most popular charts in practice because of their simplicity, ease of application, and the fact that these versatile charts are quite efficient in detecting moderate to large shifts. To describe the Shewhart chart in more detail, assume that $X_{i1}, X_{i2}, \dots, X_{in}$ denote a random sample (i.e. measurements from some quality characteristic) of size $n \geq 1$ form the process at time $i = 1,2,3,\dots$. Let w be a sample statistic that measures some quality characteristic of interest, and suppose that the mean of w is μ_w, the variance of w is σ_w^2 and the standard deviation of w is σ_w. Then the control limits and CL are given by

$$\begin{aligned} UCL &= \mu_w + k\sigma_w \\ CL &= \mu_w \\ LCL &= \mu_w - k\sigma_w \end{aligned} \tag{1.1}$$

where $k > 0$ is the charting constant which is a design parameter that determines the 'distance' of the control limits from the CL expressed in standard deviation units. When a charting statistic plots on or outside either of the control limits it is said that a signal has been observed and the process is declared OOC. Typically, a search for assignable causes is then started.

1.9.2. CUSUM-type control charts

While the Shewhart-type charts are widely known and most often used in practice because of their simplicity and global performance, other classes of charts, such as the CUSUM charts, are useful and sometimes more naturally appropriate in the process control environment in view of the sequential nature of data collection. CUSUM control charts were first introduced by Page (1954) (although not in its present form) and have been studied by many authors, for example, Barnard (1959), Ewan and Kemp (1960), Johnson (1961), Goldsmith and Whitfield (1961), Page (1961), Ewan (1963), Hawkins (1992, 1993), Woodall and Adams (1993) and Hawkins and Olwell (1998).

These charts, typically based on the cumulative sums of a charting statistic, obtained as data accumulate over time, are known to be more efficient for detecting certain types of shifts in the process. The normal theory CUSUM chart for the mean is typically based on the cumulative sum of the deviations of the individual observations (or the subgroup means) from the specified target mean.

To describe the CUSUM chart in more detail, assume that $X_{i1}, X_{i2}, X_{i3}, \dots, X_{in}$ denote a sample (subgroup) of size $n \geq 1$ on the process output at each sampling instance i, $i = 1,2,\dots$, from a process with a known process mean μ_0 and a known process standard deviation σ_0. A statistic

$$\psi_i = \psi(x_{i1}, x_{i2}, \dots, x_{in}) \tag{1.2}$$

is constructed using the data in the i^{th} sample, $i = 1,2,\dots$. The statistic in Equation (1.2) is referred to as the basic (pivot) statistic; see Bakir (2011).

The upper one-sided CUSUM works by accumulating deviations from $\mu_0 + k$ that are above target. For the upper one-sided CUSUM chart we use

$$C_i^+ = max[0, \psi_i - k + C_{i-1}^+] \text{ for } i = 1,2,3... \tag{1.3}$$

to detect positive deviations from μ_0 with starting value $C_0^+ = 0$ and the so-called reference value $k \geq 0$. A signalling event occurs for the first i such that $C_i^+ \geq H$, where $H > 0$ is the decision interval. The lower one-sided CUSUM works by accumulating deviations from $\mu_0 - k$ that are below target

$$C_i^- = min[0, \psi_i + k + C_{i-1}^-] \text{ for } i = 1,2,3... \quad (1.4)$$

or

$$C_i^{-^*} = max[0, -k - \psi_i + C_{i-1}^{-^*}] \text{ for } i = 1,2,3... \quad (1.5)$$

and is used to detect negative deviation from μ_0 with starting value $C_0^- = C_0^{-^*} = 0$. Here a signalling event occurs for the first i such that $C_i^- \leq -H$ (if Expression (1.4) is used) or $C_i^{-^*} \geq H$ (if Expression (1.5) is used). For a visually appealing chart, Expression (1.4) will be used to construct the lower one-sided CUSUM. The two-sided CUSUM chart signals for the first i at which either one of the two inequalities is satisfied, that is, either $C_i^+ \geq H$ or $C_i^- \leq -H$. For the CUSUM chart there are quantities or counters, N^+ and N^-, which indicate the number of consecutive periods that the CUSUM's C_i^+ and C_i^- have been non-zero which helps in identifying at what point in time the shift may have taken place. This is illustrated later on in Chapter 4. Both k and H are design parameters of the chart which are needed in order to implement the CUSUM chart. This is discussed next.

The design parameters k and H are chosen so that the chart has a specified nominal ARL_0 and is capable of detecting a shift, specially a small shift, as soon as possible. The first step in this direction is to choose k. For the parametric CUSUM chart for the normal mean, the choice of k has been discussed by many authors; see e.g. Lucas (1985), Hawkins and Olwell (1998), Kim et al. (2007) and Montgomery (2009). Lucas (1985) stated "The CUSUM parameter k is determined by the acceptable mean level (μ_a) and by the unacceptable mean (μ_d) level which the CUSUM scheme is to detect quickly. For normally distributed variables the k value is chosen half way between the acceptable mean level and the unacceptable mean level." In the more recent literature, see e.g. Montgomery (2009), it is agreed that in the normal theory setting k is typically chosen relative to the size of the shift we want to detect, that is, $k = \frac{1}{2}\delta$, where δ is the size of the shift in the mean expressed in standard deviation units. More details on the choice of δ is given later in this section. Hawkins and Olwell (1998; page 54), investigated the sensitivity of the *ARL* of the CUSUM chart for the normal mean to the choice of k. They considered four values of k, namely k = 0.25, 0.5, 1 and 2 and concluded that "… the CUSUM with k = 0.25 is the best of the four for all Δ less than 0.73. The k = 0.50 CUSUM, which is tuned to shifts of size Δ = 1 then takes the lead and is the best of the four in the range 0.73 < Δ < 1.46. The CUSUM k = 1 leads in the range 1.46 < Δ < 2.87, and the k = 2 CUSUM is the best of these four for Δ value above 2.87." Take note that, in their

conclusion, Δ denotes the size of the actual mean shift[ii]. For the parametric CUSUM chart for the normal mean, Kim et al. (2007) considered two values of the reference value k, namely, $k = 0$ and $k = 0.5$ and found that the CUSUM chart with $k = 0$ is more effective in detecting shifts of size $0.25\sigma_Y$, where σ_Y is the process standard deviation, whereas the chart with $k = 0.5$ detects any shift exceeding $0.25\sigma_Y$ much faster. Hawkins and Olwell (1998; page 35) made the following comment concerning the choice of $k = 0$ for the parametric CUSUM chart for the normal mean: "The in-control *ARL* of the CUSUM depends on the value of k and h. Larger values of either of these parameters lead to larger *ARL*s. At the extremes, if k and h are both zero, then the *ARL* is 1, since the first point will necessarily give a value of at least 0."

After choosing k, the next step is to find the decision interval H, in conjunction with the chosen k, so that a specified nominal ARL_0 is attained. Note, however, for a discrete random variable the chances are that H cannot always be found such that the specified nominal ARL_0 is attained exactly and hence using a conservative approach, H is found so that the attained ARL_0 is less than or equal to the specified nominal ARL_0. The decision interval, H, is found using a grid search algorithm using 100 000 Monte Carlo simulations using SAS® v 9.3.

Let us consider the parametric CUSUM chart for monitoring of normal mean with individual data ($n = 1$) with no reference sample. In this case, the pivot statistic in Equations (1.3), (1.4) and (1.5) is replaced by X_i where X_i follows a normal distribution. To examine the impact of k, we examine the out-of-control *ARL* (denoted ARL_δ) for the normal distribution in Figure 1.2, taking the IC mean $\mu_0 = 0$ and standard deviation $\sigma = 1$ (without loss of generality) and setting the nominal $ARL_0 = 500$, for $\mu_1 = 0.1, 0.25, 0.5$ and 1.0. Note that μ_1 represents the increased value of μ to be detected 'quickly' from $\mu_0 = 0$; hence μ_1 represents the true shift in the mean, that is, $\delta = \mu_1$.

[ii] Relationship between δ and Δ: Let μ_0 denote the target IC mean and let μ_1 denote the OOC value of the mean. Then δ is the size of the shift in the mean expressed in standard deviation units, i.e. $\mu_1 = \mu_0 + \delta\sigma$ so that $\delta = |\mu_1 - \mu_0|/\sigma$. In Hawkins and Olwell (1998) Δ denotes the size of the actual mean shift, i.e. $\Delta = \delta\sigma$.

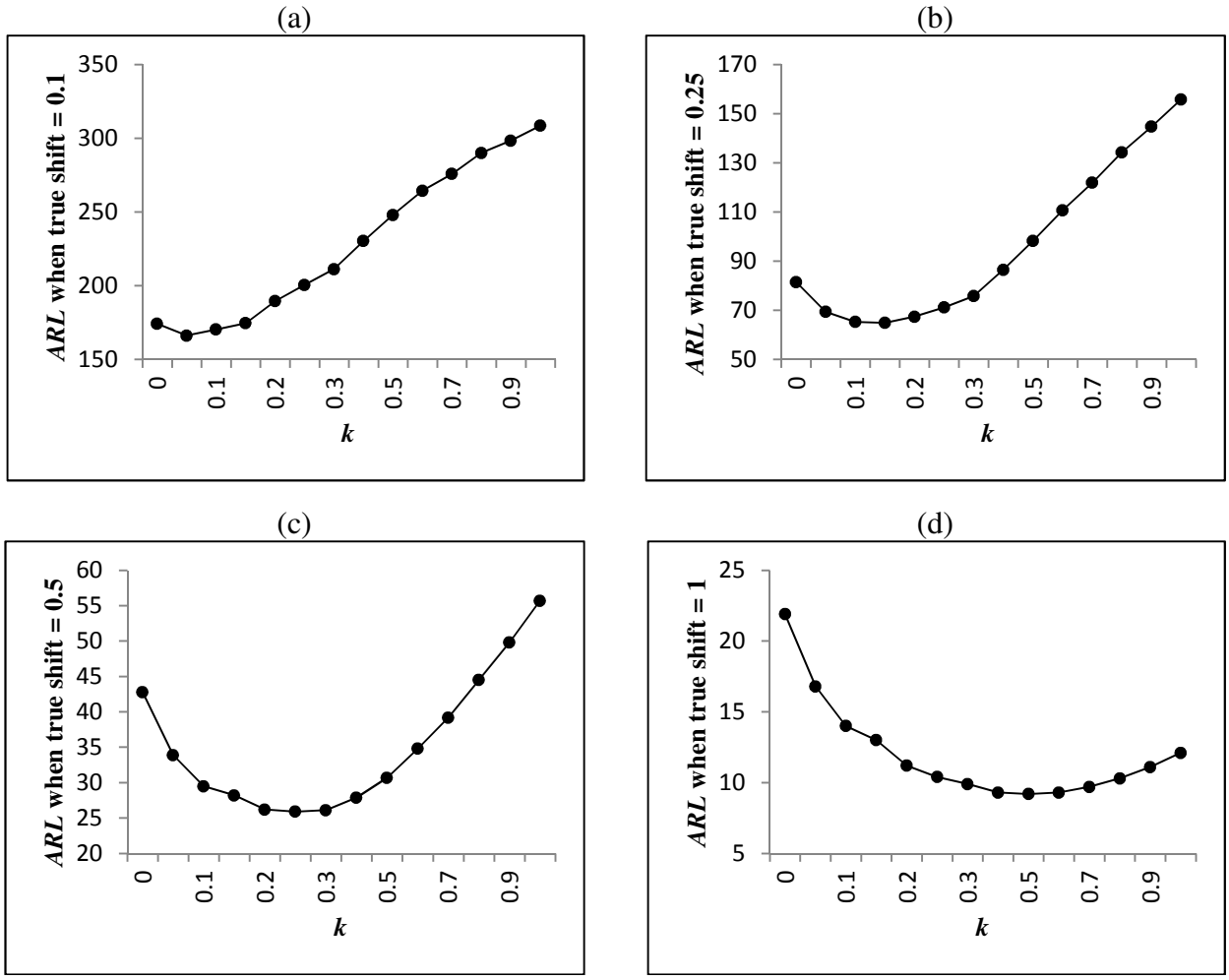

Figure 1.2. ARL_δ values of the traditional CUSUM chart with the nominal $ARL_0 = 500$ for different values of k and $\mu_1 = 0.1, 0.25, 0.5$ and 1.0

From Figure 1.2 several interesting observations can be made. When the shift is small (see panels (a) and (b) of Figure 1.2) and a larger value of k is chosen, the ARL_δ values become unacceptably high. On the other hand, if the shift is large (see panels (c) and (d) of Figure 1.2) and a smaller value of k is chosen, the ARL_δ values are also high, but not as high as in the latter case. This suggests that when there is little or no a-priori information regarding the size of the shift, a smaller value of k is the safest choice (to protect against any unnecessary delays in detection). Later we shall see that similar conclusions can be drawn about nonparametric CUSUM charts (see Section 4.3). Note that although we are considering an unknown shift, we are primarily interested in detecting a smaller and moderate shift with a CUSUM chart. Therefore, we recommend using $k = 0$ (or letting δ tend to 0).

Note that this general discussion regarding the CUSUM chart is for Case K, i.e. when the process parameters are known. However, in Case U the process parameters are unknown and need to be estimated. More details are given on Case U in Chapter 4.

With so much work done with parametric control charts, it is natural to consider analogs of these charts using nonparametric charting statistics. This approach has led to NPCUSUM charts considered in this work to be discussed later. The reader is referred to Hawkins and Olwell (1998) for a detailed overview on parametric CUSUM charts.

1.9.3. EWMA-type control charts

Another popular class of control charts is the exponentially weighted moving average (EWMA) charts. The EWMA charts also take advantage of the sequentially (time ordered) accumulating nature of the data arising in a typical SPC environment and are known to be efficient in detecting smaller shifts but are easier to implement than the CUSUM charts (see e.g. Montgomery (2009) page 419). The classical EWMA charts for the mean were introduced by Roberts (1959) and they contain the Shewhart-type charts as a special case. The literature on EWMA charts is enormous and continues to grow at a substantial pace (see e.g. the overview in the *Encyclopedia of Statistics in Quality and Reliability* by Ruggeri et al. (2007) and the references therein). Some more recent references include Capizzi and Masarotto (2012) and Ross et al. (2012).

To describe the EWMA chart in more detail, assume that $X_{i1}, X_{i2}, X_{i3}, \ldots, X_{in}$ denote a sample (subgroup) of size $n \geq 1$ on the process output at each sampling instance i, $i = 1,2,\ldots$, from a process with a known process mean μ_0 and a known process standard deviation σ_0. The charting statistic for the EWMA control chart is defined as

$$Z_i = \lambda\psi_i + (1-\lambda)Z_{i-1} \quad \text{for} \quad i = 1,2,3... \tag{1.6}$$

where $0 < \lambda \leq 1$ is a constant called the smoothing parameter and ψ_i is the pivot statistic defined in Equation (1.2). The starting value Z_0 is typically taken to be the process mean, i.e. $Z_0 = \mu_0$. The expected value and variance of Z_i are given by

$$E(Z_i) = \mu_0 \tag{1.7}$$

and

$$VAR(Z_i) = \sigma_0^2 \left(\frac{\lambda}{2-\lambda}\right)\left(1-(1-\lambda)^{2i}\right) \tag{1.8}$$

respectively (see Appendix 1A for the derivations). The exact control limits and the center line of the EWMA control chart are given by

$$UCL = E(Z_i) + L \times STDEV(Z_i) = \mu_0 + L\sigma_0\sqrt{\left(\frac{\lambda}{2-\lambda}\right)(1-(1-\lambda)^{2i})}$$

$$CL = E(Z_i) = \mu_0 \tag{1.9}$$

$$LCL = E(Z_i) - L \times STDEV(Z_i) = \mu_0 - L\sigma_0\sqrt{\left(\frac{\lambda}{2-\lambda}\right)(1-(1-\lambda)^{2i})}$$

where $L > 0$ is a charting constant. The steady-state control limits (which are typically used when the EWMA chart has been running for several time periods so that the term $\left(1-(1-\lambda)^{2i}\right)$ in (1.9) approaches unity) are given by

$$UCL = \mu_0 + L\sigma_0\sqrt{\left(\frac{\lambda}{2-\lambda}\right)}$$

and (1.10)

$$LCL = \mu_0 - L\sigma_0\sqrt{\left(\frac{\lambda}{2-\lambda}\right)}.$$

The two-sided EWMA chart is constructed by plotting Z_i against the sample number i (or time). If the charting statistic Z_i falls between the two control limits, that is, $LCL < Z_i < UCL$, the process is considered to be IC. If the charting statistic Z_i falls on or outside one of the control limits, that is $Z_i \leq LCL$ or $Z_i \geq UCL$, the process is considered to be OOC and a search for assignable causes is necessary.

The two-sided EWMA can be modified to form a one-sided statistic in much the same way a CUSUM can be made into a one-sided statistic. For example, an upper one-sided EWMA is given by $Z_i^+ = \max[\mu_0, \lambda\psi_i + (1-\lambda)Z_{i-1}]$ for $i = 1,2,3...$ with starting value $z_0^+ = \mu_0$ where μ_0 is the IC process mean or the target value. If the charting statistic Z_i plots on or above the UCL the process is considered to be OOC and a search for assignable causes is necessary.

The design parameters L and λ are chosen so that the chart has a specified nominal ARL_0 and is capable of detecting a shift, specially a small shift, as soon as possible. Montgomery (2009, page 422) states that "The optimal design procedure would consist of specifying the desired in-control and out-of-control average run-lengths and the magnitude of the process shift that is anticipated, and then to select the combination of λ and L that provide the desired ARL performance." The EWMA chart is designed by specifying λ and L so that a specified ARL_0 is achieved. The constant λ $(0 < \lambda \leq 1)$ is the smoothing parameter ($\lambda = 1$ yields the well-known Shewhart chart) and is selected depending on the magnitude of the shift to be detected while the constant $L > 0$ is the distance of the control limits from the CL (the larger the value of L, the wider the control limits and vice versa) and is selected in combination with the value of the smoothing parameter λ. With regard to the implementation of the EWMA chart, the first step is to choose λ. The recommendation is to choose a small λ, say equal to 0.05, when small shifts are of interest, if moderate shifts are of greater concern, choose $\lambda = 0.10$, whereas choose $\lambda = 0.20$ if larger shifts are of interest (see e.g. Montgomery (2005) page 423)). After λ is chosen, the second step involves choosing L, so that a desired ARL_0 is attained.

Note that this general discussion regarding the EWMA chart is for Case K, i.e. when the process parameters are known. However, in Case U the process parameters are unknown and need to be estimated. More details are given on Case U in Chapter 4.

With so much work done with parametric control charts, it is natural to consider analogs of these charts using nonparametric charting statistics. This approach has led to nonparametric EWMA (NPEWMA) charts considered in this work to be discussed later.

1.10. Methods to calculate the run-length distribution

There are four methods to calculate (or at least approximate) a control chart's run-length distribution. These methods are

i. The exact approach (for Shewhart and some Shewhart-type charts)
ii. The Markov chain approach
iii. The integral equation approach
iv. The computer simulations (the Monte Carlo) approach

A discussion on each method follows.

1.10.1. The exact approach (for Shewhart and some Shewhart-type charts)

For Shewhart control charts and some Shewhart-type control charts it is possible to calculate the characteristics of the run-length distribution exactly. For an example the reader is referred to Bakir (2004) where the *ARL* of the nonparametric Shewhart signed-rank control chart is computed exactly.

1.10.2. The Markov chain approach

A simple and unified method, which is based on a finite homogenous Markov chain, can be used to evaluate the run-length distribution and the characteristics of the run-length distribution of various types of control charts. These include the Shewhart-type chart (see e.g. Klein (2000), Khoo (2003), Khoo and Ariffin (2006) and Human et al. (2010a)), the EWMA-type chart (see e.g. Saccucci and Lucas (1990), Borror et al. (1998) and Reynolds and Arnold (2001)) and the CUSUM-type chart (see e.g. Brook and Evans (1972), Bakir and Reynolds (1979), Woodall (1984), Crosier (1986), Reynolds et al. (1990) and Reynolds (2012)). In this section, definitions, results and theorems are provided that give the necessary background to calculate the characteristics of the run-length distribution via the Markov chain approach. The theorems and results are critical to the following chapters.

The Markov chain approach for calculating the run-length distribution entails that the charting statistic is viewed as following a Markov chain, characterized by a state space S and a transition probability matrix M. The state space consists of two types of states:

i. one absorbing state (i.e. this state is entered when the chart signals, that is when the charting statistic is greater than or equal to the *UCL* or less than or equal to the *LCL*) and

ii. ν transient or non-absorbing states, so that there are $\nu + 1$ states in total.

The ν transient states correspond to ν equal length subintervals obtained by dividing the interval between the upper and the lower control limits. The choice of ν is important; its value directly impacts the accuracy of the results (i.e. the larger the value of ν, the more exact / accurate the approximate results are). For convenience, ν is taken to be an odd positive integer, equal to

$2s + 1$ with $s \geq 1$ so that there is a unique middle subinterval between the upper and lower control limits, i.e. the transient states range from $-s, -s + 1, \ldots, 0, \ldots s - 1, s$ with state 0 representing the middle subinterval between the upper and lower control limits; for a graphical representation the reader is referred to Figure 3.2 in Section 3.2.3.1. Later on we define the initial probability vector so that we start in state 0 with probability one, ensuring that the process starts in-control. The $(v + 1) \times (v + 1)$ transition probability matrix, M, is written in a partitioned form,

$$M_{(v+1)\times(v+1)} = \begin{pmatrix} Q_{v\times v} & | & \underline{p}_{v\times 1} \\ - & - & - \\ \underline{0}'_{1\times v} & | & 1_{1\times 1} \end{pmatrix} \tag{1.11}$$

where the sub-matrix $Q_{v\times v}$ contains all the probabilities of going from one transient state to another and is called the essential transition probability matrix; the column vector $\underline{p}_{v\times 1}$ contains all the probabilities of going from each transient state to the absorbing state; $\underline{0}'_{1\times v}$ a row vector of zeros which contains all the probabilities of going from the absorbing state to each transient state and the scalar value 1 is the probability of going from the absorbing state to the absorbing state. Note that the key component in using the Markov chain approach is to obtain the essential transition probability sub-matrix $Q_{v\times v}$.

The run-length random variable N of the control chart is the waiting time for the Markov chain to enter the absorbing state for the first time. Using this analogy and assuming that the process starts IC when the chart is implemented, the probability mass function, the expected value (*ARL*), the *SDRL* and the cumulative distribution function of N are given by (see Fu and Lou (2003; Theorems 5.2 and 7.4 pages 68 and 143, respectively))

$$P(N = t) = \underline{\xi} Q^{t-1}(I - Q)\underline{1} \quad \text{for} \quad t = 1,2,3, \ldots \tag{1.12}$$

$$E(N) = \underline{\xi}(\mathrm{I} - Q)^{-1}\underline{1} \tag{1.13}$$

$$SD(N) = \sqrt{\underline{\xi}(I + Q)(I - Q)^{-2}\underline{1} - (E(N))^2} \tag{1.14}$$

$$P(N \leq t) = 1 - \underline{\xi} Q^{t}\underline{1} \quad \text{for} \quad t = 1,2,3, \ldots \tag{1.15}$$

respectively, where $I = I_{v\times v}$ is the identity matrix, $Q = Q_{v\times v}$ is the essential transition probability sub-matrix, $\underline{1} = \underline{1}_{v\times 1}$ is a column vector with all elements equal to one and $\underline{\xi} = \underline{\xi}_{1\times v}$ is a row

vector called the initial probability vector which contains the probabilities that the Markov chain starts in a given state. The vector $\underline{\xi} = (\xi_{-s}, \ldots, \xi_s)$ is typically chosen such that $\sum_{i=-s}^{s} \xi_i = 1$. For a detailed discussion on the choice of the initial probability vector, see the Appendix of Lucas and Saccucci (1990). We take $\xi_0 = 1$ and $\xi_i = 0$ for all $i \neq 0$, which implies that the Markov chain starts in state zero (i.e., $Z_0 = 0$) with probability one. This essentially implies that the process is IC when we start monitoring the process. The steps for discretizing the infinite state transition probability matrix are as follows:

Step 1: Divide the interval between the *LCL* and the *UCL* into $\nu = 2s + 1$ subintervals of width $2\tau = (UCL - LCL)/\nu$ (see Figure 1.3) where each subinterval corresponds to a transient (or an accessible) state of the Markov chain; state j is said to be accessible from state i if and only if, starting in state i, it is possible that the process will at some stage enter state j. Note that $2\tau = (UCL - LCL)/\nu$ will equal $2\tau = 2UCL/\nu$ so that $\tau = UCL/\nu$ if the control limits are symmetrically placed around zero, i.e. $-LCL = UCL$.

Step 2: Choose the number of discretized subintervals ν to be an odd positive integer so that there is a unique middle entry.

Step 3: Declare the charting statistic, Z_i, to be in the transient state j at time i if $S_j - \tau < Z_i \leq S_j + \tau$ for $j = -s, -s+1, \ldots, s-1$ and $S_j - \tau < Z_i < S_j + \tau$ for $j = s$, where S_j denotes the midpoint of the j^{th} interval.

Step 4: Calculate the one-step transition probabilities (p_{ij}'s) where p_{ij} denotes the probability of moving from state i to state j in one step at any point in time.

Step 5: Construct the transition probability matrix, consisting of the one-step transition probabilities, to find the run-length distribution.

It should be noted that the midpoints (defined in Step 3) can be found using the following general calculation formula

$$S_j = LCL + (2(s+j)+1)\tau \text{ and } S_0 = 0$$

since we assume (for simplicity) that $-LCL = UCL$. The charting statistic is said to be in the absorbing or OOC state (i.e. $j = s + 1$) if Z_i falls on or outside the control limits. This region is considered absorbing since the process is stopped when a signal is given by the chart. Hence, the process is declared to be OOC whenever Z_i is in the absorbing state, whereas the process is considered to be IC whenever Z_i is in a transient state (also referred to as an IC state). Therefore, the IC region consists of v non-absorbing states, whereas the OOC region is treated as a single absorbing state.

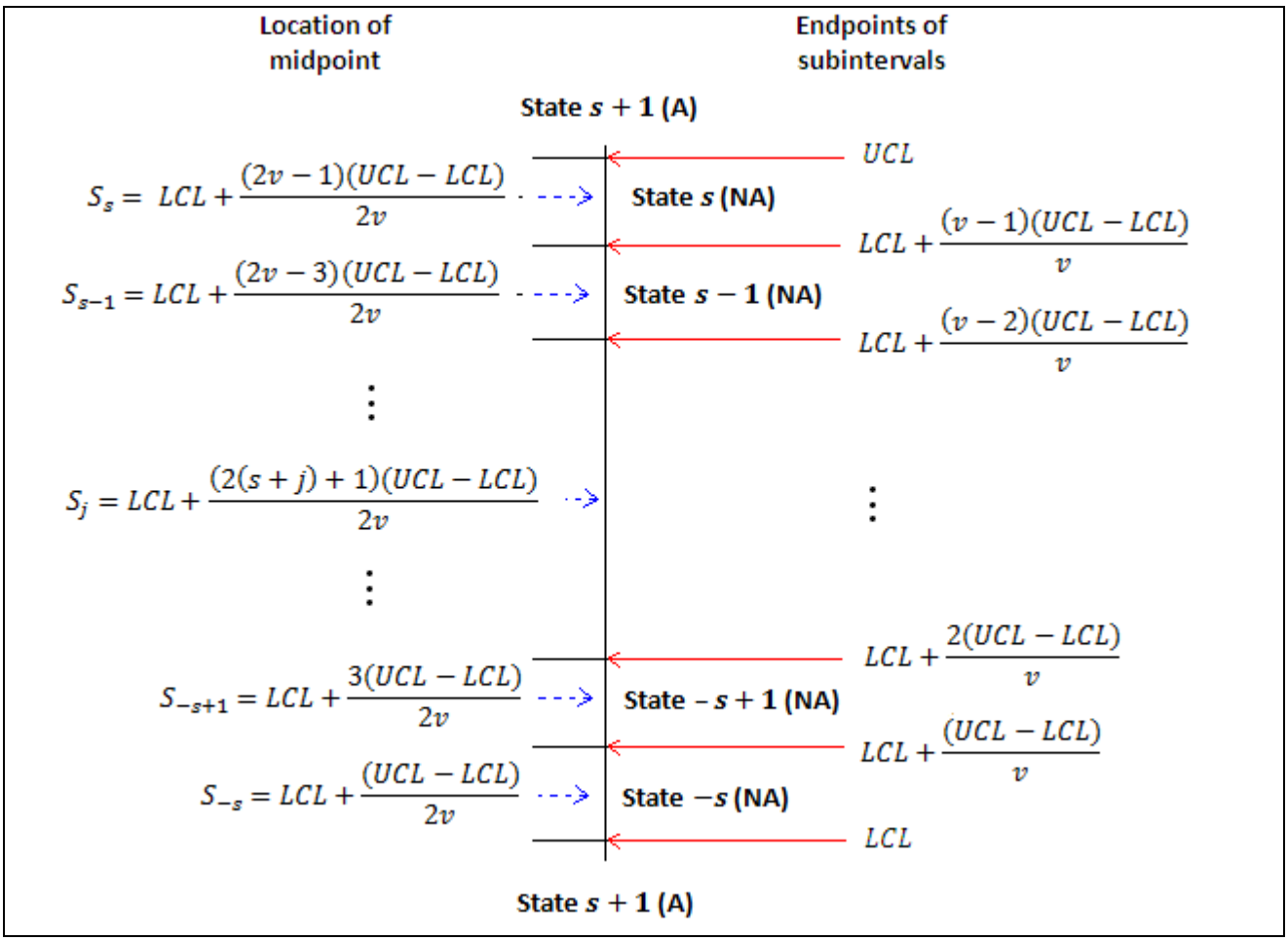

Figure 1.3. Partitioning of the interval between the *LCL* and the *UCL* into $v = 2s + 1$ subintervals

Next, we need expressions for the signalling probabilities. The elements inside of the transition probability matrix are called the one-step transition probabilities; $Q = [p_{ij}]$ for $i, j = -s, -s+1, \ldots, s-1, s$. In order to calculate these probabilities we assume that the charting statistic is equal to S_i whenever it is in state i. However, for each control chart under consideration, the one-step transition probabilities are calculated differently. This is considered in later chapters as various control charts are considered.

1.10.3. The integral equation approach

The integral equation approach utilizes mathematics and combinatorics to find a closed form expression of the run-length distribution. This approach is sometimes challenging, in that the expression obtained is typically complex or difficult to evaluate numerically. Very often the exact expression of the run-length distribution can be found, but simulations are done instead, since it is much easier. An example of where the run-length distribution is found using the exact approach is Jones et al. (2004) and Human et al. (2009) used combinatorics to calculate the run-length distributions of nonparametric Shewhart-type control charts.

1.10.4. The computer simulations (the Monte Carlo) approach

Monte Carlo simulations can be used to calculate the characteristics of the run-length distribution. The popularity of this method stems from the fact that no matter how complicated the run-length distribution is, computer simulations can almost always be used with relative ease to calculate the run-length distribution and its associated characteristics fairly accurately, provided the simulation size is big enough. In this body of work we use 100 000 simulations, since it is well known that the error of a run-length characteristic can be bounded by increasing the simulation size sufficiently. Chakraborti and Van de Wiel (2008) stated the 10% error band (i.e. run-length characteristic + 0.1(run-length characteristic)) might be too wide to detect practical departures of the simulated results from the target value. They used a narrower 2% error band to examine the robustness of a nonparametric chart with regards to its *ARL*. For all simulations in this body of work SAS® v 9.3 is used. The programs are made available in the Appendices at the end of each chapter.

A stepwise computer simulation procedure to calculate the run-length distribution for a two sided control chart, where the charting statistic is calculated from a random sample, is given as follows:

Step 1: After specifying some necessary parameters, such as the subgroup size, calculate the control limits.

Step 2: Generate random subgroups from some process distribtuion, say, the normal distribution.

Step 3: Calculate the charting statistic for each subgroup and compare it to the control limits calculated in Step 1.

Step 4: The number of subgroups needed until the charting statistics plots on or outside the control limits is recorded as an observation from the run-length distribution.

Step 5: Repeat steps 1 to 4 a total of 100 000 times.

Step 6: Once we have obtained a 'dataset' with 100 000 observations from the run-length distribution, proc univariate of SAS®v 9.3 was used to obtain the run-length characteristics.

Examples of where the run-length distribution or characteristics of the run-length distribution is found through computer simulations or Monte Carlo simulations are Bodden and Ridgon (1999) and Molnau et al. (2001).

1.11. Appendices

1.11.1. Appendix 1A: Some mathematical results

Proof to Equation (1.8)

The exponentially weighted moving average is defined as

$$Z_i = \lambda\psi_i + (1-\lambda)Z_{i-1} \text{ with } Z_0 = \mu_0 \tag{A1.1}$$

By expanding Equation (A1.1) we find

$$\begin{aligned} Z_i &= \lambda\psi_i + (1-\lambda)Z_{i-1} \\ &= \lambda\psi_i + (1-\lambda)(\lambda X_{i-1} + (1-\lambda)Z_{i-2}) \\ &\vdots \\ &= \lambda\sum_{j=0}^{i-1}(1-\lambda)^j\psi_{i-j} + (1-\lambda)^i Z_0 \end{aligned}$$

Thus, by continuing to recursively substitute for Z_{i-j}, $j = 2, 3, \ldots, t$, we obtain

$$Z_i = \lambda\sum_{j=0}^{i-1}(1-\lambda)^j\psi_{i-j} + (1-\lambda)^i Z_0 \tag{A1.2}$$

$$\begin{aligned} VAR(Z_i) &= VAR\left(\lambda \sum_{j=0}^{i-1}(1-\lambda)^j \psi_{i-j} + (1-\lambda)^i Z_0\right) \\ &= \lambda^2 VAR\left(\sum_{j=0}^{i-1}(1-\lambda)^j \psi_{i-j}\right) \text{ since } (1-\lambda)^i Z_0 \text{ is constant} \\ &= \lambda^2 \left(VAR\left(X_i + (1-\lambda)\psi_{i-1} + (1-\lambda)^2\psi_{i-2} + \cdots + (1-\lambda)^{i-2}\psi_2 + (1-\lambda)^{i-1}\psi_1\right)\right) \\ &= \lambda^2\left(\sigma^2 + (1-\lambda)^2\sigma^2 + (1-\lambda)^4\sigma^2 + \cdots + (1-\lambda)^{2i-4}\sigma^2 + (1-\lambda)^{2i-2}\sigma^2\right) \end{aligned}$$

Thus,

$$VAR(Z_i) = \lambda^2\sigma^2\left(1 + (1-\lambda)^2 + (1-\lambda)^4 + \cdots + (1-\lambda)^{2i-4} + (1-\lambda)^{2i-2}\right) \quad \text{(A1.3)}$$

In general, for a finite geometric series the sum of the first n terms of a geometric series is

$$\sum_{j=0}^{n-1} ar^j = a\frac{1-r^n}{1-r} \text{ with } r \neq 1 \quad \text{(A1.4)}$$

By using a geometric series (Equation (A1.4)) and applying it to Equation (A1.3) we obtain

$$\begin{aligned} VAR(Z_i) &= \lambda^2\sigma^2\left(\frac{1-\left((1-\lambda)^2\right)^i}{1-(1-\lambda)^2}\right) \\ &= \lambda^2\sigma^2\left(\frac{1-(1-\lambda)^{2i}}{2\lambda-\lambda^2}\right) \\ &= \lambda\sigma^2\left(\frac{1-(1-\lambda)^{2i}}{2-\lambda}\right) \end{aligned}$$

Thus,

$$VAR(Z_i) = \sigma^2\left(\frac{\lambda}{2-\lambda}\right)\left(1-(1-\lambda)^{2i}\right) \quad \text{(A1.5)}$$

1.11.2. Appendix 1B: Distributions considered in this study

A list of the distributions considered in this study is given below along with general formulae to calculate their means, medians and variances. Note the following regarding these distributions:

- All distributions have been adjusted / standardized i.e. shifted and / or scaled, such that the mean / median equals 0 and the standard deviation equals 1 (when the process is IC), so that the results are easily comparable across the different distributions.

- Only those distributions for which the parameters could not be tweaked or chosen such that the mean is zero and the variance is one have been adjusted.

- Asymmetric distributions were not transformed to become more symmetric; only there means and variances were adjusted.

The adjustment of the distributions was done as follows:

Suppose $X \sim F_X$ with the expected value and variance of X given by $E(X) = \mu$ and $VAR(X) = \sigma^2$, respectively. Then, it is well-known that we can standardize the variable X by subtracting the mean and dividing by the standard deviation i.e. $Y \stackrel{d}{=} \frac{X-\mu}{\sigma}$, and we have that $E(Y) = 0$ and $VAR(Y) = 1$.

Distribution	Probability density function (pdf)	Mean	Median	Variance	Transformation	Cases considered
Standard Normal $X \sim N(0,1)$ $x \in (-\infty, \infty)$	$f(x) = \frac{1}{\sqrt{2\pi}} e^{-\frac{1}{2}x^2}$	0	0	1	None necessary	$N(0,1)$
Student's *t* $X \sim t(v)$ $x \in (-\infty, \infty)$ $v > 0$ denotes the degrees of freedom	$f(x) = \frac{\Gamma\left(\frac{v+1}{2}\right)}{\sqrt{v\pi}\Gamma\left(\frac{v}{2}\right)} \left(1 + \frac{x^2}{v}\right)^{-\left(\frac{v+1}{2}\right)}$	0	0	$\frac{v}{v-2}$ for $v > 2$ ∞ for $v = 2$ else undefined	$Y = \frac{X-0}{\sqrt{\frac{v}{v-2}}} = \sqrt{\frac{v-2}{v}} X$	$t(3)$ $t(4)$ $t(8)$
Gamma[iii] $X \sim GAM(\alpha, \beta)$ $x \in [0, \infty)$ $\alpha > 0$ and $\beta > 0$ denote the shape and scale parameters	$f(x) = x^{\alpha-1} \frac{e^{-x/\beta}}{\Gamma(\alpha)\beta^{\alpha}}$	$\alpha\beta$	No simple closed form	$\alpha\beta^2$	$Y = \frac{X-\alpha\beta}{\sqrt{\alpha}\beta}$	$GAM(0.5,1)$ $GAM(1,1)$ $GAM(3,1)$
Logistic $X \sim Logistic(\alpha, \beta)$ $x \in (-\infty, \infty)$ $-\infty < \alpha < \infty$ and $\beta > 0$ denote the location and scale parameters	$f(x) = \frac{e^{-(x-\alpha)/\beta}}{\beta\left(1+e^{-(x-\alpha)/\beta}\right)^2}$	α	α	$\frac{\pi^2}{3}\beta^2$	$Y = \frac{X-\alpha}{\frac{\pi}{\sqrt{3}}\beta}$	$Logistic\left(0, \sqrt{3}/\pi\right)$ with $E(X) = 0$ & $VAR(X) = 1$ (no transformation needed)

[iii] Note that the Gamma distribution is positively skewed and the skewness of the Gamma distribution increases as the shape parameter α decreases. Also note that the $GAM(1,1)$ distribution is the Exponential distribution with mean 1, $EXP(1)$.

Distribution	Probability density function (pdf)	Mean	Median	Variance	Transformation	Cases considered
Log-Logistic $X \sim Log\text{-}Logistic(\alpha, \beta)$ $x \in [0, \infty)$ $\alpha > 0$ and $\beta > 0$ denote the scale and shape parameters	$f(x) = \frac{\beta/\alpha (x/\alpha)^{\beta-1}}{(1+(x/\alpha)^{\beta})^2}$	$\frac{\alpha\tau}{sin(\tau)}$ $\tau = \frac{\pi}{\beta}$ $\beta > 1$ else undefined	α	$\alpha^2 \left(\frac{2\tau}{sin(2\tau)} - \frac{(\tau)^2}{(sin(\tau))^2} \right)$ with $\tau = \frac{\pi}{\beta}$ for $\beta > 2$ else undefined	$Y = \frac{X - \frac{\alpha\tau}{sin(\tau)}}{\alpha \sqrt{\frac{2\tau}{sin(2\tau)} - \frac{(\tau)^2}{(sin(\tau))^2}}}$ with $\tau = \frac{\pi}{\beta}$	$Log\text{-}Logistic(1, 2.5)$
Laplace or Double Exponential $X \sim DE(\alpha, \beta)$ $x \in (-\infty, \infty)$ $-\infty < \alpha < \infty$ and $\beta > 0$ denote the location and scale parameters	$f(x) = \frac{1}{2\beta} e^{-\frac{\lvert x-\alpha \rvert}{\beta}}$	α	α	$2\beta^2$	$Y = \frac{X - \alpha}{\sqrt{2}\beta}$	$DE\left(0, \frac{1}{\sqrt{2}}\right)$ with $E(X) = 0$ & $VAR(X) = 1$ (no transformation needed) and $DE(0,1)$ (transformation needed)
Uniform distribution $X \sim U(a, b)$ $x \in [a, b]$ $-\infty < a < b < \infty$	$f(x) = \frac{1}{b-a}$	$\frac{a+b}{2}$	$\frac{a+b}{2}$	$\frac{(b-a)^2}{12}$	$Y = \frac{X - \frac{a+b}{2}}{\frac{(b-a)}{\sqrt{12}}}$	$U(-1,1)$
Contaminated or Mixture Normal	Since the formulae for the Contaminated or Mixture Normal distribution is too lengthy to fit into this table, a discussion follows below.					

Contaminated or Mixture Normal distribution

The Contaminated Normal (*CN*) distribution (also referred to as the Mixture Normal distribution), is a linear combination of two normal random variables: $(1-\varepsilon)N(\mu_1,\sigma_1^2)+\varepsilon N(\mu_2,\sigma_2^2)$, where $0<\varepsilon<1$ denotes the level of contamination.

If $X\sim(1-\varepsilon)N(\mu_1,\sigma_1^2)+\varepsilon N(\mu_2,\sigma_2^2)$ then the pdf is given by

$$f(x)=(1-\varepsilon)\phi(\mu_1,\sigma_1)+\varepsilon\phi(\mu_2,\sigma_2)$$

where $\phi(\mu,\sigma)$ is the pdf of a Normal distribution with mean μ and variance σ^2. The expected value and variance of the *CN* distribution are given by

$$E(X)=(1-\varepsilon)\mu_1+\varepsilon\mu_2$$

and

$$VAR(X)=(1-\varepsilon)(\mu_1^2+\sigma_1^2)+\varepsilon(\mu_2^2+\sigma_2^2)-\big((1-\varepsilon)\mu_1+\varepsilon\mu_2\big)^2,$$

respectively. Thus, the *CN* distribution is shifted and scaled such that the mean / median equals 0 and the standard deviation equals 1 by using the following transformation:

$$Y=\frac{X-(1-\varepsilon)\mu_1+\varepsilon\mu_2}{\sqrt{(1-\varepsilon)(\mu_1^2+\sigma_1^2)+\varepsilon(\mu_2^2+\sigma_2^2)-\big((1-\varepsilon)\mu_1+\varepsilon\mu_2\big)^2}}.$$

In this dissertation we consider the following *CN* distributions:

i. $0.95N\left(\mu_1 = 0, \sigma_1^2 = \frac{1}{1.15}\right) + 0.05N\left(\mu_2 = 0, \sigma_2^2 = \frac{4}{1.15}\right)$

ii. $0.6N\left(\mu_1 = 0, \sigma_1^2 = \frac{1}{16}\right) + 0.4N(\mu_2 = 0, \sigma_2^2 = 16)$

iii. $0.6N\left(\mu_1 = 0.25, \sigma_1^2 = \frac{1}{16}\right) + 0.4N(\mu_2 = 0, \sigma_2^2 = 16)$

iv. $0.6N\left(\mu_1 = -0.25, \sigma_1^2 = \frac{1}{16}\right) + 0.4N(\mu_2 = 0, \sigma_2^2 = 16)$

Note that, for the symmetric distributions listed in (i) and (ii), the median will be equal to the mean. However, for the asymmetric distributions listed in (iii) and (iv), the cumulative distribution function (cdf) will have to be used in order to calculate the median. The steps are as follows:

The $100q^{th}$ percentile $(0 < q < 1)$ is defined as the smallest integer j such that the cumulative probability is at least q, i.e. $P(N \leq j) \geq q$. Thus, we set $q = 0.5$ for the median and use the cdf of the *CN* distribution given by

$$F(x) = (1 - \varepsilon)\Phi(\mu_1, \sigma_1) + \varepsilon\Phi(\mu_2, \sigma_2)$$

where $\Phi(\mu, \sigma)$ is the cdf of a Normal distribution with mean μ and variance σ^2.

Chapter 2

Phase I control charts

2.1. Introduction

As noted in Section 1.8, Phase I control charting is an iterative process where these problem (OOC) subgroups are first investigated and possibly discarded, and then based on the remaining subgroups the parameters are re-estimated, the control limits are recalculated and the control charting procedure is repeated. This trial-and-error process is continued until at some stage all the charting statistics plot between the most recent control limits, leading to a decision that the process is IC. The final set of subgroups (data) is often referred to as the in-control or reference data, from which any necessary parameters are estimated and used to find appropriate control limits which are used for prospective process monitoring in Phase II. The problem under a Phase I control charting scenario is similar in principle to that in a testing of hypothesis problem for homogeneity, where one tests whether the data from various groups come from the same IC process distribution. This is noted, for example, by Champ and Jones (2004). Under this motivation, the *FAP*, which is the probability of at least one false alarm, is used to measure and evaluate Phase I control limits. Hence a Phase I control chart is designed by specifying a nominal false alarm probability, say FAP_0, typically taken to be 0.01, 0.05 or 0.10, and not the *FAR*, which is the probability for a single charting statistic to plot outside the estimated limits under an IC process. It may be noted that this objective is different from designing Phase II control charts based on IC data, where typically, one specifies some attribute of the IC run-length distribution, such as the average run-length, to determine the control limits.

A number of research outputs related to and based on this thesis have seen the light. In Chapter 5 we provide a list with the details of the technical reports and the peer-reviewed articles that have been published, the articles that have been accepted for publication, the local and international conferences where papers have been presented and draft articles that have been submitted and are currently under review. Here, we solely mention the peer-reviewed articles that have been published based on this chapter.

i. Chakraborti, S., Human, S.W. and Graham, M.A. (2009). "Phase I statistical process control charts: An overview and some results." *Quality Engineering*, 21 (1), 52-62.

ii. Graham, M.A., Human, S.W. and Chakraborti, S. (2010). "A Phase I nonparametric Shewhart-type control chart based on the median." *Journal of Applied Statistics,* 37 (11), 1795-1813.

2.1.1. False alarm probability

Without any loss of generality, we assume that m denotes the 'final' number of reference samples at the end of a Phase I analysis. Thus the reference data set is assumed to have $N = mn$ observations. An OOC situation is indicated when a charting statistic falls on or outside either of the control limits. This important event is often called a signal or a signalling event. It is convenient to consider the complementary event, that is when a subgroup does not signal, called the non-signalling event. Thus, for the i^{th} subgroup, $E_i = \{L\hat{C}L < C_i < U\hat{C}L\}$, $i = 1,2,...,m$, denotes the non-signalling event. Note that $L\hat{C}L$ and $U\hat{C}L$ denote the estimated Phase I control limits and that C_i denotes the charting statistic. As we discussed earlier, the *FAP* is usually the recommended chart design criterion adopted in Phase I (see e.g. Chakraborti et al. (2009)). This probability can be expressed as follows:

$$\begin{aligned} FAP &= P(\text{At least one false alarm from the } m \text{ subgroups}) \\ &= 1 - P(\text{No signal among the } m \text{ subgroups } |\text{IC}) \\ &= 1 - P(E_1, E_2, \ldots, E_m \mid \text{IC}) \\ &= 1 - P\left(\bigcap_{i=1}^{m} \{L\hat{C}L < C_i < U\hat{C}L\} \middle| \text{IC}\right). \end{aligned} \tag{2.1}$$

Equation (2.1) equals $= 1 - \int_{L\hat{C}L}^{U\hat{C}L} \int_{L\hat{C}L}^{U\hat{C}L} \cdots \int_{L\hat{C}L}^{U\hat{C}L} f_{C_1,C_2,\ldots,C_m}(c_1, c_2, \ldots, c_m) dc_1 \ldots dc_m$ if the joint distribution of the C_i's is continuous where $f_{C_1,C_2,\ldots,C_m}(c_1, c_2, \ldots, c_m)$ denotes the joint probability density function of the charting statistics $C_1, C_2, \ldots, C_m$ when the process is IC.

If the joint distribution of the C_i's is discrete then $P\left(\bigcap_{i=1}^{m}\{L\hat{C}L < C_i < U\hat{C}L\}\middle|\text{IC}\right)$ can be re-written as $P\left(\bigcap_{i=1}^{m}\{L\hat{C}L + 1 \leq C_i \leq U\hat{C}L - 1\}\middle|\text{IC}\right)$ and consequently Equation (2.1) equals $= 1 - \sum_{c_1=L\hat{C}L+1}^{U\hat{C}L-1}\sum_{c_2=L\hat{C}L+1}^{U\hat{C}L-1}\cdots\sum_{c_m=L\hat{C}L+1}^{U\hat{C}L-1} f_{C_1,C_2,\ldots,C_m}(c_1,c_2,\ldots,c_m)dc_1\ldots dc_m$ where $f_{C_1,C_2,\ldots,C_m}(c_1,c_2,\ldots,c_m)$ denotes the joint probability mass function of the charting statistics $C_1, C_2, \ldots, C_m$ when the process is IC.

Thus the *FAP* involves the m non-signalling (or, equivalently, signalling) events simultaneously and depends on the fact that the control limits are estimated in Case U. Note that these events are dependent since the charting statistics are all compared with the same pair of control limits. Hence, calculation of the *FAP* requires knowledge of the joint distribution of the charting statistics, when the process is IC. Derivation of this and determination of the control limits (and the associated charting constants; which differs depending on the type of control chart under consideration) pose some important practical challenges, particularly in an SPC context where the number of comparisons (m) can be as few as 25 or as high as 300 or more.

2.1.2. False alarm rate

The false alarm rate, which is the probability of a single charting statistic plotting on or outside the control limits when the process is IC, can be expressed as

$$FAR = 1 - P\left(L\hat{C}L < C_i < U\hat{C}L|\text{IC}\right). \tag{2.2}$$

Equation (2.2) equals $= 1 - \int_{L\hat{C}L}^{U\hat{C}L} g_{C_i}(c_i)\,dc_i$ if the marginal distribution of C_i is continuous where $g_{C_i}(c_i)$ denotes the marginal pdf of any of the charting statistic C_i when the process is IC and Equation (2.2) equals $= \sum_{L\hat{C}L+1}^{U\hat{C}L-1} g_{C_i}(c_i)$ if the marginal distribution of C_i is discrete where $g_{C_i}(c_i)$ denotes the marginal pmf of the charting statistic C_i when the process is IC. From Equation (2.2) it can be seen that the *FAR* involves a single non-signalling event and thus calculation of this probability requires only the marginal distribution of the i^{th} charting statistic C_i when the process is IC. It should be noted that Equation (2.2) is the general formula to calculate a *FAR* regardless of the phase the process is in. However, the *FAR* has interpretability problems in Phase I since the charting statistics are dependent. For more details on the application of *FAR* in Phase II control charting the reader is referred to Chapters 3 and 4.

2.1.3. Implementation of Shewhart-type Phase I control charts

Montgomery (2009) recommends that Shewhart-type charts are particularly suitable in Phase I applications. There are primarily two methods in the literature for constructing Phase I Shewhart-type control charts in Case U.

Method 1: *FAR*-based control limits

Hillier (1969) and Yang and Hillier (1970) proposed a methodology in which the probability of a false alarm or *FAR* is controlled at a desired level such as 0.0027 in order to determine the control limits. Although they did consider the effects of parameter estimation, they did not explicitly consider (i) the fact that the subgroups are all compared to the same control limits so the signals, or the signalling events, are statistically dependent and (ii) that many subgroups are all compared to the same control limits at the same time (so there is the issue of simultaneous comparisons that needs to be accounted for). As noted by several authors in the literature, these reasons limit the applicability of their methods in a Phase I setting since there will be too many false alarms with a chart constructed for a fixed *FAR*.

Method 2: *FAP*-based control limits

Under this method the control limits are calculated for a specified nominal false alarm probability (FAP_0, say). This method correctly takes into account the fact that the signalling events are dependent and uses the relevant joint (multivariate) distribution, plus it accounts for the issue of simultaneity. Hence this is the method to be used in practice.

Method 3: Bonferroni control limits

While the *FAR* (see Method 1) is an important chart performance criterion in some applications, as noted before, the typical chart performance criterion in Phase I applications is the *FAP* (see Method 2). By using Bonferroni's inequality (see e.g. Casella and Berger (2002)) it can be seen that one can find an upper bound for the *FAP* as a function of the *FAR*; this upper bound is given by

$$\begin{aligned} FAP &= 1 - P\left(\bigcap_{i=1}^{m}\{E_i\} \mid \text{IC}\right) \\ &\leq m - \sum_{i=1}^{m} P(\{E_i\} \mid \text{IC}) \\ &= m - \sum_{i=1}^{m}(1 - FAR) \\ &= mFAR. \end{aligned} \tag{2.3}$$

Note that for the derivation of Equation (2.3) equal sample sizes were assumed. If it is desired that the $FAP \leq FAP_0$, it is seen from Equation (2.3) that setting $mFAR = FAP_0$ i.e. setting the false alarm rate equal to $FAR = FAP_0/m$, would meet the requirement; in this case the symmetrically placed control limits are given by the

$$(FAP_0/2m)100^{th} \text{ and } \big(1 - (FAP_0/2m)\big)100^{th}$$

percentiles of the marginal IC distribution of a single charting statistic.

The three methods are illustrated in Figure 2.1 for Case U. For this illustration it was assumed that m = 15 random samples each of size n = 5 are available. The control limits for each method is given in Table 2.1 and illustrated in Figure 2.1.

Table 2.1. The *FAR*-based, the *FAP*-based and the Bonferroni control limits

FAR-based control limits	*FAP*-based control limits	Bonferroni control limits
$\pm$ 0.2411	$\pm$ 0.3064	$\pm$ 0.3453

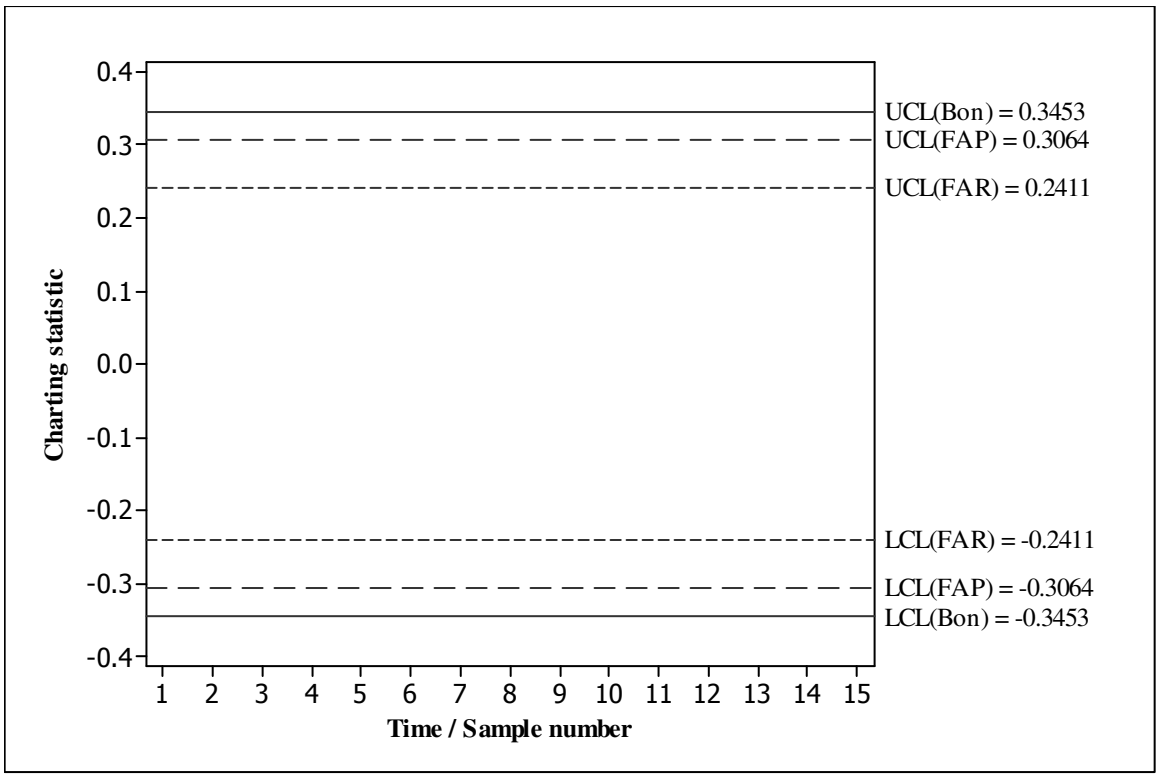

Figure 2.1. The *FAR*-based, the *FAP*-based and the Bonferroni control limits

The *FAR*-based and *FAP*-based control limits are denoted by LCL(FAR), UCL(FAR), LCL(FAP) and UCL(FAP), respectively. From Figure 2.1 it is seen that there can be many more false alarms if the control limits are based on the *FAR* criterion, that is, Method 1. The Bonferroni control limits, denoted by LCL(Bon) and UCL(Bon), respectively, are slightly wider than the *FAP*-based control limits and it is thus likely that one would observe less false alarms if one uses the Bonferroni control limits instead of the *FAP*-based control limits. Although less false alarms are appealing from a practical point of view, if the control limits are too wide, unwanted variation might go undetected. Consequently, we will focus on the method that controls the *FAP*.

2.2. Phase I median control chart

In Section 2.1 we considered some existing Phase I control charts. In this section a nonparametric Phase I Shewhart-type control chart is proposed to check if the process is IC, that is, if the medians are all equal.

2.2.1. Introduction

A nonparametric Shewhart-type Phase I control chart based on the joint median test (see e.g. Gibbons and Chakraborti (2010) page 241) is considered to monitor the location of a continuous

process distribution. This methodology can be applied when the process distribution is continuous but unknown. The proposed chart is shown to be distribution-free so that its application does not require the assumption of a parametric model (such as normality) about the underlying process. All in-control properties of distribution-free control charts remain the same for all continuous distributions. This is by design and is the definition of a nonparametric chart (refer to Section 1.6). This is of practical significance since the corresponding properties for a parametric chart depends on the distribution and would generally vary across applications, sometimes substantially, depending on the shape of the distribution and the amount of available data. This is not the case with nonparametric charts. The reader is referred to Human et al. (2011) for a detailed discussion on the robustness of parametric charts.

2.2.2. Model assumptions

Let $(X_{i1}, X_{i2}, \ldots, X_{in_i})$ denote an independent random sample (subgroup) of size $n_i \geq 1$, taken from the i^{th} population with a continuous cdf F_i, $i = 1,2,\ldots,m$. It is often the case that the samples (subgroups) are all of the same size, n, so that the subscript i in n_i can be suppressed. However, unequal sample sizes can be considered, but it is not investigated here. Thus suppose that there are m independent random samples each of size n and these mn data points are used in a Phase I analysis. We assume the location model $F_i(x) = F(x - \theta_i)$, where F is some arbitrary continuous cdf and θ_i denotes the location parameter of interest. To keep matters simple we consider the case where the location parameter θ_i is the median of the i^{th} population. We focus on the median because of its robustness properties and the simplicity of the resulting control charts. Note that, although we focus on the median from the point of view of robustness and simplicity, other percentiles can be considered and this is discussed in more detail in Section 2.2.6. We propose a distribution-free Shewhart-type control chart to check if the process is IC, that is, if the medians are all equal. The chart consists of plotting m charting statistics (denoted U_i, $i = 1,2,\ldots,m$) and comparing them simultaneously to a $L\hat{C}L$ and an $U\hat{C}L$. The control limits are estimated from the data. Note that there is no *CL* defined for this chart. If the U_i's all plot between the control limits we say that the process is IC. If this is the case, the data at hand are called IC or reference data and are subsequently used for constructing control limits for Phase II process monitoring. However, if one or more of the U_i's plot on or outside the control limits there is evidence that at least one of the medians is different from the others and the process is declared OOC. In this case the data at hand do not constitute an IC or a reference sample and the usually iterative process of examining, retesting and possibly removing the problem samples is started and continued until the IC state is

established. At that point the existing data constitute a reference or IC dataset and Phase II process monitoring begins on the basis of such data after calculating Phase II limits which may be different from the Phase I limits.

The chart is constructed as follows. First, pool the m samples together and find the pooled or overall median M of the combined sample of $N = mn$ observations. Thus

$$M = \begin{cases} X_{((N+1)/2)} & \text{if} \quad N \text{ is odd} \\ (X_{(N/2)} + X_{((N+2)/2)})/2 & \text{if} \quad N \text{ is even} \end{cases}$$

where $X_{(1)} < X_{(2)} < \cdots < X_{(N)}$ denotes the order statistics of the combined sample. Second, find the observed value u_i of U_i (where $U_i \in \{0,1,2,\ldots,n\}$), the random number of observations less than M in the i^{th} sample, i.e. $U_i = \sum_{j=1}^{n} I(X_{ij} < M)$ for $i = 1,2,\ldots,m$, where $I(A) = 1$ or 0 according as A is true or false, respectively. Finally, plot the m observed values $u_1, u_2, \ldots, u_m$ of the charting statistics on the control chart and simultaneously compare them to the $\hat{LCL}$ and the $\hat{UCL}$ in order to assess whether or not the process is IC. Finding the appropriate control limits is considered next.

2.2.3. Design of the control chart

A Phase I control chart is designed for a given *FAP*, that is, the probability of *at least one* false alarm out of the m samples, where a false alarm is the event that a (single) charting statistic plots on or outside the control limits when the process is IC. Thus a Phase I chart is designed by specifying a nominal false alarm probability, say FAP_0, which is typically taken to be 0.01, 0.05 or 0.10 (see e.g. Chakraborti et al. (2009)). The event, when a charting statistic falls on or outside of either control limit, is called a signalling event. Since the *FAP* is the probability of a composite event that deals with the m charting statistics simultaneously and the corresponding signalling events are dependent (all the charting statistics are compared with the same estimated control limits), the IC joint distribution of the charting statistics is necessary in order to calculate the *FAP*.

IC Joint probability distribution of the charting statistics

Because the charting statistics $(U_1, U_2, \dots, U_m)$ all depend on the combined sample median M they are dependent random variables. It can be shown that (see Appendix 2A) the IC joint distribution of $U_1, U_2, \dots, U_m$ is the multivariate hypergeometric distribution, given by

$$f_{U_1,U_2,\dots,U_m}(u_1, u_2, \dots, u_m) = \frac{\binom{n}{u_1}\binom{n}{u_2}\cdots\binom{n}{u_m}}{\binom{N}{u_T}} = \frac{\prod_i^{m-1}\binom{n}{u_i}\binom{n}{u_T - u_1 - \cdots - u_{m-1}}}{\binom{N}{u_T}} \qquad (2.4)$$

(see e.g. Lehmann (1975) page 381). Note that $u_T = \sum_{i=1}^{m} u_i$ denotes the total number of observations among the combined sample of $N = mn$ observations that are less than the median M Thus, while each u_i is an integer value between and including 0 and n, u_T is a fixed number equal to $N/2$ or $(N-1)/2$ depending on whether N is odd or even.

The expression in (2.4) makes it clear that the IC joint distribution of the charting statistics depends only on m and n and not on the underlying process distributions $F_1, F_2, \dots, F_m$. Thus any control charting procedure based on the statistics, i.e. charting statistics, $U_1, U_2, \dots, U_m$, is distribution-free, as long as the underlying distributions are continuous. Next this joint distribution is used to calculate the false alarm probability.

The false alarm probability

The FAP is most conveniently calculated by considering the complement of a signalling event, i.e. the event when a charting statistic plots between the control limits, which is called a non-signalling event and is denoted by $E_i = \{L\hat{C}L < U_i < U\hat{C}L\}$, $i = 1,2, \dots, m$. Since the FAP depends on the number of samples, m, the sample size, n, (both of these quantities are specified by the practitioner) and the estimated control limits, it is denoted by $FAP(m, n, L\hat{C}L, U\hat{C}L)$ and calculated as follows (refer back to Equation (2.1))

$$\begin{aligned} FAP(m, n, L\hat{C}L, U\hat{C}L) &= P(\text{At least one false alarm from the } m \text{ samples} \mid \text{IC}) \\ &= 1 - P(\text{No signal among the } m \text{ samples} \mid \text{IC}) \end{aligned}$$

No signal among the m samples indicate that all the charting statistics plot between the estimated control limits, i.e. $\bigcap_{i=1}^{m}\{L\hat{C}L < U_i < U\hat{C}L\}$, so that

$$FAP(m,n,L\hat{C}L,U\hat{C}L) = 1 - P\left(\bigcap_{i=1}^{m}\{L\hat{C}L < U_i < U\hat{C}L\}|\text{ IC}\right)$$

and since $\{L\hat{C}L < U_i < U\hat{C}L\}$ can be written as $\{L\hat{C}L + 1 \leq U_i \leq U\hat{C}L - 1\}$ we obtain

$$FAP(m,n,L\hat{C}L,U\hat{C}L) = 1 - \sum_{u_1=L\hat{C}L+1}^{U\hat{C}L-1}\sum_{u_2=L\hat{C}L+1}^{U\hat{C}L-1}\cdots\sum_{u_m=L\hat{C}L+1}^{U\hat{C}L-1} f_{U_1,U_2,\ldots,U_m}(u_1,u_2,\ldots,u_m) \qquad (2.5)$$

where $f_{U_1,U_2,\ldots,U_m}(u_1,u_2,\ldots,u_m)$ is the IC joint distribution of $U_1,U_2,\ldots,U_m$ given in Equation (2.4). From Equation (2.5) it can be seen that the *FAP* is a function of m, n, $L\hat{C}L$ and $U\hat{C}L$. However, since the number of samples, m, the sample size, n, are specified by the practitioner, we focus on finding the $L\hat{C}L$ and $U\hat{C}L$ next.

Marginal distribution of a charting statistic and the false alarm rate

The *FAR* is the probability of a false alarm at any sample. While the joint probability distribution of the charting statistics $U_1,U_2,\ldots,U_m$ is necessary to calculate the *FAP*, only the IC marginal distribution of the i^{th} charting statistic is necessary to calculate the *FAR*. Again, it can be shown (see e.g. Lehmann (1975) page 339) that the IC marginal distribution of U_i, $i = 1,2,\ldots,m$, is the well-known univariate hypergeometric distribution with pmf, expected value and variance given by

$$g_{U_i}(u_i) = \frac{\binom{n}{u_i}\binom{N-n}{u_T-u_i}}{\binom{N}{u_T}} = \frac{\binom{n}{u_i}\binom{(m-1)n}{u_T-u_i}}{\binom{N}{u_T}}, \qquad (2.6)$$

$$E(U_i) = n\frac{u_T}{N}, \qquad (2.7)$$

$$VAR(U_i) = \frac{u_T(N-u_T)\frac{n}{N}\left(1-\frac{n}{N}\right)}{N-1}, \qquad (2.8)$$

respectively. The covariance and correlation between any U_i and U_j for $i \neq j$ are given by

$$COV(U_i, U_j) = -u_T \frac{(N - u_T)}{(N-1)} \frac{n^2}{N^2} \tag{2.9}$$

and

$$CORR(U_i, U_j) = -\frac{1}{m-1} \tag{2.10}$$

respectively. From Equation (2.10) it can be seen that the correlation between any two charting statistics approaches zero for 'large' values of m and, consequently, we can approximate the control limits by ignoring the dependence among the charting statistics and by simply using the marginal univariate hypergeometric distribution of the U_i's. For example, when m equals 20, 50 and 100, respectively, the values of the correlation between any two charting statistics (from Equation (2.10)) equal -0.053, -0.020 and -0.010, respectively. Clearly, the correlation between any two charting statistics approaches zero as m increases. A more thorough discussion on this point follows later when the approximate control limits are proposed.

Returning to the IC marginal distribution of U_i, $i = 1,2, \ldots, m$, (given in Equation (2.6)), the *FAR* can be calculated from

$$FAR = 1 - P(L\hat{C}L < U_i < U\hat{C}L \mid \text{IC}) = 1 - \sum_{u_i = L\hat{C}L+1}^{U\hat{C}L-1} g_{U_i}(u_i). \tag{2.11}$$

While the *FAR* is an important chart performance criterion in some applications, as noted before, the typical chart performance criterion in Phase I applications is the *FAP*. By using Bonferroni's inequality (see Method 3 in Section 2.1.3) it can be seen that one can find an upper bound for the *FAP* as a function of the *FAR*; this upper bound is given by $FAP \leq mFAR$ (see Equation (2.3)) and in case the signalling events are independent, it is easy to show that $FAP = 1 - (1 - FAR)^m$. To see this, from Equations (2.1) and (2.2) and using the fact that if m is large, the common IC correlation among the charting statistics approaches zero (see Equation (2.10)) and the charting statistics are approximately independent, it can be seen that

$$FAP \approx 1 - \prod_{i=1}^{m} P(E_i \mid \text{IC}) = 1 - \left(1 - P(E_i \mid \text{IC})\right)^m = 1 - (1 - FAR)^m \qquad (2.12)$$

so that

$$FAR \approx 1 - (1 - FAP)^{\frac{1}{m}}. \qquad (2.13)$$

The latter relationship will be used in constructing approximate control limits later. More discussions on *FAP* and *FAR* in a Phase I context can be found in Chakraborti et al. (2009).

Exact control limits

The design of a Phase I chart entails that for the m and n at hand the practitioner specifies a *FAP* value, say FAP_0, and find the corresponding control limits. Thus we need to find values for $L\hat{C}L$ and $U\hat{C}L$, denoted by a and b, respectively, that satisfies

$$\begin{aligned} FAP_0 &= FAP(m, n, L\hat{C}L = a, U\hat{C}L = b) \\ &= 1 - \sum_{u_1=a+1}^{b-1} \sum_{u_2=a+1}^{b-1} \cdots \sum_{u_m=a+1}^{b-1} f_{U_1,U_2,\ldots,U_m}(u_1, u_2, \ldots, u_m) \end{aligned} \qquad (2.14)$$

where $0 \leq a < b \leq n$. This requires that two unknowns, a and b, be solved from one equation which could be computationally challenging. This is necessary when asymmetrically placed control limits are used, which sometimes, occur in practice. However, the IC joint distribution of $U_1, U_2, \ldots, U_m$ is symmetric about its mean, given by $E(\underline{U}) = \left(E(U_1), \ldots, E(U_m)\right)$ where $E(U_i)$ equals $n/2$ when *N* is even and $(n/2) \times \left((N-1)/N\right)$ when *N* is odd (see e.g. Lehmann (1975) page 381). Accordingly, it is reasonable to use symmetrically placed (equidistant from both ends) control limits and set $b = n - a$ so that only the charting constant a needs to be found. This implies that instead of solving for both a and b from Equation (2.14) we need to solve only for a from

$$FAP_0 = 1 - \sum_{u_1=a+1}^{n-a-1} \sum_{u_2=a+1}^{n-a-1} \cdots \sum_{u_{m-1}=a+1}^{n-a-1} f_{U_1,U_2,\ldots,U_m}(u_1, u_2, \ldots, u_m). \qquad (2.15)$$

However, since the joint distribution of the U_i's is discrete, chances are that the equality in (2.15) will not be attained exactly and using a conservative approach a is found so that the attained *FAP* is less than or equal to the specified *FAP*. Thus

$$a = max\left\{c: FAP_0 \geq 1 - \sum_{u_1=c+1}^{n-c-1}\sum_{u_2=c+1}^{n-c-1}\cdots\sum_{u_{m-1}=c+1}^{n-c-1} f_{U_1,U_2,\ldots,U_m}(u_1,u_2,\ldots,u_m)\right\}. \quad (2.16)$$

so that a is the largest integer which ensures that the attained or actual *FAP* is less than or equal to the specified (or desired or stipulated) *FAP*.

In Tables 2.2, 2.3 and 2.4 values are provided for the control limits (a and $b = n - a$) and the corresponding *FAP* values, called attained *FAP* values, when the desired or nominal *FAP* value (FAP_0) equals 0.01, 0.05 and 0.10, respectively, for m = 4(1)10 and n = 3(1)24. These values were obtained by solving Equation (2.16) using R® Version 2.6.1 (see Appendix 2B) and are referred to as the exact limits. Note that for the same FAP_0 value, the attained *FAP* values can be different for different combinations of m and n values since the IC distribution of the charting statistic is discrete and depends (only) on m and n; using Equation (2.16) we take the solution as the largest integer so that the *FAP* is at most equal to the specified FAP_0.

Table 2.2. Attained *FAP* values and the control limits (a, b)[i] for $FAP_0 = 0.01$

		Number (m) of Phase I samples						
		4	**5**	**6**	**7**	**8**	**9**	**10**
Sample size (n)	**3**	0.4740 (0,3)	0.6224 (0,3)	0.7001 (0,3)	0.7830 (0,3)	0.8302 (0,3)	0.8764 (0,3)	0.9041 (0,3)
	4	0.2429 (0,4)	0.3344 (0,4)	0.4157 (0,4)	0.4875 (0,4)	0.5508 (0,4)	0.6064 (0,4)	0.6553 (0,4)
	5	0.1137 (0,5)	0.1707 (0,5)	0.2163 (0,5)	0.2672 (0,5)	0.3092 (0,5)	0.3540 (0,5)	0.3918 (0,5)
	6	0.0508 (0,6)	0.0780 (0,6)	0.1052 (0,6)	0.1321 (0,6)	0.1584 (0,6)	0.1841 (0,6)	0.2092 (0,6)
	7	0.0222 (0,7)	0.0366 (0,7)	0.0494 (0,7)	0.0642 (0,7)	0.0775 (0,7)	0.0920 (0,7)	0.1052 (0,7)
	8	0.0095 (0,8)	0.0160 (0,8)	0.0228 (0,8)	0.0299 (0,8)	0.0370 (0,8)	0.0442 (0,8)	0.0513 (0,8)
	9	0.0041 (0,9)	0.0073 (0,9)	0.0104 (0,9)	0.0141 (0,9)	0.0174 (0,9)	0.0212 (0,9)	0.0247 (0,9)
	10	0.0017 (0,10)	0.0032 (0,10)	0.0047 (0,10)	0.0064 (0,10)	0.0082 (0,10)	0.0100 (0,10)	0.0118 (0,10)
	11	0.0007 (0,11)	0.0014 (0,11)	0.0022 (0,11)	0.0030 (0,11)	0.0038 (0,11)	0.0047 (0,11)	0.0056 (0,11)
	12	0.0070 (1,11)	0.0006 (0,12)	0.0010 (0,12)	0.0014 (0,12)	0.0018 (0,12)	0.0022 (0,12)	0.0026 (0,12)
	13	0.0032 (1,12)	0.0059 (1,12)	0.0086 (1,12)	0.0006 (0,13)	0.0008 (0,13)	0.0010 (0,13)	0.0013 (0,13)
	14	0.0015 (1,13)	0.0028 (1,13)	0.0042 (1,13)	0.0058 (1,13)	0.0074 (1,13)	0.0090 (1,13)	0.0006 (0,14)
	15	0.0083 (2,13)	0.0013 (1,14)	0.0020 (1,14)	0.0029 (1,14)	0.0037 (1,14)	0.0046 (1,14)	0.0054 (1,14)
	16	0.0041 (2,14)	0.0072 (2,14)	0.0010 (1,15)	0.0014 (1,15)	0.0018 (1,15)	0.0023 (1,15)	0.0027 (1,15)
	17	0.0020 (2,15)	0.0037 (2,15)	0.0055 (2,15)	0.0076 (2,15)	0.0096 (2,15)	0.0011 (1,16)	0.0014 (1,16)
	18	0.0084 (3,15)	0.0018 (2,16)	0.0028 (2,16)	0.0039 (2,16)	0.0050 (2,16)	0.0062 (2,16)	0.0074 (2,16)
	19	0.0043 (3,16)	0.0077 (3,16)	0.0014 (2,17)	0.0020 (2,17)	0.0026 (2,17)	0.0033 (2,17)	0.0039 (2,17)
	20	0.0022 (3,17)	0.0040 (3,17)	0.0061 (3,17)	0.0082 (3,17)	0.0014 (2,18)	0.0017 (2,18)	0.0020 (2,18)
	21	0.0078 (4,17)	0.0021 (3,18)	0.0032 (3,18)	0.0045 (3,18)	0.0057 (3,18)	0.0071 (3,18)	0.0084 (3,18)
	22	0.0041 (4,18)	0.0074 (4,18)	0.0017 (3,19)	0.0024 (3,19)	0.0031 (3,19)	0.0038 (3,19)	0.0046 (3,19)
	23	0.0022 (4,19)	0.0041 (4,19)	0.0061 (4,19)	0.0083 (4,19)	0.0017 (3,20)	0.0021 (3,20)	0.0025 (3,20)
	24	0.0070 (5,19)	0.0021 (4,20)	0.0033 (4,20)	0.0046 (4,20)	0.0059 (4,20)	0.0073 (4,20)	0.0087 (4,20)

[i] The rows of each cell show the attained *FAP* value and the control limits (a, b)

Table 2.3. Attained *FAP* values and the control limits (a, b)[ii] for $FAP_0 = 0.05$

		Number (m) of Phase I samples						
		4	**5**	**6**	**7**	**8**	**9**	**10**
Sample size (n)	**3**	0.4740 (0,3)	0.6224 (0,3)	0.7001 (0,3)	0.7830 (0,3)	0.8302 (0,3)	0.8764 (0,3)	0.9041 (0,3)
	4	0.2429 (0,4)	0.3344 (0,4)	0.4157 (0,4)	0.4875 (0,4)	0.5508 (0,4)	0.6064 (0,4)	0.6553 (0,4)
	5	0.1137 (0,5)	0.1707 (0,5)	0.2163 (0,5)	0.2672 (0,5)	0.3092 (0,5)	0.3540 (0,5)	0.3918 (0,5)
	6	0.0508 (0,6)	0.0780 (0,6)	0.1052 (0,6)	0.1321 (0,6)	0.1584 (0,6)	0.1841 (0,6)	0.2092 (0,6)
	7	0.0222 (0,7)	0.0366 (0,7)	0.0494 (0,7)	0.0642 (0,7)	0.0775 (0,7)	0.0920 (0,7)	0.1052 (0,7)
	8	0.0095 (0,8)	0.0160 (0,8)	0.0228 (0,8)	0.0299 (0,8)	0.0370 (0,8)	0.0442 (0,8)	0.0513 (0,8)
	9	0.0041 (0,9)	0.0073 (0,9)	0.0104 (0,9)	0.0141 (0,9)	0.0174 (0,9)	0.0212 (0,9)	0.0247 (0,9)
	10	0.0315 (1,9)	0.0500 (1,9)	0.0047 (0,10)	0.0064 (0,10)	0.0082 (0,10)	0.0100 (0,10)	0.0118 (0,10)
	11	0.0150 (1,10)	0.0252 (1,10)	0.0350 (1,10)	0.0459 (1,10)	0.0038 (0,11)	0.0047 (0,11)	0.0056 (0,11)
	12	0.0070 (1,11)	0.0121 (1,11)	0.0175 (1,11)	0.0231 (1,11)	0.0289 (1,11)	0.0347 (1,11)	0.0405 (1,11)
	13	0.0328 (2,11)	0.0059 (1,12)	0.0086 (1,12)	0.0117 (1,12)	0.0147 (1,12)	0.0179 (1,12)	0.0210 (1,12)
	14	0.0167 (2,12)	0.0274 (2,12)	0.0387 (2,12)	0.0058 (1,13)	0.0074 (1,13)	0.0090 (1,13)	0.0107 (1,13)
	15	0.0083 (2,13)	0.0144 (2,13)	0.0205 (2,13)	0.0272 (2,13)	0.0337 (2,13)	0.0406 (2,13)	0.0472 (2,13)
	16	0.0305 (3,13)	0.0486 (3,13)	0.0107 (2,14)	0.0143 (2,14)	0.0181 (2,14)	0.0219 (2,14)	0.0257 (2,14)
	17	0.0161 (3,14)	0.0270 (3,14)	0.0377 (3,14)	0.0493 (3,14)	0.0096 (2,15)	0.0117 (2,15)	0.0139 (2,15)
	18	0.0479 (4,14)	0.0144 (3,15)	0.0208 (3,15)	0.0275 (3,15)	0.0343 (3,15)	0.0411 (3,15)	0.0480 (3,15)
	19	0.0267 (4,15)	0.0434 (4,15)	0.0113 (3,16)	0.0152 (3,16)	0.0191 (3,16)	0.0232 (3,16)	0.0272 (3,16)
	20	0.0146 (4,16)	0.0243 (4,16)	0.0345 (4,16)	0.0450 (4,16)	0.0105 (3,17)	0.0128 (3,17)	0.0152 (3,17)
	21	0.0398 (5,16)	0.0137 (4,17)	0.0196 (4,17)	0.0261 (4,17)	0.0324 (4,17)	0.0391 (4,17)	0.0456 (4,17)
	22	0.0227 (5,17)	0.0369 (5,17)	0.0110 (4,18)	0.0147 (4,18)	0.0186 (4,18)	0.0226 (4,18)	0.0266 (4,18)
	23	0.0127 (5,18)	0.0216 (5,18)	0.0305 (5,18)	0.0401 (5,18)	0.0495 (5,18)	0.0129 (4,19)	0.0153 (4,19)
	24	0.0326 (6,18)	0.0122 (5,19)	0.0177 (5,19)	0.0235 (5,19)	0.0295 (5,19)	0.0355 (5,19)	0.0415 (5,19)

[ii] The rows of each cell show the attained *FAP* value and the control limits (a, b)

Table 2.4. Attained *FAP* values and the control limits (a, b)[iii] for $FAP_0 = 0.10$

		Number (m) of Phase I samples						
		4	**5**	**6**	**7**	**8**	**9**	**10**
Sample size (n)	**3**	0.4740 (0,3)	0.6224 (0,3)	0.7001 (0,3)	0.7830 (0,3)	0.8302 (0,3)	0.8764 (0,3)	0.9041 (0,3)
	4	0.2429 (0,4)	0.3344 (0,4)	0.4157 (0,4)	0.4875 (0,4)	0.5508 (0,4)	0.6064 (0,4)	0.6553 (0,4)
	5	0.1137 (0,5)	0.1707 (0,5)	0.2163 (0,5)	0.2672 (0,5)	0.3092 (0,5)	0.3540 (0,5)	0.3918 (0,5)
	6	0.0508 (0,6)	0.0780 (0,6)	0.1052 (0,6)	0.1321 (0,6)	0.1584 (0,6)	0.1841 (0,6)	0.2092 (0,6)
	7	0.0222 (0,7)	0.0366 (0,7)	0.0494 (0,7)	0.0642 (0,7)	0.0775 (0,7)	0.0920 (0,7)	0.1052 (0,7)
	8	0.0095 (0,8)	0.0160 (0,8)	0.0228 (0,8)	0.0299 (0,8)	0.0370 (0,8)	0.0442 (0,8)	0.0513 (0,8)
	9	0.0648 (1,8)	0.0073 (0,9)	0.0104 (0,9)	0.0141 (0,9)	0.0174 (0,9)	0.0212 (0,9)	0.0247 (0,9)
	10	0.0315 (1,9)	0.0500 (1,9)	0.0688 (1,9)	0.0877 (1,9)	0.0082 (0,10)	0.0100 (0,10)	0.0118 (0,10)
	11	0.0150 (1,10)	0.0252 (1,10)	0.0350 (1,10)	0.0459 (1,10)	0.0561 (1,10)	0.0670 (1,10)	0.0772 (1,10)
	12	0.0632 (2,10)	0.0963 (2,10)	0.0175 (1,11)	0.0231 (1,11)	0.0289 (1,11)	0.0347 (1,11)	0.0405 (1,11)
	13	0.0328 (2,11)	0.0528 (2,11)	0.0717 (2,11)	0.0920 (2,11)	0.0147 (1,12)	0.0179 (1,12)	0.0210 (1,12)
	14	0.0167 (2,12)	0.0274 (2,12)	0.0387 (2,12)	0.0502 (2,12)	0.0618 (2,12)	0.0735 (2,12)	0.0850 (2,12)
	15	0.0563 (3,12)	0.0873 (3,12)	0.0205 (2,13)	0.0272 (2,13)	0.0337 (2,13)	0.0406 (2,13)	0.0472 (2,13)
	16	0.0305 (3,13)	0.0486 (3,13)	0.0671 (3,13)	0.0858 (3,13)	0.0181 (2,14)	0.0219 (2,14)	0.0257 (2,14)
	17	0.0836 (4,13)	0.0270 (3,14)	0.0377 (3,14)	0.0493 (3,14)	0.0605 (3,14)	0.0721 (3,14)	0.0833 (3,14)
	18	0.0479 (4,14)	0.0743 (4,14)	0.0208 (3,15)	0.0275 (3,15)	0.0343 (3,15)	0.0411 (3,15)	0.0480 (3,15)
	19	0.0267 (4,15)	0.0434 (4,15)	0.0597 (4,15)	0.0770 (4,15)	0.0936 (4,15)	0.0232 (3,16)	0.0272 (3,16)
	20	0.0681 (5,15)	0.0243 (4,16)	0.0345 (4,16)	0.0450 (4,16)	0.0556 (4,16)	0.0628 (4,16)	0.0769 (4,16)
	21	0.0398 (5,16)	0.0630 (5,16)	0.0856 (5,16)	0.0261 (4,17)	0.0324 (4,17)	0.0391 (4,17)	0.0456 (4,17)
	22	0.0903 (6,16)	0.0369 (5,17)	0.0516 (5,17)	0.0665 (5,17)	0.0815 (5,17)	0.0964 (5,17)	0.0266 (4,18)
	23	0.0549 (6,17)	0.0851 (6,17)	0.0305 (5,18)	0.0401 (5,18)	0.0495 (5,18)	0.0592 (5,18)	0.0686 (5,18)
	24	0.0326 (6,18)	0.0518 (6,18)	0.0715 (6,18)	0.0913 (6,18)	0.0295 (5,19)	0.0355 (5,19)	0.0415 (5,19)

[iii] The rows of each cell show the attained *FAP* value and the control limits (a, b)

The attained *FAP* values are illustrated graphically in Figures 2.2, 2.3 and 2.4 for desired *FAP* values equal to 0.01, 0.05 and 0.10, respectively. Note that although the values of n we taken to be $n = 3(1)24$, not all n are illustrated on the same graph.

For $FAP_0 = 0.01$ it can be seen that $3 \leq n \leq 10$ give attained *FAP* values greater than the desired *FAP* value of 0.01, whereas $11 \leq n \leq 24$ give attained *FAP* values less than the desired *FAP* value of 0.01. Accordingly, $3 \leq n \leq 10$ is graphically illustrated in Figure 2.2a and $11 \leq n \leq 24$ is graphically illustrated in Figure 2.2b.

For $FAP_0 = 0.05$ it can be seen that $3 \leq n \leq 8$ give attained *FAP* values greater than the desired *FAP* value of 0.05, whereas $9 \leq n \leq 24$ give attained *FAP* values less than the desired *FAP* value of 0.05. Accordingly, $3 \leq n \leq 8$ is graphically illustrated in Figure 2.3a and $9 \leq n \leq 24$ is graphically illustrated in Figure 2.3b.

For $FAP_0 = 0.10$ it can be seen that $3 \leq n \leq 7$ give attained *FAP* values greater than the desired *FAP* value of 0.10, whereas $8 \leq n \leq 24$ give attained *FAP* values less than the desired *FAP* value of 0.10. Accordingly, $3 \leq n \leq 7$ is graphically illustrated in Figure 2.4a and $8 \leq n \leq 24$ is graphically illustrated in Figure 2.4b.

From Tables 2.2, 2.3 and 2.4 and Figures 2.2,a 2.3a and 2.4a it can be seen that ‘small’ values of n do not give desirable results, since some of the attained *FAP* values are greater than the desired *FAP* values.

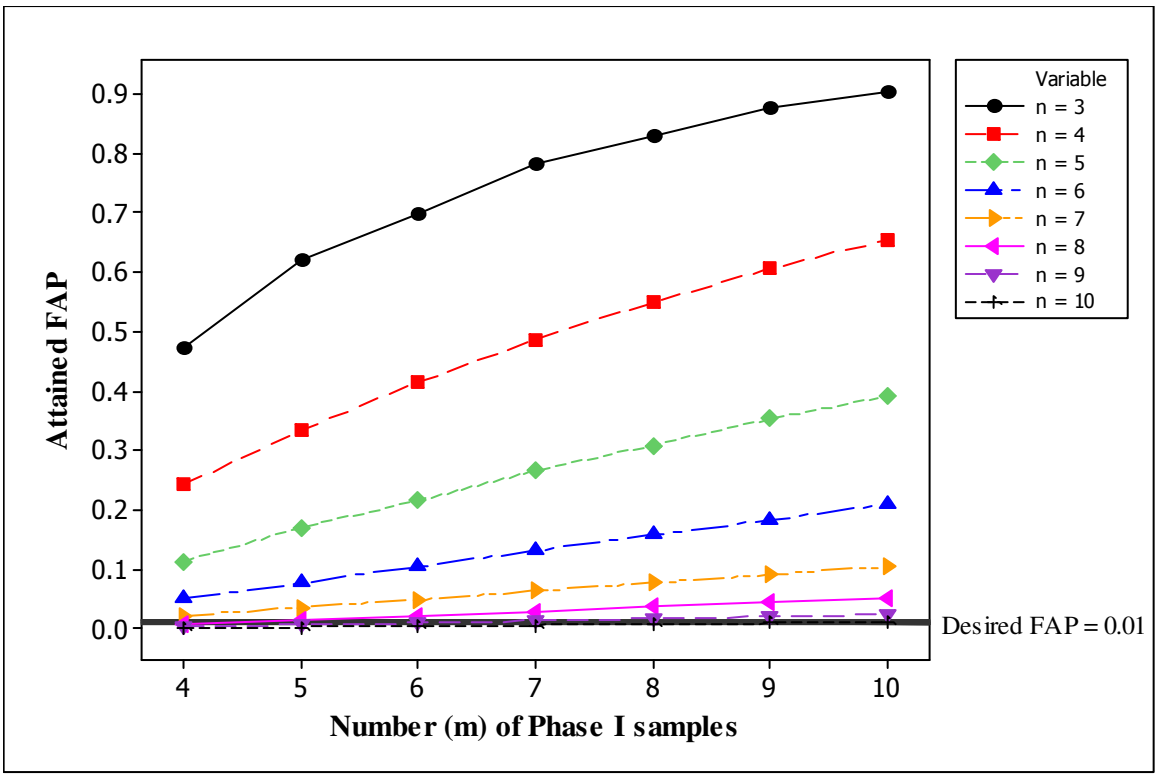

Figure 2.2a. Attained *FAP* values for $3 \leq n \leq 10$ for a desired $FAP_0 = 0.01$

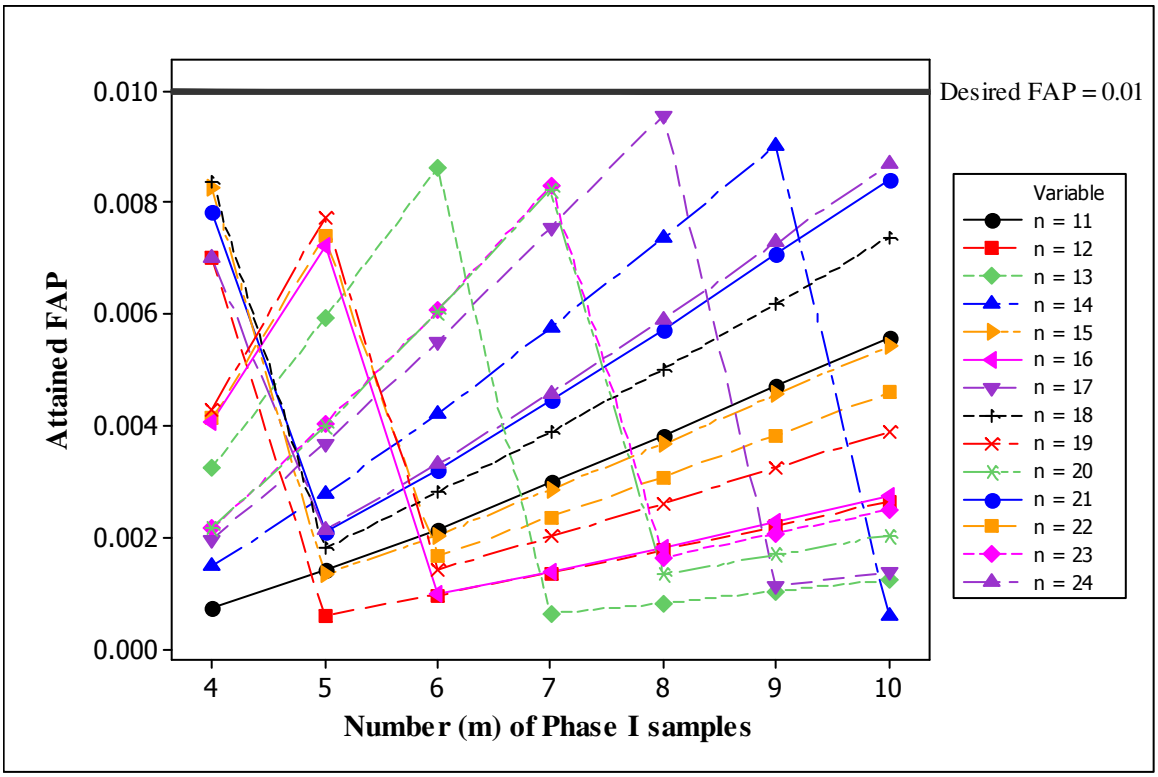

Figure 2.2b. Attained *FAP* values for $11 \leq n \leq 24$ for a desired $FAP_0 = 0.01$

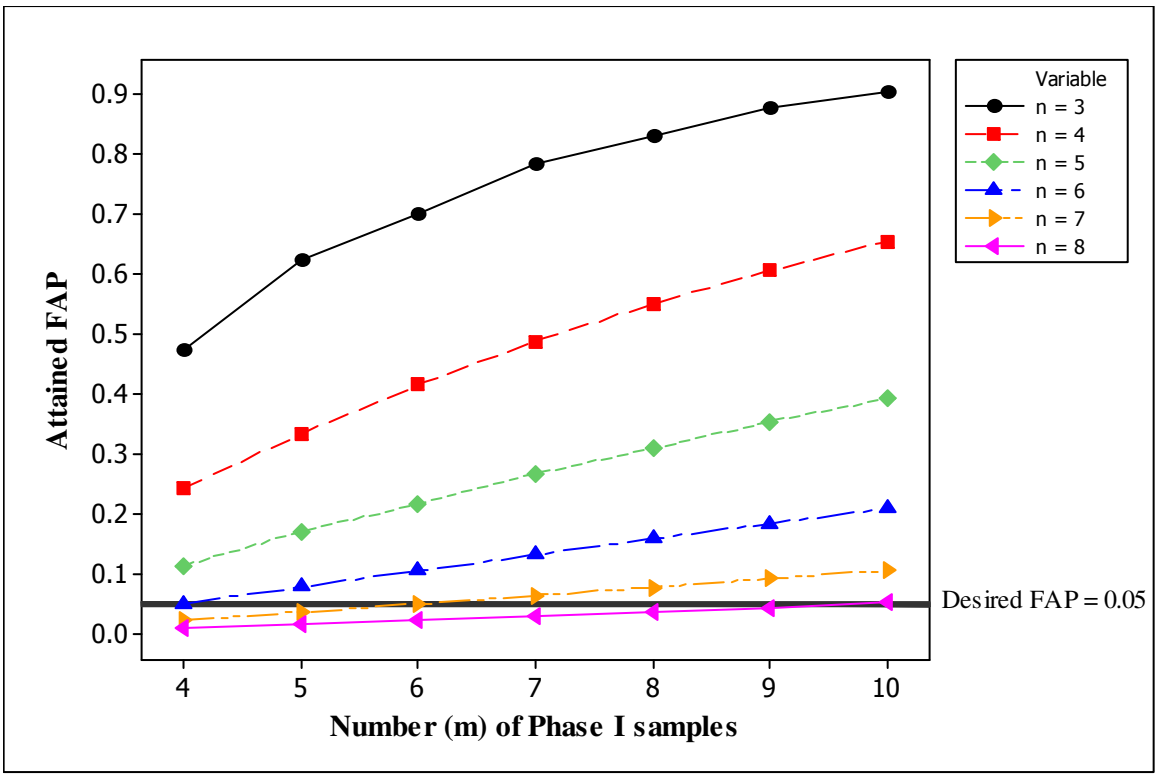

Figure 2.3a. Attained *FAP* values for $3 \leq n \leq 8$ for a desired $FAP_0 = 0.05$

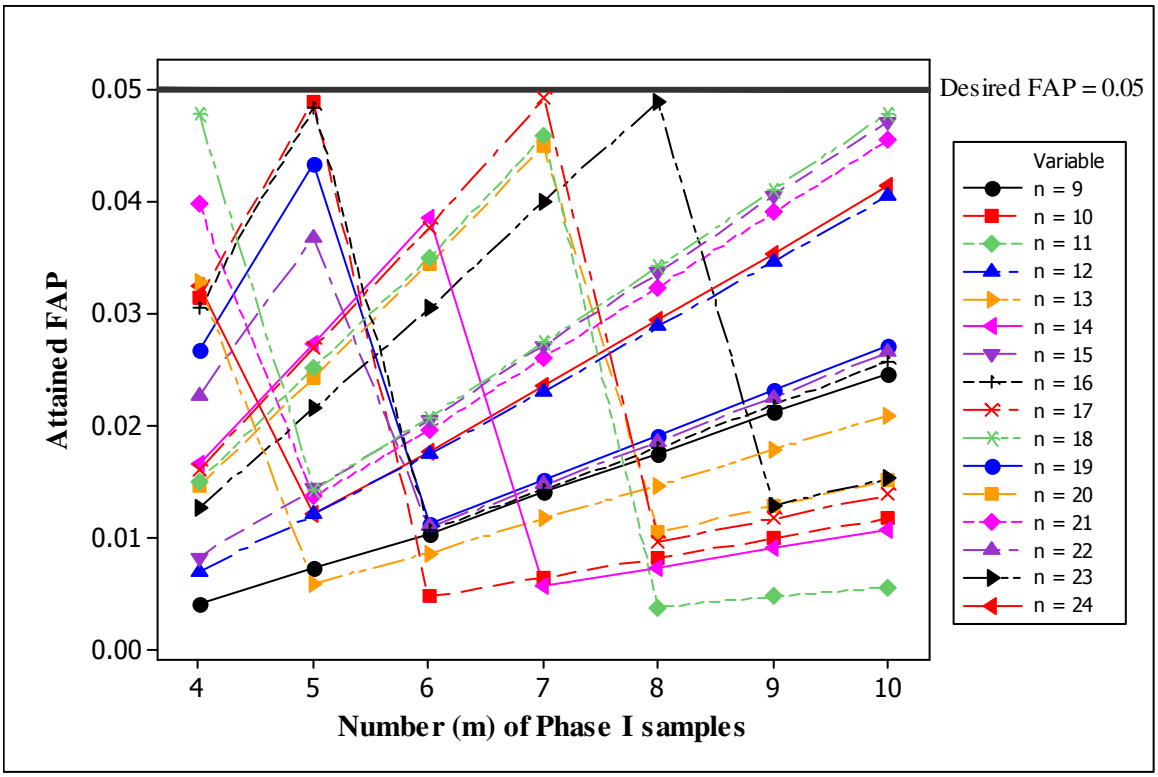

Figure 2.3b. Attained *FAP* values for $9 \leq n \leq 24$ for a desired $FAP_0 = 0.05$

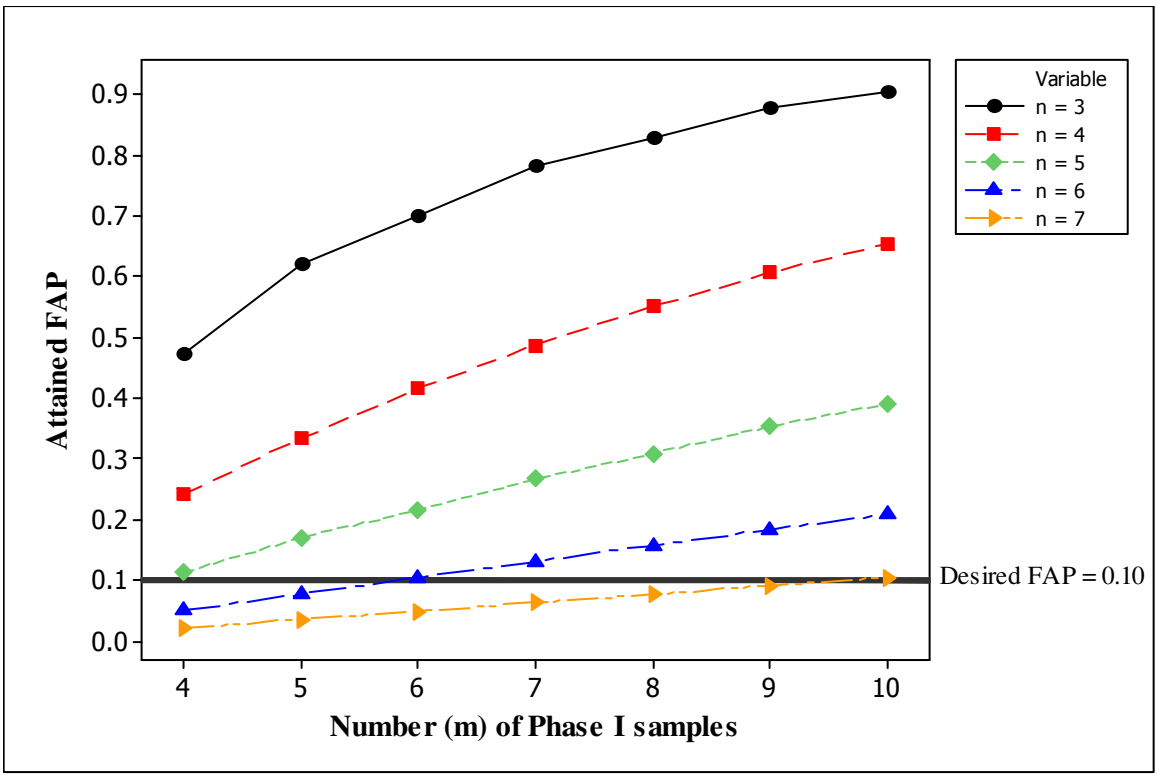

Figure 2.4a. Attained *FAP* values for $3 \leq n \leq 7$ for a desired $FAP_0 = 0.10$

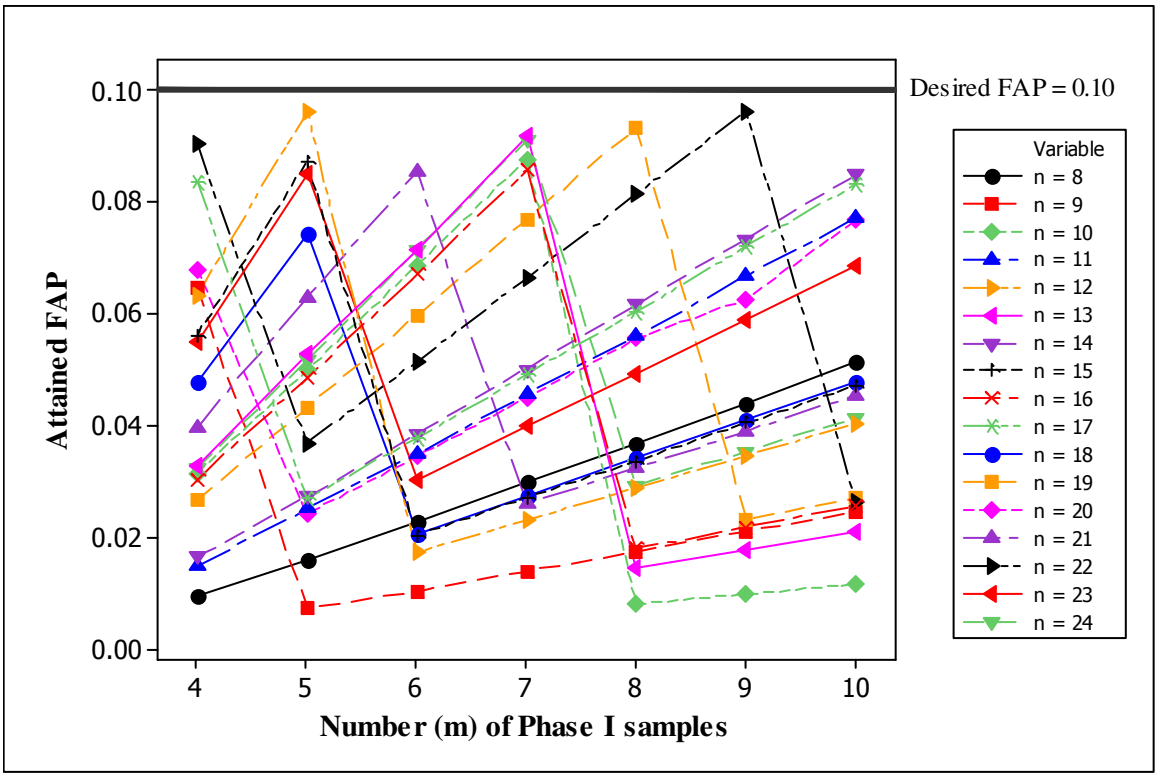

Figure 2.4b. Attained *FAP* values for $8 \leq n \leq 24$ for a desired $FAP_0 = 0.10$

In Figures 2.5, 2.6 and 2.7 the choice of the number of Phase I samples (m) is investigated for a desired *FAP* value (FAP_0) equal to 0.01, 0.05 and 0.10, respectively. Note that it was found that the subgroup size n needs to be larger than the number of subgroups m in order to achieve a small attained *FAP* value. This may be due to the discreteness of the IC distribution of the charting statistic. For example, from Figures 2.5, 2.6 and 2.7 it can be seen that smaller values of m are performing better. Note, however, that for a fixed value of m, a larger value of n will not always give a better attained *FAP* value. For example, from Table 2.4 it can be seen that for m = 10 and n = 17 the attained *FAP* equals 0.0833 which is much closer to the desired *FAP* of 0.10 than in the case of m = 10 and n = 24 where the attained *FAP* equals 0.0415. The nature of the relationship among the *FAP*, m and n can be explored further.

The situation (the subgroup size n needs to be larger than the number of subgroups m) appears to be similar to control charting with attributes data, where typically the subgroup size n is taken to be much larger than the number of subgroups m; see e.g. all the examples and problems in Chapter 7 of Montgomery (2009). This raises an interesting question as to how to design a Phase I study and allocate resources fairly, optimally and economically. For example, if a total of 100 Phase I observations are to be used, how should these be collected, in 20 groups of 5 or in 5 groups of 20? The answer depends on the particular situation. Let us consider an example. Suppose 240 observations are available. The question is should we take 24 groups of 10 or 10 groups of 24? For m = 24 and n = 10 we find attained *FAP* values of 0.0380 and 0.3651 for (a, b) = (0,10) and (1,9), respectively. For m = 10 and n = 24 we find attained *FAP* values of 0.0097 and 0.0384 for (a, b) = (4,20) and (5,19), respectively. Therefore, the attained *FAP* values of 0.0380 and 0.0384 are close to the desired *FAP* value of 0.05, so either 24 groups of 10 could be used with control limits (a, b) = (0,10) or 10 groups of 24 could be used with control limits (a, b) = (5,19).

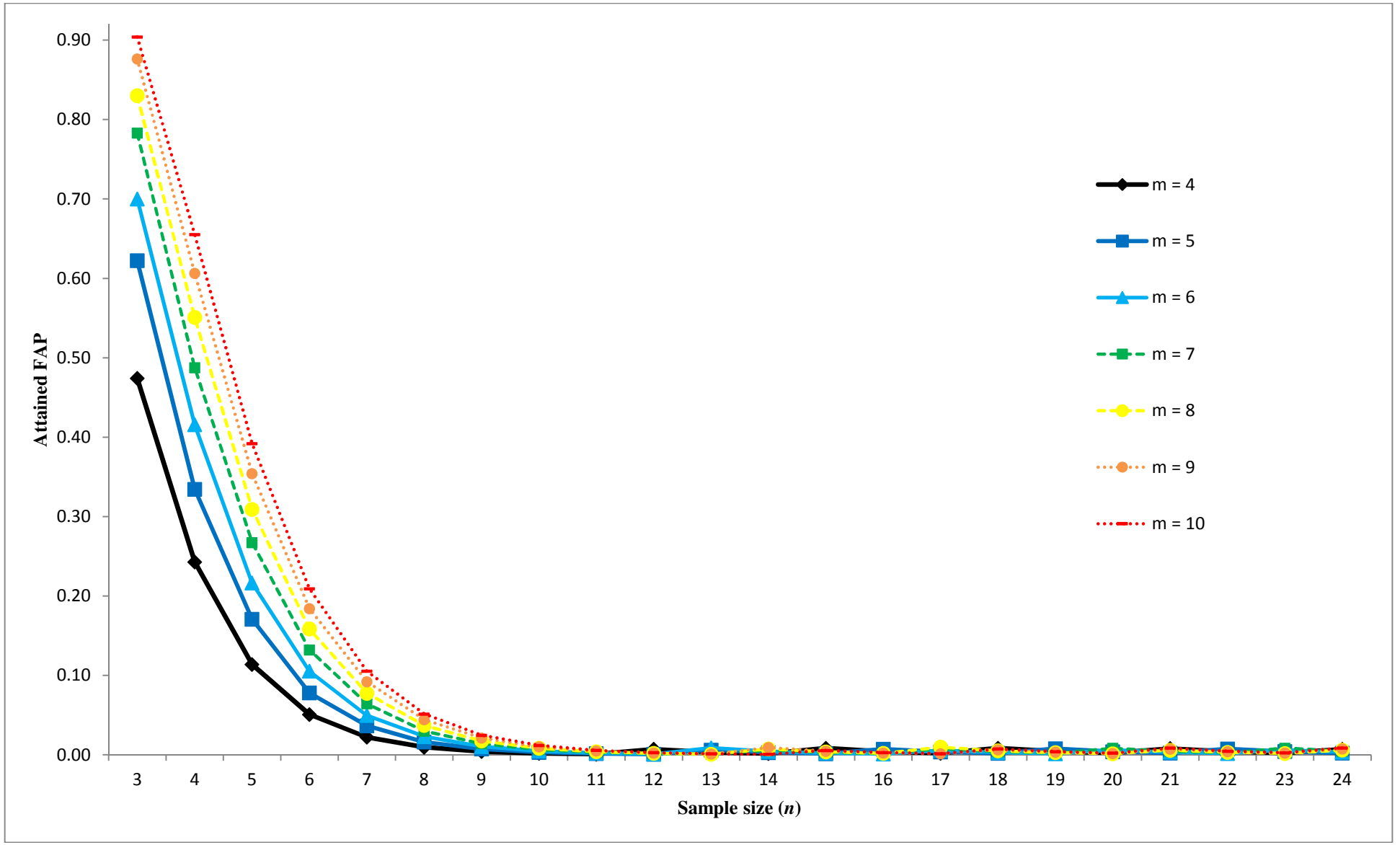

Figure 2.5. Attained *FAP* values for a desired $FAP_0 = 0.01$

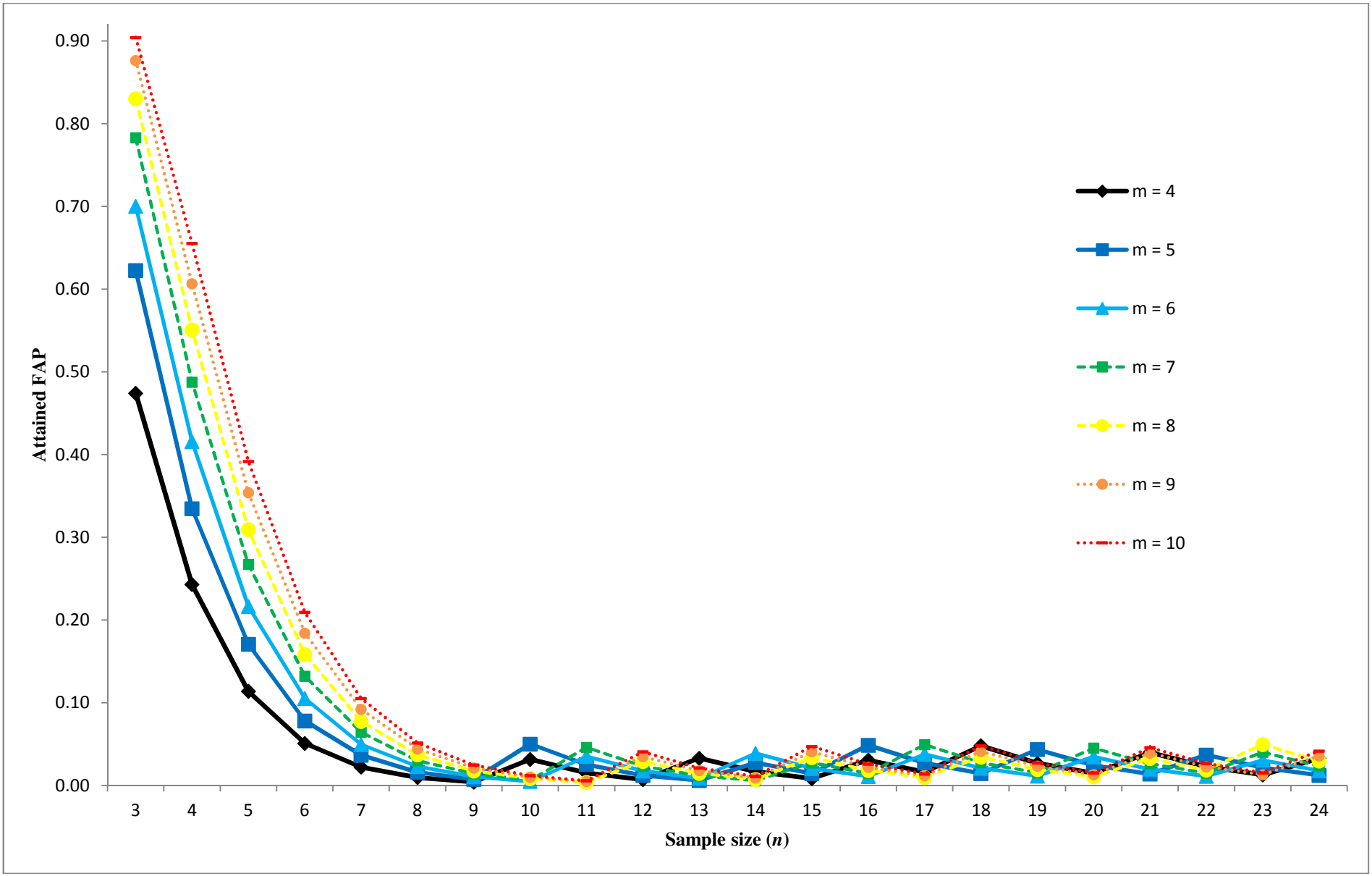

Figure 2.6. Attained *FAP* values for a desired $FAP_0 = 0.05$

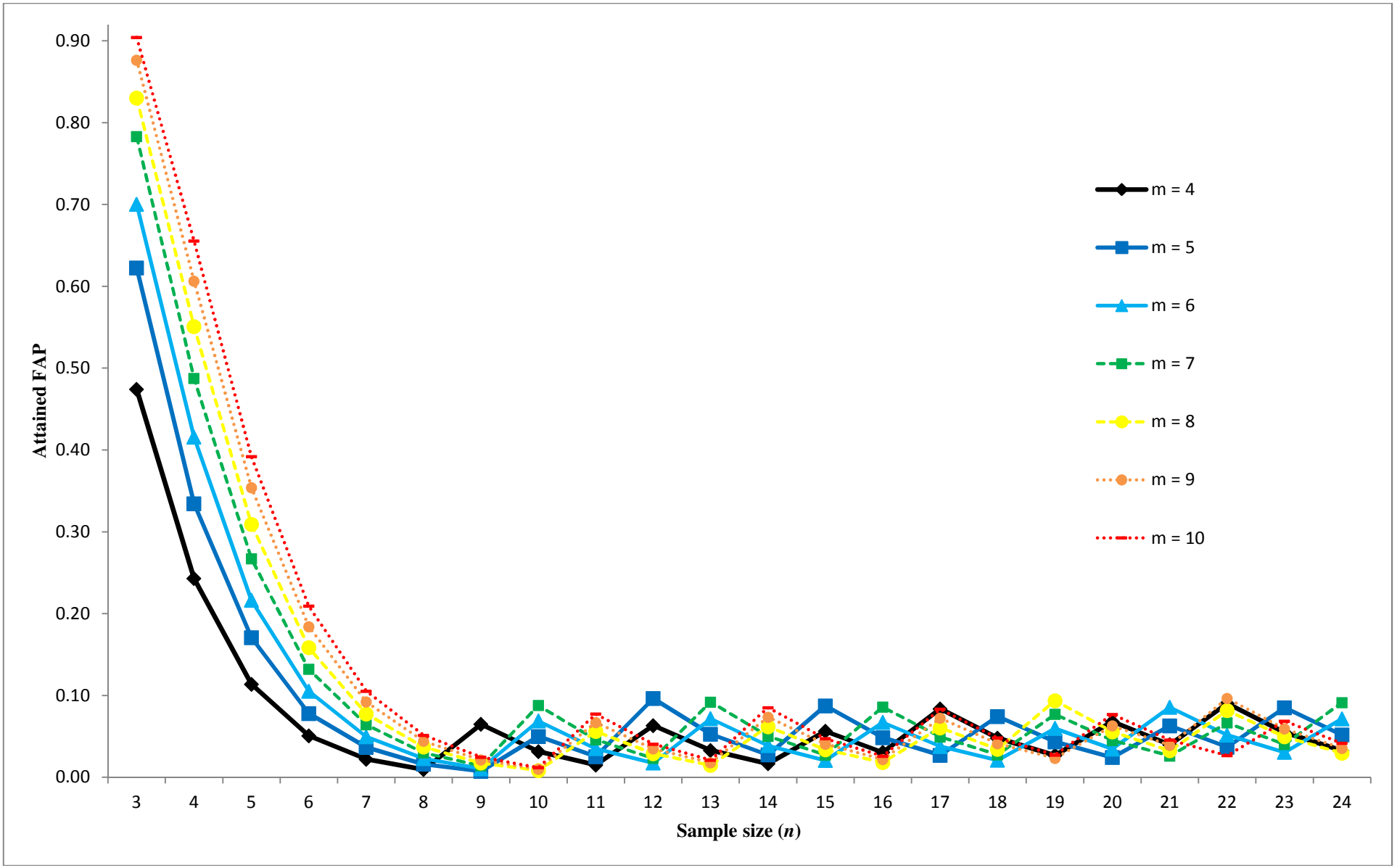

Figure 2.7. Attained *FAP* values for a desired $FAP_0 = 0.10$

Approximate control limits

Hypergeometric approximation

Computations and computer resources for the exact control limits can take a considerable amount of time, particularly when m and / or n are large, say $m \geq 10$. Since the correlation between any two charting statistics equals $-1/(m-1)$ when the process is IC (given in Equation (2.10)) and approaches zero for 'large' values of m, we can approximate the control limits by ignoring the dependence among the charting statistics and using simply the marginal univariate hypergeometric distribution of the U_i's. Thus for 'large' m the FAP of the median chart can be approximated by using Equation (2.12), i.e. $FAP \approx 1-(1-FAR)^m$. Hence for large m, the FAP can be expressed as a simple function of the FAR (which is a function of m, n, $L\hat{C}L = a$ and $U\hat{C}L = b$), and one can approximate the control limits from the distribution of a single charting statistic. This is a considerable simplification. In passing note that, when the process parameters are known or specified (referred to as Case K), it is well known that $ARL_0 = 1/FAR$ and the charting statistics are independent. Thus, in Case K, $FAP = 1-(1-1/ARL_0)^m$.

From Equation (2.13) it follows that the control limits a and b can be approximated by $\tilde{a}$ and $\tilde{b}$ by solving the following expression

$$(1-FAP_0)^{\frac{1}{m}} \leq 1-FAR = P(\tilde{a} < U_i < \tilde{b} \mid \text{IC}). \tag{2.17}$$

Because the in-control marginal distribution of U_i is symmetric when the percentile of interest is the median, we have $P(U_i \leq \tilde{a} \mid \text{IC}) = P(U_i \geq n-\tilde{a} \mid \text{IC})$ and we can again use symmetric control limits and set $\tilde{b} = n-\tilde{a}$. Consequently, the expression in (2.17) can be re-written as $(1-FAP_0)^{\frac{1}{m}} \leq 1-2P(U_i \leq \tilde{a} \mid \text{IC})$ which means that we need to solve only for $\tilde{a}$ from

$$P(U_i \leq \tilde{a} \mid \text{IC}) \leq \frac{1}{2}\left(1-(1-FAP_0)^{\frac{1}{m}}\right) \tag{2.18}$$

where FAP_0 is specified and m is known. For any particular set of values of m, n and FAP_0, Expression (2.18) can be solved uniquely by setting $\tilde{a}$ equal to

$$\tilde{a} = max\left\{d: P(U_i \leq d \mid \text{IC}) \leq \frac{1}{2}\left(1-(1-FAP_0)^{\frac{1}{m}}\right)\right\} \tag{2.19}$$

where U_i follows the hypergeometric (N, m, n, u_T) distribution shown in Equation (2.6). In order to illustrate why the maximum is taken in Equation (2.19) an illustrative example is given (see Example 2.2). The attained *FAP* in this case is equal to $1 - \left(1 - 2P(U_i \leq \tilde{a} \mid \text{IC})\right)^m$. The accuracy of this approximation is examined later.

Normal approximation

The charting constants can also be obtained by a normal approximation to the univariate hypergeometric distribution (see Lehmann (1975) page 216). These are given by

$$\hat{a} = \left[\frac{1}{2}\left(n + c_l\sqrt{\frac{n^2(m-1)}{mn-1}}\right)\right] \text{ and } \hat{b} = n - \hat{a} \tag{2.20}$$

where $c_l = \Phi^{-1}\{0.5[1 - (1 - FAP_0)^{1/m}]\}$ and $[x]$ denotes the greatest integer not exceeding x. In our comparisons, both sets of approximate solutions were quite close to the exact solutions for m = 10 and n greater than 15.

Exact control limits vs. approximate control limits

Since computations for the exact control limits can take a considerable amount of time, particularly when m and / or n are large, it is recommended that either one of the approximations (hypergeometric or normal) be used when m and / or n are large in order to save the practitioner time. In addition, from a practical point of view there are advantages to using the approximate solutions $(\tilde{a}, \tilde{b})$ and $(\hat{a}, \hat{b})$ since most software packages provide standard normal and hypergeometric probabilities.

2.2.4. Illustrative examples

Example 2.1

The median chart is illustrated by building on a dataset from Montgomery (2005, Table 5.3, page 223) on the inside diameters of piston rings manufactured by a forging process. In this dataset there are 25 samples (m = 25) each of size 5 (n = 5). However, we need n to be much larger than m for the attainable *FAP* values to be closer to some typical values of FAP_0 used in practice and so we

took $n = 24$ and $m = 7$. Thus 7 samples of each of size 24 are assumed to be available for a Phase I analysis. Our data were generated from a normal distribution, with the same mean and standard deviation as those of the original dataset. The simulated observations, along with the charting statistics, are given in Table 2.5. We plot the seven charting statistics on the control chart shown in Figure 2.8 and compare them to three sets of control limits obtained from Tables 2.2. 2.3 and 2.4 for three nominal *FAP* values, 0.01, 0.05 and 0.10, respectively.

Table 2.5. The data for Example 2.1 and the corresponding charting statistics for the Phase I median control chart and the Phase I $\overline{X}$ control chart

Sample number i	Observations												U_i	$\overline{X}_i$
	Overall Median M = 74.000													
1	74.004	74.012	73.982	73.987	74.002	74.001	74.000	74.001	74.007	74.013	74.009	73.999	9	74.001
	73.985	74.013	73.999	73.996	73.998	74.000	74.011	74.002	74.007	73.991	73.995	74.013		
2	73.998	73.990	74.001	74.001	74.019	74.010	74.004	74.004	74.021	74.003	74.011	74.016	6	74.004
	74.009	74.013	73.998	74.002	73.987	74.002	74.001	73.991	74.004	74.009	73.992	74.002		
3	73.995	73.987	74.004	74.015	74.015	74.013	73.982	74.017	73.999	74.021	73.990	74.010	12	74.002
	74.000	74.006	73.993	73.999	74.008	73.999	74.023	73.990	74.008	73.997	73.991	73.991		
4	73.990	74.002	73.996	74.016	73.996	74.001	74.005	73.990	73.999	73.998	73.997	73.995	15	73.997
	74.011	73.969	73.997	73.983	73.988	74.001	74.005	74.000	73.996	73.996	73.986	74.009		
5	74.000	74.000	73.990	74.001	74.000	73.989	73.998	73.992	74.005	74.000	73.987	74.010	12	73.997
	74.012	73.981	74.008	73.999	73.973	74.013	73.992	73.998	74.013	74.008	73.978	73.985		
6	73.998	73.984	73.978	74.031	74.001	73.992	73.997	73.995	73.999	73.996	73.988	73.998	18	73.998
	73.984	73.994	74.015	73.994	74.017	74.020	73.996	73.985	74.019	73.990	73.984	73.989		
7	73.983	74.010	74.005	74.017	74.009	73.987	74.009	74.009	73.979	74.005	74.004	73.993	7	74.003
	74.011	74.000	74.014	74.032	73.995	74.003	73.997	73.978	74.014	74.012	74.002	74.015		

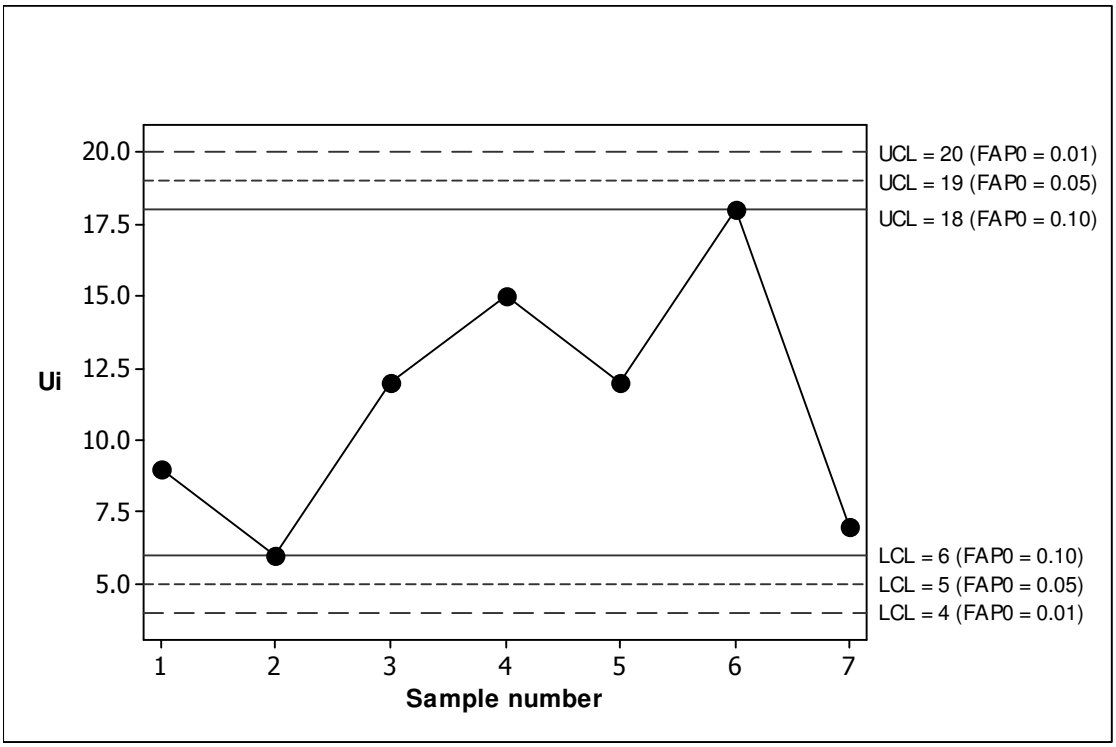

Figure 2.8. The Phase I median control chart for $m = 7$ and $n = 24$

Note that the practitioner would specify the desired *FAP*; in this example we consider three values for the desired *FAP*, namely a FAP_0 = 0.01, 0.05 and 0.10, respectively. As might be expected, the lower the FAP_0, the wider the IC region (the further are the control limits from each other) and vice versa and this can affect the assessment of whether or not the process is IC; wider control limits lead to lower *FAP* values and narrower control limits lead to higher *FAP* values. For example, for a FAP_0 of 0.01, we have *LCL* = 4 and *UCL* = 20 with an attained *FAP* of 0.0046. But for a FAP_0 of 0.05, *LCL* = 5 and *UCL* = 19 with an attained *FAP* of 0.0235. In both of these cases the seven charting statistics all fall between the control limits, indicating that the process is IC. However, for a FAP_0 of 0.10, *LCL* = 6 and *UCL* = 18 (with an attained *FAP* of 0.0913) and in this case, the second and the sixth samples plot on the *LCL* and *UCL*, respectively. Thus, at a FAP_0 of 0.10 the conclusion is that the process is OOC; hence, when the desired *FAP* equals 0.10, the data cannot be thought of as a reference sample and a search for assignable causes is necessary. Note that since these were simulated data, we know that samples 2 and 6 are not from an OOC process but the fact that the chart indicates that they are is not entirely surprising since, there is about a 10% chance of at least one false alarm by design. For illustration of the iterative implementation in Phase I, suppose that upon further investigation by the management, samples 2 and 6 are deleted from the analysis. The lower and upper control limits for the remaining data are then obtained from Table 2.4, but for m = 5 and n = 24. For a FAP_0 of 0.10, these limits are found to be equal to 6 and 18 and hence all five of the charting statistics plot IC. This final set of 120 data points constitutes an IC or a reference sample at FAP_0 = 0.10, from which, for example, one can estimate any necessary parameters (which is this case is the charting constant a) and construct the control limits to be used in Phase II process monitoring. Finally, note that for the complete data set (m = 7 and n = 24) the lower and upper control limits for the Shewhart-type Phase I $\overline{X}$ chart, as proposed in Champ and Jones (2004), are found to be 73.995 and 74.005, respectively, for FAP_0 = 0.10, so that no points are declared OOC under this chart.

Example 2.2

Suppose that m = 15, n = 30 and FAP_0 = 0.20 (a combination of values for m, n and FAP_0 not covered by Tables 2.2, 2.3 and 2.4). In this case, the IC correlation between any two charting statistics equals $-\frac{1}{m-1} = -\frac{1}{15-1} = -0.0714$, which can be thought to be small and we can approximate the control limits. Recall that, from earlier discussions, when m is 'large' enough, the correlation between the charting statistics approaches zero and we can approximate the control limits by ignoring the dependence among the charting statistics. In this case U_i follows a

hypergeometric $(N = 450, m = 15, n = 30, u_T = 225)$ distribution. The pmf and cdf for the hypergeometric $(N = 450, m = 15, n = 30, u_T = 225)$ distribution is given in Table 2.6 and for $FAP_0 = 0.20$ the lower control limit $\tilde{a}$ is found from Equation (2.19)

$$\tilde{a} = max\left\{d: P(U_i \leq d \mid \text{IC}) \leq \frac{1}{2}\left(1 - (1 - 0.20)^{1/15}\right)\right\} = 8$$

with $\frac{1}{2}\left(1 - (1 - 0.20)^{1/15}\right) = 0.00738$ so that $\tilde{b} = n - \tilde{a} = 30 - 8 = 22$, which results in an approximately attained FAP of $1 - \left(1 - 2P(U_i \leq 8 \mid \text{IC})\right)^{15} = 0.1760$, which is quite 'close' to the specified FAP_0 of 0.20. To explore the accuracy of the approximation further, we show in Table 2.7 the approximate charting constants ($\tilde{a}$ and $\tilde{b} = n - \tilde{a}$) and the approximate attained FAP values for m = 15 and n = 30 for a specified FAP_0 = 0.01, 0.05, 0.10 and 0.20, respectively.

Table 2.6. The pmf and cdf for the hypergeometric $(N = 450, m = 15, n = 30, u_T = 225)$ distribution

x	pmf	cdf	
0	0.0000	0.0000	
1	0.0000	0.0000	
2	0.0000	0.0000	
3	0.0000	0.0000	
4	0.0000	0.0000	
5	0.0001	0.0001	
6	0.0004	0.0005	
7	0.0014	0.0019	
8	0.0045	0.0064	$\tilde{a} = max\{d: P(U_i \leq d \mid \text{IC}) \leq 0.00738\}$
9	0.0116	0.0180	
10	0.0257	0.0438	
11	0.0488	0.0926	
12	0.0799	0.1724	
13	0.1133	0.2857	
14	0.1395	0.4252	
15	0.1495	0.5748	
16	0.1395	0.7143	
17	0.1133	0.8276	
18	0.0799	0.9074	
19	0.0488	0.9562	
20	0.0257	0.9820	
21	0.0116	0.9936	
22	0.0045	0.9981	
23	0.0014	0.9995	
24	0.0004	0.9999	
25	0.0001	1.0000	
26	0.0000	1.0000	
27	0.0000	1.0000	
28	0.0000	1.0000	
29	0.0000	1.0000	
30	0.0000	1.0000	

Table 2.7. Approximate[iv] charting constants based on the marginal distribution of U_i ($\tilde{a}$ and $\tilde{b} = n - \tilde{a}$) for m = 15 and n = 30

FAP_0	$\frac{1-(1-FAP_0)^{\frac{1}{m}}}{2}$	$\tilde{a}$	$\tilde{b}$	Approximate attained $FAP = 1-\left(1-2P(U_i \leq \tilde{a} \mid \text{IC})\right)^m$
0.01	0.00033	5	25	0.0031
0.05	0.00171	6	24	0.0147
0.10	0.00350	7	23	0.0566
0.20	0.00738	8	22	0.1760

Looking at the entries of Table 2.7 it might first appear that the approximation is not so satisfactory since the values in the last column are not very close to those in the first unless FAP_0 gets large. However, we need to keep in mind the discreteness of the charting statistics and the conservative answers, i.e. attained $FAP \leq$ desired FAP, we sought in the first place. To clarify this point, we further examine this issue in Table 2.8 by listing the approximate control limits ($\tilde{a}$ and $\tilde{b} = n - \tilde{a}$), the corresponding approximately attained FAP, the exact control limits (a and b) as well as the exact attained FAP (the last two figures obtained from Tables 2.2, 2.3 and 2.4) for m = 7 and n = 24 (i.e. the (m,n) values of Example 2.1), for a specified FAP_0 = 0.01, 0.05, 0.10 and 0.20, respectively. This throws new light on the efficacy of the proposed approximation. We observe that:

i. In all cases the approximate charting constants are equal to the exact charting constants (illustrating that accuracy of the approximations).

ii. The approximate attained FAP is either exactly equal or is 'very close' to the exact attained FAP. Thus a value of m as low as 7 might be large enough for one to use the easily found approximate control limits in practice.

Table 2.8. Approximate[v] charting constants based on the marginal distribution of U_i and exact charting constants and corresponding FAP values for m = 7 and n = 24

	Approximate				**Exact**		
Desired / Nominal FAP_0	$\frac{1-(1-FAP_0)^{\frac{1}{m}}}{2}$	$\tilde{a}$	$\tilde{b}$	Approximate attained $FAP = 1-\left(1-2P(U_i \leq \tilde{a} \mid \text{IC})\right)^m$	a	b	Exact attained FAP (from Tables 2.2, 2.3 and 2.4)
0.01	0.00072	4	20	0.0046	4	20	0.0046
0.05	0.00365	5	19	0.0238	5	19	0.0235
0.10	0.00747	6	18	0.0939	6	18	0.0913
0.20	0.01569	6	18	0.0939	NA[vi]	NA	NA

2.2.5. Performance comparison

[iv] The hypergeometric approximation is used.
[v] The hypergeometric approximation is used.
[vi] The exact charting constants and exact attained FAP for a desired FAP_0 of 0.20 is not available (NA) from Tables 2.2, 2.3 and 2.4.

As noted earlier, evaluating the performance of Phase I control charts requires a different paradigm than evaluating the performance of Phase II charts. In the latter case, the performance is usually compared by looking at characteristics associated with their run-length distributions such as, for example, the *FAR* and the *ARL*. In contrast, the *FAP* (the probability of at least one signal) is used to evaluate and compare the performance of Phase I charts.

We compare both the IC and the OOC performance of Phase I control charts. The IC performance indicates how robust the chart is with respect to the specified nominal *FAP* value; the nonparametric charts are expected to be IC robust (because they are distribution-free) but it is of interest to see what the attained *FAP* values are and how far off they might be from the nominal values. On the other hand, the OOC comparison involves comparing the probabilities of alarm (at least one signal) under some 'out-of-control condition' when the charts have roughly the same nominal *FAP* (i.e. the same IC performance). The chart with the highest probability of at least one signal under the OOC condition is favored. Since our proposed Shewhart-type Phase I chart is for monitoring the location of a continuous process distribution, it is appropriate to compare its performance with the parametric Phase I $\overline{X}$ chart for the mean (see e.g. Champ and Jones (2004)) assuming a normal distribution. Their Phase I $\overline{X}$ chart is designed using $\hat{\mu}_0 = \overline{\overline{X}}$ where $\overline{\overline{X}}$ is the grand mean, i.e. $\overline{\overline{X}} = \frac{1}{mn}\sum_{i=1}^{m}\sum_{j=1}^{n} X_{ij}$, $\hat{\sigma}_{0,V} = \frac{1}{c_4}\left[\frac{1}{m}\sum_{i=1}^{m} S_i^2\right]^{\frac{1}{2}}$ where c_4 is an unbiasing constant and S_i^2 is the i^{th} sample variance. It follows that (see Equation (1.1)), $UCL\ /\ LCL = \hat{\mu}_0 \pm k_V\, \hat{\sigma}_{0,V}/\sqrt{n}$ where tables for the charting constant k_V are provided by Champ and Jones (2004) for m = 4(1)10,15, n = 3(1)10 and for a FAP_0 of 0.10, 0.05 and 0.01, respectively. In some cases, a more extensive set of tables was used by Nelson et al. (2005) to calculate the charting constant. Four process distributions are considered in the simulation study:

i. The standard Normal distribution ($N(0,1)$),

ii. the Student's t-distribution with four degrees of freedom ($t(4)$) which is symmetric but with heavier tails than the normal,

iii. the Gamma distribution ($GAM(1,1)$) which is positively skewed, and

iv. the Uniform distribution ($U(-1,1)$) which is symmetric but with a different kurtosis and lighter tails than the normal distribution.

Note that, wherever necessary, the distributions in the study have been shifted and scaled such that the mean / median equals 0 and the standard deviation equals 1, so that the results are easily comparable across the distributions. The details for these steps are shown in Appendix 1B.

We compare the nonparametric Phase I median chart to the parametric Phase I $\overline{X}$ chart (see Champ and Jones (2004)). However, although Champ and Jones (2004) proposed the Phase I $\overline{X}$ chart and examined methods for obtaining probability limits for the $\overline{X}$ chart when the process mean and standard deviation are estimated, they did not investigate the OOC performance of the chart. Thus, in order find out what types of shifts have been considered in the literature regarding Phase I control charting applications, we turned to Jones-Farmer et al. (2009) who proposed a nonparametric Phase I control chart based on standardized subgroup mean-ranks and Coelho et al. (2013) who gave a performance comparison between the three nonparametric charts, i.e. the Phase I median chart proposed here, the Phase I $\overline{X}$ chart proposed by Champ and Jones (2004) and the Phase I mean-rank chart proposed by Jones-Farmer et al. (2009). Both Jones-Farmer et al. (2009) and Coelho et al. (2013) considered shifts of size γ in units of population standard deviations and, without loss of generality, this shift was added to the first subgroup. Following what has been done in the literature and in order to have a fair comparison between the proposed chart and the Phase I $\overline{X}$ chart, a shift of γ = -2(0.25)2 in terms of population standard deviations is added to the first subgroup in this chapter.

Simulation is used to compare the performance of the Phase I median chart to that of the Phase I $\overline{X}$ chart using SAS® v9.3 (see Appendix 2B). Simulation was used, because Champ and Jones (2004) only provided tables for the charting constant k_V for n = 3(1)10, and here larger values of n are considered. The steps in the simulation study were:

Step 1: Generate m samples each of size n from one of the four distributions.

Step 2: Add a shift (γ = -2(0.25)2) in terms of population standard deviations to the first subgroup.

Step 3: Find the control limits: For the median chart use Tables 2.2, 2.3 and 2.4 for FAP_0 of 0.01, 0.05 and 0.10, respectively. For the $\overline{X}$ chart the tables by Champ and Jones (2004) and Nelson et al. (2005) can be used for certain values of m and n, however, for values of m and n not provided by the tables the SAS® program in Appendix 2B should be used to obtain the charting constant k_V.

Step 4: Calculate the charting statistics for both the Phase I median and Phase I $\overline{X}$ chart, respectively. For each of the charts we then check if at least one of the respective charting statistics plots on or outside the control limits, in which case a counter is incremented.

Steps 1 to 4 are repeated 100 000 times and the proportion of times there is at least one signal is obtained by dividing the final value of the counter by 100 000. This proportion estimates the alarm probability of a chart and this estimate is referred to as the empirical (or the simulated) alarm probability of the corresponding Phase I control chart. Note that 100 000 simulations are used to achieve an acceptable error rate.

It is important to note that, in the simulation study, for the Phase I median chart the control limits were selected from Tables 2.2, 2.3 and 2.4 for FAP_0 = 0.01, 0.05 and 0.10, respectively. These control limits were kept fixed at all times when running the simulations for the IC robustness study. However, for the OOC simulations the process is stopped and a counter is incremented. In practice, at this point, one would stop the manufacturing process, search for assignable causes and take corrective action.

In-control robustness

Since the proposed Phase I chart is nonparametric, the statistical properties of the chart, such as the *FAP*, should remain the same for all continuous distributions. The empirical (simulated) *FAP* values of the Phase I median chart and that of the Phase I $\overline{X}$ chart are shown in Tables 2.9, 2.10 and

2.11 and are displayed in Figure 2.9 for various combinations of (m,n) under all four the distributions where the FAP_0 equals of 0.01, 0.05 and 0.10, respectively.

Table 2.9. Empirical *FAP* values of the Phase I median control chart and the Phase I $\overline{X}$ control chart for $FAP_0 = 0.01$

		(4,15)	**(4,20)**	**(4,24)**	**(7,15)**	**(7,20)**	**(7,24)**	**(10,15)**	**(10,20)**	**(10,24)**
Median	***N*(0,1)**	0.0080	0.0021	0.0073	0.0031	0.0083	0.0047	0.0057	0.0021	0.0080
	***t*(4)**	0.0079	0.0022	0.0070	0.0026	0.0082	0.0045	0.0055	0.0022	0.0087
	***GAM*(1,1)**	0.0083	0.0021	0.0069	0.0030	0.0080	0.0045	0.0051	0.0021	0.0091
	***U*(-1,1)**	0.0086	0.0024	0.0070	0.0029	0.0084	0.0047	0.0054	0.0022	0.0088
$\overline{X}$	***N*(0,1)**	0.0097	0.0100	0.0102	0.0097	0.0098	0.0101	0.0099	0.0100	0.0099
	***t*(4)**	0.0092	0.0094	0.0097	0.0116	0.0118	0.0120	0.0143	0.0144	0.0139
	***GAM*(1,1)**	0.0110	0.0104	0.0107	0.0166	0.0162	0.0151	0.0208	0.0185	0.0179
	***U*(-1,1)**	0.0102	0.0100	0.0105	0.0099	0.0099	0.0100	0.0101	0.0098	0.0103

Table 2.10. Empirical *FAP* values of the Phase I median control chart and the Phase I $\overline{X}$ control chart for $FAP_0 = 0.05$

		(4,15)	**(4,20)**	**(4,24)**	**(7,15)**	**(7,20)**	**(7,24)**	**(10,15)**	**(10,20)**	**(10,24)**
Median	***N*(0,1)**	0.0081	0.0146	0.0328	0.0272	0.0460	0.0234	0.0471	0.0157	0.0414
	***t*(4)**	0.0085	0.0148	0.0323	0.0269	0.0450	0.0240	0.0469	0.0154	0.0419
	***GAM*(1,1)**	0.0080	0.0147	0.0327	0.0270	0.0453	0.0236	0.0465	0.0144	0.0419
	***U*(-1,1)**	0.0083	0.0144	0.0320	0.0273	0.0450	0.0232	0.0480	0.0154	0.0415
$\overline{X}$	***N*(0,1)**	0.0083	0.0146	0.0326	0.0272	0.0450	0.0235	0.0472	0.0152	0.0415
	***t*(4)**	0.0500	0.0498	0.0499	0.0493	0.0505	0.0487	0.0506	0.0497	0.0508
	***GAM*(1,1)**	0.0478	0.0499	0.0496	0.0543	0.0543	0.0544	0.0635	0.0627	0.0607
	***U*(-1,1)**	0.0479	0.0493	0.0505	0.0569	0.0549	0.0550	0.0676	0.0641	0.0614

Table 2.11. Empirical *FAP* values of the Phase I median control chart and the Phase I $\overline{X}$ control chart for $FAP_0 = 0.10$

		(4,15)	**(4,20)**	**(4,24)**	**(7,15)**	**(7,20)**	**(7,24)**	**(10,15)**	**(10,20)**	**(10,24)**
Median	***N*(0,1)**	0.0561	0.0677	0.0329	0.0261	0.0444	0.0903	0.0483	0.0775	0.0415
	***t*(4)**	0.0560	0.0673	0.0315	0.0274	0.0447	0.0907	0.0480	0.0777	0.0419
	***GAM*(1,1)**	0.0557	0.0671	0.0338	0.0271	0.0453	0.0917	0.0477	0.0764	0.0419
	***U*(-1,1)**	0.0558	0.0669	0.0329	0.0271	0.0455	0.0900	0.0468	0.0751	0.0403
$\overline{X}$	***N*(0,1)**	0.0563	0.0681	0.0326	0.0272	0.0450	0.0913	0.0472	0.0769	0.0415
	***t*(4)**	0.1002	0.1001	0.1000	0.1009	0.0996	0.1020	0.1005	0.1019	0.1002
	***GAM*(1,1)**	0.0976	0.0993	0.0984	0.1090	0.1083	0.1081	0.1226	0.1191	0.1163
	***U*(-1,1)**	0.0952	0.0966	0.0956	0.1059	0.1043	0.1030	0.1175	0.1141	0.1108

To make the comparisons easier, the empirical *FAP* values of the median chart are shown as vertical bars whereas the *FAP* values of the $\overline{X}$ chart are depicted by line graphs in Figures 2.9a, b and c for $FAP_0 = 0.01$, 0.05 and 0.10, respectively.

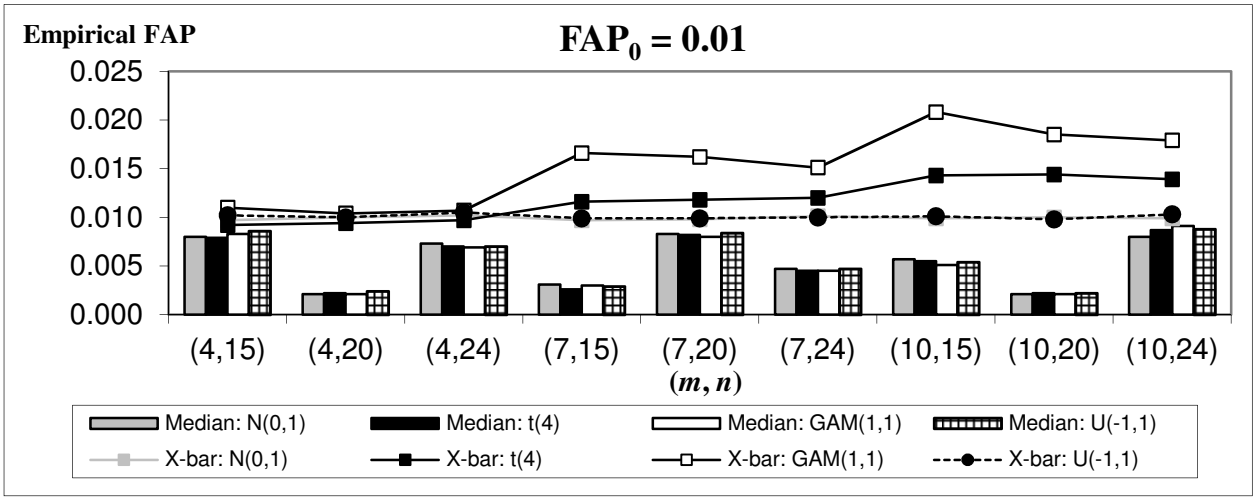

Figure 2.9a. Simulated / Empirical *FAP* values of the Phase I median control chart and the Phase I $\overline{X}$ control chart for $FAP_0 = 0.01$

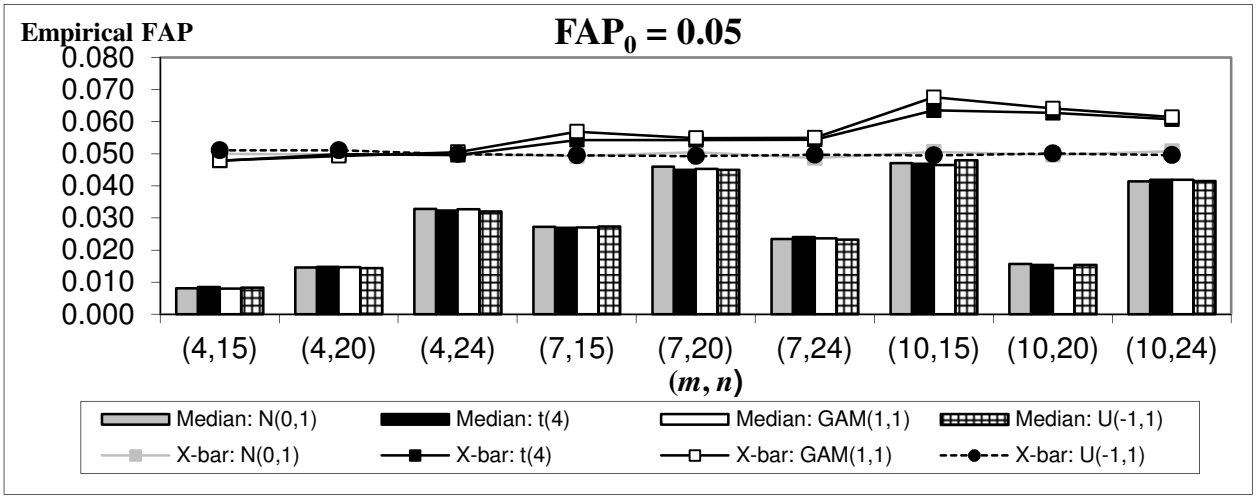

Figure 2.9b. Simulated / Empirical *FAP* values of the Phase I median control chart and the Phase I $\overline{X}$ control chart for $FAP_0 = 0.05$

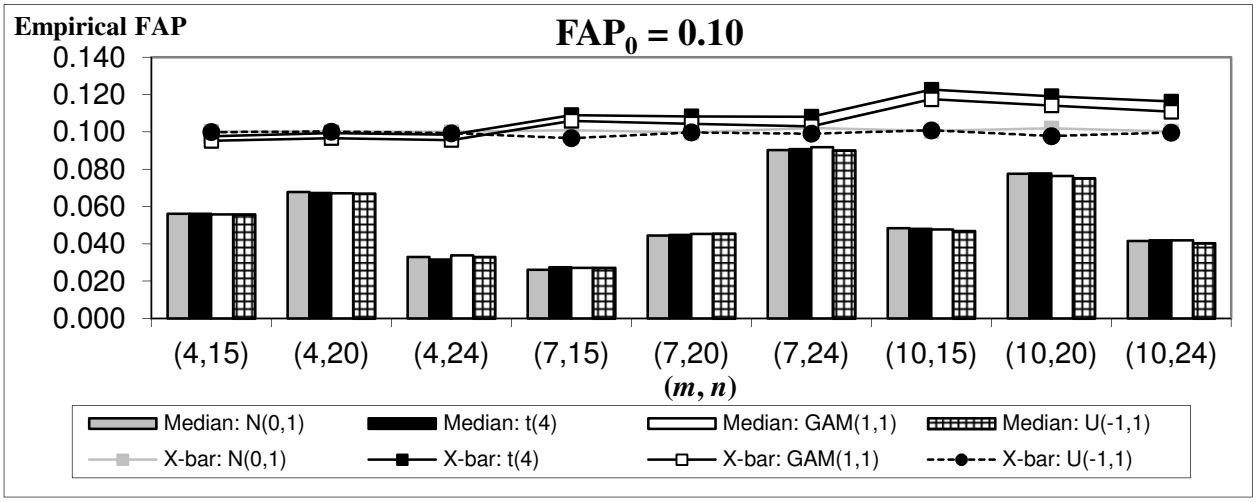

Figure 2.9c. Simulated / Empirical *FAP* values of the Phase I median control chart and the Phase I $\overline{X}$ control chart for $FAP_0 = 0.10$

From Tables 2.9, 2.10 and 2.11 and Figure 2.9 several observations can be made:

i. The empirical *FAP* values of the Phase I median chart are nearly indistinguishable from the attained *FAP* values (calculated theoretically) for all four the distributions. For example, for $m = 10$, $n = 15$ and $FAP_0 = 0.10$, the attained *FAP* equals 0.0472 as shown in Table 2.4, while the empirical *FAP* values for the $N(0,1)$, $t(4)$, $GAM(1,1)$ and $U(-1,1)$ distributions equal 0.0483, 0.0480, 0.0477 and 0.0468, respectively, as shown in Table 2.11. This provides convincing evidence that the proposed distribution-free Phase I median chart is IC robust i.e. the empirical *FAP* values remain the same for all continuous distributions for a given m and n.

ii. By design, the Phase I median chart is conservative in that its attained *FAP* values are less than or equal to the FAP_0 values.

iii. The Phase I $\overline{X}$ chart does not have the IC robustness property of the nonparametric Phase I median chart. Although for the normal and the uniform distributions the Phase I $\overline{X}$ chart has empirical *FAP* values 'very near' the FAP_0 values, for the heavy-tailed $t(4)$ and the skewed $GAM(1,1)$ distributions, the $\overline{X}$ chart has empirical *FAP* values much higher than the FAP_0 value. The non-robustness of the $\overline{X}$ chart is known in the literature for Phase II applications (see e.g. Chakraborti et al. (2004)) but this study confirms it for the Phase I case as well. What seems to be a more serious problem is that there appears to be an upward trend developing in the empirical *FAP* values of the $\overline{X}$ chart for the *t* and Gamma distributions as m, the number of subgroups, increases from 4. This is bound to be problematic in practice. Hence the empirical alarm probabilities for the $\overline{X}$ chart do not allow a meaningful performance comparison in the OOC (discussed next) case for the *t* and the Gamma distributions. These results are shown here because the $\overline{X}$ chart is the most familiar control chart in practice.

Out-of-control chart performance

Tables 2.12, 2.13 and 2.14 contain the empirical alarm probabilities of the Phase I median and the Phase I $\overline{X}$ chart for shifts $\gamma = -2(0.25)2$ when the FAP_0 equals 0.01, 0.05 and 0.10, respectively, and (m, n) = (4, 20) and (10, 24), respectively. These are displayed in Figures 2.10, 2.11 and 2.12 for FAP_0 = 0.01, 0.05 and 0.10, respectively. Note that these particular values of (m, n) are shown for illustration purposes; other combinations were considered and the results were comparable. Recall that the empirical *FAP* values of the Phase I $\overline{X}$ chart for the *t* and the Gamma distributions were found to be not close to the FAP_0 values when the process is IC so that it is not practically meaningful to compare the OOC performance of the Phase I $\overline{X}$ chart with that of the median chart. However, this was still done for reference purposes by recalculating the $\overline{X}$ chart constants (i.e. k_V) so that the empirical *FAP* values were close to the FAP_0 values.

Table 2.12a. Empirical alarm probabilities of the Phase I median and the Phase I $\overline{X}$ charts with m = 4, n = 20 and FAP_0 = 0.01

	Phase I median chart				**Phase I $\overline{X}$ chart**			
	***N*(0,1)**	***t*(4)**	***GAM*(1,1)**	***U*(-1,1)**	***N*(0,1)**	***t*(4)**	***GAM*(1,1)**	***U*(-1,1)**
γ	**(a, b) = (3,17)**				**k_v = 3.000**	**k_v = 3.100**	**k_v = 3.125**	**k_v = 3.130**
-2.00	0.9845	0.9954	0.9224	0.9523	1.0000	0.9991	0.9996	1.0000
-1.75	0.9344	0.9841	0.8486	0.7999	0.9998	0.9953	0.9970	0.9999
-1.50	0.8026	0.9423	0.7196	0.5421	0.9951	0.9846	0.9848	0.9981
-1.25	0.5710	0.8255	0.5379	0.2991	0.9511	0.9417	0.9339	0.9578
-1.00	0.3070	0.5824	0.3278	0.1204	0.7692	0.7925	0.7790	0.7742
-0.75	0.1139	0.2700	0.1469	0.0423	0.4250	0.4809	0.4781	0.4249
-0.50	0.0280	0.0691	0.0437	0.0110	0.1379	0.1677	0.1634	0.1375
-0.25	0.0057	0.0094	0.0075	0.0034	0.0278	0.0314	0.0293	0.0272
0.00	0.0021	0.0022	0.0021	0.0025	0.0094	0.0100	0.0101	0.0098
0.25	0.0060	0.0091	0.0104	0.0035	0.0270	0.0313	0.0318	0.0273
0.50	0.0282	0.0686	0.1222	0.0120	0.1378	0.1676	0.1531	0.1366
0.75	0.1137	0.2724	0.5540	0.0413	0.4261	0.4806	0.4510	0.4239
1.00	0.3030	0.5763	0.9203	0.1214	0.7685	0.7923	0.7706	0.7741
1.25	0.5726	0.8241	0.9948	0.2891	0.9531	0.9419	0.9418	0.9579
1.50	0.8049	0.9421	0.9999	0.5411	0.9955	0.9856	0.9908	0.9971
1.75	0.9359	0.9842	1.0000	0.8006	0.9997	0.9954	0.9991	0.9999
2.00	0.9849	0.9956	1.0000	0.9524	1.0000	0.9981	1.0000	1.0000

Table 2.12b. Empirical alarm probabilities of the Phase I median and the Phase I $\overline{X}$ charts with $m = 10$, $n = 24$ and $FAP_0 = 0.01$

	Phase I median chart				**Phase I $\overline{X}$ chart**			
	***N*(0,1)**	***t*(4)**	***GAM*(1,1)**	***U*(-1,1)**	***N*(0,1)**	***t*(4)**	***GAM*(1,1)**	***U*(-1,1)**
γ	$(a, b) = (4,20)$				$k_v =$ **3.300**	$k_v =$ **3.440**	$k_v =$ **3.555**	$k_v =$ **3.310**
-2.00	0.9993	0.9997	0.9735	1.0000	1.0000	0.9992	1.0000	1.0000
-1.75	0.9934	0.9982	0.9336	0.9909	1.0000	0.9920	0.9998	1.0000
-1.50	0.9579	0.9897	0.8515	0.8830	0.9999	0.9976	0.9974	0.9998
-1.25	0.8276	0.9492	0.7012	0.5962	0.9941	0.9825	0.9754	0.9945
-1.00	0.5604	0.8063	0.4878	0.2865	0.9116	0.8823	0.8561	0.9096
-0.75	0.2498	0.4916	0.2477	0.1014	0.5828	0.5428	0.5185	0.5746
-0.50	0.0683	0.1597	0.0832	0.0314	0.1816	0.1547	0.1261	0.1726
-0.25	0.0154	0.0247	0.0199	0.0118	0.0286	0.0230	0.0164	0.0261
0.00	0.0089	0.0085	0.0090	0.0084	0.0111	0.0103	0.0108	0.0100
0.25	0.0157	0.0243	0.0289	0.0116	0.0288	0.0234	0.0228	0.0260
0.50	0.0690	0.1572	0.3560	0.0306	0.1816	0.1563	0.1294	0.1725
0.75	0.2500	0.4963	0.9679	0.1011	0.5869	0.5464	0.4709	0.5731
1.00	0.5611	0.8080	1.0000	0.2877	0.9111	0.8833	0.8565	0.9099
1.25	0.8307	0.9506	1.0000	0.5967	0.9940	0.9835	0.9883	0.9944
1.50	0.9593	0.9899	1.0000	0.8836	0.9999	0.9971	0.9998	0.9999
1.75	0.9935	0.9979	1.0000	0.9909	1.0000	0.9993	1.0000	1.0000
2.00	0.9996	0.9997	1.0000	0.9999	1.0000	0.9997	1.0000	1.0000

Table 2.13a. Empirical alarm probabilities of the Phase I median and the Phase I $\overline{X}$ charts with $m = 4$, $n = 20$ and $FAP_0 = 0.05$

	Phase I median chart				**Phase I $\overline{X}$ chart**			
	***N*(0,1)**	***t*(4)**	***GAM*(1,1)**	***U*(-1,1)**	***N*(0,1)**	***t*(4)**	***GAM*(1,1)**	***U*(-1,1)**
γ	$(a, b) = (4,16)$				$k_v =$ **2.530**	$k_v =$ **2.540**	$k_v =$ **2.542**	$k_v =$ **2.540**
-2.00	0.9978	0.9995	0.9813	0.9891	1.0000	1.0000	1.0000	1.0000
-1.75	0.9861	0.9978	0.9525	0.9293	1.0000	0.9983	0.9993	1.0000
-1.50	0.9353	0.9874	0.8878	0.7710	0.9993	0.9948	0.9955	0.9998
-1.25	0.7945	0.9440	0.7658	0.5238	0.9886	0.9799	0.9763	0.9913
-1.00	0.5472	0.7988	0.5688	0.2911	0.9110	0.9073	0.8986	0.9157
-0.75	0.2778	0.5066	0.3368	0.1352	0.6668	0.6900	0.6867	0.6640
-0.50	0.1012	0.1971	0.1379	0.0522	0.3217	0.3467	0.3542	0.3180
-0.25	0.0304	0.0433	0.0370	0.0218	0.1024	0.1072	0.1084	0.1011
0.00	0.0146	0.0144	0.0149	0.0144	0.0477	0.0471	0.0463	0.0489
0.25	0.0303	0.0438	0.0465	0.0219	0.1024	0.1073	0.1042	0.1010
0.50	0.1015	0.1946	0.2791	0.0523	0.3196	0.3469	0.3290	0.3178
0.75	0.2792	0.5064	0.7487	0.1353	0.6679	0.6892	0.6707	0.6639
1.00	0.5454	0.8030	0.9711	0.2922	0.9115	0.9074	0.9082	0.9158
1.25	0.7943	0.9433	0.9989	0.5249	0.9897	0.9797	0.9852	0.9911
1.50	0.9369	0.9877	1.0000	0.7704	0.9994	0.9947	0.9987	0.9997
1.75	0.9860	0.9978	1.0000	0.9294	1.0000	0.9982	0.9990	1.0000
2.00	0.9979	0.9997	1.0000	0.9892	1.0000	1.0000	1.0000	1.0000

Table 2.13b. Empirical alarm probabilities of the Phase I median and the Phase I $\overline{X}$ charts with $m = 10$, $n = 24$ and $FAP_0 = 0.05$

	Phase I median chart				**Phase I $\overline{X}$ chart**			
	***N*(0,1)**	***t*(4)**	***GAM*(1,1)**	***U*(-1,1)**	***N*(0,1)**	***t*(4)**	***GAM*(1,1)**	***U*(-1,1)**
γ	$(a, b) = (5,19)$				$k_v = 2.800$	$k_v = 2.893$	$k_v = 2.915$	$k_v = 2.800$
-2.00	0.9999	1.0000	0.9941	1.0000	1.0000	0.9999	1.0000	1.0000
-1.75	0.9991	0.9998	0.9809	0.9980	1.0000	0.9998	1.0000	1.0000
-1.50	0.9897	0.9982	0.9444	0.9600	1.0000	0.9991	0.9994	1.0000
-1.25	0.9355	0.9868	0.8582	0.7876	0.9987	0.9947	0.9935	0.9989
-1.00	0.7595	0.9234	0.6928	0.4950	0.9678	0.9545	0.9468	0.9705
-0.75	0.4493	0.7026	0.4485	0.2401	0.7666	0.7486	0.7462	0.7651
-0.50	0.1794	0.3266	0.2062	0.1004	0.3541	0.3357	0.3478	0.3532
-0.25	0.0641	0.0859	0.0728	0.0517	0.1009	0.0919	0.0872	0.0990
0.00	0.0413	0.0408	0.0409	0.0415	0.0524	0.0501	0.0491	0.0508
0.25	0.0630	0.0870	0.0954	0.0518	0.0990	0.0919	0.0865	0.0990
0.50	0.1788	0.3271	0.5618	0.1005	0.3557	0.3371	0.3011	0.3532
0.75	0.4511	0.7048	0.9896	0.2402	0.7664	0.7463	0.7146	0.7650
1.00	0.7601	0.9254	1.0000	0.4945	0.9696	0.9570	0.9632	0.9704
1.25	0.9356	0.9875	1.0000	0.7877	0.9989	0.9945	0.9989	0.9988
1.50	0.9897	0.9985	1.0000	0.9595	1.0000	0.9992	1.0000	1.0000
1.75	0.9993	0.9997	1.0000	0.9982	1.0000	0.9996	1.0000	1.0000
2.00	0.9999	1.0000	1.0000	1.0000	1.0000	0.9999	1.0000	1.0000

Table 2.14a. Empirical alarm probabilities of the Phase I median and the Phase I $\overline{X}$ charts with $m = 4$, $n = 20$ and $FAP_0 = 0.10$

	Phase I median chart				**Phase I $\overline{X}$ chart**			
	***N*(0,1)**	***t*(4)**	***GAM*(1,1)**	***U*(-1,1)**	***N*(0,1)**	***t*(4)**	***GAM*(1,1)**	***U*(-1,1)**
γ	$(a, b) = (5,15)$				$k_v = 2.230$	$k_v = 2.240$	$k_v = 2.240$	$k_v = 2.240$
-2.00	0.9998	1.0000	0.9966	0.9985	1.0000	1.0000	1.0000	1.0000
-1.75	0.9979	0.9999	0.9890	0.9806	1.0000	1.0000	0.9996	1.0000
-1.50	0.9846	0.9982	0.9667	0.9111	0.9999	0.9968	0.9982	1.0000
-1.25	0.9258	0.9869	0.9081	0.7531	0.9954	0.9886	0.9873	0.9967
-1.00	0.7730	0.9289	0.7843	0.5284	0.9530	0.9440	0.9371	0.9556
-0.75	0.5155	0.7375	0.5704	0.3150	0.7730	0.7883	0.7802	0.7735
-0.50	0.2611	0.4078	0.3202	0.1665	0.4462	0.4720	0.4796	0.4450
-0.25	0.1093	0.1449	0.1308	0.0904	0.1814	0.1892	0.1915	0.1801
0.00	0.0694	0.0680	0.0668	0.0683	0.0982	0.0980	0.0926	0.0986
0.25	0.1122	0.1449	0.1525	0.0905	0.1798	0.1892	0.1813	0.1800
0.50	0.2616	0.4094	0.5023	0.1667	0.4485	0.4718	0.4556	0.4454
0.75	0.5167	0.7384	0.8856	0.3148	0.7726	0.7884	0.7773	0.7736
1.00	0.7702	0.9296	0.9919	0.5285	0.9535	0.9441	0.9507	0.9555
1.25	0.9256	0.9868	0.9998	0.7530	0.9955	0.9887	0.9933	0.9966
1.50	0.9843	0.9982	1.0000	0.9110	0.9999	0.9969	0.9996	1.0000
1.75	0.9976	0.9999	1.0000	0.9807	1.0000	1.0000	1.0000	1.0000
2.00	0.9998	1.0000	1.0000	0.9981	1.0000	1.0000	1.0000	1.0000

Table 2.14b. Empirical alarm probabilities of the Phase I median and the Phase I $\overline{X}$ charts with $m = 10$, $n = 24$ and $FAP_0 = 0.10$

	Phase I median chart				**Phase I $\overline{X}$ chart**			
	***N*(0,1)**	***t*(4)**	***GAM*(1,1)**	***U*(-1,1)**	***N*(0,1)**	***t*(4)**	***GAM*(1,1)**	***U*(-1,1)**
γ	$(a, b) = (5,19)$				$k_v =$ **2.550**	$k_v =$ **2.620**	$k_v =$ **2.600**	$k_v =$ **2.550**
-2.00	0.9999	1.0000	0.9941	1.0000	1.0000	1.0000	1.0000	1.0000
-1.75	0.9991	0.9998	0.9809	0.9980	1.0000	0.9997	1.0000	1.0000
-1.50	0.9897	0.9982	0.9444	0.9596	1.0000	0.9994	0.9998	1.0000
-1.25	0.9355	0.9868	0.8582	0.7878	0.9995	0.9972	0.9964	0.9994
-1.00	0.7595	0.9234	0.6928	0.4946	0.9831	0.9752	0.9710	0.9840
-0.75	0.4493	0.7026	0.4485	0.2400	0.8408	0.8295	0.8329	0.8415
-0.50	0.1794	0.3266	0.2062	0.1004	0.4698	0.4579	0.4912	0.4684
-0.25	0.0641	0.0859	0.0728	0.0518	0.1740	0.1652	0.1720	0.1717
0.00	0.0413	0.0408	0.0409	0.0415	0.1070	0.1025	0.1023	0.1026
0.25	0.0630	0.0870	0.0954	0.0518	0.1748	0.1652	0.1610	0.1718
0.50	0.1788	0.3271	0.5618	0.1005	0.4717	0.4579	0.4350	0.4684
0.75	0.4511	0.7048	0.9896	0.2402	0.8422	0.8296	0.8226	0.8415
1.00	0.7601	0.9254	1.0000	0.4945	0.9836	0.9753	0.9852	0.9841
1.25	0.9356	0.9875	1.0000	0.7877	0.9996	0.9971	0.9998	0.9996
1.50	0.9897	0.9985	1.0000	0.9595	1.0000	0.9993	1.0000	1.0000
1.75	0.9993	0.9997	1.0000	0.9982	1.0000	0.9998	1.0000	1.0000
2.00	0.9999	1.0000	1.0000	1.0000	1.0000	1.0000	1.0000	1.0000

From Tables 2.12, 2.13 and 2.14 and Figures 2.10, 2.11 and 2.12 we see that:

i. For symmetric distributions such as the normal, the *t* and the uniform, the direction of the shift doesn't seem to affect the detection capability of the charts (since symmetrically placed control limits were used), whereas for the right-skewed Gamma distribution, it does.

ii. The $\overline{X}$ chart has higher alarm probabilities than the median chart for the normal and the uniform distributions. This is not surprising, since the assumed distribution underlying the former chart is normal and the uniform distribution is comparable to the normal, but with different kurtosis.

iii. For the *t*(4) distribution the median chart compares very favourably to the $\overline{X}$ chart.

iv. For the *GAM*(1,1) distribution, the median chart performs better than the $\overline{X}$ chart for positive shifts of approximately 0.5 and greater, while the opposite is true for positive shifts smaller than 0.5 and for negative shifts.

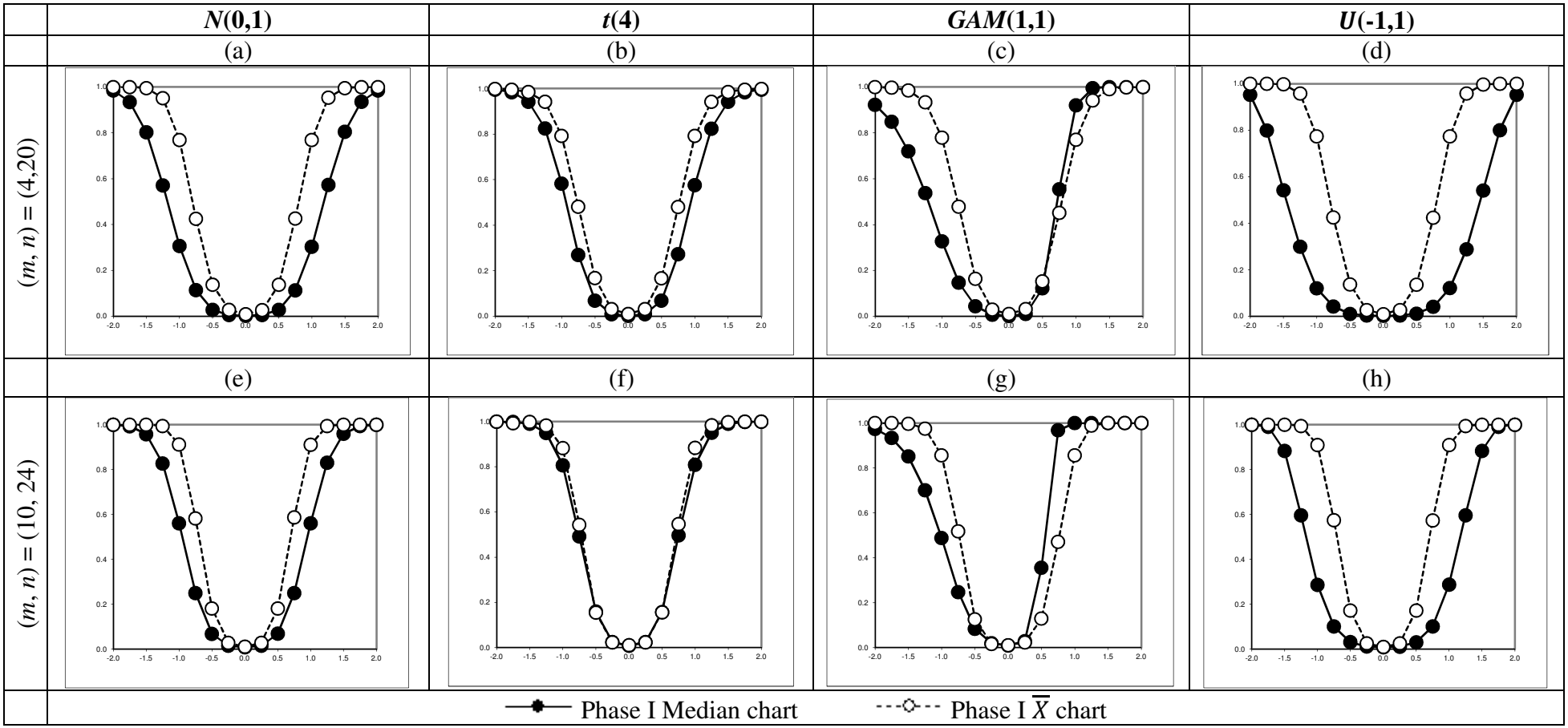

Figure 2.10[vii]. Out-of-control empirical alarm probabilities of the Phase I median and the Phase I $\overline{X}$ charts for the $N(0,1)$, $t(4)$, $U(-1,1)$ and $GAM(1,1)$ distributions for $FAP_0 = 0.01$

[vii] The horizontal and vertical axes in Figure 2.10 represent the shift ($\gamma = -2(0.025)2$) and the empirical alarm probability, respectively.

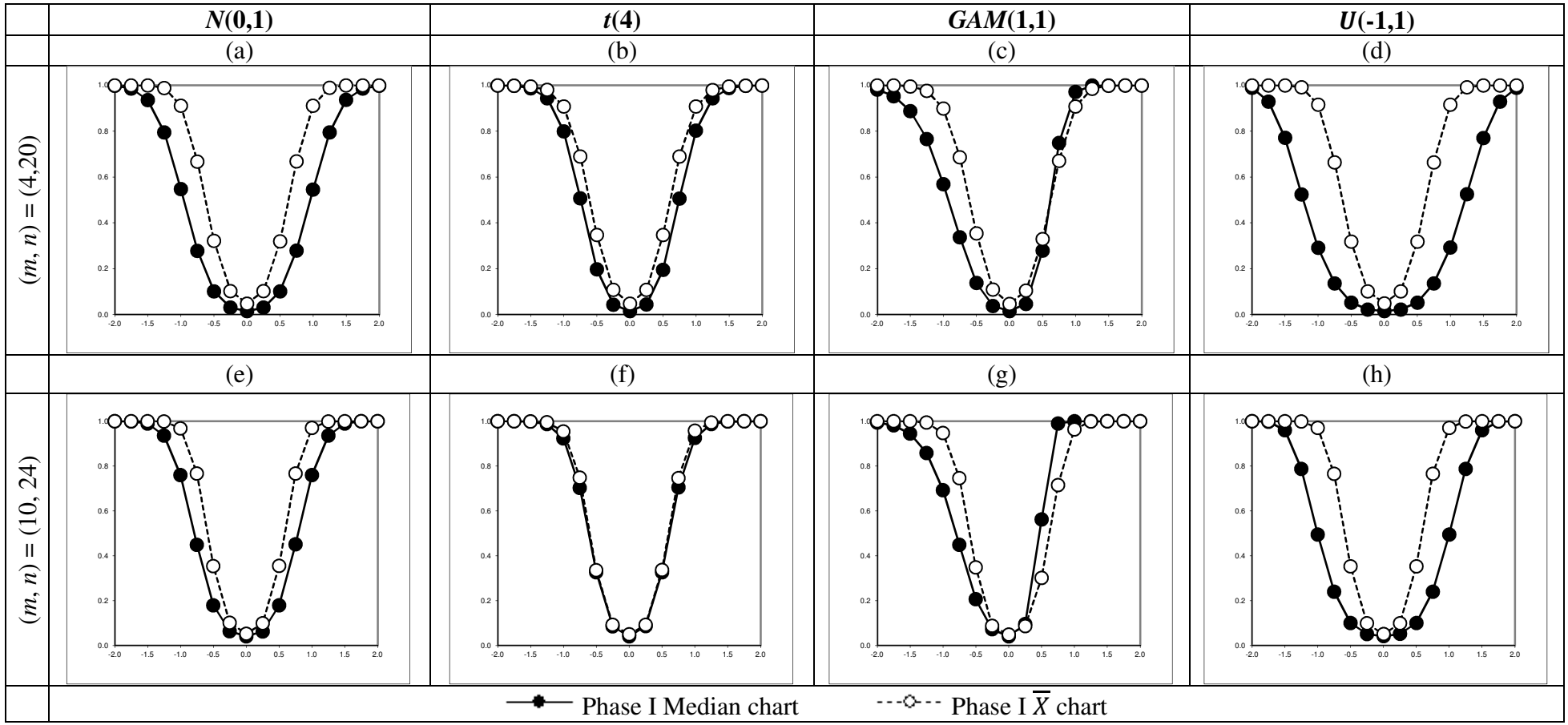

Figure 2.11[viii]. Out-of-control empirical alarm probabilities of the Phase I median and the Phase I $\overline{X}$ charts for the $N(0,1)$, $t(4)$, $U(-1,1)$ and $GAM(1,1)$ distributions for $FAP_0 = 0.05$

[viii] The horizontal and vertical axes in Figure 2.11 represent the shift ($\gamma = -2(0.025)2$) and the empirical alarm probability, respectively.

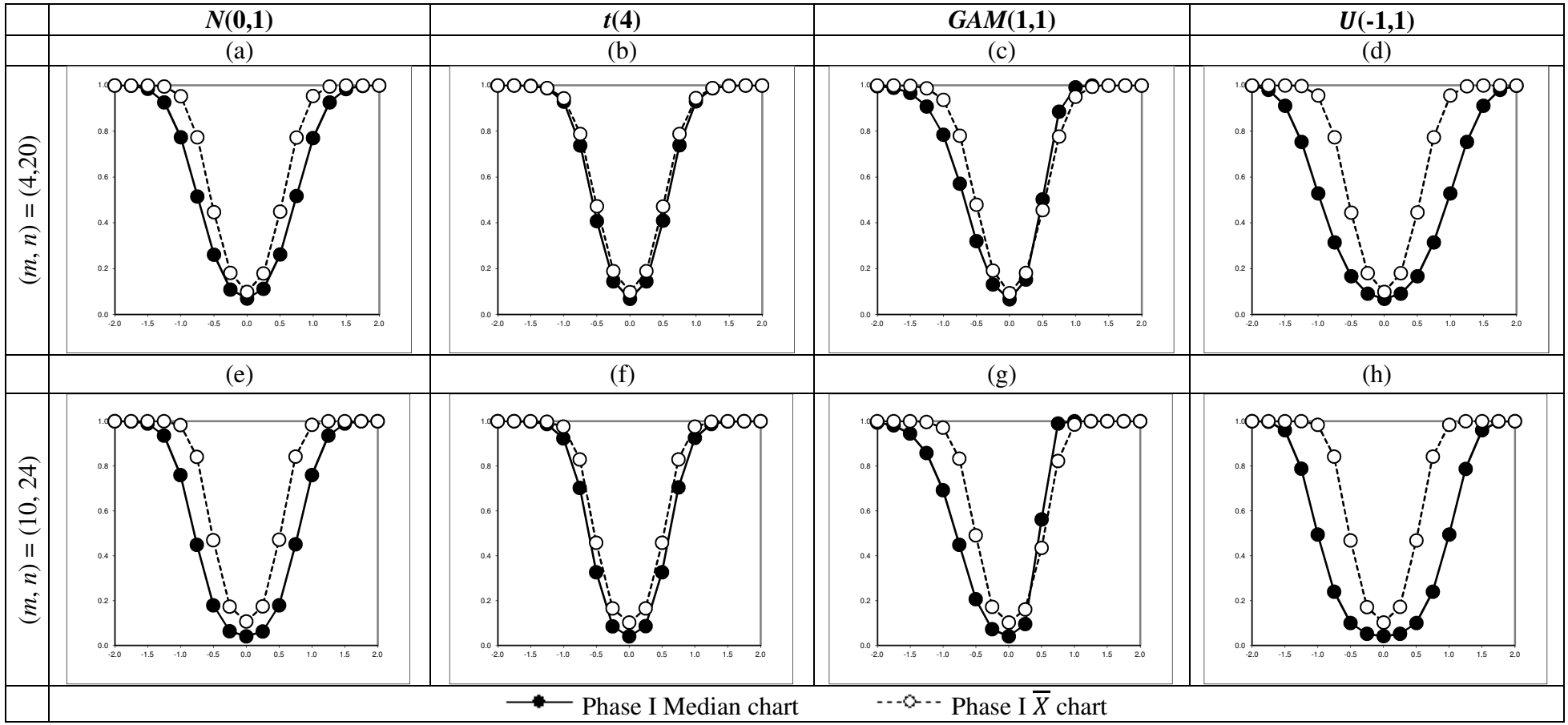

Figure 2.12[ix]. Out-of-control empirical alarm probabilities of the Phase I median and the Phase I $\overline{X}$ charts for the $N(0,1)$, $t(4)$, $U(-1,1)$ and $GAM(1,1)$ distributions for $FAP_0 = 0.10$

[ix] The horizontal and vertical axes in Figure 2.12 represent the shift ($\gamma = -2(0.025)2$) and the empirical alarm probability, respectively.

Our overall conclusion is that in Phase I applications, the proposed nonparametric median chart is IC robust and outperforms the $\overline{X}$ chart in some situations. However, even though the $\overline{X}$ chart seems to have slightly better OOC performance, we emphasize that its performance is unstable and non-robust in the IC case for the *t* and the Gamma distributions.

Unequal variances

The median chart is primarily designed to detect a location shift under equal scales (or variances). Thus the effect of unequal variances on the IC robustness and OOC performance may be of interest. For the IC case, we examined the robustness of the median chart for constant mean but unequal variances, in terms of the simulated empirical *FAP* values for all four distributions, when the first group variance increases from 1.0 to 2.0 in increments of 0.25. The simulated / empirical *FAP* values are given in Tables 2.15, 2.16 and 2.17 and are displayed in Figures 2.13 to 2.16, for various combinations of (m, n) when the FAP_0 equals 0.01, 0.05 and 0.10, respectively.

Table 2.15. Empirical *FAP* values of the Phase I median chart with unequal variances

$FAP_0 = 0.01$		**(*m*,*n*)**								
Dist	**Var**	**(4,15)**	**(4,20)**	**(4,24)**	**(7,15)**	**(7,20)**	**(7,24)**	**(10,15)**	**(10,20)**	**(10,24)**
***N*(0,1)**	**1.00**	0.0080	0.0021	0.0073	0.0031	0.0083	0.0047	0.0057	0.0021	0.0080
	1.25	0.0080	0.0021	0.0074	0.0029	0.0084	0.0043	0.0054	0.0019	0.0087
	1.50	0.0081	0.0020	0.0073	0.0033	0.0084	0.0047	0.0054	0.0022	0.0089
	1.75	0.0088	0.0021	0.0070	0.0028	0.0082	0.0049	0.0051	0.0019	0.0089
	2.00	0.0086	0.0024	0.0075	0.0027	0.0082	0.0043	0.0058	0.0019	0.0089
***t*(4)**	**1.00**	0.0079	0.0022	0.0070	0.0026	0.0082	0.0045	0.0055	0.0022	0.0087
	1.25	0.0087	0.0020	0.0066	0.0028	0.0081	0.0048	0.0054	0.0020	0.0094
	1.50	0.0084	0.0022	0.0071	0.0030	0.0083	0.0044	0.0052	0.0021	0.0084
	1.75	0.0086	0.0020	0.0072	0.0029	0.0082	0.0045	0.0053	0.0020	0.0083
	2.00	0.0083	0.0022	0.0069	0.0029	0.0080	0.0047	0.0057	0.0020	0.0092
***GAM*(1,1)**	**1.00**	0.0083	0.0021	0.0069	0.0030	0.0080	0.0045	0.0051	0.0021	0.0091
	1.25	0.0085	0.0022	0.0070	0.0028	0.0078	0.0043	0.0052	0.0018	0.0085
	1.50	0.0082	0.0023	0.0072	0.0028	0.0087	0.0045	0.0054	0.0018	0.0088
	1.75	0.0089	0.0024	0.0073	0.0029	0.0083	0.0048	0.0051	0.0022	0.0087
	2.00	0.0086	0.0022	0.0076	0.0029	0.0088	0.0045	0.0054	0.0023	0.0086
***U*(-1,1)**	**1.00**	0.0086	0.0024	0.0070	0.0029	0.0084	0.0047	0.0054	0.0022	0.0088
	1.25	0.0086	0.0024	0.0074	0.0029	0.0080	0.0048	0.0053	0.0021	0.0084
	1.50	0.0082	0.0020	0.0071	0.0032	0.0080	0.0046	0.0054	0.0018	0.0087
	1.75	0.0085	0.0024	0.0073	0.0028	0.0079	0.0045	0.0056	0.0021	0.0088
	2.00	0.0085	0.0021	0.0072	0.0029	0.0080	0.0050	0.0052	0.0020	0.0087

Table 2.16. Empirical *FAP* values of the Phase I median chart with unequal variances

$FAP_0 = 0.05$		(m,n)								
Dist	**Var**	**(4,15)**	**(4,20)**	**(4,24)**	**(7,15)**	**(7,20)**	**(7,24)**	**(10,15)**	**(10,20)**	**(10,24)**
***N*(0,1)**	**1.00**	0.0081	0.0146	0.0328	0.0272	0.0460	0.0234	0.0471	0.0157	0.0414
	1.25	0.0081	0.0145	0.0332	0.0280	0.0453	0.0236	0.0480	0.0153	0.0412
	1.50	0.0081	0.0146	0.0326	0.0267	0.0458	0.0237	0.0460	0.0155	0.0421
	1.75	0.0088	0.0149	0.0327	0.0269	0.0452	0.0240	0.0472	0.0149	0.0419
	2.00	0.0086	0.0151	0.0327	0.0278	0.0466	0.0233	0.0475	0.0151	0.0403
***t*(4)**	**1.00**	0.0085	0.0148	0.0323	0.0269	0.0450	0.0240	0.0469	0.0154	0.0419
	1.25	0.0084	0.0146	0.0331	0.0282	0.0454	0.0229	0.0481	0.0157	0.0419
	1.50	0.0084	0.0145	0.0334	0.0277	0.0451	0.0245	0.0470	0.0153	0.0407
	1.75	0.0086	0.0153	0.0332	0.0276	0.0460	0.0243	0.0478	0.0156	0.0426
	2.00	0.0083	0.0142	0.0339	0.0270	0.0456	0.0230	0.0475	0.0151	0.0412
***GAM*(1,1)**	**1.00**	0.0080	0.0147	0.0327	0.0270	0.0453	0.0236	0.0465	0.0144	0.0419
	1.25	0.0083	0.0145	0.0339	0.0284	0.0450	0.0239	0.0467	0.0151	0.0424
	1.50	0.0082	0.0149	0.0329	0.0269	0.0449	0.0243	0.0472	0.0157	0.0412
	1.75	0.0089	0.0149	0.0334	0.0275	0.0444	0.0234	0.0466	0.0154	0.0412
	2.00	0.0086	0.0154	0.0342	0.0287	0.0453	0.0245	0.0476	0.0154	0.0416
***U*(-1,1)**	**1.00**	0.0083	0.0144	0.0320	0.0273	0.0450	0.0232	0.0480	0.0154	0.0415
	1.25	0.0090	0.0146	0.0324	0.0278	0.0458	0.0243	0.0475	0.0155	0.0415
	1.50	0.0082	0.0144	0.0330	0.0280	0.0450	0.0244	0.0469	0.0153	0.0420
	1.75	0.0085	0.0151	0.0338	0.0279	0.0453	0.0234	0.0491	0.0156	0.0411
	2.00	0.0085	0.0156	0.0336	0.0280	0.0454	0.0233	0.0468	0.0153	0.0418

Table 2.17. Empirical *FAP* values of the Phase I median chart with unequal variances

$FAP_0 = 0.10$		(m,n)								
Dist	**Var**	**(4,15)**	**(4,20)**	**(4,24)**	**(7,15)**	**(7,20)**	**(7,24)**	**(10,15)**	**(10,20)**	**(10,24)**
***N*(0,1)**	**1.00**	0.0561	0.0677	0.0329	0.0261	0.0444	0.0903	0.0483	0.0775	0.0415
	1.25	0.0564	0.0690	0.0325	0.0272	0.0447	0.0916	0.0473	0.0768	0.0408
	1.50	0.0572	0.0695	0.0326	0.0267	0.0458	0.0927	0.0460	0.0784	0.0421
	1.75	0.0552	0.0687	0.0327	0.0269	0.0452	0.0899	0.0472	0.0765	0.0419
	2.00	0.0575	0.0707	0.0327	0.0278	0.0466	0.0933	0.0475	0.0764	0.0403
***t*(4)**	**1.00**	0.0560	0.0673	0.0315	0.0274	0.0447	0.0907	0.0480	0.0777	0.0419
	1.25	0.0575	0.0680	0.0323	0.0270	0.0444	0.0929	0.0475	0.0766	0.0416
	1.50	0.0575	0.0683	0.0334	0.0277	0.0451	0.0917	0.0470	0.0786	0.0407
	1.75	0.0583	0.0697	0.0332	0.0276	0.0460	0.0921	0.0478	0.0766	0.0426
	2.00	0.0583	0.0684	0.0339	0.0270	0.0456	0.0921	0.0475	0.0783	0.0412
***GAM*(1,1)**	**1.00**	0.0557	0.0671	0.0338	0.0271	0.0453	0.0917	0.0477	0.0764	0.0419
	1.25	0.0565	0.0693	0.0327	0.0278	0.0444	0.0921	0.0482	0.0770	0.0423
	1.50	0.0576	0.0681	0.0329	0.0269	0.0449	0.0909	0.0472	0.0776	0.0412
	1.75	0.0572	0.0687	0.0334	0.0275	0.0444	0.0913	0.0466	0.0772	0.0412
	2.00	0.0579	0.0715	0.0342	0.0287	0.0453	0.0928	0.0476	0.0787	0.0416
***U*(-1,1)**	**1.00**	0.0558	0.0669	0.0329	0.0271	0.0455	0.0900	0.0468	0.0751	0.0403
	1.25	0.0575	0.0695	0.0339	0.0267	0.0446	0.0926	0.0467	0.0764	0.0415
	1.50	0.0575	0.0690	0.0330	0.0280	0.0450	0.0890	0.0469	0.0765	0.0420
	1.75	0.0577	0.0704	0.0338	0.0279	0.0453	0.0924	0.0491	0.0773	0.0411
	2.00	0.0583	0.0704	0.0336	0.0280	0.0454	0.0919	0.0468	0.0766	0.0418

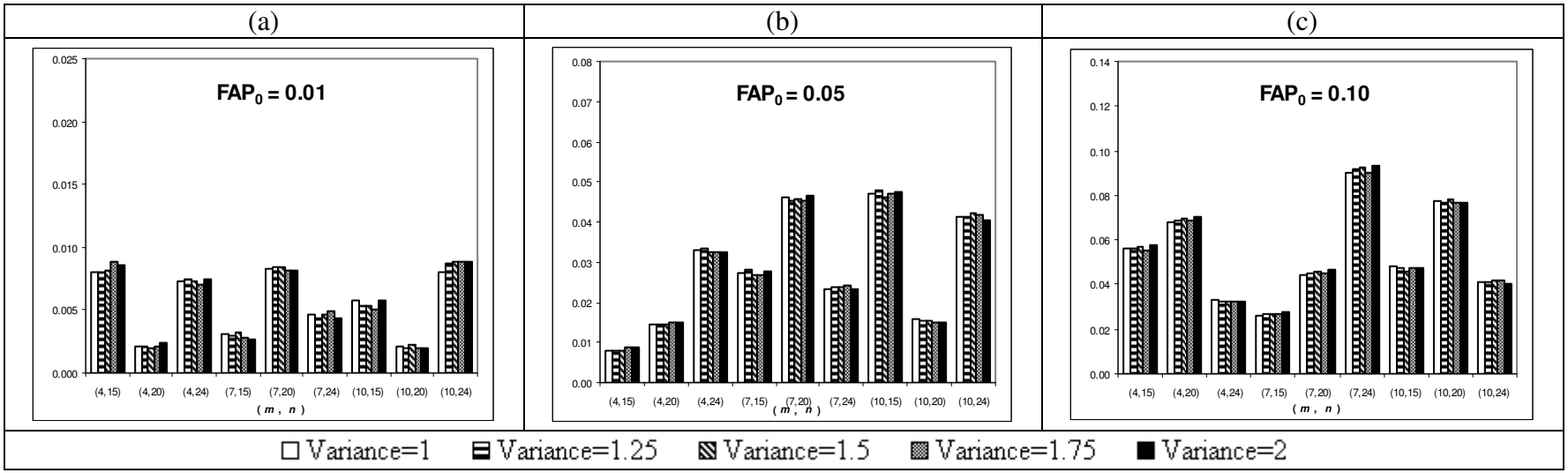

Figure 2.13. Simulated / Empirical *FAP* values of the Phase I median chart for the $N(0,1)$ distribution with unequal variances

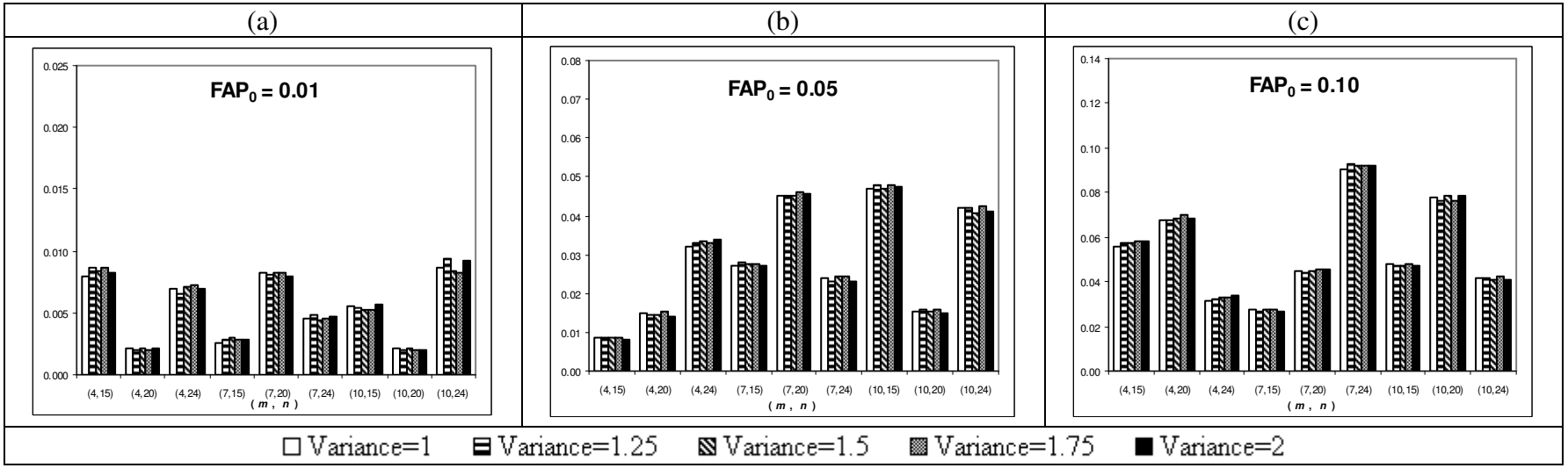

Figure 2.14. Simulated / Empirical *FAP* values of the Phase I median chart for the $t(4)$ distribution with unequal variances

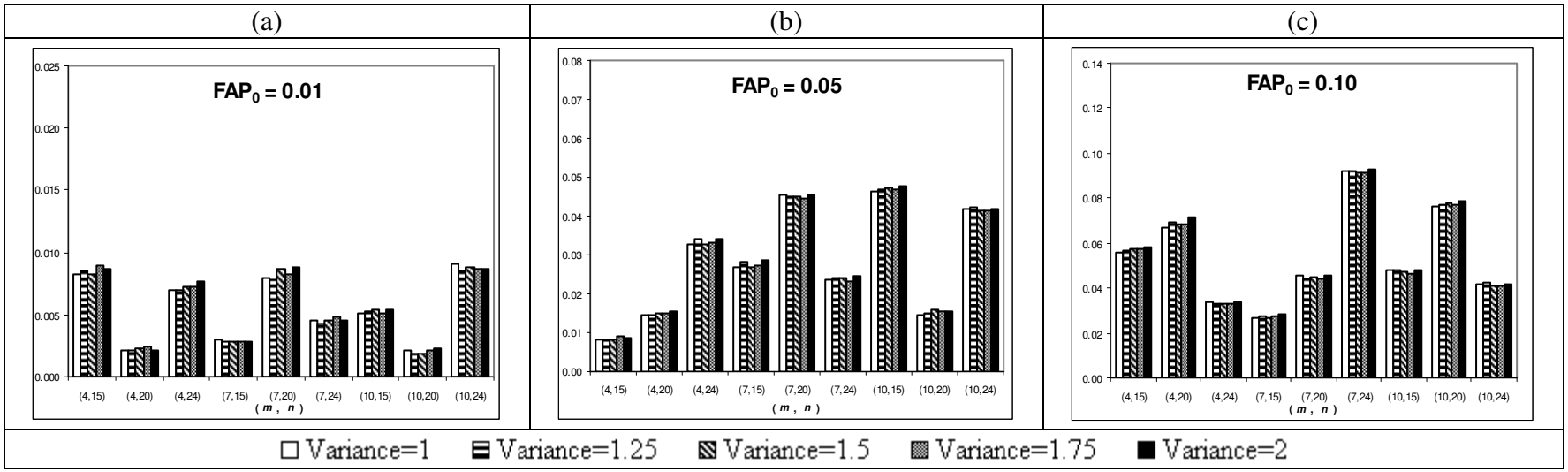

Figure 2.15. Simulated / Empirical *FAP* values of the Phase I median chart for the *GAM*(1,1) distribution with unequal variances

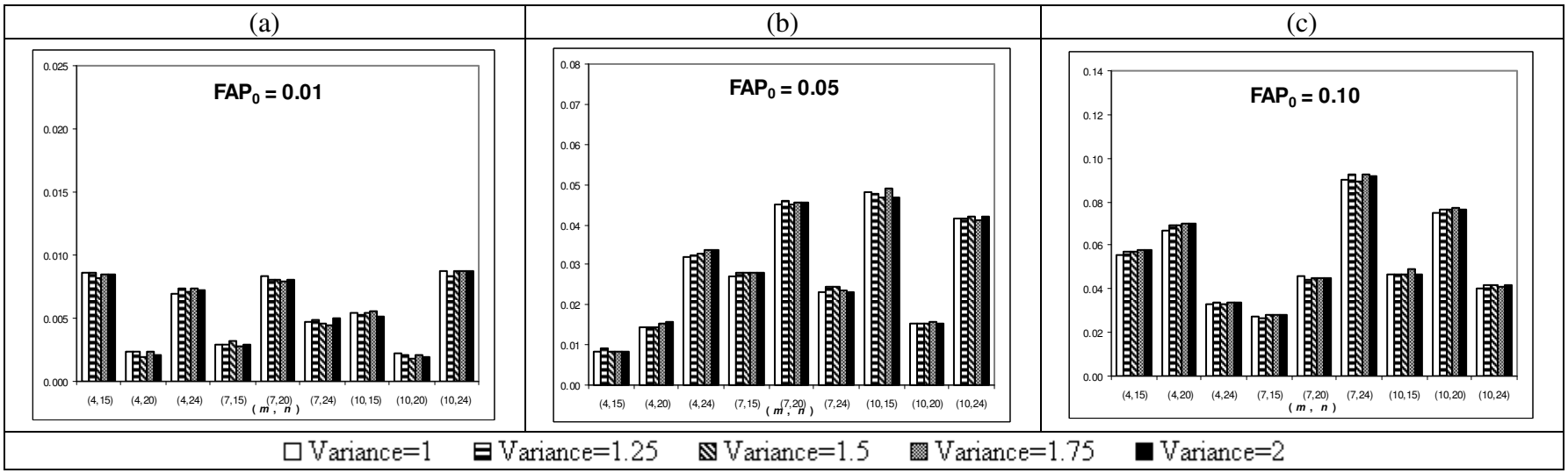

Figure 2.16. Simulated / Empirical *FAP* values of the Phase I median chart for the *U*(-1,1) distribution with unequal variances

From Figures 2.13 to 2.16, it is seen that in each case the empirical *FAP* values are nearly indistinguishable and remain at or below the FAP_0 value as the variance increases from 1.0 to 2.0 in increments of 0.25. For example, consider Figure 2.13a for $m = 4$, $n = 15$, $FAP_0 = 0.01$, where the data are from a normal distribution. The five bars represent the five empirical *FAP* values, when the variance increases from 1.0 to 2.0 in increments of 0.25, with the first bar representing the IC case (variance = 1.0). The simulated *FAP* values are seen to remain close to the IC value for increased variance. In other words the empirical *FAP* values do not change significantly from the IC value as the variance increases. The same conclusion appears to hold for other combinations of (m,n) and FAP_0 values and across all four distributions (in each case the heights of the five bars are close to each other). This suggests that the Phase I median chart maintains its IC robustness when the variances are not highly unequal.

The OOC results for the Phase I median chart are shown in Tables 2.18, 2.19 and 2.20 and are displayed in Figures 2.17, 2.18 and 2.19, respectively for FAP_0 = 0.01, 0.05 and 0.10, respectively, for the $N(0,1)$ distribution.

Table 2.18. Empirical alarm probabilities of the Phase I median chart for the $N(0,1)$ distribution for $m = 4$, $n = 20$ and $FAP_0 = 0.01$

Mean / Variance	0.25	0.75	1.00	1.25	1.75
-0.75	0.5343	0.1668	0.1139	0.0844	0.0538
-0.50	0.1582	0.0412	0.0280	0.0218	0.0152
-0.25	0.0200	0.0067	0.0057	0.0051	0.0038
0.00	0.0030	0.0021	0.0021	0.0021	0.0021
0.25	0.0200	0.0067	0.0060	0.0054	0.0038
0.50	0.1582	0.0412	0.0282	0.0218	0.0152
0.75	0.5343	0.1668	0.1137	0.0836	0.0538

Table 2.19. Empirical alarm probabilities of the Phase I median chart for the $N(0,1)$ distribution for $m = 4$, $n = 20$ and $FAP_0 = 0.05$

Mean / Variance	0.25	0.75	1.00	1.25	1.75
-0.75	0.7550	0.3676	0.2817	0.2291	0.1607
-0.50	0.3393	0.1294	0.0996	0.0838	0.0649
-0.25	0.0704	0.0317	0.0267	0.0280	0.0239
0.00	0.0201	0.0148	0.0142	0.0156	0.0165
0.25	0.0720	0.0347	0.0295	0.0258	0.0244
0.50	0.3416	0.1336	0.1030	0.0879	0.0657
0.75	0.7508	0.3733	0.2770	0.2304	0.1592

Table 2.20. Empirical alarm probabilities of the Phase I median chart for the $N(0,1)$ distribution for $m = 4$, $n = 20$ and $FAP_0 = 0.10$

Mean / Variance	0.25	0.75	1.00	1.25	1.75
-0.75	0.8953	0.6088	0.5057	0.4458	0.3569
-0.50	0.5827	0.3195	0.2588	0.2281	0.1867
-0.25	0.1927	0.1192	0.1076	0.0996	0.0923
0.00	0.0768	0.0694	0.0707	0.0689	0.0706
0.25	0.1904	0.1264	0.1128	0.1067	0.0996
0.50	0.5739	0.3010	0.2588	0.2281	0.1895
0.75	0.9010	0.6074	0.5192	0.4527	0.3677

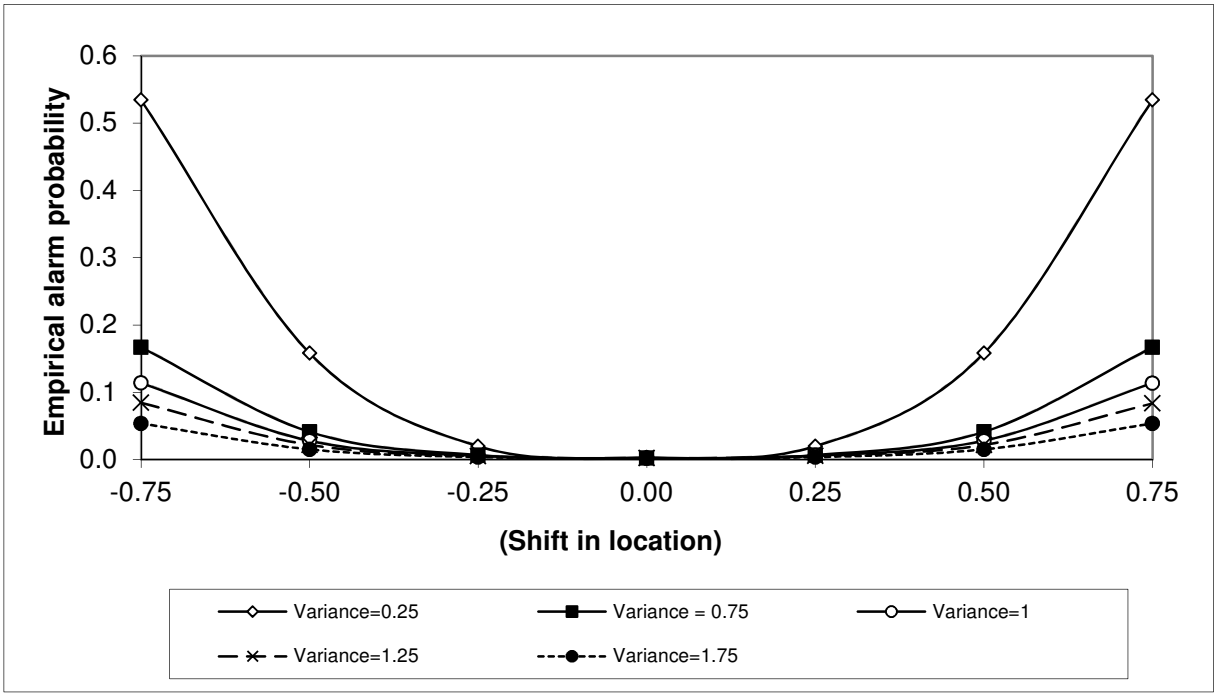

Figure 2.17. Out-of-control empirical alarm probabilities of the Phase I median chart for the $N(0,1)$ distribution for $m = 4$, $n = 20$ and $FAP_0 = 0.01$

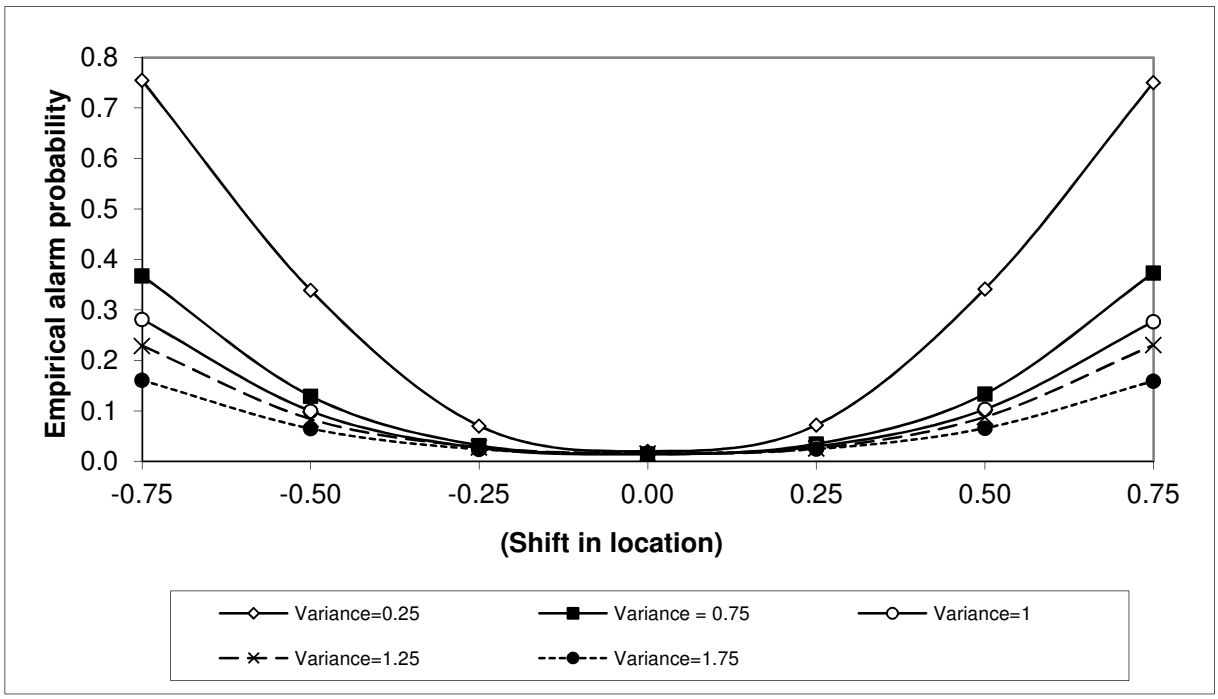

Figure 2.18. Out-of-control empirical alarm probabilities of the Phase I median chart for the $N(0,1)$ distribution for $m = 4$, $n = 20$ and $FAP_0 = 0.05$

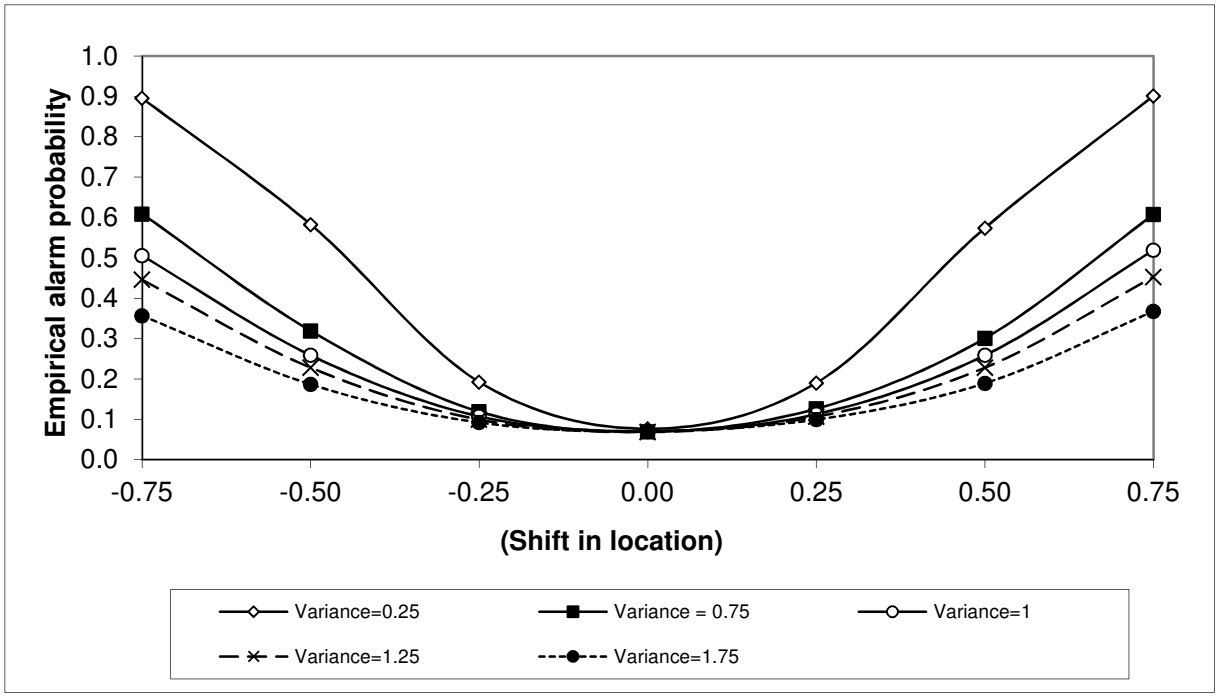

Figure 2.19. Out-of-control empirical alarm probabilities of the Phase I median chart for the $N(0,1)$ distribution for $m = 4$, $n = 20$ and $FAP_0 = 0.10$

From Figures 2.17, 2.18 and 2.19 it is seen that the empirical alarm probabilities are affected by unequal variances; the probabilities increase as the variance decreases from 1.75 to 0.25. This is not surprising, as we would expect the detection capability of a chart to be better for smaller variance. On the other hand, however, when the variance increases, the alarm probabilities decrease. This is also not surprising since the median chart was established for the location model. Finally,

similar conclusions appear to hold (not shown here) for other shifts in mean and variance, other combinations of (m, n) and FAP_0 values and across all four distributions.

2.2.6. Phase I control charts for other percentiles

We have focussed mainly on monitoring the median from the point of view of robustness and the simplicity of the resulting charts. However, we can consider using some other (say the p^{th}) percentile of a process if that's more suitable in a particular (practical) situation. In that case the IC joint probability distribution of the charting statistics is similar to Equation (2.4) but it is not symmetrically distributed. Thus for a two-sided control chart one would need to simultaneously solve for a and b from

$$FAP_0 \geq 1 - \binom{N}{u_T}^{-1} \sum_{u_1=a+1}^{b-1} \sum_{u_2=a+1}^{b-1} \cdots \sum_{u_{m-1}=a+1}^{b-1} \binom{n}{u_1}\binom{n}{u_2}\cdots\binom{n}{u_T - u_1 - \cdots - u_{m-1}}, \qquad (2.21)$$

where u_i now denotes the observed value of U_i, the number of observations in the i^{th} sample that are less than the p^{th} percentile in the combined sample, and $u_T = Np$. For a unique solution (i.e. a unique pair of (a, b)-values) we could use an equal tailed approach which means that we would find the charting constants a and b such that the probability for at least one charting statistic to plot on or above the *UCL* is equal to the probability for at least one charting statistic to plot on or below the *LCL* when the process is IC. We do not pursue this any further here.

2.3. Concluding remarks

Nonparametric Shewhart-type Phase I control charts can make a valuable contribution to the overall SPC regime. These charts require minimal assumptions and are especially useful in applications where not much is known about the underlying process distribution, which is typically the situation in Phase I. The proposed median chart requires simple calculations and can be easily implemented on the production floor. The median chart is IC robust but the $\overline{X}$ chart is not. For symmetric and heavy-tailed distributions the median chart compares favourably to the $\overline{X}$ chart in terms of OOC performance, whereas for right-skewed distributions (such as the Gamma), the median chart performs better for positive shifts of size approximately 0.5 and greater. It may be noted that the median chart can be applied when the only information available is whether or not an observation is less (or higher) than the pooled median of the combined Phase I samples. This can be

an advantage in some situations. In terms of future research one could consider a Phase I control chart for monitoring scale and simultaneously monitoring the location and scale of a process. However, in this essay the focus is on monitoring the location of a process and discussion on monitoring scale and / or simultaneously monitoring location and scale is better postponed for the future.

2.4. Appendices

2.4.1. Appendix 2A: Some mathematical results

Proof of Equation (2.4)

Combinatoric proofs of this result can be found in Lehmann (1975; page 381). Here sketches of two different outlines of the proof are given below.

Suppose there is a finite population of N items and each item belongs to one of m exclusive and exhaustive categories. Suppose that n_i of the N items belong to the i^{th} category ($n_1 + n_2 + \cdots + n_m = N$) and that a random sample of size u_T is drawn from the population. If $U_1, U_2, \ldots, U_m$ denote the random variables of items in the sample belonging to categories 1,2,…,m (so that $u_1 + u_2 + \cdots + u_m = u_T$), the joint distribution of the U's is the multiple (multivariate) hypergeometric distribution given by

$$P(U_1 = u_1, U_2 = u_2, \ldots, U_m = u_m) = \frac{\binom{n_1}{u_1} \cdots \binom{n_m}{u_m}}{\binom{N}{u_T}}. \qquad \text{(A.1)}$$

To see this, note that in the IC case, N observations are drawn from the same continuous distribution; $\binom{n_i}{u_i}$ is the number of ways of selecting u_i items from the n_i items of category i and $\binom{N}{u_T}$ is the number of ways of selecting u_T items out of the total sample of N items.

Lehmann (1975) gives an alternative expression for this distribution

$$P(U_1 = u_1, U_2 = u_2, \dots, U_m = u_m) = \frac{\binom{u_T}{u_1, \dots, u_m}\binom{N - u_T}{n_1 - u_1, \dots, n_m - u_m}}{\binom{N}{n_1, \dots, n_m}} \tag{A.2}$$

which can be seen to be equal to (A.1) after algebraic simplification, noting that

$$\binom{N}{u_1, \dots, u_m} = \frac{N!}{u_1! \dots u_m!}.$$

As explained in Lehmann (1975), to see a second way in which this distribution arises, note that each of the N items belongs to one of two exclusive and exhaustive categories A (for us less than M) and B (greater than or equal to M), with u_T belonging to A and $N - u_T$ belonging to B. Samples of sizes $n_1, n_2, \dots, n_m$ $(\sum_{i=1}^{m} n_i = N)$ are drawn, and U_i denotes the number of items in the i^{th} sample belonging to category A. Then the distribution of the U's is again given by (A.2). This is seen by noting that the denominator of (A.2) gives the total number of possible assignments of the N items to the m samples, while the numerator provides the number of such assignments for which $U_1 = u_1, U_2 = u_2, \dots, U_m = u_m$.

2.4.2. Appendix 2B: SAS® and R® programs

2.4.2.1. SAS® program to compute the false alarm and the OOC alarm probabilities for the Phase I $\overline{X}$ control chart for a shift in location when the underlying process distribution is normal

```
proc iml;
do k = 2 to 4 by 0.0001;
keep=0;
z=100000;          * Number of simulations;
m=15;              * Number of samples;
n=5;               * Number of observations;
gamma=0;           * Shift;
do sim = 1 to z;
* Generating observations from the Normal distribution;
obs = j(m,n,.);
call randgen(obs, "normal", 0,1);
obs[1,1:n]= obs[1,1:n]+gamma;
xbar_vector=j(m,1,.);
do i = 1 to m;
      xbar_vector[i,]=sum(obs[i,1:n])/n;
end;
diff_sq=j(m,n,.);
do i = 1 to m;
      do j = 1 to n;
      diff_sq[i,j]=(obs[i,j]-xbar_vector[i,])#(obs[i,j]-xbar_vector[i,]);
      end;
end;
variance_vector=j(m,1,.);
do i = 1 to m;
      variance_vector[i,]=sum(diff_sq[i,1:n])/(n-1);
end;
xbarbar=sum(obs)/(m*n);
UCL = xbarbar + k * sqrt((sum(variance_vector))/m) * sqrt((m-1)/(m*n));
LCL = xbarbar - k * sqrt((sum(variance_vector))/m) * sqrt((m-1)/(m*n));
signal_ucl=j(m,1,.);
signal_lcl=j(m,1,.);
do i = 1 to m;
      if xbar_vector[i,]>=ucl then signal_ucl[i,]=1; else signal_ucl[i,]=0;
      if xbar_vector[i,]<=lcl then signal_lcl[i,]=1; else signal_lcl[i,]=0;
end;
* Signalling event;
signal=signal_ucl + signal_lcl;
at_least=sum(signal);
if at_least>0 then FAP_sum=1; else FAP_sum=0;
      keep=keep//FAP_sum;
end;
FAP=(sum(keep))/z;
print       lcl [label='Lower control limit'],
            ucl [label='Upper control limit'],
            k [label = 'Constant in control limits'],
            m [label = 'Number of samples'],
            n [label = 'Number of observations in each sample'],
            gamma [label='shift'],
            FAP [format = .4];
end;
```

2.4.2.2. SAS® program to compute the false alarm and the OOC alarm probabilities for the Phase I median control chart for a shift in location when the underlying process distribution is normal

```
proc iml;
z=100000;          * Number of simulations;
m=10;              * Number of samples;
n=15;              * Number of observations;
lcl=1;             * Lower control limit;
ucl=n-lcl;         * Upper control limit;
gamma=2;           * Shift;
* Generating observations from the N(mu, var) distribution;
mu = 0;
var = 1;
obs = j(m*z,n,.);
call randgen(obs, "normal", mu, sqrt(var));
do i = 1 to z;
      obs[(i*m-(m-1)),]=obs[(i*m-(m-1)),]+gamma;
end;
do i = 1 to z;
      vector=0;
      apart=j(m,n,.);
      apart[1:m,] = obs[(i*m-(m-1)):(i*m),];
      do o = 1 to n;
            vector=vector//apart[,o];
      end;
      vector = vector [2:nrow(vector),];
      me=median(vector);
      do k = 1 to nrow(apart);
            do l = 1 to ncol(apart);
                  if apart[k,l]<me then apart[k,l]=1; else apart[k,l]=0;
            end;
      end;
      sum=apart[,+];
      signal_ucl=j(nrow(sum),1,.);
      signal_lcl=j(nrow(sum),1,.);
      do p = 1 to nrow(signal_ucl);
            if sum[p,] >= ucl then signal_ucl[p,]=1; else signal_ucl[p,]=0;
            if sum[p,] <= lcl then signal_lcl[p,]=1; else signal_lcl[p,]=0;
      end;
      signal=signal_lcl||signal_ucl;
      at_least=sum(signal);
      if at_least>0 then FAP_sum=1; else FAP_sum=0;
      keep=keep//FAP_sum;
end;
total=sum(keep);
FAP=total/z;
print       lcl [label='Lower control limit'],
            ucl [label='Upper control limit'],
            m [label='Number of samples'],
            n [label='Number of observations in each sample'],
            gamma [label='shift'],
            FAP [format=.4];
```

2.4.2.3. Necessary amendment to the SAS® programs in Sections 2.4.2.1 and 2.4.2.2 when the underlying process distribution is non-normal

Distribution	Necessary amendments

t(4)	`* Degrees of freedom for the t-distribution;`
	`df=4;`
	`obs1 = j(m*z,n,.);`
	`call randgen(obs1,"t",df);`
	`*Shift and scale such that mean = 0 and stdev = 1;`
	`obs=(1/sqrt(2))# obs1;`

GAM(1,1)	`* Parameter for the Gamma(1,1) distribution;`
	`kappa=1;`
	`obs1 = j(m*z,n,.);`
	`*Shift and scale such that mean = 0 and stdev = 1;`
	`call randgen(obs1, "gamma", kappa );`
	`obs = obs1 - j(m*z,n,1);`

U(-1,1)	`call randgen(obs, "uniform");`
	`*Shift and scale such that mean = 0 and stdev = 1;`
	`obs=(2#obs-j(m*z,n,1))#sqrt(3);`

2.4.2.4. SAS® program for to compute the false alarm and the OOC alarm probabilities for the Phase I median control chart for a shift in spread when the underlying process distribution is non-normal

```
proc iml;
z=100000;          * Number of simulations;
m=4;               * Number of samples;
n=20;              * Number of observations;
lcl=3;             * Lower control limit;
ucl=n-lcl;         * Upper control limit;
do sim = 1 to z;
ic_obs = j(m-1,n,.);
ooc_obs = j(1,n,.);
* Generating observations from the IC N(0,1) distribution;
call randgen(ic_obs, "normal", 0, 1);
* Generating observations from the OOC Normal distribution;
call randgen(ooc_obs, "normal", 1.75, sqrt(0.25));
* Combining the 2 so that the 1st sample (row) is OOC and the rest are IC;
obs=ooc_obs//ic_obs;
* Calculating the grand median of the all the N=mn observations;
begin=0;
do o = 1 to n;
      begin=begin//obs[,o];
end;
begin=begin[2:nrow(begin)];
me=median(begin);
* Checking whether observation is smaller than or greater than median;
do k = 1 to m;
      do l = 1 to n;
            if obs[k,l]<me then obs[k,l]=1; else obs[k,l]=0;
      end;
end;
sum=obs[,+];
* Signalling event;
signal_ucl=j(nrow(sum),1,.);
      signal_lcl=j(nrow(sum),1,.);
      do p = 1 to nrow(signal_ucl);
            if sum[p,] >= ucl then signal_ucl[p,]=1; else signal_ucl[p,]=0;
            if sum[p,] <= lcl then signal_lcl[p,]=1; else signal_lcl[p,]=0;
      end;
signal=signal_lcl||signal_ucl;
at_least=sum(signal);
if at_least>0 then FAP_sum=1; else FAP_sum=0;
keep=keep//FAP_sum;
end;
* Calculating the FAP;
FAP=(sum(keep))/z;
print       lcl [label='Lower control limit'],
            ucl [label='Upper control limit'],
            m [label='Number of samples'],
            n [label='Number of observations in each sample'],
            FAP [format=.4];
```

2.4.2.5. Necessary amendment to the SAS® program in Section 2.4.2.4 when the underlying process distribution is non-normal

Distribution	Necessary amendments

t(4)	`* Generating observations from the t(4) distribution with mean=0 and var=1;`
	`call randgen(ic_obs, "t", 4);`
	`ic_obs=(1/sqrt(2))#ic_obs;`
	`* Generating observations from the t(4) distribution with mean=0 and var>1;`
	`call randgen(ooc_obs, "t", 4);`

GAM(1,1)	`* Generating observations from the Gamma(1,1) distribution with mean=0 and var=1;`
	`call randgen(ic_obs, "gamma",1);`
	`ic_obs=ic_obs - j(m-1,n,1);`
	`* Generating observations from the Gamma(2,1) distribution with mean=0 and var>1;`
	`call randgen(ooc_obs, "gamma",2);`
	`ooc_obs=ooc_obs-j(1,n,2);`

U(-1,1)	`* Generating observations from the Uniform(-1,1) distribution with mean=0 and var=1;`
	`call randgen(ic_obs, "uniform");`
	`ic_obs=(2#ic_obs-j(m-1,n,1))#sqrt(3);`
	`* Generating observations from the Uniform(-1,1) with mean=0 and var>1;`
	`call randgen(ooc_obs, "uniform");`
	`ooc_obs=(2#ooc_obs-j(1,n,1))#sqrt(6);`

2.4.2.6. R® program for obtaining the obtaining the charting constants (a and $b = n - a$) for the Phase I median control chart

I would like to acknowledge Phillip Labuschagne for some programming assistance with regards to R® programming.

```
# Lower bound for a :
a.lb <- 0
# Upper bound for a :
a.ub <-9
# Lower bound for n :
n.lb <- 3
# Upper bound for n :
n.ub <- 24
# Lower bound for m :
m.lb <- 4
# Upper bound for m :
m.ub <- 4
# Transforming a
a.lb <- a.lb + 1
a.ub  <- a.ub + 1
# The functions
erhs <- function(er.u) {
      erha.out <- 1
      for (i in c(1:length(er.u))){
      erhs.out <- erhs.out*choose(g.n,er.u[i])
      }
erhs.out
}
foo <- function(foo.a){
      foo.uvals <- unique(foo.a)
      foo.num_occur <- rep(0,length(foo.uvals))
      foo.b <- 1
      foo.len <- length(foo.a)
      for (i in c (1:(length(foo.uvals)))){
            foo.num_occur <- length(foo.a[foo.a==foo.uvals[i]])
            foo.b=foo.b*choose(foo.len,foo.num_occur)
            foo.len <- foo.len-foo.num_occur
      }
      foo.b
}
isp <- function(isp.m,isp.uT,isp.a,isp.b){
isp.out <- rep(0,isp.m)
isp.sum <- isp.uT
isp.j <- isp.a
for (isp.i in c (1:(isp.m-1))){
      isp.done <- FALSE
      while (isp.done == FALSE) {
            if ((isp.sum-isp.j)/(isp.m-isp.i)>isp.b) {isp.j <- isp.j+1
            }
            else {
                  isp.out[isp.i] <- isp.j
                  isp.sum <- isp.sum-isp.j
                  isp.done <- TRUE
            }
      }
}
isp.out[isp.m] <- isp.sum
if ((isp.sum>isp.b)||(isp.sum<isp.a)) {c("CRAP",isp.out)} else {isp.out}
}
```

```
mx2 <- function(x2.b) {          # Increases the first element and
      if (x2.b[1]<x2.b[2]-1) {  # decreases the second element if allowed
            mx2.out <- c(x2.b[1]+1,x2.b[2]-1)
      }
      else {
            mx2.out <- c(x2.b)
      }
      mx2.out
}
ife <- function(i.x){          # Increases first element of the vector
      i.m <- length(i.x)       # given to the function
      i.sum <- sum(i.x)
      i.out <- i.x
      i.j <- i.x[1]+1
      i.out[1] <- i.j
      i.busy <- TRUE
      i.i <- 1
      while (i.busy == TRUE) {
            if (i.out[i.i] > i.out[i,i+1]) {
                i.out[i,i+1] <- i.out[i.i]
            }
            else {i.busy <- FALSE
            }
            i.i <- i.i+1
            if (i.i == i.m) {i.busy <- FALSE}
      }
i.busy <- TRUE
i.i <- 1
while (i.busy == TRUE) {
      if (i.out[i.i] < i.out[i.i+1]) {
          i.out[i,i+1] <- i.out[i.i+1]-1
          if (sum(i.out) == i.sum) {i.busy <- FALSE}
      }
      else {
            i.i <- i.i+1
            if (i.i==i.m) {i.busy <- FALSE}
      }
}
if (sum(i,out) !=i.sum) {i.out <- c("no",i.out[-i.m])}
i.out
}
mx <- function(x,v){
      levelss <- 0
      x.m <- length(x.v)
      mx.out <- t(as.matrix(x.v))
      x.sp <- t(matrix(mx.out,x.m,x.m-2))
      x.done <- FALSE
      x.level <- 1
      # for (mx.i in c(1:25)) {
      while (x.done==FALSE) {
      if (x.level==1) {
          x.pos <- x.m-x.level
          x.f <- x.sp[1,-c(x.pos:(x.pos+1))]
          x.b <- c(x.sp[1,c(x.pos:(x.pos+1))])
          if (x.b[1]>=x.b[2]-1) {x.b[3] <- 0}
            else {x.b[3] <- 1}
          while (x.b[3] == 1) {
            x.b <- mx2(x.b[1:2])
            mx.out <- rbind(mx.out,c(x.f,x.b[1:2]))
            if (x.b[1] >= x.b[2]-1) {
                x.b[3] <- 0
            }
            else {
```

```
                x.b[3] <- 1
            }
        }
x.level <- 2
}
else {
      x.pos <- x.m-x.level
      mx.hold2 <- x.sp[(x.level-1),c(x.pos:x.m)]
      if (mx.hold2[2]>mx.hold2[1]+1) {
          mx.hold1 <- mx2(x.sp[(x.level-1),c(x.pos,x.pos+1)])
          x.sp[(x.level-1),c(x.pos,x.pos+1)] <- mx.hold1
          for (mx.i2 in c(1:(x.level-2))){
            x.sp[mx.i2,] <- x.sp[(x.level-1),]
      }
      mx.out <- rbind(mx.out,x.sp[(x.level-1),c(1:x.m)])
      x.level <- x.level-1
}
else {
      if (sum(mx.hold2) > (mx.hold2[1])*length(mx.hold2)) {
          x.pos <- x.pos-1
          if (x.pos==0) {
            mx.hold1 <- ife(x.sp[(x.level-1),])
          }
      else {
          mx.hold1 <- ife(x.sp[(x.level-1),-c(1:x.pos)])
      }
      if (mx.hold1[1]== "no") {
          x.level <- x.level+1
      }
      else {
          if (x.pos==0){
            for (mx.i2 in c(1:(x.level-1))){
                  x.sp[mx.i2,] <- mx.hold1
            }
            x.level <- 2
          }
          else {
            for (mx.i2 in c(1:(x.level-1))){
                  x.sp[mx.i2,-c(1:x.pos)] <- mx.hold1
            }
          x.level <- 2
      }
      x.level <- x.level-1
      mx.out <- rbind(mx.out,x.sp[(x.level),c(1:x.m)])
      }
}
else {
     x.level <- x.level+1
     }
}
}
if (x.level==x.m) {x.done <- TRUE}
levelss <- c(levelss,x.level)
}
mx.out
}
# Constructing the table containing the distribution of FAP
the.out <- array(0,dim=c((a.ub-a.lb+1),(n.ub-n.lb+1),(m.ub-m.lb+1)))
attr(the.out, "dimnames")<-list(c((a.lb-1):(a.ub-1)),c(n.lb:n.ub),c(m.lb:m.ub))
names(attr(the.out, "dimnames")) <- c("a","n","m")
start.time <- Sys.time()
m.pos <- 0
# Constructing the table
```

```
for (g.m in c(m.lb:m.ub)) {
  m.pos <- m.pos+1
  n.pos <- 0
  for (g.n in c(n.lb:n.ub)) {
    n.pos <- n.pos+1
    a.pos <- 0
    g.uT <- trunc((g.m*g.n)/2)
    for (g.a in c(a.lb:a.ub)) {
      a.pos <- a.pos+1
      if (g.a>trunc(g.n/2)) {the.sums <- (NA)}
      else {
        g.b <- g.n-g.a
        dom <- mx(isp(g.m, g.uT, g.a, g.b))
        vals <- cbind(apply(dom,1,erhs),apply(dom,1,foo))
        the.sums<as.numeric(((t(vals[,1])%*%vals[,2])/choose(g.n*g.m,g.uT)))
      }
      the.out[a.pos,n.pos,m.pos] <- (1-the.sums)
    }
  }
}

time.taken <- Sys.time()-start.time

# Build the FAP table from the table with the distribution of FAP
the.outt <- the.out
d <- dim(the.outt)
b <- 0

# Initialize and name the matrices that will store the data
FAP010a <- matrix(0,d[2],d[3])
rownames(FAP010a) <- attr(the.outt, "dimnames")$n
colnames(FAP010a) <- attr(the.outt, "dimnames")$m
names(attr(FAP010a, "dimnames")) <- c("n","m")
FAP010prob <- FAP010a
attr(FAP010prob, "dimnames") <- attr(FAP010a, "dimnames")

FAP005a <- FAP010a
attr(FAP005a, "dimnames") <- attr(FAP010a, "dimnames")
FAP005prob <- FAP010a
attr(FAP005prob, "dimnames") <- attr(FAP010a, "dimnames")

FAP001a <- FAP010a
attr(FAP001a, "dimnames") <- attr(FAP010a, "dimnames")
FAP001prob <- FAP010a
attr(FAP001prob, "dimnames") <- attr(FAP010a, "dimnames")

# Build the actual FAP tables
for (mm in c(1:d[3])) {
      for (nn in c(1:d[2])) {
            done <- FALSE
            done01 <- FALSE
            done005 <- FALSE
            done001 <- FALSE
            aa <- 0
            while (done == FALSE) {
                  aa <- aa+1
                  if ((the.outt[aa,nn,mm]>0.1)&&(done01==FALSE)) {
                        FAP010a[nn,mm] <- max(0,aa-2)
                        FAP010prob[nn,mm] <- the.outt[max(aa-1,1),nn,mm]
                        done01 <- TRUE
            }
            if ((the.outt[aa,nn,mm]>0.05)&&(done005==FALSE)) {
               FAP005a[nn,mm] <- max(0,aa-2)
```

```
                FAP005prob[nn,mm] <- the.outt[max(aa-1,1),nn,mm]
                done005 <- TRUE
             }
             if ((the.outt[aa,nn,mm]>0.01)&&(done001==FALSE)) {
                FAP001a[nn,mm] <- max(0,aa-2)
                FAP001prob[nn,mm] <- the.outt[max(aa-1,1),nn,mm]
                done001 <- TRUE
             }
             if ((done01 == TRUE) &&
                   (done005 == TRUE) &&
                   (done001 == TRUE)) {done <- TRUE}
             if (aa == d[1]) {done <- TRUE}
             }
      }
}

FAP010a
```

Chapter 3

Phase II control charts – parameters known

3.1 Introduction

When the underlying parameters of the process distribution are known or specified it is referred to as the 'standard(s) known' case and is denoted Case K. This will happen in high volume manufacturing processes where ample reliable information is available so that it is possible to specify values for the parameters (see e.g. Human (2009) page 127). Studying Case K sets the stage for the situation when the parameters are unknown, i.e. the 'standard(s) unknown' which is denoted Case U. Studying Case K also helps us understand the operation and the performance of the charts in the simplest of cases.

Recall that the number of charting statistics to be plotted on a control chart before the first signal is called the run-length of a chart. The discrete random variable defining the run-length is called the run-length random variable and is denoted by N. The distribution of N is called the run-length distribution. For Case K the run-length distribution follows a Geometric distribution with probability of success $1-\beta$ so that we write, symbolically, $N \sim GEO(1-\beta)$. This follows by assuming the subgroups are independent and that the probability of a signal is the same for all samples. The run-length distribution is given by

$$P(N = j) = \beta^{j-1}(1-\beta) \text{ for } j = 1,2,\ldots \tag{3.1}$$

where β denotes the probability of no signal. From the properties of the Geometric distribution the ARL is the expected value of N so that

$$ARL = E(N) = \frac{1}{1-\beta}. \tag{3.2}$$

Other characteristics of the run-length distribution are also of interest. For example, in addition to the mean we should also look at the standard deviation of the run-length distribution to get an idea about the variation or spread. From the properties of the Geometric distribution, the standard deviation of the run-length distribution, denoted by $SDRL$, is given by

$$SDRL = STDEV(N) = \frac{\sqrt{\beta}}{1-\beta}. \tag{3.3}$$

Since the Geometric distribution is skewed to the right the mean and the standard deviation become questionable measures of central tendency and spread so that additional descriptive measures are useful. The percentiles, along with the mean and the standard deviation, provide a clearer picture of the run-length distribution (see e.g. Radson and Boyd (2005) and Chakraborti (2007)). The $100q^{th}$ percentile $(0 < q < 1)$ is defined as the smallest integer j such that the cumulative probability is at least q, i.e. $P(N \leq j) \geq q$. Focusing on the median, since it is a robust measure of performance, from the properties of the Geometric distribution, the median of the run-length distribution, denoted by *MRL*, is given by

$$MRL = \frac{-1}{log_2(\beta)}. \tag{3.4}$$

These properties of the Geometric distribution will be used later on.

Next, to set the stage, a brief literature overview of nonparametric control charts for Case K is given. For a more thorough overview on the area of nonparametric control charts the reader is referred to Chakraborti et al. (2001), Chakraborti and Graham (2007) and Chakraborti et al. (2011).

In Section 1.9 the three main classes of control charts are discussed: namely the Shewhart chart, the cumulative sum (CUSUM) chart and the exponentially weighted moving average (EWMA) chart. For monitoring the known location (Case K) of a process several nonparametric Shewhart, CUSUM and EWMA control charts have been developed and we mention some of the important and interesting contributions here.

Nonparametric Shewhart control charts:

i. Amin et al. (1995) and Bakir (2004) proposed nonparametric Shewhart-type control charts based on the well-known sign (SN) and Wilcoxon signed-rank (WSR) statistics, respectively. It should be noted that Amin et al. (1995) also incorporated warning limits into their Shewhart-type sign chart in order to improve the performance of the chart.

ii. Chakraborti and Eryilmaz (2007) improved Bakir (2004)'s Shewhart-type signed-rank chart by incorporating runs-rules and, more recently, Human et al. (2010a) improved Amin et al. (1995)'s Shewhart-type sign chart by incorporating runs-rules. The rules considered include the following:

a. A single charting statistic plots on or outside the control limits (the *1-of-1* rule).

b. k consecutive charting statistics plot on or outside the control limits (the k-*of*-k rule).

c. k of the last w ($k \leq w$) charting statistics plot on or outside the control limits (the k-*of*-w rule).

Runs-rules are implemented in order to improve the performance of the charts.

iii. Amin and Widmaier (1999) studied the Shewhart-type sign chart with variable sampling intervals. A variable sampling interval (VSI) control chart allows the sampling intervals to vary according to what is being observed in the current sample. For more details on VSI schemes, the reader is referred to Reynolds et al. (1990), Saccucci et al. (1992) and Reynolds (1996).

Nonparametric CUSUM (denoted NPCUSUM) control charts:

i. McGilchrist and Woodyer (1975) developed a distribution-free CUSUM test and applied it to the problem of detecting a change in the median of a rainfall distribution (note that although they did not construct a control chart, their proposed test can be used for constructing a distribution-free control chart).

ii. Amin et al. (1995) and Bakir and Reynolds (1979) proposed NPCUSUM charts based on the well-known sign and signed-rank statistics, respectively.

Nonparametric EWMA (denoted NPEWMA) control charts:

i. Amin and Searcy (1991) proposed a NPEWMA chart based on the signed-rank statistic.

From the literature overview, it is clear that the NPEWMA chart based on the well-known sign test statistic is missing from the list and in this dissertation this gap is filled. Thus, in the next section (Section 3.2) we propose a NPEWMA chart based on the SN test statistic; this new chart is labeled the NPEWMA-SN chart. Following this, in Section 3.3 we thoroughly investigate the NPEWMA chart based on the WSR test statistic; this chart is labeled NPEWMA-SR chart.

A number of research outputs related to and based on this thesis have seen the light. In Chapter 5 we provide a list with the details of the technical reports and the peer-reviewed articles that have been published, the articles that have been accepted for publication, the local and international conferences where papers have been presented and draft articles that have been submitted and are currently under review. Here, we solely mention the peer-reviewed articles that have been published based on Sections 3.2 and 3.3, respectively:

i. Graham, M.A., Chakraborti, S. and Human, S.W. (2011). “A nonparametric EWMA sign chart for location based on individual measurements.” *Quality Engineering*, 23 (3), 227-241.

ii. Graham, M.A., Chakraborti, S. and Human, S.W. (2011). “A nonparametric exponentially weighted moving average signed-rank chart for monitoring location.” *Computational Statistics and Data Analysis*, 55 (8), 2490-2503.

3.2 Nonparametric EWMA control chart based on the sign statistic

3.2.1 Introduction

In typical applications of the EWMA chart it is usually assumed that the underlying process distribution is distributed normally (or, at least, approximately so) and, what is more, is that this assumption is typically taken for granted even in cases where there is individuals data or not much is known about the process distribution. Against this backdrop, Human et al. (2011) showed that the typical parametric EWMA control chart (denoted EWMA-$\overline{X}$) based on the assumption of normality lacks IC robustness for some non-normal distributions (such as the symmetric bi-modal and the contaminated normal distribution) and therefore recommended using a NPEWMA chart when normality is a concern. A major advantage of a nonparametric control chart (see e.g. Chakraborti et al. (2001)) is that it has exactly the same IC run-length distribution for all continuous process distributions and is therefore naturally robust; this implies that the IC performance of a nonparametric control chart stays unchanged for all continuous processes, which provides the practitioner more flexibility in its application. So, in a NPEWMA chart one can combine the advantages of nonparametric charts (e.g. IC robustness) and that of EWMA-type charts (e.g. better small shift detection capability). To this end, Amin and Searcy (1991) proposed a NPEWMA chart based on the well-known Wilcoxon signed-rank (WSR) test statistic (see Section 3.3), which is a nonparametric test for the median of a symmetric continuous distribution, and investigated its properties using computer simulation. Their simulation results showed that although their proposed chart is less efficient than the EWMA-$\overline{X}$ chart when the underlying process distribution is normal, it is considerably more efficient for heavy-tailed distributions. This is typically the story with nonparametric tests and control charts. With this motivation, in this chapter, we consider some NPEWMA charts. First we propose a NPEWMA chart based on the well-known sign statistic for monitoring the location of a continuous process; the NPEWMA-SN chart. The sign test is one of the simplest nonparametric tests for any percentile of any continuous distribution and is thus more generally applicable than the WSR test which requires the distribution to be symmetric. Another practical advantage to using the sign statistic is that one does not require the exact numerical values of the observations in order to apply the sign test; the only information that is needed is whether the observation is larger or smaller than the specified parameter of interest. Moreover, it is known (see Gibbons and Chakraborti (2010) page 218) that the simpler sign has higher asymptotic relative efficiency than the WSR test in certain situations. The sign test statistic is defined in the next section.

It should be noted at this point that NPCUSUM charts also combine the advantages of nonparametric charts (e.g. IC robustness) and that of CUSUM-type charts (e.g. better small shift detection capability). However, the CUSUM charts based on the SN and WSR statistics have already been proposed and studied in depth, by Amin et al. (1995) and Bakir and Reynolds (1979), respectively, and will not be discussed any further here. Nonetheless, a new NPCUSUM chart is proposed in Chapter 4 and it is important to note that all NPCUSUM charts enjoy the same advantages as listed above for NPEWMA charts.

3.2.2 The sign test statistic

Let $X_{i1}, X_{i2}, \ldots, X_{in}$ denote the i^{th} $(i = 1,2,\ldots)$ sample or subgroup of independent observations of size $n \geq 1$ from a process with an unknown continuous distribution function F. Let θ_0 denote the known or specified value of the median of F when the process is IC, then θ_0 is called the target value. Let n_i^+ (n_i^-) denote the number of obsered values x_{ij} with values greater (less) than θ_0 in the i^{th} sample. Provided there are no ties, i.e. none of the values are equal to θ_0, we have that $n_i^+ + n_i^- = n$. Define

$$SN_i = \sum_{j=1}^{n} sign(x_{ij} - \theta_0) \tag{3.5}$$

for $i = 1,2,3,\ldots$ where the *sign* function is defined by

$$sign(x) = \begin{cases} 1 & \text{if} \quad x > 0 \\ 0 & \text{if} \quad x = 0 \\ -1 & \text{if} \quad x < 0. \end{cases}$$

Then it can be seen that $SN_i = n_i^+ - n_i^-$ i.e. SN_i is the difference between the number of observations with values greater than θ_0 and the number of observations with values less than θ_0 in the i^{th} sample. From $SN_i = n_i^+ - n_i^-$, it follows that $SN_i + n = 2n_i^+$ assuming no ties, so that

$$n_i^+ = \frac{SN_i + n}{2}. \tag{3.6}$$

The random variable n_i^+ denotes that number of observations greater than θ_0 in the i^{th} sample. To be more consistent with the literature, we denote, from this point on,

$$n_i^+ = T_i = \sum_{j=1}^{n} \Psi(X_{ij} - \theta_0), \tag{3.7}$$

where $\Psi(A) = \begin{cases} 0 & \text{if } A \leq 0 \\ 1 & \text{if } A > 0. \end{cases}$ By substituting $n_i^+ = T_i$ into Equation (3.6) and re-writing the equation, we obtain

$$SN_i = 2\,T_i - n. \tag{3.8}$$

The advantage to using the sign test based on SN_i is the fact that its expected value in the IC case is 0 (this is proven later on). However, in the (nonparametric) literature the statistic T_i is the more well-known version, on which the sign test is based, and is referred to as the *sign test statistic* (see e.g. Gibbons and Chakraborti (2010) page 168). For the purpose of this study, however, we use SN_i and refer to it as the sign test statistic.

The Shewhart-type sign control chart

It should be noted at this point that the statistic, SN_i, is the charting statistic used when constructing the Shewhart-type sign chart by Amin et al. (1995). The control limits for the Shewhart-type sign chart are given by $UCL/LCL = \pm c$ where c is an integer value between 0 and n (including n) and the center line equals zero, i.e. $CL = 0$. The charting constant c is found such that the attained *FAR* is close to some nominal *FAR* (the industry value of 0.0027 is typically used) value. It is worth noting the similarities between the control limits for the sign chart and those for the fraction nonconforming (p) chart. The latter are given by $\hat{p} \pm z_{\frac{\alpha}{2}}\sqrt{\frac{\hat{p}(1-\hat{p})}{n}}$ where $\hat{p} = \frac{X}{n}$ is the sample proportion of successes and $z_{\frac{\alpha}{2}}$ is the $100(1 - {}^{\alpha}/_{2})$th percentile of the standard normal distribution; these control limits are based on the Wald confidence interval (Brown et al. (2001)); the latter and other articles (see, for example, Ghosh (1979), Blyth and Still (1983) and Vollset (1993)) pointed out that the coverage properties of the Wald interval can be erratically poor for many combinations of n and p. However, alternative intervals have been proposed; see for example Agresti-Coull (1998) who proposed an interval that lowered the discrepancy between the actual and nominal coverage probability. This issue has implications in relation with the false alarm rate of sign control chart and in general for control charts for attributes data and can be a topic of further research in the SPC context.

Zero differences

For a continuous random variable, X, the probability of any particular value is zero; thus, $P(X = a) = 0$ for any $a \in \mathrm{R}$. Since the distribution of the observations is assumed to be continuous we have that $P(X_{ij} - \theta_0 = 0) = 0$. Theoretically, the case where $sign(x_{ij} - \theta_0) = 0$ should thus occur with zero probability, but in practice zero differences do occur as a result of, for example, truncation or rounding of the observed values. A common practice (see e.g. Gibbons and Chakraborti (2010) page 171) in such cases is to discard all the observations leading to zero differences and to redefine n as the number of nonzero differences.

Distributional properties of SN_i

The random variable T_i has a binomial distribution with parameters n and $p = P(X_{ij} > \theta_0)$, i.e. $T_i \sim BIN(n, p)$. The properties of the binomial distribution are well-known and they are given in the second column of Table 3.1. We can find the distribution of SN_i via the linear relationship given in Equation (3.8) and this is given in the last column of Table 3.1.

Table 3.1. Moments and the pmf of the T_i and SN_i statistics, respectively

	T_i	SN_i
Expected value	$E(T_i) = np$	$E(SN_i) = E(2T_i - n) = n(2p-1)$
Variance	$VAR(T_i) = np(1-p)$	$VAR(SN_i) = VAR(2T_i - n) = 4np(1-p)$
Standard deviation	$STDEV(T_i) = \sqrt{np(1-p)}$	$STDEV(SN_i) = 2\sqrt{np(1-p)}$
Probability mass function (pmf)	$f(t) = P(T_i = t) = \binom{n}{t} p^t (1-p)^{n-t}$ $t = 0,1,2,\ldots,n$	$f(s) = P(SN_i = s) = P(2T_i - n = s) = P\left(T_i = \frac{n+s}{2}\right)$ $s = -n, -n+1, \ldots, n-1, n$

The probability distributions of T_i and SN_i are both symmetric[i] in the IC case, when the median is equal to θ_0. Hence, when the process is IC we have that:

- the probability distributions, given by the pmf's, are referred to as the *in-control* probability distributions;
- $p = P(X_{ij} > \theta_0 | \text{IC}) = 0.5$; and
- since the IC distribution of the charting statistic SN_i is symmetric about 0, the control limits will be equal distances away from 0, assuming the importance of detecting an upward and downward shift is the same.

Figure 3.1 illustrates the IC probability distributions of T_i and SN_i for n = 10. It is seen that the discrete distributions are symmetric about their means, that is, T_i is symmetric around its mean of np = 10×0.5 = 5 and SN_i is symmetric around its mean of $n(2p-1)$ = 10(2×0.5−1) = 0. We continue to work with SN_i to propose our control chart.

[i] T_i and SN_i are symmetric about np and zero, respectively, as long as the median remains at θ_0.

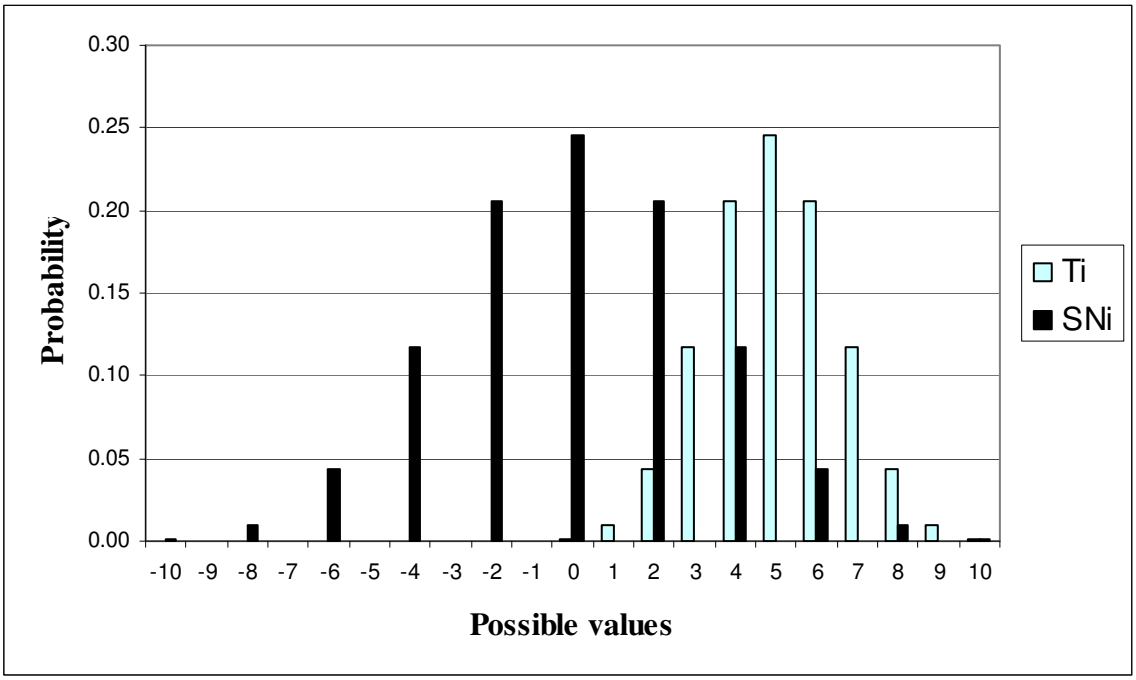

Figure 3.1. The IC probability distribution of T_i and SN_i for $n = 10$

3.2.3 The NPEWMA-SN control chart

3.2.3.1 Design of the chart

The proposed NPEWMA-SN chart is an analog of the parametric EWMA chart given in Section 1.9.3 with SN_i substituted for ψ_i in Equation (1.6). The charting statistic of the proposed NPEWMA-SN chart is obtained by sequentially accumulating the statistics $SN_1, SN_2, SN_3, \ldots,$ and is defined as

$$Z_i = \lambda SN_i + (1-\lambda)Z_{i-1} \text{ for } i = 1,2,3 \ldots \tag{3.9}$$

where $0 < \lambda \leq 1$ is a design parameter called the smoothing constant. The starting value, Z_0, which is required with the first sample at $i = 1$, is set equal to the target value or the expected value of Z_i when the process is IC i.e. $Z_0 = 0$ (see Result 3.1 below).

The *CL* and the control limits of the NPEWMA-SN chart are functions of the IC mean and the IC standard deviation of the charting statistic, Z_i, which are given in the following result.

Result 3.1

$E(Z_i|\text{IC}) = 0$ and $\sigma_{Z_i|\text{IC}} = \sqrt{\frac{\lambda}{2-\lambda}(1-(1-\lambda)^{2i})n}$, respectively.

Proof

By the definition of the charting statistic (see Equation (3.9)) and using recursive substitution (see Appendix 1A) we obtain the following result:

$$E(Z_i|\text{IC}) = E(\lambda SN_i + (1-\lambda)Z_{i-1}|\text{IC}) = E\left(\lambda\sum_{j=0}^{i-1}(1-\lambda)^j SN_{i-j} + (1-\lambda)^i Z_0|\text{IC}\right).$$

Using the fact that $E\left(SN_{i-j}|\text{IC}\right) = 0$ (see Table 3.1) and $Z_0 = 0$ we have that

$$E(Z_i|\text{IC}) = \lambda\sum_{j=0}^{i-1}(1-\lambda)^j E\left(SN_{i-j}|\text{IC}\right) + (1-\lambda)^i Z_0 = 0.$$

In order to obtain the variance similar steps are followed, i.e. we once again use the definition of the charting statistic (see Equation (3.9)) and recursive substitution (see Appendix 1A). However, we also use the result for the sum of a finite geometric series (see Equation (A1.4) in Appendix 1A) and the fact that $VAR\left(SN_{i-j}|\text{IC}\right) = n$ (see Table 3.1 with $p = 0.5$). Consequently, we have that

$$\begin{aligned}
VAR(Z_i|\text{IC}) &= VAR\left(\lambda\textstyle\sum_{j=0}^{i-1}(1-\lambda)^j SN_{i-j} + (1-\lambda)^i Z_0|\text{IC}\right) \\
&= \lambda^2\sum_{j=0}^{i-1}(1-\lambda)^{2j} VAR\left(SN_{i-j}|\text{IC}\right) \\
&= n\lambda^2\sum_{j=0}^{i-1}(1-\lambda)^{2j} \\
&= n\lambda^2\left(\frac{1-(1-\lambda)^{2i}}{1-(1-\lambda)^2}\right) \\
&= n\lambda\left(\frac{1-(1-\lambda)^{2i}}{2-\lambda}\right).
\end{aligned}$$

Therefore, $STDEV(Z_i|\text{IC}) = \sigma_{Z_i|\text{IC}} = \sqrt{\frac{\lambda n}{2-\lambda}(1-(1-\lambda)^{2i})}$.

In analogy with the parametric EWMA, the exact control limits and the *CL* of the NPEWMA-SN control chart are thus given by

$$UCL = E(Z_i|\text{IC}) + L\sigma_{Z_i|\text{IC}} = +L\sqrt{\frac{\lambda n}{2-\lambda}(1-(1-\lambda)^{2i})}$$

$$CL = E(Z_i|\text{IC}) = 0 \tag{3.10}$$

$$LCL = E(Z_i|\text{IC}) - L\sigma_{Z_i|\text{IC}} = -L\sqrt{\frac{\lambda n}{2-\lambda}(1-(1-\lambda)^{2i})}$$

where $L > 0$ is a charting constant. The steady-state control limits (which are typically used when the NPEWMA-SN chart has been running for several time periods so that the term $\left(1-(1-\lambda)^{2i}\right)$ in (3.10) approaches unity) are given by

$$UCL = +L\sqrt{\frac{\lambda n}{2-\lambda}}$$

and (3.11)

$$LCL = -L\sqrt{\frac{\lambda n}{2-\lambda}}.$$

The NPEWMA-SN chart is a plot of the Z_i's (together with the *CL* and the control limits) on the vertical axis versus the sample number or time, i, on the horizontal axis. If any Z_i plots on or outside either of the two control limits the process is declared to be OOC and a search for assignable causes is started. Otherwise, the process is considered IC and the charting procedure continues. Note that, in the developments that follow, we:

i. Consider monitoring the 50th percentile (or median) of the process so that θ_0 actually denotes the known or specified value of the process median. Because the IC probability distribution of the charting statistic is symmetric when monitoring the median it makes sense to use symmetric control limits which results in a visually appealing control chart. However, it should be pointed out that our methodology is flexible enough and can be used to monitor any percentile of interest and can be used with asymmetric control limits (e.g. when detecting an upward and a downward shift is not equally important).

ii. Study two-sided charts only. In applications where a one-sided chart is more meaningful or practical the methodology can be easily modified (this is illustrated in Section 1.9.3).

iii. Use the steady-state control limits; this significantly simplifies the calculation of the run-length distribution via the Markov chain approach and will be discussed in more detail below. However, it should be noted that using the exact control limits with say, simulation, will give more accurate results.

iv. We assume that $n = 1$, which means that we deal with individual observations and then we simply assign a value of 1 to the statistic SN_i if the observation is greater than θ_0, zero if it equals θ_0 and -1 if it is less than θ_0. We focus on the special case of $n = 1$ because the usual EWMA-$\overline{X}$ control chart is typically used with individual observations (see e.g. Montgomery (2009) page 419) and simplifies the performance comparison of the various charts considered in the performance comparison.

Also, note that, the two design parameters of the chart i.e. λ and L, directly influences the NPEWMA chart's performance and suitable combinations should be used. The choice of λ and L is discussed in more detail later.

Run-length distribution

We use a Markov chain approach (see Section 1.10.1) to evaluate / approximate the run-length distribution of the NPEWMA-SN chart. The approach will be discussed in more detail below. We then calculate and evaluate some associated chart performance characteristics (such as the mean (*ARL*), the standard deviation (*SDRL*), the median (*MRL*) and some lower and higher order percentiles etc.). The percentiles, along with the mean and the standard deviation, provide a

clearer picture of the run-length distribution (see e.g. Radson and Boyd (2005) and Chakraborti (2007)).

For an EWMA statistic, we have a continuous state Markov chain (with an infinite state transition probability matrix) and its values are discretized into a finite state Markov chain so that (approximate) results can be obtained relatively easily. Recall that the state space consists of two types of states:

i. one absorbing state (i.e. this state is entered when the chart signals, that is when the EWMA statistic is greater than or equal to the *UCL* or less than or equal to the *LCL*) and

ii. ν transient or non-absorbing states, so that there are $\nu + 1$ states in total.

The ν transient states correspond to ν equal length subintervals of width 2τ obtained by dividing the interval between the upper and lower control limits. For convenience, ν is taken to be an odd positive integer, equal to $2s + 1$ with $s \geq 1$ so that there is a unique middle subinterval between the upper and lower control limits. In this dissertation $\nu = 1001$ is used unless otherwise stated (see Appendix 3B for a motivation on the choice of the number of subintervals between the control limits). From Section 1.10.1 recall that we are interested in calculating the one-step transition probabilities; $M = [p_{ij}]$ for $i, j = -s, -s+1, \ldots, s-1, s$. In order to calculate these probabilities we assume that the charting statistic is equal to S_i whenever it is in state i. For j non-absorbing we obtain

$$p_{ij} = P(S_j - \tau < Z_k \leq S_j + \tau \mid \text{in } S_i) \;\; \forall j \;\; (j \neq s)$$
$$\text{and} \qquad (3.12)$$
$$p_{ij} = P(S_j - \tau < Z_k < S_j + \tau \mid \text{in } S_i) \;\; \text{for} \;\; j = s.$$

Note that the subscript k does not indicate that the charting statistic is time dependent; it simply refers to the charting statistic under consideration. For j absorbing we use the fact that the rows of a M must add to one and therefore the probabilities of going from a transient state to the absorbent state are found by subtraction. Finding the essential probability sub-matrix, Q (see Equation (1.11)), involves finding the transition probabilities of going from one transient state to another. In order to calculate the transition probabilities for the NPEWMA-SN control chart we use the charting statistic given in Equation (3.9) and substitute this into (3.12) to obtain

$$p_{ij} = P\left(\left(\left(\frac{(S_j-\tau)-(1-\lambda)S_i}{\lambda}\right)+1\right)/2 < T_k \leq \left(\left(\frac{(S_j+\tau)-(1-\lambda)S_i}{\lambda}\right)+1\right)/2\right) \ \forall j \ (j \neq s)$$

and (3.13)

$$p_{ij} = P\left(\left(\left(\frac{(S_j-\tau)-(1-\lambda)S_i}{\lambda}\right)+1\right)/2 < T_k < \left(\left(\frac{(S_j+\tau)-(1-\lambda)S_i}{\lambda}\right)+1\right)/2\right) \text{ for } j = s.$$

Since the values τ, λ, S_i and S_j are known constants, (λ is chosen by the practitioner and τ, S_i and S_j are calculated), the binomial probabilities in Expression (3.13) can easily be calculated. The proof of Equation (3.13) and an illustrative example follows.

Proof

For j non-absorbing, i.e. $j = -s, -s+1, \ldots, s-1$, we obtain the one-step transition probabilities $p_{ij} = P(S_j - \tau < Z_k \leq S_j + \tau \mid \text{in } S_i)$. This is the probability that Z_k is within state j, conditioned on Z_{k-1} being equal to the midpoint of state i. By using the definition of the charting statistic given in Equation (3.9) and the fact that $SN_k = 2T_k - n$ with $n = 1$ and where T_k is binomially distributed with parameters n and $p = P(X_{ij} > \theta_0)$, this transition probability can be written as

$$\begin{aligned}
p_{ij} &= P(S_j - \tau < \lambda SN_k + (1-\lambda)Z_{k-1} \leq S_j + \tau | Z_{k-1} = S_i) \\
&= P(S_j - \tau < \lambda SN_k + (1-\lambda)S_i \leq S_j + \tau) \\
&= P\left(\frac{(S_j-\tau)-(1-\lambda)S_i}{\lambda} < SN_k \leq \frac{(S_j+\tau)-(1-\lambda)S_i}{\lambda}\right) \\
&= P\left(\frac{(S_j-\tau)-(1-\lambda)S_i}{\lambda} < 2T_k - 1 \leq \frac{(S_j+\tau)-(1-\lambda)S_i}{\lambda}\right) \\
&= P\left(\left(\frac{(S_j-\tau)-(1-\lambda)S_i}{\lambda}+1\right)/2 < T_k \leq \left(\frac{(S_j+\tau)-(1-\lambda)S_i}{\lambda}+1\right)/2\right).
\end{aligned}$$

Example 3.1

Numerical results for the NPEWMA-SN chart with design parameters $\lambda = 0.05$, $L = 2$ and $v = 2s + 1 = 9$ (so that $s = 4$, that is we divide the interval between the control limits into nine subintervals (see Figure 3.2) resulting in a 'small' transition probability matrix with only ten rows and ten columns, respectively) are given. The steady-state control limits are given by $LCL = -0.320$ and $UCL = 0.320$ which are obtained by substituting $\lambda = 0.05$, $L = 2$ and $n = 1$ into Equation (3.11).

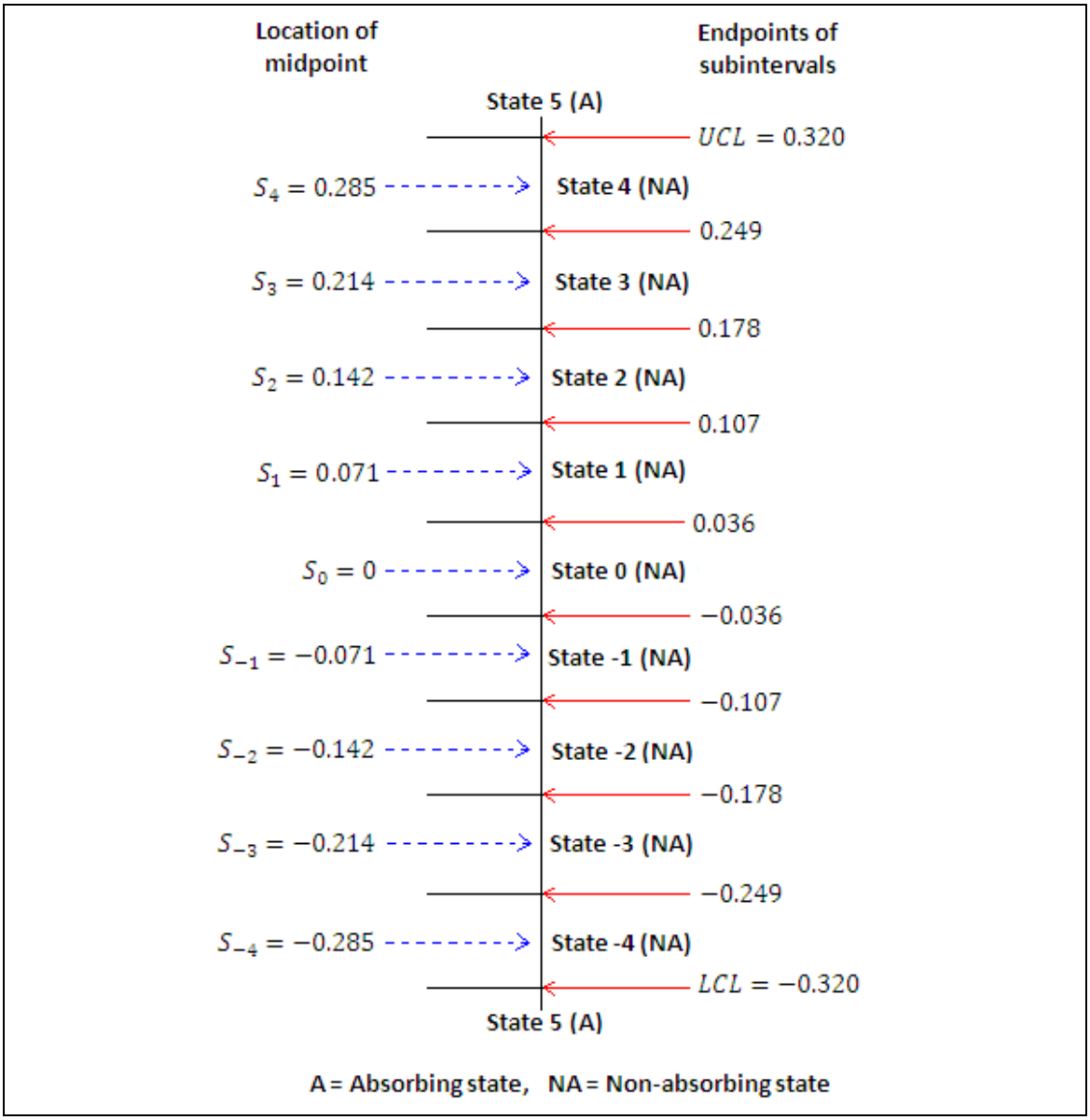

Figure 3.2. Partitioning of the interval between the *LCL* and the *UCL* into $v = 9$ subintervals for $\lambda = 0.05$ and $L = 2$

Using nine IC states, the transition probability matrix is given by

$$M_{10\times10} = \begin{pmatrix} Q_{9\times9} & | & \underline{p}_{9\times1} \\ - & - & - \\ \underline{0}'_{1\times9} & | & 1_{1\times1} \end{pmatrix}$$

$$= \left(\begin{array}{ccccccccc|c} p_{(-4)(-4)} & p_{(-4)(-3)} & p_{(-4)(-2)} & p_{(-4)(-1)} & p_{(-4)0} & p_{(-4)1} & p_{(-4)2} & p_{(-4)3} & p_{(-4)4} & p_{(-4)5} \\ p_{(-3)(-4)} & p_{(-3)(-3)} & p_{(-3)(-2)} & p_{(-3)(-1)} & p_{(-3)0} & p_{(-3)1} & p_{(-3)2} & p_{(-3)3} & p_{(-3)4} & p_{(-3)5} \\ p_{(-2)(-4)} & p_{(-2)(-3)} & p_{(-2)(-2)} & p_{(-2)(-1)} & p_{(-2)0} & p_{(-2)1} & p_{(-2)2} & p_{(-2)3} & p_{(-2)4} & p_{(-2)5} \\ p_{(-1)(-4)} & p_{(-1)(-3)} & p_{(-1)(-2)} & p_{(-1)(-1)} & p_{(-1)0} & p_{(-1)1} & p_{(-1)2} & p_{(-1)3} & p_{(-1)4} & p_{(-1)5} \\ p_{0(-4)} & p_{0(-3)} & p_{0(-2)} & p_{0(-1)} & p_{00} & p_{01} & p_{02} & p_{03} & p_{04} & p_{05} \\ p_{1(-4)} & p_{1(-3)} & p_{1(-2)} & p_{1(-1)} & p_{10} & p_{11} & p_{12} & p_{13} & p_{14} & p_{15} \\ p_{2(-4)} & p_{2(-3)} & p_{2(-2)} & p_{2(-1)} & p_{20} & p_{21} & p_{22} & p_{23} & p_{24} & p_{25} \\ p_{3(-4)} & p_{3(-3)} & p_{3(-2)} & p_{3(-1)} & p_{30} & p_{31} & p_{32} & p_{33} & p_{34} & p_{35} \\ p_{4(-4)} & p_{4(-3)} & p_{4(-2)} & p_{4(-1)} & p_{40} & p_{41} & p_{42} & p_{43} & p_{44} & p_{45} \\ - & - & - & - & - & - & - & - & - & - \\ p_{5(-4)} & p_{5(-3)} & p_{5(-2)} & p_{5(-1)} & p_{50} & p_{51} & p_{52} & p_{53} & p_{54} & p_{55} \end{array}\right)$$

$$= \frac{1}{2}\left(\begin{array}{ccccccccc|c} 0 & 1 & 0 & 0 & 0 & 0 & 0 & 0 & 0 & 1 \\ 1 & 0 & 1 & 0 & 0 & 0 & 0 & 0 & 0 & 0 \\ 0 & 1 & 0 & 1 & 0 & 0 & 0 & 0 & 0 & 0 \\ 0 & 0 & 1 & 0 & 1 & 0 & 0 & 0 & 0 & 0 \\ 0 & 0 & 0 & 1 & 0 & 1 & 0 & 0 & 0 & 0 \\ 0 & 0 & 0 & 0 & 1 & 0 & 1 & 0 & 0 & 0 \\ 0 & 0 & 0 & 0 & 0 & 1 & 0 & 1 & 0 & 0 \\ 0 & 0 & 0 & 0 & 0 & 0 & 1 & 0 & 1 & 0 \\ 0 & 0 & 0 & 0 & 0 & 0 & 0 & 1 & 0 & 1 \\ - & - & - & - & - & - & - & - & - & - \\ 0 & 0 & 0 & 0 & 0 & 0 & 0 & 0 & 0 & 2 \end{array}\right)$$

where the transition probabilities are calculated using Equation (3.13). The calculation of p_{01} is given below for illustration purposes.

$$p_{01}$$
$$= P\left(\left(\left(\frac{(S_1-\tau)-(1-\lambda)S_0}{\lambda}\right)+1\right)/2 < T_k \leq \left(\left(\frac{(S_1+\tau)-(1-\lambda)S_0}{\lambda}\right)+1\right)/2\right)$$
$$= P\left(\left(\left(\frac{(0.071-0.036)-(1-0.05)0}{0.05}\right)+1\right)/2 < T_k \leq \left(\left(\frac{(0.071+0.036)-(1-0.05)0}{0.05}\right)+1\right)/2\right)$$
$$= P(0.856 < T_k \leq 1.568)$$
$$= P(T_k = 1) = \frac{1}{2}.$$

The second last equality follows from the fact that the random variable, T_k, having a $BIN(n = 1, p = 0.5)$ distribution, takes on only nonnegative integer values ($T_k \in \{0,1\}$).

Once the one-step transition probabilities are calculated and the essential transition probability sub-matrix Q is found, the IC run-length characteristics are obtained using equations (1.13), (1.14) and (1.15). This yields $ARL_0 = 25.00$ and $SDRL_0 = 20.00$ with the IC 5^{th}, 25^{th}, 50^{th}, 75^{th} and 95^{th} percentiles being equal to 5, 11, 19, 33 and 65, respectively. The ARL_0 indicates that, when the process is IC, the first signal would be observed, on average, at every 25^{th} plotted point. The first quartile is 11, so we know that a false alarm will not occur within the first 11 plotted points, with a probability of at most 75%. As another example, the $MRL_0 = 19$, which indicates that the first false alarm will be observed, within the first 19 plotted points, at least 50% of the time.

3.2.3.2 Implementation of the chart

The reader is referred to Section 1.9.3 for a detailed discussion on the choice of the design parameters, λ and L. Here we simply state that three values of λ, corresponding to small (roughly 0.5 standard deviations or less), moderate (roughly between 0.5 and 1.5 standard deviations) and large shifts (roughly 1.5 standard deviations or more), were used along with values of L ranging from 2 to 3 in increments of 0.1. Note that, the first row of each cell in Table 3.2 shows the ARL_0 and $SDRL_0$ values, respectively, whereas the second row shows the in-control 5^{th}, 25^{th}, 50^{th}, 75^{th} and 95^{th} percentiles (in this order); these descriptive statistics help summarize the IC run-length distribution, in terms of its shape, typical value (location) and spread.

From Table 3.2 we observe that for a specified / fixed value of λ, the ARL_0 and other characteristics of the IC run-length distribution all increase as L increases. Also, the IC run-length distribution is positively skewed (as is expected) since $ARL_0 > MRL_0$ for all combinations of (λ, L).

This table is useful for a practical implementation of the control chart. For example, from Table 3.2 we observe that for ($\lambda = 0.05$, $L = 2.5$) the $ARL_0 = 396.36$ and for ($\lambda = 0.05$, $L = 2.6$) the $ARL_0 = 514.42$, which implies that the value of L that leads to an ARL_0 of 500 is between 2.5 and 2.6. Refining the search algorithm leads to ($\lambda = 0.05$, $L = 2.583$) with an ARL_0 of 497.75 (see Table 3.3); more details are given below.

Table 3.2. The characteristics[ii] of the IC run-length distribution for the NPEWMA-SN chart

L	Small shifts	Moderate shifts	Large shifts
	$\lambda = 0.05$	$\lambda = 0.10$	$\lambda = 0.20$
2.0	123.00 (113.05) 15, 43, 88, 167, 349	72.74 (67.34) 9, 25, 52, 99, 207	52.92 (49.69) 5, 17, 38, 72, 152
2.1	151.82 (141.14) 18, 51, 109, 206, 433	93.78 (86.78) 11, 32, 67, 127, 267	73.84 (69.03) 8, 25, 53, 100, 212
2.2	192.64 (180.74) 21, 64, 137, 262, 553	118.77 (111.94) 13, 39, 84, 162, 342	104.63 (100.29) 9, 33, 74, 143, 305
2.3	243.29 (230.53) 24, 79, 173, 332, 703	156.91 (148.70) 16, 51, 111, 214, 454	157.08 (151.13) 14, 49, 111, 215, 459
2.4	310.64 (296.68) 29, 99, 220, 425, 903	208.58 (200.28) 19, 66, 147, 286, 608	254.90 (247.71) 20, 78, 179, 351, 749
2.5	396.36 (381.58) 34, 125, 279, 544, 1158	281.06 (271.63) 23, 88, 198, 386, 823	444.74 (436.71) 30, 134, 311, 613, 1316
2.6	514.42 (498.32) 42, 160, 362, 707, 1509	376.57 (366.84) 29, 115, 264, 518, 1109	883.01 (873.93) 54, 260, 615, 1221, 2627
2.7	688.49 (671.00) 52, 211, 483, 948, 2028	544.25 (533.21) 38, 164, 381, 750, 1608	2143.60 (2133.50) 120, 624, 1489, 2968, 6401
2.8	914.52 (896.17) 64, 276, 640, 1261, 2703	798.32 (787.09) 52, 238, 557, 1102, 2369	***
2.9	1262.27 (1242.56) 83, 377, 881, 1742, 3742	1170.49 (1158.06) 72, 346, 815, 1618, 3482	***
3.0	1722.6 (1701.96) 108, 510, 1200, 2380, 5119	1820.61 (1807.21) 106, 533, 1266, 2519, 5427	***

*** For the NPEWMA-SN chart to signal one must have that

$$L^2\left(\frac{\lambda}{2-\lambda}\right) \leq 1. \tag{3.14}$$

The reader is referred to Appendix 3A for the derivation of this limitation. Also note that, the closer $L^2\left(\frac{\lambda}{2-\lambda}\right)$ gets to one, the larger the ARL_0 (and the other characteristics of the IC run-length distribution) get. Hence, if the expression in (3.14) isn't satisfied or the IC run-length characteristics become unreasonably large, these values are omitted as they are not considered useful in practice.

With regard to the implementation of the NPEWMA-SN chart, the first step is to choose λ. The recommendation (see Section 1.9.3) is to choose a small λ, say equal to 0.05, when small shifts are of interest, if moderate shifts are of greater concern, choose $\lambda = 0.10$, whereas choose $\lambda = 0.20$ if larger shifts are of interest. Note that these recommendations are consistent with those for the EWMA-$\overline{X}$ chart (see e.g. Montgomery (2009) page 423)). After λ is chosen, the second step involves choosing L, so that a desired ARL_0 is attained.

[ii] The first row of each cell shows the ARL_0 and $SDRL_0$ values, respectively, whereas the second row shows the values of the in-control 5th, 25th, 50th, 75th and 95th percentiles (in this order).

In order to aid the practitioner in the design of the NPEWMA-SN chart, Table 3.3 lists some (λ, L)-combinations for popular nominal ARL_0 values of 370 and 500, respectively. In each case, the ARL_0 values, obtained using the Markov chain approach, called the attained ARL_0 values, are also provided. Note that because of the discreteness of the sign statistic, the nominal ARL values are not attained exactly, however, it is remarkable that the NPEWMA-SN chart can attain ARL_0 values pretty close to the nominal values which make these charts useful in practice.

Table 3.3. (λ, L)-combinations for the NPEWMA-SN chart for nominal $ARL_0 = 370$ and 500

	Nominal $ARL_0 = 370$		**Nominal $ARL_0 = 500$**	
Shift to be detected	**(λ, L)**	**Attained ARL_0**	**(λ, L)**	**Attained ARL_0**
Small	(0.05, 2.472)	369.49	(0.05, 2.583)	497.75
Moderate	(0.10, 2.585)	370.74	(0.10, 2.667)	500.15
Large	(0.20, 2.471)	364.61	(0.20, 2.521)	497.61

So, for example, in order to detect a small shift in the median with the NPEWMA-SN chart with an ARL_0 of approximately 500, one can use the (λ, L)-combination: (0.05, 2.583). Table 3.3 should be useful for implementing the NPEWMA-SN chart in practice. A SAS® program is provided (see Appendix 3C) if the practitioner wishes to obtain some other (λ, L)-combinations for other nominal ARL_0 values.

3.2.3.3 Performance comparison with other charts

In-control robustness

The IC performance of a chart is typically used to assess its robustness (i.e. the sensitivity of or, the change in, the properties of the run-length distribution) to different distributional assumptions whereas the OOC performance of the chart is examined to assess its efficacy in detecting a shift in the underlying process.

This study includes a wide collection of non-normal distributions and considers light tailed and heavy-tailed, symmetric and asymmetric, uni-modal and bi-modal, positively skewed as well as the Contaminated Normal (*CN*) distributions, which are particularly useful to study the effects of outliers. Note that, wherever necessary, all distributions have been shifted and scaled such that the mean / median equals 0 and the standard deviation equals 1, so that the results are easily comparable across the distributions. The details for these steps are shown in Appendix 1B. Specifically, the distributions considered in the study are:

i. The Standard Normal distribution, $N(0,1)$.

ii. The Student's t-distribution, $t(\nu)$, with degrees of freedom $\nu = 4$ and 8, respectively, which is symmetric but with heavier tails than the Normal.

iii. The Gamma distribution, $GAM(\alpha, \beta)$, with parameters $(\alpha, \beta) = (0.5,1)$, $(1,1)$ and $(3,1)$, respectively, which is positively skewed.

iv. The Laplace (or Double Exponential) distribution, $DE(0,1/\sqrt{2})$, with location parameter 0 and the scale parameter set equal to $1/\sqrt{2}$.

v. The Logistic distribution with location parameter 0 and the scale parameter set equal to $\sqrt{3}/\pi$.

vi. The Contaminated Normal (CN) distribution, which is a linear combination of two Normal random variables with the same location but different variance:

$$0.95N\left(0, \frac{1}{1.15}\right) + 0.05N\left(0, \frac{4}{1.15}\right)$$

where the σ_i's are chosen so that the standard deviation of the distribution equals 1, that is, $0.95\sigma_1^2 + 0.05\sigma_2^2 = 1$. We consider the case where $\sigma_2/\sigma_1 = 2$. The contaminated normal distribution is often used to study the effects of outliers.

The NPEWMA-SN chart is compared[iii] to the parametric EWMA-$\overline{X}$ chart. The results are shown in Table 3.4. Because the proposed NPEWMA-SN chart is nonparametric, the IC run-length distribution and the associated characteristics remain the same for all continuous distributions. However, this is not true for the EWMA-$\overline{X}$ chart. Note that, the values of L were chosen such that the $ARL_0 \approx 500$ for each chart and that, in case of the EWMA-$\overline{X}$ chart, the values of L were chosen (using a search algorithm) such that the $ARL_0 \approx 500$ when the underlying distribution is $N(0,1)$.

[iii] Comparison studies have been done in the literature on Phase II control charts (see e.g. Das (2009)).

Table 3.4. The IC performance characteristics[iv] of the run-length distribution for the NPEWMA-SN and the EWMA-$\overline{X}$ charts for selected (λ, L)-combinations

	NPEWMA-SN		
	(λ, L) = (0.05, 2.583)	**(λ, L) = (0.10, 2.667)**	**(λ, L) = (0.20, 2.521)**
For all distributions	497.75 (481.72) 41, 155, 350, 684, 1459	500.15 (489.29) 36, 152, 350, 689, 1477	497.61 (489.44) 33, 149, 347, 687, 1474
	EWMA-$\overline{X}$		
Distribution	**(λ, L) = (0.05, 2.613)**	**(λ, L) = (0.10, 2.820)**	**(λ, L) = (0.20, 2.962)**
***N*(0,1)**	496.80 (481.23) 39, 154, 349, 683, 1456	500.84 (496.97) 34, 151, 352, 698, 1507	497.21 (491.12) 30, 147, 346, 689, 1473
***t*(4)**	439.19 (428.37) 32, 133, 308, 605, 1298	336.80 (332.23) 22, 100, 234, 465, 1000	219.01 (217.18) 13, 64, 153, 303, 651
***t*(8)**	471.89 (457.49) 37, 146, 332, 649, 1383	428.78 (420.63) 28, 128, 301, 593, 1265	325.68 (323.01) 20, 96, 228, 451, 969
Laplace	443.87 (432.60) 34, 136, 311, 609, 1305	360.35 (353.91) 24, 108, 251, 496, 1071	236.91 (234.55) 15, 70, 164, 327, 706
Logistic	477.10 (464.89) 37, 146, 335, 655, 1411	432.79 (424.59) 29, 130, 305, 597, 1276	331.57 (328.54) 21, 98, 231, 457, 987
***GAM*(0.5,1)**	429.69 (425.65) 27, 127, 298, 594, 1273	266.00 (263.73) 16, 78, 185, 367, 793	146.25 (146.08) 8, 42, 101, 202, 439
***GAM*(1,1)**	464.97 (457.19) 31, 139, 324, 643, 1376	325.51 (323.16) 19, 95, 226, 449, 970	185.76 (184.71) 11, 54, 130, 256, 555
***GAM*(3,1)**	487.45 (473.27) 36, 149, 343, 673, 1430	419.24 (415.31) 26, 124, 292, 580, 1244	282.46 (279.81) 17, 83, 195, 391, 842
CN	450.23 (467.54) 9, 116, 305, 632, 1385	434.59 (442.18) 15, 120, 300, 605, 1311	357.60 (355.41) 16, 101, 247, 497, 1078

[iv] The first row of each cell shows the ARL_0 and $SDRL_0$ values, respectively, whereas the second row shows the values of the in-control 5th, 25th, 50th, 75th and 95th percentiles (in this order).

For a better understanding of the values presented in Table 3.4, let us consider the first cell. The value of $ARL_0 = 497.75$ in the first row indicates that, for the NPEWMA-SN chart with design parameters $\lambda = 0.05$ and $L = 2.583$, when the process is IC, the first false alarm would be observed, on average, at every 498th plotted point. The first quartile is 155, so we know that a false alarm will not occur within the first 155 plotted points, with a probability of at most 75%. As another example, the $MRL_0 = 350$, which indicates that the first false alarm will be observed, within the first 350 plotted points, at least 50% of the time.

For a visual representation of the IC run-length distributions, the values given in Table 3.4 are displayed in some boxplot-like graphs (see Radson and Boyd (2005)) and shown in Figure 3.3. Each boxplot shows the mean of the distribution as a square and the median as a circle inside the box. The 'whiskers' are extended to the 5th and the 95th percentiles instead of the usual minimum and maximum. Note that only one boxplot is shown for the NPEWMA-SN chart (the first boxplot on the left), since its IC run-length characteristics are the same for all continuous distributions and that a reference line was inserted on the vertical axis at 500, which is the desired nominal ARL_0 value in this case.

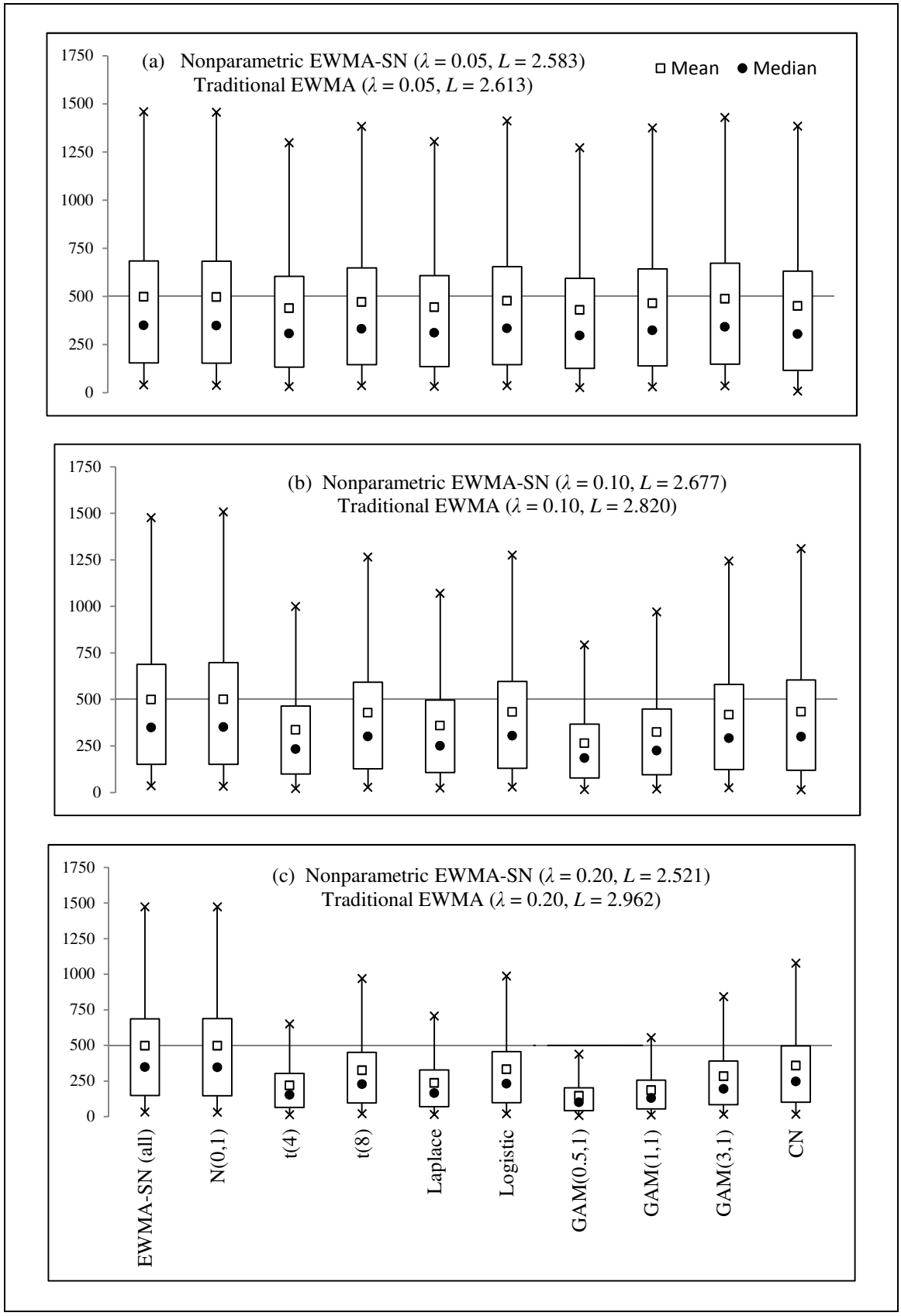

Figure 3.3. Boxplot-like graphs of the IC run-length distributions of the NPEWMA-SN chart (first boxplot on the left) and the EWMA-$\overline{X}$ chart (remaining 9 boxplots on the right)

From Figure 3.3 several observations can be made. As expected, the run-length distributions are all skewed right. The EWMA-$\overline{X}$ chart does not have the IC robustness property of the NPEWMA-SN chart, given that its ARL_0 values vary (as the underlying distribution changes) and sometimes vary quite dramatically. For example, for $\lambda = 0.20$ (see panel (c) of Figure 3.3 together with the values in Table 3.4) the ARL_0 of the EWMA-$\overline{X}$ chart varies from 497.21 (when the underlying distribution is $N(0,1)$) to 146.25 (when the underlying distribution is $GAM(0.5,1)$). In addition, for some of the distributions, the ARL_0 values of the EWMA-$\overline{X}$ chart are significantly smaller than 500, which is clearly problematic since they indicate more false alarms. For example, from Table 3.4 it can be seen that for the $GAM(0.5,1)$ distribution, the $ARL_0 = 146.25$ for the EWMA-$\overline{X}$ chart when $\lambda = 0.20$. This is roughly a third of the nominal ARL_0 value of 500. Although it is possible to tune the EWMA-$\overline{X}$ chart for each distribution by using a grid search algorithm to find the design parameter L such that the nominal $ARL_0 \approx 500$, in general, it raises reasons for concern regarding false alarms while using it in situations where the underlying distribution is not sufficiently known or is (markedly) non-normal. The NPEWMA-SN chart does not suffer from this potential shortcoming.

Out-of-control chart performance

While the IC performance raises excessive false alarm concerns for the EWMA-$\overline{X}$ chart, it is important to also examine the OOC performance for a more complete comparison. This is presented now. In analogy with the parametric charts, the OOC properties depend on the underlying process distribution and on some information about the noncentrality parameter. For the NPEWMA-SN chart all OOC properties depend on the underlying process distribution through the probability that an observation exceeds the median, i.e. $P(X_i > \theta_0)$, where X_i denotes the i^{th} $(i = 1,2,\ldots)$ observation. In order to compare the traditional and nonparametric EWMA charts:

i. It is straight forward to show using Equations (3.2) and (3.3) that the *SDRL* is always less than the *ARL*, i.e. $SDRL < ARL$, and holds whether the process is IC or OOC and this is also what we observe from Tables 3.4 (for the IC case) and Tables 3.5, 3.6 and 3.7 (for the OOC case).

ii. The ARL_0 values of all the charts are fixed at or close to 500 (for the NPEWMA-SN chart we use the same value for L over all distributions, whereas for the EWMA-$\overline{X}$ chart we had to use different values for L over the different distributions).

iii. We compare the NPEWMA-SN chart to the EWMA-$\overline{X}$ chart with known parameters (see Roberts (1959) and Steiner (1999)). The shift considered by Roberts (1959; page 242) for the EWMA-$\overline{X}$ chart is given by $\Delta = \frac{\delta}{\sigma_{\overline{X}}}$ with $\sigma_{\overline{X}} = {}^{\sigma}/_{\sqrt{n}}$. The shift considered by Steiner (1999; page 78) for the EWMA-$\overline{X}$ chart is given by $\frac{\mu_X}{\sigma_{\overline{X}}}$ with $\sigma_{\overline{X}} = {}^{\sigma}/_{\sqrt{n}}$. Thus, in order to have a fair comparison between the proposed NPEWMA-SN chart and the EWMA-$\overline{X}$ chart, a shift of $\delta = \gamma {}^{\sigma}/_{\sqrt{n}}$ where $-\infty < \gamma < \infty$, $\gamma \neq 0$ is used for all charts. Note, however, that since individuals data is considered we have that $n = 1$ and the population standard deviation also equals one, i.e. $\sigma = 1$, in our case, so that $\delta = \gamma$ and can be used interchangeably.

iv. Both positive and negative shifts were considered for the Gamma distribution; for symmetric distributions the direction of the shift does not seem to affect the detection capability of the charts, whereas for the right-skewed Gamma distribution, it does. The reader is referred to Figures 2.10, 2.11 and 2.12 in Chapter 2 for an illustration of this.

Tables 3.5 and 3.6 give the OOC characteristics of the run-length distribution, for the EWMA-$\overline{X}$ chart and the NPEWMA-SN chart, respectively, for positive shifts (γ is taken to be 0.5 to 2.0 in increments of 0.5). The largest value of γ under consideration is $\gamma = 2.0$, since, for larger shifts, the run-length characteristics of the charts tend to converge; this convergence is illustrated in the technical report by Graham et al. (2009) where larger shifts, i.e. larger than $\gamma = 2.0$ were considered. Also, taking the largest value of γ equal to 2.0 is consistent with the shifts considered in Chapter 1 and the rest of the dissertation. Table 3.7 gives the OOC characteristics of the run-length distribution, for the EWMA-$\overline{X}$ chart and the NPEWMA-SN chart, respectively, for the Gamma distribution for negative shifts (γ is taken to be -2.0 to -0.5 in increments of 0.5).

Note that in order to allow for a signal after one observation, the maximum allowable *UCL* for the NPEWMA-SN chart is λ and, in general, in order to allow for a signal after the i^{th} observation, the maximum allowable *UCL* is $(1-(1-\lambda)^i)$. This can be easily shown by substituting the maximum value of SN_i (which equals 1) into Equation (3.9) and rewriting the charting statistic as $Z_i = \lambda \sum_{j=0}^{i-1} (1-\lambda)^j SN_{i-j} + (1-\lambda)^i Z_0$. Thus, the first time the chart can signal is on the first observation number i such that

$$i \geq ln(1 - UCL) / ln(1 - \lambda). \quad (3.15)$$

The proof of this result is given in Appendix 3A. The other point to keep in mind when examining the OOC performance of EWMA charts, is the problem of inertia. The term 'inertia' refers to a measure of the resistance of a chart to signaling a particular process shift. For example, if the EWMA charting statistic happens to be close to the *LCL* at the time when an upward shift occurs, the time required to reach the *UCL* will be longer than if the EWMA statistic was close to the *CL*. It has been shown (Woodall and Mahmoud (2005)) that the EWMA charts have more of an inertia problem than the CUSUM charts; particularly when we are interested in both upward and downward shifts (i.e. two-sided control charts) as the EWMA is implemented by means of a single charting statistic as opposed to a CUSUM procedure that use two separate (upper and lower) charting statistics. Therefore, although the EWMA is easier to implement in practice, its 'worst-case' OOC performance is worse than that of a CUSUM, in which one of the schemes will detect a shift, since the value of the upper one-sided CUSUM never drops below zero and the value of the lower one-sided CUSUM never rises above zero. Many authors have discussed possible solutions to the inertia problem: Spliid (2010) proposed a one-sided EWMA procedure with resetting, Woodall and Mahmoud (2005) recommended that EWMA charts always be used in conjunction with Shewhart limits and Capizzi and Masarotto (2003) proposed an adaptive EWMA (AEWMA) approach that combined the EWMA and the Shewhart approaches in a smoother way than using an EWMA chart in conjunction with Shewhart limits. Similar adaptations of the nonparametric EWMA chart are possible and will be considered in the future. However, note that there are some authors who do not think that the inertia is a big concern (see e.g. Yashchin (1993, page 56) and Ryan (2000, page 247)).

Table 3.5. OOC characteristics[v] of the run-length distribution for the EWMA-$\overline{X}$ control chart for positive shifts

Distribution	Shift (γ)	0.5	1.0	1.5	2.0	Shift (γ)	0.5	1.0	1.5	2.0
	L	$\lambda = 0.05$				L	$\lambda = 0.10$			
$N(0,1)$	2.613	28.68 (16.62) 10, 17, 25, 36, 61	11.37 (4.23) 6, 8, 11, 14, 19	7.10 (2.05) 4, 6, 7, 8, 11	5.22 (1.28) 3, 4, 5, 6, 7	2.820	31.44 (22.59) 8, 16, 25, 41, 76	10.37 (4.77) 5, 7, 9, 13, 19	6.12 (2.13) 3, 5, 6, 7, 10	4.37 (1.25) 3, 3, 4, 5, 7
$t(4)$	2.682	30.94 (17.73) 11, 18, 27, 39, 65	11.76 (4.21) 6, 9, 11, 14, 20	7.29 (2.01) 5, 6, 7, 8, 11	5.34 (1.25) 4, 5, 5, 6, 8	3.039	41.89 (31.94) 10, 20, 33, 54, 105	11.86 (5.32) 5, 8, 11, 15, 22	6.69 (2.16) 4, 5, 6, 8, 11	4.72 (1.29) 3, 4, 5, 5, 7
$t(8)$	2.640	29.53 (16.99) 10, 18, 25, 37, 62	11.50 (4.22) 6, 9, 11, 14, 19	7.18 (2.05) 4, 6, 7, 8, 11	5.27 (1.27) 4, 4, 5, 6, 8	2.883	34.16 (24.53) 9, 17, 27, 44, 83	10.77 (4.92) 5, 7, 10, 13, 20	6.28 (2.17) 3, 5, 6, 7, 10	4.47 (1.25) 3, 4, 4, 5, 7
Laplace	2.666	30.48 (17.58) 11, 18, 26, 38, 65	11.68 (4.27) 6, 9, 11, 14, 20	7.24 (2.05) 4, 6, 7, 8, 11	5.32 (1.27) 4, 4, 5, 6, 8	2.965	38.30 (28.66) 9, 18, 30, 50, 95	11.27 (5.13) 5, 8, 10, 14, 21	6.46 (2.11) 4, 5, 6, 8, 10	4.60 (1.27) 3, 4, 4, 5, 7
Logistic	2.635	29.46 (17.00) 10, 17, 25, 37, 62	11.47 (4.22) 6, 8, 11, 14, 19	7.17 (2.05) 4, 6, 7, 8, 11	5.26 (1.27) 4, 4, 5, 6, 8	2.885	34.08 (25.08) 8, 17, 27, 44, 83	10.84 (4.90) 5, 7, 10, 13, 20	6.29 (8.14) 3, 5, 6, 7, 10	4.46 (1.25) 3, 4, 4, 5, 7
$GAM(0.5,1)$	2.721	33.75 (20.97) 9, 19, 29, 43, 74	12.57 (4.56) 6, 9, 12, 15, 21	7.52 (1.97) 4, 6, 8, 9, 11	5.45 (1.19) 3, 5, 6, 6, 7	3.323	51.54 (42.48) 9, 22, 40, 68, 136	14.84 (7.55) 5, 9, 13, 19, 29	7.81 (2.51) 4, 6, 8, 9, 12	5.28 (1.30) 3, 4, 5, 6, 7
$GAM(1,1)$	2.652	31.29 (19.13) 9, 18, 27, 40, 68	12.03 (4.45) 6, 9, 12, 15, 20	7.31 (2.01) 4, 6, 7, 9, 11	5.31 (1.21) 3, 5, 5, 6, 7	3.112	42.24 (33.56) 8, 19, 33, 55, 109	12.81 (6.25) 5, 8, 12, 16, 25	7.16 (2.38) 4, 6, 7, 9, 11	4.90 (1.28) 3, 4, 5, 6, 7
$GAM(3,1)$	2.623	29.78 (17.73) 10, 17, 26, 38, 64	11.66 (4.35) 6, 9, 11, 14, 20	7.21 (2.05) 4, 6, 7, 8, 11	5.26 (1.24) 3, 4, 5, 6, 7	2.901	34.27 (25.92) 8, 16, 27, 45, 85	11.13 (5.29) 5, 7, 10, 14, 21	6.44 (2.21) 3, 5, 6, 8, 10	4.52 (1.25) 3, 4, 5, 7
CN	2.656	24.49 (18.26) 3, 11, 20, 33, 59	7.42 (4.73) 2, 4, 6, 10, 16	3.82 (2.20) 1, 2, 3, 5, 8	2.45 (1.28) 1, 2, 2, 3, 5	2.856	32.86 (23.70) 8, 16, 26, 43, 80	10.60 (4.84) 5, 7, 10, 13, 20	6.22 (2.15) 3, 5, 6, 7, 10	4.44 (128) 3, 4, 4, 5, 7
	L	$\lambda = 0.20$								
$N(0,1)$	2.962	41.68 (36.20) 7, 16, 31, 56, 114	10.56 (6.43) 4, 6, 9, 13, 23	5.50 (2.43) 3, 4, 5, 7, 10	3.75 (1.34) 2, 3, 4, 4, 6					
$t(4)$	3.550	110.57 (104.97) 11, 35, 78, 152, 318	18.36 (12.36) 5, 10, 15, 23, 43	7.49 (3.34) 3, 5, 7, 9, 14	4.69 (1.58) 3, 4, 4, 5, 8					
$t(8)$	3.154	57.16 (50.91) 8, 21, 42, 77, 160	12.48 (7.74) 4, 7, 10, 16, 27	6.11 (2.72) 3, 4, 6, 7, 11	4.02 (1.39) 2, 3, 4, 5, 7					
Laplace	3.351	75.92 (68.83) 9, 26, 55, 105, 217	15.11 (9.95) 5, 8, 12, 19, 35	6.71 (2.95) 3, 5, 6, 8, 12	4.36 (1.49) 2, 3, 4, 5, 7					
Logistic	3.135	55.38 (49.05) 8, 21, 41, 74, 156	12.17 (7.48) 4, 7, 10, 15, 27	5.98 (2.65) 3, 4, 5, 7, 11	4.01 (1.43) 2, 3, 4, 5, 7					
$GAM(0.5,1)$	4.093	103.00 (97.97) 9, 33, 73, 140, 301	28.56 (23.20) 5, 12, 22, 37, 75	11.55 (6.64) 4, 7, 10, 15, 24	6.29 (2.25) 3, 5, 6, 8, 10					
$GAM(1,1)$	3.708	77.04 (72.19) 8, 26, 55, 104, 221	20.03 (14.82) 5, 10, 16, 26, 49	8.79 (4.50) 3, 6, 8, 11, 17	5.24 (1.84) 3, 4, 5, 6, 8					
$GAM(3,1)$	3.295	54.90 (49.59) 7, 20, 40, 74, 154	14.20 (9.52) 4, 8, 12, 18, 33	6.80 (3.24) 3, 5, 6, 8, 13	4.40 (1.55) 2, 3, 4, 5, 7					
CN	3.098	52.32 (46.36) 8, 19, 38, 71, 144	11.86 (7.30) 4, 7, 10, 15, 26	5.90 (2.62) 3, 4, 5, 7, 11	3.95 (1.38) 2, 3, 4, 5, 7					

[v] The first row of each cell shows the *ARL* and *SDRL* values, respectively, whereas the second row shows the values of the 5th, 25th, 50th, 75th and 95th percentiles (in this order).

Table 3.6. OOC characteristics[vi] of the run-length distribution for the NPEWMA-SN control chart for positive shifts

Shift (γ)	0.5	1.0	1.5	2.0	0.5	1.0	1.5	2.0
Distribution	$\lambda = 0.05$ and $L = 2.583$				$\lambda = 0.10$ and $L = 2.667$			
***N*(0,1)**	42.19 (26.46) 14, 23, 35, 53, 94	18.03 (6.38) 11, 13, 16, 21, 30	13.16 (2.73) 11, 11, 13, 14, 19	11.65 (1.35) 11, 11, 11, 11, 14	48.35 (36.61) 12, 22, 38, 63, 121	17.53 (7.79) 10, 12, 15, 21, 33	12.17 (3.05) 10, 10, 10, 13, 18	10.64 (1.45) 10, 10, 10, 10, 14
***t*(4)**	29.70 (15.61) 13, 19, 26, 37, 60	15.34 (4.38) 11, 11, 14, 17, 24	12.56 (2.23) 11, 11, 11, 14, 17	11.68 (1.38) 11, 11, 11, 11, 14	31.07 (20.70) 9, 16, 25, 39, 72	13.75 (5.31) 9, 9, 12, 16, 24	10.69 (2.65) 9, 9, 9, 12, 16	9.73 (1.64) 9, 9, 9, 9, 13
***t*(8)**	36.53 (21.45) 13, 21, 31, 46, 79	16.82 (5.48) 11, 13, 16, 19, 27	12.93 (2.54) 11, 11, 11, 14, 18	11.72 (1.42) 11, 11, 11, 11, 14	39.82 (28.98) 11, 19, 31, 51, 97	15.43 (6.72) 9, 9, 14, 18, 29	11.09 (3.02) 9, 9, 9, 12, 17	9.77 (1.69) 9, 9, 9, 9, 13
Laplace	27.52 (13.81) 13, 18, 24, 34, 54	15.68 (4.64) 11, 13, 14, 18, 25	12.90 (2.52) 11, 11, 11, 14, 18	11.86 (1.58) 11, 11, 11, 13, 15	28.32 (18.15) 9, 16, 23, 36, 64	14.14 (5.63) 9, 9, 13, 17, 25	11.06 (3.00) 9, 9, 9, 12, 17	9.93 (1.88) 9, 9, 9, 9, 13
Logistic	35.79 (20.80) 13, 21, 30, 45, 77	16.80 (5.47) 11, 13, 16, 19, 27	12.97 (2.57) 11, 11, 13, 14, 18	11.75 (1.46) 11, 11, 11, 13, 14	38.87 (28.06) 11, 19, 31, 50, 95	15.41 (6.70) 9, 9, 14, 18, 29	11.13 (3.06) 9, 9, 9, 13, 17	9.81 (1.74) 9, 9, 9, 9, 13
***GAM*(0.5,1)**	11.00 (0.00) 11, 11, 11, 11, 11	11.00 (0.00) 11, 11, 11, 11, 11	11.00 (0.00) 11, 11, 11, 11, 11	11.00 (0.00) 11, 11, 11, 11, 11	9.00 (0.00) 9, 9, 9, 9, 9	9.00 (0.00) 9, 9, 9, 9, 9	9.00 (0.00) 9, 9, 9, 9, 9	9.00 (0.00) 9, 9, 9, 9, 9
***GAM*(1,1)**	19.46 (7.45) 11, 14, 18, 23, 34	11.00 (0.00) 11, 11, 11, 11, 11	11.00 (0.00) 11, 11, 11, 11, 11	11.00 (0.00) 11, 11, 11, 11, 11	18.49 (9.34) 9, 12, 16, 22, 37	9.00 (0.00) 9, 9, 9, 9, 9	9.00 (0.00) 9, 9, 9, 9, 9	9.00 (0.00) 9, 9, 9, 9, 9
***GAM*(3,1)**	32.43 (17.91) 13, 20, 28, 40, 67	13.31 (2.84) 11, 11, 13, 14, 19	11.00 (11.07) 11, 11, 11, 11, 11	11.00 (0.00) 11, 11, 11, 11, 11	34.54 (23.96) 9, 18, 28, 44, 82	11.50 (3.39) 9, 9, 9, 13, 18	9.00 (0.08) 9, 9, 9, 9, 9	9.00 (0.00) 9, 9, 9, 9, 9
CN	39.43 (24.00) 14, 22, 33, 49, 87	17.39 (5.90) 11, 13, 16, 20, 29	12.98 (2.57) 11, 11, 13, 14, 18	11.63 (1.33) 11, 11, 11, 11, 14	43.60 (32.59) 12, 21, 34, 56, 108	16.08 (7.27) 9, 11, 14, 19, 30	11.14 (3.07) 9, 9, 9, 13, 17	9.68 (1.58) 9, 9, 9, 9, 13
	$\lambda = 0.20$ and $L = 2.521$							
***N*(0,1)**	61.48 (52.97) 11, 24, 45, 82, 167	18.65 (10.88) 9, 11, 15, 23, 40	11.66 (4.05) 9, 9, 9, 13, 20	9.76 (1.88) 9, 9, 9, 9, 14				
***t*(4)**	38.55 (30.28) 9, 17, 29, 50, 99	14.63 (7.00) 9, 9, 12, 17, 29	10.89 (3.23) 9, 9, 9, 12, 18	9.80 (1.92) 9, 9, 9, 9, 14				
***t*(8)**	51.03 (42.60) 11, 21, 38, 68, 136	16.80 (9.10) 9, 9, 14, 20, 35	11.43 (3.82) 9, 9, 9, 13, 19	9.84 (1.98) 9, 9, 9, 9, 14				
Laplace	34.64 (26.44) 9, 16, 27, 45, 87	15.13 (7.48) 9, 9, 13, 18, 30	11.33 (3.70) 9, 9, 9, 13, 19	10.02 (3.70) 9, 9, 13, 18, 30				
Logistic	49.67 (41.25) 11, 20, 37, 66, 132	16.78 (9.07) 9, 9, 14, 20, 35	11.41 (3.79) 9, 9, 9, 13, 19	9.89 (2.04) 9, 9, 9, 9, 14				
***GAM*(0.5,1)**	9.00 (0.09) 9, 9, 9, 9, 9	9.00 (0.09) 9, 9, 9, 9, 9	9.00 (0.09) 9, 9, 9, 9, 9	9.00 (0.09) 9, 9, 9, 9, 9				
***GAM*(1,1)**	20.90 (13.05) 9, 12, 17, 26, 47	9.00 (0.09) 9, 9, 9, 9, 9	9.00 (0.09) 9, 9, 9, 9, 9	9.00 (0.09) 9, 9, 9, 9, 9				
***GAM*(3,1)**	43.51 (35.16) 9, 19, 33, 57, 114	11.85 (4.25) 9, 9, 9, 13, 20	9.00 (0.09) 9, 9, 9, 9, 9	9.00 (0.00) 9, 9, 9, 9, 9				
CN	56.38 (47.91) 11, 22, 42, 75, 152	17.66 (9.92) 9, 11, 15, 21, 37	11.42 (3.80) 9, 9, 9, 13, 19	9.74 (1.85) 9, 9, 9, 9, 14				

[vi] The first row of each cell shows the *ARL* and *SDRL* values, respectively, whereas the second row shows the values of the 5th, 25th, 50th, 75th and 95th percentiles (in this order).

Table 3.7. OOC characteristics[vii] of the run-length distribution for the EWMA-$\overline{X}$ and the EWMA-SN control charts for negative shifts

Distribution	L	EWMA-$\overline{X}$				NPEWMA-SN			
		Shift (γ)				Shift (γ)			
		-0.5	-1.0	-1.5	-2.0	-0.5	-1.0	-1.5	-2.0
		$\lambda = 0.05$				$\lambda = 0.05$ and $L = 2.583$			
***GAM*(0.5,1)**	2.721	29.99 (15.87) 13, 19, 26, 37, 61	11.56 (4.01) 7, 9, 11, 13, 19	7.27 (2.05) 5, 6, 7, 8, 11	5.35 (1.31) 4, 4, 5, 6, 8	34.29 (19.51) 13, 20, 29, 43, 73	19.05 (7.14) 11, 14, 17, 22, 33	15.03 (4.15) 11, 11, 14, 17, 23	13. 31 (2.84) 11, 11, 13,14, 19
***GAM*(1,1)**	2.652	28.67 (15.53) 12, 18, 25, 35, 59	11.30 (4.05) 7, 8, 10, 13, 19	7.12 (2.04) 5, 6, 7, 8, 11	5.26 (1.28) 4, 4, 5, 6, 8	40.37 (24.83) 14, 23, 34, 51, 89	19.99 (7.86) 11, 14, 18, 24, 35	15.13 (4.23) 11, 11, 14, 17, 23	13.19 (2.74) 11, 11, 13, 14, 19
***GAM*(3,1)**	2.623	28.30 (15.78) 11, 17, 24, 35, 59	11.26 (4.12) 6, 8, 10, 13, 19	7.07 (2.05) 5, 6, 7, 8, 11	5.22 (1.28) 4, 4, 5, 6, 8	43.90 (28.00) 15, 24, 36, 55, 99	20.10 (7.94) 11, 14, 18, 24, 35	14.74 (3.94) 11, 11, 14, 16, 22	12.74 (2.38) 11, 11, 11, 14, 17
		$\lambda = 0.10$				$\lambda = 0.10$ and $L = 2.820$			
***GAM*(0.5,1)**	3.323	70.14 (52.72) 18, 33, 55, 91, 175	12.92 (5.35) 7, 9, 12, 15, 24	7.23 (2.29) 5, 6, 7, 8, 12	5.10 (1.34) 4, 4, 5, 6, 8	45.12 (33.26) 12, 22, 36, 58, 111	20.61 (10.39) 10, 13, 18, 25, 41	15.07 (5.62) 10, 10, 14, 18, 26	12.82 (3.76) 10, 10, 12, 14, 20
***GAM*(1,1)**	3.112	45.80 (33.30) 13, 22, 36, 59, 113	11.60 (4.98) 6, 8, 10, 14, 21	6.69 (2.18) 4, 5, 6, 8, 11	4.95 (1.31) 3, 4, 4, 5, 7	56.28 (43.66) 13, 25, 43, 74, 140	22.16 (11.72) 10, 14, 19, 27, 45	15.31 (5.76) 10, 10, 14, 18, 26	12.76 (3.72) 10, 10, 12, 14, 20
***GAM*(3,1)**	2.901	34.52 (24.32) 10, 17, 28, 44, 83	10.55 (4.72) 5, 7, 9, 13, 20	6.24 (2.13) 4, 5, 6, 7, 10	4.44 (1.27) 3, 4, 4, 5, 7	62.51 (49.29) 14, 28, 47, 82, 160	22.06 (11.39) 10, 14, 19, 27, 44	14.74 (5.30) 10, 10, 13, 17, 25	12.19 (3.21) 10, 10, 10, 14, 19
		$\lambda = 0.20$				$\lambda = 0.20$ and $L = 2.962$			
***GAM*(0.5,1)**	4.093	2782.84 (2841.79) 126, 788, 1898, 3855, 8381	43.63 (32.99) 12, 20, 34, 57, 107	9.35 (3.90) 5, 7, 8, 11, 17	5.56 (1.76) 4, 4, 5, 6, 9	1760.70 (1760.84) 106, 512, 1220, 2424, 5175	172.07 (155.59) 25, 61, 125, 234, 478	62.86 (46.37) 20, 30, 49, 80, 154	39.22 (22.72) 20, 22, 32, 48, 85
***GAM*(1,1)**	3.708	3229.53 (3230.87) 171, 2274, 4473, 9574	20.54 (13.33) 7, 11, 17, 26, 47	7.66 (3.22) 4, 5, 7, 9, 14	4.84 (1.62) 3, 4, 4, 6, 8	3160.12 (3136.82) 179, 928, 2197, 4423, 9489	213.42 (195.78) 28, 74, 154, 288, 617	65.60 (48.80) 20, 31, 50, 85, 162	38.33 (22.17) 20, 22, 31, 47, 83
***GAM*(3,1)**	3.295	123.38 (114.96) 15, 42, 89, 173, 358	13.24 (7.88) 5, 8, 11, 17, 29	6.28 (2.68) 3, 4, 6, 7, 11	4.18 (1.45) 3, 3, 4, 5, 7	4103.70 (4141.72) 228, 1190, 2849, 5611, 12412	212.03 (189.25) 28, 75, 153, 288, 591	58.80 (42.31) 20, 29, 46, 74, 144	33.69 (17.41) 20, 20, 28, 40, 68

[vii] The first row of each cell shows the *ARL* and *SDRL* values, respectively, whereas the second row shows the values of the 5th, 25th, 50th, 75th and 95th percentiles (in this order).

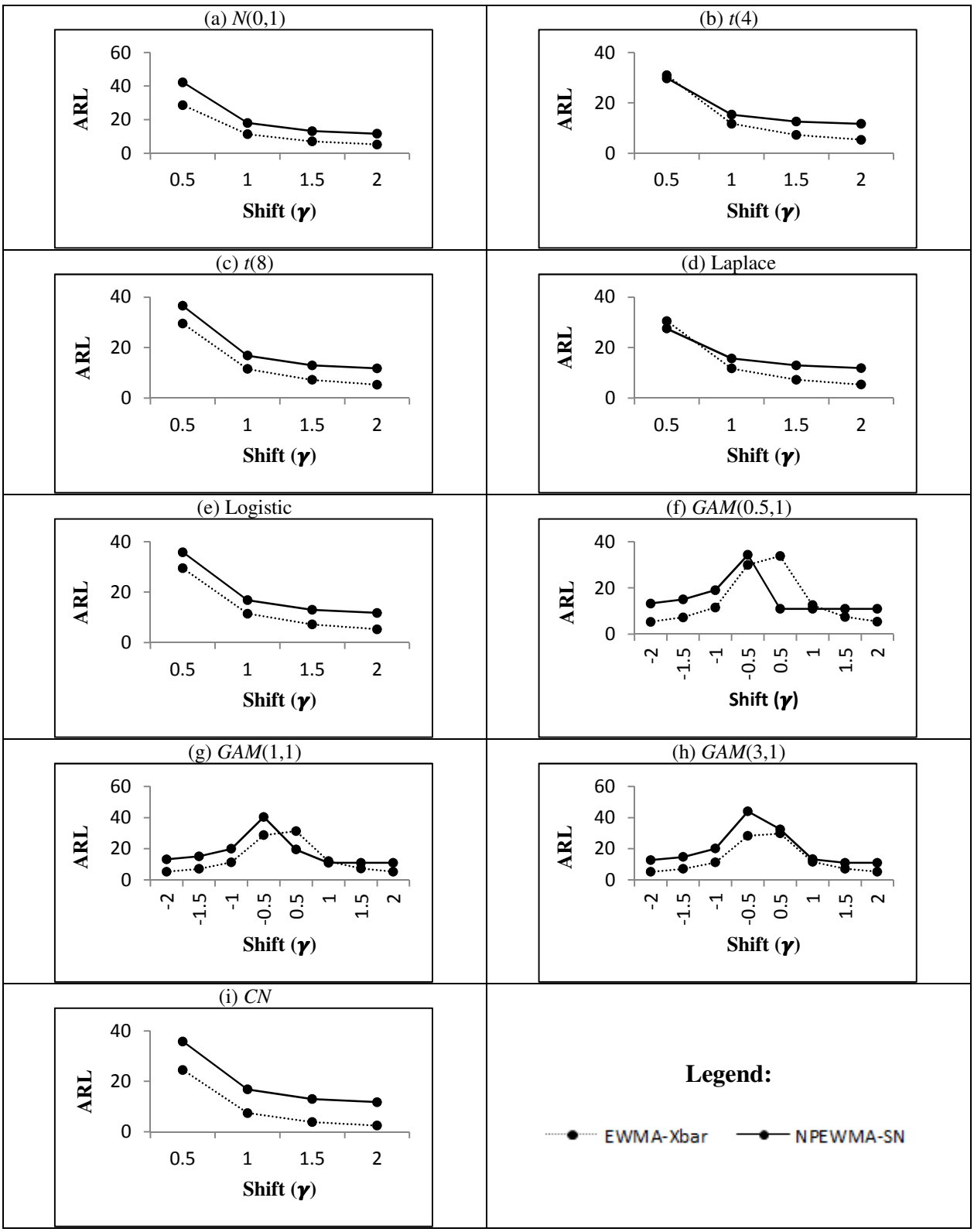

Figure 3.4. OOC *ARL* values for the EWMA- $\overline{X}$ control chart and the NPEWMA-SN control chart for $\lambda = 0.05$

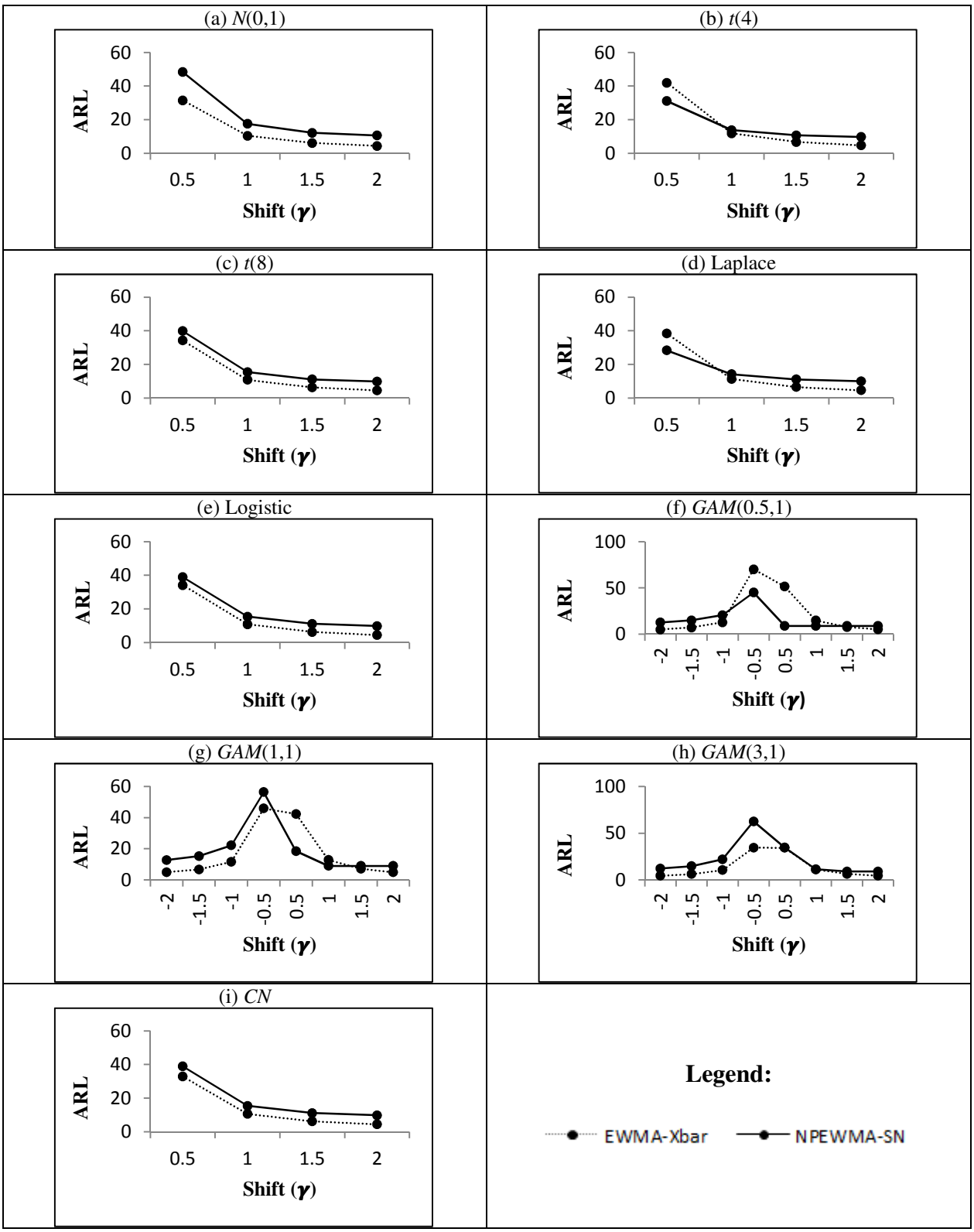

Figure 3.5. OOC *ARL* values for the EWMA-$\overline{X}$ control chart and the NPEWMA-SN control chart for $\lambda = 0.10$

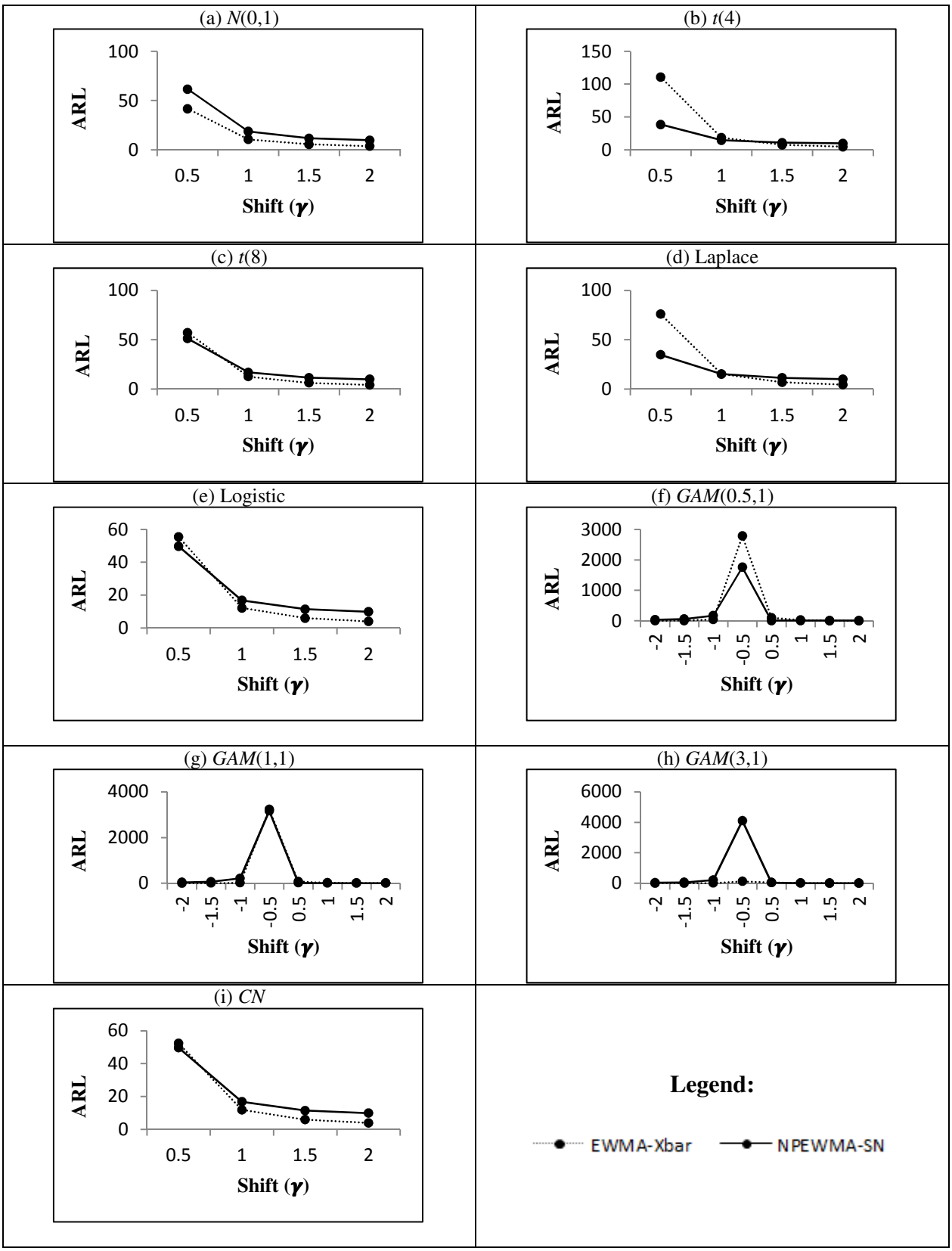

Figure 3.6. OOC *ARL* values for the EWMA-$\overline{X}$ control chart and the NPEWMA-SN control chart for $\lambda = 0.20$

It may be noted that there is some bias in the *ARL* (the ARL_δ is bigger than the ARL_0) of the charts for the Gamma distribution when the shift is small (see Figures 3.6 (f), (g) and (h)). This could be due to many extreme long run-lengths observed in the simulation of the *ARL*, which could be a result of the right-skewness of the Gamma distribution coupled with the fact that the run-length distribution is itself highly right-skewed with a long right tail. The bias could also be a result of simulation error because these ARL_δ values are very close to the ARL_0 values. Some authors have considered *ARL*-unbiased parametric charts and this would be a topic of further research in the context of nonparametric charts. On the other hand, Steiner and Jones (2010), among others, have recommended examining the median run-length instead "which is easier to simulate and gives arguably a better summary." This approach is considered in Chapter 4.

A summary of our observations from the OOC comparisons is as follows:

- When the underlying process distribution is $N(0,1)$, we find that for all λ and for all magnitudes of shifts the EWMA-$\overline{X}$ chart outperforms the NPEWMA-SN chart, which is not surprising, since traditional normal theory methods typically outperform their nonparametric counterparts when the assumption of normality is satisfied. The same conclusion can be drawn for the *CN* distribution. This could be attributed to the fact that we have a small level of contamination and, consequently, the EWMA-$\overline{X}$ chart performs best overall.

- For the $t(8)$ and the Logistic distributions, the EWMA-$\overline{X}$ chart outperforms the NPEWMA-SN chart for all λ and for all magnitudes of shifts, except for $\lambda = 0.20$ and $\gamma = 0.50$ where the NPEWMA-SN is performing slightly better.

- For the heavier tailed $t(4)$ distribution, for $\lambda = 0.05$ and 0.10, the NPEWMA-SN chart performs best for small shifts ($\gamma = 0.50$), whereas the EWMA-$\overline{X}$ chart performs best for all other shifts under consideration. For $\lambda = 0.20$, the NPEWMA-SN chart performs best for small to moderate shifts ($\gamma = 0.50$ and 1.00), whereas the EWMA-$\overline{X}$ chart performs best for all other shifts under consideration.

- For the heavy-tailed Laplace distribution, we find that for all λ the NPEWMA-SN chart performs best for small shifts ($\gamma = 0.50$), whereas the EWMA-$\overline{X}$ chart performs best for all other shifts under consideration.

- For the Gamma distribution, both positive and negative shifts were considered; for symmetric distributions the direction of the shift does not seem to affect the detection capability of the charts, whereas for the right-skewed Gamma distribution, it does.

    - Positive shifts: For the $GAM(3,1)$ distribution and for all λ, the performances of the two charts are very similar. For the more highly skewed $GAM(1,1)$ and $GAM(0.5,1)$ distributions and for all λ, the NPEWMA-SN chart performs best for small to moderate shifts (γ = 0.50 and 1.00), whereas the EWMA-$\overline{X}$ chart performs best for all other shifts under consideration.

    - Negative shifts: The EWMA-$\overline{X}$ chart performs best, except for (i) a small shift of γ = -0.50 for the $GAM(0.5,1)$ distribution for λ = 0.10 and 0.20 where the NPEWMA-SN chart performs best and (ii) and for a small shift of γ = -0.50 for the $GAM(1,1)$ distribution for λ = 0.20 where the charts perform similarly.

- For moderate to large shifts (γ = 1.5 and 2.00), the run-length characteristics of the NPEWMA-SN chart tend to 11 as the shift increases, this is due to the restriction shown in Equation (3.15), whereas those of the EWMA-$\overline{X}$ chart can (and do) get smaller. Similar conclusions can be drawn for λ = 0.10 and 0.20 where the run-length characteristics of the NPEWMA-SN chart tend to 10 and 9, respectively, as the shift increases.

3.2.3.4 Illustrative examples

Example 3.2

We illustrate the NPEWMA-SN chart using a set of data from Montgomery (2005; Table 8.1). The first 20 of these observations were drawn from a normal distribution with mean and standard deviation equal to 10 and 1, respectively, whereas the last 10 observations were drawn from a normal distribution with mean and standard deviation equal to 11 and 1, respectively. Consequently, we can think of these last 10 observations as having been drawn from the process when it was OOC. Montgomery (2005) applied the EWMA-$\overline{X}$ chart with λ = 0.10 and L = 2.7 to these data (this choice of design parameters results in an $ARL_0 \approx 370$). It should be noted that although Montgomery (2005) used exact control limits in his example, here we calculated steady-state control limits for a fair comparison (recall that we use steady-state control limits for the

NPEWMA-SN chart since this significantly simplifies the calculation of the run-length distribution via the Markov chain approach). For the NPEWMA-SN chart we set the design parameters $\lambda = 0.10$ and $L = 2.585$ and use $v = 1001$ to obtain an $ARL_0 = 370.74$. The steady-state control limits were calculated using Equation (3.11) and they equal ±0.593, respectively, with $CL = 0$. The NPEWMA-SN charting statistics were calculated using Equation (3.9) and are given in Table 3.8 along with the original individual observations.

Table 3.8. The individual observations and the NPEWMA-SN charting statistics for Example 3.2

Observation number (i)	x_i	**NPEWMA-SN**	**Observation number (i)**	x_i	**NPEWMA-SN**
1	9.45	-0.100	16	9.37	0.024
2	7.99	-0.190	17	10.62	0.121
3	9.29	-0.271	18	10.31	0.209
4	11.66	-0.144	19	8.52	0.088
5	12.16	-0.030	20	10.84	0.179
6	10.18	0.073	21	10.90	0.261
7	8.04	-0.034	22	9.33	0.135
8	11.46	0.069	23	12.29	0.222
9	9.20	-0.037	24	11.50	0.300
10	10.34	0.066	25	10.60	0.370
11	9.03	-0.040	26	11.08	0.433
12	11.47	0.064	27	10.38	0.489
13	10.51	0.157	28	11.62	0.540
14	9.40	0.042	29	11.31	0.586
15	10.08	0.137	30	10.52	0.628

From Figures 3.7 and 3.8 we see that the NPEWMA-SN control chart signals at observation 30, whereas the EWMA-$\overline{X}$ chart signaled earlier at sample number 29, indicating that the latter chart may be performing better. While this is not surprising, since traditional normal theory methods typically outperform their nonparametric counterparts when the assumption of normality is satisfied, it is encouraging to see the NPEWMA-SN chart performing comparably against the EWMA-$\overline{X}$ chart.

It is interesting to note it seems that the charting statistics are alternating up and down for the NPEWMA-SN chart. Although there is a set of decision rules for detecting non-random patterns on control charts (see the Western Electronic Handbook (1956)), these rules are typically implemented with the Shewhart-type charts in order to increase their sensitivity for detecting small shifts and will not apply here (with an EWMA-type chart).

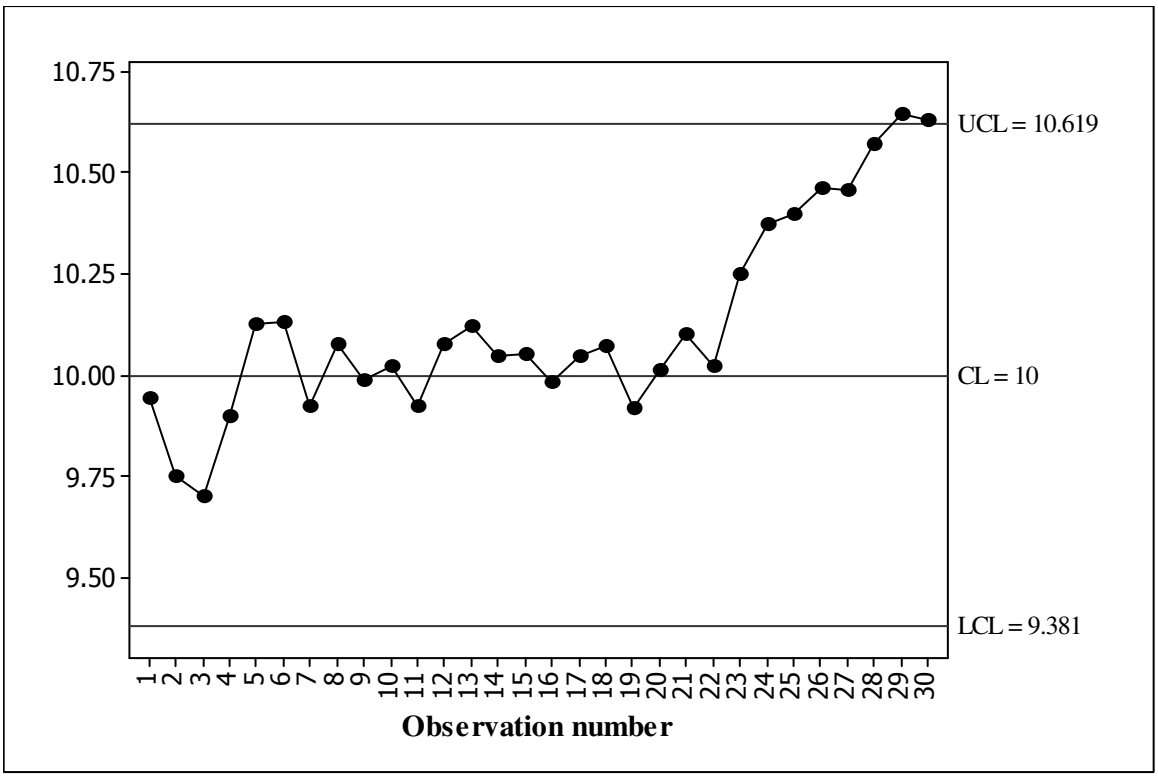

Figure 3.7. The EWMA- $\overline{X}$ control chart for Example 3.2

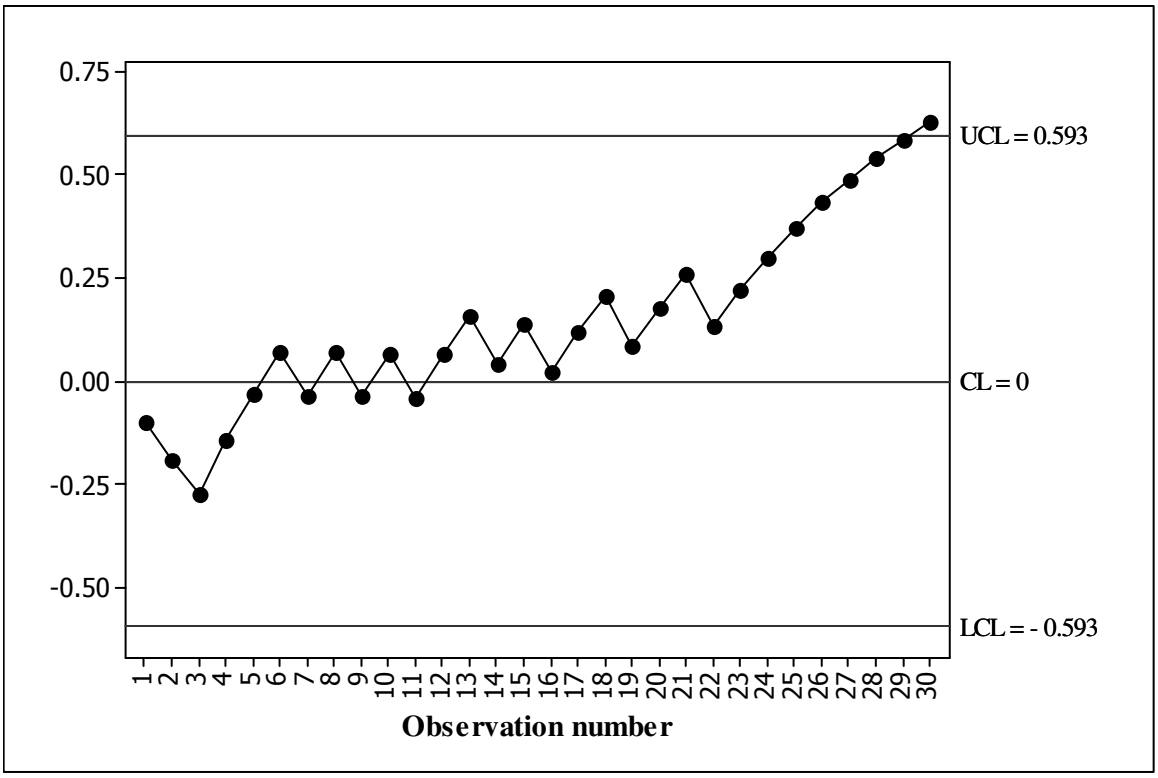

Figure 3.8. The NPEWMA-SN control chart for Example 3.2

For our first example, the data did not reject a goodness of fit test for normality. Nonparametric charts are useful for all continuous distributions and asymmetric and heavier tailed distributions are of particular interest in practice as they can give rise to more outliers which do not

necessarily indicate an OOC process. So we illustrate the NPEWMA-SN chart when the data follow a right skewed distribution with a heavy tail.

Example 3.3

To illustrate the utility and the application of the proposed nonparametric chart, we consider data from a right skewed distribution with a heavy tail. The first 20 data points were generated from a Pareto $\left(2/\sqrt{3}, 3\right)$ distribution. This distribution has a median equal to $\left(2/\sqrt{3}\right)\left(\sqrt[3]{2}\right) \approx 1.455$ and a variance equal to 1. Then each of these data points was transformed (shifted) by subtracting the median so that the transformed observations have a median of zero and a standard deviation of 1. Similarly, the last 10 observations were generated by transforming the observations from a Pareto $\left(2/\sqrt{3}, 3\right)$ distribution so that the resulting observations have a median of 0.5 and a standard deviation equal to 1. Consequently, these last 10 observations can be thought of as having been drawn from a process that is out-of-control in the median. The two Pareto probability density functions (pdf's) in use are shown in Figure 3.9.

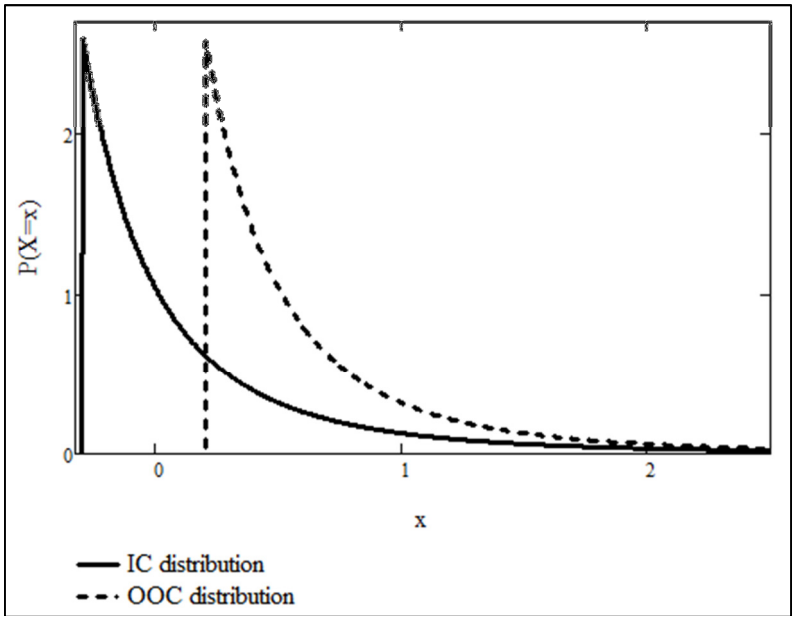

Figure 3.9. The in- and out-of-control Pareto pdf's used in Example 3.3

For the NPEWMA-SN chart, we use $\lambda = 0.10$ and $L = 2.585$ from Table 3.3 for an $ARL_0 = 370.74$. The values of the NPEWMA-SN charting statistics were calculated using Equation (3.9) and are shown in Table 3.9 along with the original simulated observations. For the EWMA-$\overline{X}$ chart we use $\lambda = 0.10$ and $L = 2.703$ for $ARL_0 \approx 370$ (see Montgomery (2005) page 412). The EWMA-$\overline{X}$ and the NPEWMA-SN control charts are shown in Figures 3.10 and 3.11, respectively.

Table 3.9. The individual observations and the NPEWMA-SN charting statistics for Example 3.3

Observation number (i)	x_i	**NPEWMA-SN**	**Observation number (i)**	x_i	**NPEWMA-SN**
1	-0.184	-0.100	16	-0.129	-0.083
2	0.453	0.010	17	-0.278	-0.175
3	-0.234	-0.091	18	1.320	-0.058
4	0.152	0.018	19	-0.117	-0.152
5	-0.287	-0.084	20	0.116	-0.037
6	0.578	0.025	21	0.310	0.067
7	-0.300	-0.078	22	0.472	0.160
8	3.948	0.030	23	0.201	0.244
9	-0.111	-0.073	24	0.523	0.320
10	-0.228	-0.166	25	0.871	0.388
11	-0.177	-0.249	26	0.475	0.449
12	0.626	-0.124	27	0.933	0.504
13	-0.154	-0.212	28	2.614	0.554
14	0.112	-0.091	29	0.323	0.598
15	1.349	0.018	30	0.589	0.639

From Figures 3.10 and 3.11 we see that the NPEWMA-SN control chart signals at observation 29, whereas the EWMA-$\overline{X}$ chart does not signal at all. In fact, the charting statistics in both charts start to develop an upward trend from time point 20, but the trend in the nonparametric chart is far more pronounced and steeper. In addition, the NPEWMA-SN chart has the practical advantage that it does not require normality or any other specific parametric model assumption about the underlying process distribution. Thus a nonparametric chart is in-control robust by definition. However, although, in principle, the EWMA-$\overline{X}$ chart can be designed for a specific application to be fairly robust to the violation of the underlying distributional assumptions (see Borror et al. (1999)), this is bound to be cumbersome and, consequently, not expected to be satisfactory in all applications in practice (see Human et al. (2011)). Note that, although this is an example using simulated data, it clearly shows that there are situations in practice where the NPEWMA-SN chart can offer a viable alternative to the EWMA-$\overline{X}$ chart.

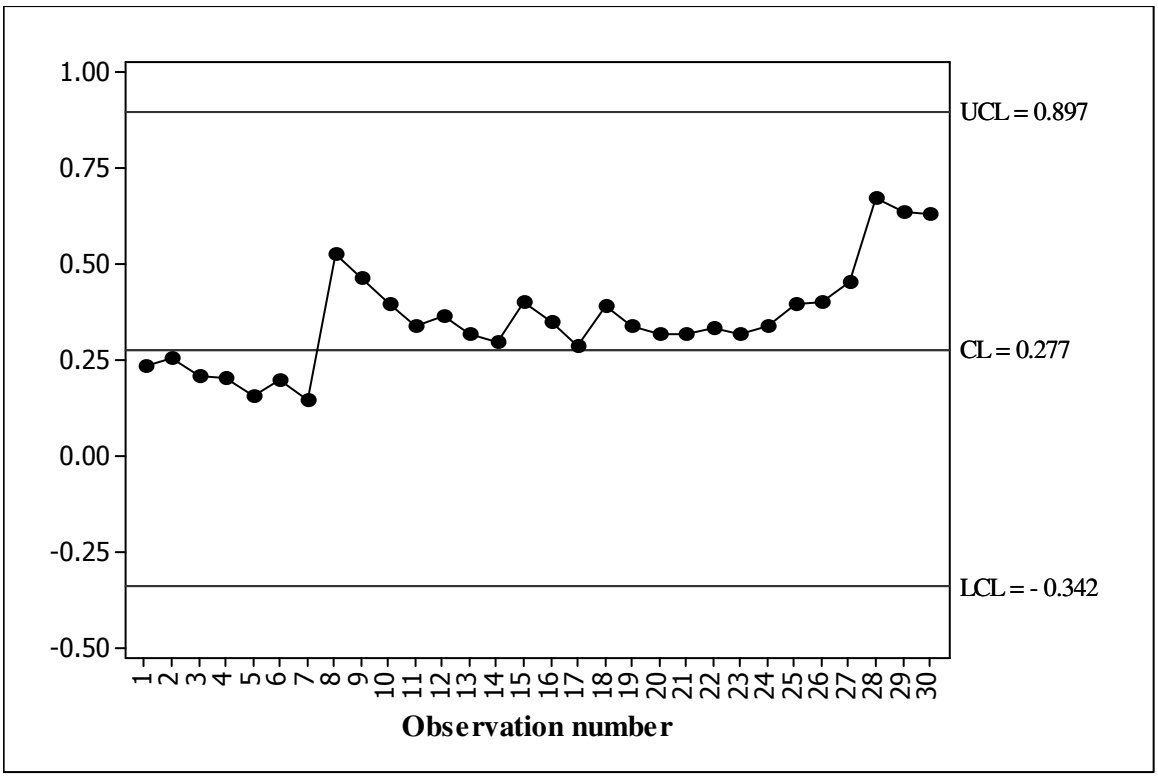

Figure 3.10. The EWMA-$\overline{X}$ control chart for Example 3.3

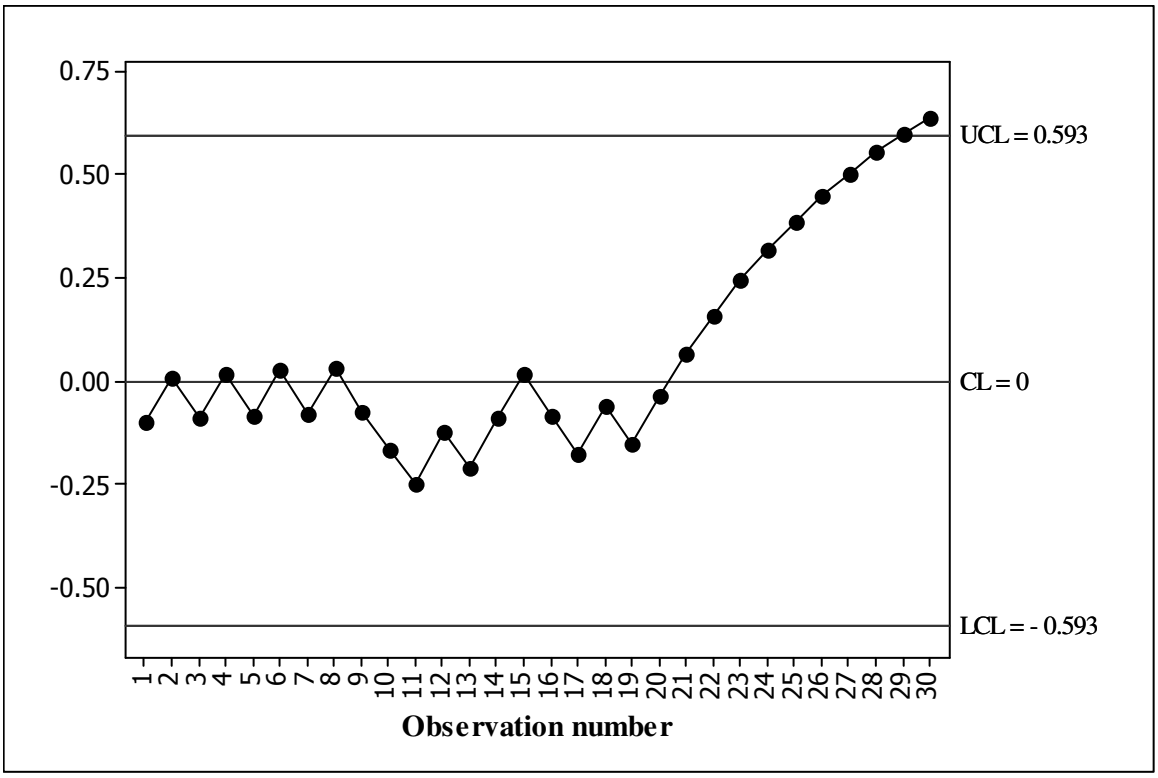

Figure 3.11. The NPEWMA-SN control chart for Example 3.3

3.2.4 Summary

EWMA charts are among the most popular control charts used in practice; they take advantage of the sequential accumulation of evidence arising in a typical SPC environment and are known to be more efficient than the Shewhart charts in detecting smaller shifts. However, the traditional parametric EWMA charts suffer from a lack of IC robustness and as a result the possibility of varying, inflated and unknown false alarm rates is a serious practical concern. These concerns are amplified for individuals data, where the central limit theorem does not offer any protection. NPEWMA charts offer an attractive alternative in such situations as they combine the inherent advantages of nonparametric charts (IC robustness) with the better small shift detection capability of EWMA-type charts. We propose a NPEWMA control chart for i.i.d. individuals data based on the sign statistic and study its properties via the IC and OOC run-length distribution using a Markov chain approach. It is seen that although the NPEWMA-SN chart is perfectly IC robust, it generally has somewhat of an inferior OOC performance relative to the EWMA-$\overline{X}$ chart for some light-tailed symmetric distributions such as the Normal, Logistic and Contaminated Normal distributions. However, when the underlying process distribution is more heavy-tailed like the Laplace distribution or highly right-skewed like the Gamma distribution the NPEWMA-SN chart has superior performance in some cases. Moreover, the nonparametric chart is expected to be less sensitive to outliers and a knowledge or specification of the process variance is not necessary. Next, we consider a NPEWMA control chart based on the signed-rank statistic.

3.3 Nonparametric EWMA control chart based on the signed-rank statistic

3.3.1 Introduction

Amin and Searcy (1991) considered a NPEWMA chart based on the Wilcoxon signed-rank (SR) statistic for monitoring the known or the specified or the target value of the median of a process; we label this the NPEWMA-SR chart. However, much work remained to be done. Chakraborti and Graham (2007), noted that "…more work is necessary on the practical implementation of the (NPEWMA-SR) charts…". Given the potential practical benefits of this control chart, in this thesis we perform an in-depth study to gain insight into its design, implementation and performance. More precisely:

i. We use a Markov-chain approach to calculate the IC run-length distribution and the associated performance characteristics.

ii. We examine the *ARL* as a performance measure and, for a more thorough assessment of the chart's performance, we also calculate and study the *SDRL*, the *MRL*, the 1st and 3rd quartiles as well as the 5th and 95th percentiles for an overall assessment of the run-length distribution.

iii. We provide easy to use tables for the chart's design parameters to aid practical implementation.

iv. We do an extensive simulation-based performance study comparison with competing traditional and nonparametric charts.

Next, some statistical background information is given and the NPEWMA-SR chart is defined. Following this, the computational aspects of the run-length distribution plus the design and implementation of the chart are discussed. Then the IC and OOC chart performance are compared to those of the EWMA-$\overline{X}$ chart and the NPEWMA-SN chart. We conclude with an illustrative example and a summary.

3.3.2 The signed-rank test statistic

The Wilcoxon signed-rank (SR) test is a popular nonparametric alternative to the one-sample *t*-test for testing hypotheses (or setting-up confidence intervals) about the location parameter (mean / median) of a symmetric continuous distribution. Note that for a *t*-test to be valid the assumption of normality is needed, but that is not necessary for the SR test. The SR test is quite efficient, the asymptotic relative efficiency (ARE) of the SR test relative to the *t*-test is 0.955, 1, 1.097 and 1.5 for the Normal, Uniform, Logistic and Laplace distribution, respectively (see e.g. Gibbons and Chakraborti (2010) page 218). This indicates that the SR test is more powerful for some heavier tailed distributions. In fact, it can be shown that the ARE of the SR test to the *t*-test is at least 0.864 for any symmetric continuous distribution. So, very little seems to be lost and much to be gained in terms of efficiency when the SR test is used instead of the *t*-test. In Section 3.2 we proposed a NPEWMA chart based on the sign (SN) statistic, the so-called NPEWMA-SN chart. Although both the sign and the signed-rank charts are nonparametric, the SR chart is expected to be more efficient since the SR test is more efficient than the SN test for a number of light to moderately heavy-tailed normal-like distributions (see e.g. Gibbons and Chakraborti (2010) page 218). Thus the NPEWMA-SR chart is an exceptionally viable alternative to the traditional EWMA and the NPEWMA-SN charts.

Let $X_{i1}, X_{i2}, \ldots, X_{in}$ denote the i^{th} ($i = 1,2,\ldots$) sample or subgroup of independent observations of size $n > 1$ from a process with an unknown symmetric continuous distribution function F. Let θ_0 denote the known or specified value of the median when the process is IC, then θ_0 is the target value. Let R_{ij}^{+} denote the rank of the absolute deviations, $|X_{ij} - \theta_0|$, within the subgroup $(|X_{i1} - \theta_0|, |X_{i2} - \theta_0|, \ldots, |X_{in} - \theta_0|)$ for $i = 1,2,3\ldots$. Then R_{ij}^{+} is referred to as the within-group absolute rank of the deviations. Define

$$SR_i = \sum_{j=1}^{n} sign(X_{ij} - \theta_0) R_{ij}^{+} \tag{3.16}$$

for $i = 1,2,3\ldots$ where the *sign* function is defiend by

$$sign(x) = \begin{cases} 1 & \text{if} \quad x > 0 \\ 0 & \text{if} \quad x = 0 \\ -1 & \text{if} \quad x < 0. \end{cases}$$

The SR_i statistic is linearly related to the well-known Wilcoxon signed-rank statistic T_n^{+} through the formula (see Bakir (2003), page 424)

$$SR_i = 2T_n^{+} - \frac{n(n+1)}{2} \tag{3.17}$$

where $T_n^{+} = \sum_{j=1}^{n} \Psi(X_{ij} - \theta_0) R_{ij}^{+}$ and $\Psi(A) = \begin{cases} 0 & \text{if} \quad A \leq 0 \\ 1 & \text{if} \quad A > 0. \end{cases}$

Clearly, T_n^{+} is the sum of the ranks of the absolute values of the deviations corresponding to the positive deviations. By using the null distribution of the Wilcoxon signed-rank statistic (which is well documentated, see e.g. Gibbons and Charakraborti (2010) page 195) we can easily compute probabilities associated with SR_i through the use of the linear relationship given in Equation (3.17). The advantage to using the SR_i statistic is the fact that its expected value in the IC case is 0 (this is proven later on). However, in the (nonparametric) literature the statistic T_n^{+} is the more well-known version, on which the signed-rank test is based, and is referred to as the *Wilcoxon signed-rank statistic*.

Zero differences

For a continuous random variable, X, the probability of any particular value is zero; thus, $P(X = a) = 0$ for any $a \in \mathrm{R}$. Since the distribution of the observations is assumed to be continuous we have that $P(X_{ij} - \theta_0 = 0) = 0$. Theoretically, the case where $sign(x_{ij} - \theta_0) = 0$ should thus occur with zero probability, but in practice zero differences do occur as a result of, for example, truncation or rounding of the observed values. A common practice (see e.g. Gibbons and Chakraborti (2010) page 202) in such cases is to discard all the observations leading to zero differences and to redefine n as the number of nonzero differences.

Distributional properties of SR_i

The properties of the T_n^+ are well-known (see e.g. Gibbons and Chakraborti (2010) page 195) and they are given in the second column of Table 3.10. We can find the distribution of SR_i via the linear relationship given in Equation (3.17) and this is given in the last column of Table 3.10.

The probability distributions of T_n^+ and SR_i are both symmetric[viii] in the IC case, when the median is equal to θ_0. Hence, when the process is IC we have that:

- the probability distributions, given by the pmf's, are referred to as the *in-control* probability distributions; and

- since the IC distribution of the charting statistic SR_i is symmetric about 0, the control limits will be equal distances away from 0, assuming the importance of detecting an upward and downward shift is the same.

[viii] T_n^+ and SR_i are symmetric about $n(n+1)/4$ and zero, respectively, as long as the median remains at θ_0.

Table 3.10. Moments and the pmf of the T_n^+ and SR_i statistics, respectively

	$\boldsymbol{T_n^+}$	$\boldsymbol{SR_i}$
Expected value	$E(T_n^+) = \frac{n(n+1)}{4}$	$E(SR_i) = E\left(2T_n^+ - \frac{n(n+1)}{2}\right) = 0$
Variance	$VAR(T_n^+) = \frac{n(n+1)(2n+1)}{24}$	$VAR(SR_i) = VAR\left(2T_n^+ - \frac{n(n+1)}{2}\right) = \frac{n(n+1)(2n+1)}{6}$
Standard deviation	$STDEV(T_n^+) = \sqrt{\frac{n(n+1)(2n+1)}{24}}$	$STDEV(SR_i) = \sqrt{\frac{n(n+1)(2n+1)}{6}}$
Probability mass function (pmf)	$f(t) = P(T_n^+ = t) = \frac{u_n(t)}{2^n}$ $t = 0,1,\ldots,\frac{n(n+1)}{2}$ where $u_n(t)$ is the number of possible ways to assign signs so that the sum of the positive integers equals t	$f(s) = P(SR_i = s) = P\left(2T_n^+ - \frac{n(n+1)}{2} = s\right) = P\left(T_n^+ = \frac{s}{2} + \frac{n(n+1)}{4}\right)$ $s = -\frac{n(n+1)}{2}, -\frac{n(n+1)}{2} + 1, \ldots, \frac{n(n+1)}{2}$

Figure 3.12 illustrates the IC probability distributions of T_n^+ and SR_i for $n = 5$. It is seen that the discrete distributions are symmetric about their means, that is, T_n^+ is symmetric around its mean of $\frac{n(n+1)}{4} = \frac{(5)(6)}{4} = 7.5$ and SR_i is symmetric around its mean of 0. We continue to work with SR_i to propose our control chart.

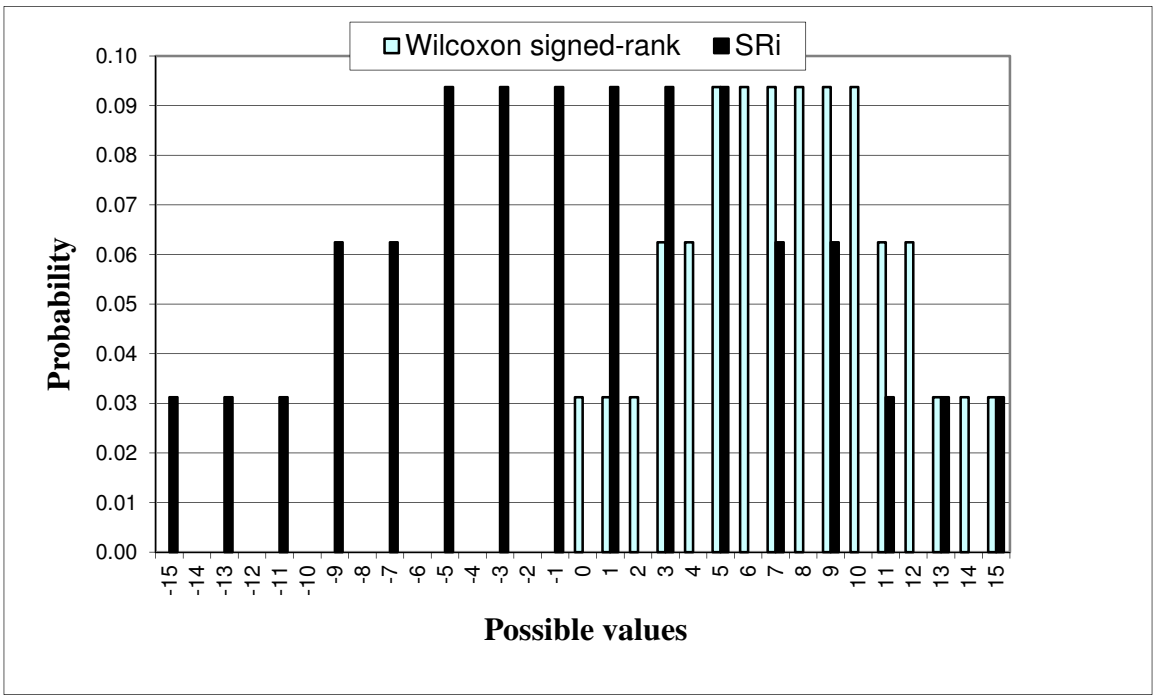

Figure 3.12. The IC probability distribution of T_n^+ and SR_i for $n = 5$

3.3.3 The NPEWMA-SR control chart

3.3.3.1 Design of the chart

The proposed NPEWMA-SR chart is an analog of the parametric EWMA chart given in Section 1.9.3 with SR_i substituted for ψ_i in Equation (1.6). The charting statistic of the proposed NPEWMA-SR chart is obtained by sequentially accumulating the statistics $SR_1, SR_2, SR_3, \ldots,$ and is defined as

$$Z_i = \lambda\, SR_i + (1-\lambda)Z_{i-1} \quad \text{for} \quad i = 1,2,3,\ldots \tag{3.18}$$

where $0 < \lambda \leq 1$ is a design parameter called the smoothing constant. The starting value, Z_0, which is required with the first sample at $i = 1$, is set equal to the target value or the expected value of Z_i when the process is IC i.e. $Z_0 = 0$ (see Result 3.2 below). Note that $\lambda = 1$ yields the Shewhart-type signed-rank chart of Bakir (2004).

The *CL* and the control limits of the NPEWMA-SR chart are functions of the IC mean and the IC standard deviation of the charting statistic, Z_i, which are given in the following result.

Result 3.2

$E(Z_i|\text{IC}) = 0$ and $\sigma_{Z_i|\text{IC}} = \sqrt{\left(\frac{n(n+1)(2n+1)}{6}\right)\left(\frac{\lambda}{2-\lambda}\right)(1-(1-\lambda)^{2i})}$, respectively.

Proof

These values are obtained as follows. By the definition of the charting statistic (see Equation (3.18)) and using recursive substitution (see Appendix 1A) we obtain the following result:

$$E(Z_i|\text{IC}) = E(\lambda SR_i + (1-\lambda)Z_{i-1}|\text{IC}) = E\left(\lambda\sum_{j=0}^{i-1}(1-\lambda)^j SR_{i-j} + (1-\lambda)^i Z_0|\text{IC}\right)$$

Using the fact that $E\left(SR_{i-j}|\text{IC}\right) = 0$ (see Table 3.10) and $Z_0 = 0$ we have that

$$E(Z_i|\text{IC}) = \lambda\sum_{j=0}^{i-1}(1-\lambda)^j E\left(SR_{i-j}|\text{IC}\right) + (1-\lambda)^i Z_0 = 0.$$

In order to obtain the variance similar steps are followed, i.e. we once again use the definition of the charting statistic (see Equation (3.18)) and recursive substitution (see Appendix 1A). However, we also use the result for the sum of a finite geometric series (see Equation (A1.4) in Appendix 1A) and the fact that $VAR(SR_i|\text{IC}) = \frac{n(n+1)(2n+1)}{6}$ (see Table 3.10). Consequently, we have that

$$\begin{aligned}
VAR(Z_i|\text{IC}) &= VAR\left(\lambda\sum_{j=0}^{i-1}(1-\lambda)^j SR_{i-j} + (1-\lambda)^i Z_0|\text{IC}\right)\\
&= \lambda^2\sum_{j=0}^{i-1}(1-\lambda)^{2j} VAR\left(SR_{i-j}|\text{IC}\right)\\
&= \left(\frac{n(n+1)(2n+1)}{6}\right)\lambda^2\sum_{j=0}^{i-1}(1-\lambda)^{2j}\\
&= \left(\frac{n(n+1)(2n+1)}{6}\right)\lambda^2\left(\frac{1-(1-\lambda)^{2i}}{1-(1-\lambda)^2}\right)
\end{aligned}$$

Therefore, $STDEV(Z_i|\text{IC}) = \sqrt{\left(\frac{n(n+1)(2n+1)}{6}\right)\left(\frac{\lambda}{2-\lambda}\right)(1-(1-\lambda)^{2i})}$.

In analogy with the parametric EWMA, the exact control limits and the *CL* of the NPEWMA-SR control chart are thus given by

$$UCL = E(Z_i|\text{IC}) + L\sigma_{Z_i|\text{IC}} = +L\sqrt{\left(\frac{n(n+1)(2n+1)}{6}\right)\left(\frac{\lambda}{2-\lambda}\right)(1-(1-\lambda)^{2i})}$$

$$CL = E(Z_i|\text{IC}) = 0 \tag{3.19}$$

$$LCL = E(Z_i|\text{IC}) - L\sigma_{Z_i|\text{IC}} = -L\sqrt{\left(\frac{n(n+1)(2n+1)}{6}\right)\left(\frac{\lambda}{2-\lambda}\right)(1-(1-\lambda)^{2i})}$$

where $L > 0$ is a charting constant. The steady-state control limits (which are typically used when the NPEWMA-SR chart has been running for several time periods so that the term $\left(1-(1-\lambda)^{2i}\right)$ in (3.19) approaches unity) are given by

$$UCL = +L\sqrt{\left(\frac{n(n+1)(2n+1)}{6}\right)\left(\frac{\lambda}{2-\lambda}\right)}$$

and (3.20)

$$LCL = -L\sqrt{\left(\frac{n(n+1)(2n+1)}{6}\right)\left(\frac{\lambda}{2-\lambda}\right)}.$$

The NPEWMA-SR chart is a plot of the Z_i's (together with the *CL* and the control limits) on the vertical axis versus the sample number or time, i, on the horizontal axis. If any Z_i plots on or outside either of the two control limits the process is declared to be OOC and a search for assignable causes is started. Otherwise, the process is considered IC and the charting procedure continues. It should be noted that because T_n^+ is known to be distribution-free for all symmetric continuous distributions (see e.g. Gibbons and Chakraborti (2010) page 195) so is the statistic *SR* and hence the NPEWMA-SR chart. In the developments that follow:

i. We study two-sided charts with symmetrically placed control limits i.e. equidistant from the *CL*. This is the typical application of the EWMA-$\overline{X}$ chart. The methodology can be easily modified where a one-sided chart is more meaningful (this is illustrated in Section 1.9.3).

ii. Use the steady-state control limits; this significantly simplifies the calculation of the run-length distribution via the Markov chain approach and will be discussed in more detail below. However, it should be noted that using the exact control limits with say, simulation, will give more accurate results.

iii. We investigate the entire run-length distribution in terms of the mean (*ARL*), the standard deviation (*SDRL*), the median run-length (*MRL*), the 1st and the 3rd quartiles as well as the 5th and the 95th percentiles (Amin and Searcy (1991) only evaluated the *ARL*). It's a well-known fact that important information about the performance of a control chart may be missed by focusing only on the *ARL*, because the run-length distribution is highly right-skewed (see e.g. Radson and Boyd (2005) and Chakraborti (2007)).

Run-length distribution

We use a Markov chain approach (see Section 1.10.1) to evaluate / approximate the run-length distribution of the NPEWMA-SR chart. The Markov chain approach is discussed in detail in Section 1.10.1 (in general) and in Section 3.2.3 (for the NPEWMA-SN chart). Accordingly, the reader is referred to those sections and we simply derive the one-step transition probabilities here. By substituting the charting statistic given in Equation (3.18) into the general formulae for one-step transition probabilities given in Equation (3.12) we obtain

$$\begin{aligned} &P\left(S_j-\tau<\lambda SR_k+(1-\lambda)Z_{k-1}\le S_j+\tau \mid Z_{k-1}=S_i\right)\\ &=P\left(S_j-\tau<\lambda SR_k+(1-\lambda)S_i\le S_j+\tau\right)\\ &=P\left(\frac{\left(S_j-\tau\right)-(1-\lambda)S_i}{\lambda}<SR_k\le\frac{\left(S_j+\tau\right)-(1-\lambda)S_i}{\lambda}\right)\\ &=P\left(\left(\frac{(S_j-\tau)-(1-\lambda)S_i}{\lambda}+\frac{n(n+1)}{2}\right)/2<T_n^+\le\left(\frac{(S_j+\tau)-(1-\lambda)S_i}{\lambda}+\frac{n(n+1)}{2}\right)/2\right). \end{aligned}$$

Since the values τ, λ, S_i and S_j are known constants, (λ is chosen by the practitioner and τ, S_i and S_j are calculated), the probability above can easily be calculated.

3.3.3.2 Implementation of the chart

The reader is referred to Section 1.9.3 for a detailed discussion on the choice of the design parameters, λ and L. Here we simply state that three values of λ, corresponding to small (roughly

0.5 standard deviations or less), moderate (roughly between 0.5 and 1.5 standard deviations) and large shifts (roughly 1.5 standard deviations or more), were used along with values of L ranging from 2 to 3 in increments of 0.1 for subgroup sizes $n = 5$ and 10 (for a detailed discussion on the choice of n see Bakir and Reynolds (1979) wherein they concluded that the best subgroup size is somewhere between 5 and 10 depending on the desired ARL_0 and the size of the shift to be detected).

Tables 3.11 and 3.12 give the IC run-length characteristics for the NPEWMA-SR chart for $n = 5$ and 10, respectively, and we observe that for a specified / fixed value of λ, the ARL_0 and other characteristics of the IC run-length distribution all increase as L increases. Also, the IC run-length distribution is positively skewed (as is expected) since $ARL_0 > MRL_0$ for all combinations of (λ, L). These tables are useful for a practical implementation of the control chart. For example, from Table 3.11 for $n = 5$, we observe that for ($\lambda = 0.05$, $L = 2.6$) the $ARL_0 = 496.96$ and for ($\lambda = 0.05$, $L = 2.7$) the $ARL_0 = 640.44$, which implies that the value of L that leads to an ARL_0 of 500 is between 2.6 and 2.7 and close to 2.6. Refining the search algorithm leads to ($\lambda = 0.05$, $L = 2.602$) with an ARL_0 of 499.83 (see Table 3.13); more details are given below.

Table 3.11. Performance characteristics[ix] of the IC run-length distribution for the NPEWMA-SR chart with $n = 5$

L	**Small shifts**	**Moderate shifts**	**Large shifts**
	$\lambda = 0.05$	**$\lambda = 0.10$**	**$\lambda = 0.20$**
2.0	127.18 (117.83) 15, 43, 91, 173, 362	73.72 (68.60) 9, 25, 53, 100, 211	46.05 (43.21) 5, 15, 33, 63, 132
2.1	156.62 (146.42) 17, 52, 112, 213, 449	91.51 (85.95) 10, 30, 65, 125, 263	58.07 (54.94) 6, 19, 41, 79, 168
2.2	194.21 (183.14) 20, 64, 138, 265, 560	114.41 (108.39) 12, 37, 81, 156, 331	73.92 (70.50) 7, 24, 52, 101, 215
2.3	242.64 (230.66) 24, 78, 172, 332, 703	144.31 (137.82) 14, 46, 102, 198, 419	95.16 (91.52) 8, 30, 67, 131, 278
2.4	305.68 (292.78) 28, 97, 216, 419, 890	183.97 (177.00) 16, 58, 130, 252, 537	123.83 (119.93) 10, 38, 87, 170, 363
2.5	386.96 (373.15) 33, 121, 273, 531, 1132	236.12 (228.68) 19, 73, 166, 324, 692	163.43 (159.27) 12, 50, 115, 225, 481
2.6	496.96 (481.21) 39, 153, 348, 682, 1456	307.15 (299.22) 23, 94, 215, 423, 904	220.15 (215.72) 16, 66, 154, 303, 651
2.7	640.44 (624.75) 48, 195, 449, 882, 1887	404.57 (396.15) 29, 122, 283, 558, 1195	300.03 (295.35) 20, 90, 209, 414, 889
2.8	838.61 (821.99) 59, 253, 586, 1156, 2479	541.06 (532.15) 36, 162, 378, 747, 1603	417.77 (412.83) 26, 124, 291, 577, 1242
2.9	1108.26 (1090.69) 74, 331, 774, 1530, 3285	730.87 (721.46) 46, 217, 510, 1010, 2171	590.31 (585.08) 35, 174, 411, 816, 1758
3.0	1471.46 (1452.99) 93, 437, 1026, 2033, 4371	997.49 (987.60) 61, 294, 694, 1379, 2968	856.39 (850.86) 49, 250, 595, 1185, 2554

[ix] The first row of each cell shows the ARL_0 and $SDRL_0$ values, respectively, whereas the second row shows the values of the in-control 5th, 25th, 50th, 75th and 95th percentiles (in this order).

Table 3.12. Performance characteristics[x] of the IC run-length distribution for the NPEWMA-SR chart with $n = 10$

L	Small shifts	Moderate shifts	Large shifts
	$\lambda = 0.05$	$\lambda = 0.10$	$\lambda = 0.20$
2.0	526.24 (484.78) 64, 182, 378, 714, 1493	230.19 (212.76) 28, 79, 165, 312, 655	127.34 (118.12) 15, 43, 91, 173, 363
2.1	643.37 (597.91) 74, 218, 461, 875, 1836	282.21 (263.15) 32, 95, 202, 384, 807	156.79 (146.74) 17, 52, 112, 214, 450
2.2	790.58 (740.97) 86, 264, 564, 1077, 2269	347.75 (327.01) 37, 115, 248, 474, 1000	193.83 (182.93) 20, 64, 138, 265, 559
2.3	976.99 (923.11) 100, 320, 694, 1334, 2819	431.42 (408.95) 43, 140, 306, 590, 1247	241.48 (229.70) 23, 78, 171, 330, 700
2.4	1211.01 (1152.78) 117, 391, 858, 1657, 3511	538.45 (514.21) 50, 172, 381, 737, 1565	302.73 (290.07) 27, 96, 214, 415, 882
2.5	1520.23 (1457.55) 137, 483, 1073, 2083, 4429	676.74 (650.72) 59, 213, 477, 928, 1975	383.02 (369.46) 33, 120, 270, 526, 1120
2.6	1916.65 (1849.51) 162, 600, 1350, 2631, 5607	857.99 (830.16) 70, 267, 603, 1179, 2515	488.46 (473.99) 39, 151, 343, 672, 1434
2.7	2438.25 (2366.61) 193, 753, 1712, 3353, 7161	1096.87 (1067.23) 84, 337, 770, 1509, 3227	630.57 (615.18) 47, 192, 442, 868, 1858
2.8	3131.18 (3055.01) 233, 955, 2194, 4311, 9228	1415.89 (1384.45) 103, 430, 991, 1951, 4179	817.76 (801.47) 57, 247, 572, 1127, 2417
2.9	4056.22 (3975.58) 285, 1225, 2837, 5592, 11990	1853.14 (1819.89) 127, 557, 1295, 2556, 5485	1076.12 (1058.94) 72, 322, 751, 1485, 3189
3.0	5298.98 (5213.92) 353, 1585, 3699, 7313, 15704	2430.95 (2395.95) 158, 724, 1696, 3357, 7213	1427.59 (1409.53) 90, 424, 995, 1972, 4241

With regard to the implementation of the NPEWMA-SR chart, the first step is to choose λ. The recommendation (see Section 1.9.3) is to choose a small λ, say equal to 0.05, when small shifts are of interest, if moderate shifts are of greater concern, choose $\lambda = 0.10$, whereas choose $\lambda = 0.20$ if larger shifts are of interest. Note that these recommendations are consistent with those for the EWMA-$\overline{X}$ chart (see e.g. Montgomery (2009) page 423)). After λ is chosen, the second step involves choosing L, so that a desired ARL_0 is attained.

In order to aid the practitioner in the design of the NPEWMA-SR chart, Table 3.13 lists some (λ, L)-combinations for popular nominal ARL_0 values of 370 and 500 and $n = 5$ and 10. In each case, the ARL_0 values, obtained using the Markov chain approach, called the attained ARL_0 values, are also provided. Note that because of the discreteness of the sign statistic, the nominal ARL values are not attained exactly, however, it is remarkable that the NPEWMA-SR chart can attain ARL_0 values pretty close to the nominal values which make these charts useful in practice.

[x] The first row of each cell shows the ARL_0 and $SDRL_0$ values, respectively, whereas the second row shows the values of the in-control 5th, 25th, 50th, 75th and 95th percentiles (in this order).

Table 3.13. (λ, L)-combinations for the NPEWMA-SR chart[1] for nominal ARL_0 = 370 and 500

	Nominal ARL_0 = 370		Nominal ARL_0 = 500	
Shift to be detected	**(λ, L)**	**Attained ARL_0**	**(λ, L)**	**Attained ARL_0**
	n = 5			
Small	(0.05, 2.481)	370.29	(0.05, 2.602)	499.83
Moderate	(0.10, 2.668)	370.13	(0.10, 2.775)	500.11
Large	(0.20, 2.764)	369.91	(0.20, 2.852)	499.27
	n = 10			
Small	(0.05, 2.486)	370.49	(0.05, 2.610)	500.67
Moderate	(0.10, 2.684)	370.09	(0.10, 2.794)	500.13
Large	(0.20, 2.810)	370.19	(0.20, 2.905)	498.92

[1] Table 3.13 is more extensive and unlike in Amin and Searcy (1991) who give some (λ, UCL)-values.

So, for example, suppose n = 5 and one is interested in detecting a small shift in the location with a NPEWMA-SR with an ARL_0 of 370. Then one can use the (λ, L)-combination: (0.05, 2.481) which yields an attained ARL_0 of 370.29. Table 3.13 should be very useful for implementing the NPEWMA-SR chart in practice. A SAS® program is provided (see Appendix 3C) if the practitioner wishes to obtain some other (λ, L)-combinations for other nominal ARL_0 values.

3.3.3.3 Performance comparison with other charts

In-control robustness

The IC performance of a chart is typically used to assess its robustness (i.e. the sensitivity of or, the change in, the properties of the run-length distribution) to different distributional assumptions whereas the OOC performance of the chart is examined to assess its efficacy in detecting a shift in the underlying process.

This study includes only symmetric distributions, since the assumption of symmetry is needed for WSR and signed-rank test statistics. Note that, wherever necessary, all distributions have been shifted and scaled such that the mean / median equals 0 and the standard deviation equals 1, so that the results are easily comparable across the distributions. The details for these steps are shown in Appendix 1B. Specifically, the distributions considered in the study are:

i. The Standard Normal distribution, $N(0,1)$.

ii. The Student's t-distribution, $t(\nu)$, with degrees of freedom $\nu = 4$ and 8, respectively, which is symmetric but with heavier tails than the Normal.

iii. The Laplace (or Double Exponential) distribution, $DE(0,1/\sqrt{2})$.

iv. The Logistic distribution, $LG(0,\sqrt{3}/\pi)$.

v. The Contaminated Normal (CN) distribution, which is a linear combination of two Normal random variables with the same location but different variance:

$$0.95N\left(0,\frac{1}{1.15}\right) + 0.05N\left(0,\frac{4}{1.15}\right)$$

where the σ_i's are chosen so that the standard deviation of the distribution equals 1, that is, $0.95\sigma_1^2 + 0.05\sigma_2^2 = 1$. We consider the case where $\sigma_2/\sigma_1 = 2$. The contaminated normal distribution is often used to study the effects of outliers.

The NPEWMA-SR chart is compared to the parametric EWMA-$\overline{X}$ chart and the nonparametric EWMA-SN chart. Because the NPEWMA-SR and the NPEWMA-SN charts are nonparametric, the IC run-length distribution and the associated characteristics should remain the same for all symmetric continuous distributions. A Markov chain approach was used in the calculations for the two NPEWMA charts whereas for the EWMA-$\overline{X}$ chart, the values of the IC run-length characteristics were estimated using 100 000 simulations as the exact closed-form expressions for the run-length distribution is not available for all the distributions considered in the study; the main stumbling block being the exact distribution of the mean (i.e $\overline{X}$) for small subgroup sizes. The results are shown in Table 3.14 for $\lambda = 0.05$, 0.10 and 0.20, respectively, and $n = 10$. Note that, the values of L were chosen such that in each case $ARL_0 \approx 500$ and, in case of the EWMA-$\overline{X}$ chart, the values of L were chosen (using a search algorithm) such that the $ARL_0 \approx 500$ when the underlying distribution is $N(0,1)$. The first row of each cell in Table 3.14 shows the ARL_0 and $SDRL_0$ values, respectively, whereas the second row shows the values of the 5th, 25th, 50th, 75th and 95th percentiles (in this order).

Table 3.14. The IC performance characteristics of the run-length distribution for the NPEWMA-SR, the NPEWMA-SN and the EWMA-$\overline{X}$ charts for selected (λ, L)-combinations and $n = 10$

NPEWMA-SR			
(λ, L)	**(0.05, 2.610)**	**(0.10, 2.794)**	**(0.20, 2.905)**
For all symmetric continuous distributions	500.67 (486.10) 40, 154, 352, 688, 1471	500.13 (491.61) 34, 150, 349, 690, 1481	498.92 (494.15) 30, 147, 347, 690, 1485
NPEWMA-SN			
(λ, L)	**(0.05, 2.612)**	**(0.10, 2.797)**	**(0.20, 2.933)**
For all continuous distributions	501.04 (486.58) 39, 155, 352, 689, 1472	500.25 (491.88) 34, 150, 349, 690, 1482	499.64 (495.00) 30, 147, 348, 691, 1488
EWMA-$\overline{X}$			
Dist **(λ, L)**	**(0.05, 2.613)**	**(0.10, 2.815)**	**(0.20, 2.962)**
***N*(0,1)**	496.37 (482.62) 39, 152, 350, 681, 1462	498.96 (490.01) 34, 149, 349, 689, 1475	497.31 (492.20) 30, 147, 346, 688, 1479
***t*(4)**	480.84 (470.36) 38, 148, 337, 661, 1421	441.57 (436.35) 29, 131, 308, 608, 1309	367.65 (365.04) 22, 108, 255, 509, 1094
***t*(8)**	494.13 (478.31) 39, 153, 349, 682, 1445	490.80 (479.81) 33, 147, 344, 678, 1445	471.10 (466.43) 28, 137, 329, 653, 1407
Laplace	491.87 (479.56) 39, 150, 345, 675, 1450	477.52 (473.51) 32, 142, 331, 657, 1423	438.70 (434.15) 26, 129, 305, 607, 1300
Logistic	491.81 (479.10) 39, 152, 345, 677, 1452	491.58 (485.19) 33, 147, 342, 676, 1462	473.63 (471.09) 28, 138, 328, 654, 1416
CN	494.67 (479.24) 39, 152, 349, 683, 1448	487.51 (477.50) 33, 148, 343, 671, 1438	476.14 (473.16) 29 ,140, 331, 662, 1411

For a better understanding of the way the values are presented in Table 3.14, let us consider the first cell. The value of $ARL_0 = 500.67$ in the first row indicates that, for the NPEWMA-SR chart with design parameters $\lambda = 0.05$ and $L = 2.610$, when the process is IC, the first false alarm would be observed, on average, at every 501st plotted point. The first quartile is 154, so we know that a false alarm will not occur within the first 154 plotted points, with a probability of at most 75%. As another example, the $MRL_0 = 352$, which indicates that the first false alarm will be observed, within the first 352 plotted points, at least 50% of the time.

For a visual presentation of the IC run-length distributions, the values of Table 3.14 were used to construct boxplot-like graphs (see Radson and Boyd (2005)) shown in Figure 3.13. Each boxplot shows the mean of the run-length distribution as a square and the median as a circle inside the box and the 'whiskers' are extended to the 5th and the 95th percentiles instead of the usual minimum and maximum. Note that only one boxplot is shown for each of the two NPEWMA charts (the first two boxplots on the left), because their IC run-length characteristics are the same for all symmetric continuous distributions and that a reference line was inserted on the vertical axis at 500, which is the desired nominal ARL_0 value in this case.

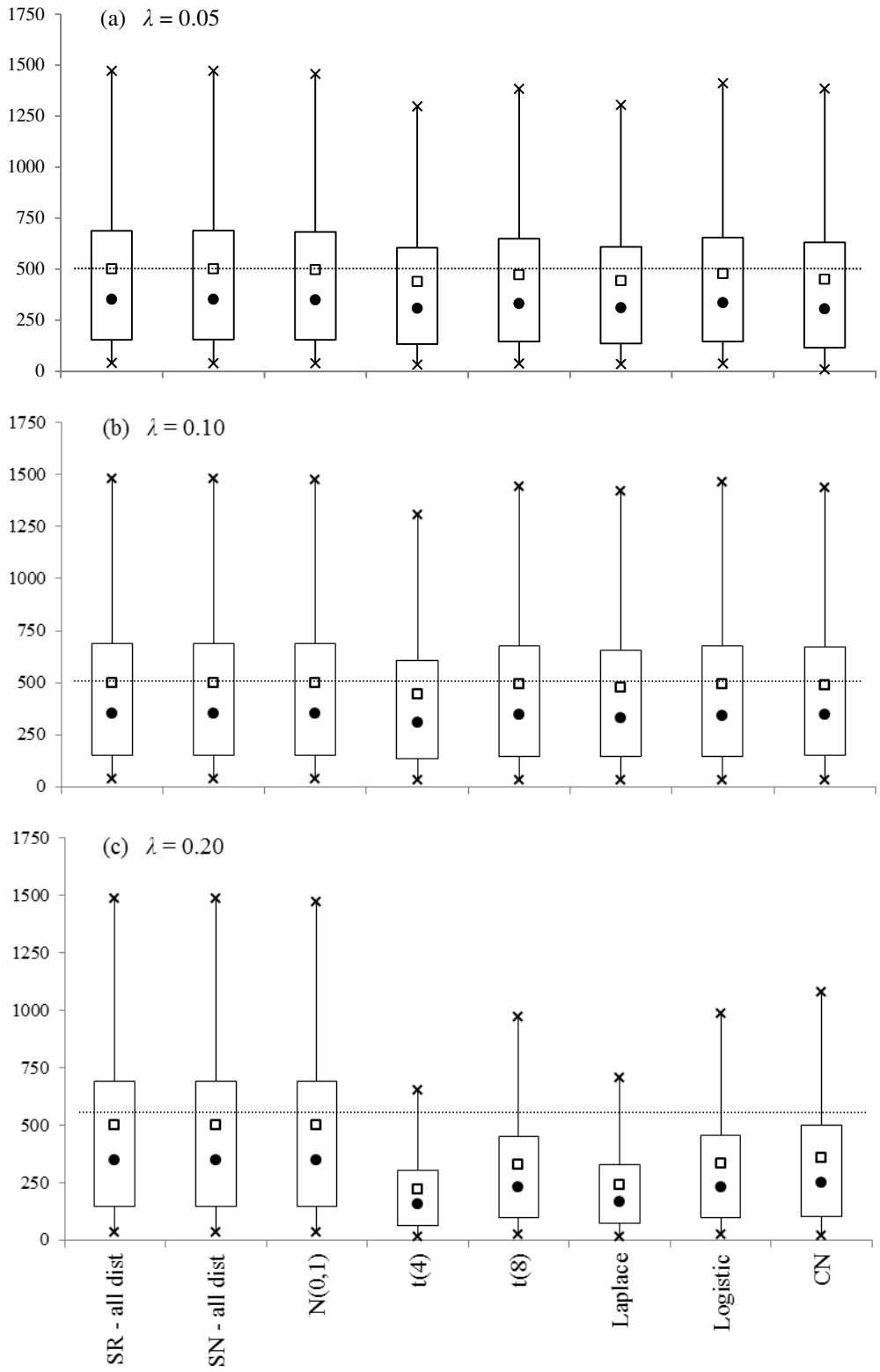

Figure 3.13[xi]. Boxplot-like graphs of the IC run-length distributions of the NPEWMA-SR chart (first boxplot on the left), the NPEWMA-SN chart (second boxplot to the left) and the EWMA- $\overline{X}$ chart (remaining 6 boxplots on the right)

[xi]Panel (a): NPEWMA-SR (λ=0.05, L=2.610); NPEWMA-SN (λ=0.05, L=2.612); EWMA- $\overline{X}$ (λ=0.05, L=2.613)
Panel (b): NPEWMA-SR (λ=0.10, L=2.794); NPEWMA-SN (λ=0.10, L=2.797); EWMA- $\overline{X}$ (λ=0.10, L=2.815)
Panel (c): NPEWMA-SR (λ=0.20, L=2.905); NPEWMA-SN (λ=0.20, L=2.933); EWMA- $\overline{X}$ (λ=0.20, L=2.962)

Several interesting observations can be made from Table 3.14 and Figure 3.13:

i. As expected, both NPEWMA charts are IC robust for all λ and for all distributions under consideration, including the *CN* distribution, indicating that the nonparametric charts are more resistant to outliers. Also, the IC run-length distributions of the NPEWMA-SN and the NPEWMA-SR charts look almost identical.

ii. The EWMA-$\overline{X}$ chart is not IC robust and its run-length distribution has a higher variance as seen from the interquartile ranges. Its IC characteristics vary (sometimes dramatically) as the underlying distribution changes. For example, focusing on the ARL_0 as a measure of location, for $\lambda = 0.20$ (see Figure 3.13 (c) and Table 3.14) the ARL_0 of the EWMA-$\overline{X}$ chart varies from 497.31 (when the underlying distribution is $N(0,1)$) to 367.65 (when the underlying distribution is $t(4)$). In addition, for $\lambda = 0.20$, the ARL_0 values of the EWMA-$\overline{X}$ chart are much smaller than 500 (farther below the reference line) for all distributions other than the normal. This is problematic as there will be many more false alarms than what is nominally expected.

iii. The EWMA-$\overline{X}$ chart appears to be less IC robust for larger values of λ, especially for the *CN* distribution. Thus, this chart may be problematic when outliers are likely to be present.

Out-of-control chart performance

For the OOC chart performance comparison it is customary to ensure that the ARL_0 values of the competing charts are fixed at (or very close to) an acceptably high value, such as 500 in this case, and then compare their out-of-control *ARL*'s (denoted ARL_δ) values, for specific values of the shift δ; the chart with the smaller ARL_δ value is generally preferred. We compare the NPEWMA-SR chart to the NPEWMA-SN chart and the EWMA-$\overline{X}$ chart with known parameters (see Roberts (1959) and Steiner (1999)).

Tables 3.15, 3.16 and 3.17 give the OOC characteristics of the run-length distribution for the EWMA-$\overline{X}$ chart, the NPEWMA-SN chart and the NPEWMA-SR chart, respectively, for n = 10 and γ = 0.5(0.5)2.0. Note that negative shifts are not considered in this section since, for symmetric distributions, the direction of the shift does not seem to affect the detection capability of the charts (see Section 3.2.3 for a detailed discussion on this point).

It may be noted that in order for the NPEWMA-SR chart to be able to signal after one subgroup (i.e. to obtain an ARL_δ of 1), the maximum allowable value for the UCL is $\lambda n(n+1)/2$ and, in general, in order for the chart to be able to signal after the i^{th} subgroup, the maximum allowable UCL is $(1-(1-\lambda)^i)n(n+1)/2$. This result can be established by substituting the maximum value of SR_i (which equals $n(n+1)/2$) into Equation (3.18) and rewriting the charting statistic as $Z_i = \lambda\sum_{j=0}^{i-1}(1-\lambda)^j SR_{i-j} + (1-\lambda)^i Z_0$. Thus, the first time the chart can signal is on the subgroup number i such that

$$i \geq \frac{ln(1-2UCL/(n(n+1))}{ln(1-\lambda)}. \qquad (3.21)$$

The proof to the restriction is given in Appendix 3A. For example, for n = 10, λ = 0.05 and L = 2.610 (this (λ, L)-combination can be used for a desired ARL_0 of 500 (see Table 3.13)) we get UCL = 8.200 from Equation (3.20) and then the right-hand side of (3.21) equals 3.148. Thus the NPEWMA-SR chart can only signal for the first time on or beyond subgroup number 4 when n = 10 and λ = 0.05, which is confirmed from Table 3.17. A similar restriction applies to the performance of the NPEWMA-SN chart (see Equation (3.15)).

Table 3.15. OOC characteristics[xii] of the run-length distribution for the EWMA-$\overline{X}$ control chart for $n = 10$

Distribution	Shift (γ)	0.5	1.0	1.5	2.0	Shift (γ)	0.5	1.0	1.5	2.0
	L	$\lambda = 0.05$				*L*	$\lambda = 0.10$			
***N*(0,1)**	**2.613**	28.35 (15.45) 11, 17, 25, 35, 58	11.32 (4.26) 6, 8, 11, 13, 19	7.14 (2.06) 4, 6, 7, 8, 11	5.22 (1.26) 4, 4, 5, 6, 8	**2.815**	31.58 (4.80) 8, 15, 25, 40, 77	10.39 (4.850) 5, 7, 9, 13, 19	6.08 (2.12) 3, 5, 6, 7, 10	4.37 (1.24) 3, 4, 4, 5, 7
***t*(4)**	**2.682**	30.94 (17.73) 11, 18, 27, 39, 65	11.76 (4.21) 6, 9, 11, 14, 20	7.31 (1.94) 5, 6, 7, 8, 11	5.44 (1.01) 4, 5, 5, 6, 7	**2.865**	33.23 (24.24) 8, 16, 27, 43, 81	10.64 (4.88) 5, 7, 10, 13, 20	6.21 (2.13) 3, 5, 6, 7, 10	4.76 (1.20) 3, 4, 5, 5, 7
***t*(8)**	**2.640**	29.53 (16.99) 10, 18, 25, 37, 62	11.50 (4.22) 6, 9, 11, 14, 19	7.18 (2.05) 4, 6, 7, 8, 11	5.27 (1.27) 4, 4, 5, 6, 8	**2.824**	31.71 (22.69) 8, 16, 25, 41, 76	10.43 (4.80) 5, 7, 9, 13, 20	6.10 (2.14) 3, 5, 6, 7, 10	4.38 (1.25) 3, 4, 4, 5, 7
Laplace	**2.666**	30.48 (17.58) 11, 18, 26, 38, 65	11.68 (4.27) 6, 9, 11, 14, 20	7.24 (2.05) 4, 6, 7, 8, 11	5.61 (1.27) 4, 4, 5, 6, 8	**2.830**	32.12 (23.25) 8, 16, 26, 42, 78	10.40 (4.71) 5, 7, 9, 13, 19	6.13 (2.09) 3, 5, 6, 7, 10	4.68 (1.27) 3, 3, 4, 5, 7
Logistic	**2.635**	29.46 (17.00) 10, 17, 25, 37, 62	11.47 (4.22) 6, 8, 11, 14, 19	7.17 (2.05) 4, 6, 7, 8, 11	5.26 (1.27) 4, 4, 5, 6, 8	**2.820**	31.51 (22.84) 8, 15, 25, 41, 77	10.39 (4.79) 5, 7, 9, 13, 20	6.09 (2.11) 3, 5, 6, 7, 10	4.39 (1.25) 3, 4, 4, 5, 7
CN	**2.656**	24.49 (18.26) 3, 11, 20, 33, 59	7.42 (4.73) 2, 4, 6, 10, 16	3.82 (2.20) 1, 2, 3, 5, 8	2.45 (1.28) 1, 2, 2, 3, 5	**2.825**	31.68 (23.33) 8, 16, 25, 41, 77	10.38 (4.77) 5, 7, 9, 13, 19	6.11 (2.13) 3, 5, 6, 7, 10	4.36 (1.24) 3, 3, 4, 5, 7
	L	$\lambda = 0.20$								
***N*(0,1)**	**2.962**	41.46 (35.53) 7, 17, 31, 54, 112	10.53 (6.31) 4, 6, 9, 13, 23	5.55 (2.57) 3, 4, 5, 7, 10	3.75 (1.34) 2, 3, 4, 4, 6					
***t*(4)**	**3.100**	52.40 (46.45) 8, 19, 39, 70, 146	11.89 (7.29) 4, 7, 10, 15, 26	5.91 (2.69) 3, 4, 5, 7, 11	4.08 (1.36) 2, 3, 4, 5, 7					
***t*(8)**	**2.983**	43.30 (37.35) 7, 17, 32, 57, 120	10.63 (6.49) 4, 6, 9, 13, 23	5.54 (2.42) 3, 4, 5, 7, 10	3.79 (1.32) 2, 5, 4, 4, 6					
Laplace	**3.005**	45.07 (39.71) 7, 17, 33, 60, 124	11.02 (6.76) 4, 6, 9, 14, 25	5.62 (2.48) 3, 4, 5, 7, 10	3.95 (1.36) 2, 3, 4, 4, 6					
Logistic	**2.980**	42.98 (37.49) 7, 16, 31, 57, 120	10.69 (6.48) 4, 6, 9, 13, 24	5.56 (2.43) 3, 4, 5, 7, 10	3.77 (1.35) 2, 3, 4, 4, 6					
CN	**2.981**	42.92 (37.08) 7, 17, 32, 57, 117	10.73 (6.64) 4, 6, 9, 13, 24	5.53 (2.44) 3, 4, 5, 7, 10	3.78 (1.33) 2, 3, 4, 4, 6					

[xii] The first row of each cell shows the *ARL* and *SDRL* values, respectively, whereas the second row shows the values of the 5th, 25th, 50th, 75th and 95th percentiles (in this order).

Table 3.16. OOC characteristics[xiii] of the run-length distribution for the NPEWMA-SN control chart for $n = 10$

Shift (γ)	0.5	1.0	1.5	2.0	0.5	1.0	1.5	2.0
Distribution	$\lambda = 0.05$ and $L = 2.612$				$\lambda = 0.10$ and $L = 2.797$			
***N*(0,1)**	41.33 (26.47) 13, 22, 34, 54, 93	15.48 (6.60) 7, 11, 14, 19, 28	9.43 (3.15) 5, 7, 9, 11, 15	7.10 (1.85) 5, 6, 7, 8, 11	46.29 (35.01) 10, 21, 37, 60, 118	14.87 (7.64) 6, 9, 13, 19, 30	8.37 (3.18) 4, 6, 8, 10, 14	6.11 (1.99) 4, 5, 6, 7, 10
***t*(4)**	26.62 (14.77) 10, 16, 23, 33, 55	11.08 (3.81) 6, 8, 10, 13, 18	7.29 (2.01) 5, 6, 7, 8, 11	5.34 (1.25) 3, 4, 5, 5, 7	28.70 (19.95) 8, 15, 23, 37, 67	9.98 (4.30) 5, 7, 9, 12, 18	6.20 (1.96) 4, 5, 6, 7, 10	4.50 (0.98) 3, 4, 4, 5, 6
***t*(8)**	34.35 (20.70) 12, 20, 29, 43, 74	13.41 (5.31) 7, 10, 12, 16, 24	8.49 (2.53) 5, 7, 8, 10, 13	6.47 (1.55) 4, 5, 6, 7, 9	38.43 (29.33) 9, 18, 30, 50, 97	12.58 (6.25) 5, 8, 11, 15, 25	7.42 (2.71) 4, 5, 7, 9, 12	5.45 (1.55) 4, 4, 5, 6, 8
Laplace	20.42 (10.15) 8, 13, 18, 25, 40	9.71 (3.12) 6, 7, 9, 11, 15	6.82 (1.71) 5, 6, 7, 8, 10	5.56 (1.14) 4, 5, 5, 6, 8	20.96 (12.98) 7, 12, 18, 26, 46	8.55 (3.43) 4, 6, 8, 10, 15	5.82 (1.76) 4, 5, 6, 7, 9	4.64 (1.13) 3, 4, 4, 5, 7
Logistic	33.52 (20.62) 11, 19, 28, 43, 75	13.31 (5.15) 7, 10, 12, 16, 23	8.39 (2.417) 5, 7, 8, 10, 13	6.40 (1.52) 4, 5, 6, 7, 9	37.27 (27.87) 9, 18, 29, 49, 93	12.24 (5.88) 5, 8, 11, 15, 24	7.31 (2.61) 4, 5, 7, 9, 12	5.39 (1.55) 4, 4, 5, 6, 8
CN	37.76 (23.62) 12, 21, 32, 47, 83	14.59 (5.95) 7, 10, 14, 18, 26	9.13 (2.81) 5, 7, 9, 11, 14	6.82 (1.70) 5, 6, 7, 8, 10	43.12 (33.37) 10, 19, 34, 57, 109	13.75 (7.12) 6, 9, 12, 17, 28	7.92 (3.00) 4, 6, 7, 9, 14	5.75 (1.70) 4, 5, 5, 7, 9
	$\lambda = 0.20$ and $L = 2.933$							
***N*(0,1)**	68.76 (65.55) 10, 24, 49, 91, 199	16.67 (11.72) 4, 8, 13, 22, 39	8.01 (4.19) 3, 5, 7, 10, 16	5.35 (2.18) 3, 4, 5, 6, 10				
***t*(4)**	37.68 (31.72) 7, 15, 28, 50, 102	10.07 (5.84) 4, 6, 9, 13, 21	5.64 (2.35) 3, 4, 5, 7, 10	4.07 (1.31) 2, 3, 4, 5, 6				
***t*(8)**	53.04 (47.57) 8, 20, 39, 71, 146	13.37 (8.54) 4, 7, 11, 17, 30	6.97 (3.32) 3, 5, 6, 9, 13	4.80 (1.75) 3, 4, 4, 6, 8				
Laplace	25.10 (19.47) 6, 11, 19, 33, 64	8.30 (4.39) 3, 5, 7, 10, 17	5.14 (1.99) 3, 4, 5, 6, 9	3.94 (1.24) 2, 3, 4, 5, 6				
Logistic	51.53 (45.87) 8, 20, 38, 69, 145	13.17 (8.48) 4, 7, 11, 17, 30	6.84 (3.22) 3, 5, 6, 8, 13	4.76 (1.76) 3, 4, 4, 6, 8				
CN	60.25 (52.82) 8, 22, 45, 82, 164	14.92 (10.06) 5, 8, 12, 19, 35	7.60 (3.74) 3, 5, 7, 9, 15	5.12 (1.92) 3, 4, 5, 6, 9				

[xiii] The first row of each cell shows the *ARL* and *SDRL* values, respectively, whereas the second row shows the values of the 5th, 25th, 50th, 75th and 95th percentiles (in this order).

Table 3.17. OOC characteristics[xiv] of the run-length distribution for the NPEWMA-SR control chart for $n = 10$

Shift (γ)	0.5	1.0	1.5	2.0	0.5	1.0	1.5	2.0
Distribution	**$\lambda = 0.05$ and $L = 2.610$**				**$\lambda = 0.10$ and $L = 2.794$**			
***N*(0,1)**	31.14 (18.12) 11, 18, 26, 39, 66	12.55 (4.66) 7, 9, 12, 15, 22	8.06 (2.14) 5, 7, 8, 9, 12	8.18 (1.29) 4, 5, 6, 7, 8	34.28 (25.41) 9, 17, 27, 44, 85	11.50 (5.32) 5, 8, 10, 14, 22	6.91 (2.29) 4, 5, 6, 8, 11	5.17 (1.31) 4, 4, 5, 6, 8
***t*(4)**	23.27 (11.96) 9, 15, 20, 29, 46	10.13 (3.35) 6, 8, 10, 12, 16	6.82 (1.59) 5, 6, 7, 8, 10	4.75 (1.19) 3, 4, 5, 5, 7	24.75 (16.36) 7, 13, 20, 32, 57	8.92 (3.52) 5, 6, 8, 11, 16	5.77 (1.65) 4, 5, 5, 7, 9	4.46 (1.27) 3, 4, 4, 5, 7
***t*(8)**	28.42 (15.41) 11, 18, 25, 35, 57	11.51 (4.05) 6, 9, 11, 14, 19	7.65 (1.94) 5, 6, 7, 9, 11	5.87 (1.17) 4, 5, 6, 7, 8	30.36 (21.21) 8, 15, 25, 39, 72	10.43 (4.50) 5, 7, 9, 13, 19	6.49 (2.03) 4, 5, 6, 8, 10	4.92 (1.17) 3, 4, 5, 6, 7
Laplace	21.84 (10.66) 9, 14, 20, 27, 42	9.83 (3.11) 6, 8, 9, 12, 16	6.87 (1.66) 5, 6, 7, 8, 10	5.53 (1.05) 4, 5, 5, 6, 7	22.59 (14.45) 7, 12, 19, 28, 51	8.67 (3.36) 5, 6, 8, 10, 15	5.79 (1.66) 4, 5, 6, 7, 9	4.55 (1.04) 3, 4, 4, 5, 6
Logistic	28.11 (15.53) 11, 17, 25, 35, 57	11.43 (3.99) 6, 8, 11, 13, 19	7.57 (1.96) 5, 6, 7, 9, 11	5.90 (1.19) 4, 5, 6, 7, 8	30.26 (21.34) 8, 15, 24, 39, 72	10.41 (4.48) 5, 7, 10, 13, 19	6.46 (2.00) 4, 5, 6, 7, 10	4.92 (1.19) 3, 4, 5, 6, 7
CN	30.01 (17.78) 11, 17, 25, 37, 65	12.06 (4.33) 7, 9, 11, 14, 20	7.82 (2.09) 5, 6, 7, 9, 12	6.03 (1.24) 4, 5, 6, 7, 8	33.30 (24.10) 9, 16, 26, 42, 83	10.87 (4.77) 5, 7, 10, 13, 20	6.72 (2.13) 4, 5, 6, 8, 11	5.05 (1.24) 3, 4, 5, 6, 7
	$\lambda = 0.20$ and $L = 2.905$							
***N*(0,1)**	46.99 (40.84) 8, 18, 35, 63, 128	11.86 (7.27) 4, 7, 10, 15, 26	6.36 (2.77) 3, 4, 6, 8, 12	4.49 (1.42) 3, 3, 4, 5, 7				
***t*(4)**	30.54 (24.73) 6, 13, 23, 40, 80	8.60 (4.54) 4, 5, 7, 11, 17	5.06 (1.81) 3, 4, 5, 6, 9	3.83 (1.03) 3, 3, 4, 4, 6				
***t*(8)**	40.39 (34.24) 7, 16, 30, 54, 109	10.68 (6.13) 4, 6, 9, 13, 23	5.83 (2.41) 3, 4, 5, 7, 10	4.21 (1.27) 3, 3, 4, 5, 7				
Laplace	27.59 (22.23) 6, 12, 21, 36, 71	8.34 (4.35) 4, 5, 7, 10, 17	5.04 (1.87) 3, 4, 5, 6, 9	3.88 (1.11) 3, 3, 4, 4, 6				
Logistic	39.66 (33.39) 7, 16, 29, 53, 106	10.53 (6.03) 4, 6, 9, 13, 22	5.83 (2.36) 3, 4, 5, 7, 10	4.19 (1.29) 3, 3, 4, 5, 7				
CN	44.30 (37.44) 8, 17, 33, 60, 117	11.08 (6.43) 4, 7, 9, 14, 24	6.06 (2.57) 3, 4, 5, 7, 11	4.33 (1.36) 3, 3, 4, 5, 7				

[xiv] The first row of each cell shows the *ARL* and *SDRL* values, respectively, whereas the second row shows the values of the 5th, 25th, 50th, 75th and 95th percentiles (in this order).

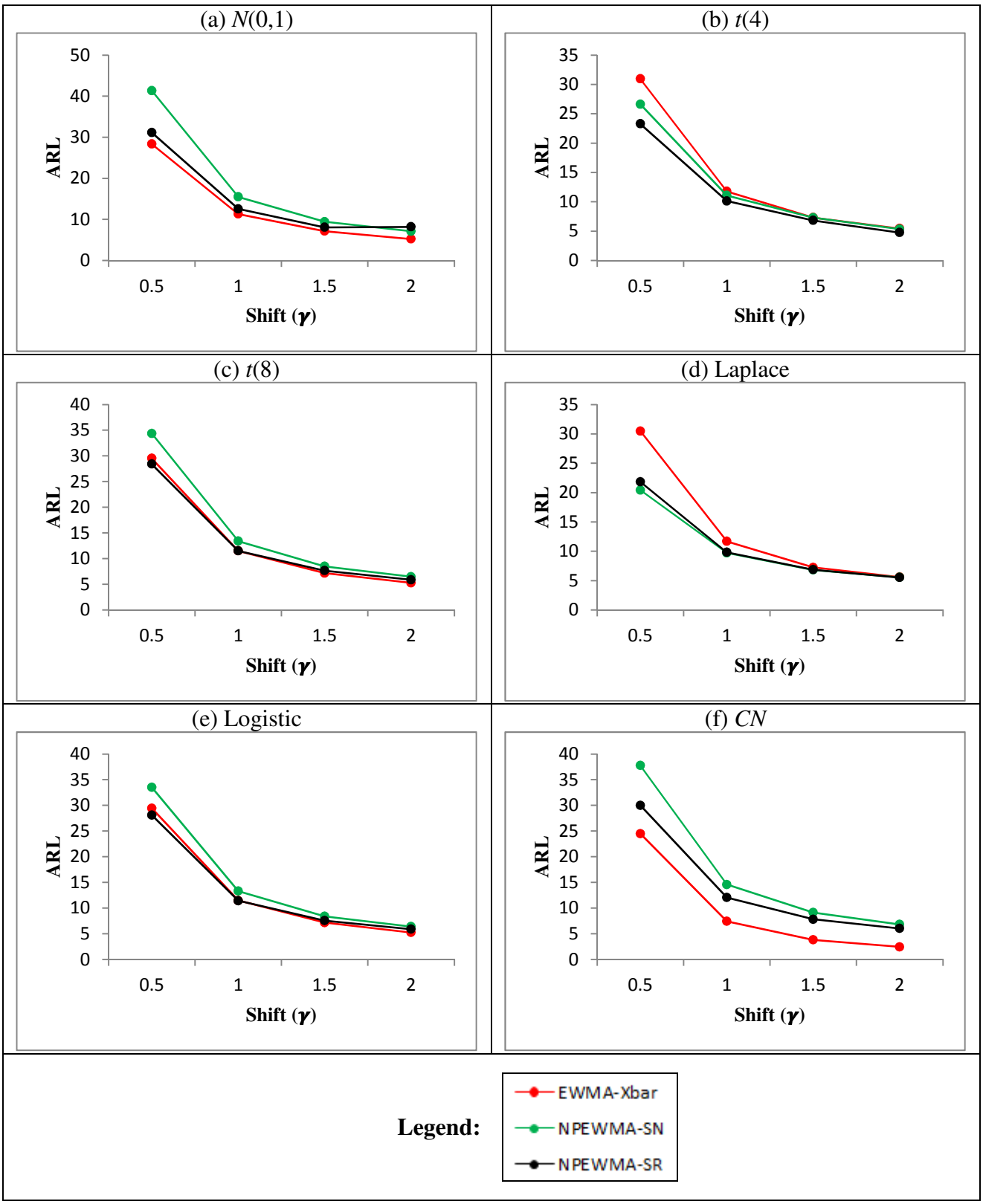

Figure 3.14. OOC *ARL* values for the EWMA-$\overline{X}$ chart, the NPEWMA-SN chart and the NPEWMA-SR chart for $\lambda = 0.05$

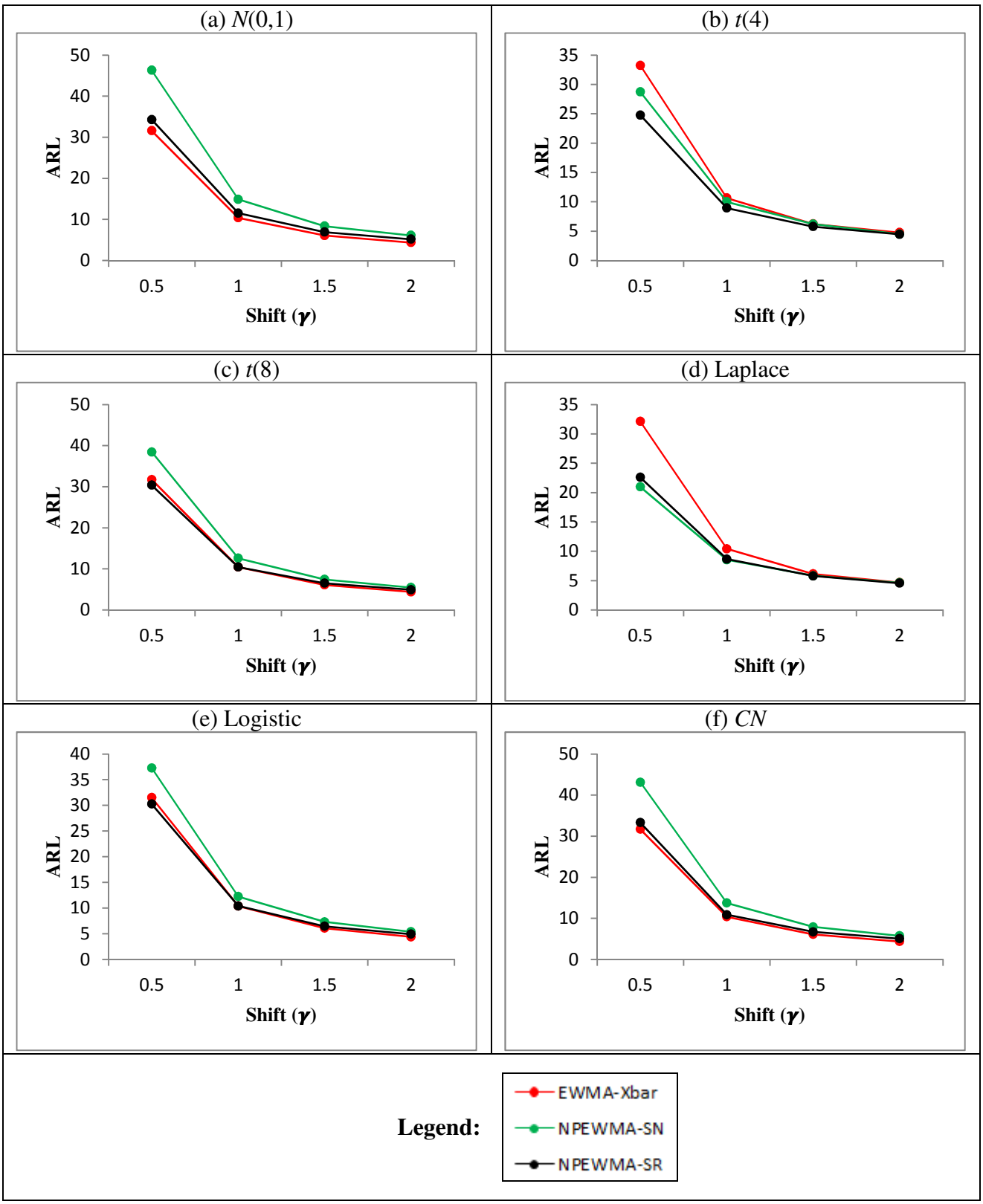

Figure 3.15. OOC *ARL* values for the EWMA-$\overline{X}$ chart, the NPEWMA-SN chart and the NPEWMA-SR chart for $\lambda = 0.10$

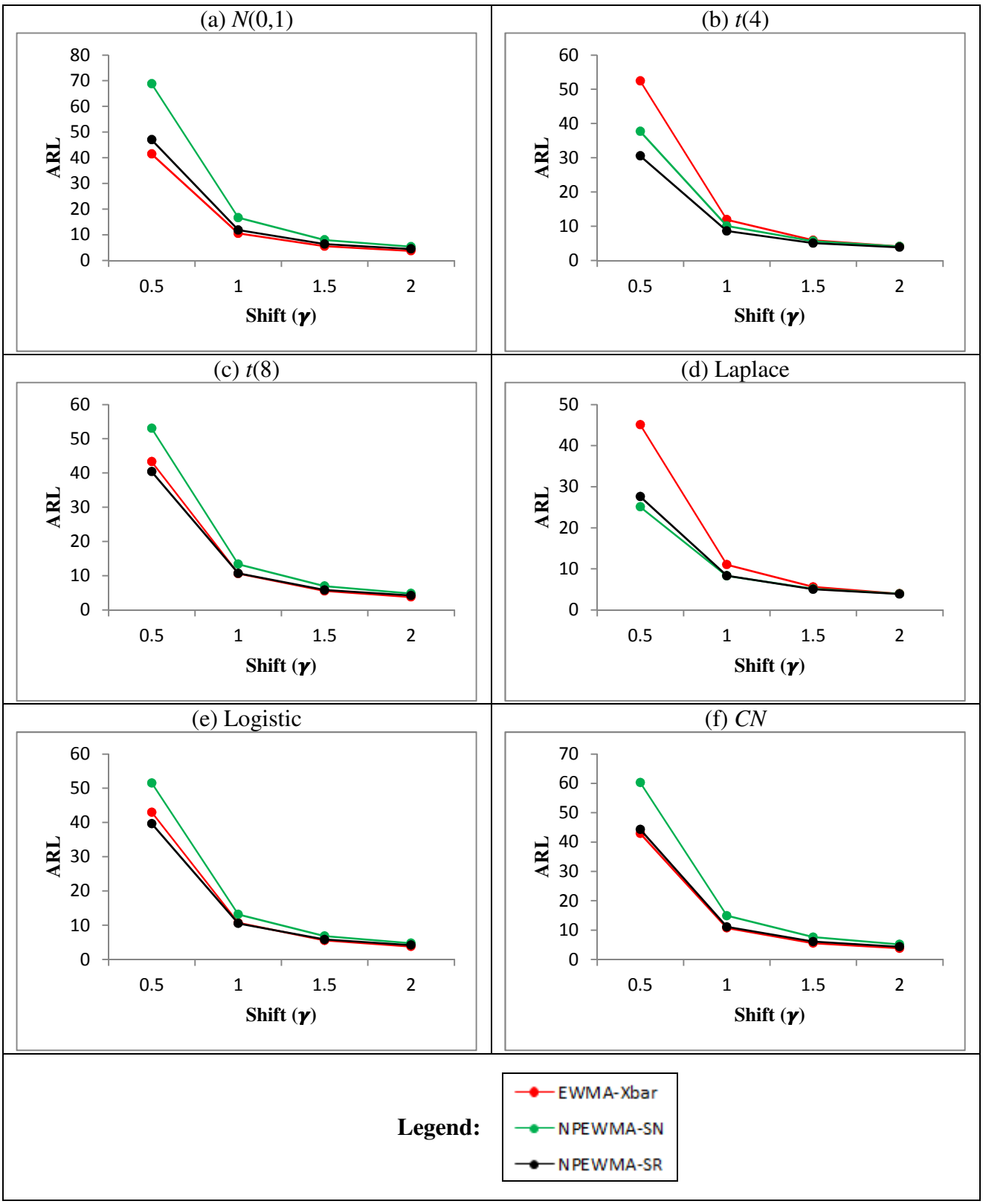

Figure 3.16. OOC *ARL* values for the EWMA-$\overline{X}$ chart, the NPEWMA-SN chart and the NPEWMA-SR chart for $\lambda = 0.20$

A summary of our observations from the OOC performance characteristics is as follows:

i. When the underlying process distribution is $N(0,1)$, the EWMA-$\overline{X}$ chart outperforms both nonparametric charts. This is not surprising, as it is typical for parametric methods to outperform their nonparametric counterparts when all assumptions are met. The NPEWMA-SR performs second best, whereas the NPEWMA-SN chart performs the worst. We obtain the same results for the *CN* distribution. This could be attributed to the fact that we have a small level of contamination and, consequently, the EWMA-$\overline{X}$ chart outperforms both nonparametric charts.

ii. When the underlying process distribution is $t(4)$, the NPEWMA-SR chart performs best followed by the NPEWMA-SN chart. The EWMA-$\overline{X}$ chart performs the worst, which is expected.

iii. It is well-known that as the degrees of freedom for the t-distribution increases, the t-distribution tends to the normal distribution. When we consider the $t(8)$ distribution, we find that the performance of the EWMA-$\overline{X}$ chart and the NPEWMA-SR chart is very similar. This is not surprising, since the $t(8)$ distribution is more normal-like than the $t(4)$ distribution. The NPEWMA-SN chart performs the worst, although it seems that, for larger shifts ($\gamma \geq 1.50$) the performance of all three charts is very similar.

iv. The NPEWMA-SR chart outperforms the NPEWMA-SN chart for all distributions under consideration except for the Laplace distribution, for which the performances of the charts are very similar. The EWMA-$\overline{X}$ chart performs the worst when the underlying process distribution is Laplace.

v. When the underlying process distribution is Logistic, the NPEWMA-SR chart performs the best for small shifts ($\gamma = 0.50$). For all other shifts the performance of the EWMA-$\overline{X}$ chart and the NPEWMA-SR chart is very similar. The NPEWMA-SN chart performs the worst.

3.3.3.4 Illustrative examples

Example 3.4

We first illustrate the NPEWMA-SR chart using a well-known dataset from Montgomery (2001; Table 5.2) on the inside diameters of piston rings manufactured by a forging process. Table 5.2 contains fifteen prospective samples each of five observations (n = 5). We assume that the underlying process distribution is symmetric (since a goodness of fit test for normality is not rejected for these data) with a known median of 74mm. For the three EWMA charts we choose the design parameters (λ, L) so that $ARL_0 \approx 370$. More specifically, we set λ = 0.05 and L equal to 2.488, 2.484 and 2.481 for the EWMA-$\overline{X}$, NPEWMA-SN and NPEWMA-SR charts, respectively. The values of the SR_i statistics and the NPEWMA-SR charting statistics were calculated using Equations (3.16) and (3.18), respectively, and are presented in Table 3.18.

Table 3.18. The SR_i statistics and the NPEWMA-SR charting statistics, Z_i

Subgroup number	SR_i	Z_i
1	8	0.400
2	4	0.580
3	-14	-0.149
4	7	0.208
5	-3	0.048
6	9	0.496
7	10	0.971
8	-6	0.622
9	12	1.191
10	14	1.832
11	4	1.940
12	15	2.593
13	15	3.213
14	15	3.803
15	14	4.313

From Figures 3.17, 3.18 and 3.19 we see that the EWMA-$\overline{X}$ control chart is the first to signal at subgroup number 12, whereas the NPEWMA-SN and the NPEWMA-SR charts both signal later at subgroup number 13. This is not surprising, as normal theory counterparts typically outperform nonparametric methods when the assumptions are met and a goodness-of-fit test does not reject normality for these data. In this example the EWMA-$\overline{X}$ slightly outperformed the nonparametric charts, but it should be noted that the assumptions necessary for the parametric chart seemed to be met. Typically in practice, however, normality can be in

doubt or may not be justified for lack of information or data and a nonparametric method may be more desirable. The next example illustrates this.

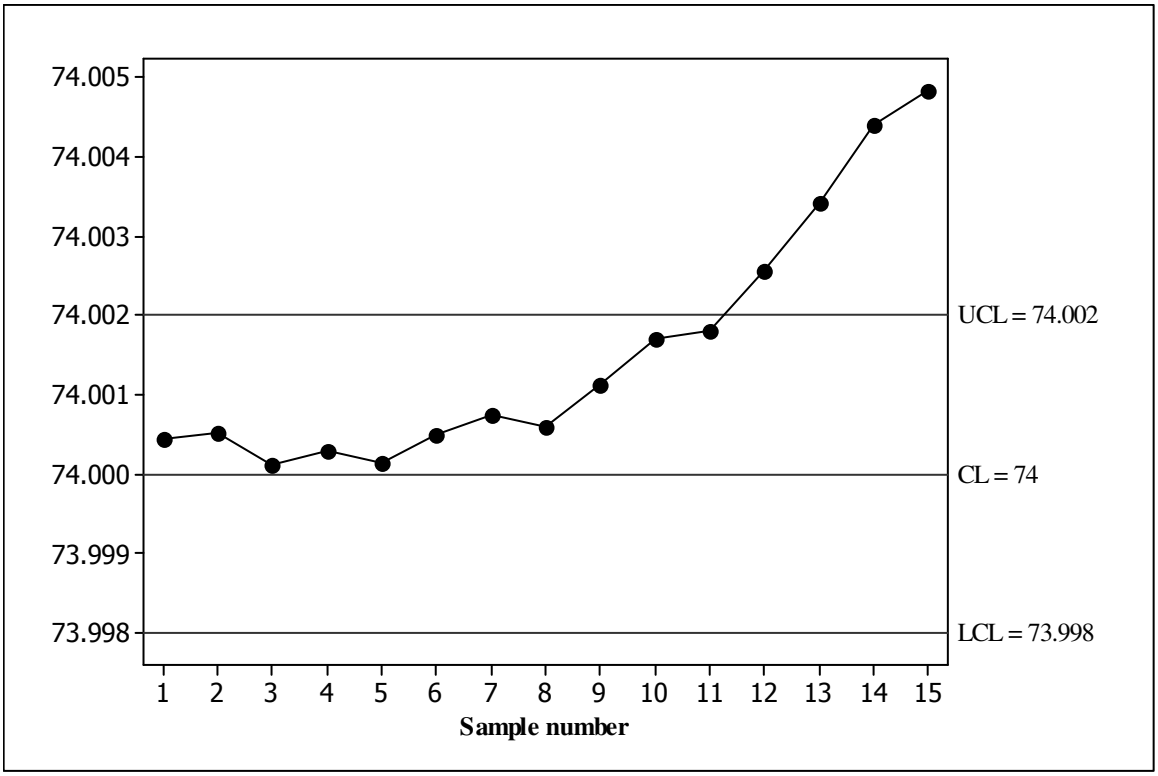

Figure 3.17. The EWMA- $\overline{X}$ control chart for the Montgomery piston ring data

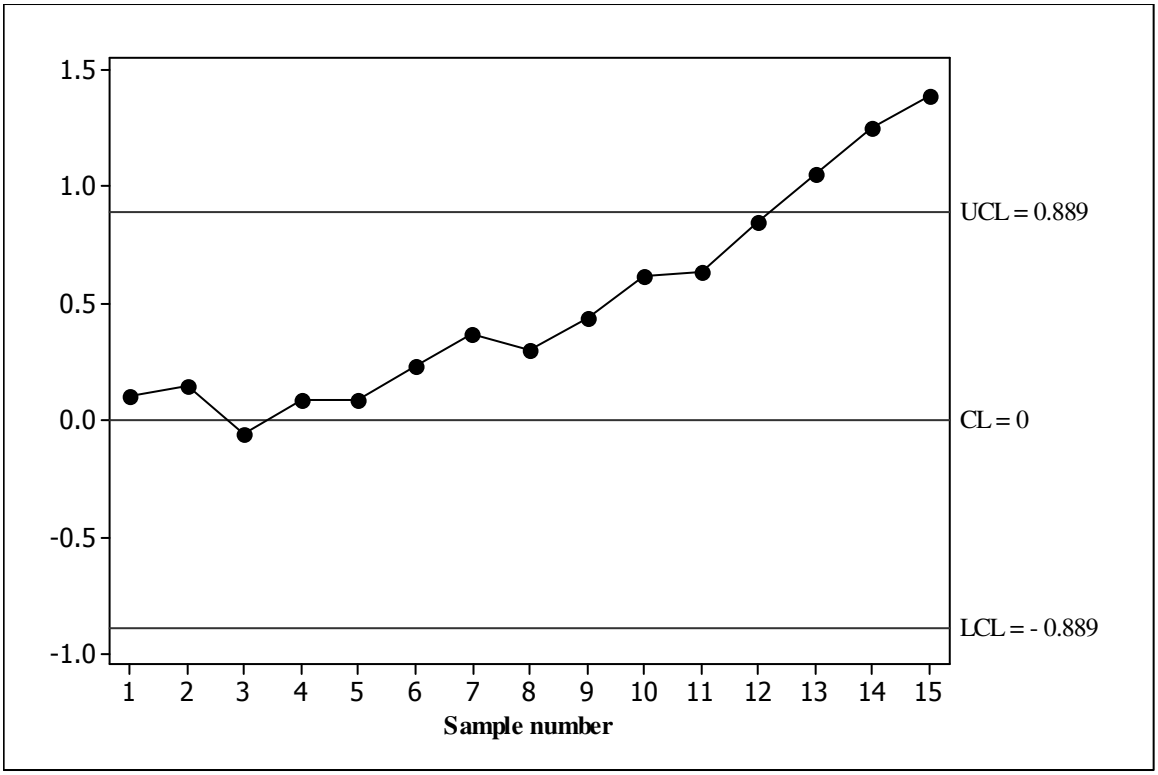

Figure 3.18. The NPEWMA-SN control chart for the Montgomery piston ring data

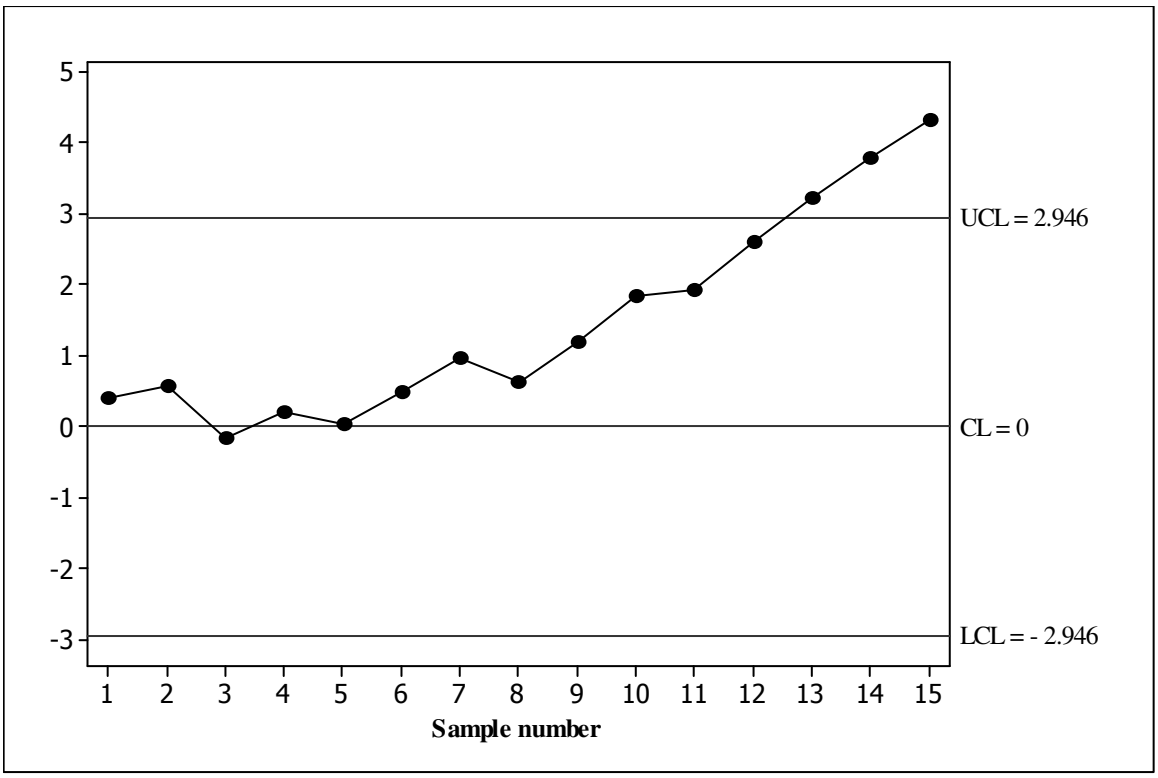

Figure 3.19. The NPEWMA-SR control chart for the Montgomery piston ring data

Example 3.5

The second example is to illustrate the effectiveness and the application of the nonparametric chart when normality is in doubt using some simulated data from a Logistic distribution with location parameter 0 and scale parameter $\sqrt{3}/\pi$: $LG(0, \sqrt{3}/\pi)$, so that the observations come from a symmetric distribution with a median of zero and a standard deviation of 1. Suppose that the median increases or has sustained an upward step shift of 0.5. Accordingly, subgroups each of size 5 (n = 5) were generated from the Logistic distribution with the same scale parameter but with the location parameter equal to 0.5, resulting in observations that have a median of 0.5 and a standard deviation of 1. For the three EWMA charts we choose the design parameters (λ, L) so that $ARL_0 \approx 500$. More specifically, we set λ = 0.10 and L equal to 2.701, 2.682 and 2.668 for the EWMA-$\overline{X}$, NPEWMA-SN and NPEWMA-SR charts, respectively.

The control charts are shown Figures 3.20, 3.21 and 3.22 and we observe that the nonparametric EWMA control charts are the first to signal at sample number 7, whereas the EWMA-$\overline{X}$ chart signals later at sample number 9.

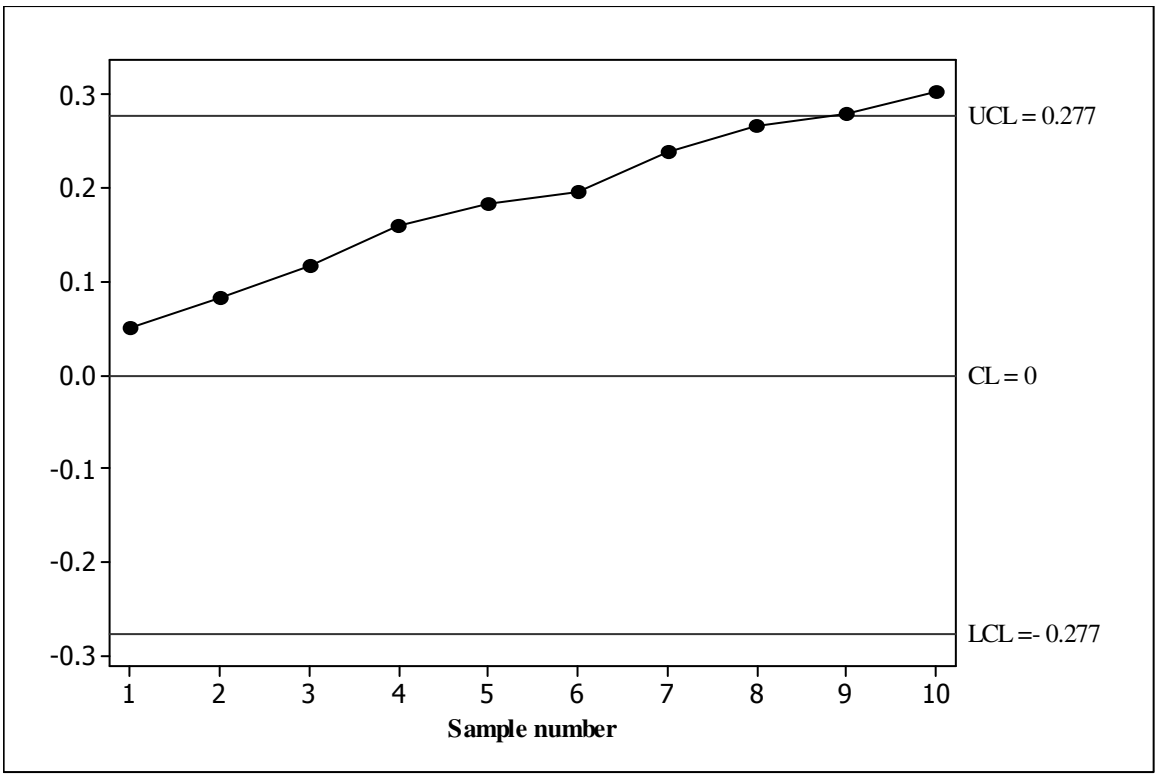

Figure 3.20. The EWMA- $\overline{X}$ control chart for the simulated data

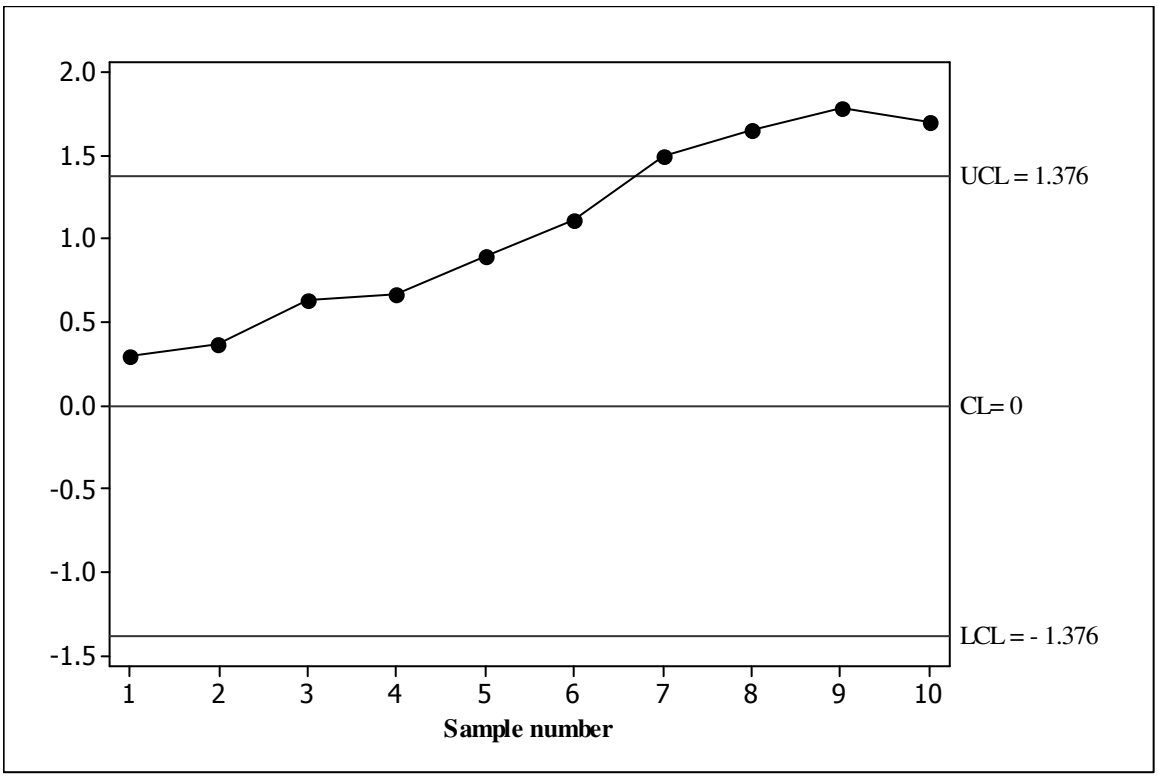

Figure 3.21. The NPEWMA-SN control chart for the simulated data

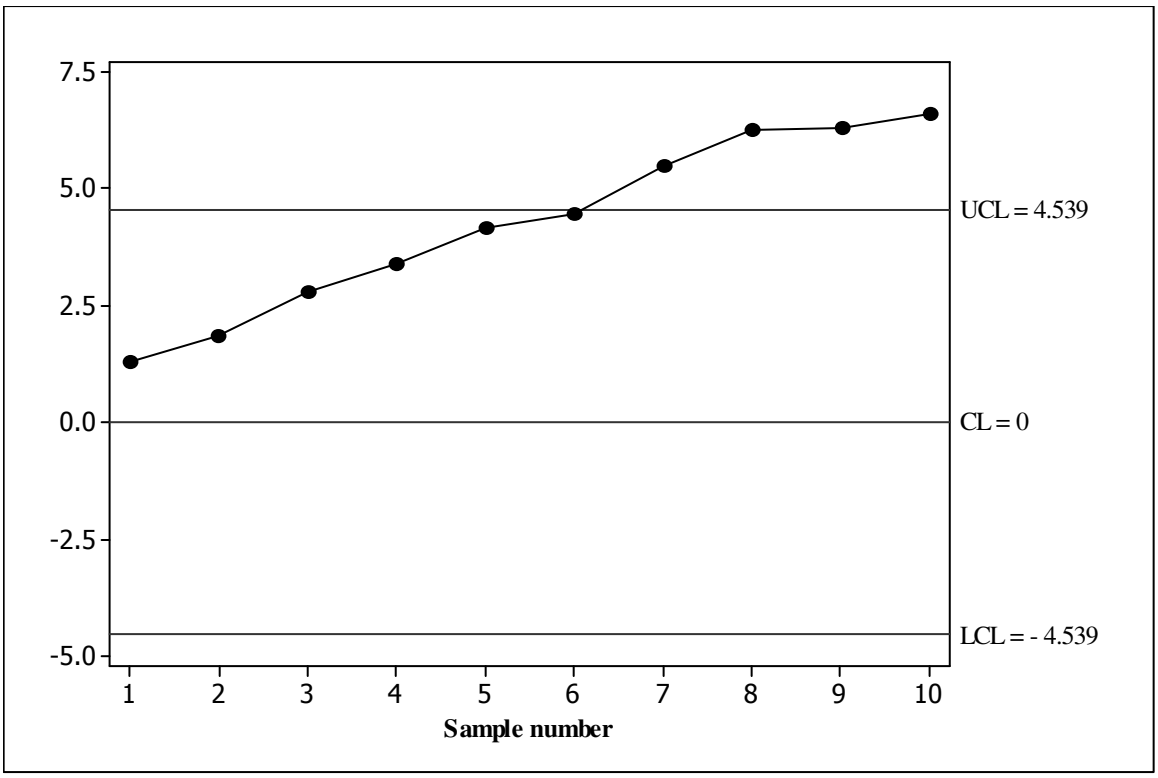

Figure 3.22. The NPEWMA-SR control chart for the simulated data

3.3.4 Summary

We studied the NPEWMA-SR chart and its properties via the IC and OOC run-length distribution using a Markov chain approach and simulation, respectively. A performance comparison of the NPEWMA-SR chart is done with its competitors: the EWMA-$\overline{X}$ chart and the NPEWMA-SN chart, and it is seen that the NPEWMA-SR chart performs as well as and, in many cases, better than its competitors.

3.4 Concluding remarks

EWMA charts take advantage of the sequentially (time ordered) accumulating nature of the data arising in a typical SPC environment and are known to be more efficient in detecting smaller shifts. The parametric EWMA-$\overline{X}$ chart can lack IC robustness and as such the corresponding false alarm rates can be a practical concern. NPEWMA charts offer an attractive alternative in such situations as they combine the inherent advantages of nonparametric charts (IC robustness) with the better small shift detection capability of EWMA-type charts. In Chapter 3 we proposed two NPEWMA charts based on the sign and signed-rank statistics and showed that on the basis of minimal required assumptions, robustness of the IC run-length distribution and OOC performance, the NPEWMA-SN and NPEWMA-SR charts are strong contenders in practical SPC applications.

3.5 Appendices

3.5.1 Appendix 3A: Some mathematical results

Note that although the proofs and derivations below are done using the steady-state *UCL*, they can also be derived in a similar manner using the steady-state *LCL*.

Proof to Equation (3.14)

Note that this proof is given in general for any sample size n. However, in order to get to the expression given in (3.14) substitute $n = 1$ into the derivations below.

In order for the NPEWMA-SN chart to signal one must have that the maximum value, that the charting statistic can take on, must be less than or equal to the upper control limit, i.e. $\max(SN_i) \leq UCL$.

Since the $\max(SN_i) = n$ and the steady-state $UCL = L\sqrt{\frac{\lambda n}{2-\lambda}}$, we find that $n \leq L\sqrt{\frac{\lambda n}{2-\lambda}}$ which simplifies to $L^2\left(\frac{\lambda}{2-\lambda}\right) \leq 1$.

Proof to Equation (3.15)

Note that this proof is given in general for any sample size n. However, in order to get to the expression given in (3.15) substitute $n = 1$ into the derivations below.

The chart will signal for the first i such that $Z_i \geq UCL$

$\lambda \sum_{j=0}^{i-1}(1-\lambda)^j SN_{i-j} + (1-\lambda)^i z_0 \geq UCL$ from recursive substitution

$\lambda \sum_{j=0}^{i-1}(1-\lambda)^j SN_{i-j} \geq UCL$ since $z_0 = 0$

$\lambda \sum_{j=0}^{i-1}(1-\lambda)^j (2T_{i-j} - n) \geq UCL$

$\lambda \sum_{j=0}^{i-1}(1-\lambda)^j (2n - n) \geq UCL$ since n is the max value that T_{i-j} can take on

$n\lambda \sum_{j=0}^{i-1}(1-\lambda)^j \geq UCL$

$\lambda \left(\frac{1-(1-\lambda)^i}{1-(1-\lambda)}\right) \geq \frac{UCL}{n}$ by using a geometric series

$(1-\lambda)^i \leq 1 - \frac{UCL}{n}$

$iln(1-\lambda) \leq ln\left(1 - \frac{UCL}{n}\right)$

$i \geq \frac{ln\left(1-\frac{UCL}{n}\right)}{ln(1-\lambda)}$ since $ln(1-\lambda) < 0$

Proof to Equation (3.21)

The chart will signal for the first i such that $Z_i \geq UCL$

$\lambda \sum_{j=0}^{i-1}(1-\lambda)^j SR_{i-j} + (1-\lambda)^i z_0 \geq UCL$ from recursive substitution

$\lambda \sum_{j=0}^{i-1}(1-\lambda)^j SR_{i-j} \geq UCL$ since $z_0 = 0$

$\lambda \sum_{j=0}^{i-1}(1-\lambda)^j \left(2T^+_{n,i-j} - \frac{n(n+1)}{2}\right) \geq UCL$

$\lambda \sum_{j=0}^{i-1}(1-\lambda)^j \left(2\frac{n(n+1)}{2} - \frac{n(n+1)}{2}\right) \geq UCL$ since $\frac{n(n+1)}{2}$ is the max value that T_{i-j} can take on

$\frac{n(n+1)}{2}\lambda \sum_{j=0}^{i-1}(1-\lambda)^j \geq UCL$

$\lambda\left(\frac{1-(1-\lambda)^i}{1-(1-\lambda)}\right) \geq \frac{2UCL}{n(n+1)}$ by using a geometric series

$(1-\lambda)^i \leq 1 - \frac{2UCL}{n(n+1)}$

$iln(1-\lambda) \leq ln\left(1 - \frac{2UCL}{n(n+1)}\right)$

$i \geq \frac{ln\left(1-\frac{2UCL}{n(n+1)}\right)}{ln(1-\lambda)}$ since $ln(1-\lambda) < 0$

3.5.2 Appendix 3B: A note on the number of subintervals between the control limits

For the Markov chain approach, when the number of subintervals ν is sufficiently large, the finite approach provides an effective method that allows the run-length properties of the EWMA control scheme to be accurately approximated. In practice, values of ν around 100 yield satisfactory approximations (see Yu (2007); page 20). Verification of the Markov chain approach using Monte Carlo simulation suggests that the discrepancies are within 2% of the simulated values when $\nu = 1001$ (see Table B3.1). Taking larger values of ν would result in more accurate answers, but in doing so, some run-length characteristics could not be computed within a practical period of time. Therefore, in this body of work, we obtained the run-length characteristics using the Interactive Matric Language (IML) procedure of SAS® using $\nu = 1001$.

Table B3.1. ARL_0 values and the absolute percentage difference between the simulated values[xv] and the values obtained using the Markov chain approach for the NPEWMA-SN chart for various values of ν

			$\lambda = 0.05$, $L = 2.472$		$\lambda = 0.10$, $L = 2.588$	
Markov chain approach	ν	**51**	439.07	(18.62%)	384.92	(4.06%)
		59	386.23	(4.34%)	420.36	(13.64%)
		67	379.34	(2.48%)	337.55	(8.75%)
		75	410.76	(10.97%)	360.21	(2.62%)
		83	410.48	(10.90%)	423.25	(14.42%)
		101	396.12	(7.02%)	357.42	(3.38%)
		151	380.61	(2.83%)	358.61	(3.05%)
		201	391.25	(5.70%)	330.66	(10.61%)
		251	368.50	(0.45%)	354.17	(4.26%)
		301	369.42	(0.20%)	379.63	(2.63%)
		401	365.71	(1.20%)	370.68	(0.21%)
		501	377.47	(1.98%)	377.33	(2.01%)
		1001	369.49	(0.18%)	373.80	(1.05%)
100 000 simulations			370.15		369.91	

From Table B3.1 we can see that the larger the value of ν, the smaller the percentage difference between the simulated values and the values obtained using the Markov chain approach, for example, when the design parameters are taken to be $\lambda = 0.05$ and $L = 2.472$, we have a large percentage difference of 18.62% when ν is taken to be small ($\nu = 51$) as opposed to a small percentage difference of 0.18% when ν is taken to be large ($\nu = 1001$).

[xv] Note that steady state control limits were used in both the simulations and the Markov chain approach in order to make the comparisons fair.

3.5.3 Appendix 3C: SAS® programs

3.5.3.1 SAS® program using Monte Carlo simulation to compute the run-length characteristics of the EWMA-$\overline{X}$ chart when the underlying process distribution is normal

```
quit;
proc iml;
* Number of simulations;
sim = 100000;
runl = j(sim,1,.);
* Design parameters of the EWMA-Xbar control chart;
lambda = 0.2;
L = 2.962;
* Sample size;
n = 10;
*Shift;
gamma = 2;
stdev = 1;
mean  = gamma * (stdev/sqrt(n));
* Steady state control limits;
UCL = 0 + L*(1/sqrt(n))*sqrt((lambda/(2-lambda)));
LCL = 0 - L*(1/sqrt(n))*sqrt((lambda/(2-lambda)));
do k = 1 to sim;
      * Initializing values;
      indicator = 0;
      count = 0;
      zi_1 = 0;
      do i = 1 to 1000000000000000 until (indicator = 1);
      count = count + 1;
      * Generating observations from the Normal distribution;
      xi = j(n,1,.);
      call randgen(xi,'NORMAL',mean,1);
      x_bar = xi[+,]/n;
      * Charting statistic;
    zi = lambda*x_bar + (1 - lambda) * zi_1;
      * Comparing charting statistic to the steady state control limits;
      if (zi<UCL) & (zi>LCL) then do; indicator = 0; end;
      if (zi>UCL) | (zi<LCL) then do; indicator = 1; end;
      zi_1 = zi;
      end;
      runl[k,1] = count;
end;
create EWMA from runl[colname={RL}];
append from runl;
proc univariate data = EWMA noprint;
histogram;
inset mean std p5 q1 median q3 p95 / format=10.2;
run;
```

3.5.3.2 SAS® program using Monte Carlo simulation to compute the run-length characteristics of the NPEWMA-SN chart when the underlying process distribution is normal

```
quit;
proc iml;
* Number of simulations;
sim = 100000;
runlength = j(sim,1,.);
* Design parameters of EWMA control chart;
lambda = 0.2;
L = 2.933;
* Sample size;
n = 10;
gamma = 2;
stdev = 1;
mean = gamma * stdev/sqrt(n);
xi = j(n,1,.);
ti_vec = j(n,1,.);
* Steady state control limits;
UCL_steady = 0 + L*sqrt(n)*sqrt((lambda/(2-lambda)));
LCL_steady = 0 - L*sqrt(n)*sqrt((lambda/(2-lambda)));
do j = 1 to sim;
*initializing values;
indicator = 0;
count = 0;
zi_1 = 0;
do i = 1 to 1000000000000000 until (indicator = 1);
count = count + 1;
* Generating observations from the Normal distribution;
call randgen(xi,'normal', mean,1);
do o = 1 to nrow(xi);
if xi[o,]>=0 then ti_vec[o,]=1;
else ti_vec[o,]=0;
end;
ti = ti_vec[+,];
sni = 2*ti - n;
* Charting statistic;
zi = lambda*sni + (1 - lambda) * zi_1;
* Comparing the charting statistic to the steady state control limits;
if (zi<UCL_steady) & (zi>LCL_steady) then do; indicator = 0; end;
if (zi>UCL_steady) | (zi<LCL_steady) then do; indicator = 1; end;
zi_1 = zi;
end;
runlength[j,1] = count;
end;
create EWMA from runlength[colname={RL}];
append from runlength;
proc univariate data = EWMA noprint;
histogram;
inset mean std p5 q1 median q3 p95 / format=10.2;
run;
```

3.5.3.3 SAS® program using Monte Carlo simulation to compute the run-length characteristics of the NPEWMA-SR chart when the underlying process distribution is normal

```
proc iml;
* Number of simulations;
sim = 100000;
runl = j(sim,1,.);
* Design parameters of EWMA control chart;
lambda = 0.2;
L = 2.905;
* Sample size;
n = 10;
* Shift;
gamma = 2;
stdev = 1;
mean = gamma * stdev / sqrt(n);
* Steady state control limits;
UCL = L * sqrt( (lambda / (2-lambda) )) * sqrt ( (n*(n+1)*(2*n+1))/6 );
LCL = -UCL;
do k = 1 to sim;
      indicator = 0;
      count = 0;
      zi_1 = 0;
      do i = 1 to 10000000000 until (indicator=1);
      count = count + 1;
      * Generating observations from the Normal distribution;
      tv = 0; * Median of the normal distribution;
      xi = j(n,1,.);
      sign = j(n,1,.);
      abs_diff = j(n,1,.);
      sri = j(n,1,.);
      call randgen (xi, 'normal', mean, 1);
      do j = 1 to n;
            if xi[j,1] > tv then sign[j,1] = 1;
            if xi[j,1] < tv then sign[j,1] = -1;
            if xi[j,1] = tv then sign[j,1] = 0;
      end;
      do j = 1 to n;
            abs_diff[j,1] = abs(xi[j,1]-tv);
      end;
      rank_abs_diff = rank(abs_diff);
      do j = 1 to n;
            sri[j,1] = sign[j,1] # rank_abs_diff[j,1];
      end;
      signed_rank = sum(sri);
      *Charting statistic;
      zi = lambda*signed_rank + (1-lambda)*zi_1;
      * Comparing the charting statistic to the control limits;
      if (zi<UCL) & (zi>LCL) then do; indicator = 0; end;
      if (zi>UCL) | (zi<LCL) then do; indicator = 1; end;
      zi_1=zi;
end;
runl[k,1] = count;
end;
create EWMA from runl[colname={RL}];
append from runl;
proc univariate data = EWMA noprint;
histogram;
inset mean std p5 q1 median q3 p95 / format = 10.2;
run;
```

3.5.3.4 Necessary amendments to the SAS® programs given in Sections 3.5.3.1, 3.5.3.2 and 3.5.3.3 when the underlying process is non-normal

Dist	Necessary amendments

$t(\nu)$	`* Generating values from the t distribution with mean=0 and variance=1;`
	`df = 4;  *Or df = 8;`
	`call randgen(xi,"t", df);`
	`xi=xi*sqrt( (df-2)/df ) + gamma*(stdev/sqrt(n));`

Laplace	`stdev = sqrt(2);`
	`* Generating values from the Laplace distribution with mean=0 and variance=1;`
	`uni=j(n,1,.);`
	`xi=j(n,1,.);`
	`call randgen(uni,'UNIFORM');`
	`xi = quantile('laplace',uni,gamma*(stdev/sqrt(n)),1);`
	`xi = (1/sqrt(2))*xi;`

Logistic	`* Generating values from the logistic distribution with mean=0 and variance=1;`
	`y=j(n,1,.);`
	`xi=j(n,1,.);`
	`* Based on the Probability Integral Transformation (PIT);`
	`call randgen (y, 'UNIFORM');`
	`xi=log(y/(1-y))#j(n,1,sqrt(3)/(constant('PI')))+j(n,1,gamma*stdev/sqrt(n));`

$GAM(\alpha,\beta)$	`* Generating values from the logistic distribution with mean=0 and variance=1;`
	`shape = 0.5;  * Or = 1 or = 3`
	`call randgen(xi,'gamma',shape);`
	`xi = (xi - shape)/sqrt(shape) + gamma*stdev/sqrt(n);`

CN	`* Generating values from the contaminated normal distribution with mean=0 and variance=1;`
	`ep = 0.05;`
	`y = ranuni(0);`
	`sig1 = SQRT(1/1.15);`
	`sig2 = SQRT(4/1.15);`
	`mu1 = 0;`
	`mu2 = 0;`
	`if y > ep then xi = RAND('NORMAL',mu1,sig1);`
	`else xi = RAND('NORMAL',mu2,sig2);`
	`mean = (1-ep)*mu1 + ep*mu2;`
	`var  = ((1-ep)*(mu1*mu1+sig1*sig1)+ep*(mu2*mu2+sig2*sig2))-(mean**2);`
	`stdev = sqrt(var);`
	`xi = xi + gamma*stdev/sqrt(n);`

3.5.3.5 SAS® program using the Markov chain approach to compute the run-length characteristics of the NPEWMA-SN chart when the underlying process distribution is normal

```
proc iml;
* Number of subintervals between UCL and LCL;
r=1001;
* Sample size;
n=1;
* Design parameters of the EWMA control chart;
L=2;
lambda=0.05;
* Shift;
gamma=0;
* Parameter of the Binomial distribution;
p=0.5;
* Calculating the steady-state control limits;
UCL = L * sqrt(n) * sqrt(lambda/(2-lambda));
LCL = -UCL;
* Interval between LCL and UCL divided into subintervals of width 2*tau;
S=j(r,1,0);
tau = ((UCL-LCL)/r)/2;
S[1,1] = UCL - tau;
do i = 2 to r;
      S[i,1]=S[i-1,1]-2*tau;
end;
Q_a=j(r,r,0);
Q_b=j(r,r,0);
Q=j(r,r,0);
do i = 1 to r;
      do j = 1 to r;
      Q_a[i,j]=floor(((((S[j,]-tau) - (1-lambda)*S[i,])/lambda) + n)/2);
      end;
end;
do i = 1 to r;
      do j = 1 to r;
      Q_b[i,j]=floor(((((S[j,]+tau) - (1-lambda)*S[i,])/lambda) + n)/2);
      end;
end;
do i = 1 to r;
      do j = 1 to r;
      Q[i,j]=cdf('BINOMIAL',(Q_b[i,j]),p,n)-cdf('BINOMIAL',(Q_a[i,j]),p,n);
      end;
end;
* Defining the eta row vector;
eta=j(1,r,0);
eta[1,((1+r)/2)]=1;
* Defining the vector 'one' used in Equations (1.12) to (1.15);
one=j(r,1,1);
* Defining the identity matrix used in Equations (1.12) to (1.15);
identity = I(r);
* Calculation of moments;
indicator0 = 0;
survival  = 0;
Qh = I(r);
do i = 1 to 10000000000 until (indicator0=1);
Qc = Qh*Q;
survival0 = eta * Qc * one;
survival = survival // survival0;
Qh = Qc;
```

```
if survival[i+1,] < 0.04 then indicator0=1;
end;
cdf1 = 1 - survival;
cdf = cdf1;
index=j(nrow(cdf),1,1);
do i = 2 to nrow(cdf);
      index[i,]=index[i-1,]+1;
end;
* Calculating the average run length (ARL);
ARL = eta*ginv(identity-Q)*one;
* Calculating the second moment;
N2 = eta * (identity + Q) * (ginv((identity-Q)**2)) * one;
* Calculating the standard deviation;
SDRL = sqrt (N2 - ((ARL)**2) );
* Printing the output;
print_cdf=index||cdf;
* Calculations of the percentiles;
p_5th=0;
p_25th=0;
p_50th=0;
p_75th=0;
p_95th=0;
do i = 1 to nrow(cdf);
      if print_cdf[i,2]<0.05 then p_5th=print_cdf[i,1];
      if print_cdf[i,2]<0.25 then p_25th=print_cdf[i,1];
      if print_cdf[i,2]<0.50 then p_50th=print_cdf[i,1];
      if print_cdf[i,2]<0.75 then p_75th=print_cdf[i,1];
      if print_cdf[i,2]<0.95 then p_95th=print_cdf[i,1];
end;
print       n [label='Sample size'],
            L [label = 'Multiplier'],
            lambda [label = 'lambda'],
            p [label='probability'],
            r [label = 'Number of subintervals between UCL and LCL'],
            UCL [label='Upper control limit'],
            LCL [label='Lower control limit'],
            S [label='midpoints'],
            Q [label='Transition probability matrix'],
            ARL [label = 'Average run length' format=.2],
            SDRL [label = 'Standard deviation of the run length' format=.2],
            p_5th p_25th p_50th p_75th p_95th;
```

3.5.3.6 SAS® program using the Markov chain approach to compute the run-length characteristics of the NPEWMA-SR chart when the underlying process distribution is normal

```
proc iml;
* Number of subintervals between UCL and LCL;
r = 1001;
* Sample size;
n = 5;
* Design parameters of the EWMA chart;
L = 2.668;
lambda = 0.1;
* The IC standard deviation of the signed-rank statistic;
stdev = sqrt (n*(n+1)*(2*n+1)/6);
* Wilcoxon singed-rank probabilities for a sample size of 4;
if n = 4 then do;
      T4 = j((n*(n+1)/2)+1,1,1);
      T4[1:3,]=1;
      T4[4:8,]=2;
      T4[9:11,]=1;
      T = T4/(2**n);
end;
* Wilcoxon singed-rank probabilities for a sample size of 5;
if n = 5 then do;
      T5 = j((n*(n+1)/2)+1,1,1);
      T5[1:3,]=1;
      T5[4:5,]=2;
      T5[6:11,]=3;
      T5[12:13,]=2;
      T5[14:16,]=1;
      T = T5/(2**n);
end;
* Wilcoxon singed-rank probabilities for a sample size of 6;
if n = 6 then do;
      T6 = j((n*(n+1)/2)+1,1,1);
      T6[1:3,]=1;
      T6[4:5,]=2;
      T6[6,]=3;
      T6[7:9,]=4;
      T6[10:13,]=5;
      T6[14:16,]=4;
      T6[17,]=3;
      T6[18:19,]=2;
      T6[20:22,]=1;
      T = T6/(2**n);
end;
* Wilcoxon singed-rank probabilities for a sample size of 7;
if n = 7 then do;
      T7 = j((n*(n+1)/2)+1,1,1);
      T7[1:3,]=1;
      T7[4:5,]=2;
      T7[6,]=3;
      T7[7,]=4;
      T7[8:9,]=5;
      T7[10,]=6;
      T7[11:12,]=7;
      T7[13:17,]=8;
      T7[18:19,]=7;
      T7[20,]=6;
      T7[21:22,]=5;
```

```
        T7[23,]=4;
        T7[24,]=3;
        T7[25:26,]=2;
        T7[27:29,]=1;
        T = T7/(2**n);
end;
* Wilcoxon singed-rank probabilities for a sample size of 8;
if n = 8 then do;
        T8 = j((n*(n+1)/2)+1,1,1);
        T8[1:3,]=1;
        T8[4:5,]=2;
        T8[6,]=3;
        T8[7,]=4;
        T8[8,]=5;
        T8[9,]=6;
        T8[10,]=7;
        T8[11,]=8;
        T8[12,]=9;
        T8[13,]=10;
        T8[14,]=11;
        T8[15,]=12;
        T8[16:18,]=13;
        T8[19,]=14;
        T8[20:22,]=13;
        T8[23,]=12;
        T8[24,]=11;
        T8[25,]=10;
        T8[26,]=9;
        T8[27,]=8;
        T8[28,]=7;
        T8[29,]=6;
        T8[30,]=5;
        T8[31,]=4;
        T8[32,]=3;
        T8[33:34,]=2;
        T8[35:37,]=1;
        T = T8/(2**n);
end;
* Wilcoxon singed-rank probabilities for a sample size of 9;
if n = 9 then do;
        T9 = j((n*(n+1)/2)+1,1,1);
        T9[1:3,]=1;
        T9[4:5,]=2;
        T9[6,]=3;
        T9[7,]=4;
        T9[8,]=5;
        T9[9,]=6;
        T9[10,]=8;
        T9[11,]=9;
        T9[12,]=10;
        T9[13,]=12;
        T9[14,]=13;
        T9[15,]=15;
        T9[16,]=17;
        T9[17,]=18;
        T9[18,]=19;
        T9[19:20,]=21;
        T9[21,]=22;
        T9[22:25,]=23;
        T9[26,]=22;
        T9[27:28,]=21;
        T9[29,]=19;
        T9[30,]=18;
```

```
        T9[31,]=17;
        T9[32,]=15;
        T9[33,]=13;
        T9[34,]=12;
        T9[35,]=10;
        T9[36,]=9;
        T9[37,]=8;
        T9[38,]=6;
        T9[39,]=5;
        T9[40,]=4;
        T9[41,]=3;
        T9[42:43,]=2;
        T9[44:46,]=1;
        T = T9/(2**n);
end;
* Wilcoxon singed-rank probabilities for a sample size of 10;
if n = 10 then do;
        T10 = j((n*(n+1)/2)+1,1,1);
        T10[1:3,]=1;
        T10[4:5,]=2;
        T10[6,]=3;
        T10[7,]=4;
        T10[8,]=5;
        T10[9,]=6;
        T10[10,]=8;
        T10[11,]=10;
        T10[12,]=11;
        T10[13,]=13;
        T10[14,]=15;
        T10[15,]=17;
        T10[16,]=20;
        T10[17,]=22;
        T10[18,]=24;
        T10[19,]=27;
        T10[20,]=29;
        T10[21,]=31;
        T10[22,]=33;
        T10[23,]=35;
        T10[24,]=36;
        T10[25,]=38;
        T10[26:27,]=39;
        T10[28:29,]=40;
        T10[30:31,]=39;
        T10[32,]=38;
        T10[33,]=36;
        T10[34,]=35;
        T10[35,]=33;
        T10[36,]=31;
        T10[37,]=29;
        T10[38,]=27;
        T10[39,]=24;
        T10[40,]=22;
        T10[41,]=20;
        T10[42,]=17;
        T10[43,]=15;
        T10[44,]=13;
        T10[45,]=11;
        T10[46,]=10;
        T10[47,]=8;
        T10[48,]=6;
        T10[49,]=5;
        T10[50,]=4;
        T10[51,]=3;
```

```
      T10[52:53,]=2;
      T10[54:56,]=1;
      T = T10/(2**n);
end;
* Calculating the control limits;
UCL = L * stdev * sqrt(lambda/(2-lambda));
LCL = -UCL;
* Calculating the midpoints;
S=j(r,1,0);
* The interval between the UCL and LCL are divided into subintervals;
tau = ((UCL-LCL)/r)/2;
S[1,1] = UCL - tau;
do i = 2 to r;
      S[i,1]=S[i-1,1]-2*tau;
end;
Q_a=j(r,r,0);
Q_b=j(r,r,0);
Q=j(r,r,0);
do i = 1 to r;
      do j = 1 to r;
      Q_a[i,j]=floor(((((S[j,]-tau) - (1-lambda)*S[i,])/lambda) +
      n*(n+1)/2)/2);
      end;
end;
do i = 1 to r;
      do j = 1 to r;
      Q_b[i,j]=floor(((((S[j,]+tau) - (1-lambda)*S[i,])/lambda) +
      n*(n+1)/2)/2);
      end;
end;
do i = 1 to r;
      do j = 1 to r;
      lower = Q_a[i,j];
      upper = Q_b[i,j];
      if lower < 0 then if lower*upper > 0 then Q[i,j]=0;
      if lower > n*(n+1)/2 then lower_term = 1;
      else if lower < 0 then lower_term = 0;
      else lower_term = sum(T[1:(lower+1),]);
      if upper > n*(n+1)/2 then upper_term = 1;
      else if upper < 0 then upper_term = 0;
      else upper_term = sum(T[1:(upper+1),]);
      Q[i,j] = upper_term - lower_term;
      end;
end;
* Defining the eta row vector;
eta=j(1,r,0);
eta[1,((1+r)/2)]=1;
* Defining the column vector filled with one;
one=j(r,1,1);
* Defining the identity matrix;
identity = I(r);
* Calculation of moments;
indicator0 = 0;
 survival  = 0;
        Qh = I(r);
do i = 1 to 1000000 until (indicator0=1);
             Qc = Qh*Q;
    survival0 = eta * Qc * one;
       survival = survival // survival0;
             Qh = Qc;
      if survival[i+1,] < 0.04 then indicator0=1;
end;
cdf1 = 1 - survival;
```

```
cdf = cdf1;
index=j(nrow(cdf),1,1);
do i = 2 to nrow(cdf);
      index[i,]=index[i-1,]+1;
end;
* Calculating the average run length (ARL);
ARL = eta*ginv(identity-Q)*one;
* Calculating the second moment;
N2 = eta * (identity + Q) * (ginv((identity-Q)**2)) * one;
* Calculating the standard deviation;
SDRL = sqrt (N2 - ((ARL)**2) );
* Printing the output;
print_cdf=index||cdf;
* Calculations of the percentiles;
p_5th=0;
p_25th=0;
p_50th=0;
p_75th=0;
p_95th=0;
do i = 1 to nrow(cdf);
      if print_cdf[i,2]<0.05 then p_5th=print_cdf[i,1];
      if print_cdf[i,2]<0.25 then p_25th=print_cdf[i,1];
      if print_cdf[i,2]<0.50 then p_50th=print_cdf[i,1];
      if print_cdf[i,2]<0.75 then p_75th=print_cdf[i,1];
      if print_cdf[i,2]<0.95 then p_95th=print_cdf[i,1];
end;

print       n [label='Sample size'],
            L [label = 'Multiplier'],
            lambda [label = 'lambda'],
            r [label = 'Number of subintervals between UCL and LCL'],
            UCL [label='Upper control limit'],
            LCL [label='Lower control limit'],
            ARL [label = 'Average run length' format=.2],
            SDRL [label = 'Standard deviation of the run length' format=.2],
            p_5th p_25th p_50th p_75th p_95th;
```

3.5.3.7 Necessary amendments to the SAS® programs in Sections 3.5.3.5 and 3.5.3.6 when the underlying process distribution is non-normal

Because the NPEWMA-SN and the NPEWMA-SR charts are nonparametric, the IC run-length distribution and the associated characteristics should remain the same for all symmetric continuous distributions. A Markov chain approach was used in the calculations of the run-length characteristics for the two NPEWMA charts when the process is IC using the SAS® programs given in Sections 3.5.3.5 and 3.5.3.6, respectively. However, for the OOC chart performance comparison, 100 000 Monte Carlo simulations[xvi] were used since matrix inversion is often troublesome and we have shown (see Appendix 3B) that the percentage difference between the simulated values and the values obtained using the Markov chain approach are very small when 100 000 simulations are used.

[xvi] See Sections 3.5.3.2 and 3.5.3.3 for the SAS® programs using Monte Carlo simulations for the NPEWMA-SN and NPEWMA-SR charts, respectively

Chapter 4

Phase II control charts – parameters unknown

4.1 Introduction

In Chapter 3 two nonparametric EWMA charts were proposed based on the sign and signed-rank statistics for the situation when the IC process median is specified or known. In many practical situations, the process median may not be known and would have to be estimated using a Phase I reference sample. This situation is referred to as the 'standard(s) unknown' case and is denoted Case U. It is well-known that ignoring the effects of estimation of parameters can be costly as the run-length properties of the chart are greatly impacted which can lead to, for example, many more false alarms than nominally expected (see e.g. Jensen et al. (2006)).

In Section 1.9 the three main classes of control charts are discussed: namely the Shewhart chart, the cumulative sum (CUSUM) chart and the exponentially weighted moving average (EWMA) chart. For Case U several Shewhart, CUSUM and EWMA control charts have been developed and we mention some of the important and interesting contributions here.

Nonparametric Shewhart control charts:

i. Janacek and Meikle (1997) proposed a nonparametric Shewhart-type chart where the charting statistic is the median of each Phase II sample and the control limits are given by two order statistics obtained from a reference sample. Chakraborti et al. (2004) generalized the work of Janacek and Meikle (1997) by using the j^{th} order statistic $Y_{(j:n)}$, $j = 1,2,...,n$, of a Phase II sample as the charting statistic; these charts are referred to as Shewhart-type precedence charts.

ii. Chakraborti et al. (2009) considered enhancing the Shewhart-type precedence charts of Chakraborti et al. (2004) by incorporating the *2-of-2* DR and the *2-of-2* KL runs-rules. The reader is referred to Derman and Ross (1997) and Klein (2000) for details on the DR and KL runs-rules schemes, respectively.

iii. Balakrishnan et al. (2010) noted a potential drawback of the Shewhart-type precedence charts proposed by Chakraborti et al. (2004): The fact that these charts are based on a single order statistic $Y_{(j:n)}$ of each Phase II sample could be a drawback since even if the bulk of the Phase II sample observations lie outside the control limits, the Shewhart-type precedence chart will not signal (when it should) if the $Y_{(j:n)}$ plots between the control limits. Consequently, Balakrishnan et al. (2010) proposed a nonparametric Phase II chart using $Y_{(j:n)}$ and R where R denotes the number of Phase II sample observations that lie between the control limits. This procedure can be viewed as running two charts simultaneously, a Shewhart-type precedence chart plotting $Y_{(j:n)}$ and a chart plotting R.

iv. The same authors, i.e. Balakrishnan, Triantafyllou and Koutras, also proposed three relatively flexible nonparametric Phase II charts in the year 2009 (see Balakrishnan et al. (2009)). These charts, like the charts by Chakraborti et al. (2004, 2009) and Balakrishnan et al. (2010), monitor an order statistic of the Phase II sample using two order statistics from a Phase I reference sample as control limits along with a chart based on a run or rank-based charting statistic defined on the Phase II sample observations that lie between the Phase I control limits.

v. Bakir (2006) considered signed-rank like statistics in Case U and used these to construct nonparametric Shewhart-type charts for the median.

vi. Chakraborti and Van de Wiel (2008) proposed a nonparametric Shewhart-type chart based on the well-known Mann-Whitney test statistic for monitoring the location of a process.

Nonparametric CUSUM (denoted NPCUSUM) control charts:

i. McDonald (1990) considered a CUSUM procedure for individual observations based on the statistics called ‘sequential ranks’.

ii. Bakir (2006) considered signed-rank like statistics in Case U and used these to construct NPCUSUM-type charts for the median.

iii. Chatterjee and Qiu (2009) proposed NPCUSUM control charts using bootstrap control limits.

iv. Li et al. (2010) proposed a NPCUSUM-type chart based on the well-known Mann-Whitney test statistic for monitoring the location of a process.

v. Yang and Cheng (2011) proposed a NPCUSUM chart for variables data to monitor the process mean.

Nonparametric EWMA (denoted NPEWMA) control charts:

i. Bakir (2006) considered signed-rank like statistics in Case U and used these to construct NPEWMA-type charts for the median.

ii. Li et al. (2010) proposed a NEWMA-type chart based on the well-known Mann-Whitney test statistic for monitoring the location of a process.

Hawkins et al. (2003) brought a new perspective to the standards unknown case by the introduction of the change-point model. Although they considered normally distributed data, there have been recent developments in the nonparametric change-point area for monitoring the location of a process by Zhou et al. (2009) and Hawkins and Deng (2010), respectively. More recently, Ross and Adams (2012) considered two nonparametric control charts for detecting arbitrary distribution changes.

In this chapter we consider a nonparametric CUSUM chart and a nonparametric EWMA chart for monitoring the unknown median based on a reference sample. The proposed charts are based on what are known as precedence or exceedance test statistics (see e.g. Fligner and Wolfe (1976) and Balakrishnan and Ng (2006)).

Firstly, the precedence / exceedance statistics are defined in Section 4.2. Following this, the NPCUSUM control chart based on the exceedance statistics (denoted NPCUSUM-EX) is proposed in Section 4.3. Thereafter, the NPEWMA control chart based on the exceedance statistics (denoted NPEWMA-EX) is proposed in Section 4.4. A summary and concluding remarks are given in Section 4.5.

A number of research outputs related to and based on this thesis have seen the light. In Chapter 5 we provide a list with the details of the technical reports and the peer-reviewed articles

that have been published, the articles that have been accepted for publication, the local and international conferences where papers have been presented and draft articles that have been submitted and are currently under review. Here, we solely mention the peer-reviewed articles that have been published based on Sections 4.3 and 4.4, respectively:

i. Mukherjee, A., Graham, M.A. and Chakraborti, S. (2013). "Distribution-free exceedance CUSUM control charts for location." *Communications in Statistics - Simulation and Computation*, 42 (5), 1153-1187.

ii. Graham, M.A., Mukherjee, A. and Chakraborti, S. (2012). "Distribution-free exponentially weighted moving average control charts for monitoring unknown location." *Computational Statistics and Data Analysis*, 56 (8), 2539–2561.

4.2 The exceedance statistic

The precedence test is a two-sample nonparametric test based on the number of observations from one of the samples that precedes a specified (say the r^{th}) order statistic of the second sample. The precedence statistic is linearly related to the exceedance statistic, which is the number of observations from one of the samples that exceed the r^{th} order statistic of the other sample, so that precedence and exceedance tests are equivalent (the reader is referred to Fligner and Wolfe (1976) where the distributional properties of the exceedance statistics have been discussed in detail). Precedence / exceedance tests have been found to be useful in a number of applications including quality control and reliability studies with lifetime data. The reader is referred to Balakrishnan and Ng (2006) for the vast literature on precedence / exceedance tests. In particular, they note that (see page 51 of their textbook) "Wilcoxon's rank-sum test performs better than the precedence tests if the underlying distributions are close to symmetry, such as the normal distribution, gamma distribution with large values of shape parameter, and lognormal distribution with small values of shape parameter. However, under some right-skewed distributions such as the exponential distribution, gamma distribution with shape parameter 2.0, and lognormal distribution with shape parameter 0.5, the precedence tests have higher power values than the Wilcoxon's rank-sum test for small values of r. It is evident that the more right-skewed the underlying distribution is, the more powerful the precedence test is." Some statistical background on precedence / exceedance statistics follows.

Assume that a Phase I reference sample $X_1, X_2, \ldots, X_m$ $(m > 1)$ is available from an IC process with a cdf $F(x)$. Let $Y_{j1}, Y_{j2}, \ldots, Y_{jn}$, $(n \geq 1)$ $j = 1,2, \ldots$, denote the j^{th} test Phase II sample of size n from a cdf $G(y)$. Both F and G are unknown continuous distribution functions and the process is IC when $F = G$. For detecting a change in the location, we use the location model $G_Y(x) = F(x - \theta)$ where $\theta \epsilon (-\infty, \infty)$ is the location parameter. Let $U_{j,r}$ denote the number of exceedances, that is, the number of Y observations in the j^{th} Phase II sample that exceeds $X_{(r)}$, the r^{th} ordered observation in the Phase I reference sample. The statistic $U_{j,r}$ is called an exceedance statistic and the probability $p_r = P(Y > X_{(r)} | X_{(r)})$ is called an exceedance probability. Note that this exceedance probability is a conditional probability given (conditionally) on $X_{(r)}$. More detail on the exceedance probability is given in Result 4.1 below. The number of Y observations in the j^{th} Phase II sample that precede $X_{(r)}$ is called a precedence statistic and this statistic was used by Chakraborti et al. (2004) to study the Shewhart-type precedence charts; this paper has been the starting point for a number of follow-up papers in this area.

Shewhart-type charts are popular in practice because of their simplicity and ease of application. While it is known (see e.g. Montgomery (2009) page 400) that these charts are effective in detecting larger process shifts (of roughly 2 standard deviations and greater) they are less able to detect smaller process shifts quickly enough. Consequently, control charts that use accumulated data up to and including the most recent time point, such as the EWMA and CUSUM charts, are preferred. Using this motivation, next, we propose the NPCUSUM control chart based on the exceedance statistics. It can be shown that the unconditional joint distribution of exceedance statistics is distribution-free (see Result 4B.2 in Appendix 4B) and hence the proposed NPEWMA-EX and NPCUSUM-EX charts are unconditionally distribution-free.

4.3 Nonparametric CUSUM control chart based on the exceedance statistic

4.3.1 Statistical background

For a detailed discussion on the CUSUM-$\overline{X}$ chart the reader is referred to Section 1.9.2. Here, a NPCUSUM chart based on the exceedance statistic is proposed. Given $X_{(r)} = x_{(r)}$ from the Phase I reference sample, it can be shown (see Result 4B.1 in Appendix 4B) that each $U_{j,r}$ follows a binomial distribution with parameters (n, p_r) and thus, conditionally on $X_{(r)}$, we can construct a binomial-type CUSUM chart based on the $U_{j,r}$'s to monitor the process location (via the exceedance

probabilities). Since $U_{j,r}|X_{(r)} \sim BIN(n, p_r)$ we have, from the properties of the binomial distribution, that $E\left(U_{j,r}\middle|X_{(r)}\right) = np_r$ for any $j = 1,2,3,\ldots$. However, since the conditional probability p_r is unknown we suggest replacing it by its unconditional IC value. The effect of this substitution, although motivated by the need for a practical solution, can be investigated further. For the interim, we motivate this substitution by noting that the conditional probability focusses on a specific observed value of some statistic or random variable whereas the unconditional probability can be viewed as a weighted average across all possible values that could have been observed for that statistic / variable on which was conditioned. Hence, the unconditional probability is a better measure than the conditional probability. In addition, the conditional probability p_r converges in probability to the unconditional IC value.

Result 4.1

The unconditional exceedance probability $P\left(Y > X_{(r)}\right)$ equals $(m - r + 1) / (m + 1)$ when the process is IC.

Proof

Note that $P\left(Y > X_{(r)}\right) = E\left(P\left(Y > X_{(r)}\middle|X_{(r)}\right)\right) = E(p_r)$. When the process is IC, $F = G$ and then $p_r = 1 - F\left(X_{(r)}\right) = 1 - V_r$ (say). Since $X_{(r)}$ is the r^{th} order statistic in a random sample of size m from F, using the probability integral transform, it can be shown (see e.g. Gibbons and Chakraborti (2010) page 39) that V_r follows the distribution of the r^{th} order statistic in a random sample of size m from the uniform $(U(0,1))$ distribution as long as F is continuous. This latter distribution is known to be a beta distribution with parameters r and $m - r + 1$, respectively. Moreover, when the process is IC, p_r follows a beta distribution with parameters $m - r + 1$ and r. Thus

$$E(p_r) = P\left(Y > X_{(r)}\right) = 1 - \frac{r}{m+1} = \frac{m-r+1}{m+1},$$

when the process is IC using the expectation formula for a beta distribution.

Thus, from Result 4.1 the unconditional exceedance probability $P\left(Y > X_{(r)}\right)$ equals

$$d = \frac{m - r + 1}{m + 1} \tag{4.1}$$

when the process is IC. Hence, once $X_{(r)}$ is observed, one can construct the NPCUSUM-EX, in analogy with the CUSUM-$\overline{X}$ (see Equations (1.3) and (1.4) in Section 1.9.2 with the pivot statistic ψ_i replaced by X_i (for individual data) or $\overline{X}_i$ (for subgroup data)). Consequently, for the upper one-sided NPCUSUM-EX we use

$$C_j^+ = max[0, C_{j-1}^+ + (U_{j,r} - nd) - k] \text{ for } j = 1,2,3... \tag{4.2}$$

and for the lower one-sided NPCUSUM-EX we use

$$C_j^- = min[0, C_{j-1}^- + (U_{j,r} - nd) + k] \text{ for } j = 1,2,3... \tag{4.3}$$

with starting values $C_0^+ = C_0^- = 0$ and where $k \geq 0$ is the so-called reference value. For the two-sided NPCUSUM-EX both C_j^- and C_j^+ are plotted simultaneously and the chart signals a possible OOC situation for the first j at which either $C_j^- \leq -H$ or $C_j^+ \geq H$, where $H > 0$ is the so-called decision interval. Otherwise, the process is considered IC and process monitoring continues without interruption. Recall that (see Section 1.9.2) for the CUSUM-$\overline{X}$ chart the quantities (counters) N^+ and N^- indicate the number of consecutive periods that the CUSUM's C_j^+ and C_j^- have been non-zero which helps in identifying at what point in time the shift may have taken place. In NPCUSUM charts these counters can be used in a similar manner. This is illustrated later on.

In this section, and as used in Chakraborti et al. (2004), $X_{(r)}$ is taken to be the median of the reference sample. The reasons for focusing on the median are clear; it is robust and a better representative of the central reference value. The performance of the NPCUSUM-EX median chart is compared both a parametric and a nonparametric CUSUM chart, respectively, namely the parametric CUSUM-$\overline{X}$ chart and the NPCUSUM-Rank chart. For more details on the NPCUSUM-Rank chart, the reader is referred to Li et al. (2010). These charts are candidates to monitor small shifts in the location. The comparisons are based on the ARL_δ with a given ARL_0. In addition, the use of winsorization is illustrated in this section for the *ARL*-based method. Winsorization is used in the performance comparison, since the *ARL* isn't a robust measure, i.e. it is dramatically impacted by the presence of outliers. Since $X_{(r)}$ is taken to be the median of the reference sample we find that

$d = 0.5$ (see Equation (4.1)). By replacing $d = 0.5$ into Equation (4.2), the upper one-sided NPCUSUM-EX chart based on the reference sample median, is given by the charting statistic

$$C_j^+ = \max[0, C_{j-1}^+ + (U_{j,r} - n/2) - k] \text{ for } j = 1,2,3... \quad (4.4)$$

with a starting value $C_0^+ = 0$. Note that an upper one-sided chart is considered in this section, since the two-sided NPCUSUM-EX chart will be considered in the Section 4.3.5. In addition, this is done in order to illustrate to the practitioner how a one-sided CUSUM chart is implemented.

4.3.2 Implementation of the chart

The design parameters (k, H) are chosen so that the chart has a specified nominal ARL_0 and is capable of detecting a shift, specially a small shift, as soon as possible. For a detailed discussion on the choice of k and H the reader is referred to Section 1.9.2 and, in that section, the choice of k for the CUSUM-$\overline{X}$ chart is discussed in detail. It was found that when there is little or no a-priori information regarding the size of the shift, a smaller value of k is the safest choice (to protect against any unnecessary delays in detection). Note that although we are considering an unknown shift, we are primarily interested in detecting a smaller and moderate shift with a CUSUM chart. Therefore, we recommend using $k = 0$ (or letting δ tend to 0). First, we consider $k = 0$.

This study includes a collection of non-normal distributions that are heavy-tailed, symmetric and skewed. Note that, wherever necessary, the distributions in the study have been shifted and scaled such that the mean / median equals 0 and the standard deviation equals 1, so that the results are easily comparable across the distributions. The details for these steps are shown in Appendix 1B. Specifically, the distributions considered in the study are:

i. The Standard Normal distribution, $N(0,1)$.

ii. The Gamma distribution, $GAM(\alpha, \beta)$, with parameters $(\alpha, \beta) = (1,1)$[i] and $(3,1)$, respectively, which is positively skewed.

[i] Note that the $GAM(1,1)$ distribution is the standard exponential distribution with mean 1, $EXP(1)$.

iii. The Student's t-distribution, $t(v)$, with degrees of freedom (df) $v = 3$, which is symmetric about 0 but with heavier tails than the $N(0,1)$.

iv. The Laplace (or Double Exponential $DE(0,1)$) distribution with mean 0 and variance 2, which is also symmetric but highly leptokurtic and has heavier tails.

Tables 4.1 and 4.2 list different values of H with $k = 0$ for the industry standard ARL_0 values of 370 and 500 and for $m = 500$ and 1000, respectively. These tables should be useful for implementing the NPCUSUM-EX median chart in practice.

Table 4.1. The IC characteristics[ii] of the run-length distribution of the NPCUSUM-EX median chart for different n with $m = 500$, $d = 0.5$ and $k = 0$

	Nominal ARL_0 = 370	**Nominal ARL_0 = 500**
Distribution	**$n = 5, H = 13.0$**	**$n = 5, H = 13.5$**
***N*(0,1)**	394.06 (2279.96) 29, 63, 126, 294, 1266	480.12 (3542.63) 31, 67, 134, 321, 1494
***EXP*(1)**	406.99 (2707.59) 29, 63, 125, 293, 1278	467.90 (2669.46) 31, 67, 135, 319, 1483
***GAM*(3,1)**	343.78 (2025.18) 28, 59, 117, 269, 1104	453.43 (2129.83) 31, 67, 136, 324, 1489
***t*(3)**	409.22 (3368.77) 29, 63, 126, 294, 1290	488.18 (5288.29) 31, 67, 134, 320, 1496
***DE*(0,1)**	404.24 (3566.87) 29, 62, 124, 291, 1280	486.71 (3590.93) 31, 67, 135, 322, 1501
Distribution	**$n = 11, H = 14.5$**	**$n = 11, H = 15.5$**
***N*(0,1)**	361.20 (3476.82) 17, 37, 76, 191, 1050	544.91 (8365.88) 19, 40, 85, 223, 1387
***EXP*(1)**	365.10 (3824.06) 17, 36, 75, 189, 1047	538.40 (6505.87) 19, 40, 84, 222, 1203
***GAM*(3,1)**	370.11 (3638.60) 17, 36, 75, 176, 931	520.73 (4004.53) 19, 40, 84, 207, 1221
***t*(3)**	370.71 (4236.95) 17, 37, 75, 191, 1071	463.24 (6987.13) 18, 38, 79, 206, 1213
***DE*(0,1)**	347.59 (2205.70) 17, 36, 75, 192, 1081	533.52 (8816.49) 19, 41, 85, 226, 1378
Distribution	**$n = 25, H = 15.5$**	**$n = 25, H = 16.5$**
***N*(0,1)**	335.38 (4094.52) 9, 19, 41, 115, 815	555.66 (11960.87) 10, 21, 46, 138, 1059
***EXP*(1)**	319.67 (4547.30) 9, 19, 41, 114, 801	450.18 (8130.46) 9, 20, 44, 123, 938
***GAM*(3,1)**	375.91 (4185.58) 9, 19, 39, 105, 696	460.32 (15327.72) 9, 20, 44, 123, 928
***t*(3)**	350.98 (4977.05) 9, 20, 42, 114, 827	452.32 (13780.67) 9, 21, 44, 122, 911
***DE*(0,1)**	341.56 (4254.38) 9, 20, 41, 115, 809	550.84 (14802.36) 10, 21, 46, 133, 1067

Firstly, it is seen that the IC run-length characteristics of the proposed chart are approximately the same for all continuous distributions for fixed m and n which confirms its nonparametric characteristics. Secondly, the proposed chart can attain the industry standard ARL_0 values of 370 and 500 almost exactly.

[ii] Note that, the first row of each of the cells shows the *ARL* and *SDRL* values whereas the second row shows the 5th, 25th, 50th, 75th and 95th percentiles (in this order). Also note that these values were obtained via simulation and not the Markov chain approach; see Appendix4A for the motivation behind this.

Table 4.2. The IC characteristics[iii] of the run-length distribution of the NPCUSUM-EX median chart for different n with m =1000, d = 0.5 and k = 0

	Nominal ARL_0 = 370	**Nominal ARL_0 = 500**
Distribution	**n = 5, H = 15.5**	**n = 5, H = 16.5**
***N*(0,1)**	394.68 (911.58) 42, 91, 173, 366, 1361	487.10 (1548.10) 46, 102, 198, 439, 1690
***EXP*(1)**	384.42 (972.02) 42, 89, 173, 372, 1291	474.69 (1668.50) 46, 99, 195, 426, 1585
***GAM*(3,1)**	383.33 (1048.65) 42, 89, 172, 370, 1273	470.56 (1395.70) 46, 99, 194, 427, 1571
***t*(3)**	389.89 (1084.26) 42, 89, 174, 373, 1289	470.19 (1277.29) 46, 99, 195, 428, 1586
***DE*(0,1)**	385.70 (918.64) 42, 90, 173, 371, 1300	475.51 (1628.32) 47, 99, 194, 422, 1590
Distribution	**n = 11, H = 18.5**	**n = 11, H = 20.0**
***N*(0,1)**	371.10 (1810.85) 27, 58, 116, 272, 1204	516.43 (3079.99) 30, 65, 133, 326, 1631
***EXP*(1)**	355.46 (1428.46) 26, 56, 114, 260, 1174	505.77 (3121.91) 30, 66, 135, 331, 1591
***GAM*(3,1)**	381.93 (2315.71) 27, 58, 117, 273, 1203	552.18 (5437.10) 30, 66, 133, 328, 1613
***t*(3)**	372.83 (2008.43) 27, 58, 116, 273, 1202	536.60 (4091.31) 31, 66, 134, 325, 1602
***DE*(0,1)**	368.17 (2172.19) 27, 58, 116, 272, 1190	528.42 (4412.10) 31, 66, 133, 322, 1611
Distribution	**n = 25, H = 21.5**	**n = 25, H = 22.5**
***N*(0,1)**	369.96 (2451.44) 16, 34, 73, 190, 1104	486.27 (11749.40) 17, 36, 75, 203, 1409
***EXP*(1)**	370.80 (2219.84) 16, 36, 76, 192, 1211	493.66 (7470.19) 17, 38, 79, 218, 1504
***GAM*(3,1)**	416.70 (4703.45) 16, 35, 72, 188, 1136	555.21 (10451.15) 17, 37, 78, 213, 1405
***t*(3)**	375.78 (4808.40) 15, 33, 69, 181, 1047	510.02 (9028.25) 17, 36, 75, 200, 1286
***DE*(0,1)**	425.33 (6523.23) 16, 35, 72, 190, 1140	539.45 (5942.58) 17, 37, 79, 214, 1428

Note that the ARL_0 values in Tables 4.1 and 4.2 were obtained for relatively large reference samples m (= 500 and 1000, respectively). While these m values seem large, note that m = 500 means 100 samples each of size 5 from Phase I, which is reasonable. Several authors have discussed and made recommendations about the size of the reference sample and the consensus seems to be around 300 to 500. For smaller reference sample sizes, the calculations are rather difficult and need special care. A modified approach based on winsorization is discussed in Appendix 4C for this case.

[iii] Note that, the first row of each of the cells shows the *ARL* and *SDRL* values whereas the second row shows the 5th, 25th, 50th, 75th and 95th percentiles (in this order). Also note that these values were obtained via simulation and not the Markov chain approach; see Appendix4A for the motivation behind this.

Effect of the Phase II test sample size

In order to examine the effect of the Phase II test sample size, Tables 4.3 to 4.7 show the shift detection capability of the NPCUSUM-EX median chart as n increases.

Table 4.3. The OOC[iv] characteristics[v] of the run-length distribution for different n with $m = 1000$, $d = 0.5$ and $k = 0$ for the $N(0,1)$ distribution

	Nominal $ARL_0 = 370$	**Nominal $ARL_0 = 500$**
γ	$n = 5, \quad H = 15.5$	$n = 5, \quad H = 16.5$
0.25	70.60 (53.31) 24, 39, 56, 84, 164	74.57 (55.70) 26, 42, 60, 89, 173
0.50	36.38 (16.08) 18, 25, 33, 44, 67	38.52 (16.78) 19, 27, 35, 46, 70
0.75	24.72 (8.53) 14, 19, 23, 29, 41	26.35 (8.82) 15, 20, 25, 31, 43
1.00	19.07 (5.51) 12, 15, 18, 22, 29	20.72 (5.60) 13, 16, 19, 23, 30
1.50	13.40 (2.94) 10, 11, 13, 15, 19	14.13 (2.96) 10, 12, 16, 18, 20
2.00	10.64 (1.84) 8, 9, 10, 12, 14	11.30 (1.92) 8, 10, 11, 12, 15
γ	$n = 11, \quad H = 18.5$	$n = 11, \quad H = 20.0$
0.25	61.83 (79.05) 17, 29, 43, 69, 158	67.94 (80.43) 19, 31, 47, 75, 181
0.50	30.25 (17.84) 13, 19, 26, 36, 62	32.41 (19.15) 14, 21, 28, 38, 65
0.75	20.30 (8.48) 10, 14, 18, 24, 36	21.59 (8.56) 11, 16, 20, 26, 38
1.00	15.22 (5.13) 9, 12, 14, 18, 25	16.53 (5.47) 10, 13, 15, 19, 27
1.50	10.54 (2.74) 7, 9, 10, 12, 16	11.33 (2.84) 7, 9, 11, 13, 17
2.00	8.20 (1.76) 6, 7, 8, 9, 12	8.82 (1.84) 6, 7, 9, 10, 12
γ	$n = 25, \quad H = 21.5$	$n = 25, \quad H = 22.5$
0.25	59.22 (120.60) 11, 20, 32, 57, 174	61.74 (123.92) 12, 21, 33, 58, 183
0.50	25.32 (25.05) 9, 14, 19, 29, 59	26.58 (26.16) 9, 14, 20, 30, 62
0.75	17.27 (9.24) 7, 10, 14, 19, 32	16.83 (9.76) 8, 11, 15, 20, 33
1.00	12.08 (5.16) 6, 9, 11, 14, 22	12.67 (5.38) 6, 9, 12, 15, 23
1.50	8.23 (2.60) 5, 6, 8, 10, 13	8.56 (2.66) 5, 7, 8, 10, 14
2.00	6.31 (1.65) 4, 5, 6, 7, 9	6.55 (1.66) 4, 5, 6, 8, 10

[iv] Shifts: $\delta = \gamma \sigma / \sqrt{n}$ are considered; a detailed motivation regarding the choice of shift is given in the next section.

[v] Note that, the first row of each of the cells shows the *ARL* and *SDRL* values whereas the second row shows the 5th, 25th, 50th, 75th and 95th percentiles (in this order).

Table 4.4. The OOC characteristics[vi] of the run-length distribution for different n with $m = 1000$, $d = 0.5$ and $k = 0$ for the $EXP(1)$ distribution

	Nominal $ARL_0 = 370$	**Nominal $ARL_0 = 500$**
γ	$n = 5, \quad H = 15.5$	$n = 5, \quad H = 16.5$
0.25	54.58 (36.53) 21, 33, 45, 65, 118	58.15 (38.03) 23, 35, 49, 70, 124
0.50	26.24 (9.98) 14, 20, 24, 31, 45	27.60 (10.23) 15, 20, 26, 32, 46
0.75	16.67 (4.54) 11, 14, 16, 19, 25	17.70 (4.72) 12, 14, 17, 20, 26
1.00	11.92 (2.53) 8, 10, 12, 13, 16	12.60 (2.62) 9, 11, 12, 14, 18
1.50	7.30 (0.56) 7, 7, 7, 8, 8	7.56 (0.70) 7, 7, 7, 8, 9
2.00	7.00 (0.00) 7, 7, 7, 7, 7	7.00 (0.00) 7, 7, 7, 7 7
γ	$n = 11, \quad H = 18.5$	$n = 11, \quad H = 20.0$
0.25	47.78 (47.76) 16, 25, 36, 55, 114	52.88 (56.47) 17, 27, 39, 60, 129
0.50	22.75 (11.01) 11, 16, 20, 27, 43	24.17 (11.35) 12, 17, 22, 29, 45
0.75	14.49 (5.04) 8, 11, 14, 17, 24	15.59 (5.29) 9, 12, 15, 18, 25
1.00	10.41 (2.88) 7, 8, 10, 12, 16	11.29 (3.07) 7, 9, 11, 13, 17
1.50	6.60 (1.27) 5, 6, 6, 7, 9	7.08 (1.34) 5, 6, 7, 8, 9
2.00	4.59 (0.66) 4, 4, 4, 5, 6	5.01 (0.60) 4, 5, 5, 5, 6
γ	$n = 25, \quad H = 21.5$	$n = 25, \quad H = 22.5$
0.25	44.17 (85.33) 10, 17, 26, 44, 122	47.50 (96.67) 11, 18, 28, 46, 126
0.50	19.13 (20.13) 8, 11, 16, 22, 40	19.92 (16.39) 8, 12, 16, 23, 42
0.75	12.01 (5.43) 6, 8, 11,14, 22	12.61 (5.85) 6, 9, 11, 15, 23
1.00	8.85 (3.30) 5, 7, 8, 10, 15	9.18 (3.28) 5, 7, 8, 11, 15
1.50	5.69 (1.48) 4, 5, 6, 6, 8	5.91 (1.52) 4, 5, 6, 7, 9
2.00	4.14 (0.83) 3, 4, 4, 5, 6	4.30 (0.86) 3, 4, 4, 5, 6

[vi] Note that, the first row of each of the cells shows the *ARL* and *SDRL* values whereas the second row shows the 5th, 25th, 50th, 75th and 95th percentiles (in this order).

Table 4.5. The OOC characteristics[vii] of the run-length distribution for different n with $m = 1000$, $d = 0.5$ and $k = 0$ for the *GAM*(3,1) distribution

	Nominal $ARL_0 = 370$	**Nominal $ARL_0 = 500$**
γ	$n = 5, \quad H = 15.5$	$n = 5, \quad H = 16.5$
0.25	64.43 (46.09) 24, 37, 52, 77, 147	70.35 (51.39) 25, 40, 57, 84, 159
0.50	32.53 (13.68) 16, 23, 30, 39, 59	34.01 (14.21) 18, 24, 32, 41, 61
0.75	21.68 (6.96) 13, 17, 20, 25, 34	22.98 (7.20) 14, 18, 22, 27, 36
1.00	16.28 (4.34) 10, 13, 16, 18, 24	17.20 (4.35) 12, 14, 16, 20, 25
1.50	10.96 (2.01) 8, 10, 11, 12, 14	11.62 (2.09) 9, 10, 11, 13, 16
2.00	8.56 (1.07) 7, 8, 8, 9, 10	9.04 (1.12) 8, 8, 9, 10, 11
γ	$n = 11, \quad H = 18.5$	$n = 11, \quad H = 20.0$
0.25	57.66 (66.31) 17, 28, 41, 65, 142	63.10 (75.50) 19, 30, 45, 71, 159
0.50	27.42 (15.10) 12, 18, 24, 33, 55	29.74 (16.19) 13, 19, 26, 35, 69
0.75	17.98 (7.04) 10, 13, 16, 21, 31	19.43 (7.58) 11, 14, 18, 23, 33
1.00	13.56 (4.35) 8, 10, 13, 16, 22	14.51 (4.53) 9, 11, 14, 17, 23
1.50	8.98 (2.15) 6, 8, 9, 10, 13	9.68 (2.22) 7, 8, 9, 11, 14
2.00	6.83 (1.28) 5, 6, 7, 8, 9	7.30 (1.31) 5, 6, 7, 8, 10
γ	$n = 25, \quad H = 21.5$	$n = 25, \quad H = 22.5$
0.25	53.57 (107.16) 11, 19, 30, 52, 154	58.41 (110.50) 12, 20, 32, 56, 177
0.50	23.00 (19.17) 8, 13, 18, 26, 53	24.25 (23.68) 9, 14, 19, 28, 54
0.75	14.87 (8.03) 7, 10, 13, 18, 29	15.43 (8.20) 7, 10, 14, 18, 30
1.00	10.90 (4.45) 6, 8, 10, 13, 19	11.45 (4.80) 6, 8, 10, 14, 20
1.50	7.22 (2.14) 4, 6, 7, 8, 11	7.54 (2.23) 5, 6, 7, 9, 12
2.00	5.44 (1.32) 4, 4, 5, 6, 8	5.69 (1.34) 4, 5, 6, 6, 8

[vii] Note that, the first row of each of the cells shows the *ARL* and *SDRL* values whereas the second row shows the 5th, 25th, 50th, 75th and 95th percentiles (in this order).

Table 4.6. The OOC characteristics[viii] of the run-length distribution for different n with $m = 1000$, $d = 0.5$ and $k = 0$ for the $t(3)$ distribution

	Nominal $ARL_0 = 370$	**Nominal $ARL_0 = 500$**
γ	$n = 5, \quad H = 15.5$	$n = 5, \quad H = 16.5$
0.25	45.20 (23.68) 20, 30, 40, 54, 89	47.84 (24.83) 21, 31, 42, 57, 94
0.50	23.59 (7.81) 14, 18, 22, 28, 38	25.13 (8.23) 14, 19, 24, 29, 40
0.75	16.52 (4.24) 11, 14, 16, 19, 24	17.64 (4.42) 12, 14, 17, 20, 26
1.00	13.20 (2.75) 9, 11, 13, 15, 18	13.96 (2.88) 10, 12, 14, 16, 19
1.50	10.02 (1.58) 8, 9, 10, 11, 13	10.58 (1.61) 8, 10, 10, 12, 14
2.00	8.64 (1.06) 7, 8, 8, 9, 10	9.14 (1.12) 8, 8, 9, 10, 11
γ	$n = 11, \quad H = 18.5$	$n = 11, \quad H = 20.0$
0.25	38.08 (29.33) 14, 22, 31, 45, 84	41.26 (29.24) 16, 24, 34, 49, 90
0.50	18.97 (7.55) 10, 14, 18, 22, 33	20.52 (7.94) 11, 15, 19, 24, 35
0.75	13.13 (3.97) 8, 10, 12, 15, 20	14.16 (4.21) 9, 11, 13, 16, 22
1.00	10.17 (2.56) 7, 8, 10, 12, 15	10.93 (2.70) 7, 9, 11, 12, 16
1.50	7.31 (1.40) 5, 6, 7, 8, 10	7.84 (1.46) 6, 7, 8, 9, 11
2.00	6.00 (0.93) 5, 5, 6, 6, 8	6.46 (1.02) 5, 6, 6, 7, 8
γ	$n = 25, \quad H = 21.5$	$n = 25, \quad H = 22.5$
0.25	33.20 (47.53) 10, 16, 23, 36, 81	35.23 (48.64) 10, 16, 24, 38, 90
0.50	15.19 (7.99) 7, 10, 13, 18, 29	16.04 (8.44) 8, 11, 14, 19, 31
0.75	10.24 (3.85) 6, 8, 9, 12, 18	10.75 (4.01) 6, 8, 10, 13, 18
1.00	7.79 (2.35) 5, 6, 7, 9, 12	8.15 (2.43) 5, 6, 8, 9, 13
1.50	5.45 (1.28) 4, 5, 5, 6, 8	5.70 (1.33) 4, 5, 6, 6, 8
2.00	4.34 (0.84) 3, 4, 4, 5, 6	4.53 (0.86) 3, 4, 4, 5, 6

[viii] Note that, the first row of each of the cells shows the *ARL* and *SDRL* values whereas the second row shows the 5th, 25th, 50th, 75th and 95th percentiles (in this order).

Table 4.7. The OOC characteristics[ix] of the run-length distribution for different n with $m = 1000$, $d = 0.5$ and $k = 0$ for the $DE(0,1)$ distribution

	Nominal $ARL_0 = 370$	**Nominal $ARL_0 = 500$**
γ	$n = 5, \quad H = 15.5$	$n = 5, \quad H = 16.5$
0.25	43.10 (21.54) 19, 28, 38, 52, 83	46.10 (21.90) 21, 31, 41, 55, 86
0.50	23.99 (7.89) 14, 18, 23, 28, 39	25.50 (8.27) 15, 20, 24, 30, 41
0.75	17.45 (4.56) 11, 14, 17, 20, 26	18.45 (4.77) 12, 15, 18, 21, 27
1.00	14.07 (3.11) 10, 12, 14, 16, 20	15.05 (3.26) 10, 13, 15, 17, 21
1.50	10.90 (1.90) 8, 10, 11, 12, 14	11.59 (1.96) 9, 10, 11, 13, 15
2.00	9.35 (1.36) 8, 8, 9, 10, 12	9.89 (1.38) 8, 9, 10, 11, 12
γ	$n = 11, \quad H = 18.5$	$n = 11, \quad H = 20.0$
0.25	35.20 (23.20) 14, 21, 29, 42, 76	38.60 (25.82) 15, 23, 32, 46, 82
0.50	18.73 (7.23) 10, 14, 17, 22, 32	20.30 (7.55) 11, 15, 19, 24, 34
0.75	13.32 (3.98) 8, 10, 13, 16, 21	14.26 (4.14) 9, 11, 14, 17, 22
1.00	10.58 (2.72) 7, 9, 10, 12, 16	11.33 (2.77) 7, 9, 11, 13, 16
1.50	7.89 (1.60) 6, 7, 8, 9, 11	8.45 (1.65) 6, 7, 8, 9, 11
2.00	6.55 (1.10) 5, 6, 6, 7, 8	7.00 (1.15) 5, 6, 7, 8, 9
γ	$n = 25, \quad H = 21.5$	$n = 25, \quad H = 22.5$
0.25	30.07 (42.88) 9, 15, 22, 34, 71	32.05 (42.75) 10, 16, 23, 55, 78
0.50	14.37 (6.93) 7, 10, 13, 17, 26	15.06 (6.90) 7, 10, 14, 18, 28
0.75	10.09 (3.58) 6, 8, 10, 12, 17	10.52 (3.66) 6, 8, 10, 12, 17
1.00	7.83 (2.31) 5, 6, 8, 9, 12	8.18 (2.40) 5, 6, 8, 10, 13
1.50	5.67 (1.33) 4, 5, 6, 6, 8	5.92 (1.37) 4, 5, 6, 7, 8
2.00	4.61 (0.92) 3, 4, 4, 5, 6	4.81 (0.95) 4, 4, 5, 5, 6

[ix] Note that, the first row of each of the cells shows the *ARL* and *SDRL* values whereas the second row shows the 5th, 25th, 50th, 75th and 95th percentiles (in this order).

In order to examine the effect of the Phase II test sample size, Figures 4.1 and 4.2 show the shift detection capability of the NPCUSUM-EX median chart as n increases for a nominal $ARL_0 = 370$ and 500, respectively.

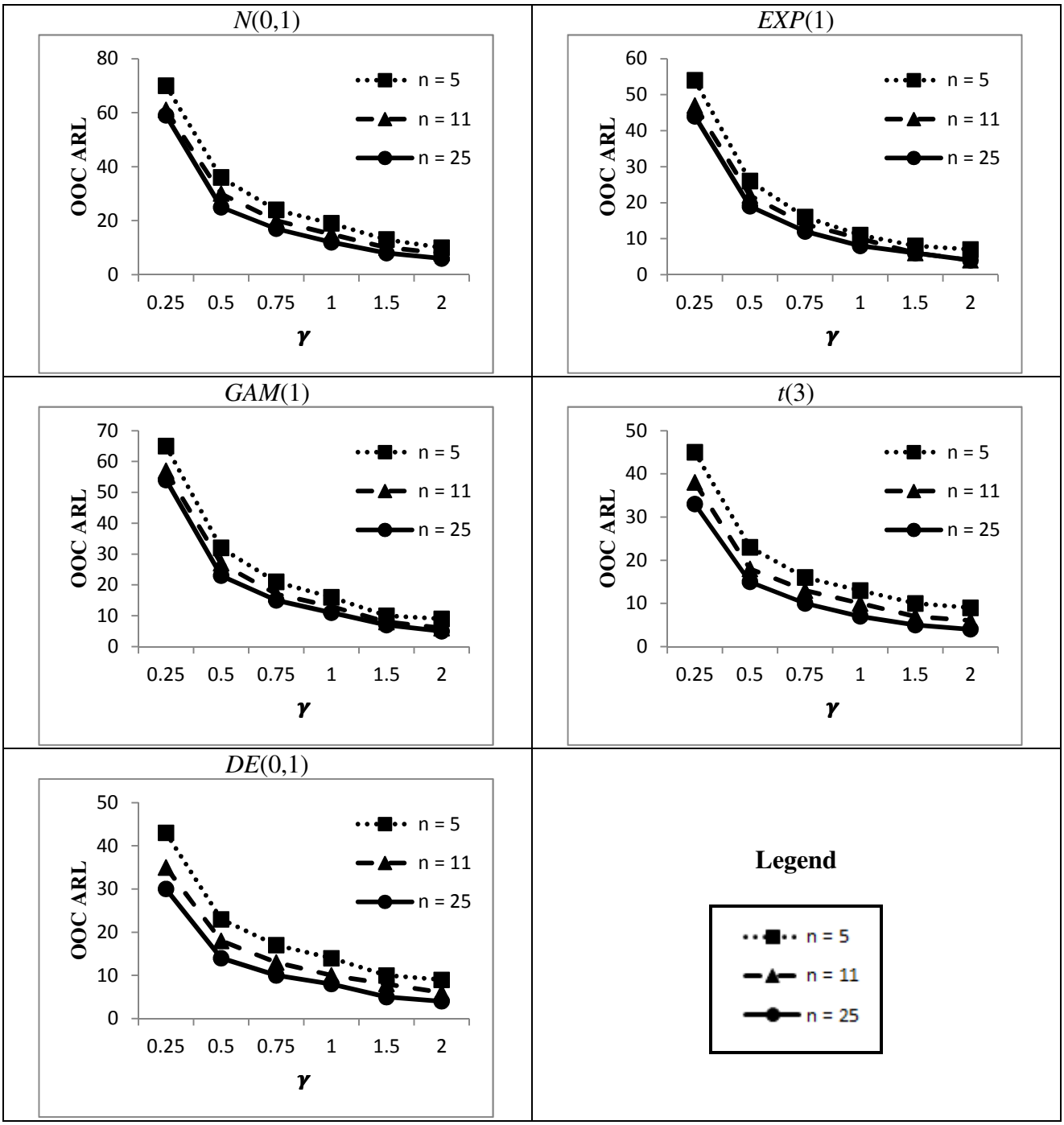

Figure 4.1. OOC performance comparison of the NPCUSUM-EX median chart for different values of n and various distributions for nominal $ARL_0 = 370$, $m = 1000$, $d = 0.5$ and $k = 0$

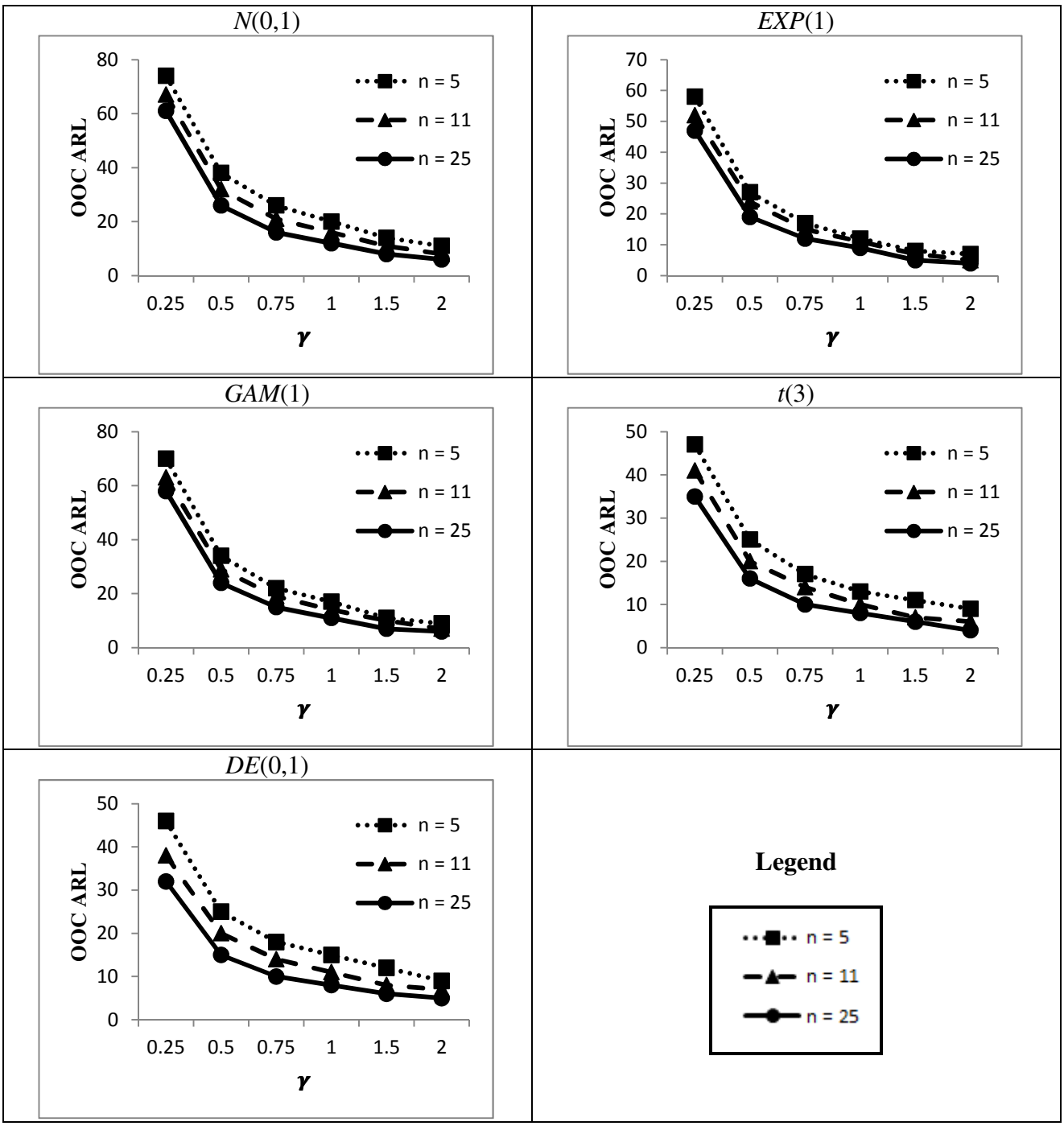

Figure 4.2. OOC performance comparison of the NPCUSUM-EX median chart for different values of n and various distributions for nominal $ARL_0 = 500$, $m = 1000$, $d = 0.5$ and $k = 0$

From Figures 4.1 and 4.2 we see that the shift detection capability of the chart increases as n increases for all distributions under consideration, which is to be expected. Thus, $n = 25$ performs best. However, it is typical for control charting with variables data, to take the subgroup size n much smaller than the number of subgroups m and, consequently, we recommend using $n = 5$ or 11. From this point forward we use $n = 5$ for illustration purposes. Note that this recommendation is

the opposite to control charting with attributes data, where typically the subgroup size n is taken to be much larger than the number of subgroups m.

4.3.3 Performance comparison with other charts

We compare the NPCUSUM-EX chart to the adjusted[x] CUSUM-$\overline{X}$ chart (see Jones et al. (2004)) and the NPEWMA-Rank chart (see Li et al. (2010)). The shift considered by Jones (2004; page 97) for the adjusted CUSUM-$\overline{X}$ chart is given by $\delta = \frac{\mu-\mu_0}{\sigma/\sqrt{n}}$. The shift considered by Li et al. (2010; page 215) for the NPCUSUM-Rank chart is measured by the subgroup standard deviation $\sigma/\sqrt{n}$. Thus, in order to have a fair comparison between the proposed NPCUSUM-EX chart and its competitors, a shift of $\delta = \gamma\,\sigma/\sqrt{n}$ where $-\infty < \gamma < \infty$, $\gamma \neq 0$ is used for all charts. In this chapter the values of γ under consideration are γ = 0.25(0.25)1.00, 1.50 and 2.00. The largest value of γ under consideration is γ = 2.0, since, for larger shifts, the run-length characteristics of the charts tend to converge to some small values, i.e if the shift is large enough the any of the charts will signal (almost) immediately (see Tables 4.8 to 4.12).

The results are shown in Tables 4.8 to 4.12 and also graphically represented in Figures 4.3 and 4.4 for m = 100 and n = 5 for each distribution under consideration. In Tables 4.8 to 4.12 the first row of each of the cells shows the *ARL* and *SDRL* values whereas the second row shows the 5th, 25th, 50th, 75th and 95th percentiles (in this order). It should be noted that:

i. The ARL_0 values of all the charts under comparison are fixed at or close to 500 and the chart with the smallest ARL_δ performs the best.

ii. For the CUSUM-$\overline{X}$ chart the standards (parameters) are estimated from a Phase I reference sample duly taking care of the issues related to estimation.

iii. Two values of the reference value k are considered, namely, $k = 0$ with $d^* = 0.5$ and $k = n(d^* - d)$ with $d^* = 0.5\sqrt{\frac{n(m+n+1)}{4(m+2)}}$.

[x] Adjusted: Case U; the parameters have to be estimated using a Phase I reference sample.

Table 4.8. The IC and OOC characteristics[xi] of the run-length distribution for $m = 100$ and $n = 5$ for the $N(0,1)$ distribution with nominal $ARL_0 = 500$ and winsorization at the 5000th step

	Chart Type					
	Parametric CUSUM-$\overline{X}$ chart with parameters estimated from a Phase I sample		NPCUSUM-Rank chart		NPCUSUM-EX median chart	
Winsorization level	WL = 95.4	WL = 96.6	WL = 95.6	WL = 97.7	WL = 95.9	WL = 97.3
Control limits	$H = 8.50$	$H = 5.17$	$H = 563.0$	$H = 225$	$H = 9.55$	$H = 5.18$
k	0	$0.5\sigma/\sqrt{n}$	0	$0.5\sqrt{mn(m+n+1)/12}$	0	$k = n(d^* - d)$
d^* / γ	NA	NA	NA	NA	0.50	$0.5\sqrt{\frac{n(m+n+1)}{4(m+2)}} \approx 0.57$
0.00	507.44 (1177.56) 14, 31, 72, 256, 4449	493.51 (1070.55) 11, 32, 99, 337, 3139	503.52 (1171.43) 16,33, 74, 264, 4236	505.53 (972.27) 12, 48, 144, 444, 2499	503.24 (1137.31) 14, 31, 70, 252, 3880	502.27 (1023.94) 10, 37, 113, 404, 2844
0.25	92.00 (380.94) 10, 17, 27, 51, 240	97.55 (307.37) 7, 14, 29, 68, 346	93.33 (343.36) 12, 19, 29, 56, 255	137.73 (351.71) 8, 19, 44, 114, 521	122.89 (464.30) 11, 19, 32, 65, 380	146.06 (430.42) 8, 17, 39, 105, 547
0.50	24.81 (61.19) 7, 11, 16, 25, 56	26.74 (69.05) 5, 9, 14, 25, 76	26.98 (72.05) 10, 14, 19, 27, 59	41.09 (114.10) 6, 11, 19, 40, 129	35.97 (143.89) 9, 13, 20, 31, 83	49.78 (180.86) 6, 11, 19, 40, 153
0.75	13.52 (8.15) 6, 9, 12, 16, 27	12.93 (16.50) 4, 6, 10, 15, 31	16.15 (9.80) 8, 11, 14,18, 30	18.11 (26.46) 5, 8, 12, 19, 48	18.21 (22.74) 7, 10, 14, 20, 39	20.22 (30.90) 5, 8, 12, 21, 58
1.00	9.93 (4.28) 5, 7, 9, 12, 18	8.22 (5.12) 3, 5, 7, 10, 17	12.43 (4.73) 7, 9, 11, 14, 21	11.35 (13.77) 5, 6, 9, 13, 26	12.97 (7.39) 6, 9, 11, 15, 24	12.17 (11.72) 4, 6, 9, 14, 29
1.50	6.62 (2.08) 4, 5, 6, 8, 10	5.00 (2.01) 3, 4, 5, 6, 9	8.96 (2.08) 6, 8, 9,10, 13	6.77 (2.67) 4, 5, 6, 8, 12	8.76 (2.82) 6, 7, 8, 10, 14	6.77 (3.37) 3, 4, 6, 8, 13
2.00	5.01 (1.29) 3, 4, 5, 6, 7	3.67 (1.19) 2, 3, 3, 4, 6	7.41 (1.23) 6, 7, 7, 8, 10	5.31 (1.38) 4, 5, 6, 8, 20	6.95 (1.69) 5, 6, 6, 8, 10	4.99 (1.87) 3, 4, 5, 6, 8

[xi] Note that, the first row of each of the cells shows the *ARL* and *SDRL* values whereas the second row shows the 5th, 25th, 50th, 75th and 95th percentiles (in this order).

Table 4.9. The IC and OOC characteristics[xii] of the run-length distribution for $m = 100$ and $n = 5$ for the $EXP(1)$ distribution with nominal $ARL_0 = 500$ and winsorization at the 5000th step

	Chart Type					
	Parametric CUSUM-$\bar{X}$ chart with parameters estimated from a Phase I sample		NPCUSUM-Rank chart		NPCUSUM-EX median chart	
Winsorization level	WL = 95.7	WL = 96.6	WL = 95.6	WL = 97.9	WL = 95.5	WL = 97.2
Control limits	$H = 8.00$	$H = 5.25$	$H = 563.0$	$H = 225.0$	$H = 9.55$	$H = 5.18$
k	0	$0.5\sigma/\sqrt{n}$	0	$0.5\sqrt{mn(m+n+1)/12}$	0	$k = n(d^* - d)$
d^* / γ	NA	NA	NA	NA	0.50	$0.5\sqrt{\frac{n(m+n+1)}{4(m+2)}} \approx 0.57$
0.00	497.99 (1151.67) 11, 28, 69, 262, 3990	494.40 (1080.71) 9, 29, 89, 332, 3220	502.40 (1155.50) 16, 33, 74, 257, 4067	500.02 (953.54) 12, 47, 141, 448, 2464	501.01 (1158.61) 14, 31, 72, 264, 4223	491.60 (1021.17) 10, 37, 110, 383, 2763
0.25	112.39 (475.83) 8, 15, 25, 51, 329	171.68 (584.54) 6, 14, 30, 87, 636	49.89 (216.36) 11, 15, 22, 34, 107	108.92 (338.02) 7, 14, 30, 75, 401	97.27 (400.71) 10, 16, 26, 51, 248	123.30 (399.82) 7, 14, 30, 81, 440
0.50	28.47 (91.94) 6, 10, 16, 26, 68	51.78 (247.44) 4, 9, 15, 30, 149	15.84 (16.01) 9, 11, 13, 17, 29	25.24 (73.72) 6, 8, 12, 21, 73	27.69 (142.54) 7, 10, 15, 23, 58	30.71 (110.29) 4, 8, 13, 24, 92
0.75	14.06 (15.56) 5, 8, 11, 16, 30	17.64 (56.61) 4, 6, 10, 17, 44	11.19 (3.48) 7, 9, 10, 13, 17	10.52 (17.21) 5, 6, 8, 11, 21	12.26 (12.33) 6, 8, 10, 14, 25	11.54 (22.89) 3, 5, 8, 12, 29
1.00	9.99 (6.25) 4, 6, 9, 12, 19	10.12 (31.63) 3, 5, 7, 11, 22	9.05 (1.95) 7, 8, 9, 10, 13	7.14 (3.10) 5, 5, 6, 8, 12	8.25 (3.95) 5, 6, 7, 9, 15	6.60 (7.87) 3, 4, 5, 8, 15
1.50	6.45 (2.44) 3, 5, 6, 8, 11	5.32 (2.62) 2, 4, 5, 6, 10	7.24 (1.00) 6, 7, 7, 8, 9	5.18 (0.98) 4, 5, 5, 6, 7	4.79 (1.28) 4, 4, 4, 5, 7	3.39 (1.01) 3, 3, 3, 3, 5
2.00	4.82 (1.48) 3, 4, 5, 6, 7	3.82 (1.45) 2, 3, 4, 4, 6	6.37 (0.61) 6, 6, 6, 7, 7	4.50 (0.62) 4, 4, 4, 5, 5	4.02 (0.20) 4, 4, 4, 4, 4	3.01 (0.08) 3, 3, 3, 3, 3

[xii] Note that, the first row of each of the cells shows the *ARL* and *SDRL* values whereas the second row shows the 5th, 25th, 50th, 75th and 95th percentiles (in this order).

Table 4.10. The IC and OOC characteristics[xiii] of the run-length distribution for $m = 100$ and $n = 5$ for the *GAM*(3,1) distribution with nominal $ARL_0 = 500$ and winsorization at the 5000th step

	Chart Type					
	Parametric CUSUM-$\overline{X}$ chart with parameters estimated from a Phase I sample		NPCUSUM-Rank chart		NPCUSUM-EX median chart	
Windsorization level	WL = 95.6	WL = 96.5	WL = 95.7	WL = 97.9	WL = 95.3	WL = 97.2
Control limits	$H = 8.50$	$H = 5.20$	$H = 563.0$	$H = 225.0$	$H = 9.55$	$H = 5.18$
k	0	$0.5\sigma/\sqrt{n}$	0	$0.5\sqrt{mn(m+n+1)/12}$	0	$k = n(d^* - d)$
d^* / γ	NA	NA	NA	NA	0.50	$0.5\sqrt{\frac{n(m+n+1)}{4(m+2)}} \approx 0.57$
0.00	494.98 (1152.81) 12, 29, 70, 255, 4117	504.68 (1085.77) 10, 30, 90, 352, 3226	496.82 (1138.20) 16, 33, 74, 262, 3752	494.35 (945.50) 11, 45, 140, 450, 2393	509.83 (1186.24) 14, 31, 74, 269, 4546	493.35 (1013.53) 11, 38, 108, 364, 2739
0.25	109.26 (443.83) 9, 16, 27, 55, 303	139.34 (477.73) 6, 14, 29, 79, 505	90.09 (371.13) 12, 18, 27, 49, 222	143.62 (391.30) 8, 18, 41, 108, 555	126.09 (494.92) 10, 18, 29, 61, 356	143.49 (435.83) 7, 16, 36, 100, 534
0.50	27.76 (101.83) 7, 11, 16, 25, 61	37.35 (137.94) 5, 9, 15, 29, 109	23.54 (39.17) 10, 13, 17, 24, 49	39.89 (101.63) 6, 10, 18, 35, 131	34.02 (142.31) 8, 12, 18, 28, 76	45.05 (142.86) 5, 9, 17, 36, 145
0.75	14.13 (17.18) 6, 8, 11, 16, 30	15.82 (72.91) 4, 6, 10, 16, 38	14.45 (7.44) 8, 10, 13, 16, 26	17.15 (55.18) 5, 8, 11, 17, 43	16.60 (53.03) 7, 9, 12, 18, 34	17.70 (36.70) 4, 7, 10, 18, 49
1.00	10.03 (5.87) 5, 7, 9, 12, 19	8.88 (8.02) 3, 5, 7, 10, 20	11.25 (3.51) 7, 9, 10, 13, 17	9.65 (6.38) 5, 6, 8, 11, 20	11.23 (6.82) 6, 8, 10, 13, 21	9.91 (14.59) 3, 5, 8, 11, 23
1.50	6.54 (2.27) 4, 5, 6, 8, 11	5.19 (2.38) 3, 4, 5, 6, 10	8.24 (1.54) 6, 7, 8, 9, 11	6.14 (1.88) 4, 5, 6, 7, 9	7.29 (2.18) 5, 6, 7, 8, 11	5.34 (2.52) 3, 4, 5, 6, 10
2.00	4.92 (1.40) 3, 4, 5, 6, 7	3.75 (1.31) 2, 3, 4, 4, 6	6.97 (0.94) 6, 6, 7, 7, 9	4.97 (0.95) 4, 4, 5, 5, 7	5.60 (1.16) 4, 5, 5, 6, 8	3.79 (1.16) 3, 3, 3, 4, 6

[xiii] Note that, the first row of each of the cells shows the *ARL* and *SDRL* values whereas the second row shows the 5th, 25th, 50th, 75th and 95th percentiles (in this order).

Table 4.11. The IC and OOC characteristics[xiv] of the run-length distribution for $m = 100$ and $n = 5$ for the $t(3)$ distribution with nominal $ARL_0 = 500$ and winsorization at the 5000th step

	Chart Type					
	Parametric CUSUM-$\bar{X}$ chart with parameters estimated from a Phase I sample		NPCUSUM-Rank chart		NPCUSUM-EX median chart	
Winsorization level	WL = 95.2	WL = 96.6	WL = 95.6	WL = 98.0	WL = 95.7	WL = 97.4
Control limits	$H = 8.02$	$H = 5.05$	$H = 563.0$	$H = 225.0$	$H = 9.55$	$H = 5.18$
k	0	$0.5\sigma/\sqrt{n}$	0	$0.5\sqrt{mn(m+n+1)/12}$	0	$k = n(d^* - d)$
d^* / γ	NA	NA	NA	NA	0.50	$0.5\sqrt{\frac{n(m+n+1)}{4(m+2)}} \approx 0.57$
0.00	496.93 (1179.16) 13, 28, 64, 230, 4539	501.25 (1104.27) 9, 31, 90, 319, 3331	501.88 (1142.80) 16, 32, 71, 256, 3931	492.11 (944.01) 12, 47, 138, 435, 2434	498.96 (1139.02) 14, 31, 71, 258, 3933	494.62 (1010.80) 10, 37, 111, 375, 2748
0.25	111.54 (514.50) 8, 15, 24, 45, 237	169.39 (655.76) 6, 13, 26, 66, 519	49.81 (189.48) 11, 16, 24, 39, 114	83.73 (221.83) 7, 15, 30, 71, 303	62.42 (267.48) 10, 15, 24, 40, 148	78.14 (242.04) 6, 13, 25, 60, 273
0.50	34.96 (247.14) 6, 10, 15, 22, 52	56.46 (366.38) 5, 8, 13, 24, 89	16.97 (10.60) 9, 11, 15,19, 33	21.22 (37.98) 5, 8, 13, 22, 60	16.69 (12.84) 7, 10, 14, 19, 34	18.09 (29.15) 4, 8, 12, 20, 49
0.75	15.00 (95.56) 5, 8, 10, 14, 26	29.29 (293.97) 4, 6, 9, 13, 31	11.78 (4.01) 7, 9, 11, 13, 19	10.24 (7.67) 5, 6, 8,12, 22	11.05 (4.55) 6, 8, 10, 13, 19	9.46 (6.84) 4, 6, 8, 11, 21
1.00	10.37 (75.34) 4, 6, 8, 10, 17	17.23 (202.69) 3, 5, 6, 9, 17	9.50 (2.37) 7, 8, 9, 11, 14	7.33 (3.13) 4, 5, 6, 8, 13	8.57 (2.68) 6, 7, 8, 10, 14	6.60 (3.08) 3, 4, 6, 8, 12
1.50	6.71 (53.64) 3, 5, 6, 7, 10	6.88 (100.17) 2, 3, 4, 5, 9	7.31 (1.22) 6, 6, 7, 8, 10	5.23 (1.28) 4, 4, 5, 6, 8	6.48 (1.36) 5, 6, 6, 7, 9	4.53 (1.47) 3, 3, 4, 5, 8
2.00	5.13 (50.05) 3, 4, 4, 5, 7	5.47 (99.93) 2, 3, 3, 4, 6	6.31 (0.79) 5, 6, 6, 7, 8	4.42 (0.92) 4, 4, 4, 5, 6	5.56 (0.92) 4, 5, 6, 6, 7	3.73 (0.91) 3, 3, 4, 4, 5

[xiv] Note that, the first row of each of the cells shows the *ARL* and *SDRL* values whereas the second row shows the 5th, 25th, 50th, 75th and 95th percentiles (in this order).

Table 4.12. The IC and OOC characteristics[xv] of the run-length distribution for $m = 100$ and $n = 5$ for the $DE(0,1)$ distribution with nominal $ARL_0 = 500$ and winsorization at the 5000th step

	Chart Type					
	Parametric CUSUM-$\overline{X}$ chart with parameters estimated from a Phase I sample		NPCUSUM-Rank chart		NPCUSUM-EX median chart	
Winsorization level	WL = 95.5	WL = 96.7	WL = 95.5	WL = 97.6	WL = 95.7	WL = 97.0
Control limits	$H = 8.25$	$H = 5.15$	$H = 563.0$	$H = 225$	$H = 9.55$	$H = 5.18$
k	0	$0.5\sigma/\sqrt{n}$	0	$0.5\sqrt{mn(m+n+1)/12}$	0	NA
d^* \ γ	NA	NA	NA	NA	0.50	$0.5\sqrt{\frac{n(m+n+1)}{4(m+2)}} \approx 0.57$
0.00	492.36 (1164.91) 13, 29, 68, 241, 4367	505.43 (1085.83) 10, 32, 93, 341, 3169	508.74 (1160.94) 16, 33, 73, 269, 4103	507.43 (987.93) 12, 46, 143, 450, 2661	493.02 (1138.46) 14, 31, 72, 270, 3953	507.55 (1051.32) 10, 37, 112, 384, 3043
0.25	94.44 (388.64) 9, 16, 26, 51, 247	123.21 (442.64) 7, 14, 29, 72, 383	64.02 (259.88) 11, 17, 26, 43, 144	110.76 (313.85) 7, 16, 35, 87, 390	58.15 (249.72) 10, 15, 23, 38, 132	71.41 (238.15) 6, 13, 25, 54, 221
0.50	22.44 (58.34) 7, 11, 16, 23, 52	27.55 (72.73) 5, 9, 14, 25, 77	19.48 (17.22) 9, 12, 16, 22, 39	26.73 (54.03) 6, 9, 14, 26, 77	16.94 (17.05) 8, 10, 14, 19, 33	17.82 (27.62) 5, 8, 12, 20, 46
0.75	13.17 (8.19) 6, 8, 11, 15, 26	12.64 (14.38) 4, 6, 9, 14, 31	13.16 (5.32) 8, 10, 12, 15, 22	12.55 (11.21) 5, 7, 9, 14, 30	11.48 (4.76) 6, 8, 10, 13, 20	9.83 (6.80) 4, 6, 8, 11, 22
1.00	9.68 (4.42) 5, 7, 9, 11, 18	8.31 (6.16) 3, 5, 7, 10, 17	10.44 (3.06) 7, 8, 10, 12, 16	8.46 (4.62) 4, 6, 7, 10, 16	9.17 (2.88) 6, 7, 9, 10, 14	7.22 (3.51) 3, 5, 7, 8, 14
1.50	6.40 (2.06) 4, 5, 6, 7, 10	4.95 (2.07) 3, 4, 5, 6, 9	7.95 (1.54) 6, 7, 8, 9, 11	5.81 (1.67) 4, 5, 5, 6, 9	7.06 (1.63) 5, 6, 7, 8, 10	5.08 (1.81) 3, 4, 5, 6, 8
2.00	4.88 (1.32) 3, 4, 5, 6, 7	3.66 (1.24) 2, 3, 3, 4, 6	6.78 (0.99) 6, 6, 7, 7, 9	4.82 (1.04) 4, 4, 5, 5, 7	6.03 (1.12) 4, 5, 6, 6, 8	4.16 (1.19) 3, 3, 4, 5, 6

[xv] Note that, the first row of each of the cells shows the *ARL* and *SDRL* values whereas the second row shows the 5th, 25th, 50th, 75th and 95th percentiles (in this order).

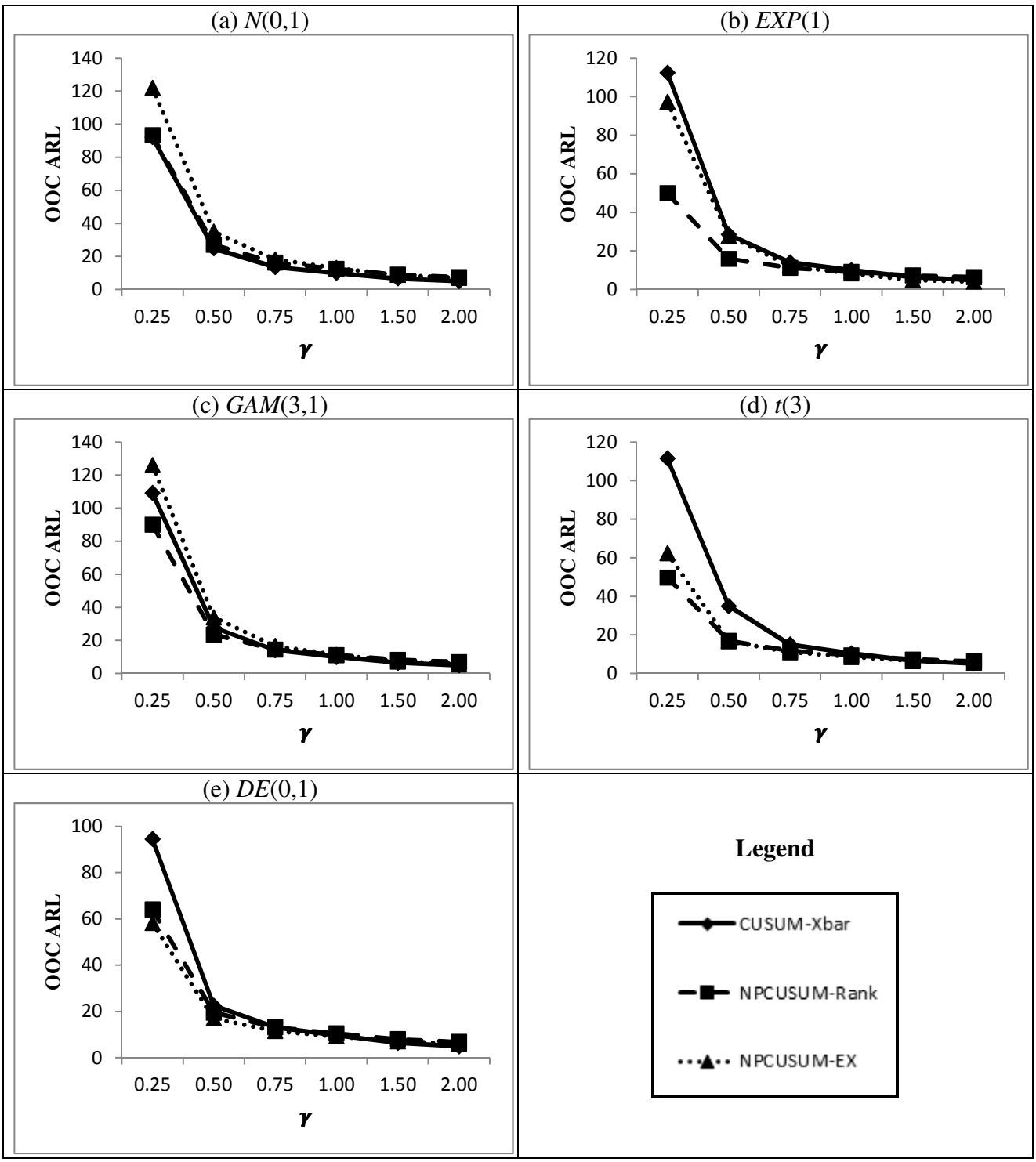

Figure 4.3. *ARL* performance comparison of the competing charts for various distributions with $m = 100$, $n = 5$, nominal $ARL_0 = 500$ and $k = 0$

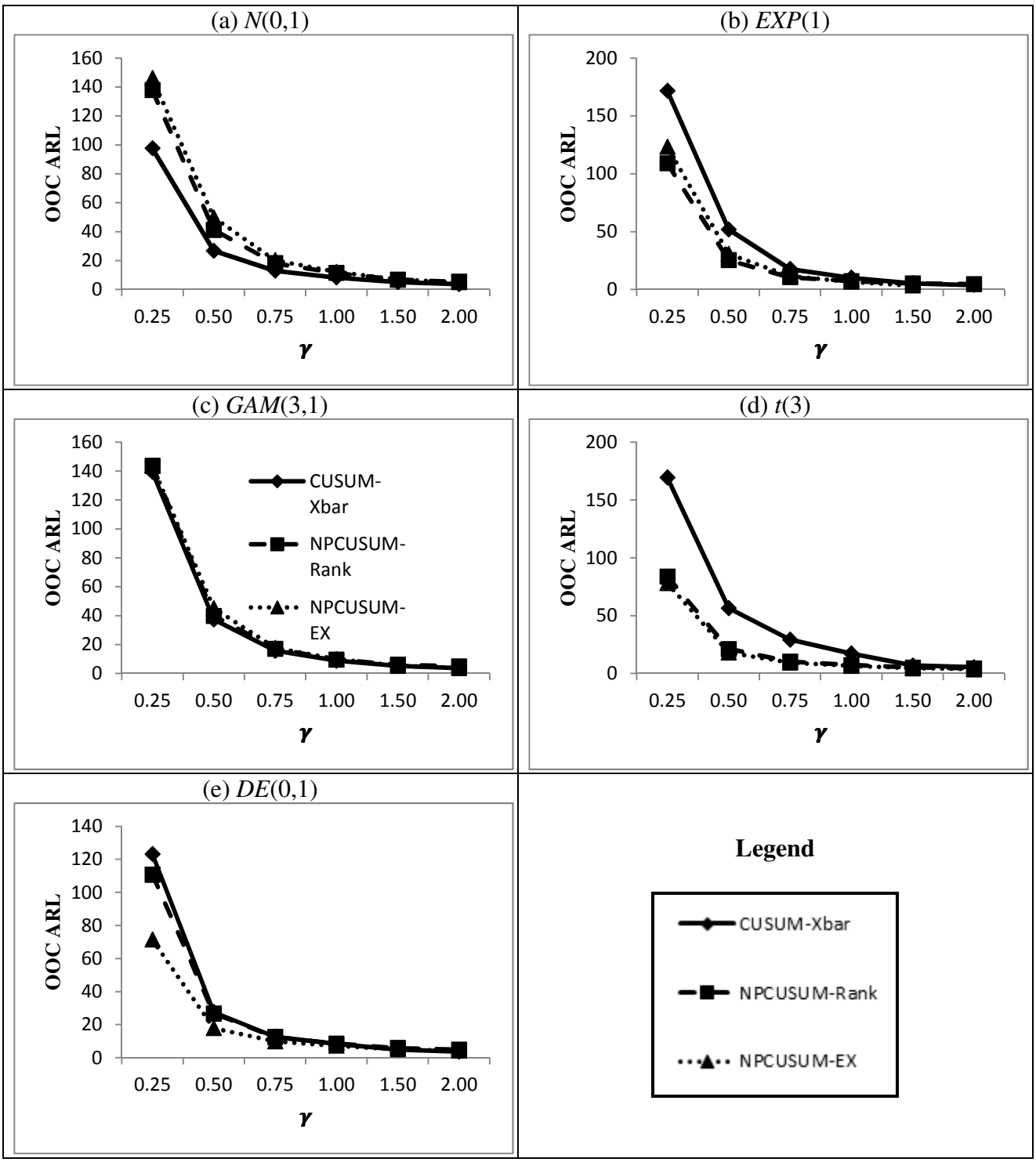

Figure 4.4. *ARL* performance comparison of the competing charts for various distributions with $m = 100$, $n = 5$, nominal $ARL_0 = 500$ and $k > 0$

From Figures 4.3(a) and 4.4(a) we see that for all k and when the underlying process distribution is $N(0,1)$, the CUSUM-$\overline{X}$ chart outperforms the other charts, which is not surprising, since it is natural for parametric methods to outperform their nonparametric counterparts when all assumptions are satisfied. We also find that the NPCUSUM-EX chart outperforms the NPCUSUM-Rank chart for larger ($\gamma > 1.5$) magnitudes of shifts.

From Figures 4.3(b) and 4.4(b) we see that when the underlying process distribution is $EXP(1)$, although the proposed chart and the CUSUM-$\overline{X}$ chart have a very similar performance for $k = 0$, the proposed chart outperforms the CUSUM-$\overline{X}$ chart for $k > 0$. In addition, for all k and for shifts of moderately larger ($\gamma > 0.75$) magnitudes, the NPCUSUM-EX chart outperforms the NPCUSUM-Rank chart.

From Figures 4.3(c) and 4.4(c) we see that for all k and when the underlying process distribution is $GAM(3,1)$, the proposed chart and the CUSUM-$\overline{X}$ chart have a very similar performance. In addition, for all k and for shifts of moderately larger ($\gamma > 0.75$) magnitudes, the NPCUSUM-EX chart outperforms the NPCUSUM-Rank chart.

From Figures 4.3(d) and 4.4(d) we see that when the underlying process distribution is $t(3)$, the NPCUSUM-EX chart outperforms the competing charts for shifts of moderate ($0.25 < \gamma < 2.00$) magnitudes for $k = 0$ and the superiority is even more visible for $k > 0$. The NPCUSUM-EX chart is the best for the $DE(0,1)$ distribution. It outperforms the competing charts for all k and for shifts all magnitudes for the $DE(0,1)$ distribution and this can be observed from Figures 4.3(e) and 4.4(e).

In summary, it is seen that in comparison with the CUSUM-$\overline{X}$ chart, the NPCUSUM-EX median chart is outperformed only when the underlying distribution is Normal. In all other cases the performances of the two charts are either similar or the NPCUSUM-EX median chart has superior performance. Finally, the NPCUSUM-EX median chart outperforms the NPCUSUM-Rank chart in all instances.

It is important to note that, in Tables 4.8 – 4.12, m was taken to be even from a practical point of view and, in this case, the median (and the other quantiles) may not be uniquely defined. However, note that the computations were done in SAS which uses the empirical distribution function and calculates sample percentiles as follows: arrange the data in ascending order and calculate an index $i = \left(\frac{per}{100}\right)m$ where per denotes the percentile of interest. If i is an integer, the percentile of interest is the average of the values in positions i and $i + 1$. If i is not an integer, then round up, and the percentile of interest is the value in that position. We recommend this scheme in practice for calculation of percentiles. Our calculations for some odd values of m close to the even values used here show that the results are fairly close. For example, the run-length characteristics for m = 100 and m = 99 are seen to be not very far apart. One will obviously use the particular value of m one has at hand, in practice, odd or even.

4.3.4 Illustrative examples

Example 4.1

We illustrate the NPCUSUM-EX median chart using a well-known dataset from Montgomery (2001; Tables 5.1 and 5.2) on the inside diameters of piston rings manufactured by a forging process. The data given in Table 5.1 contains twenty-five retrospective or Phase I samples, each of size five, that were collected when the process was thought to be IC, i.e. m = 125. These data are considered to be the Phase I reference data for which a goodness of fit test for normality is not rejected. The reference sample has a median equal to 74.001, i.e. $X_{(r)} = 74.001$.

Table 5.2 of Montgomery (2001) contains fifteen prospective (Phase II) samples each of five observations (n = 5). For the NPCUSUM-EX median chart we use k = 0 and set H = 7.5 for an $ARL_0 \approx 370$. The values of the exceedance and the NPCUSUM-EX statistics are shown for illustration in Table 4.13. For the CUSUM-$\overline{X}$ and NPCUSUM-Rank charts we also use k = 0 and set H = 18 and H = 580, respectively, for an $ARL_0 \approx 370$. It should be noted that these values of H was found using a grid search algorithm. The CUSUM-$\overline{X}$, the NPCUSUM-Rank and the NPCUSUM-EX median charts are shown in Figures 4.5, 4.6 and 4.7, respectively.

Table 4.13. The exceedance and the NPCUSUM-EX median statistics

j	1	2	3	4	5	6	7	8	9	10	11	12	13	14	15
$U_{j,r}$	3	2	0	4	1	4	4	1	3	4	2	5	5	5	4
C_j^+	0.5	0	0	1.5	0	1.5	3	1.5	2	3.5	3	5.5	8	10.5	12

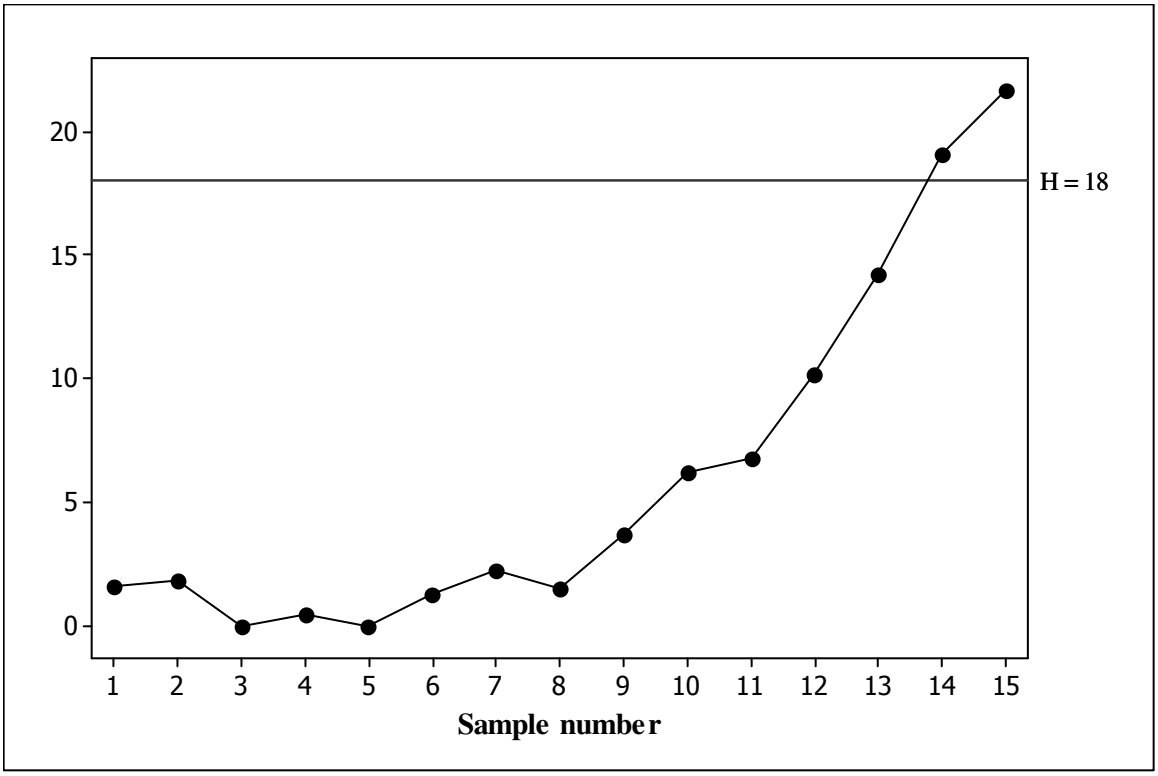

Figure 4.5. The CUSUM-$\overline{X}$ chart for the Montgomery (2001) piston ring data

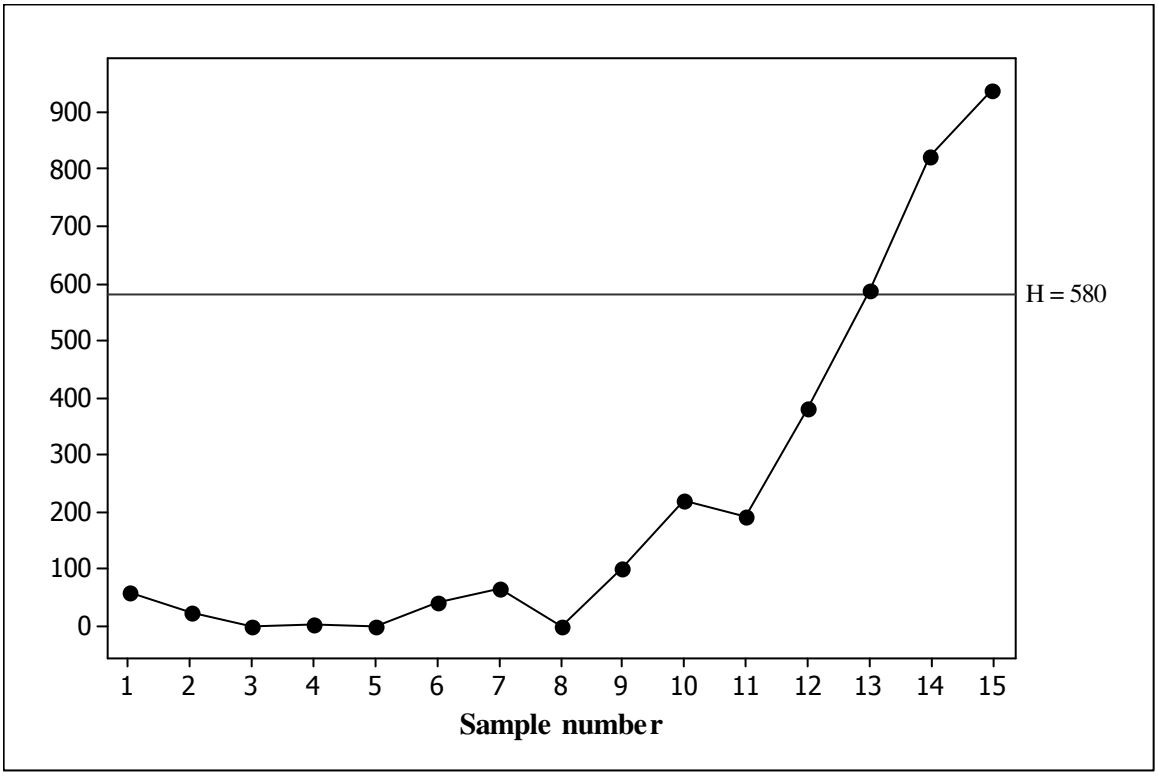

Figure 4.6. The NPCUSUM-Rank chart for the Montgomery (2001) piston ring data

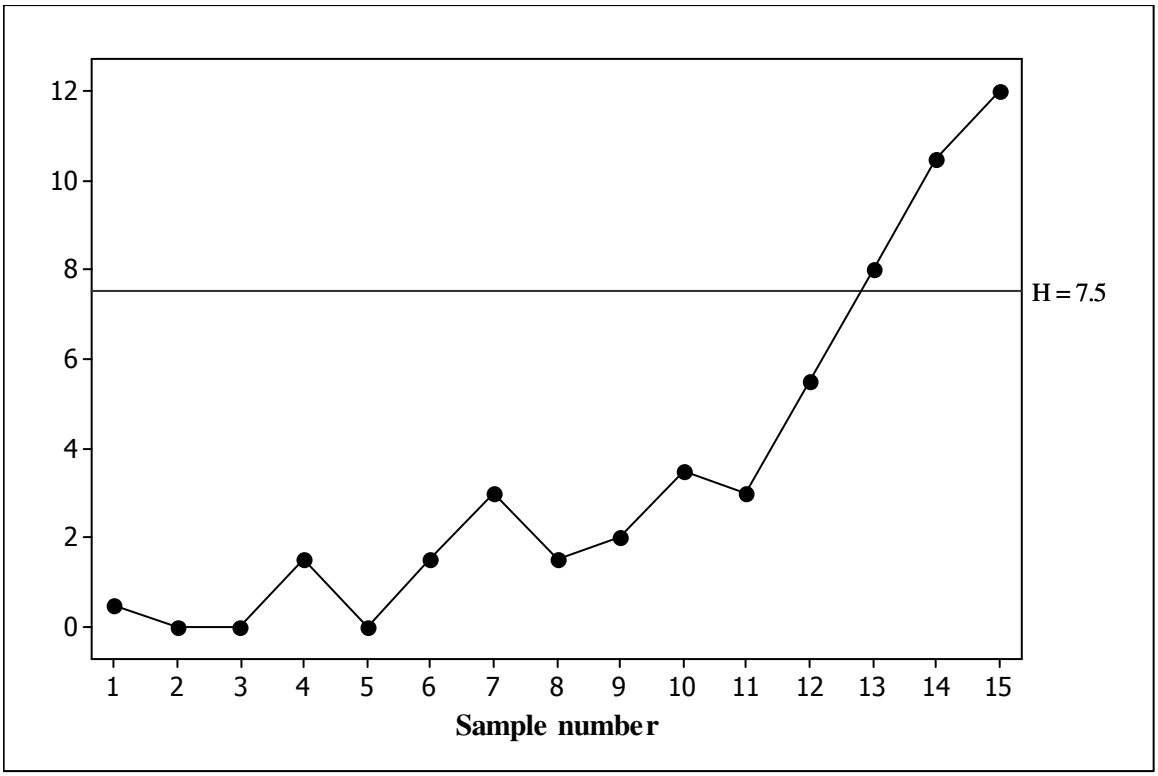

Figure 4.7. The NPCUSUM-EX chart for the Montgomery (2001) piston ring data

From Figures 4.5, 4.6 and 4.7 we can see that the performances of the charts are very similar. The NPCUSUM-EX median and NPCUSUM-Rank charts signal at sample 13, whereas the CUSUM-$\overline{X}$ chart signals at the very next sample, 14. However, recall that the NPCUSUM charts don't require normality or any distributional assumption other than continuity to guarantee the $ARL_0 \approx 370$ but the same couldn't be said about the CUSUM-$\overline{X}$ chart unless the underlying distribution was normal or close to it.

As we have mentioned before, in practice the normality assumption can be in doubt or can't be justified for lack of enough information or data and a nonparametric method may be more desirable.

4.3.5 Nonparametric CUSUM control chart based on other percentiles

Up to this point the properties of the NPCUSUM-EX chart using the median of the reference (Phase I) sample has been proposed and investigated. Here the choice of the order statistic from the reference (Phase I) sample that defines the exceedance statistic in this chart is investigated. The choice of the design parameter k of the NPCUSUM-EX chart is studied. Furthermore, observing certain shortcomings of the *ARL*, we use the median run-length (*MRL*) as the performance metric.

Median run-length (*MRL*) as performance metric

The most widely used chart performance metric is the *ARL* and determining the charting constants typically involves specifying a nominal IC *ARL* value, such as 500. This is how the control charts have been constructed in this body of work so far. However, since the run-length distribution is significantly right-skewed, researchers have advocated using other, more representative, measures for the assessment of a chart's performance. These include the standard deviation of the run-length (*SDRL*) and other percentiles of the run-length, more specifically, the median run-length (*MRL*), which provides more insightful information about the IC and OOC performances of control charts, not given by the *ARL*. The idea of looking at percentiles, in SPC, goes back to Barnard (1959) and more recently researchers such as Gan (1994), Chakraborti (2007) and Khoo et al. (2011) have advocated the use of percentiles, such as the median, for assessment of chart performance. The disadvantages of using the *ARL* as a performance measure are summarized as follows:

i. The run-length distribution of a chart is typically highly skewed and thus conclusions based on the *ARL* can be misleading.

ii. Difficulty of interpretation. As pointed out by Gan (1994), a chart having an ARL_0 of 500 (say) will have about 63% of all the run-lengths lower than 500 but 50% of all the run-lengths will be lower than 348, since the IC *MRL* (denoted MRL_0) is 348.

iii. There may be problems with the existence of the ARL_0 for some charts; see, for example, Chakraborti et al. (2004) and Graham et al. (2012), where the ARL_0 can be infinite and the authors emphasize that charts with an infinite ARL_0 are not useful in practice as this will often produce infinite or very large *ARL*'s under a shift as well.

iv. High standard deviation. Even if the ARL_0 exists it is, in most cases, associated with a high $SDRL_0$ which is undesirable. Extremely large values, for any of the run-length characteristics, means that those run-length characteristics can't be computed within a practical time, i.e. using the *ARL* as performance measure can be time-consuming.

v. Lack of robustness. As is well-known, the *ARL* isn't a robust measure, i.e. it is dramatically impacted by the presence of outliers and, consequently, using winsorization or a trimmed mean is often necessary for practical applications. When using winsorization or a trimmed mean this further complicates the interpretation.

Thus the use of the *MRL* as a measure of typical chart performance is recommended. For example, if the $MRL_0 = 250$ it means that there is at least a 50% chance that the first signal will be observed by the 250thsample although the process is actually IC. Stated differently, 50% of the IC run-lengths will be greater than or equal to 250 and 50% will be less. The ARL_0 simply does not have such an easily understood interpretation. Like the practical convention followed for the ARL_0, for an efficient control chart, the MRL_0 should be 'large' enough and the OOC *MRL* (denoted MRL_δ) should be 'small'. Also, when comparing the performance of two or more charts the MRL_0 of the charts should be fixed at an acceptably 'high' level such as 350 and the chart with the smaller MRL_δ is preferred. To this end, note that the run-length distribution of a Shewhart chart follows a Geometric distribution, i.e. $N \sim GEO(p)$ where N denotes the run-length variable and p is the probability of a success, that is, the probability of a signal. Since $N \sim GEO(p)$ it follows that its expected value, $E(N)$, which is the *ARL*, equals $\frac{1}{p}$ (by properties of the Geometric distribution (see

Section 3.1)), i.e. $ARL = \frac{1}{p}$ so that the success probability is given by $p = \frac{1}{ARL}$. For industry standard values for ARL_0 such as 500, it follows $p = \frac{1}{500} = 0.002$ and, consequently, the MRL_0 is equal to $\frac{-1}{log_2(1-p)}$ (by properties of the Geometric distribution), which, in our case equals $\frac{-1}{log_2(1-0.002)} = 346.2$. Therefore, keeping parity with the long practice of computing standards based on the traditional Shewhart-type chart in SPC, the IC target MRL_0 is recommended to be equal to 346. However, for simplicity, we take the nominal MRL_0 to be equal to 350 in this chapter.

Implementation of the chart

Practical implementation of the proposed NPCUSUM-EX chart requires specifying the following quantities:

i. The size of the IC Phase I reference sample (m).

ii. The order of the reference sample order statistic (r) and, following this, the value of $X_{(r)}$.

iii. The size of each Phase II test sample (n).

iv. A nominal value for a desired performance metric such as the ARL_0 or the MRL_0.

v. The reference value (k).

vi. The decision interval (H).

It is up to the practitioner to specify values of the chart parameters m, n and r and the nominal value for the desired performance metric in a given situation. The choice of r will be discussed later. The design parameters k and H are chosen so that the chart has a specified nominal ARL_0 or MRL_0 (the latter performance metric is used in this section) and is capable of detecting a specified shift, specially a small shift, as soon as possible (see Section 1.9.2 for a detailed discussion on the choice of the design parameters k and H).

In order to investigate the impact of the reference value on the performance of the chart more thoroughly, we consider a number of reference values, $k_l = \tau_l STDEV(U_{j,r})$ for l = 1,2,3,4,

respectively, where $\tau_l = c_l\delta$, c_l is a positive constant and $\delta = \gamma\sigma/\sqrt{n}$ is the size of the shift to be detected with γ = 0.00(0.25)1.00, 1.50 and 2.00. The constant c_l ranges from small to medium to large, namely, 0.25, 0.50, 1.00 and 2.00. Note that although shifts as large as γ = 2.00 were considered in this study, the largest value of γ reported here is γ = 1.00, since, for larger shifts we have the following considerations:

i. The run-length characteristics of the charts tend to converge and

ii. later on it is shown that for moderate to large shifts the practitioner should use the exceedance chart based on higher order percentiles, such as the 60th or the 75th percentiles, since they signal very quickly for all k under consideration.

After choosing k, the next step is to find the decision interval H, in conjunction with the chosen k, so that a desired nominal MRL_0 is attained. However, for a discrete random variable the chances are that H cannot always be found such that the desired nominal MRL_0 is attained exactly and hence using a conservative approach, H is found so that the attained MRL_0 is less than or equal to the desired nominal MRL_0. The decision interval, H, is found using a grid search algorithm using 100 000 Monte Carlo simulations. SAS® v 9.3 is used for the simulations and the results are verified using R.2.15.0.

In-control robustness

Because the NPCUSUM-EX chart is a nonparametric chart, the IC run-length distribution and the associated characteristics should be the same for all continuous distributions. In other words, the IC run-length distribution is the same by definition and thus all IC characteristics such as the *MRL* must remain the same for all continuous distributions. Next, the OOC chart performance comparison is given. The same distributions are considered as with the NPCUSUM-EX median chart.

Out-of-control chart performance comparison

Tables 4.14 to 4.17 give the OOC run-length characteristics for γ = 0.25, 0.50, 0.75 and 1.00, respectively. The first row of each cell shows the *MRL* followed by the corresponding interquartile range (*IQR*) in parentheses, whereas the second row shows the values of the 5th, 25th, 75th and 95th percentiles (in this order).

Several observations can be made from an examination of Tables 4.14 to 4.17. The decision interval, H, for the NPCUSUM-EX chart is the same for the 25th and 75th percentiles and for the 40th and 60th percentiles, respectively. Note that, since the $STDEV(U_{j,r})$ is the same for the pair of percentiles $(M - \Delta_1, M + \Delta_1)$ where M denotes the median and Δ_1 is an integer between 1 and 49, the reference value k would be the same (since k is a function of $STDEV(U_{j,r})$) and, consequently, the decision interval H would be the same (the reader is referred to Section 1.9.2 where the choice of the design parameters k and H are explained in detail).

As expected, the MRL_δ values as well as all the run-length distribution percentiles decrease sharply with increasing shift, which is expected, indicating that NPCUSUM charts are reasonably effective in detecting shifts in location. However, the effectiveness (speed of detection) of the charts varies depending on the magnitude of the shift, the underlying process distribution and the type of the reference percentile being considered in forming the exceedance statistic.

Table 4.14. OOC run-length characteristics[xvi] (target $MRL_0 = 350$, $m = 100$, $n = 5$, and $\gamma = 0.25$)

		r = 25th percentile	r = 40th percentile	r = 50th percentile	r = 60th percentile	r = 75th percentile
$c_l = 2$	**Dist / *H***	***H*=5.710**	***H*=6.500**	***H*=6.550**	***H*=6.500**	***H*=5.710**
	***N*(0,1)**	396 (954) 26, 122, 1076, 3185	269 (705) 21, 84, 789, 2571	236 (614) 18, 72, 686, 2359	206 (580) 16, 63, 643, 2267	170 (502) 13, 53, 555, 2142
	***EXP*(1)**	73 (273) 12, 27, 300, 1756	126 (415) 14, 42, 457, 2034	161 (501) 14, 48, 549, 2105	174 (521) 14, 52, 573, 2120	207 (595) 14, 60, 655, 2336
	***GAM*(3,1)**	272 (781) 21, 79, 860, 2832	218 (612) 18, 66, 678, 2420	203 (550) 16, 64, 614, 2150	205 (576) 16, 61, 637, 2215	189 (571) 14, 57, 628, 2254
	***t*(3)**	348 (846) 27, 111, 958, 3009	157 (464) 16, 54, 518, 2154	123 (386) 14, 43, 429, 1759	107 (326) 12, 36, 362, 1761	108 (355) 10, 35, 390, 1817
	***DE*(0,1)**	410 (1003) 29, 131, 1134, 3394	208 (567) 19, 67, 634, 2190	120 (333) 14, 42, 375, 1610	106 (342) 12, 36, 378, 1752	144 (459) 12, 43, 502, 1966
$c_l = 1$	**Dist / *H***	***H*=11.700**	***H*=13.500**	***H*=14.000**	***H*=13.500**	***H*=11.700**
	***N*(0,1)**	248 (896) 31, 82, 978, 4457	214 (807) 30, 74, 881, 4412	203 (773) 28, 71, 844, 4684	194 (779) 26, 66, 845, 4285	196 (752) 23, 65, 817, 3816
	***EXP*(1)**	52 (115) 18, 29, 144, 1655	87 (287) 21, 40, 327, 2827	129 (520) 23, 50, 570, 3777	166 (658) 24, 57, 715, 4065	217 (776) 24, 67, 843, 4016
	***GAM*(3,1)**	140 (528) 27,57, 585, 3519	156 (579) 26, 58, 637, 3954	180 (764) 26, 62, 826, 4506	181 (699) 25, 64, 763, 3976	214 (764) 26, 68, 832, 4018
	***t*(3)**	182 (651) 30, 71, 722, 3678	116 (392) 25, 50, 442, 3110	101 (333) 23, 46, 379, 3120	96 (334) 21, 43, 377, 3010	113 (441) 19, 44, 485, 3046
	***DE*(0,1)**	245 (889) 33, 86, 975, 4321	146 (493) 27, 59, 552, 3577	98 (352) 20, 41, 393, 3035	94 (275) 23, 46, 321, 2721	153 (577) 21, 53, 630, 3360
$c_l = 0.5$	**Dist / *H***	***H*=24.500**	***H*=28.000**	***H*=28.000**	***H*=28.000**	***H*=24.500**
	***N*(0,1)**	244 (853) 61, 114, 967, 8994	230 (896) 55, 105, 1001, 9507	218 (721) 52, 100, 821, 8127	218 (826) 50, 99, 925, 9066	222 (895) 47, 97, 992, 9420
	***EXP*(1)**	77 (98) 34, 50, 148, 1844	117 (265) 39, 66, 331, 5363	148 (438) 42, 76, 514, 6088	198 (684) 46, 90, 774, 8496	249 (1019) 49, 106, 1125, 9458
	***GAM*(3,1)**	156 (408) 49, 83, 491, 6723	175 (556) 49, 88, 644, 7928	190 (662) 47, 90, 752, 8271	218 (778) 49, 100, 878, 9277	246 (950) 49, 106, 1056, 8757
	***t*(3)**	187 (537) 57, 98, 635, 7431	136 (304) 46, 78, 382, 3569	129 (268) 43, 73, 341, 5108	127 (296) 40, 70, 366, 5523	150 (494) 38, 74, 568, 7224
	***DE*(0,1)**	250 (930) 63, 118, 1048, 9347	163 (394) 50, 87, 481, 6543	126 (337) 39, 68, 405, 5705	119 (213) 43, 70, 283, 3885	186 (659) 42, 86, 745, 9918
$c_l = 0.25$	**Dist / *H***	***H*=38.000**	***H*=43.000**	***H*=45.000**	***H*=43.000**	***H*=38.000**
	***N*(0,1)**	263 (550) 85, 146, 696, 5913	243 (528) 77, 133, 661, 5448	245 (525) 77, 133, 658, 6390	241 (523) 72, 128, 651, 5818	250 (575) 69, 130, 705, 6156
	***EXP*(1)**	101 (106) 50, 70, 176, 1123	150 (216) 57, 91, 337, 2906	186 (346) 62, 108, 454, 4565	215 (448) 65, 117, 565, 5142	266 (609) 71, 137, 746, 6250
	***GAM*(3,1)**	191 (334) 73, 115, 449, 4237	206 (405) 70, 117, 522, 4885	228 (471) 72, 127, 598, 5538	240 (515) 70, 127, 642, 5643	270 (622) 73, 140, 762, 6026
	***t*(3)**	213 (359) 80, 128, 487, 4605	166 (253) 67, 104, 357, 3147	160 (256) 63, 100, 356, 3389	156 (253) 58, 95, 348, 3060	182 (357) 57, 100, 457, 4080
	***DE*(0,1)**	258 (524) 87, 145, 669, 5997	188 (305) 72, 117, 422, 4024	156 (204) 65, 102, 306, 2688	154 (273) 58, 91, 364, 3425	213 (459) 62, 113, 572, 5231

[xvi] Note that, the first row of each of the cells shows the *MRL* and *IQR* values whereas the second row shows the 5th, 25th, 75th and 95th percentiles (in this order)

Table 4.15. OOC run-length characteristics[xvii] (target $MRL_0 = 350$, $m = 100$, $n = 5$, and $\gamma = 0.50$)

		$r = 25^{th}$ percentile	$r = 40$th percentile	$r = 50$th percentile	$r = 60$th percentile	$r = 75$th percentile
$c_l = 2$	**Dist / *H***	***H*=2.710**	***H*=2.809**	***H*=2.900**	***H*=2.730**	***H*=2.710**
	***N*(0,1)**	1658 (3475) 97, 560, 4035, 10948	293 (595) 20, 105, 700, 1917	129 (288) 10, 45, 333, 1123	108 (285) 8, 38, 323, 1441	59 (132) 5, 22, 154, 615
	***EXP*(1)**	46 (323) 11, 15, 338, 4139	60 (160) 6, 21, 181, 754	65 (204) 7, 21, 225, 1007	76 (190) 6, 26, 216, 999	80 (221) 7, 26, 247, 1100
	***GAM*(3,1)**	1639 (3626) 80, 534, 4161, 11675	189 (449) 13, 64, 513, 1638	104 (248) 8, 36, 284, 1028	106 (297) 9, 35, 332, 1571	74 (178) 6, 25, 203, 823
	***t*(3)**	2249 (4103) 148, 868, 4971, 12720	129 (290) 12, 49, 339, 1106	51 (104) 6, 20, 124, 459	38 (80) 5, 15, 95, 398	29 (64) 4, 12, 76, 319
	***DE*(0,1)**	1847 (3636) 117, 654, 4320, 11371	190 (411) 15, 70, 481, 1422	54 (102) 6, 22, 124, 422	37 (83) 5, 15, 98, 465	43 (107) 4, 15, 122, 563
$c_l = 1$	**Dist / *H***	***H*=5.75**	***H*=6.500**	***H*=6.600**	***H*=6.500**	***H*=5.750**
	***N*(0,1)**	187 (558) 20, 61, 619, 2515	102 (308) 14, 37, 345, 1666	79 (235) 12, 30, 265, 1402	68 (198) 10, 26, 224, 1169	60 (176) 9, 23, 199, 1144
	***EXP*(1)**	12 (12) 8, 9, 21, 85	23 (45) 7, 13, 58, 434	34 (89) 8, 16, 105, 771	50 (151) 9, 19, 170, 1067	84 (279) 9, 28, 307, 1671
	***GAM*(3,1)**	54 (150) 11, 24, 174, 1175	57 (157) 13, 26, 183, 1251	60 (174) 11, 24, 198, 1208	65 (193) 10, 24, 217, 1271	81 (267) 9, 28, 295, 1625
	***t*(3)**	93 (240) 17, 39, 279, 1453	38 (67) 10, 20, 87, 454	29 (48) 9, 16, 64, 283	27 (59) 6, 13, 72, 455	25 (43) 7, 13, 56, 262
	***DE*(0,1)**	166 (474) 50, 58, 532, 2258	51 (102) 11, 25, 127, 5701	29 (45) 9, 16, 61, 244	24 (42) 7, 13, 55, 366	41 (119) 7, 17, 136, 993
$c_l = 0.5$	**Dist / *H***	***H*=12.000**	***H*=13.500**	***H*=13.500**	***H*=13.500**	***H*=12.000**
	***N*(0,1)**	96 (273) 37, 49, 322, 2901	69 (158) 21, 38, 196, 2027	64 (147) 19, 34, 181, 1626	66 (177) 16, 33, 210, 2069	63 (150) 18, 33, 183, 1808
	***EXP*(1)**	18 (12) 13, 14, 26, 58	28 (30) 13, 18, 48, 253	36 (56) 14, 22, 78, 739	50 (118) 15, 27, 145, 1544	91 (351) 17, 37, 388, 3306
	***GAM*(3,1)**	46 (58) 20, 30, 88, 818	47 (76) 17, 28, 104, 1038	52 (110) 17, 29, 139, 1343	62 (161) 17, 32, 193, 2112	85 (305) 18, 37, 342, 2787
	***t*(3)**	60 (79) 24, 38, 117, 804	37 (37) 17, 25, 62, 240	31 (30) 14, 22, 52, 182	30 (31) 13, 21, 52, 212	35 (49) 12, 21, 70, 617
	***DE*(0,1)**	88 (191) 28, 48, 239, 2139	45 (50) 18, 30, 80, 329	32 (28) 15, 23, 51, 157	30 (33) 13, 20, 53, 356	46 (109) 13, 24, 133, 1557
$c_l = 0.25$	**Dist / *H***	***H*=24.000**	***H*=27.500**	***H*=28.500**	***H*=27.500**	***H*=24.000**
	***N*(0,1)**	114 (191) 45, 71, 262, 3469	97 (134) 39, 62, 196, 2414	92 (132) 37, 58, 190, 2196	92 (168) 32, 55, 223, 3174	90 (131) 35, 56, 187, 2750
	***EXP*(1)**	30 (15) 22, 25, 40, 72	45 (37) 24, 33, 70, 250	59 (66) 27, 40, 106, 784	75 (118) 29, 47, 165, 2313	117 (288) 33, 61, 349, 4724
	***GAM*(3,1)**	65 (57) 35, 48, 105, 473	71 (78) 33, 48, 126, 977	79 (107) 33, 51, 158, 1799	88 (142) 32, 54, 196, 2863	119 (305) 34, 62, 367, 5062
	***t*(3)**	79 (67) 41, 58, 125, 470	58 (41) 32, 44, 85, 214	52 (37) 29, 39, 76, 187	50 (38) 26, 37, 75, 225	55 (61) 24, 36, 97, 614
	***DE*(0,1)**	106 (140) 46, 70, 210, 1990	68 (52) 36, 50, 102, 266	50 (43) 26, 37, 80, 372	49 (40) 26, 36, 76, 325	70 (116) 26, 42, 158, 2179

[xvii] Note that, the first row of each of the cells shows the *MRL* and *IQR* values whereas the second row shows the 5^{th}, 25^{th}, 75^{th} and 95^{th} percentiles (in this order)

Table 4.16. OOC run-length characteristics[xviii] (target $MRL_0 = 350$, $m = 100$, $n = 5$, and $\gamma = 0.75$)

		r = 25th percentile	r = 40th percentile	r = 50th percentile	r = 60th percentile	r = 75th percentile
$c_l = 2$	**Dist / H**	**H=1.575**	**H=1.350**	**H=1.530**	**H=1.350**	**H=1.575**
	***N*(0,1)**	***	1422 (2695) 80, 491, 3187, 8155	73 (147) 6, 28, 175, 493	42 (82) 4, 16, 98, 306	39 (81) 4, 15, 96, 327
	***EXP*(1)**	***	76 (308) 5, 21, 329, 2322	27 (59) 3, 10, 69, 257	28 (58) 3, 11, 69, 258	51 (125) 4, 18, 143, 568
	***GAM*(3,1)**	***	729 (1771) 35, 226, 1997, 6288	53 (109) 5, 20, 129, 409	39 (80) 4, 15, 95, 327	50 (112) 4, 18, 130, 518
	***t*(3)**	***	538 (1212) 34, 191, 1403	29 (50) 3, 12, 62, 166	16 (27) 2, 7, 34, 96	16 (29) 3, 7, 36, 125
	***DE*(0,1)**	***	964 (2010) 60, 350, 2360, 6471	32 (54) 4, 14, 68, 174	16 (27) 2, 7, 34, 103	23 (52) 3, 9, 61, 257
$c_l = 1$	**Dist / H**	**H=3.500**	**H=4.100**	**H=4.200**	**H=4.100**	**H=3.500**
	***N*(0,1)**	256 (709) 20, 82, 791, 3107	62 (146) 9, 25, 171, 802	41 (90) 7, 17, 107, 497	33 (70) 6, 14, 84, 364	23 (45) 4, 10, 55, 234
	***EXP*(1)**	8 (0) 8, 8, 8, 16	9 (11) 4, 7, 18, 89	14 (25) 4, 18, 33, 167	21 (46) 4, 10, 56, 312	32 (98) 4, 12, 90, 503
	***GAM*(3,1)**	45 (108) 10, 21, 129, 834	29 (62) 7, 14, 76, 410	29 (64) 6, 13, 77, 383	31 (68) 5, 13, 81, 400	30 (68) 4, 12, 80, 409
	***t*(3)**	117 (269) 16, 46, 315, 1347	23 (34) 7, 12, 46, 146	15 (19) 5, 9, 28, 78	12 (15) 4, 7, 22, 65	10 (15) 3, 6, 21, 71
	***DE*(0,1)**	268 (676) 22, 91, 767, 2885	33 (56) 8, 16, 72, 222	17 (21) 5, 10, 31, 83	12 (15) 4, 7, 22, 73	14 (28) 3, 7, 35, 166
$c_l = 0.5$	**Dist / H**	**H=7.800**	**H=8.900**	**H=8.900**	**H=8.900**	**H=7.800**
	***N*(0,1)**	48 (87) 16, 28, 115, 747	34 (51) 12, 20, 71, 405	30 (44) 10, 19, 63, 305	28 (40) 9, 17, 57, 298	27 (44) 8, 15, 59, 369
	***EXP*(1)**	9 (0) 9, 9, 9, 14	11 (8) 7, 9, 17, 41	15 (15) 7, 10, 25, 92	20 (28) 8, 13, 41, 252	36 (92) 9, 18, 110, 1069
	***GAM*(3,1)**	22 (19) 12, 16, 35, 106	22 (24) 9, 15, 39, 157	23 (30) 9, 15, 45, 220	26 (42) 9, 16, 58, 342	35 (81) 9, 18, 99, 809
	***t*(3)**	32 (31) 14, 22, 53, 144	19 (13) 9, 14, 27, 56	16 (11) 8, 11, 22, 44	14 (10) 7, 10, 20, 44	14 (14) 6, 9, 23, 69
	***DE*(0,1)**	47 (72) 16, 28, 100, 433	23 (19) 11, 16, 35, 75	17 (12) 8, 12, 24, 47	14 (11) 7, 10, 21, 48	18 (26) 6, 11, 37, 216
$c_l = 0.25$	**Dist / H**	**H=16.200**	**H=18.500**	**H=18.500**	**H=18.500**	**H=16.200**
	***N*(0,1)**	55 (53) 26, 39, 92, 445	45 (41) 22, 32, 73, 259	41 (36) 19, 29, 65, 221	40 (39) 18, 27, 66, 253	39 (44) 16, 26, 70, 354
	***EXP*(1)**	16 (0) 16, 16, 16, 22	19 (11) 12, 15, 26, 46	24 (17) 13, 18, 35, 84	31 (31) 14, 22, 53, 219	49 (88) 16, 29, 117, 1538
	***GAM*(3,1)**	31 (18) 20, 25, 43, 83	33 (24) 18, 24, 48, 121	34 (28) 17, 24, 52, 174	38 (38) 17, 26, 64, 311	50 (79) 17, 29, 108, 1225
	***t*(3)**	42 (24) 24, 32, 56, 103	28 (14) 18, 23, 37, 59	24 (12) 15, 19, 31, 50	23 (12) 13, 18, 30, 52	23 (16) 12, 17, 33. 80
	***DE*(0,1)**	54 (42) 27, 40, 82, 255	34 (18) 20, 27, 45, 73	25 (12) 16, 21, 33, 52	23 (12) 14, 18, 30, 54	29 (29) 12, 20, 49, 226

*** Values could not be computed within a reasonable time. This indicates that the values are extremely large and the corresponding chart is performing poorly.

[xviii] Note that, the first row of each of the cells shows the *MRL* and *IQR* values whereas the second row shows the 5th, 25th, 75th and 95th percentiles (in this order)

Table 4.17. OOC run-length characteristics[xix] (target $MRL_0 = 350$, $m = 100$, $n = 5$, and $\gamma = 1.00$)

		$r = 25^{th}$ percentile	$r = 40$th percentile	$r = 50$th percentile	$r = 60$th percentile	$r = 75$th percentile
$c_l = 2$	**Dist / *H***	***H*=0.750**	***H*=0.700**	***H*=0.390**	***H*=0.700**	***H*=0.750**
	***N*(0,1)**	***	***	41 (76) 4, 17, 93, 264	11 (18) 1, 5, 23, 57	34 (66) 3, 13, 79, 246
	***EXP*(1)**	***	***	10 (21) 2, 4, 25, 92	7 (13) 1, 3, 16, 45	43 (96) 3, 16, 112, 443
	***GAM*(3,1)**	***	***	27 (51) 3, 11, 62, 195	10 (16) 1, 4, 20, 53	44 (95) 3, 16, 111, 385
	***t*(3)**	***	***	15 (24) 2, 7, 31, 73	5 (8) 1, 2, 10, 24	11 (20) 2, 5, 25, 74
	***DE*(0,1)**	***	***	18 (30) 2, 8, 38, 91	5 (8) 1, 3, 11, 25	16 (35) 2, 6, 41, 160
$c_l = 1$	**Dist / *H***	***H*=2.715**	***H*=2.701**	***H*=2.925**	***H*=2.701**	***H*=2.715**
	***N*(0,1)**	1396 (3303) 64, 431, 3734, 10821	54 (116) 8, 22, 138, 513	27 (49) 4, 12, 61, 213	17 (29) 3, 8, 37, 110	15 (27) 3, 17, 34, 111
	***EXP*(1)**	11 (0) 11, 11, 11, 11	5 (4) 4, 4, 8, 25	7 (10) 3, 4, 4, 54	9 (17) 2, 5, 22, 83	19 (43) 38, 51, 218
	***GAM*(3,1)**	76 (222) 13, 20, 252, 1976	21 (39) 5, 10, 49, 197	17 (31) 3, 8, 39, 146	14 (27) 2, 7, 34, 113	19 (42) 3, 8, 50, 203
	***t*(3)**	606 (1503) 42, 207, 1710, 6285	18 (25) 5, 10, 35, 89	10 (11) 3, 6, 17, 43	7(8) 2, 4, 12, 27	6 (7) 2, 4, 11, 32
	***DE*(0,1)**	1698 (3652) 94, 582, 4234, 11464	29 (46) 6, 14, 60, 162	12 (14) 3, 7, 21, 49	7 (8) 2, 4, 12, 29	8 (13) 2, 4, 17, 63
$c_l = 0.5$	**Dist / *H***	***H*=5.800**	***H*=6.500**	***H*=6.500**	***H*=6.500**	***H*=5.800**
	***N*(0,1)**	33 (48) 12, 20, 68, 304	21 (25) 8, 13, 38, 126	18 (21) 7, 11, 32, 99	16 (19) 6, 10, 29, 88	15 (20) 5, 9, 29, 96
	***EXP*(1)**	8 (0) 8, 8, 8, 8	6(3) 5, 5, 8, 15	8 (7) 4, 5, 12, 29	11 (12) 4, 7, 19, 67	18 (35) 5, 10, 45, 313
	***GAM*(3,1)**	14 (9) 8, 11, 20, 42	13 (11) 6, 9, 20, 51	13 (13) 5, 9, 22, 65	15 (18) 5, 9, 27, 99	19 (33) 5, 10, 43, 233
	***t*(3)**	23 (20) 11, 16, 36, 83	12 (8) 6, 9, 17, 31	10 (6) 5, 7, 13, 23	8 (5) 4, 6, 11, 21	8 (7) 4, 5, 12, 25
	***DE*(0,1)**	35 (45) 12, 21, 66, 204	15 (11) 7, 11, 22, 42	11 (7) 5, 8, 15, 25	9 (5) 4, 7, 12, 21	9 (10) 4, 6, 16, 53
$c_l = 0.25$	**Dist / *H***	***H*=11.750**	***H*=13.511**	***H*=13.905**	***H*=13.511**	***H*=11.750**
	***N*(0,1)**	32 (26) 17, 23, 49, 117	26 (18) 14, 19, 37, 83	24 (17) 12, 18, 35, 74	23 (17) 11, 16, 33, 74	21 (18) 10, 15, 33, 84
	***EXP*(1)**	12 (0) 12, 12, 12, 12	10 (5) 8, 8, 13, 19	13 (7) 8, 10, 17, 32	16 (12) 8, 12, 24, 56	25 (32) 10, 16, 48, 318
	***GAM*(3,1)**	18 (8) 13, 15, 23, 38	18 (11) 11, 14, 25, 44	19 (12) 11, 15, 27, 55	20 (15) 10, 15, 30, 76	25 (28) 10, 16, 44, 188
	***t*(3)**	25 (13) 16, 20, 33, 54	17 (7) 11, 14, 21, 31	15 (6) 10, 12, 18, 26	13 (5) 8, 11, 16, 24	12 (7) 7, 9, 16, 29
	***DE*(0,1)**	33 (24) 18, 24, 48, 92	21 (9) 13, 17, 26, 39	16 (8) 11, 13, 21, 29	13 (6) 8, 11, 17, 26	14 (10) 7, 11, 21, 51

*** Values could not be computed within a reasonable time. This indicates that the values are extremely large and the corresponding chart is performing poorly.

The observations from Tables 4.14 to 4.17 are summarized in Table 4.18 below along with some recommendations. Note that for brevity, a shorthand notation is used to describe the charts. For example, the NPCUSUM-EX chart based on the 50th percentile is denoted by EX(50), and if two charts perform similarly, for example, if the NPCUSUM-EX chart based on the 50th and 60th percentiles perform similarly, the notation EX(50,60) is used.

[xix] Note that, the first row of each of the cells shows the *MRL* and *IQR* values whereas the second row shows the 5th, 25th, 75th and 95th percentiles (in this order)

Table 4.18. Summary of the efficacy of different reference sample percentiles for the NPCUSUM-EX chart

	Size of Location Shift			
	Small ($\delta \leq 0.25$)	Small to moderate ($0.25 < \delta \leq 0.50$)	Moderate to large ($0.50 < \delta \leq 0.75$)	Large ($0.75 < \delta \leq 1.00$)
Symmetric distributions				
***N*(0,1)**	Overall the higher order percentile based charts, EX(75), EX(60) and EX(50), perform best. More specifically, for each c_l, the chart performing the best is: c_l = 0.25: EX(60) c_l = 0.5: EX(50,60) c_l = 1: EX(60,75) c_l = 2: EX(75)	The EX(75) chart performs the best for all c_l	The EX(75) chart performs the best for all c_l	For c_l = 2 the EX(60) chart performs the best. For all other values of c_l under consideration the EX(75) chart performs the best.
***t*(3)**	The EX(60) chart performs the best for all c_l	For c_l = 1 and 2, the EX(75) chart performs the best. For c_l = 0.25 and 0.5, the EX(60) chart performs the best.	The EX(60,75) charts perform similarly and the best.	Overall the higher order percentile based charts, EX(75) and EX(60) perform best. More specifically, for each c_l, the chart performing the best is: c_l = 0.25: EX(75) c_l = 0.5: EX(60,75) c_l = 1: EX(60,75) c_l = 2: EX(60)
***DE*(0,1)**	The EX(60) chart performs the best for all c_l	The EX(60) chart performs the best for all c_l	The EX(60) chart performs the best for all c_l	The EX(60) chart performs the best for all c_l
Asymmetric distributions				
***EXP*(1)**	The EX(25) chart performs the best for all c_l	The EX(25) chart performs the best for all c_l	For c_l = 2 the EX(50,60) charts perform similarly and the best. For all other values of c_l the EX(25) chart performs the best.	For c_l = 2 the EX(60) chart performs the best. For all other values of c_l the EX(40) chart performs the best.
***GAM*(3,1)**	For c_l = 2 the EX(75) chart performs the best. For all other values of c_l the EX(25) chart performs the best.	For c_l = 2 the EX(75) chart performs the best. For all other values of c_l the EX(25) chart performs the best.	c_l = 0.25, 0.5: EX(25) c_l = 1: EX(40,50) c_l = 2: EX(60)	c_l = 0.25: EX(25,40) c_l = 0.5: EX(40,50) c_l = 1 and 2: EX(60)

From Table 4.18 it is clear that a NPCUSUM-EX chart using reference sample percentiles other than the median (to define the precedence statistic in a particular situation) can provide a useful nonparametric chart in practice. In fact, it appears that the NPCUSUM-EX chart, using the higher order percentiles, such as the 60th and 75th percentiles, respectively, are good overall charts for detecting a larger location shift. This finding is an important contribution to the literature on

exceedance / precedence tests and charts. Other reference sample percentiles, such as the 25th or the 40th, can also be used when a smaller shift is expected.

Choice of the reference value

The reference value k is an important design parameter of a CUSUM chart and is generally chosen based on the size of the expected shift. In the parametric context, given the population distribution, one can choose the optimal k from the notion of a sequential probability ratio test (see e.g. Hawkins and Olwell (1998)). Traditionally, for the CUSUM-$\overline{X}$ chart it is recommended that smaller values of the reference value are preferable for detecting smaller shifts and that larger values of the reference value are preferable for detecting larger shifts (see Section 1.9.2). In the nonparametric setting, however, the choice of such k is more complicated and we investigate this issue more thoroughly, starting with revisiting the CUSUM-$\overline{X}$ chart. Note that when we suspect that the process has gone OOC, the goal is to choose that value of k which gives the shortest MRL_δ. Our simulation study suggests that for both parametric and nonparametric charts, when small shifts are under consideration, the MRL_δ values initially decrease, as the reference value k increases from 0, reaches a minimum and then sharply increases (see Figure 1.2 in Section 1.9.2 for the CUSUM-$\overline{X}$ chart and Figures 4.8 to 4.12 below for the NPCUSUM). Thus, roughly, the MRL_δ is U-shaped or V-shaped. i.e. it is a convex function, as a function of k (or, equivalently, a function of c_l). Since we are plotting the OOC MRL values, one would select the c_l value for which the value of MRL_δ is the lowest, i.e. the turning point of the convex function. The reasoning behind this follows. For an 'efficient' control chart the MRL_0 should be 'large' and the MRL_δ should be 'small'. Since the MRL_0 is fixed at the same value, the k (or, equivalently, the c_l value) with the smallest or lowest MRL_δ is selected to be the winner. For the CUSUM-$\overline{X}$ chart the U-shape (with ARL_δ on the vertical axis against k on the horizontal axis) is illustrated graphically in Figure 1.2 in Section 1.9.2. For the NPCUSUM-EX chart we illustrate the shape of the MRL_δ profile graphically in Figures 4.8 to 4.12 for different choices of percentiles of the Phase I reference sample. The line colour of the symmetric distributions is in black and the line colour of the asymmetric distributions is in red. To summarize, we see that, in the NPCUSUM setting, the choice of such k is not straightforward, since the choice depends on the reference sample order statistic, the magnitude of the shift that one wants to detect and the shape of the underlying process distribution. A detailed discussion is given below.

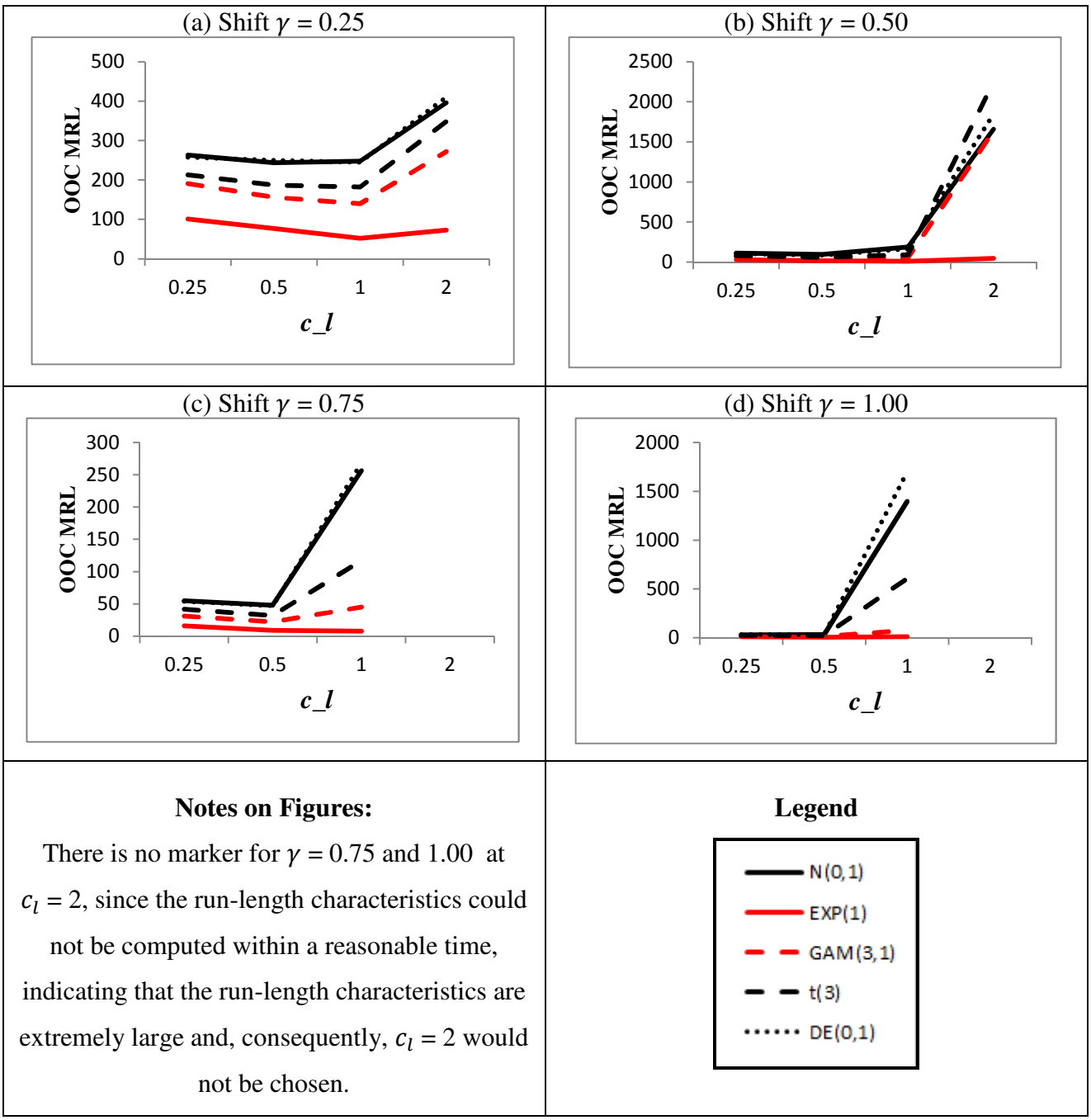

Figure 4.8. Out-of-control *MRL* values under different choices of c_l[xx] for the NPCUSUM-EX chart based on the 25th percentile of the reference sample

If we consider the MRL_δ values under different choices of c_l, for the NPCUSUM-EX chart based on the 25th percentile of the reference sample, we see that the MRL_δ values initially decline as c_l increases and reaches a minimum around $c_l = 1$ for small to moderate shifts ($\gamma = 0.25$ and 0.50) (see Figures 4.8a,b) and around $c_l = 0.5$ for moderate to large shifts ($\gamma = 0.75$ and 1.00) (see Figures 4.8c,d). After the minimum is reached the MRL_δ values begin to increase sharply. It is thus tempting to conjecture that the NPCUSUM charts have a U-shape function or a convex function

[xx] Recall the relationship between the reference value and c_l is given by $k_l = c_l \delta STDEV(U_{j,r})$

when the 25th percentile of the reference sample is used. Next, the graphs for the NPCUSUM-EX chart based on the 40th percentile of the reference sample are shown.

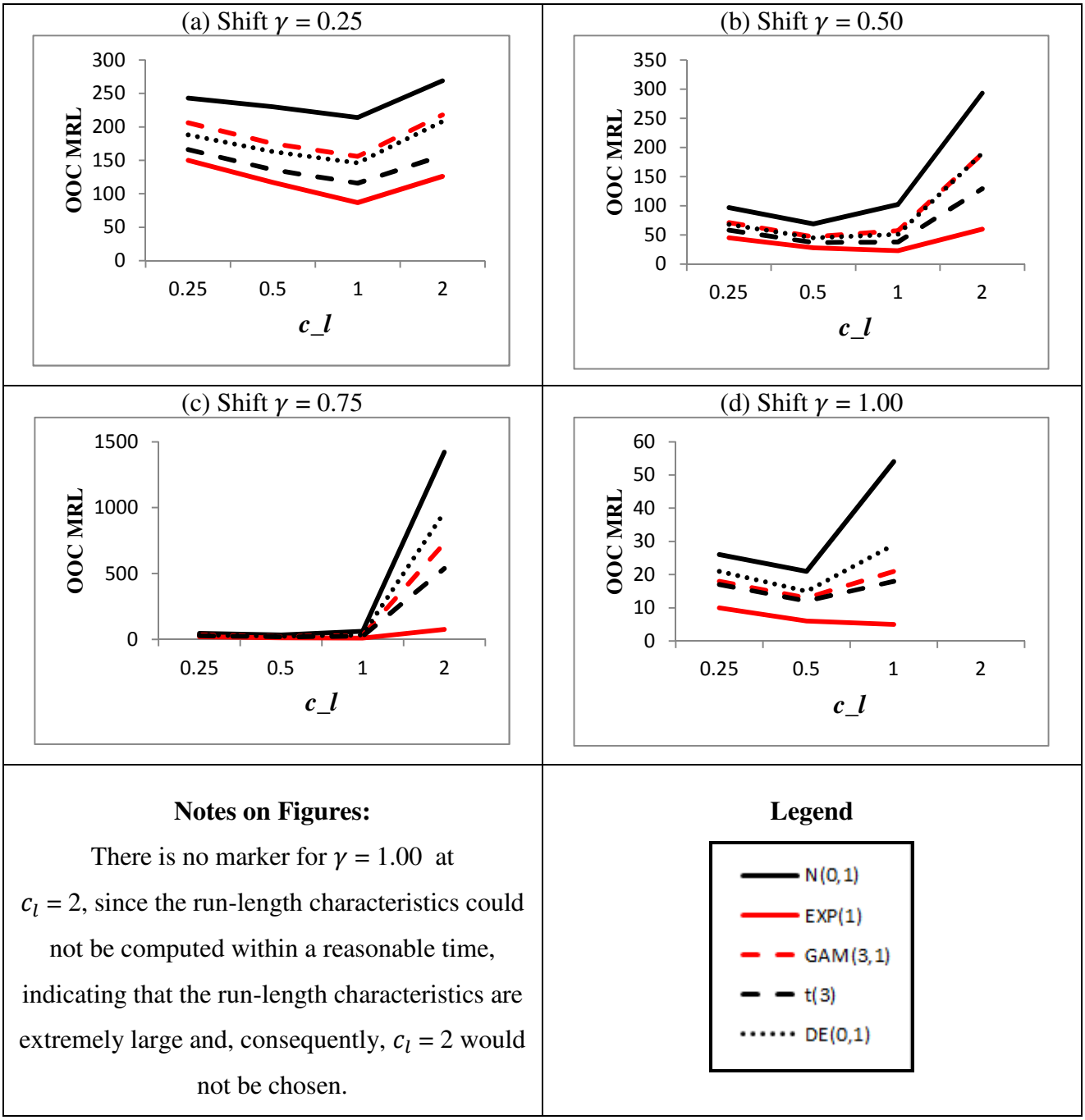

Figure 4.9. Out-of-control *MRL* values under different choices of c_l[xxi] for the NPCUSUM-EX chart based on the 40th percentile of the reference sample

From Figure 4.9 we see that a U-shape is observed in all cases with the minimum at $c_l = 1$ for $\gamma = 0.25$, 0.50 and 0.75. However, for $\gamma = 1.00$ the minimum is reached at $c_l = 0.5$ for all

[xxi] Recall the relationship between the reference value and c_l is given by $k_l = c_l \delta STDEV(U_{j,r})$

distributions except for the *EXP*(1) distribution where $c_l = 1$ is preferred. Next, the graphs for the NPCUSUM-EX chart based on the median of the reference sample are shown.

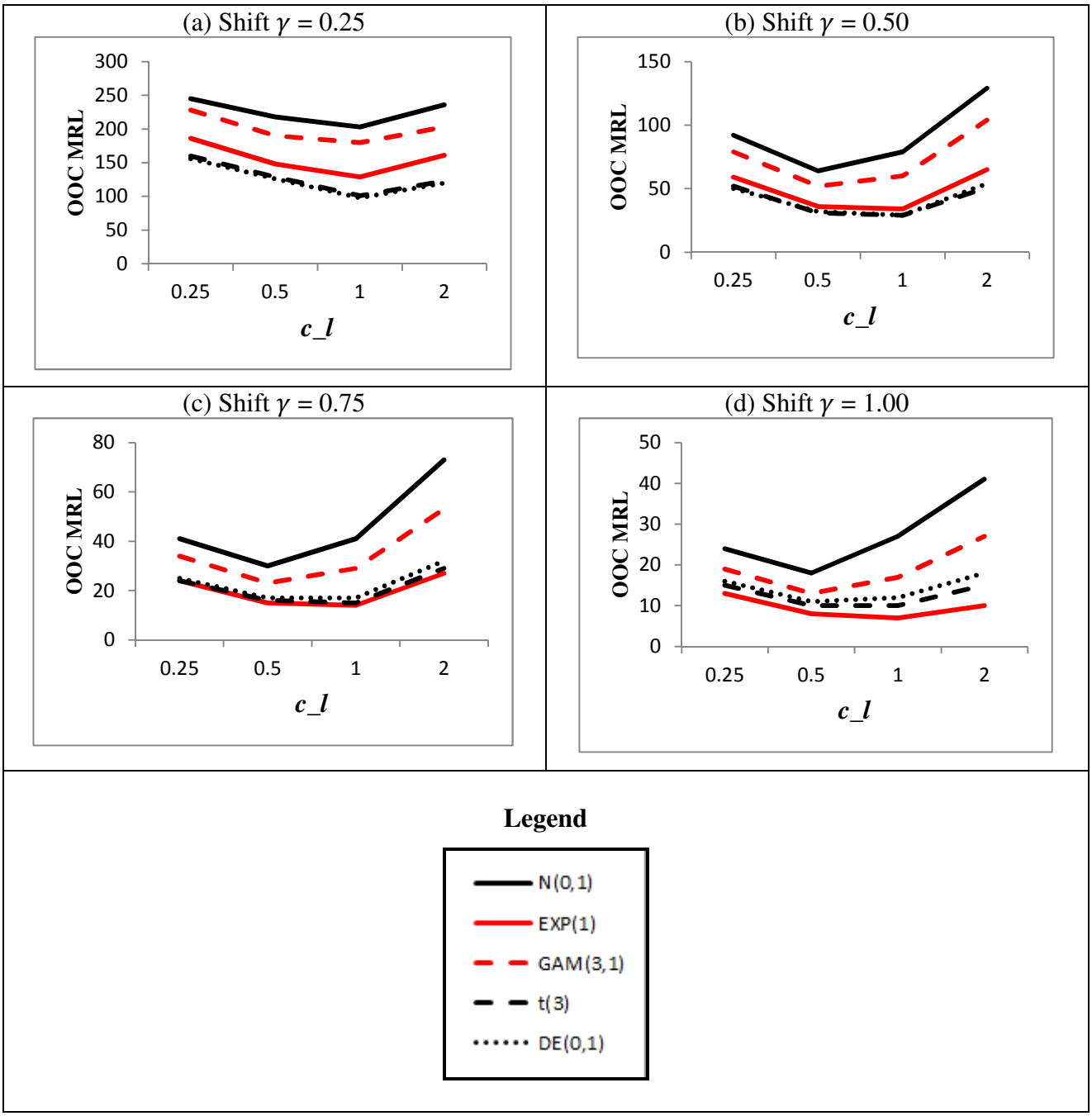

Figure 4.10. Out-of-control *MRL* values under different choices of c_l[xxii] for the NPCUSUM-EX chart based on the median of the reference sample

From Figure 4.10 again a U-shape is evident and one would select the c_l value for which the value of MRL_δ is the lowest. A summary is given in Table 4.19. Next, the graphs for the NPCUSUM-EX chart based on the 60th percentile of the reference sample are shown.

[xxii] Recall the relationship between the reference value and c_l is given by $k_l = c_l \delta STDEV(U_{j,r})$

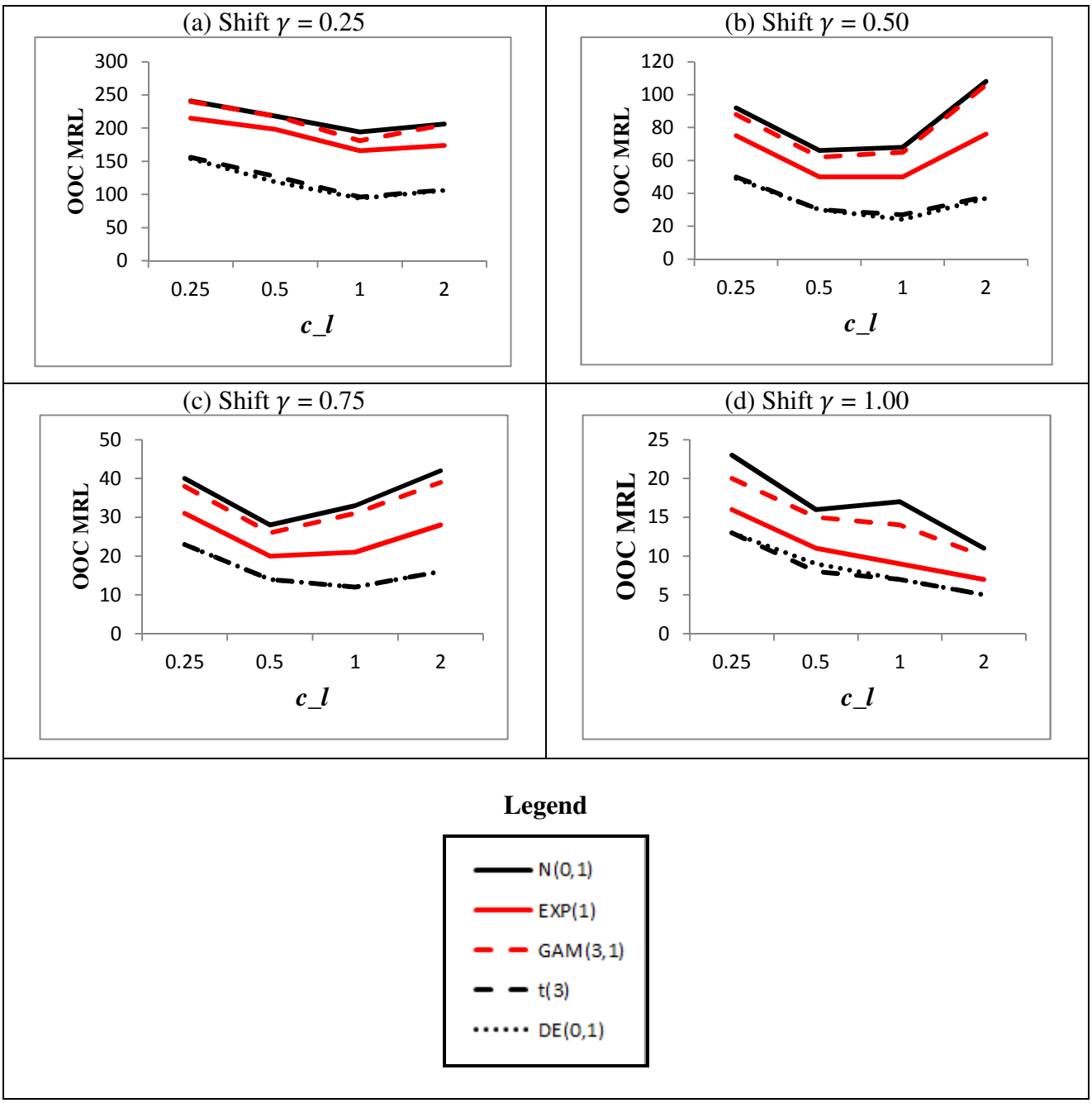

Figure 4.11. Out-of-control *MRL* values under different choices of c_l[xxiii] for the NPCUSUM-EX chart based on the 60th percentile of the reference sample

For the NPCUSUM-EX chart based on the 60th percentile of the reference sample the U-shape isn't as prominent as with the NPCUSUM-EX chart based on smaller percentiles, as it is only clearly seen for when $\gamma = 0.50$ (see Figure 4.11b). For $\gamma = 1.00$ it seems that larger values of c_l are preferred regardless of the size of this shift. Next, the graphs for the NPCUSUM-EX chart based on the 75th percentile of the reference sample are shown.

[xxiii] Recall the relationship between the reference value and c_l is given by $k_l = c_l \delta STDEV(U_{j,r})$

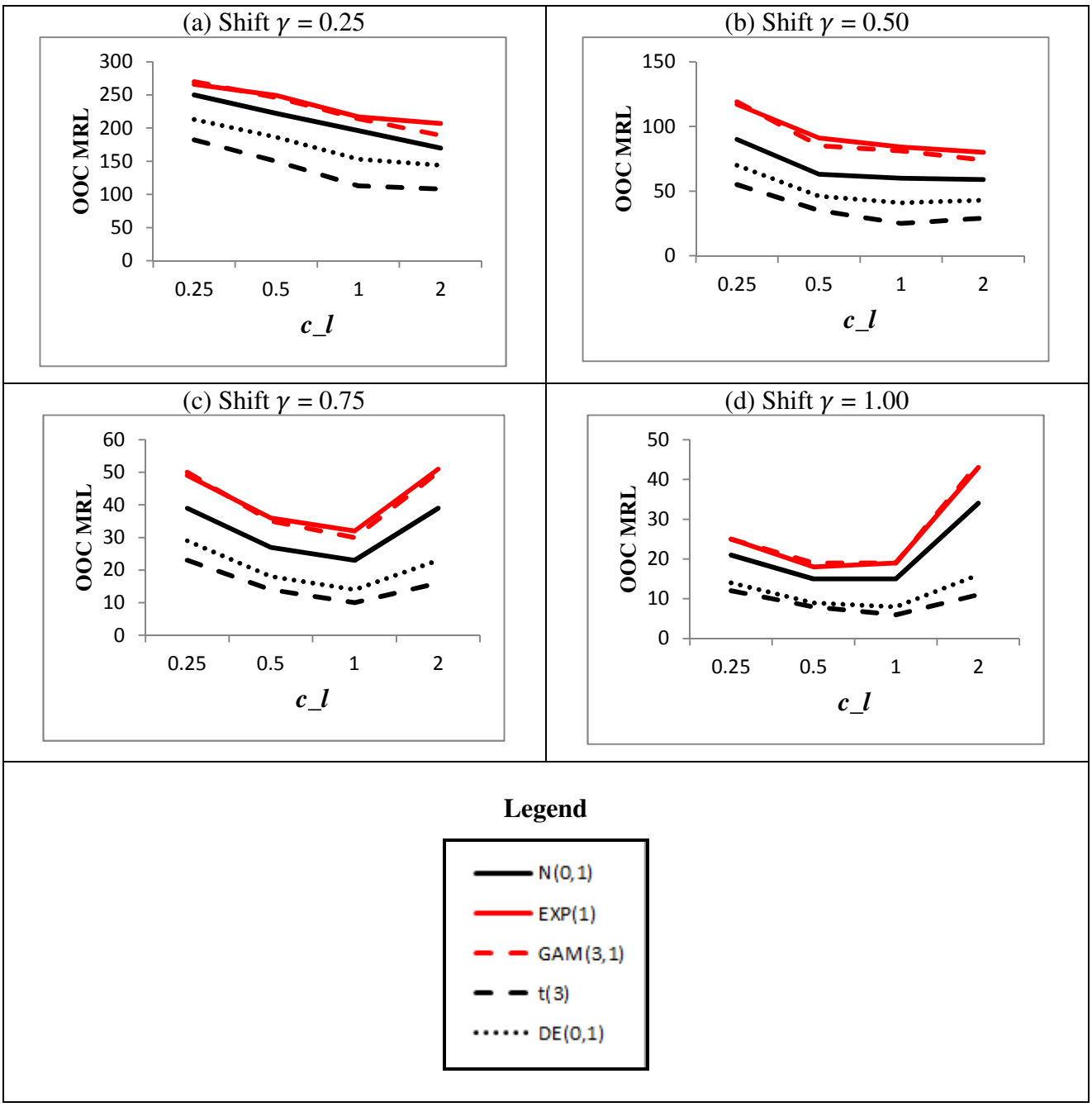

Figure 4.12. Out-of-control *MRL* values under different choices of c_l[xxiv] for the NPCUSUM-EX chart based on the 75th percentile of the reference sample

For the NPCUSUM-EX chart based on the 75th percentile of the reference sample the U-shape isn't as prominent as with the NPCUSUM-EX chart based on smaller percentiles, as it is only clearly seen when the shift is moderate to large ($\gamma = 0.75$ and 1.00) (see Figures 4.12c,d). In all other cases it seems that larger values of c_l are preferred regardless of the size of this shift. The results of Figures 4.8 to 4.12 are summarized in Table 4.19 below.

[xxiv] Recall the relationship between the reference value and c_l is given by $k_l = c_l \delta STDEV(U_{j,r})$

Table 4.19. Summary of the different reference sample percentiles and the choices of c_l

If the practitioner has reason to suspect that the underlying process distribution is symmetric					
Desired shift / Chart	**EX(25)**	**EX(40)**	**EX(50)**	**EX(60)**	**EX(75)**
0.25	$c_l = 1.00$	$c_l = 1.00$	$c_l = 1.00$	$c_l = 1.00$	Larger values of c_l are preferred, preferably $c_l \geq 1$
0.50	$c_l = 0.50$	$c_l = 0.50$	$c_l = 0.50$ or $c_l = 1.00$	$c_l = 0.50$ or $c_l = 1.00$	
0.75			$c_l = 0.50$	$c_l = 0.50$	$c_l = 1.00$
1.00	$c_l = 0.25$ or $c_l = 0.50$			Larger values of c_l are preferred, preferably $c_l \geq 1$	$c_l = 0.50$ or $c_l = 1.00$
If the practitioner has reason to suspect that the underlying process distribution is asymmetric					
0.25	$c_l = 1.00$	$c_l = 1.00$	$c_l = 1.00$	$c_l = 1.00$	Larger values of c_l are preferred, preferably $c_l \geq 1$
0.50				$c_l = 0.50$ or $c_l = 1.00$	
0.75	$c_l = 0.50$	$c_l = 0.50$ or $c_l = 1.00$	$c_l = 0.50$	$c_l = 0.50$	$c_l = 0.50$ or $c_l = 1.00$
1.00				Larger values of c_l are preferred, preferably $c_l \geq 1$	

When making inferences from Table 4.19, the practitioner should keep in mind that the relationship between the reference value (k_l) and c_l is given by $k_l = c_l \delta STDEV(U_{j,r})$. Now, from Table 4.19 it is seen that the smallest value of c_l under consideration ($c_l = 0.25$) is only listed once and, consequently, the practitioner should take caution when assigning small values to c_l and also to the reference value k. Table 4.19 should be helpful for the practitioner in implementing the NPCUSUM-EX charts.

Illustrative examples

Example 4.2

We illustrate the NPCUSUM-EX chart first using a well-known dataset from Montgomery (2001; Tables 5.1 and 5.2) on the inside diameters of piston rings manufactured by a forging process. The data given in Table 5.1 contains twenty-five retrospective or Phase I samples, each of size five, that were collected when the process was thought to be IC, i.e. $m = 125$. An analysis in Montgomery (2001) showed that these data are from an IC process and thus can be considered to be Phase I reference data. Note also that for these data, a goodness of fit test for normality is not rejected. This does not guarantee that the normality assumption for a traditional or parametric CUSUM chart is valid but often the practical implication is as such. We instead apply and contrast the proposed nonparametric exceedance charts based on the 25^{th}, 40^{th}, 50^{th} (median), 60^{th} and the 75^{th} percentile, respectively, of the reference sample. The values of the respective reference sample percentiles are as follows: 25^{th} percentile = 73.995, 40^{th} percentile = 73.998, median = 74.001, 60^{th} percentile = 74.004 and 75^{th} percentile = 74.008. All of the measurements are in mm.

In order to calculate the Phase II exceedance control charts, we use the data in Table 5.2 of Montgomery (2001) that contains fifteen prospective (Phase II) samples each of five observations ($n = 5$). For each NPCUSUM-EX chart we use $c_l = 1.00$ and, using a search algorithm, we find the value of H such that $MRL_0 \approx 350$. The desired shift to be detected was taken to be small $\gamma = 0.25$ (see Figures 4.13 to 4.17).

Table 4.20. Charting statistics and counters for the Montgomery (2001) data with $\gamma = 0.25$

25th percentile				40th percentile				50th percentile				60th percentile				75th percentile			
C_j^-	N^-	C_j^+	N^+	C_j^-	N^-	C_j^+	N^+	C_j^-	N^-	C_j^+	N^+	C_j^-	N^-	C_j^+	N^+	C_j^-	N^-	C_j^+	N^+
0.0	0	0.0	0	0.0	0	0.7	1	0.0	0	0.2	1	0.0	0	0.7	1	0.0	0	1.5	1
-0.5	1	0.0	0	0.0	0	0.4	2	-0.2	1	0.0	0	0.0	0	0.4	2	0.0	0	2.0	2
-2.0	2	0.0	0	-0.7	1	0.0	0	-2.4	2	0.0	0	-1.7	1	0.0	0	-1.0	1	0.4	3
-1.4	3	0.0	0	0.0	0	0.7	1	-0.6	3	1.2	1	-0.5	2	0.7	1	-1.0	2	0.0	0
-0.9	4	0.0	0	0.0	0	0.4	2	-1.9	4	0.0	0	-2.2	3	0.0	0	-2.1	3	0.0	0
-0.4	5	0.1	1	0.0	0	1.1	3	-0.1	5	1.2	1	-2.0	4	0.0	0	-1.1	4	0.5	1
0.0	0	0.1	2	0.0	0	1.8	4	0.0	0	2.4	2	-0.7	5	0.7	1	-1.1	5	0.0	0
0.0	0	0.1	3	-0.7	1	0.5	5	-1.2	1	0.6	3	-2.5	6	0.0	0	-2.1	6	0.0	0
0.0	0	1.1	4	0.0	0	2.2	6	-0.4	2	0.9	4	-1.2	7	0.7	1	-0.2	7	1.5	1
0.0	0	2.2	5	0.0	0	3.9	7	0.0	0	2.1	5	0.0	0	2.4	2	0.0	0	3.0	2
-0.5	1	1.2	6	0.0	0	3.7	8	-0.2	1	1.3	6	0.0	0	2.1	3	0.0	0	3.4	3
0.0	0	2.2	7	0.0	0	5.4	9	0.0	0	3.5	7	0.0	0	4.8	4	0.0	0	5.9	4
0.0	0	3.2	8	0.0	0	7.1	10	0.0	0	5.7	8	0.0	0	7.5	5	0.0	0	9.4	5
0.0	0	4.2	9	0.0	0	8.8	11	0.0	0	7.9	9	0.0	0	10.2	6	0.0	0	12.9	6
0.0	0	5.3	10	0.0	0	10.5	12	0.0	0	9.2	10	0.0	0	11.9	7	0.0	0	14.4	7

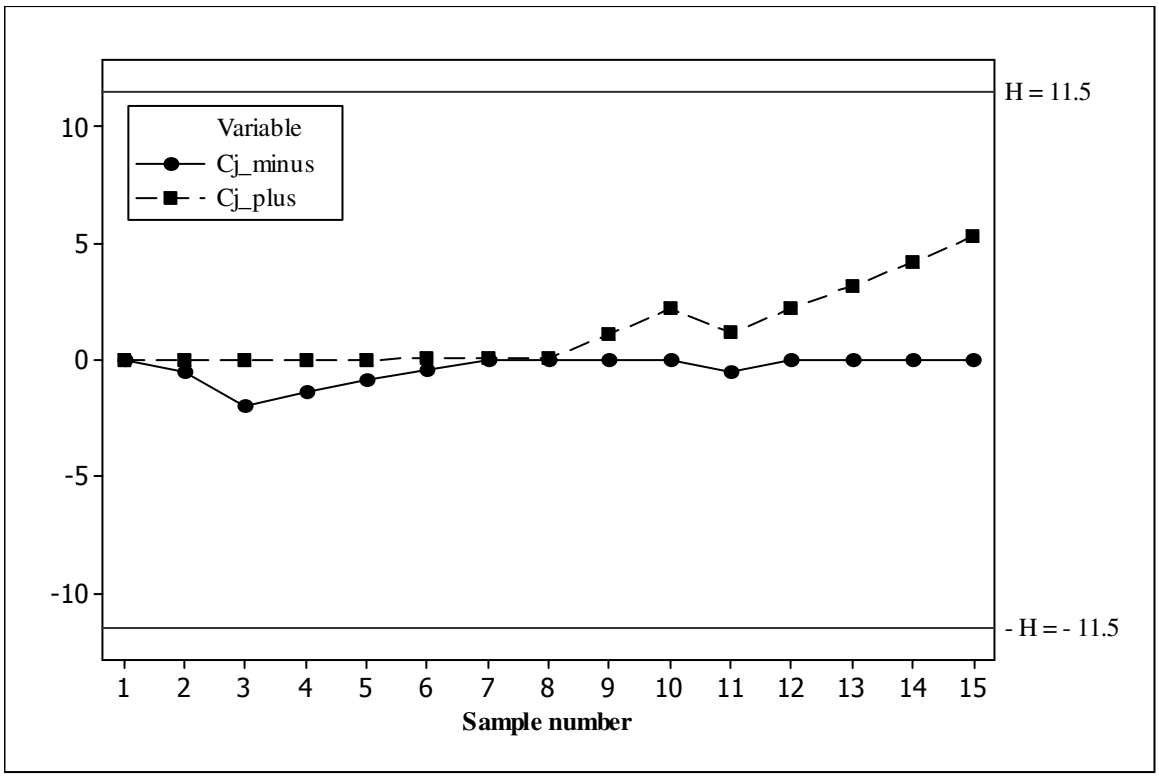

Figure 4.13. NPCUSUM-EX chart based on the 25th percentile for the Montgomery (2001) data with $\gamma = 0.25$

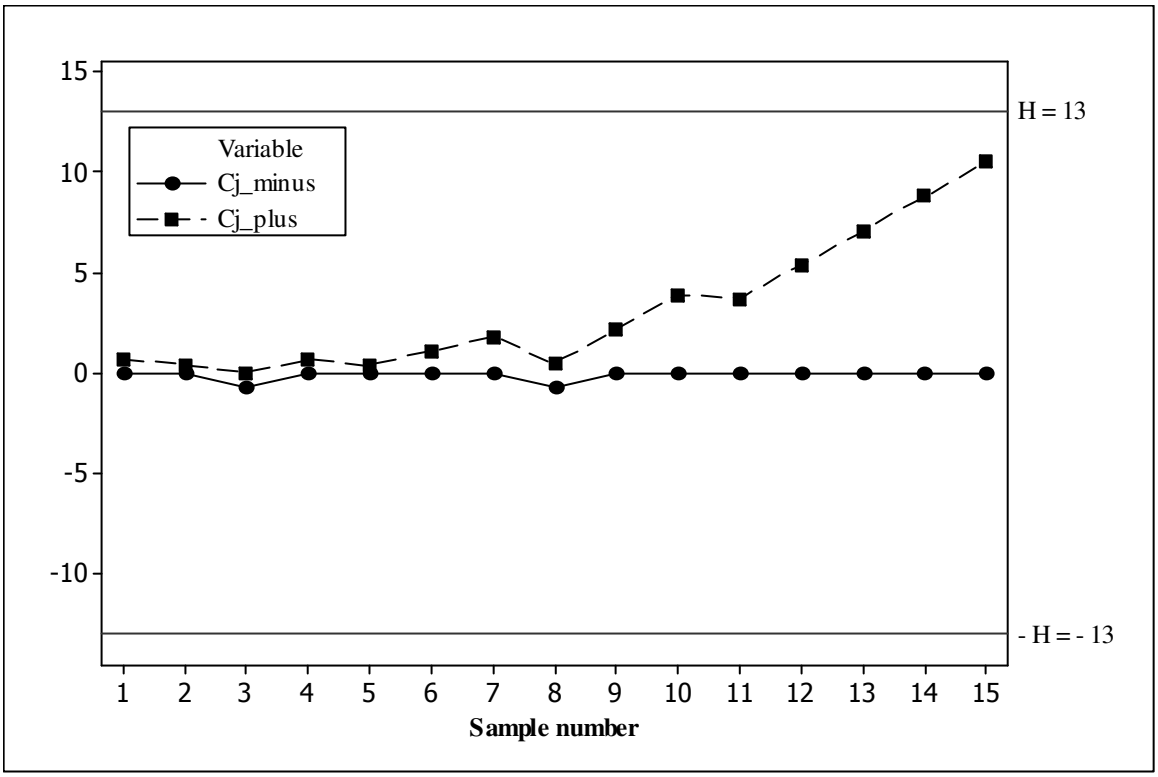

Figure 4.14. NPCUSUM-EX chart based on the 40th percentile for the Montgomery (2001) data with $\gamma = 0.25$

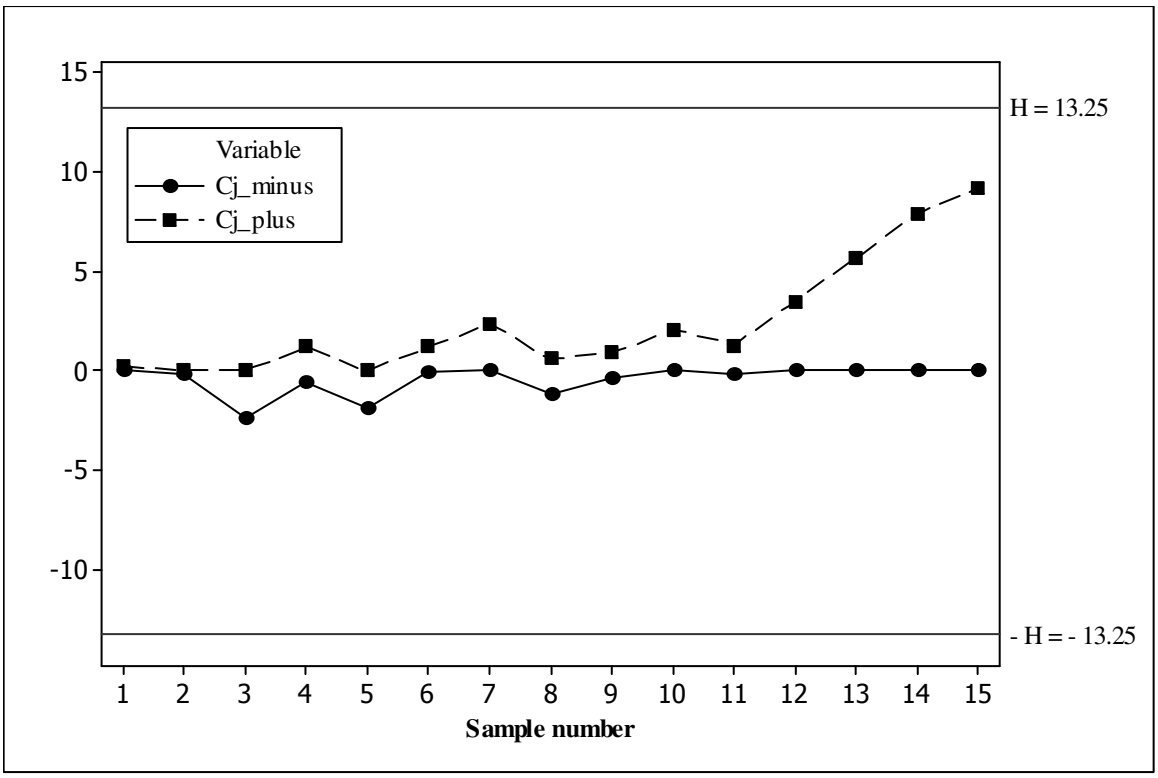

Figure 4.15. NPCUSUM-EX chart based on the 50th percentile for the Montgomery (2001) data with $\gamma = 0.25$

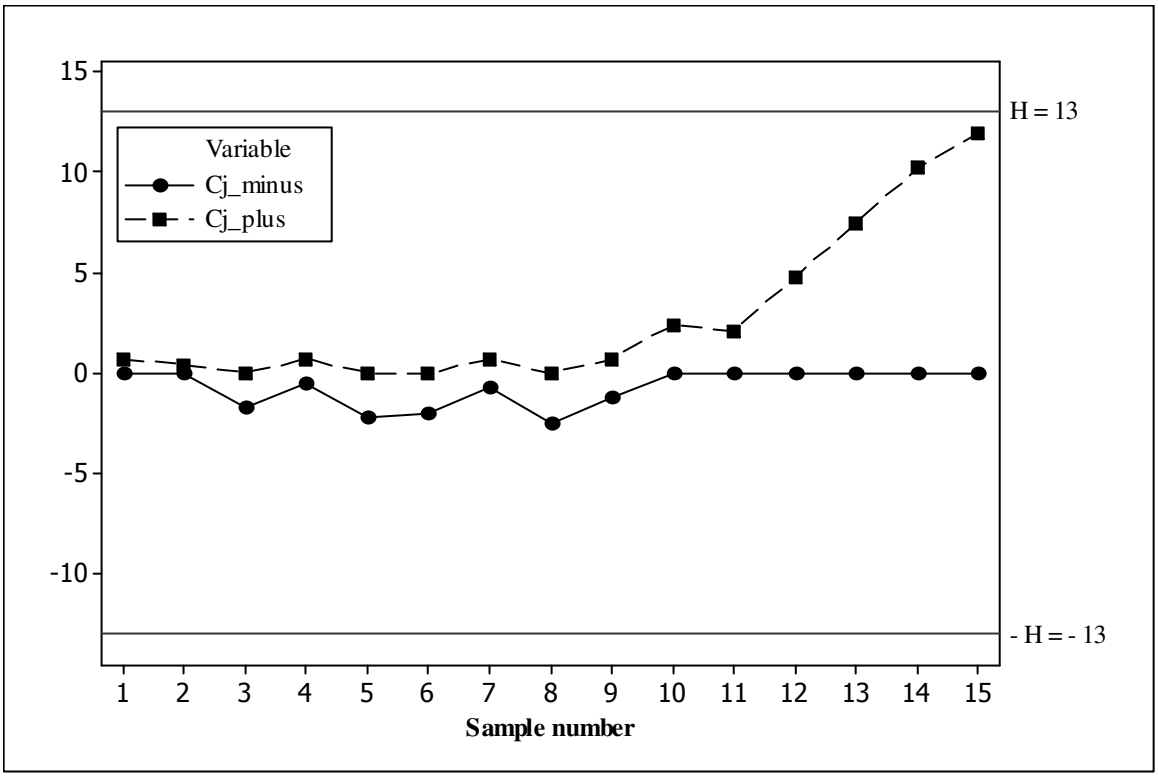

Figure 4.16. NPCUSUM-EX chart based on the 60th percentile for the Montgomery (2001) data with $\gamma = 0.25$

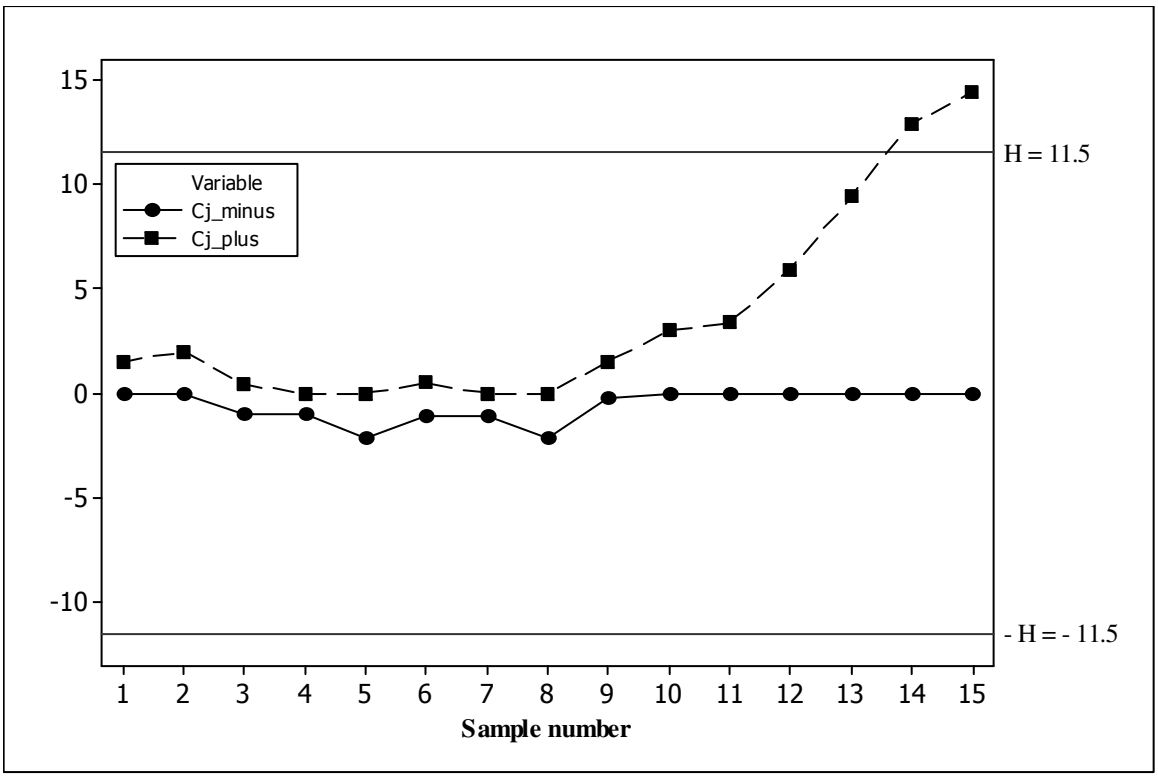

Figure 4.17. NPCUSUM-EX chart based on the 75th percentile for the Montgomery (2001) data with $\gamma = 0.25$

The NPCUSUM-EX based on the 25th percentile performs the worst and doesn't signal at all. The NPCUSUM-EX chart based on the 40th, 50th and 60th percentiles, respectively, almost signals, whereas the NPCUSUM-EX chart based on the 75th percentile actually does signal at sample number 14 with a counter of $N^+ = 6$, meaning that the shift most likely occurred at sample number 8. This isn't surprising, since Table 4.18 suggests that NPCUSUM-EX chart 75th percentile performs best when the underlying process distribution is normal and we have a small shift ($\gamma = 0.25$) and $c_l = 1.00$. In conclusion, the NPCUSUM-EX chart based on the 75th percentile performs better than its competitors, all of which are tuned at to detect a small shift of 0.25.

For our first example, the data did not reject a goodness of fit test for normality. Nonparametric charts are useful for all continuous distributions and heavier tailed distributions are of particular interest in practice as they can give rise to more outliers which do not necessarily indicate an OOC process. So we illustrate the NPCUSUM-EX chart when the data follow a symmetric yet heavier tailed distribution (than the normal) with some simulated data from the Double Exponential distribution.

Example 4.3

The second example is to illustrate the effectiveness and the application of the nonparametric chart when normality is in doubt. We simulate some data from the Double Exponential distribution; *DE*(0,1) which is known to have a median of zero and a standard deviation equal to $\sqrt{2}$. An IC reference sample of size 100 (m = 100) was generated from this distribution and each data point was scaled so that the transformed observations have a mean / median of 0 and a standard deviation of 1. Next the Phase II samples, each of size 5 (n = 5), were independently and sequentially generated by transforming the observations from a *DE*(0,1) distribution so that the resulting observations have a mean / median of $\gamma/\sqrt{n} = 0.25/\sqrt{5} = 0.112$ and a standard deviation of 1. Consequently, the Phase II samples can be thought of as having been drawn from a process that is known to be OOC in the location parameter. Again, we use $c_l = 1.00$.

Table 4.21. Charting statistics and counters for the simulated data with $\gamma = 0.25$

25th percentile				**40th percentile**				**50th percentile**				**60th percentile**				**75th percentile**			
C_j^-	N^-	C_j^+	N^+	C_j^-	N^-	C_j^+	N^+	C_j^-	N^-	C_j^+	N^+	C_j^-	N^-	C_j^+	N^+	C_j^-	N^-	C_j^+	N^+
0.0	0	0.0	0	0.0	0	0.7	1	0.0	0	0.2	1	0.0	0	0.7	1	0.0	0	0.0	0
0.0	0	0.0	0	-0.7	1	0.0	0	-1.2	1	0.0	0	-0.7	1	0.0	0	-1.1	1	0.0	0
0.0	0	0.0	0	-1.5	2	0.0	0	-1.5	2	0.0	0	-1.5	2	0.0	0	-1.1	2	0.0	0
0.0	0	0.0	0	-2.2	3	0.0	0	-1.7	3	0.0	0	-1.2	3	0.0	0	-1.2	3	0.0	0
0.0	0	0.0	0	-2.0	4	0.0	0	-2.0	4	0.0	0	-1.0	4	0.0	0	-2.2	4	0.0	0
0.0	0	0.0	0	-0.7	5	0.7	1	-0.2	5	1.2	1	0.0	0	1.7	1	-0.2	5	1.5	1
-0.5	1	0.0	0	-0.4	6	0.4	2	-0.4	6	0.4	2	0.0	0	1.4	2	-0.3	6	0.9	2
0.0	0	1.0	1	0.0	0	2.1	3	0.0	0	1.6	3	0.0	0	3.1	3	-1.3	7	0.0	0
-0.5	1	0.0	0	-0.7	1	0.8	4	-0.2	1	0.8	4	0.0	0	2.8	4	-0.3	8	0.5	1
-1.0	2	0.0	0	-0.5	2	0.5	5	-0.5	2	0.0	0	0.0	0	2.5	5	-0.4	9	0.0	0
-0.5	3	0.0	0	0.0	0	1.2	6	0.0	0	1.2	1	0.0	0	4.1	6	-0.4	10	0.0	0
-0.1	4	0.0	0	0.0	0	0.9	7	0.0	0	1.4	2	0.0	0	4.8	7	0.0	0	0.5	1
0.0	0	1.0	1	0.0	0	0.6	8	0.0	0	1.6	3	0.0	0	5.5	8	0.0	0	0.0	0
0.0	0	2.0	2	0.0	0	1.3	9	0.0	0	2.8	4	0.0	0	5.2	9	0.0	0	0.5	1
0.0	0	2.0	3	0.0	0	1.0	10	0.0	0	3.0	5	0.0	0	5.9	10	0.0	0	1.9	2

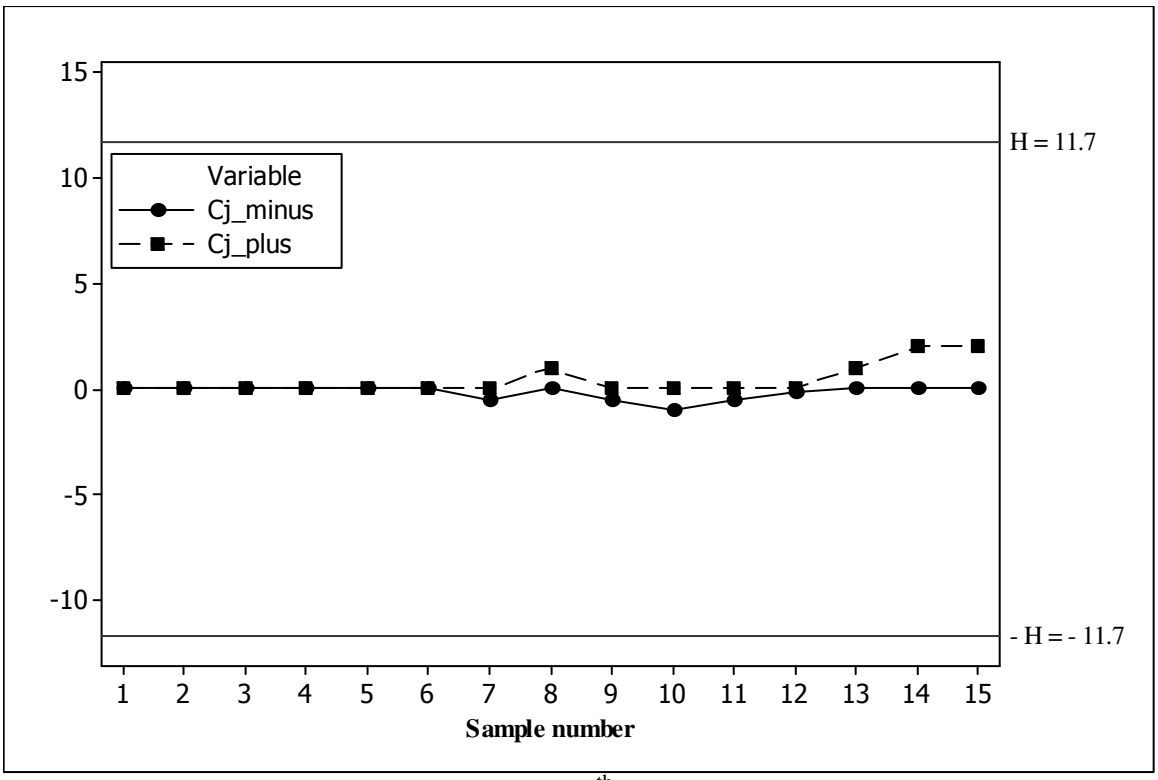

Figure 4.18. NPCUSUM-EX chart based on the 25th percentile for the simulated data with $\gamma = 0.25$

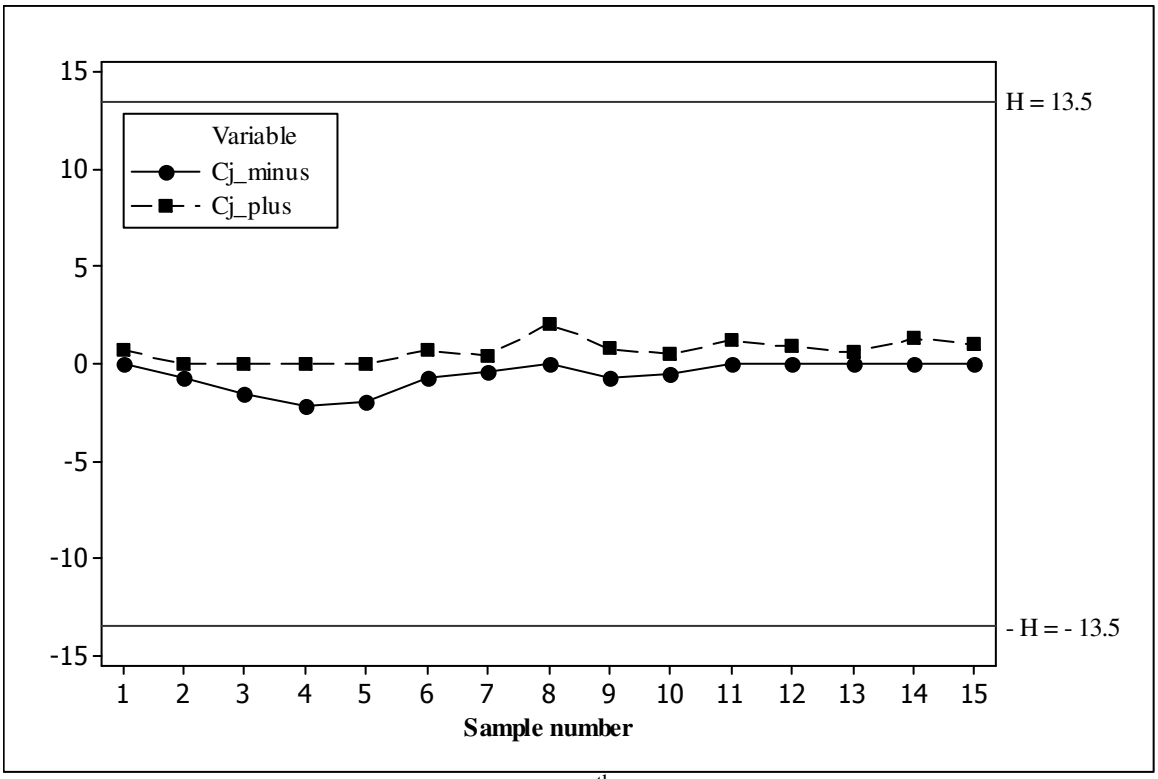

Figure 4.19. NPCUSUM-EX chart based on the 40th percentile for the simulated data with $\gamma = 0.25$

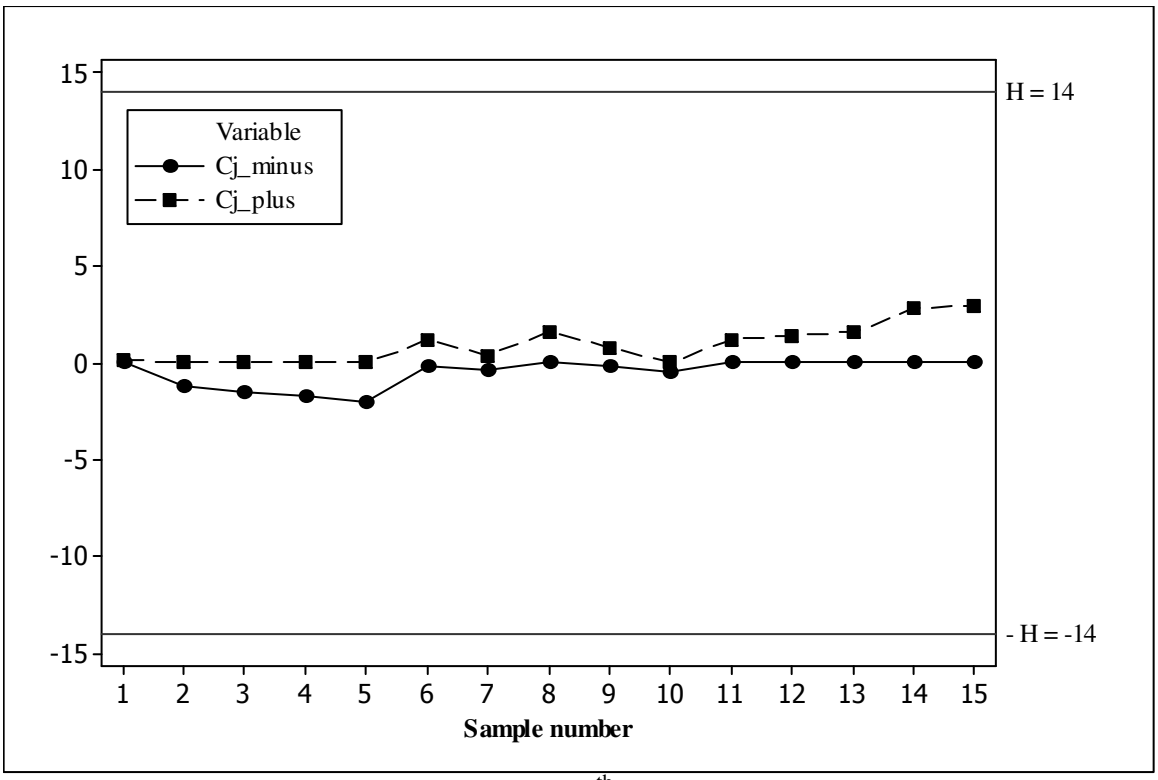

Figure 4.20. NPCUSUM-EX chart based on the 50th percentile for the simulated data with $\gamma = 0.25$

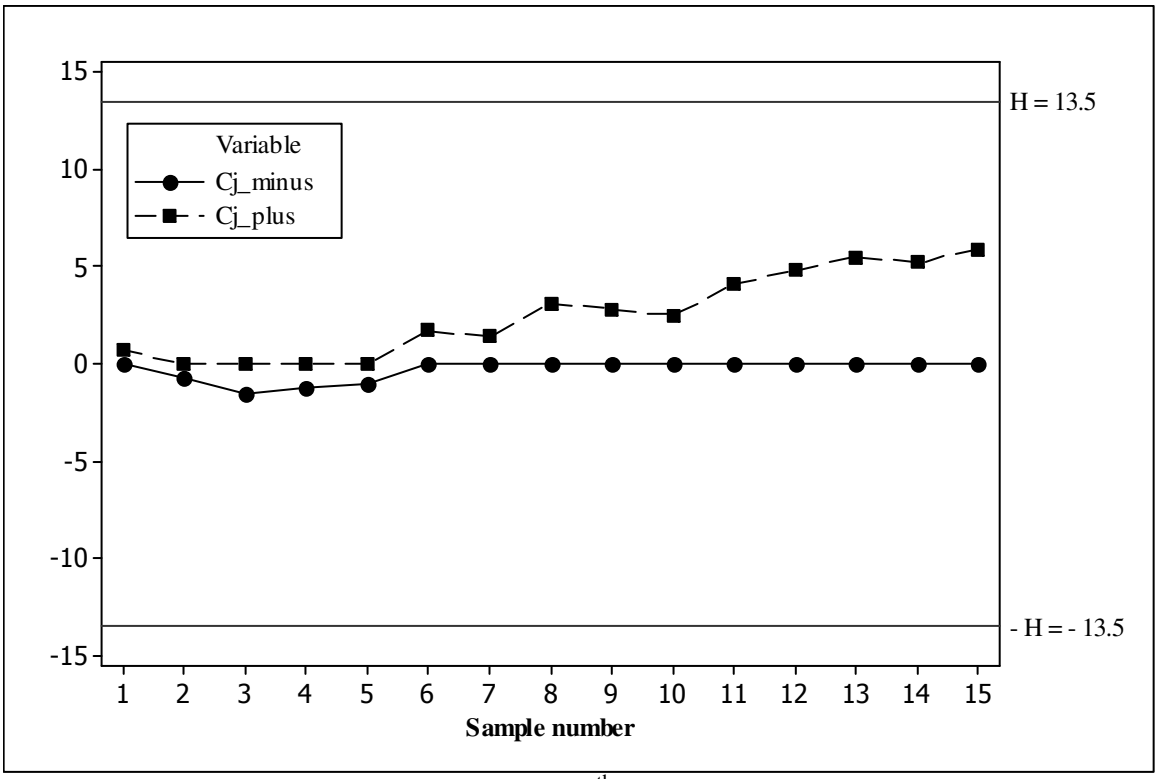

Figure 4.21. NPCUSUM-EX chart based on the 60th percentile for the simulated data with $\gamma = 0.25$

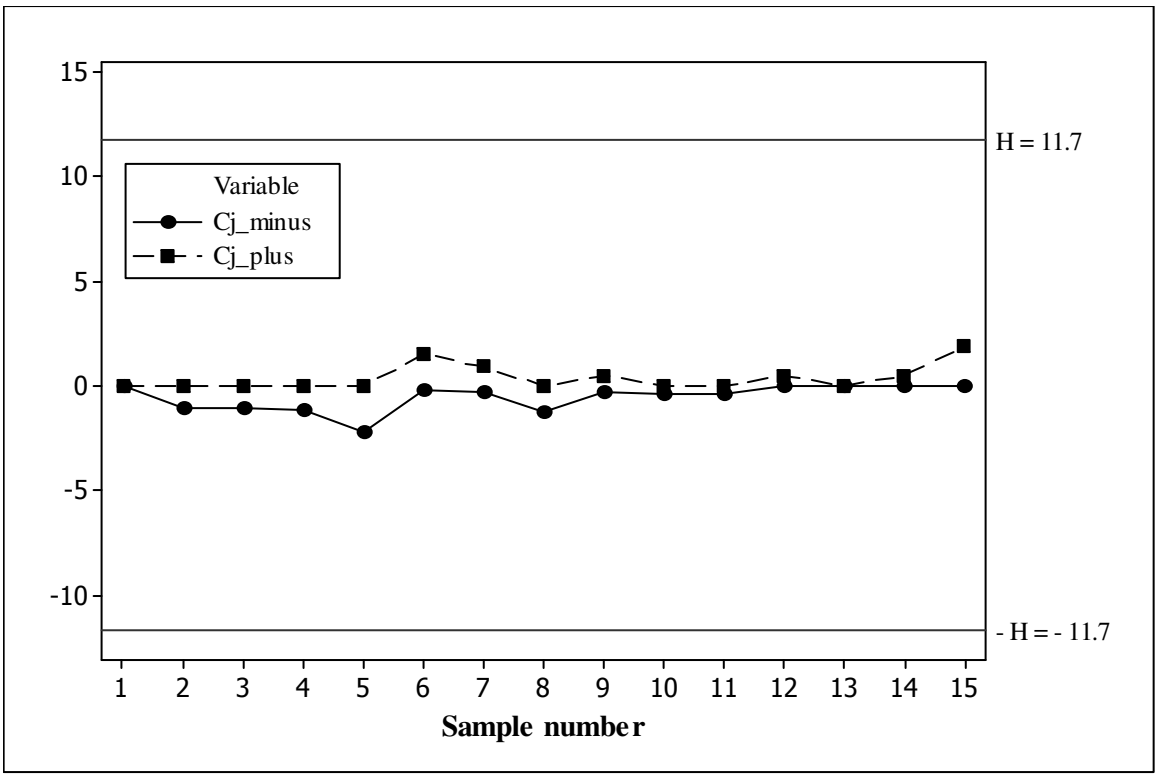

Figure 4.22. NPCUSUM-EX chart based on the 75th percentile for the simulated data with $\gamma = 0.25$

From Figures 4.18 to 4.22 we see that none of the charts signal. This is not surprizing, as the magnitude of the shift is very small ($\gamma/\sqrt{n} = 0.25/\sqrt{5} = 0.112$) and from Table 4.14 we find relatively high MRL_δ values for the $DE(0,1)$ distribution when $\gamma = 0.25$ and $c_l = 1.00$. Also, from Table 4.14, we see that the lowest MRL_δ (= 94) is associated with the NPCUSUM-EX chart based on the 60th percentile for the $DE(0,1)$ distribution when $\gamma = 0.25$ and $c_l = 1.00$. This is confirmed from Figure 4.21 where the NPCUSUM-EX chart based on the 60th percentile has the steepest incline compared to the other charts. The other MRL_δ values are 245, 146, 98 and 153 for the NPCUSUM-EX chart based on the 25th, 40th, 50th and 75th percentiles, respectively. So, for example, MRL_δ = 245 indicates that the first signal will be observed within the first 245 plotted points at least 50% of the time.

The findings above are very interesting, because the small shift ($\gamma = 0.25$) goes undetected. Also, for the same data, the CUSUM-$\overline{X}$ chart, with design parameters equal to $h = 4$ and $k = 0.5$ (the same reasoning holds for the choice of design parameters for the CUSUM-$\overline{X}$ chart as before) also doesn't signal.

4.3.6 Summary

NPCUSUM charts offer an attractive alternative in practice as they combine the inherent advantages of nonparametric charts with the better small shift detection capability of CUSUM-type charts. We have examined a class of NPCUSUM charts based on the exceedance statistic by investigating which order statistic (percentile), from the reference sample, should be used for good overall performance. We also examine the impact of the reference value, k, on the performance of the chart. We conclude that the NPCUSUM-EX chart, using the 3rd quartile of the reference sample, is a good overall chart for detecting a larger location shift. Other reference sample percentiles, such as the 25th or the 40th, can also be used when a smaller shift in location is expected. Overall, it is seen that the NPCUSUM-EX chart based on higher percentiles performs better than its competitors in many cases for a number of distributions. More specifically, for moderate to large shifts there is little doubt that the practitioner should use the exceedance chart based on the 60th or 75th percentiles, respectively, which signals quickly for all reference values under consideration. This is an interesting result in the literature on nonparametric exceedance / precedence tests and control charts. Next a class of NPEWMA charts based on the exceedance statistic is examined.

4.4 Nonparametric EWMA control chart based on the exceedance statistic

4.4.1 Statistical background

Constructing the NPEWMA-EX chart is straight forward. From Result 4B.1 in Appendix 4B we have that for a given value of the order statistic $X_{(r)} = x_{(r)}$, the variable $U_{j,r}$ follows a $BIN(n, p_r)$ distribution, conditionally on $X_{(r)}$, we can construct a binomial-type EWMA chart using the $U_{j,r}$'s to monitor the process location. Hence, once $X_{(r)}$ is observed, one can construct the NPEWMA-EX, in analogy with the parametric EWMA-$\overline{X}$ (see Equation (1.6) in Section 1.9.3 with the pivot statistic ψ_i replaced by X_i (for individual data) or $\overline{X}_i$ (for subgroup data)). Accordingly, the charting statistic of the chart is given by

$$Z_j = \lambda\, U_{j,r} + (1-\lambda) Z_{j-1} \text{ for } \quad j = 1,2,3,\ldots \tag{4.5}$$

where the starting value is taken as $Z_0 = E\left(U_{j-k,r} | X_{(r)}\right) = np_r$ and $0 < \lambda \leq 1$ is the smoothing constant. Note that we get the Shewhart-type precedence chart of Chakraborti et al. (2004) when $\lambda = 1$.

To calculate the control limits of the NPEWMA-EX chart the IC mean and IC standard deviation of Z_j are necessary. It can be shown that the unconditional IC mean and the unconditional IC standard deviation of Z_j are given by

$$E(Z_j|\,\text{IC}) = n(1-a)\left(1-(1-\lambda)^j\right)$$

and (4.6)

$$STDEV(Z_j|\,\text{IC}) = \sqrt{\left(\frac{na(1-a)}{m+2}\right)\left\{n(1-(1-\lambda)^j)^2 + \frac{\lambda(m+1)}{2-\lambda}(1-(1-\lambda)^{2j})\right\}},$$

respectively, where $a = r/(m+1)$ (see Result 4B.4 in Appendix 4B for the derivation of these formulae). Hence, the NPEWMA-EX chart has a charting statistic Z_j given in Equation (4.5) with $Z_0 = n(1-a)$ and the exact time-varying control limits and *CL* of the chart are given by

$$UCL = E(Z_j|\,\text{IC}) + L \times STDEV(Z_j|\,\text{IC})$$
$$= n(1-a)\left(1-(1-\lambda)^j\right) + L\sqrt{\left(\frac{na(1-a)}{m+2}\right)\left\{n(1-(1-\lambda)^j)^2 + \frac{\lambda(m+1)}{2-\lambda}(1-(1-\lambda)^{2j})\right\}}$$

$$CL = E(Z_j|\,\text{IC}) = n(1-a)\left(1-(1-\lambda)^j\right) \quad (4.7)$$

$$LCL = E(Z_j|\,\text{IC}) - L \times STDEV(Z_j|\,\text{IC}) =$$
$$n(1-a)\left(1-(1-\lambda)^j\right) - L\sqrt{\left(\frac{na(1-a)}{m+2}\right)\left\{n(1-(1-\lambda)^j)^2 + \frac{\lambda(m+1)}{2-\lambda}(1-(1-\lambda)^{2j})\right\}}.$$

The corresponding unconditional steady-state control limits and *CL* are given by

$$UCL = n(1-a) + L\sqrt{\left(\frac{na(1-a)}{m+2}\right)\left\{n + \frac{\lambda(m+1)}{2-\lambda}\right\}}$$

$$CL = n(1-a) \quad (4.8)$$

$$LCL = n(1-a) - L\sqrt{\left(\frac{na(1-a)}{m+2}\right)\left\{n + \frac{\lambda(m+1)}{2-\lambda}\right\}}.$$

These limits are typically used when the NPEWMA-EX chart has been running for several time periods and are obtained from (4.7) as $j \to \infty$ so that $\left(1-(1-\lambda)^{j}\right)$ and $\left(1-(1-\lambda)^{2j}\right)$ approach unity, respectively. If any Z_j plots on or outside of either of the control limits, the process is declared OOC and a search for assignable causes is started. Otherwise, the process is considered IC and the charting procedure continues. The steady-state control limits are used when proposing the NPEWMA-EX chart based on the median. However, later on, when proposing the NPEWMA-EX chart for other percentiles (other than the median), the exact time-varying control limits are used. Note that λ and L are the two design parameters of the chart which influence the chart's performance. Choice of λ and L is discussed in more detail in Section 1.9.3. Note also that the NPEWMA chart looks and operates very much like the traditional EWMA-$\overline{X}$.

4.4.2 Implementation of the chart

For implementation of the chart the design parameters (λ, L) are needed. The choice of the chart design parameters are discussed in detail in Section 1.9.3. To sum up, the first step is to choose λ. If small shifts (roughly 0.5 standard deviations or less) are of primary concern the typical recommendation is to choose a small λ, say equal to 0.05, if moderate shifts (roughly between 0.5 and 1.5 standard deviations) are of greater concern choose λ = 0.10, whereas if larger shifts (roughly 1.5 standard deviations or more) are of concern choose λ = 0.20. Next we choose L, in conjunction with the chosen λ, so that a desired nominal ARL_0 is attained.

Table 4.22 list some (λ, L)-combinations for the popular ARL_0 values of 370 and 500 for small to moderate reference sample sizes m = 49, 99 and 149 and subgroup sizes n = 5 and 10, respectively, when $X_{(r)}$ is taken to be the median. For now we only focus on the median since it is a good representative of the central reference value for distributions of all shapes and is by far the most popular percentile used in practice. However, in general, the exceedance statistic and hence the NPEWMA-EX chart can be based on other percentiles (order statistics) of the reference sample and their development would follow along similar lines (this is discussed in Section 4.4.5). It should be noted that if $X_{(r)}$ is taken to be the median it is easier to be calculated when m is odd. In each case, the run-length characteristics are calculated using simulation and are called the attained values. The first row of each cell in Table 4.22 shows the ARL_0 followed by the corresponding $SDRL_0$ in parentheses, whereas the second row shows the values of the IC 5th, 25th, 50th, 75th and 95th percentiles (in this order).

Table[xxv] 4.22. (λ, L)-combinations for the NPEWMA-EX chart for nominal $ARL_0 = 370$ and 500, respectively

		Nominal $ARL_0 = 370$		Nominal $ARL_0 = 500$	
m	**Shift**	**(λ, L)**	**Attained values**	**(λ, L)**	**Attained values**
		***n* = 5**			
49	Small	(0.05, 1.351)	372.86 (667.30) 17, 42, 110, 379, 1692	(0.05, 1.411)	499.94 (925.83) 19, 48, 136, 507, 2250
	Moderate	(0.10, 1.816)	369.39 (605.82) 14, 43, 131, 415, 1522	(0.10, 1.884)	501.49 (849.82) 16, 51, 168, 552, 2174
	Large	(0.20, 2.255)	369.16 (555.17) 12, 50, 160, 457, 1421	(0.20, 2.319)	504.22 (756.62) 14, 64, 208, 622, 2028
99	Small	(0.05, 1.669)	368.29 (546.03) 22, 61, 160, 442, 1406	(0.05, 1.743)	499.61 (804.97) 24, 70, 188, 560, 2115
	Moderate	(0.10, 2.132)	372.93 (519.76) 18, 63, 176, 460, 1387	(0.10, 2.211)	500.07 (698.94) 21, 77, 231, 630, 1861
	Large	(0.20, 2.499)	371.69 (474.05) 16, 73, 199, 483, 1303	(0.20, 2.577)	500.06 (648.69) 19, 92, 263, 650, 1788
149	Small	(0.05, 1.847)	379.76 (519.83) 25, 73, 187, 467, 1411	(0.05, 1.927)	501.17 (715.41) 28, 84, 229, 621, 1884
	Moderate	(0.10, 2.289)	371.18 (471.05) 21, 75, 200, 481, 1292	(0.10, 2.375)	499.46 (649.81) 24, 95, 256, 648, 1784
	Large	(0.20, 2.599)	369.58 (436.17) 19, 84, 217, 491, 1240	(0.20, 2.684)	500.59 (603.06) 22, 108, 289, 665, 1693
m		***n* = 10**			
49	Small	(0.05, 1.060)	369.96 (818.33) 13, 29, 73, 294, 1836	(0.05, 1.100)	499.59 (1164.46) 14, 31, 86, 381, 2516
	Moderate	(0.10, 1.466)	369.85 (737.47) 10, 27, 86, 346, 1771	(0.10, 1.516)	499.08 (1036.26) 11, 31, 103, 454, 2430
	Large	(0.20, 1.930)	370.80 (656.18) 9, 33, 114, 396, 1672	(0.20, 1.991)	501.73 (904.94) 9, 37, 144, 540, 2240
99	Small	(0.05, 1.355)	370.29 (664.74) 17, 42, 113, 385, 1640	(0.05, 1.413)	504.63 (967.66) 18, 48, 137, 493, 2320
	Moderate	(0.10, 1.812)	373.22 (617.30) 14, 43, 133, 426, 1553	(0.10, 1.880)	503.75 (857.94) 15, 50, 166, 561, 2164
	Large	(0.20, 2.266)	369.89 (542.58) 12, 51, 161, 455, 1456	(0.20, 2.338)	500.76 (756.93) 14, 63, 207, 611, 1997
149	Small	(0.05, 0.541)	369.08 (585.76) 19, 52, 138, 424, 1509	(0.05, 1.604)	498.30 (850.32) 21, 58, 167, 549, 2132
	Moderate	(0.10, 2.010)	371.881 (630.48) 17, 49, 148, 425, 1364	(0.10, 2.082)	503.22 (751.75) 18, 66, 204, 610, 2009
	Large	(0.20, 2.434)	372.19 (494.57) 14, 64, 184, 479, 1377	(0.20, 2.508)	508.27 (691.98) 17, 83, 241, 644, 1919

So, for example, in order to detect a small shift in the median with the NPEWMA-EX chart with an ARL_0 of approximately 500 and $m = 49$ and $n = 5$, one can use the (λ, L)-combination: (0.05, 1.411). A SAS® program is provided (see Appendix 4D) if the practitioner wishes to obtain some other (λ, L)-combinations for other nominal ARL_0 values.

[xxv] Note that the first row of each cell shows the *ARL* followed by the corresponding *SDRL* in parentheses, whereas the second row shows the values of the 5th, 25th, 50th, 75th and 95th percentiles (in this order).

4.4.3 Performance comparison with other charts

It is of interest to examine the performance of the nonparametric control charts and make comparisons with competing charts wherever available. However, since there is no specific model assumptions made for these charts, Monte Carlo simulation is used to this end.

We compare the NPEWMA-EX chart to the adjusted[xxvi] EWMA-$\overline{X}$ chart (see Jones (2002)) and the NPEWMA-Rank chart (see Li et al. (2010)). For the EWMA-$\overline{X}$ chart the parameters are estimated from a Phase I reference sample, duly taking care of the issues related to estimation. The shift considered by Jones (2002; page 286) for the adjusted EWMA-$\overline{X}$ chart is given by $\frac{\mu-\mu_0}{\sigma/\sqrt{n}}$ and is referred to a standardized shift in the mean. The shift considered Li et al. (2010; page 215) for the NPEWMA-Rank is measured by the subgroup standard deviation $\sigma/\sqrt{n}$. Thus, in order to have a fair comparison between the proposed NPEWMA-EX chart and its competitors, a shift of $\delta = \gamma\,\sigma/\sqrt{n}$ where $-\infty < \gamma < \infty, \gamma \neq 0$ is used for all charts.

Our study includes a collection of non-normal distributions and considers heavy-tailed, symmetric and skewed distributions. Specifically, the distributions considered in the study are:

i. The Standard Normal distribution, $N(0,1)$.

ii. The Exponential distribution with mean 1, which is $GAM(1,1)$.

iii. The Laplace (or double exponential distribution $DE(0,1)$) distribution with mean 0 and variance 2 which is standard normal like, but has heavier tails.

iv. The Symmetric Mixture Normal distribution (denoted *SymmMixN*) with parameters
$$[0.6N(\mu_1 = 0, \sigma_1 = 0.25) + 0.4N(\mu_2 = 0, \sigma_2 = 4)].$$

[xxvi] Adjusted: Case U; the parameters have to be estimated using a Phase I reference sample.

v. Two Asymmetric Mixture Normal distributions with parameters

$$[0.6N(\mu_1 = 0.25, \sigma_1 = 0.25) + 0.4N(\mu_2 = 0, \sigma_2 = 4)]$$

and

$$[0.6N(\mu_1 = -0.25, \sigma_1 = 0.25) + 0.4N(\mu_2 = 0, \sigma_2 = 4)],$$

denoted *AsymmMixN1* and *AsymmMixN2*, respectively.

vi. The Log-Logistic ($\alpha = 1,\ \beta = 2.5$) distribution. The Log-Logistic distribution (see e.g. Meeker and Escobar (1998) page 89) arises as the distribution of a positive valued random variable whose logarithm follows the familiar logistic distribution. Its shape is similar to that of a log-normal distribution but with heavier tails. This distribution is used to consider a heavy-tailed right-skewed distribution in our simulations. In the quality literature, Kantam and Rao (2005) considered CUSUM charts for Log-Logistic data.

Note that, wherever necessary, the distributions in the study have been shifted and scaled such that the mean / median equals 0 and the standard deviation equals 1, so that the results are easily comparable across the distributions. The details for these steps are shown in Appendix 1B.

Because the NPEWMA-EX chart is nonparametric, the IC run-length distribution and the associated characteristics remain the same for all continuous distributions. In other words, the IC run-length distribution is robust by definition and thus all IC characteristics such as the *ARL* would remain the same for all continuous distributions.

For the OOC chart performance comparison it is customary to ensure that the ARL_0 values of the competing charts are fixed at (or very close to) an acceptably high value, such as 500 in this case, and then compare their ARL_δ values; the chart with the smaller ARL_δ value is generally preferred. Tables 4.23 to 4.29 show the IC and OOC performance characteristics of the run-length distribution for $m = 100$, $n = 5$ and γ = 0.00(0.25)1.00, 0.50, 1.50 and 2.00, for the NPEWMA-EX, EWMA-$\overline{X}$ and NPEWMA-Rank charts, respectively. Note that the largest value of γ under consideration is γ = 2.00, since, for larger shifts, the run-length characteristics of the charts tend to converge. This is consistent with the shifts considered in the previous chapters. The first row of each cell in Tables 4.23 to 4.29 shows the *ARL* followed by the corresponding *SDRL* in parentheses, whereas the second row shows the values of the 5th, 25th, 50th, 75th and 95th percentiles (in this order).

Table[xxvii] **4.23.** Performance comparison under the $N(0,1)$ distribution for $m = 100$ and $n = 5$

			NPEWMA-EX	EWMA-$\overline{X}$	NPEWMA-Rank
	$\lambda = 0.05$				
	Control limits		1.991; 3.058	± 0.462	234.2; 295.8
IC	**0.00**		508.45 (795.41) 24, 72, 200, 590, 2106	512.42 (1009.21) 22, 64, 177, 534, 2065	503.99 (874.65) 23, 68, 189, 551, 2046
OOC	**Shift (γ)**	**0.25**	398.98 (687.24) 20, 49, 130, 417, 1738	312.72 (695.72) 15, 35, 82, 262, 1367	326.08 (705.73) 16, 37, 88, 287, 1453
		0.50	185.97 (456.32) 14, 26, 49, 129, 860	93.36 (305.26) 10, 18, 31, 62, 307	98.77 (306.09) 11, 19, 32, 66, 348
		0.75	62.22 (189.51) 10, 17, 27, 48, 176	26.76 (53.78) 8, 12, 18, 27, 64	30.18 (84.12) 9, 13, 19, 29, 70
		1.00	24.76 (34.77) 9, 13, 18, 26, 59	14.81 (11.84) 6, 9, 12, 17, 30	15.90 (14.64) 7, 10, 13, 18, 32
		1.50	12.73 (6.13) 7, 9, 11, 15, 23	8.40 (3.11) 5, 6, 8, 10, 14	9.05 (3.16) 5, 7, 8, 10, 15
		2.00	9.20 (2.64) 6, 7, 9, 10, 14	6.00 (1.71) 4, 5, 6, 7, 9	6.60 (1.68) 4, 5, 6, 7, 10
	$\lambda = 0.10$				
	Control limits		1.735; 3.314	± 0.682	219.5; 310.5
IC	**0.00**		510.77 (748.45) 21, 78, 226, 624, 1970	512.30 (947.37) 19, 68, 198, 554, 1988	512.69 (851.32) 19, 73, 215, 593, 1998
OOC	**Shift (γ)**	**0.25**	418.13 (670.26) 16, 51, 153, 480, 1766	324.52 (734.68) 12, 34, 93, 294, 1389	335.53 (660.36) 13, 37, 105, 334, 1434
		0.50	197.19 (429.69) 11, 25, 55, 164, 886	102.24 (325.86) 8, 16, 31, 72, 375	112.62 (325.32) 9, 17, 34, 80, 441
		0.75	70.73 (205.42) 8, 15, 26, 54, 238	28.45 (87.72) 6, 10, 16, 27, 78	31.53 (84.31) 6, 11, 17, 29, 87
		1.00	28.14 (63.53) 7, 11, 16, 27, 76	13.53 (13.12) 5, 7, 10, 16, 32	14.83 (19.69) 5, 8, 11, 17, 34
		1.50	11.33 (6.90) 5, 7, 10, 13, 23	7.02 (3.18) 4, 5, 6, 8, 13	7.57 (3.33) 4, 5, 7, 9, 14
		2.00	7.69 (2.73) 5, 6, 7, 9, 13	4.85 (1.63) 3, 4, 5, 6, 8	5.34 (1.62) 3, 4, 5, 6, 8
	$\lambda = 0.20$				
	Control limits		1.374; 3.675	± 1.010	198.3; 331.7
IC	**0.00**		498.81 (640.47) 20, 93, 261, 644, 1781	502.04 (1000.30) 15, 74, 214, 552, 1869	512.18 (829.96) 18, 88, 246, 614, 1850
OOC	**Shift (γ)**	**0.25**	418.33 (595.99) 15, 66, 191, 518, 1576	346.44 (784.34) 10, 38, 116, 339, 1378	348.12 (629.52) 11, 43, 130, 379, 1408
		0.50	214.28 (405.12) 9, 27, 72, 212, 910	124.84 (327.38) 6, 16, 37, 101, 482	127.09 (300.01) 7, 17, 40, 108, 517
		0.75	88.21 (233.29) 6, 14, 30, 72, 311	36.51 (107.51) 5, 9, 16, 34, 111	37.80 (85.83) 5, 10, 17, 35, 123
		1.00	32.81 (67.88) 5, 10, 17, 33, 103	14.81 (21.31) 4, 6, 10, 16, 40	15.87 (22.94) 4, 7, 10, 17, 42
		1.50	11.30 (11.09) 4, 6, 9, 13, 27	6.31 (3.84) 3, 4, 5, 8, 13	6.87 (4.05) 3, 4, 6, 8, 14
		2.00	6.82 (3.44) 3, 3, 5, 6, 8, 13	4.06 (1.72) 2, 3, 4, 5, 7	4.49 (1.74) 3, 3, 4, 5, 8

[xxvii] Note that the first row of each cell shows the *ARL* followed by the corresponding *SDRL* in parentheses, whereas the second row shows the values of the 5th, 25th, 50th, 75th and 95th percentiles (in this order).

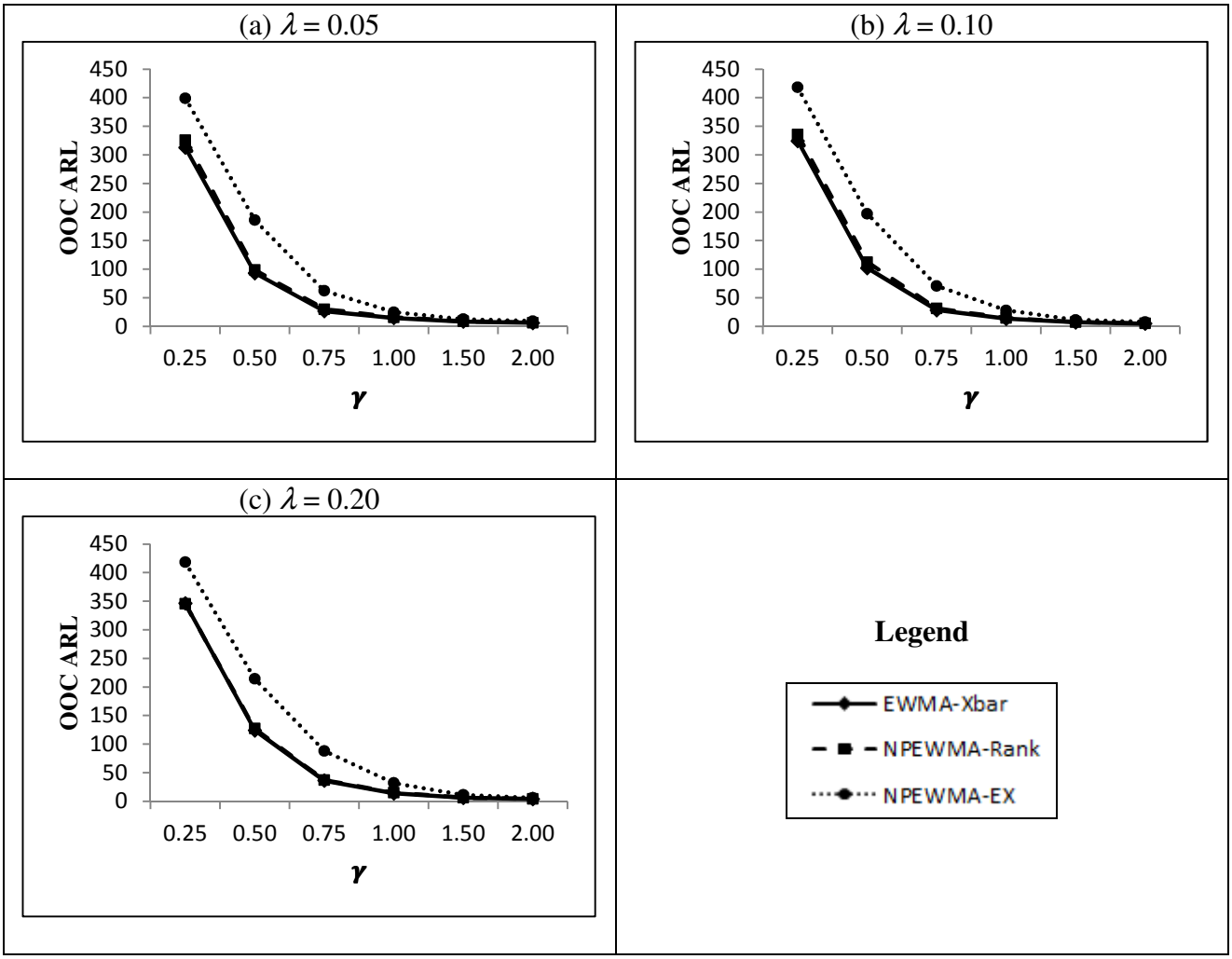

Figure 4.23. OOC *ARL* values under the $N(0,1)$ distribution for $m = 100$ and $n = 5$

A summary of our observations from the OOC comparisons for the standard normal distribution using Table 4.23 and Figure 4.23 is as follows. For all shifts under consideration the EWMA-$\overline{X}$ and NPEWMA-Rank charts perform similarly and both charts outperform the NPEWMA-EX. It isn't surprizing that the EWMA-$\overline{X}$ is superior to the NPEWMA-EX chart in this case, since it is typical for parametric methods to outperform their nonparametric counterparts when all assumptions are met.

Table[xxviii] **4.24.** Performance comparison under the $EXP(1)$ distribution for $m = 100$ and $n = 5$

			NPEWMA-EX	EWMA-$\overline{X}$	NPEWMA-Rank
	$\lambda = 0.05$				
	Control limits		1.991; 3.058	$\pm$ 0.444	234.2; 295.8
IC	**0.00**		503.27(784.58) 24, 71, 198, 578, 2000	501.57(1217.83) 20, 58, 156, 456, 1982	497.86 (851.89) 23, 66, 185, 548, 2003
OOC	**Shift (γ)**	**0.25**	317.06(641.13) 16, 36, 86, 292, 1405	588.82 (2131.56) 12, 30, 76, 292, 2441	285.71 (1263.33) 13, 24, 44, 117, 1153
		0.50	109.14 (320.47) 10, 17, 28, 64, 434	240.42 (1440.65) 8, 16, 29, 67, 639	48.25 (410.08) 9, 12, 18, 28, 81
		0.75	29.89(105.11) 7, 11, 15, 23, 65	58.22(578.88) 7, 11, 17, 28, 90	14.81 (80.81) 7, 9, 11, 15, 26
		1.00	12.74(19.09) 6, 8, 10, 13, 26	18.10(141.41) 5, 8, 12, 18, 36	9.36 (3.69) 6, 7, 9, 11, 15
		1.50	6.06(1.94) 5, 5, 5, 6, 9	8.36(4.22) 4, 6, 7, 10, 15	6.37 (1.38) 5, 5, 6, 7, 9
		2.00	5.02(0.23) 5, 5, 5, 5, 5	5.86(2.08) 3, 4, 5, 7, 10	5.14 (0.82) 4, 5, 5, 6, 7
	$\lambda = 0.10$				
	Control limits		1.735; 3.314	$\pm$ 0.640	219.5; 310.5
IC	**0.00**		501.01(713.38) 21, 78, 230, 630, 1881	486.29(1536.20) 14, 50, 145, 422, 1805	498.52 (817.35) 19, 71, 206, 584, 1913
OOC	**Shift (γ)**	**0.25**	341.02 (619.71) 13, 36, 104, 359, 1476	510.79 (2293.24) 8, 25, 69, 257, 1946	360.68 (1456.22) 10, 23, 56, 188, 1553
		0.50	113.82(317.98) 8, 15, 28, 70, 503	242.38 (1893.71) 6, 13, 27, 67, 559	59.77 (434.05) 7, 11, 16, 30, 122
		0.75	28.59(87.85) 6, 9, 13, 22, 79	47.76(550.19) 5, 9, 15, 27, 105	13.68 (50.90) 5, 7, 10, 14, 28
		1.00	11.86(36.27) 5, 6, 8, 12, 25	16.08(49.40) 4,7, 10, 16, 39	8.14 (14.79) 4, 6, 7, 9, 15
		1.50	4.86(1.64) 4, 4, 4, 5, 8	6.87(4.27) 3, 4, 6, 8, 14	5.15 (1.30) 4, 4, 5, 6, 8
		2.00	4.02(0.21) 4, 4, 4, 4, 4	4.61(1.88) 2, 3, 4, 5, 8	4.08 (0.74) 3, 4, 4, 4, 5
	$\lambda = 0.20$				
	Control limits		1.374; 3.675	$\pm$0.931	198.3; 331.7
IC	**0.00**		498.61 (653.65) 20, 94, 256, 640, 1807	518.30 (2265.32) 10, 46, 136, 403, 1735	503.07 (786.33) 17, 81, 235, 592, 1914
OOC	**Shift (γ)**	**0.25**	351.56 (543.44) 11, 43, 159, 419, 1449	468.86 (2742.07) 6, 22, 63, 220, 1525	409.95 (1350.67) 9, 27, 80, 281, 1791
		0.50	126.23 (287.26) 6, 15, 33, 102, 564	195.36 (1921.99) 4, 11, 26, 70, 473	116.93 (2322.39) 5, 10, 19, 43, 231
		0.75	38.30 (133.30) 4, 8, 13, 26, 124	49.42 (774.59) 3, 7, 13, 28, 125	17.29 (68.92) 4, 6, 9, 15, 43
		1.00	12.14 (35.93) 3, 5, 7, 11, 30	17.57 (65.41) 3, 5, 9, 16, 51	8.01 (8.16) 4, 5, 6, 9, 17
		1.50	3.84 (1.84) 3, 3, 3, 4, 7	6.35 (7.35) 2, 3, 5, 7, 15	4.36 (1.56) 3, 3, 4, 5, 7
		2.00	3.02 (0.18) 3, 3, 3, 3, 3	3.87 (2.16) 2, 3, 3, 5, 7	3.32 (0.73) 2, 3, 3, 4, 5

[xxviii] Note that the first row of each cell shows the *ARL* followed by the corresponding *SDRL* in parentheses, whereas the second row shows the values of the 5th, 25th, 50th, 75th and 95th percentiles (in this order).

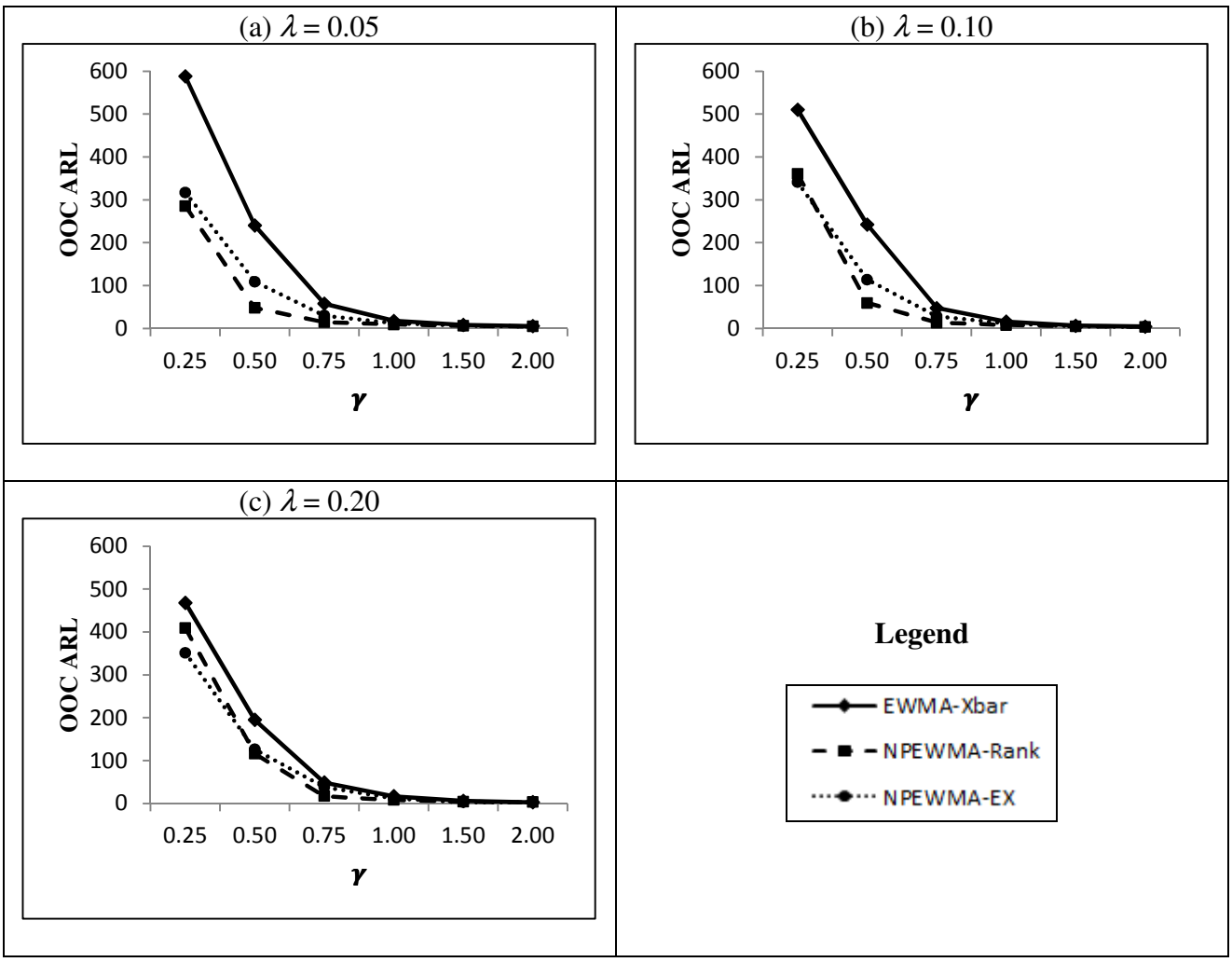

Figure 4.24. OOC *ARL* values under the *EXP*(1) distribution for $m = 100$ and $n = 5$

A summary of our observations from the OOC comparisons for the *EXP*(1) distribution using Table 4.24 and Figure 4.24 is as follows. For all shifts under consideration the EWMA-$\overline{X}$ chart performs the worst. When comparing the two nonparametric charts, the NPEWMA-EX chart performs best for $\gamma = 0.25$ ($\lambda = 0.10$ and 0.20) and for $\gamma = 1.50$ and 2.00 (for all λ). It may be noted that there is some bias in the *ARL* (the ARL_δ is bigger than the ARL_0) of the EWMA-$\overline{X}$ chart when the shift is small. This may be due to many extreme long run-lengths observed in the simulation of the *ARL*, which can be a result of the right-skewness of the *EXP*(1) distribution coupled with the fact that the run-length distribution is itself highly right-skewed with a long right tail. The bias could also be a result of simulation error because these ARL_δ values are very close to the ARL_0 values. Some authors have considered *ARL*-unbiased parametric charts and this would be a topic of further research in the context of nonparametric charts. On the other hand, Steiner and Jones (2010), among others, have recommended examining the *MRL* instead "which is easier to simulate and gives arguably a better summary." This approach is considered later on in Section 4.4.5.

Table[xxix] **4.25.** Performance comparison under the $DE(0,1)$ distribution for $m = 100$ and $n = 5$

			NPEWMA-EX	EWMA-$\overline{X}$	NPEWMA-Rank
	$\lambda = 0.05$				
	Control limits		1.991; 3.058	± 0.449	234.2; 295.8
IC	**0.00**		499.65 (784.93) 24, 70, 197, 586, 2017	498.47 (1367.32) 20, 57, 150, 443, 1962	498.75 (859.89) 23, 68, 187, 551, 2026
OOC	**Shift (γ)**	**0.25**	236.07 (500.18) 16, 34, 70, 192, 1083	324.82 (1009.33) 15, 33, 75, 235, 1353	257.97 (620.30) 14, 31, 66, 197, 1159
		0.50	50.72 (155.31) 11, 17, 25, 43, 126	96.56 (466.12) 10, 17, 29, 58, 290	56.48 (209.38) 10, 16, 24, 42, 147
		0.75	20.06 (40.58) 9, 12, 16, 22, 39	29.81 (139.13) 7, 12, 17, 26, 61	18.68 (49.11) 7, 11, 14, 20, 39
		1.00	13.57 (8.86) 7, 10, 12, 16, 24	14.26 (11.63) 6, 9, 12, 16, 29	11.75 (6.62) 6, 8, 10, 14, 21
		1.50	9.34 (2.41) 6, 8, 9, 11, 14	8.01 (3.11) 4, 6, 7, 9, 14	7.39 (2.15) 5, 6, 7, 8, 11
		2.00	7.66 (1.48) 6, 7, 7, 8, 10	5.81 (1.74) 4, 5, 6, 7, 9	5.70 (1.27) 4, 5, 5, 6, 8
	$\lambda = 0.10$				
	Control limits		1.735; 3.314	± 0.666	219.5; 310.5
IC	**0.00**		500.75 (735.73) 19, 76, 222, 618, 1937	499.84 (1655.17) 16, 58, 159, 448, 1812	511.47 (829.81) 20, 73, 215, 593, 2003
OOC	**Shift (γ)**	**0.25**	257.51 (516.17) 13, 33, 82, 243, 1117	327.31 (1053.01) 12, 31, 82, 260, 1284	279.22 (614.79) 12, 30, 76, 245, 1245
		0.50	53.04 (129.29) 9, 15, 25, 47, 161	107.21 (494.73) 8, 15, 29, 66, 355	62.42 (218.48) 7, 13, 23, 45, 196
		0.75	18.70 (21.53) 7, 10, 14, 21, 43	29.36 (89.69) 6, 10, 15, 27, 81	18.14 (39.01) 6, 9, 12, 19, 44
		1.00	11.94 (6.38) 6, 8, 10, 14, 23	13.17 (15.31) 5, 7, 10, 15, 30	10.26 (6.70) 5, 7, 9, 12, 21
		1.50	7.79 (2.47) 5, 6, 7, 9, 13	6.79 (3.21) 3, 5, 6, 8, 12	6.07 (2.14) 4, 5, 6, 7, 10
		2.00	6.35 (1.53) 5, 5, 6, 7, 9	4.65 (1.60) 3, 4, 4, 5, 8	4.56 (1.21) 3, 4, 4, 5, 7
	$\lambda = 0.20$				
	Control limits		1.374; 3.675	± 0.998	198.3; 331.7
IC	**0.00**		497.82 (633.82) 20, 95, 266, 641, 1815	495.69 (2425.21) 13, 60, 177, 469, 1833	492.57 (737.42) 18, 84, 258, 594, 1809
OOC	**Shift (γ)**	**0.25**	274.80 (455.47) 11, 38, 107, 300, 1138	340.27 (976.85) 9, 34, 98, 289, 1352	293.06 (557.20) 10, 34, 94, 296, 1236
		0.50	68.44 (176.94) 7, 15, 29, 63, 231	130.85 (417.72) 6, 15, 36, 96, 497	76.23 (224.89) 6, 13, 25, 60, 276
		0.75	22.41 (33.61) 5, 9, 14, 25, 60	39.93 (141.90) 4, 9,16, 33, 126	20.03 (31.98) 4, 7, 12, 21, 58
		1.00	12.27 (13.29) 4, 7, 10, 14, 28	15.57 (43.17) 3, 6, 9, 16, 42	10.07 (9.06) 3, 5, 8, 12, 24
		1.50	6.91 (3.07) 4, 5, 6, 8, 13	6.24 (4.16) 3,4,5,7,13	5.17 (2.39) 3, 4, 5, 6, 10
		2.00	5.28 (1.75) 3, 4, 5, 6, 9	3.97 (1.70) 2, 3, 4, 5, 7	3.75 (1.26) 2, 3, 3, 4, 6

[xxix] Note that the first row of each cell shows the *ARL* followed by the corresponding *SDRL* in parentheses, whereas the second row shows the values of the 5th, 25th, 50th, 75th and 95th percentiles (in this order).

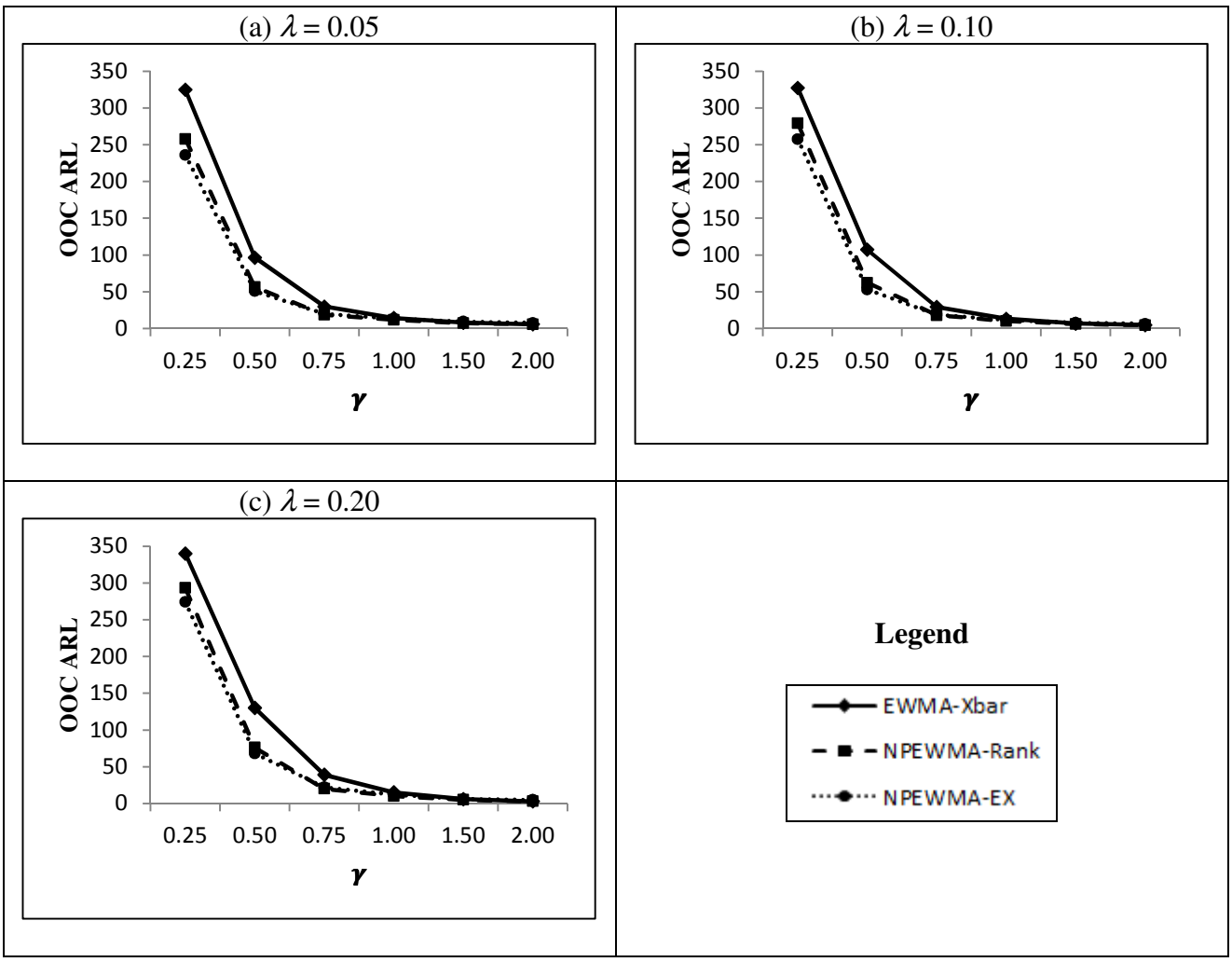

Figure 4.25. OOC *ARL* values under the *DE*(0,1) distribution for $m = 100$ and $n = 5$

A summary of our observations from the OOC comparisons for *DE*(0,1) distribution using Table 4.25 and Figure 4.25 is as follows. For all shifts under consideration the EWMA-$\overline{X}$ chart performs the worst. When comparing the two nonparametric charts, for $\gamma < 0.75$ the NPEWMA-EX chart performs the best and for all other shifts under consideration the NPEWMA-Rank chart performs the best.

Table[xxx] **4.26.** Performance comparison under the *SymmMixN* distribution for $m = 100$ and $n = 5$

			NPEWMA-EX	EWMA-$\bar{X}$	NPEWMA-Rank
	$\lambda = 0.05$				
	Control limits		1.991; 3.058	± 0.448	234.2; 295.8
IC	**0.00**		506.89 (790.60) 25, 71, 198, 597, 2042	506.34 (1361.96) 21, 58, 154, 450, 2010	487.43 (795.70) 23, 67, 187, 557, 1969
OOC	**Shift (γ)**	**0.25**	13.20 (5.28) 7, 10, 12, 15, 22	336.02 (1217.08) 14, 32, 75, 234, 1369	17.41 (55.75) 7, 10, 14, 19, 34
		0.50	8.68 (1.71) 6, 7, 8, 10, 12	107.08 (736.18) 10, 17, 29, 58, 299	8.34 (2.60) 5, 7, 8, 10, 13
		0.75	8.13 (1.47) 6, 7, 8, 9, 11	28.56 (129.92) 7, 12, 17, 26, 63	6.91 (1.87) 5, 6, 7, 8, 10
		1.00	7.83 (1.35) 6, 7, 8, 9, 10	14.54 (54.85) 6, 9, 12, 16, 29	6.32 (1.49) 4, 5, 6, 7, 9
		1.50	7.31 (1.13) 6, 7, 7, 8, 9	8.08 (3.07) 4, 6, 7, 9, 14	5.52 (1.17) 4, 5, 5, 6, 8
		2.00	6.93 (0.99) 6, 6, 7, 7, 9	5.79 (1.72) 4, 5, 6, 7, 9	4.95 (0.95) 4 ,4, 5, 5, 7
	$\lambda = 0.10$				
	Control limits		1.735; 3.314	± 0.656	219.5; 310.5
IC	**0.00**		506.84 (720.55) 21, 78, 232, 628, 1942	505.01 (1561.21) 16, 55, 155, 441, 1913	513.18 (774.04) 19, 74, 220, 619, 2005
OOC	**Shift (γ)**	**0.25**	12.17 (6.74) 6, 8, 11, 14, 23	328.51 (1110.10) 11, 30, 78, 248, 1312	15.81 (23.33) 5, 8, 12, 18, 37
		0.50	7.46 (1.82) 5, 6, 7, 8, 11	112.68 (531.66) 7, 15, 27, 63, 365	6.94 (2.66) 4, 5, 6, 8, 12
		0.75	6.91 (1.54) 5, 6, 7, 8, 10	28.98 (136.86) 5, 9, 15, 25, 73	5.62 (1.79) 3, 4, 5, 6, 9
		1.00	6.62 (1.41) 5, 6, 6, 7, 9	13.03 (25.01) 4, 7, 10, 15, 30	5.10 (1.48) 3, 4, 5, 6, 8
		1.50	6.14 (1.20) 5, 5, 6, 7, 8	6.62 (3.08) 3, 5, 6, 8, 12	4.41 (1.12) 3, 4, 4, 5, 6
		2.00	5.75 (1.04) 4, 5, 6, 6, 8	4.62 (1.60) 3, 4, 4, 5, 8	3.92 (0.90) 3, 3, 4, 4, 6
	$\lambda = 0.20$				
	Control limits		1.374; 3.675	± 0.960	198.3; 331.7
IC	**0.00**		503.65 (658.16) 20, 94, 263, 654, 1807	502, 84 (1644.98) 12, 55, 158, 435, 1829	561.41 (787.78) 18, 90, 268, 708, 2119
OOC	**Shift (γ)**	**0.25**	12.66 (9.43) 5, 7, 10, 15, 29	323.36 (924.14) 9, 30, 88, 263, 1287	17.67 (25.67) 4, 7, 11, 19, 50
		0.50	6.67 (2.37) 4, 5, 6, 8, 11	132.12 (1098.01) 5, 13, 29, 77, 427	6.11 (3.19) 3, 4, 5, 7, 12
		0.75	6.01 (1.96) 4, 5, 6, 7, 10	32.12 (113.93) 4, 8, 14, 28, 100	4.75 (1.95) 3, 3, 4, 6, 8
		1.00	5.68 (1.75) 4, 4, 5, 7, 9	13.52 (19.81) 3, 6, 9, 15, 37	4.22 (1.62) 2, 3, 4, 5, 7
		1.50	5.14 (1.45) 3, 4, 5, 6, 8	5.88 (4.12) 2, 4, 5, 7, 12	3.57 (1.15) 2, 3, 3, 4, 6
		2.00	4.71 (1.25) 3, 4, 5, 5, 7	3.81 (1.64) 2, 3, 3, 5, 7	3.13 (0.90) 2, 3, 3, 4, 5

[xxx] Note that the first row of each cell shows the *ARL* followed by the corresponding *SDRL* in parentheses, whereas the second row shows the values of the 5th, 25th, 50th, 75th and 95th percentiles (in this order).

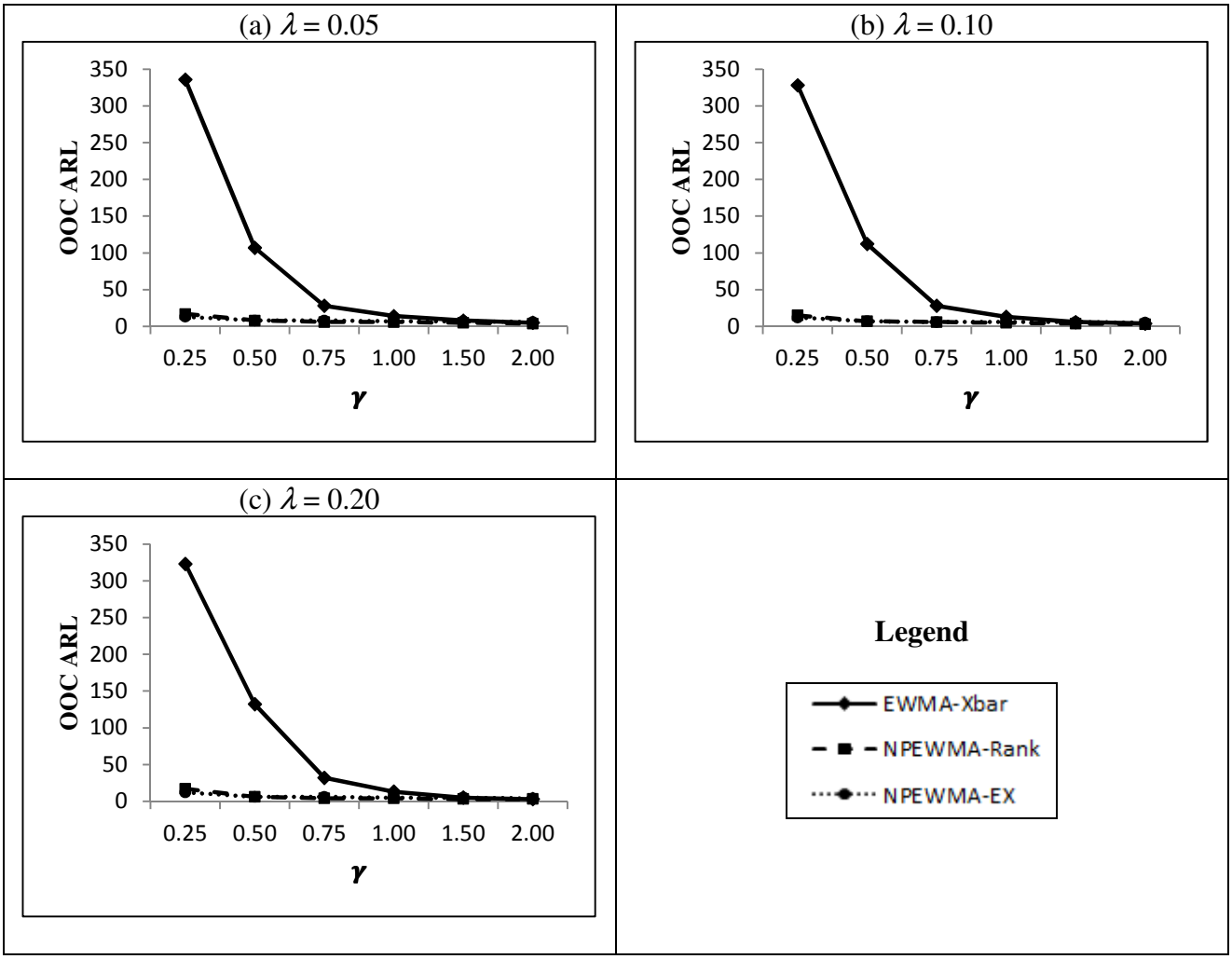

Figure 4.26. OOC *ARL* values under the *SymmMixN* distribution for $m = 100$ and $n = 5$

A summary of our observations from the OOC comparisons for the *SymmMixN* distribution using Table 4.26 and Figure 4.26 is as follows. For all shifts under consideration the EWMA-$\overline{X}$ chart performs the worst. When comparing the two nonparametric charts, for $\gamma = 0.25$ the NPEWMA-EX chart performs the best and for all other shifts under consideration the NPEWMA-Rank chart performs the best.

Table[xxxi] **4.27.** Performance comparison under the *AsymmMixN1* distribution for $m = 100$ and $n = 5$

			NPEWMA-EX	EWMA-$\bar{X}$	NPEWMA-Rank
	$\lambda = 0.05$				
	Control limits		1.991; 3.058	± 0.447	234.2; 295.8
IC	**0.00**		511.42 (803.11) 25, 71, 199, 593, 2085	509.61 (1426.34) 20, 57, 153, 447, 1991	486.57 (788.21) 23, 67, 187, 550, 1978
OOC	**Shift (γ)**	**0.25**	13.59 (8.34) 8, 10, 12, 16, 23	325.57 (1104.52) 14, 32, 74, 232, 1335	16.52 (13.34) 7, 10, 14, 19, 34
		0.50	8.90 (1.74) 7, 8, 9, 10, 12	97.51 (456.45) 10, 17, 28, 56, 294	8.36 (2.62) 5, 7, 8, 10, 13
		0.75	8.32 (1.47) 6, 7, 8, 9, 11	28.22 (150.07) 7, 12, 17, 26, 64	6.93 (1.81) 5, 6, 7, 8, 10
		1.00	8.00 (1.34) 6, 7, 8, 9, 10	14.17 (12.71) 6, 9, 12, 16, 29	6.32 (1.54) 4, 5, 6, 7, 9
		1.50	7.49 (1.17) 6, 7, 7, 8, 10	8.04 (3.09) 4, 6, 7, 9, 14	5.52 (1.19) 4, 5, 5, 6, 8
		2.00	7.08 (1.03) 6, 6, 7, 8, 9	5.76 (1.72) 4, 5, 5, 7, 9	4.96 (0.95) 4, 4, 5, 5, 7
	$\lambda = 0.10$				
	Control limits		1.735; 3.314	± 0.657	219.5; 310.5
IC	**0.00**		507.79 (723.57) 21, 80, 234, 628, 1927	501.96 (1475.70) 16, 55, 156, 448, 1937	516.08 (800.09) 20, 73, 217, 618, 2000
OOC	**Shift (γ)**	**0.25**	12.15 (6.36) 6, 8, 11, 14, 23	333.13 (1214.22) 11, 30, 78, 249, 1336	15.71 (18.43) 5, 8, 12, 18, 37
		0.50	7.45 (1.83) 5, 6, 7, 8, 11	110.22 (548.28) 7, 14, 27, 63, 364	6.93 (2.67) 4, 5, 6, 8, 12
		0.75	6.91 (1.53) 5, 6, 7, 8, 10	29.71 (151.64) 5, 9, 14, 25, 73	5.61 (1.78) 3, 4, 5, 6, 9
		1.00	6.62 (1.41) 5, 6, 6, 7, 9	13.03 (22.89) 4, 7, 10, 15, 30	5.10 (1.48) 3, 4, 5, 6, 8
		1.50	6.13 (1.20) 5, 5, 6, 7, 8	6.64 (3.08) 3, 5, 6, 8, 12	4.41 (1.13) 3, 4, 4, 5, 6
		2.00	5.75 (1.04) 4, 5, 6, 6, 8	4.61 (1.60) 3, 4, 4, 5, 8	3.93 (0.89) 3, 3, 4, 4, 6
	$\lambda = 0.20$				
	Control limits		1.374; 3.675	± 0.963	198.3; 331.7
IC	**0.00**		495.30 (642.25) 20, 96, 262, 640, 1773	511.87 (1774.70) 13, 55, 157, 437, 1837	565.06 (818.51) 18, 93, 268, 694, 2128
OOC	**Shift (γ)**	**0.25**	12.62 (9.89) 5, 7, 10, 15, 29	335.03 (1067.76) 8, 29, 87, 265, 1322	18.09 (31.14) 4, 7, 11, 19, 50
		0.50	6.61 (2.34) 4, 5, 6, 8, 11	128.88 (676.65) 6, 14, 30, 81, 456	6.16 (3.21) 3, 4, 5, 7, 12
		0.75	6.00 (1.93) 4, 5, 6, 7, 10	34.76 (132.27) 4, 8, 14, 28, 104	4.75 (1.96) 3, 3, 4, 6, 8
		1.00	5.66 (1.76) 3, 4, 5, 7, 9	13.51 (22.49) 3, 6, 9, 14, 36	4.23 (1.57) 2, 3, 4, 5, 7
		1.50	5.15 (1.46) 3, 4, 5, 6, 8	5.87 (4.01) 2, 4, 5, 7, 12	3.58 (1.16) 2, 3, 3, 4, 6
		2.00	4.72 (1.23) 3, 4, 5, 5, 7	3.81 (1.63) 2, 3, 3, 5, 7	3.15 (0.91) 2, 3, 3, 4, 5

[xxxi] Note that the first row of each cell shows the *ARL* followed by the corresponding *SDRL* in parentheses, whereas the second row shows the values of the 5th, 25th, 50th, 75th and 95th percentiles (in this order).

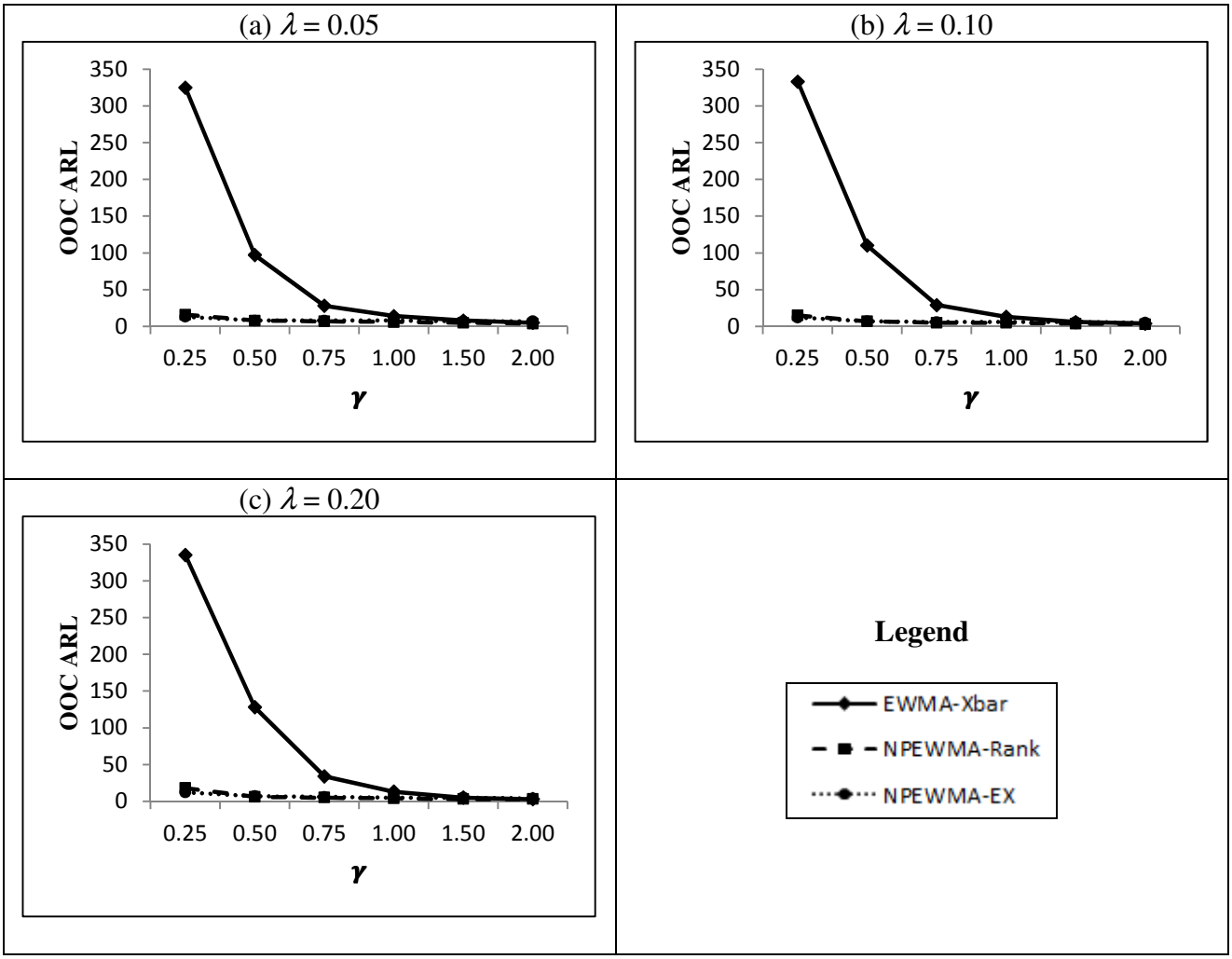

Figure 4.27. OOC *ARL* values under the *AsymmMixN1* distribution for $m = 100$ and $n = 5$

From Table 4.27 and Figure 4.27 it can be seen that similar conclusions can be drawn for the *AsymmMixN1* distribution as for the *SymmMixN* distribution. To recap, for all shifts under consideration the EWMA-$\overline{X}$ chart performs the worst. When comparing the two nonparametric charts, for $\gamma = 0.25$ the NPEWMA-EX chart performs the best and for all other shifts under consideration the NPEWMA-Rank chart performs the best.

Table[xxxii] **4.28.** Performance comparison under the *AsymmMixN2* distribution for $m = 100$ and $n = 5$

			NPEWMA-EX	EWMA-$\overline{X}$	NPEWMA-Rank
	$\lambda = 0.05$				
	Control limits		1.991; 3.058	± 0.446	234.2; 295.8
IC	**0.00**		506.54 (789.23) 25, 71, 198, 590, 2071	504.13 (1373.32) 21, 57, 150, 451, 1999	490.32 (782.31) 23, 68, 191, 558, 2006
OOC	**Shift (γ)**	**0.25**	13.52 (5.33) 8, 10, 12, 16, 23	320.87 (1068.66) 14, 32, 72, 225, 1314	16.60 (14.00) 7, 10, 14, 19, 34
		0.50	8.90 (1.73) 7, 8, 9, 10, 12	103.26 (504.63) 10, 17, 29, 58, 312	8.35 (2.60) 5, 7, 8, 10, 13
		0.75	8.31 (1.46) 6, 7, 8, 9, 11	27.65 (100.01) 7, 12, 17, 26, 63	6.92 (1.82) 5, 6, 7, 8, 10
		1.00	8.00 (1.35) 6, 7, 8, 9, 10	14.25 (22.46) 6, 9, 12, 16, 29	6.33 (1.54) 4, 5, 6, 7, 9
		1.50	7.49 (1.17) 6, 7, 7, 8, 10	8.03 (3.07) 4, 6, 7, 9, 14	5.53 (1.19) 4, 5, 5, 6, 8
		2.00	7.07 (1.03) 6, 6, 7, 8, 9	5.77 (1.72) 4, 5, 6, 7, 9	4.96 (0.95) 4, 4, 5, 5, 7
	$\lambda = 0.10$				
	Control limits		1.735; 3.314	± 0.833	219.5; 310.5
IC	**0.00**		509.83 (732.22) 21, 79, 231, 634, 1964	502.99 (1490.60) 16, 55, 156, 449, 1903	507.55 (781.94) 20, 73, 218, 612, 1972
OOC	**Shift (γ)**	**0.25**	12.17 (6.46) 6, 8, 11, 14, 23	331.96 (1083.49) 11, 30, 78, 249, 1314	15.69 (22.94) 5, 8, 12, 17, 36
		0.50	7.47 (1.84) 5, 6, 7, 8, 11	113.37 (703.62) 7, 14, 27, 63, 364	6.92 (2.66) 4, 5, 6, 8, 12
		0.75	6.91 (1.54) 5, 6, 7, 8, 10	30.19 (199.36) 5, 9, 15, 25, 74	5.63 (1.78) 3, 4, 5, 6, 9
		1.00	6.62 (1.39) 5, 6, 6, 7, 9	13.17 (37.73) 4, 7, 10, 15, 30	5.11 (1.48) 3, 4, 5, 6, 8
		1.50	6.14 (1.20) 5, 5, 6, 7, 8	6.64 (3.19) 3, 5, 6, 8, 12	4.41 (1.12) 3, 4, 4, 5, 6
		2.00	5.75 (1.03) 4, 5, 6, 6, 8	4.61 (1.61) 3, 4, 4, 5, 8	3.93 (0.90) 3, 3, 4, 4, 6
	$\lambda = 0.20$				
	Control limits		1.374; 3.675	± 0.964	198.3; 331.7
IC	**0.00**		499.44 (635.53) 21, 95, 269, 645, 1779	497.07 (1428.81) 13, 56, 158, 449, 2001	561.41 (787.78) 19, 90, 268, 708, 2219
OOC	**Shift (γ)**	**0.25**	12.52 (9.75) 5, 7, 10, 15, 29	359.58 (1248.90) 9, 31, 89, 272, 1385	18.52 (60.75) 4, 7, 11, 19, 48
		0.50	6.60 (2.38) 4, 5, 6, 8, 11	133.51 (592.08) 6, 14, 30, 80, 475	6.12 (3.12) 3, 4, 5, 7, 12
		0.75	6.01 (1.93) 4, 5,6, 7, 10	36.42 (163.25) 4, 8, 14, 28, 105	4.79 (2.02) 3, 3, 4, 6, 9
		1.00	5.66 (1.72) 3, 4, 5, 7, 9	13.82 (24.92) 3, 6, 9, 15, 38	4.23 (1.56) 2, 3, 4, 5, 6
		1.50	5.14 (1.46) 3, 4, 5, 6, 8	5.88 (3.75) 2, 4, 5, 7, 12	3.58 (1.16) 2, 3, 3, 4, 6
		2.00	4.70 (1.22) 3, 4, 5, 5, 7	3.83 (1.65) 2, 3, 3, 5, 7	3.14 (0.91) 2, 3, 3, 4, 5

[xxxii] Note that the first row of each cell shows the *ARL* followed by the corresponding *SDRL* in parentheses, whereas the second row shows the values of the 5th, 25th, 50th, 75th and 95th percentiles (in this order).

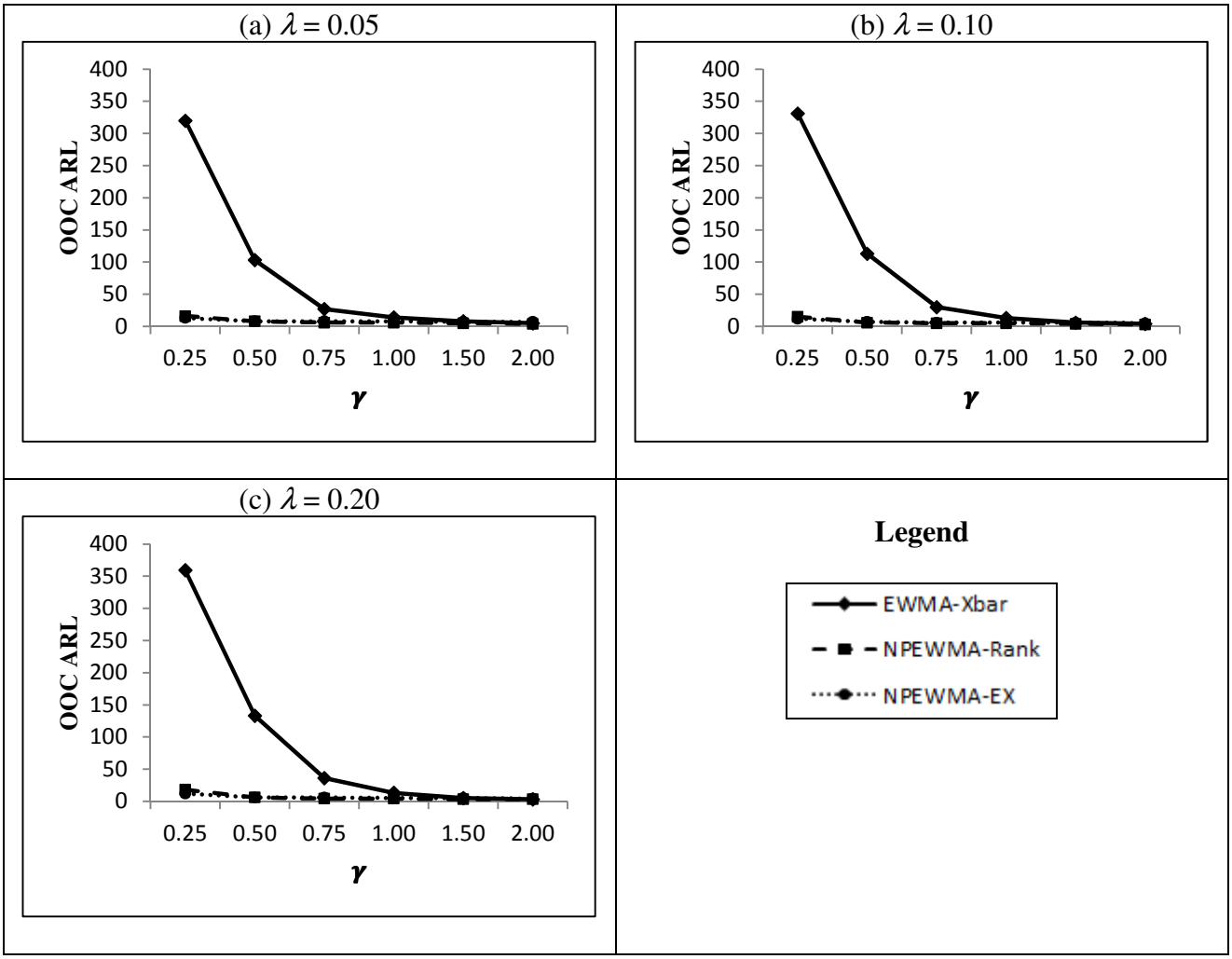

Figure 4.28. OOC *ARL* values under the *AsymmMixN2* distribution for $m = 100$ and $n = 5$

From Table 4.28 and Figure 4.28 it can be seen that similar conclusions can be drawn for the *AsymmMixN2* distribution as for the *AsymmMixN1* and the *SymmMixN* distributions. To recap, for all shifts under consideration the EWMA-$\overline{X}$ chart performs the worst. When comparing the two nonparametric charts, for $\gamma = 0.25$ the NPEWMA-EX chart performs the best and for all other shifts under consideration the NPEWMA-Rank chart performs the best.

Table[xxxiii] **4.29.** Performance comparison under the *Log-Logistic*$[\alpha = 1, \beta = 2.5]$ distribution for $m = 100$ and $n = 5$

			NPEWMA-EX	EWMA-$\overline{X}$	NPEWMA-Rank
	$\lambda = 0.05$				
	Control limits		1.991; 3.058	***	234.2; 295.8
IC	**0.00**		503.26 (788.70) 25, 71, 196, 585, 2045	***	501.83 (860.25) 23, 68, 191, 553, 2038
OOC	**Shift (γ)**	**0.25**	108.91 (326.17) 11, 18, 31, 66, 424	***	79.30 (511.05) 10, 15, 23, 41, 174
		0.50	14.31 (22.17) 7, 9, 11, 15, 28	***	11.46 (7.31) 6, 8, 10, 13, 21
		0.75	7.76 (2.60) 5, 6, 7, 8, 12	***	7.19 (1.85) 5, 6, 7, 8, 11
		1.00	5.91 (0.93) 5, 5, 6, 6, 8	***	5.60 (1.01) 4, 5, 5, 6, 7
		1.50	5.01 (0.08) 5, 5, 5, 5, 5	***	4.30 (0.50) 4, 4, 4, 5, 5
		2.00	5.00 (0.00) 5, 5, 5, 5, 5	***	3.91 (0.34) 3, 4, 4, 4, 4
	$\lambda = 0.10$				
	Control limits		1.735; 3.314	***	219.5; 310.5
IC	**0.00**		506.94 (724.35) 21, 78, 229, 628, 1939	***	507.54 (830.23) 20, 73, 215, 590, 1948
OOC	**Shift (γ)**	**0.25**	117.08 (315.08) 8, 16, 31, 78, 500	***	105.04 (718.96) 8, 13, 23, 49, 277
		0.50	13.20 (26.20) 5, 7, 9, 14, 29	***	10.31 (9.16) 5, 7, 9, 12, 21
		0.75	6.37 (2.30) 4, 5, 6, 7, 10	***	5.87 (1.84) 4, 5, 5, 7, 9
		1.00	4.76 (0.85) 4, 4, 5, 5, 6	***	4.46 (0.92) 3, 4, 4, 5, 6
		1.50	4.01 (0.07) 4, 4, 4, 4, 4	***	3.35 (0.50) 3, 3, 3, 4, 4
		2.00	4.00 (0.00) 4, 4, 4, 4, 4	***	3.03 (0.16) 3, 3, 3, 3, 3
	$\lambda = 0.20$				
	Control limits		1.374; 3.675	***	198.3; 331.7
IC	**0.00**		505.53 (644.15) 20, 94, 264, 657, 1804	***	495.88 (736.16) 19, 83, 236, 595, 1823
OOC	**Shift (γ)**	**0.25**	136.26 (321.66) 7, 16, 38, 106, 585	***	133.45 (624.10) 6, 13, 28, 75, 462
		0.50	14.41 (34.14) 4, 6, 9, 14, 37	***	11.16 (15.18) 4, 6, 8, 12, 28
		0.75	5.44 (3.98) 3, 4, 5, 6, 10	***	5.13 (2.56) 3, 4, 5, 6, 9
		1.00	3.70 (0.93) 3, 3, 3, 4, 5	***	3.64 (0.97) 3, 3, 3, 4, 5
		1.50	3.00 (0.07) 3, 3, 3, 3, 3	***	2.70 (0.51) 2, 2, 3, 3, 3
		2.00	3.00 (0.00) 3, 3, 3, 3, 3	***	2.19 (0.39) 2, 2, 2, 2, 3

*** The run-length characteristics can't be computed for the EWMA-$\overline{X}$ chart based on normal theory, since the run-length characteristics don't converge

[xxxiii] Note that the first row of each cell shows the *ARL* followed by the corresponding *SDRL* in parentheses, whereas the second row shows the values of the 5th, 25th, 50th, 75th and 95th percentiles (in this order).

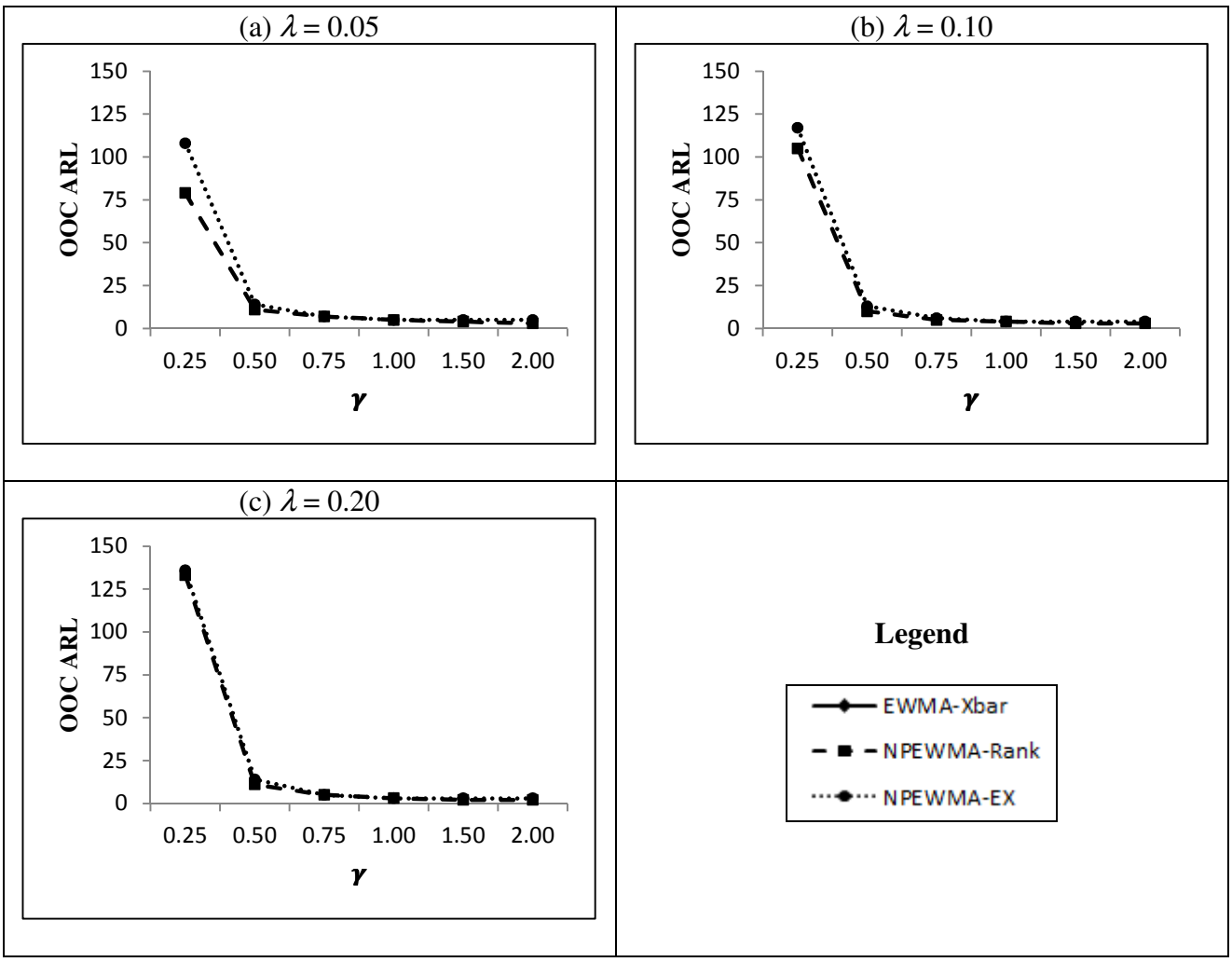

Figure 4.29. OOC *ARL* values under the Log-Logistic $[\alpha = 1, \beta = 2.5]$ distribution for $m = 100$ and $n = 5$

A summary of our observations from the OOC comparisons for the Log-Logistic distribution using Table 4.29 and Figure 4.29 is as follows. The run-length characteristics can't be computed for the EWMA-$\overline{X}$ chart based on normal theory methods, since the run-length characteristics don't converge. This is a common result for control charts based on normal theory methods (see, for example, Chakraborti et al. (2004) page 454 where a similar problem is encountered for the uniform distribution when working with the Shewhart-$\overline{X}$ chart). Although the performance for the NPEWMA-Rank chart and the NPEWMA-EX chart is very similar, the NPEWMA-Rank outperforms the NPEWMA-EX chart for all shifts under consideration.

Our overall conclusion is this. In comparison with the EWMA-$\overline{X}$ chart, when small shifts are of interest, the NPEWMA-EX chart is outperformed only when the underlying distribution is normal. However, the point to remember is that the EWMA-$\overline{X}$ chart can be non-robust in case normality is not satisfied, whereas the nonparametric charts require no distributional assumption,

which is a substantial practical advantage. In comparison with the NPEWMA-Rank chart, the NPEWMA-EX chart has either a similar or better performance. These observations coupled with the fact that the EWMA charts are generally easier to be used on the job floor and they provide one-chart monitoring for two-sided (both higher and lower shifts) monitoring make the NPEWMA-EX chart a useful tool for the data analyst.

Effect of the reference sample size

The NPEWMA-EX chart is calibrated to achieve an ARL_0 equal to a target, say 500. However, this is the unconditional IC average run-length (averaged over all possible IC Phase I samples) and users in practice may be interested in the ARL_0 depending (conditional) on the Phase I sample they have. The attained ARL_0 will vary, since the Phase I sample is a random sample, even though the chart may have been designed for a nominal ARL_0 of 500 and the Phase I sample is from an IC process.

A simulation study was conducted to investigate the effect of the reference sample size on the performance of the NPEWMA-EX chart. The reference sample size (m) was chosen to be 20, 50, 100, 500 and 1000, respectively. The smoothing constant was taken to be 0.05, i.e. $\lambda = 0.05$, and L was chosen so that $ARL_0 \approx 500$ for each reference sample size. Table 4.30 shows the IC and OOC performance characteristics of the run-length distribution for shifts of size $\gamma = 0.00(0.25)1.00$, 1.50 and 2.00 in the median, for the different reference sample sizes and $n = 5$, for the NPEWMA-EX chart under the $N(0,1)$ distribution. In addition, the results are shown for the NPEWMA-SN chart (see Section 3.2), since this is the analogue of the NPEWMA-EX chart if the process parameters were known or specified. The *ARL* values are illustrated in Figure 4.30.

From Table 4.30 and Figure 4.30 we find that as it might be expected, the larger the reference sample size, the less the uncertainty and the better the performance of the chart. Generally, when the reference sample size is not less than 100, the NPEWMA-EX chart performs well, that is it performs like what is expected unconditionally. In addition, the values, when the parameters are unknown, tend to the values if the parameters were known, which is expected, since the uncertainty decreases as the reference sample size increases. Similar conclusions were found for other (skewed and heavy-tailed) distributions.

Table[hh] 4.30. Effect of reference sample size on the NPEWMA-EX chart under the $N(0,1)$ distribution for $\lambda = 0.05$ and $n = 5$

m	**20**	**50**	**100**	**500**	**1000**	**Parameters known or specified**
Control Limits	2.039; 3.120 with $L = 1.036$	1.996; 3.102 with $L = 1.42$	1.991; 3.058 with $L = 1.75$	2.010; 3.000 with $L = 2.35$	2.019; 2.986 with $L = 2.47$	-0.931, 0.931 with $L = 2.60$
Shift (γ) 0.00	500.95 (1210.72) 13, 27, 72, 345, 2574	504.69 (953.55) 19, 49, 143, 492, 2277	508.45 (795.41) 24, 72, 200, 590, 2106	498.31 (562.59) 36, 123, 303, 672, 1616	500.58 (526.46) 40, 146, 335, 672, 1554	500.94 (482.31) 39, 156, 352, 689, 1467
0.25	488.98 (1220.19) 13, 29, 75, 327, 2516	458.66 (886.23) 17, 42, 121, 444, 2127	398.98 (687.24) 20, 49, 130, 417, 1738	222.03 (326.81) 21, 53, 111, 246, 820	172.02 (213.16) 21, 51, 102, 207, 557	118.99 (101.86) 20, 47, 89, 158, 322
0.50	430.41 (1139.25) 12, 24, 57, 252, 2266	300.54 (743.68) 13, 26, 56, 198, 1545	185.97 (456.32) 14, 26, 49, 129, 860	57.62 (67.32) 13, 25, 39, 68, 156	48.23 (38.59) 13, 23, 37, 60, 120	40.57 (26.43) 12, 22, 34, 52, 92
0.75	305.57 (938.98) 10, 18, 36, 127, 1631	148.49 (524.62) 11, 18, 30, 70, 596	62.22 (189.51) 10, 17, 27, 48, 176	27.17 (17.90) 10, 16, 23, 33, 59	25.07 (14.28) 10, 15, 22, 31, 52	22.71 (11.52) 9, 15, 20, 28, 45
1.00	223.61 (840.20) 9, 14, 24, 65, 1067	63.25 (271.63) 9, 14, 20, 34, 165	24.76 (34.77) 9, 13, 18, 26, 59	17.68 (8.43) 8, 12, 16, 21, 33	16.73 (7.88) 8, 12, 15, 20, 31	15.62 (6.51) 8, 11, 14, 19, 28
1.50	67.81 (440.12) 7, 10, 14, 22, 113	16.48 (56.58) 7, 10, 12, 17, 32	12.73 (6.13) 7, 9, 11, 15, 23	10.84 (3.49) 7, 8, 10, 13, 17	10.38 (3.27) 6, 8, 10, 12, 17	9.98 (3.05) 6, 8, 9, 12, 16
2.00	16.46 (79.83) 6, 8, 10, 14, 28	10.05 (4.10) 6, 8, 9, 11, 17	9.20 (2.64) 6, 7, 9, 10, 14	8.16 (1.99) 6, 7, 8, 9, 12	7.87 (1.89) 6, 6, 7, 9, 11	7.50 (1.83) 5, 6, 7, 9, 11

[hh] Note that the first row of each cell shows the *ARL* followed by the corresponding *SDRL* in parentheses, whereas the second row shows the values of the 5th, 25th, 50th, 75th and 95th percentiles (in this order).

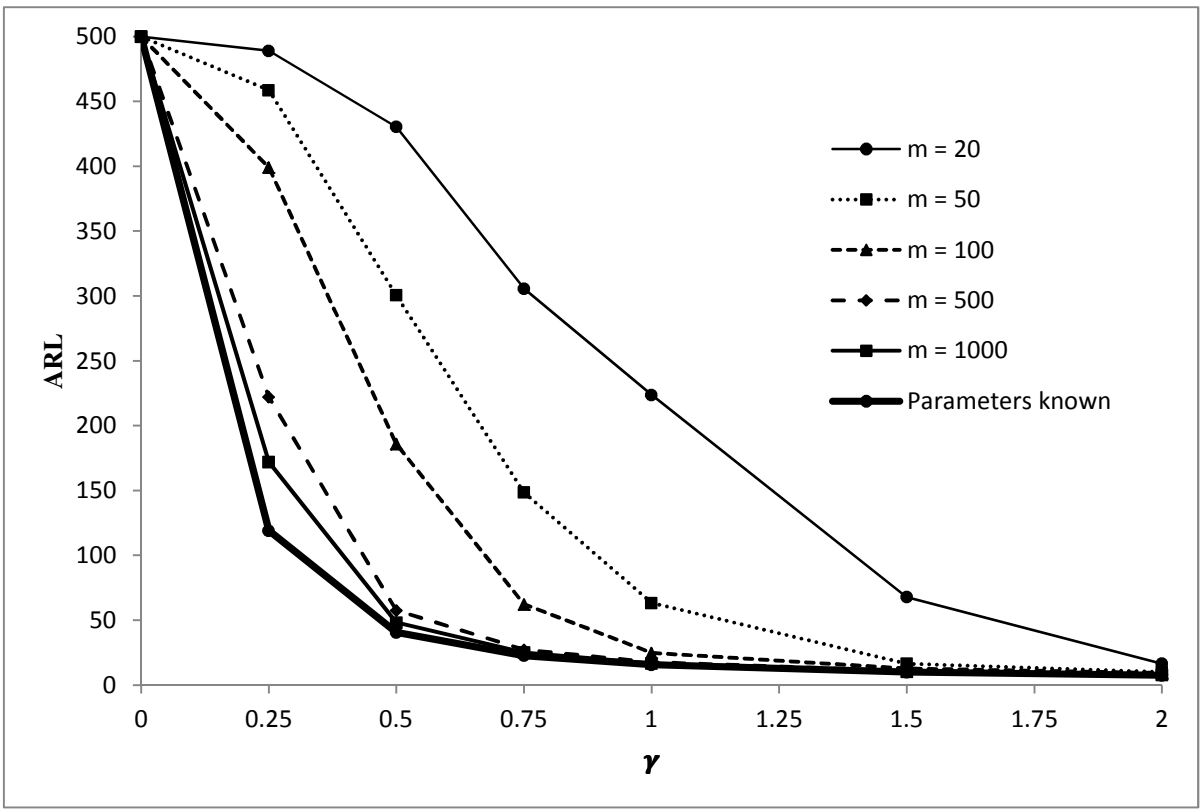

Figure 4.30 Comparison of different reference sample sizes for $n = 5$ and $\lambda = 0.05$

4.4.4 Illustrative examples

Example 4.4

First we illustrate the NPEWMA-EX chart using a well-known dataset from Montgomery (2001; Tables 5.1 and 5.2) on the inside diameters of piston rings manufactured by a forging process. The data given in Table 5.1 contain twenty-five retrospective or Phase I samples, each of size five, that were collected when the process was thought to be IC, i.e. $m = 125$. These data are considered to be the Phase I reference data for which a goodness of fit test for normality is not rejected. The reference sample has a median equal to 74.001, i.e. $r = 63$ and $X_{(63)} = 74.001$. Table 5.2 of Montgomery (2001) contains fifteen prospective (Phase II) samples each of five observations ($n = 5$). The NPEWMA-EX chart is compared to the EWMA-$\overline{X}$ chart and the NPEWMA-Rank chart, respectively. The design parameters were taken so that $ARL_0 \approx 500$ for each chart.

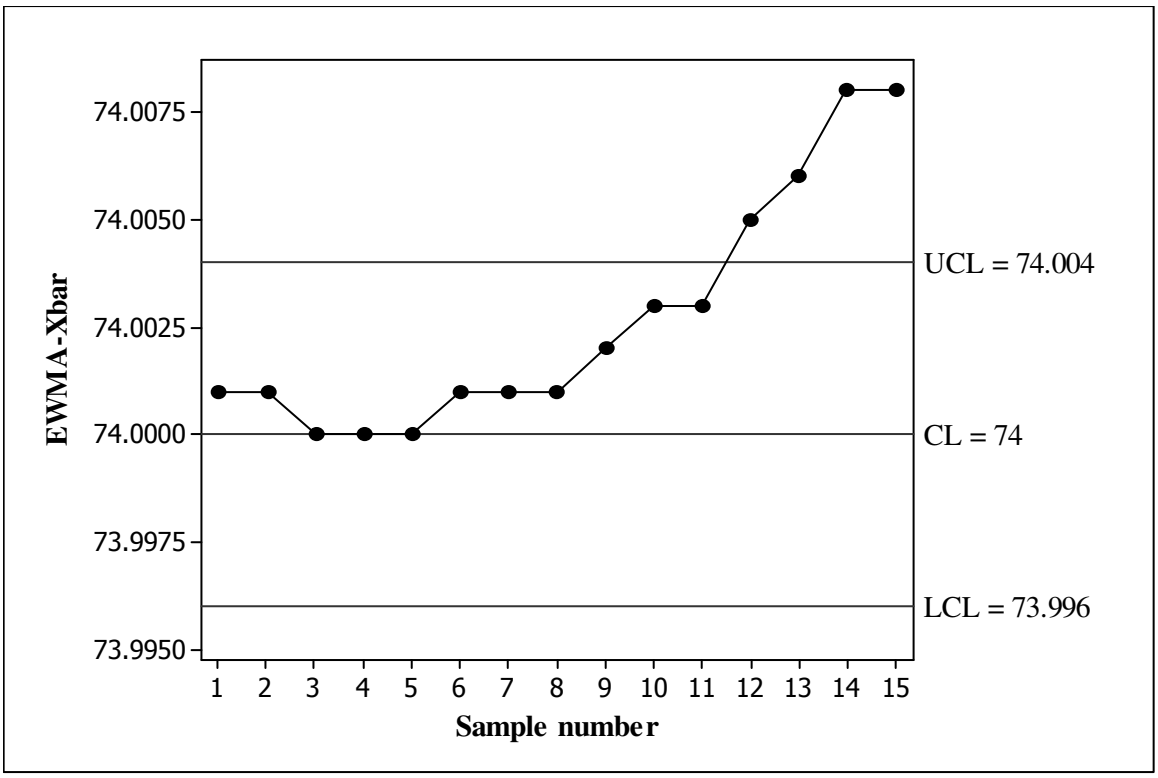

Figure 4.31. The EWMA-$\overline{X}$ chart for the Montgomery piston ring data

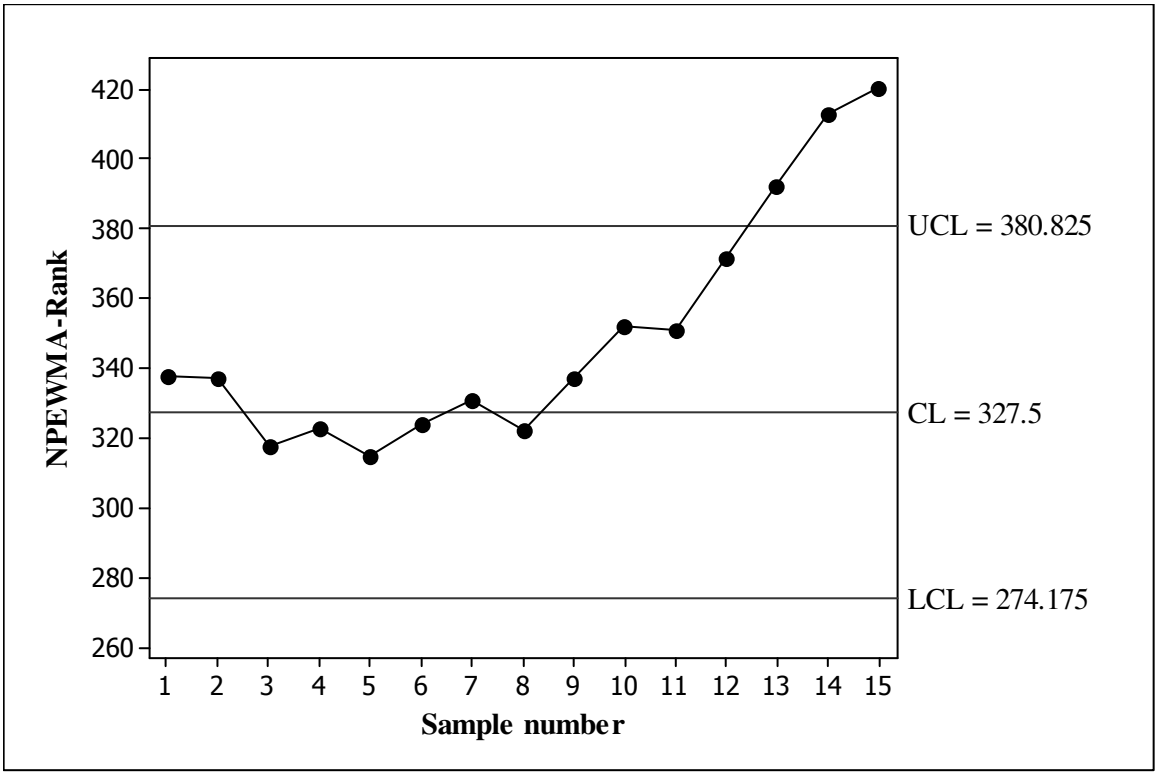

Figure 4.32. The NPEWMA-Rank chart for the Montgomery piston ring data

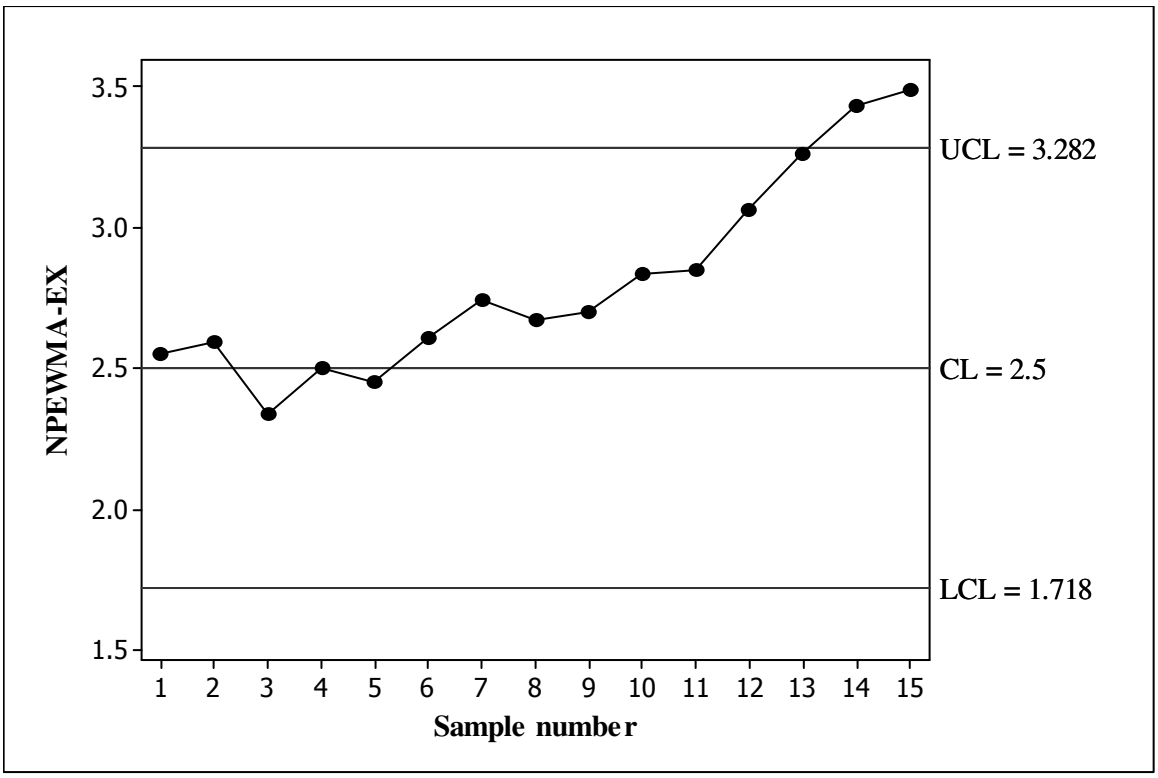

Figure 4.33. The NPEWMA-EX chart for the Montgomery piston ring data

From Figure 4.31 it can bee seen that the EWMA-$\overline{X}$ chart signals first at sample number 12, whereas the NPEWMA-Rank chart and the NPEWMA-EX chart signals later at sample number 13 (see Figure 4.32) and sample number 14 (see Figure 4.33), respectively. Thus, the the EWMA-$\overline{X}$ chart performs the best. This is not surprising, as normal theory methods usually outperform nonparametric methods when the normality assumption is satisfied. However, it should be noted that in practice normality can be in doubt or may not be justifiable for lack of information or data and a nonparametric method may be more desirable for the "just in case" scenario. The next example illustrates this type of a situation.

Example 4.5

In practice the underlying process distribution is often unknown or other than the normal and this is where the nonparametric charts can be really useful. To illustrate the application of the NPEWMA-EX chart when the data follow a symmetric yet heavier tailed distribution (than the normal) we use some simulated data from the Laplace (or double exponential) distribution; $DE(0,1)$ which is known to have a median of zero and a standard deviation equal to $\sqrt{2}$. An IC reference sample of size 100 (m = 100) was generated from this distribution and each data point was scaled so that the transformed observations have a standard deviation of 1. For the reference data we find

the median equal to -0.023. Next the Phase II samples, each of size 5 (n = 5), were independently and sequentially generated by transforming the observations from a $DE(0,1)$ distribution so that the resulting observations have a median of $\gamma/\sqrt{n}$ ($= 0.2236$ for γ = 0.5 and n = 5) and a standard deviation of 1. Consequently, the Phase II samples can be thought of as having been drawn from a process that is OOC in the median. For the NPEWMA-EX, EWMA-$\overline{X}$ and NPEWMA-Rank charts we set $\lambda = 0.05$ and L was found so that $ARL_0 \approx 500$ for each chart.

From Figures 4.35 and 4.36 we see that both the NPEWMA-Rank and the NPEWMA-EX charts signal at sample number 24, respectively. This is not surprising, as the performance of the NPEWMA-EX and NPEWMA-Rank charts are very similar for the Laplace distribution (see Table 4.25). Although both charts signal at sample number 24, it should be noted that the NPEWMA-EX chart signals at both sample numbers 24 and 25, whereas the NPEWMA-Rank only signals at sample number 24. From Figure 4.34 we see that although the EWMA-$\overline{X}$ chart has a steep incline, it doesn't signal. This example shows that there are situations in practice where the NPEWMA-EX chart offers an effective alternative over available parametric and nonparametric control charts.

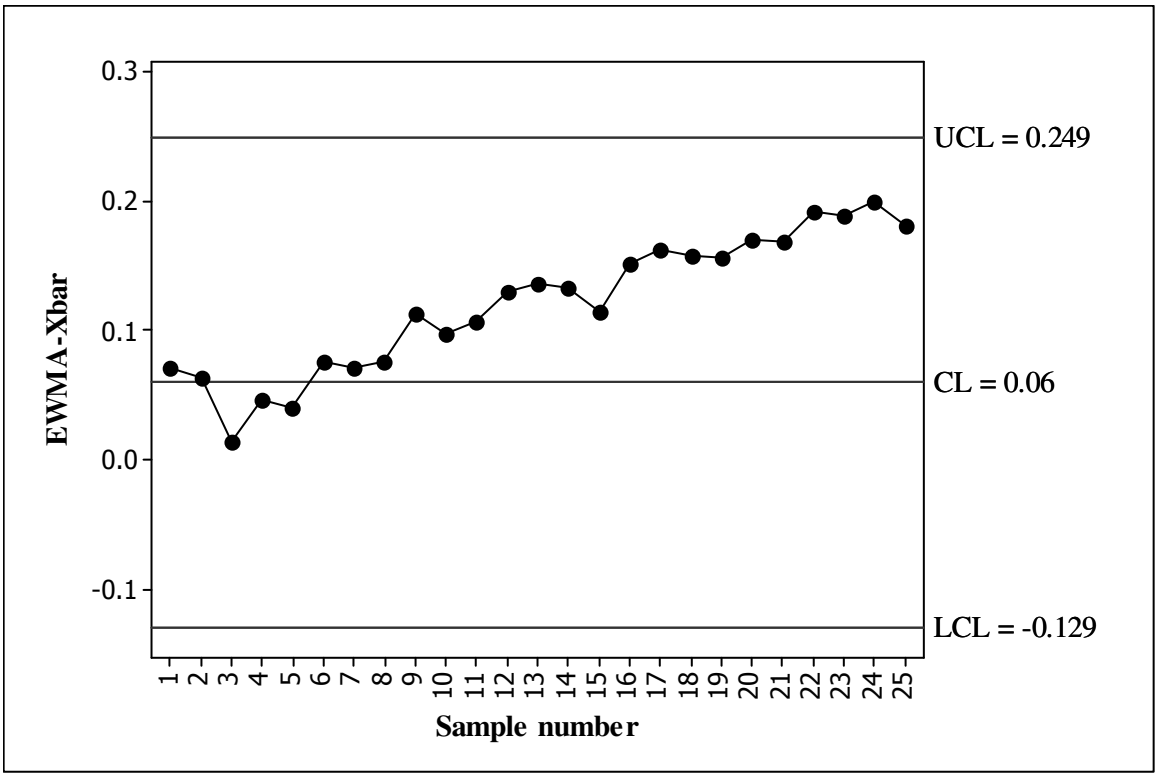

Figure 4.34. The EWMA-$\overline{X}$ chart for the simulated data

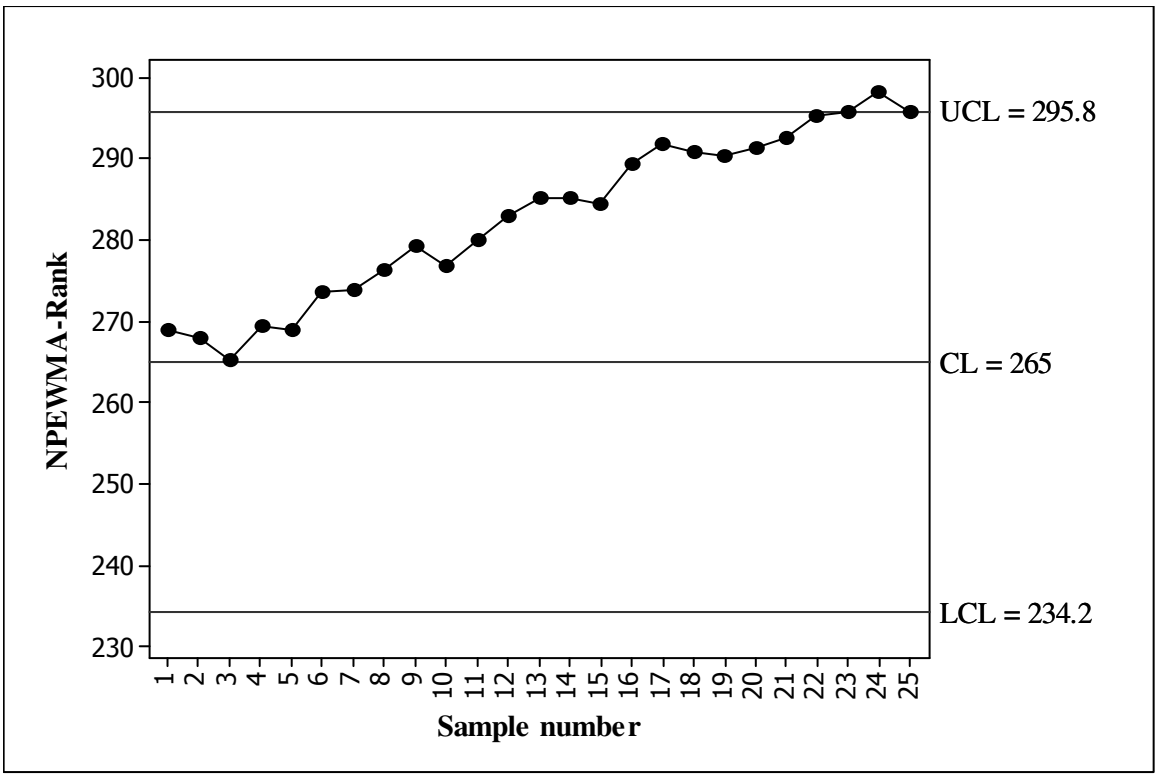

Figure 4.35. The NPEWMA-Rank chart for the simulated data

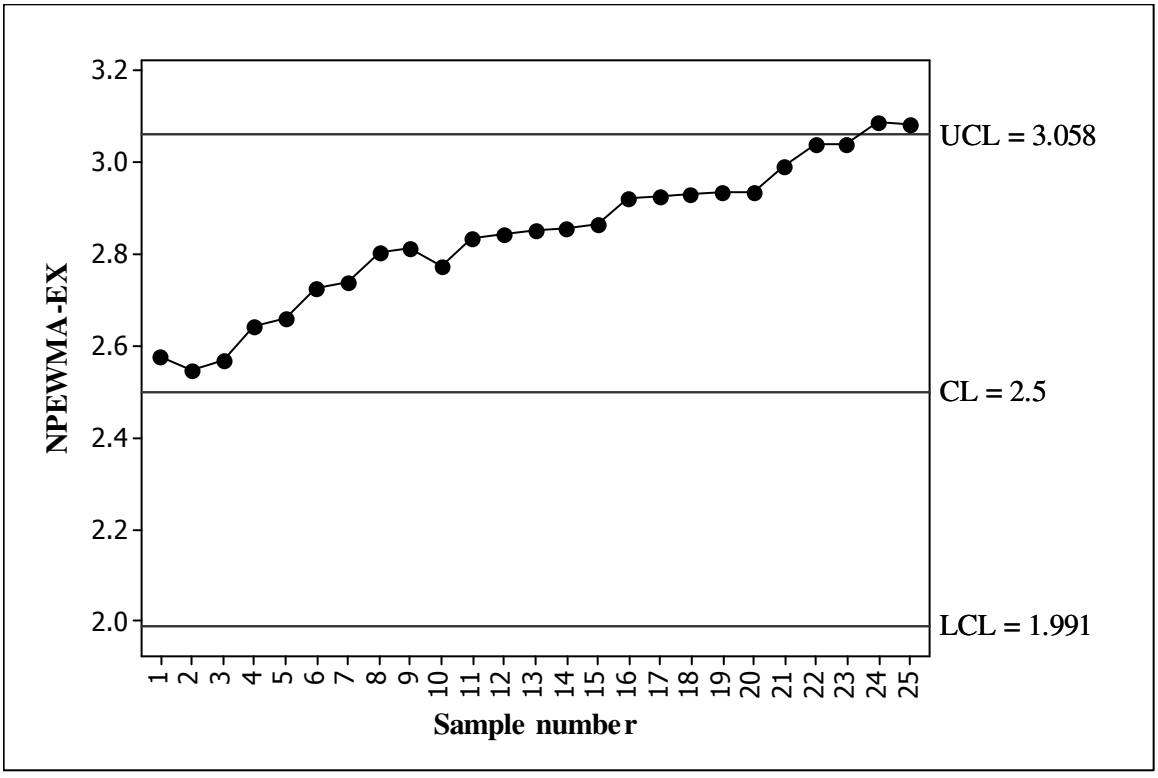

Figure 4.36. The NPEWMA-EX chart for the simulated data

4.4.5 Nonparametric EWMA control chart based on other percentiles

Up to this point the properties of the NPEWMA-EX chart using the median of the reference (Phase I) sample has been proposed and investigated. Here the choice of the order statistic from the reference (Phase I) sample that defines the exceedance statistic in this chart is investigated. Furthermore, observing certain shortcomings of the *ARL*, we use the *MRL* as the performance metric. In addition, we consider exact time-varying control limits as opposed to using steady-state control limits like in Sections 4.4.2 to 4.4.4 (for the NPEWMA-EX median chart). Steiner (1999) compared the run-length characteristics of the EWMA-$\overline{X}$ chart with exact time-varying control limits to the run-length characteristics of the EWMA-$\overline{X}$ chart with steady state control limits when the process parameters are known. Steiner (1999) used the *ARL* as performance measure and showed that, while the process is IC, the ARL_0 values of EWMA control charts with exact time-varying control limits are nearly identical to those of EWMA control charts with steady-state control limits. However, when the initial process level is OOC, i.e. if there are early process shifts, the ARL_δ values may differ substantially depending on the value of the smoothing constant λ. Steiner (1999) concluded that, in general, exact time-varying control limits are useful when λ is small, say, less than 0.3.

In-control robustness

Because the NPEWMA-EX chart is nonparametric, the IC run-length distribution and the associated characteristics remain the same for all continuous distributions. Table 4.31 shows some (λ, L)-combinations for the NPEWMA-EX chart for nominal $MRL_0 = 350$ for $m = 100$ and $n = 5$. The first row of each cell in the tables below shows the *MRL* followed by the corresponding interquartile range (*IQR*) in parentheses, whereas the second row shows the values of the 5th, 25th, 75th and 95th percentiles (in this order).

Table 4.31. (λ, L)-combinations for the NPEWMA-EX chart for nominal MRL_0= 350 for m = 100 and n = 5

	Shift	**(λ, L)**	**Attained values**
25th percentile	Small	(0.05, 2.041)	341 (1702) 3, 43, 1745, 8289
	Moderate	(0.10, 2.347)	344 (1054) 4, 80, 1134, 4139
	Large	(0.20, 2.608)	345 (961) 7, 92, 1053, 3451
40th percentile	Small	(0.05, 2.044)	342 (1710) 4, 44, 1754, 8294
	Moderate	(0.10, 2.380)	351 (1031) 5, 81, 1112, 3921
	Large	(0.20, 2.653)	356 (803) 15, 112, 915, 2540
50th percentile	Small	(0.05, 2.091)	345 (1933) 1, 30, 1963, 10496
	Moderate	(0.10, 2.384)	352 (1036) 7, 88, 1124, 3847
	Large	(0.20, 2.676)	353 (791) 17, 119, 910, 2581
60th percentile	Small	(0.05, 2.044)	342 (1627) 4, 42, 1669, 8305
	Moderate	(0.10, 2.380)	355 (1053) 5, 84, 1137, 4028
	Large	(0.20, 2.653)	345 (795) 13, 109, 904, 2581
75th percentile	Small	(0.05, 2.041)	363 (1739) 3, 46, 1785, 8910
	Moderate	(0.10, 2.347)	347 (1055) 4, 78, 1133, 3931
	Large	(0.20, 2.608)	349 (922) 9, 93, 1015, 3255

From Table 4.31 it is seen that the design parameter, L, is the same for the 25th and 75th percentiles and for the 40th and 60th percentiles, respectively. This is due to the fact that the $STDEV(U_{j,r})$ is the same for the pair of percentiles $(M - \Delta_1, M + \Delta_1)$ where M denotes the median and Δ_1 is an integer between 1 and 49. Next, we study the OOC chart performance.

Out-of-control chart performance comparison

For the OOC chart performance comparison it is customary to ensure that the MRL_0 values of the competing charts are fixed at (or very close to) an acceptably high value, such as 350 in this case, and then compare their MRL_δ values, for specific values of the shift δ, and the chart with the smaller MRL_δ value is preferred. In the previous seciton we studied the effect of the reference sample size when using the median of the reference (Phase I) sample and concluded that the larger the reference sample size, the less the uncertainty and the better the performance of the chart, and that, generally, when the reference sample size is not less than 100, the proposed chart performs well. Accordingly, in this paper, we take the size of the IC Phase I reference sample to be 100, i.e. $m = 100$. Tables 4.32 to 4.38 show the OOC performance characteristics of the run-length distrribution for $m = 100$, $n = 5$ and $\gamma = 0.25(0.25)1.00$, 1.50 and 2.00.

The first row of each cell in the tables below shows the *MRL* followed by the corresponding interquartile range (*IQR*) in parentheses, whereas the second row shows the values of the 5th, 25th, 75th and 95th percentiles (in this order). The same distributions are considered as with the NPEWMA-EX median chart; they are listed in Section 4.4.3.

Table 4.32. Performance comparison under the $N(0,1)$ distribution for $m = 100$ and $n = 5$

Shift (γ)	25th percentile	40th percentile	50th percentile	60th percentile	75th percentile
	$\lambda = 0.05$				
0.25	234 (1276) 3, 34, 1310, 8227	155 (983) 4, 23, 1006, 6054	139 (975) 1, 16, 991, 8595	129 (832) 3, 18, 850, 6247	118 (833) 2, 15, 848, 6616
0.50	60 (312) 3, 15, 327, 3759	37 (167) 3, 10, 177, 2619	31 (150) 1, 8, 158, 2532	28 (127) 2, 8, 135, 2160	27 (140) 2, 7, 147, 2547
0.75	22 (57) 3, 9, 66, 635	15 (33) 3, 7, 40, 291	12 (30) 1, 4, 34, 225	11 (28) 1, 4, 32, 241	10 (25) 1, 4, 29, 262
1.00	13 (23) 3, 6, 29, 112	9 (14) 2, 4, 18, 63	7 (13) 1, 3, 16, 55	7 (10) 1, 4, 14, 49	6 (11) 1, 3, 14, 56
1.50	7 (9) 3, 3, 12, 25	4 (4) 2, 3, 7, 16	3 (5) 1, 2, 7, 14	4 (4) 1, 2, 6, 13	3 (4) 1, 2, 6, 13
2.00	5 (5) 3, 3, 8, 13	4 (3) 2, 2, 5, 9	2 (3) 1, 1, 4, 8	2 (2) 1, 2, 4, 7	2 (2) 1, 1, 3, 7
Shift (γ)	**$\lambda = 0.10$**				
0.25	312 (1007) 9, 78, 1085, 4070	229 (807) 5, 53, 860, 3295	188 (690) 5, 43, 733, 3172	150 (628) 2, 33, 661, 3011	137 (594) 2, 26, 620, 3204
0.50	121 (454) 8, 35, 489, 2540	64 (229) 3, 19, 248, 1728	52 (185) 3, 16, 201, 1548	41 (143) 2, 12, 155, 1346	35 (123) 1, 9, 132, 1255
0.75	42 (109) 6, 17, 126, 826	24 (54) 2, 10, 64, 384	19 (43) 3, 8, 51, 298	16 (37) 2, 6, 43, 256	13 (33) 1, 5, 38, 267
1.00	22 (37) 6, 11, 48, 203	13 (20) 2, 6, 26, 94	11 (17) 2, 5, 22, 76	9 (15) 1, 4, 19, 65	7 (14) 1, 3, 17, 70
1.50	11 (10) 5, 7, 17, 38	6 (8) 2, 3, 11, 22	5 (6) 2, 3, 9, 18	4 (5) 1, 2, 7, 16	3 (4) 1, 2, 6, 15
2.00	7 (4) 5, 6, 10, 18	4 (4) 2, 2, 6, 11	3 (3) 2, 2, 5, 9	2 (2) 1, 2, 4, 8	2 (3) 1, 1, 4, 7
Shift (γ)	**$\lambda = 0.20$**				
0.25	500 (1193) 20, 158, 1351, 3920	272 (683) 13, 85, 768, 2388	230 (618) 11, 68, 686, 2344	169 (481) 6, 49, 530, 2091	115 (384) 3, 31, 415, 2081
0.50	337 (901) 18, 102, 1003, 3357	111 (323) 8, 35, 358, 1590	77 (226) 6, 26, 252, 1218	54 (152) 3, 18, 170, 957	38 (107) 2, 12, 119, 755
0.75	130 (360) 12, 44, 404, 1912	40 (91) 6, 17, 108, 554	30 (64) 4,12, 76, 370	22 (49) 2, 9, 58, 266	16 (37) 1, 6, 43, 194
1.00	54 (117) 9, 24, 141, 702	21 (36) 4, 10, 46, 170	16 (25) 3, 8, 33, 115	12 (19) 1, 6, 25, 84	9 (17) 1, 4, 21, 68
1.50	19 (25) 6, 11, 36, 102	9 (9) 3, 6, 15, 35	7 (8) 2, 4, 12, 26	5 (6) 1, 3, 9, 20	4 (6) 1, 2, 8, 19
2.00	11 (9) 6, 8, 17, 33	6 (4) 3, 4, 8, 15	4 (4) 2, 3, 7, 12	3 (3) 1, 2, 5, 10	3 (3) 1, 1, 4, 8

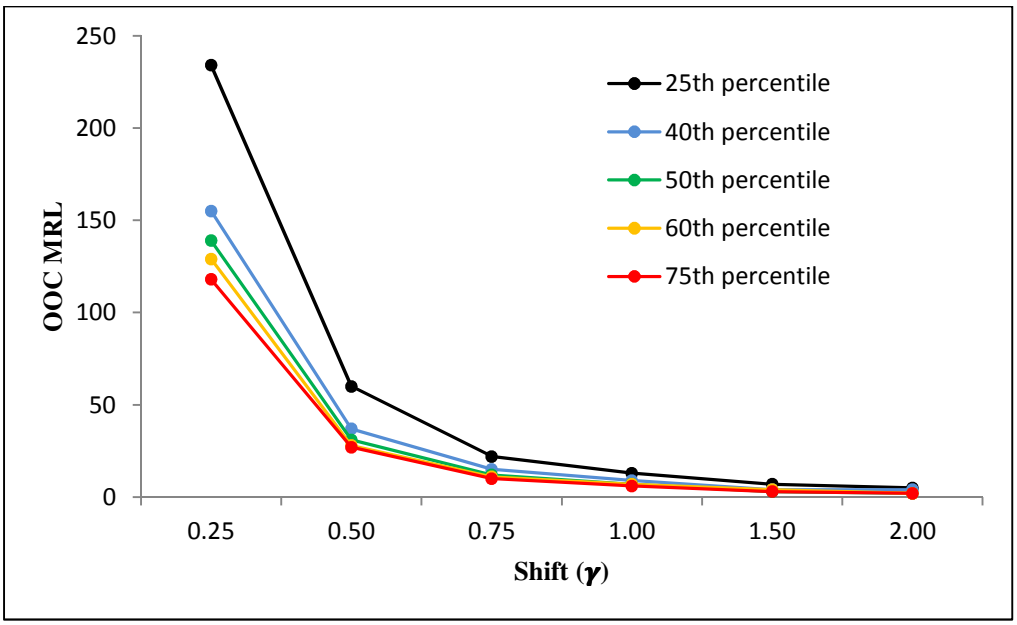

Figure 4.37a. *MRL* performance comparison of the NPEWMA-EX chart based on various percentiles of the reference sample under the $N(0,1)$ distribution with $m = 100$, $n = 5$ and $\lambda = 0.05$

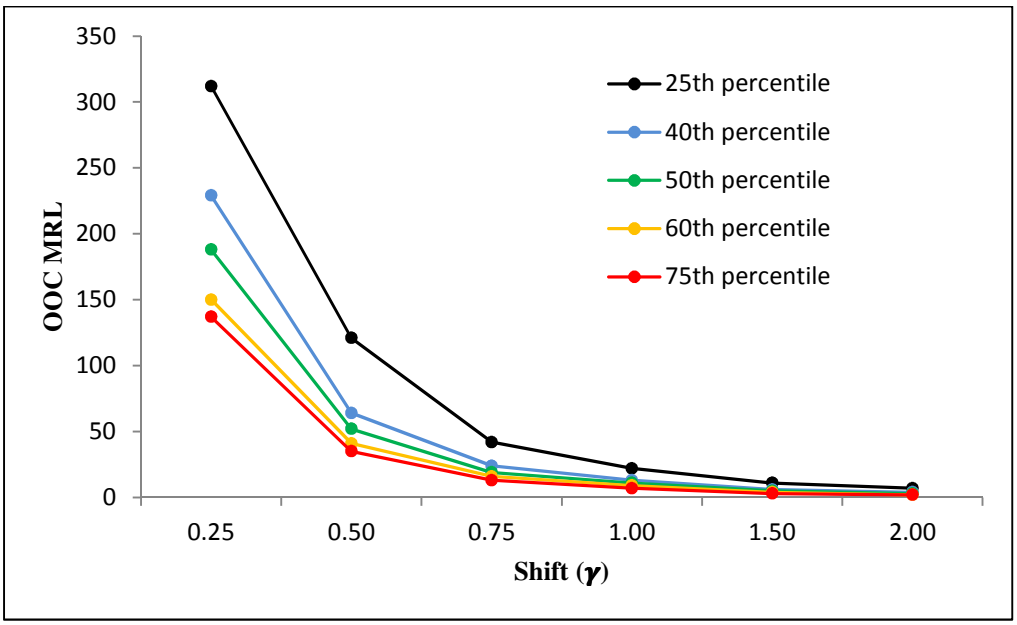

Figure 4.37b. *MRL* performance comparison of the NPEWMA-EX chart based on various percentiles of the reference sample under the $N(0,1)$ distribution with $m = 100$, $n = 5$ and $\lambda = 0.10$

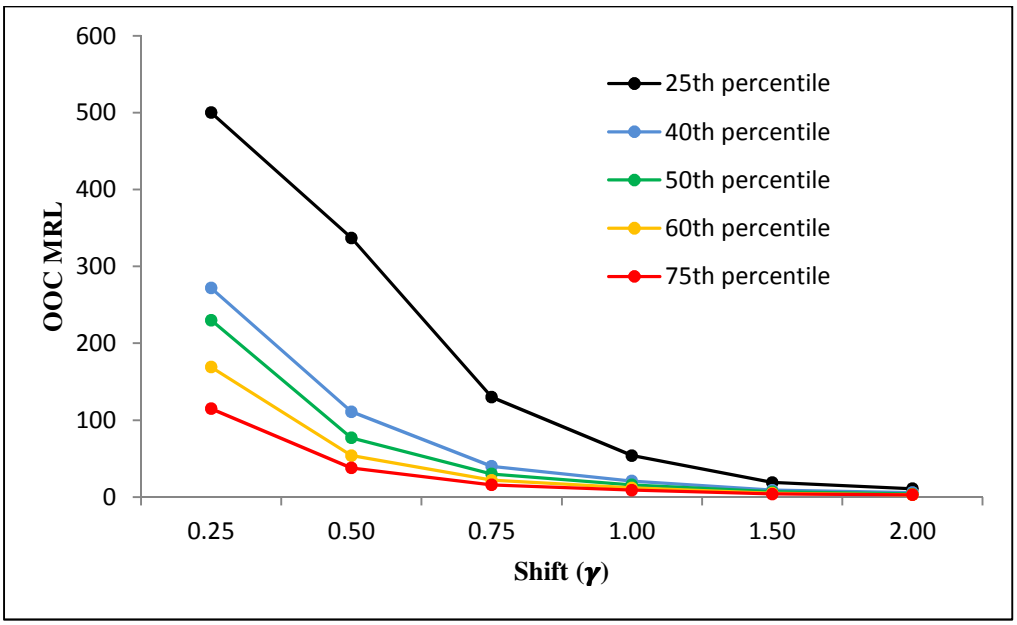

Figure 4.37c. *MRL* performance comparison of the NPEWMA-EX chart based on various percentiles of the reference sample under the $N(0,1)$ distribution with $m = 100$, $n = 5$ and $\lambda = 0.20$

From Table 4.32 it can be seen that when the underlying process distribution is $N(0,1)$, the NPEWMA-EX chart based on the 75^{th} percentile performs the best regardless of the size of the shift and choice of the smoothing constant λ. This is illustrated in Figures 4.37a,b,c for $\lambda = 0.05$, 0.10 and 0.20, respectively.

Table 4.33. Performance comparison under the $EXP(1)$ distribution for $m = 100$ and $n = 5$ when target $MRL_0 = 350$

Shift (γ)	25th percentile	40th percentile	50th percentile	60th percentile	75th percentile
			$\lambda = 0.05$		
0.25	23 (96) 3, 8, 104, 2391	49 (322) 3, 11, 333, 4271	68 (534) 1, 11, 545, 6466	98 (686) 2, 15, 701, 5805	134 (985) 2, 18, 1003, 6998
0.50	5 (5) 3, 3, 8, 32	9 (19) 2, 4, 23, 233	12 (40) 1, 5, 45, 904	20 (90) 2, 6, 96, 1892	40 (288) 2, 8, 296, 4190
0.75	3 (0) 3, 3, 3, 5	4 (4) 2, 3, 7, 23	5 (10) 1, 2, 12, 61	7 (15) 1, 4, 19, 160	14 (52) 1, 5, 57, 1262
1.00	3 (0) 3, 3, 3, 3	2 (2) 2, 2, 4, 7	3 (4) 1, 1, 5, 15	4 (7) 1, 2, 9, 32	7 (17) 1, 3, 20, 206
1.50	3 (0) 3, 3, 3, 3	2 (0) 2, 2, 2, 2	1 (0) 1, 1, 1, 3	2 (2) 1, 1, 3, 7	3 (4) 1, 2,6, 21
2.00	3 (0) 3, 3, 3, 3	2 (0) 2, 2, 2, 2	1 (0) 1, 1, 1, 2	1 (0) 1, 1, 1, 1	2 (2) 1, 1, 1, 2
Shift (γ)			$\lambda = 0.10$		
0.25	43 (170) 6, 15, 185, 1546	85 (370) 3, 21, 391, 2315	114 (491) 4, 26, 518, 2704	134 (576) 3, 27, 603, 2941	156 (658) 2, 30, 688, 3193
0.50	7 (8) 5, 5, 13, 53	14 (31) 2, 6, 37, 297	21 (60) 2, 8, 68, 718	29 (111) 2, 9, 120, 1206	48 (232) 2, 11, 243, 1974
0.75	5 (0) 5, 5, 5, 7	5 (7) 2, 3, 10, 32	8 (13) 2, 4, 17, 85	10 (23) 1, 4, 27, 213	18 (62) 1, 5, 67, 763
1.00	5 (0) 5, 5, 5, 5	2 (2) 2, 2, 4, 9	4 (5) 2, 2, 7, 20	5 (9) 1, 2, 11, 42	9 (24) 1, 3, 27, 200
1.50	5 (0) 5, 5, 5, 5	2 (0) 2, 2, 2, 4	2 (0) 2, 2, 2, 2	2 (2) 1, 1, 3, 8	3 (5) 1, 2, 7, 26
2.00	5 (0) 5, 5, 5, 5	2 (0) 2, 2, 2, 2	2 (0) 2, 2, 2, 2	1 (0) 1, 1, 1, 3	2 (2) 1, 1, 3, 8
Shift (γ)			$\lambda = 0.20$		
0.25	135 (489) 10, 37, 526, 2668	141 (450) 8, 40, 490, 1911	155 (474) 8, 44, 518, 1994	148 (456) 5, 40, 496, 1975	145 (501) 4, 36, 537, 2398
0.50	10 (17) 6, 6, 23, 156	23 (55) 4, 10, 65, 442	32 (97) 4, 12, 109, 718	40 (126) 3, 13, 139, 869	52 (183) 2, 15, 198, 1345
0.75	6 (0) 6, 6, 6, 11	7 (10) 3, 4, 14, 58	11 (19) 3, 5, 24, 128	15 (31) 1, 6, 37, 218	22 (67) 1, 8, 75, 531
1.00	6 (0) 6, 6, 6, 6	3 (2) 3, 3, 5, 13	5 (6) 2, 3, 9, 29	7 (11) 1, 4, 15, 59	11 (27) 1, 4, 31, 172
1.50	6 (0) 6, 6, 6, 6	3 (0) 3, 3, 3, 3	2 (1) 2, 2, 3, 5	3 (3) 1, 1, 4, 10	4 (7) 1, 2, 9, 30
2.00	6 (0) 6, 6, 6, 6	3 (0) 3, 3, 3, 3	2 (0) 2, 2, 2, 2	1 (0) 1, 1, 1, 3	2 (3) 1, 1, 4, 9

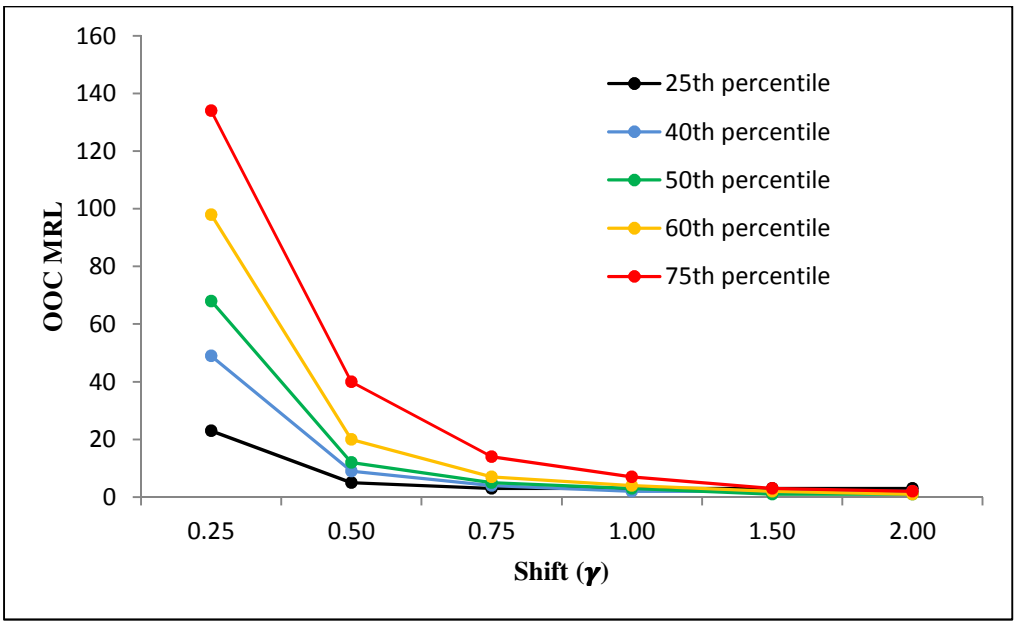

Figure 4.38a. *MRL* performance comparison of the NPEWMA-EX chart based on various percentiles of the reference sample under the *EXP*(1) distribution with $m = 100$, $n = 5$ and $\lambda = 0.05$

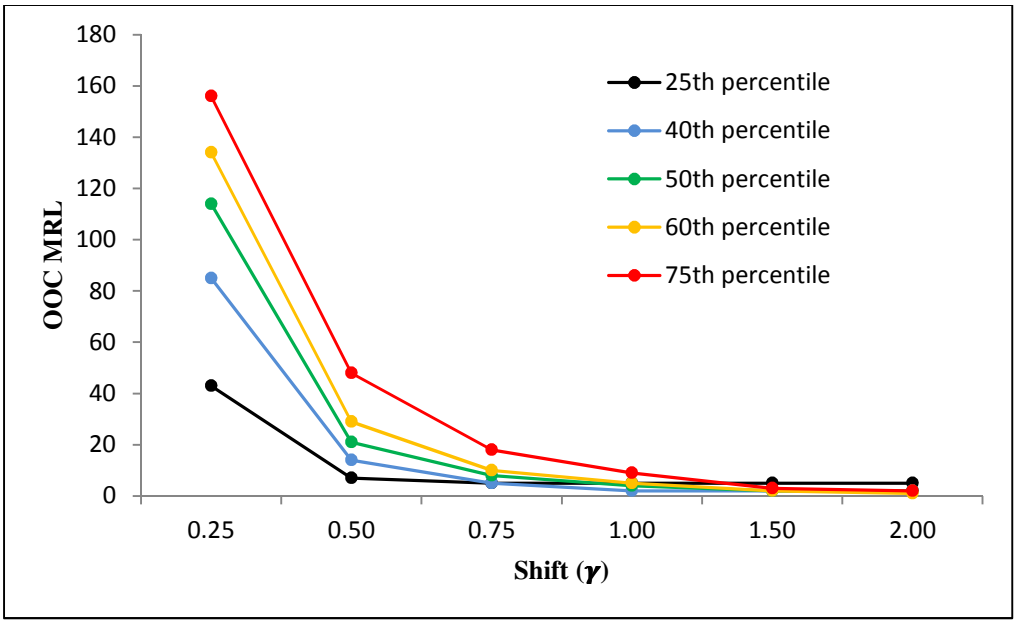

Figure 4.38b. *MRL* performance comparison of the NPEWMA-EX chart based on various percentiles of the reference sample under the *EXP*(1) distribution with $m = 100$, $n = 5$ and $\lambda = 0.10$

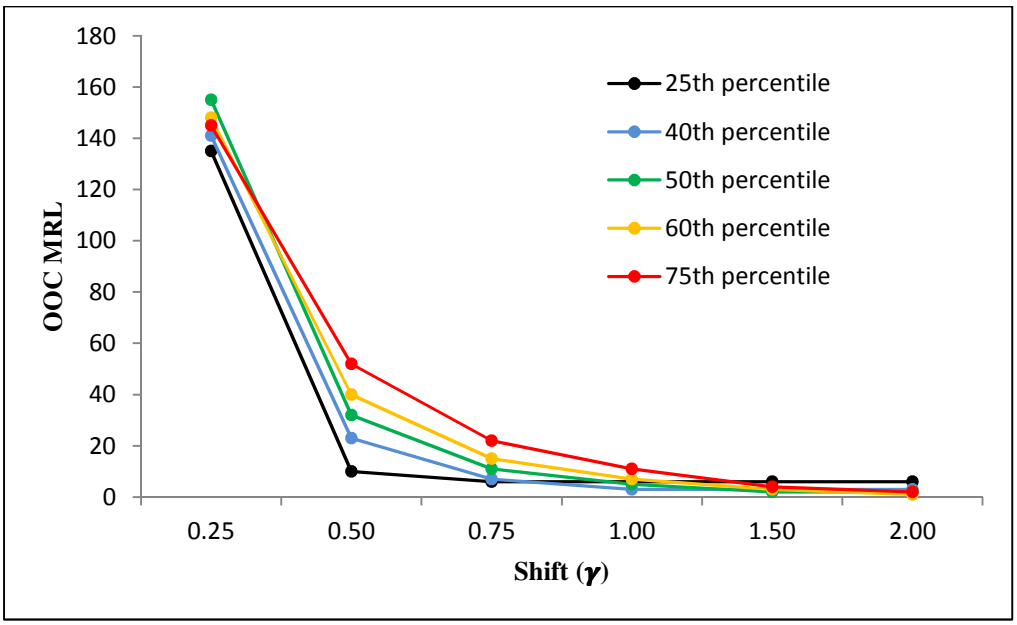

Figure 4.38c. *MRL* performance comparison of the NPEWMA-EX chart based on various percentiles of the reference sample under the *EXP*(1) distribution with $m = 100$, $n = 5$ and $\lambda = 0.20$

From Table 4.33 it can be seen that when the underlying process distribution is *EXP*(1), the choice of the order statistic from the reference sample stays the same regardless of the value of the smoothing constant λ. Thus, for all λ, the NPEWMA-EX chart based on the 25th percentile performs best for $\gamma = 0.25$, 0.50 and 0.75, the NPEWMA-EX chart based on the 40th percentile performs best for $\gamma = 1.00$ and the NPEWMA-EX chart based on the median performs best for $\gamma = 1.50$. For the largest shift under consideration, i.e. $\gamma = 2.00$, the NPEWMA-EX chart based on the 60th percentile performs best. Since the run-length characteristics seem to converge as the size of this shift increases, the recommendation would be to use the NPEWMA-EX chart based on the 60th percentile when large shifts are of concern. This is illustrated in Figures 4.38a,b,c for $\lambda = 0.05$, 0.10 and 0.20, respectively.

Table 4.34. Performance comparison under the $DE(0,1)$ distribution for $m = 100$ and $n = 5$ when target $MRL_0 = 350$

Shift (γ)	25th percentile	40th percentile	50th percentile	60th percentile	75th percentile
	$\lambda = 0.05$				
0.25	233 (1351) 3, 36, 1387, 8103	96 (549) 4, 18, 567, 5159	53 (281) 1, 10, 291, 4045	46 (311) 2, 10, 321, 4316	85 (643) 2, 12, 655, 5990
0.50	54 (225) 3, 15, 240, 2679	20 (45) 3, 8, 53, 334	11 (25) 1, 4, 29, 151	10 (22) 2, 4, 26, 281	16 (69) 1, 5, 74, 1770
0.75	23 (53) 3, 9, 62, 364	9 (14) 2, 5, 19, 54	6 (9) 1, 3, 12, 30	5 (7) 1, 3, 10, 26	7 (14) 1, 3, 17, 133
1.00	13 (21) 3, 7, 28, 88	6 (7) 2, 4, 11, 25	4 (5) 1, 2, 7, 15	3 (5) 1, 2, 7, 27	4 (4) 1, 2, 6, 12
1.50	8 (8) 3, 5, 13, 25	4 (3) 2, 3, 6, 11	3 (3) 1, 1, 4, 7	2 (2) 1, 1, 3, 6	2 (2) 1, 1, 3, 7
2.00	5 (5) 3, 3, 8, 15	3 (2) 2, 2, 4, 7	2 (2) 1, 1, 3, 5	2 (1) 1, 1, 2, 4	1 (1) 1, 1, 2, 3
Shift (γ)	**$\lambda = 0.10$**				
0.25	332 (1028) 9, 84, 1112, 3898	148 (513) 4, 37, 550, 2735	83 (280) 4, 24, 304, 1830	67 (308) 2, 16, 324, 2164	96 (467) 2, 19, 486, 2900
0.50	111 (377) 8, 35, 412, 2329	34 (77) 3, 13, 90, 461	19 (35) 3, 8, 43, 187	14 (31) 1, 5, 36, 265	22 (78) 1, 6, 84, 885
0.75	44 (92) 6, 18, 110, 542	15 (22) 2, 7, 29, 81	9 (13) 2, 4, 17, 41	6 (9) 1, 3, 12, 37	8 (18) 1, 3, 21, 146
1.00	23 (35) 6, 12, 47, 152	9 (11) 2, 5, 16, 34	6 (7) 2, 3, 10, 20	4 (5) 1, 2, 7, 15	4 (7) 1, 2, 9, 33
1.50	12 (11) 5, 8, 19, 38	5 (5) 2, 3, 8, 14	4 (3) 2, 2, 5, 9	2 (3) 1, 1, 4, 7	2 (2) 1, 1, 3, 7
2.00	8 (6) 5, 6, 12, 21	3 (4) 2, 2, 6, 9	3 (2) 2, 2, 4, 6	2 (1) 1, 1, 2, 4	1 (1) 1, 1, 2, 4
Shift (γ)	**$\lambda = 0.20$**				
0.25	564 (1269) 23, 181, 1450, 4153	219 (597) 12, 67, 644, 2030	124 (332) 8, 40, 372, 1570	87 (294) 4, 25, 319, 1518	92 (330) 3, 24, 354, 1944
0.50	346 (894) 18, 108, 1002, 3288	60 (129) 6, 23, 152, 588	29 (55) 4, 13, 68, 282	19 (41) 1, 8, 49, 297	26 (79) 1, 9, 88, 599
0.75	127 (303) 12, 46, 349, 124	24 (38) 5, 12, 50, 143	13 (18) 3, 7, 25, 63	9 (13) 1, 4, 17, 53	10 (21) 1, 4, 25, 147
1.00	61 (116) 10, 26, 142, 506	13 (16) 4, 8, 24, 55	8 (8) 3, 5, 13, 27	5 (6) 1, 3, 9, 21	5 (8) 1, 2, 10, 38
1.50	22 (28) 6, 13, 41, 98	7 (6) 3, 5, 11, 21	5 (4) 2, 3, 7, 12	3 (4) 1, 1, 5, 8	2 (3) 1, 1, 4, 8
2.00	14 (12) 6, 9, 21, 41	5 (3) 3, 4, 7, 12	4 (2) 2, 3, 5, 8	2 (2) 1, 1, 3, 5	1 (1) 1, 1, 2, 4

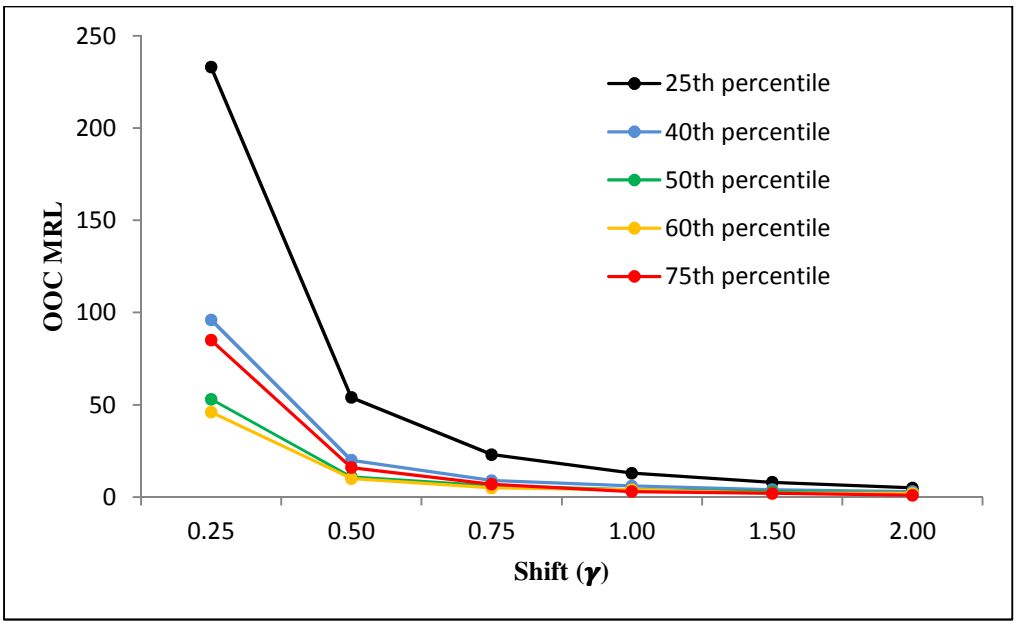

Figure 4.39a. *MRL* performance comparison of the NPEWMA-EX chart based on various percentiles of the reference sample under the *DE*(0,1) distribution with $m = 100$, $n = 5$ and $\lambda = 0.05$

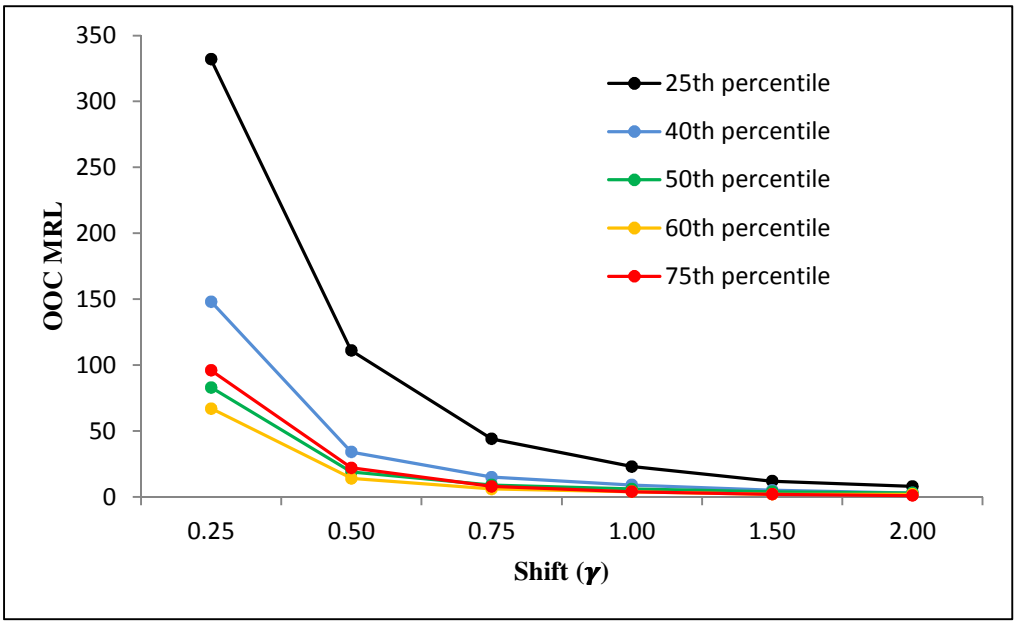

Figure 4.39b. *MRL* performance comparison of the NPEWMA-EX chart based on various percentiles of the reference sample under the *DE*(0,1) distribution with $m = 100$, $n = 5$ and $\lambda = 0.10$

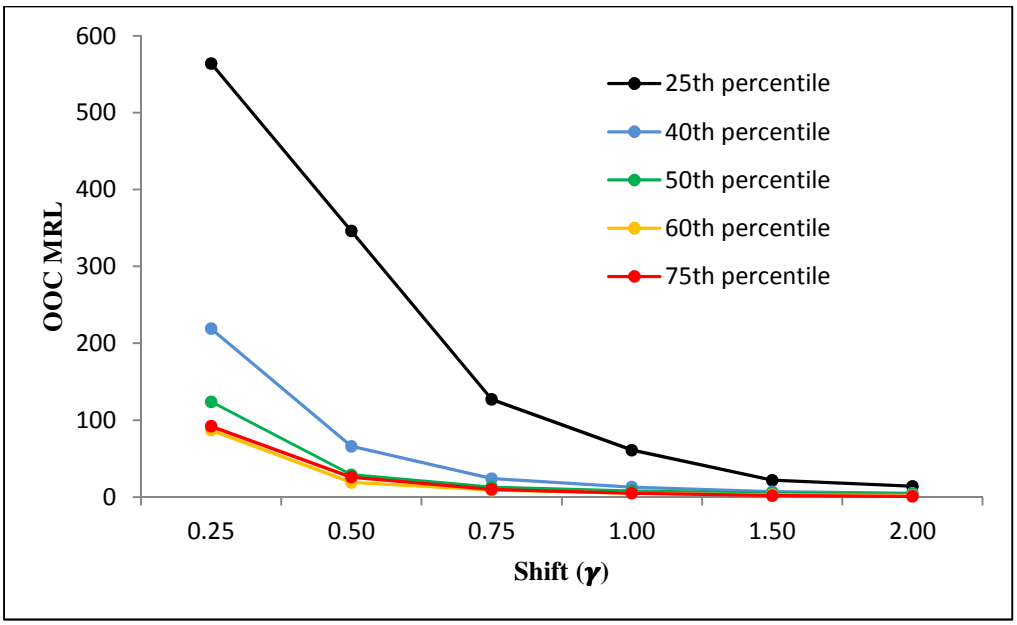

Figure 4.39c. *MRL* performance comparison of the NPEWMA-EX chart based on various percentiles of the reference sample under the *DE*(0,1) distribution with $m = 100$, $n = 5$ and $\lambda = 0.20$

From Table 4.34 it can be seen that when the underlying process distribution is *DE*(0,1), the choice of the order statistic from the reference sample stays the same regardless of the value of the smoothing constant λ. Thus, for all λ, the NPEWMA-EX chart based on the 60th percentile performs best for $\gamma \leq 1.00$, whereas the NPEWMA-EX chart based on the 75th percentile performs best when large shifts ($\gamma = 1.50$ and 2.00) are under consideration. Moreover, for the largest shift under consideration, i.e. $\gamma = 2.00$, the NPEWMA-EX chart based on the 75th percentile performs best. Since the run-length characteristics seem to converge as the size of this shift increases, the recommendation would be to use the NPEWMA-EX chart based on the 75th percentile when large shifts are of concern. This is illustrated in Figures 4.39a,b,c for $\lambda = 0.05$, 0.10 and 0.20, respectively, where it can also clearly be seen that the NPEWMA-EX chart based on the 25th percentile is performing the worst.

Table 4.35. Performance comparison under the *SymmMixN* distribution for $m = 100$ and $n = 5$ when target $MRL_0 = 350$

Shift (γ)	25th percentile	40th percentile	50th percentile	60th percentile	75th percentile
			$\lambda = 0.05$		
0.25	116 (226) 7, 40, 266, 778	8 (9) 2, 4, 13, 26	5 (5) 1, 2, 7, 15	4 (3) 1, 2, 5, 12	4 (6) 1, 2, 8, 47
0.50	46 (77) 5, 19, 96, 216	5 (3) 2, 4, 7, 12	3 (3) 1, 1, 4, 6	2 (2) 1, 1, 3, 4	1 (1) 1, 1, 2, 3
0.75	29 (43) 3, 14, 57, 122	4 (3) 2, 4, 7, 11	3 (2) 1, 1, 3, 6	2 (1) 1, 1, 2, 4	1 (0) 1, 1, 1, 2
1.00	21 (29) 3, 10, 39, 78	4 (3) 2, 3, 6, 10	2 (2) 1, 1, 3, 5	2 (1) 1, 1, 2, 3	1 (0) 1, 1, 1, 2
1.50	13 (15) 3, 7, 22, 42	4 (2) 2, 3, 5, 8	2 (2) 1, 1, 3, 5	2 (1) 1, 1, 2, 3	1 (0) 1, 1, 1, 2
2.00	9 (9) 3, 5, 14, 26	4 (2) 2, 2, 4, 7	2 (2) 1, 1, 3, 4	2 (1) 1, 1, 2, 3	1 (0) 1, 1, 1, 2
Shift (γ)			$\lambda = 0.10$		
0.25	254 (465) 19, 102, 567, 1466	12 (12) 2, 7, 19, 39	6 (6) 2, 4, 10, 20	4 (5) 1, 2, 7, 15	4 (8) 1, 2, 10, 78
0.50	102 (153) 12, 45, 198, 444	7 (6) 2, 4, 10, 17	4 (2) 2, 3, 5, 8	2 (2) 1, 1, 3, 5	1 (1) 1, 1, 2, 4
0.75	61 (88) 9, 29, 117, 242	6 (5) 2, 4, 9, 15	3 (2) 2, 2, 4, 7	2 (1) 1, 1, 2, 4	1 (0) 1, 1, 1, 2
1.00	39 (52) 8, 20, 72, 148	6 (5) 2, 3, 8, 13	3 (2) 2, 2, 4, 6	2 (1) 1, 1, 2, 3	1 (0) 1, 1, 1, 2
1.50	21 (24) 6, 12, 36, 69	4 (4) 2, 3, 7, 10	3 (2) 2, 2, 4, 6	2 (1) 1, 1, 2, 3	1 (0) 1, 1, 1, 2
2.00	14 (13) 5, 9, 22, 41	4 (3) 2, 2, 5, 8	3 (1) 2, 2, 3, 5	2 (1) 1, 1, 2, 3	1 (0) 1, 1, 1, 2
Shift (γ)			$\lambda = 0.20$		
0.25	1297 (2252) 95, 522, 2774, 7188	18 (23) 5, 10, 33, 95	9 (9) 3, 5, 14, 29	5 (6) 1, 3, 9, 19	5 (9) 1, 3, 12, 69
0.50	489 (792) 40, 200, 992, 2227	10 (8) 4, 7, 15, 28	5 (4) 2, 3, 7, 10	3 (3) 1, 1, 4, 6	1 (2) 1, 1, 3, 5
0.75	254 (396) 26, 109, 505, 1136	9 (7) 4, 6, 13, 22	4 (3) 2, 3, 6, 9	3 (2) 1, 1, 3, 5	1 (0) 1, 1, 1, 3
1.00	144 (219) 18, 64, 283, 626	8 (6) 3, 5, 11, 19	4 (2) 2, 3, 5, 8	2 (2) 1, 1, 3, 4	1 (0) 1, 1, 1, 2
1.50	58 (80) 11, 29, 109, 237	6 (4) 3, 5, 9, 14	4 (2) 2, 3, 5, 7	2 (2) 1, 1, 3, 4	1 (0) 1, 1, 1, 2
2.00	30 (37) 8, 17, 54, 111	5 (3) 3, 4, 7, 11	3 (2) 2, 2, 4, 6	2 (2) 1, 1, 3, 4	1 (0) 1, 1, 1, 2

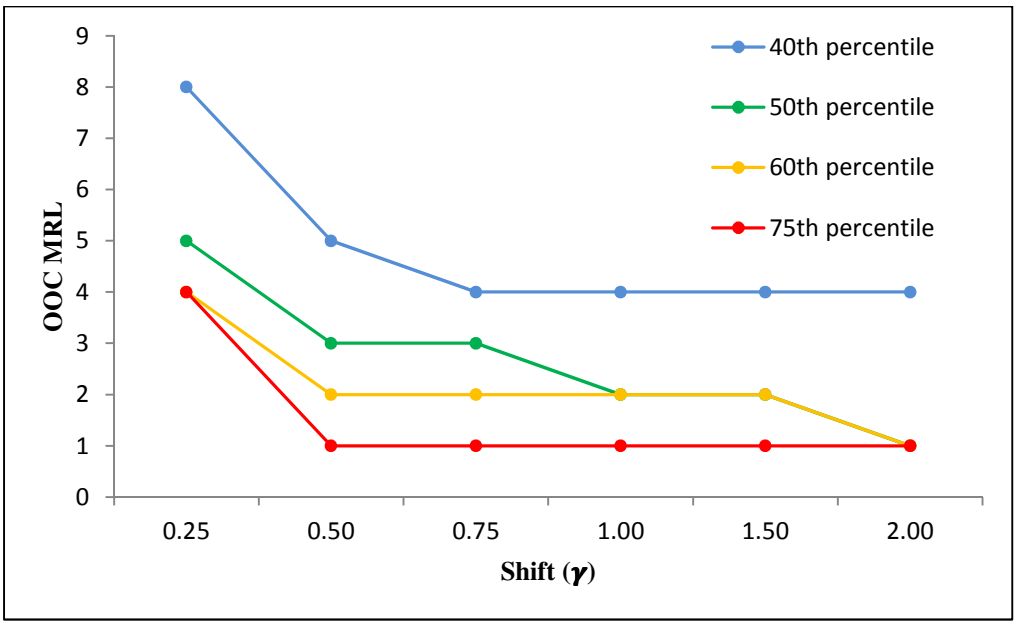

Figure 4.40a. *MRL* performance comparison of the NPEWMA-EX chart based on various percentiles[xxxv] of the reference sample under the *SymmMixN* distribution with $m = 100$, $n = 5$ and $\lambda = 0.05$

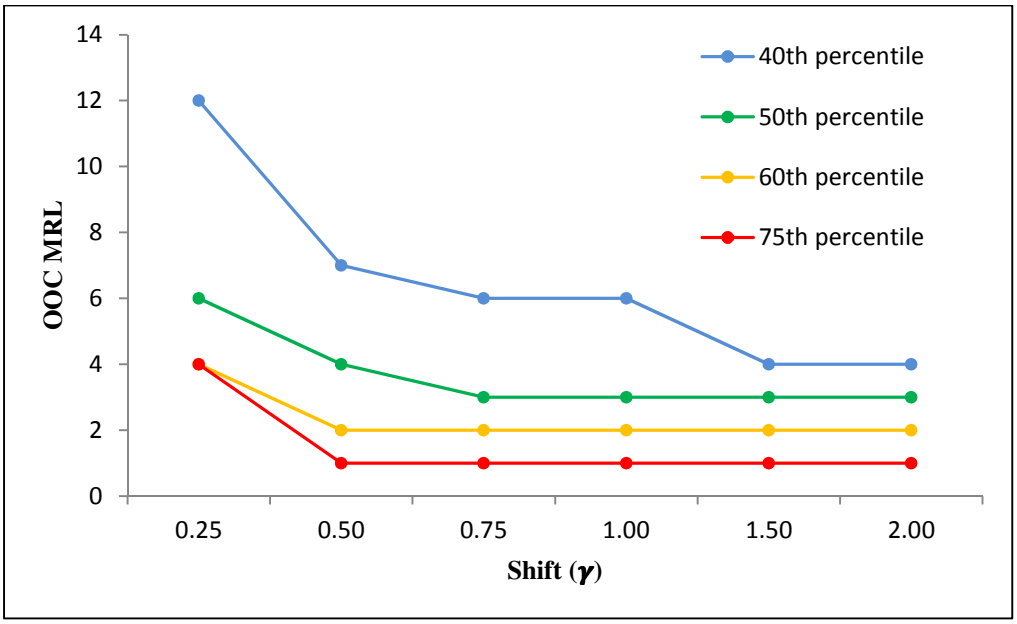

Figure 4.40b. *MRL* performance comparison of the NPEWMA-EX chart based on various percentiles[xxxv] of the reference sample under the *SymmMixN* distribution with $m = 100$, $n = 5$ and $\lambda = 0.10$

[xxxv] Note that the line graph of the 25th percentile is omitted, since it is performing the worst, i.e. it has large OOC *MRL* values. Deleting the 25th percentile makes the graph more visually appealing.

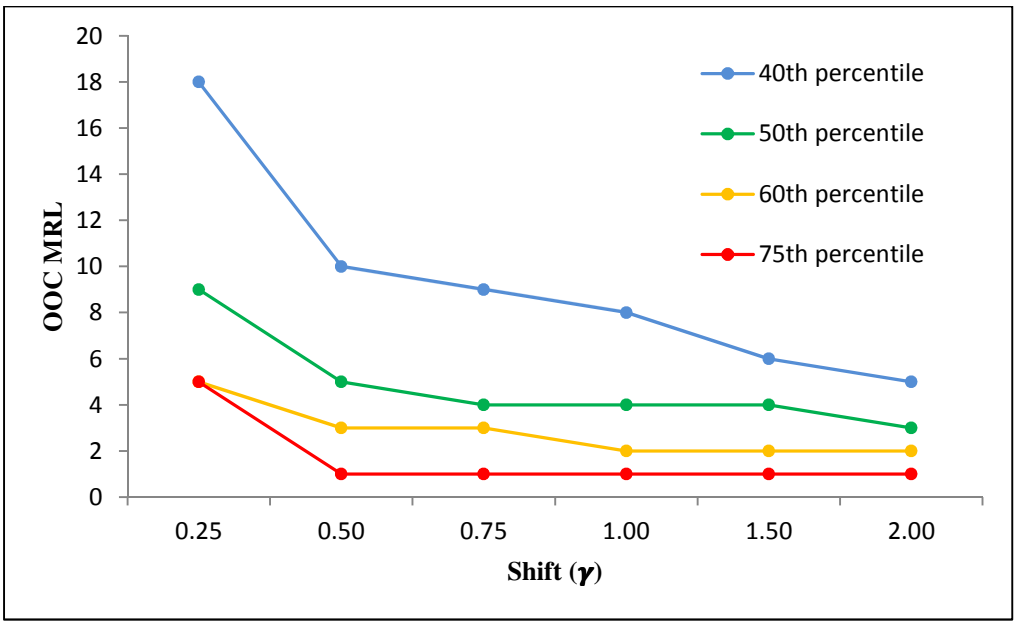

Figure 4.40c. *MRL* performance comparison of the NPEWMA-EX chart based on various percentiles[xxxvi] of the reference sample under the *SymmMixN* distribution with $m = 100$, $n = 5$ and $\lambda = 0.20$

From Table 4.35 it can be seen that when the underlying process distribution is *SymmMixN*, the choice of the order statistic from the reference sample stays the same regardless of the value of the smoothing constant λ. Thus, for all λ, the NPEWMA-EX chart based on the 60th percentile performs best for $\gamma = 0.25$, whereas the NPEWMA-EX chart based on the 75th percentile performs best for all other shifts under consideration. Again we find that for the largest shift under consideration, i.e. $\gamma = 2.00$, the NPEWMA-EX chart based on the 75th percentile performs best. Since the run-length characteristics seem to converge as the size of this shift increases, the recommendation would be to use the NPEWMA-EX chart based on the 75th percentile when large shifts are of concern. This is illustrated in Figures 4.40a,b,c for $\lambda = 0.05$, 0.10 and 0.20, respectively, where it can also clearly be seen that the NPEWMA-EX chart based on the 25th percentile is performing the worst.

[xxxvi] Note that the line graph of the 25th percentile is omitted, since it is performing the worst, i.e. it has large OOC *MRL* values. Deleting the 25th percentile makes the graph more visually appealing.

Table 4.36. Control chart performance comparison under the *AsymmMixN1* distribution for $m = 100$ and $n = 5$ when target $MRL_0 = 350$

Shift (γ)	25th percentile	40th percentile	50th percentile	60th percentile	75th percentile
	$\lambda = 0.05$				
0.25	213 (454) 8, 69, 523, 1581	8 (10) 2, 4, 14, 29	5 (5) 1, 3, 8, 15	4 (4) 1, 2, 6, 12	3 (5) 1, 2, 7, 30
0.50	76 (133) 5, 29, 162, 360	5 (4) 2, 4, 8, 14	3 (3) 1, 1, 4, 7	2 (2) 1, 1, 3, 4	1 (1) 1, 1, 2, 3
0.75	41 (65) 5, 18, 83, 186	5 (3) 2, 4, 7, 12	3 (2) 1, 1, 3, 6	2 (1) 1, 1, 2, 4	1 (0) 1, 1, 1, 2
1.00	27 (39) 3, 13, 52, 110	4 (4) 2, 3, 7, 10	2 (2) 1, 1, 3, 6	2(1) 1, 1, 2, 3	1 (0) 1, 1, 1, 2
1.50	15 (18) 3, 8, 26, 52	4 (2) 2, 3, 5, 8	2 (2) 1, 1, 3, 5	2(1) 1, 1, 2, 3	1 (0) 1, 1, 1, 2
2.00	10 (10) 3, 6, 16, 31	4 (1) 2, 3, 4, 7	2 (2) 1, 1, 3, 4	2(1) 1, 1, 2, 3	1 (0) 1, 1, 1, 2
Shift (γ)	$\lambda = 0.10$				
0.25	457 (873) 30, 174, 1047, 2857	13 (15) 2, 7, 22, 45	6 (6) 2, 4, 10, 21	4 (5) 1, 2, 7, 15	4 (6) 1, 2, 8, 38
0.50	169 (274) 16, 69, 344, 784	8 (7) 2, 5, 12, 19	4 (2) 2, 3, 5, 8	2 (2) 1, 1, 3, 5	1 (1) 1, 1, 2, 4
0.75	88 (136) 11, 40, 176, 389	7 (6) 2, 4, 10, 16	4 (3) 2, 2, 5, 7	2 (1) 1, 1, 2, 4	1 (0) 1, 1, 1, 2
1.00	53 (75) 9, 26, 101, 215	6 (6) 2, 3, 9, 14	3 (2) 2, 2, 4, 7	2 (1) 1, 1, 2, 4	1 (0) 1, 1, 1, 2
1.50	26 (31) 6, 15, 46, 91	5 (4) 2, 3, 7, 11	3 (2) 2, 2, 4, 6	2 (1) 1, 1, 2, 3	1 (0) 1, 1, 1, 2
2.00	17 (16) 6, 10, 26, 49	4 (4) 2, 2, 6, 9	3 (1) 2, 2, 3, 5	2 (1) 1, 1, 2, 3	1 (0) 1, 1, 1, 2
Shift (γ)	$\lambda = 0.20$				
0.25	2291 (4167) 153, 902, 5069, 13072	21 (28) 5, 12, 40, 87	9 (9) 3, 6, 15, 31	6 (6) 1, 3, 9, 20	5 (7) 1, 3, 10, 45
0.50	855 (1426) 64, 346, 1773, 4084	12 (11) 4, 7, 18, 33	5 (3) 2, 4, 7, 11	3 (3) 1, 1, 4, 6	1 (2) 1, 1, 3, 4
0.75	408 (670) 36, 170, 840, 1880	10 (9) 4, 16, 15, 25	5 (3) 2, 3, 6, 10	3 (2) 1, 1, 3, 5	1 (1) 1, 1, 2, 3
1.00	216 (334) 23, 93, 427, 986	9 (7) 4, 6, 13, 22	4 (3) 2, 3, 6, 9	2 (2) 1, 1, 3, 5	1 (0) 1, 1, 1, 2
1.50	81 (119) 13, 38, 157, 334	7 (5) 3, 5, 10, 16	4 (2) 2, 3, 5, 7	2 (2) 1, 1, 3, 4	1 (0) 1, 1, 1, 2
2.00	38 (50) 9, 21, 71, 147	6 (4) 3, 4, 8, 13	3 (1) 2, 3, 4, 6	2 (2) 1, 1, 3, 4	1 (0) 1, 1, 1, 2

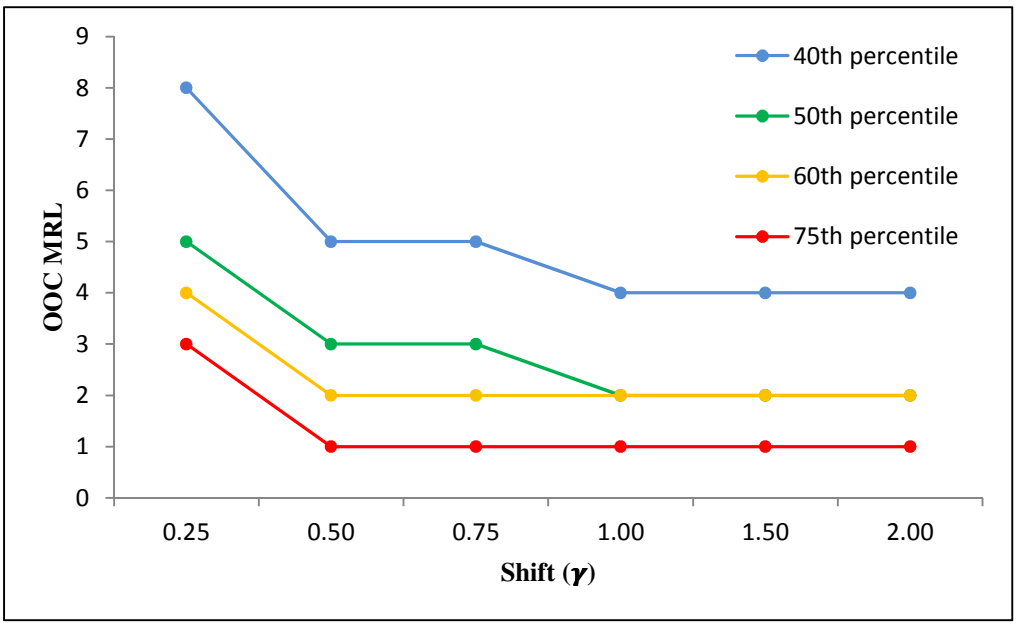

Figure 4.41a. *MRL* performance comparison of the NPEWMA-EX chart based on various percentiles[xxxvii] of the reference sample under the *AsymmMixN1* distribution with $m = 100$, $n = 5$ and $\lambda = 0.05$

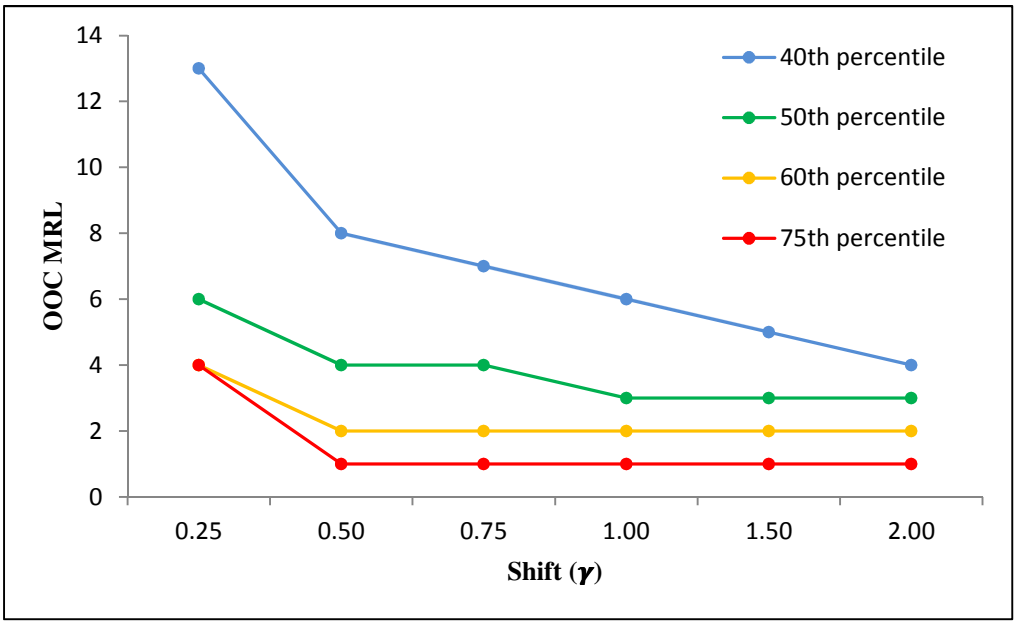

Figure 4.41b. *MRL* performance comparison of the NPEWMA-EX chart based on various percentiles[xxxvii] of the reference sample under the *AsymmMixN1* distribution with $m = 100$, $n = 5$ and $\lambda = 0.10$

[xxxvii] Note that the line graph of the 25th percentile is omitted, since it is performing the worst, i.e. it has large OOC *MRL* values. Deleting the 25th percentile makes the graph more visually appealing.

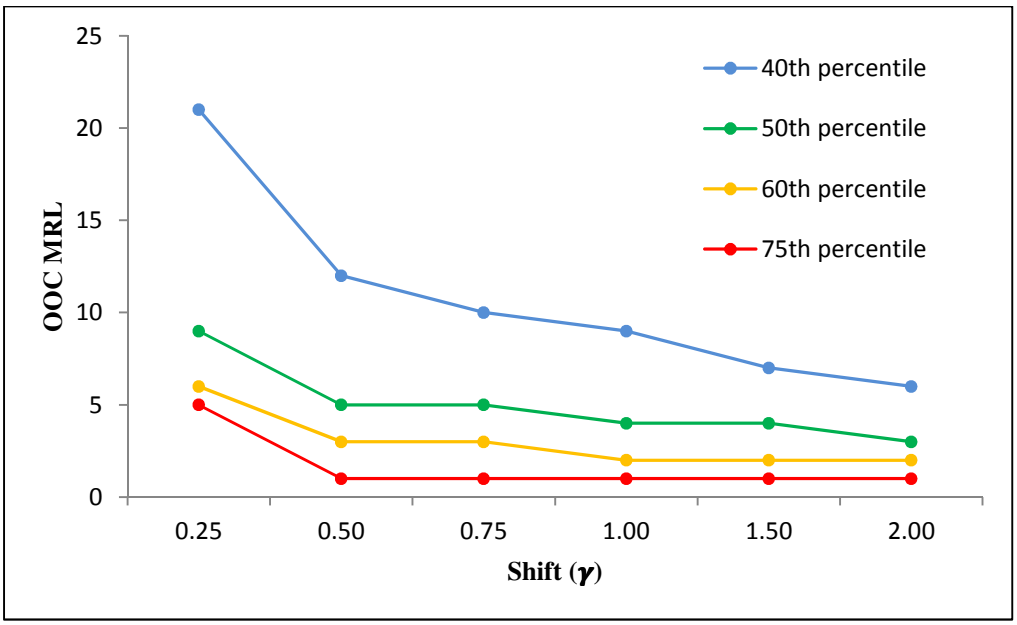

Figure 4.41c. *MRL* performance comparison of the NPEWMA-EX chart based on various percentiles[xxxviii] of the reference sample under the *AsymmMixN1* distribution with $m = 100$, $n = 5$ and $\lambda = 0.20$

From Table 4.36 it can be seen that when the underlying process distribution is *AsymmMixN1*, we have similar results to when the process distribution is *SymmMixN*, i.e. for all λ, the NPEWMA-EX chart based on the 60th percentile performs best for $\gamma = 0.25$, whereas the NPEWMA-EX chart based on the 75th percentile performs best for all other shifts under consideration. This is illustrated in Figures 4.41a,b,c for $\lambda = 0.05$, 0.10 and 0.20, respectively, where it can also clearly be seen that the NPEWMA-EX chart based on the 25th percentile is performing the worst.

[xxxviii] Note that the line graph of the 25th percentile is omitted, since it is performing the worst, i.e. it has large OOC *MRL* values. Deleting the 25th percentile makes the graph more visually appealing.

Table 4.37. Control chart performance comparison under the *AsymmMixN2* distribution for $m = 100$ and $n = 5$ when target $MRL_0 = 350$

Shift (γ)	25th percentile	40th percentile	50th percentile	60th percentile	75th percentile
			$\lambda = 0.05$		
0.25	70 (132) 5, 26, 158, 450	7 (8) 2, 4, 12, 23	4 (5) 1, 2, 7, 15	4 (4) 1, 2, 6, 12	4 (7) 1, 2, 9, 124
0.50	33 (48) 4, 15, 63, 136	4 (3) 2, 4, 7, 11	3 (2) 1, 1, 3, 6	2 (2) 1, 1, 3, 4	1 (1) 1, 1, 2, 4
0.75	22 (30) 3, 11, 41, 84	4 (3) 2, 3, 6, 10	2 (2) 1, 1, 3, 5	2 (1) 1, 1, 2, 3	1 (0) 1, 1, 1, 2
1.00	17 (21) 3, 9, 30, 60	4 (2) 2, 3, 5, 9	2 (2) 1, 1, 3, 5	2 (1) 1, 1, 2, 3	1 (0) 1, 1, 1, 2
1.50	11 (12) 3, 6, 18, 33	4 (1) 2, 3, 4, 7	2 (2) 1, 1, 3, 4	2 (1) 1, 1, 2, 3	1 (0) 1, 1, 1, 2
2.00	8 (8) 3, 5, 13, 22	3 (2) 2, 2, 4, 6	1 (1) 1, 1, 2, 3	1 (1) 1, 1, 2, 3	1 (0) 1, 1, 1, 2
Shift (γ)			$\lambda = 0.10$		
0.25	158 (272) 16, 66, 338, 889	11 (12) 2, 6, 18, 35	6 (6) 2, 4, 10, 19	4 (5) 1, 2, 7, 15	5 (9) 1, 2, 11, 137
0.50	66 (95) 10, 32, 127, 273	7 (5) 2, 4, 9, 15	4 (3) 2, 2, 5, 7	2 (2) 1, 1, 3, 4	1 (1) 1, 1, 2, 5
0.75	42 (56) 8, 22, 78, 165	6 (5) 2, 3, 8, 13	3 (2) 2, 2, 4, 6	2 (1) 1, 1, 2, 3	1 (0) 1, 1, 1, 2
1.00	30 (36) 7, 17, 53, 106	5 (5) 2, 3, 8, 11	3 (2) 2, 2, 4, 6	2 (1) 1, 1, 2, 3	1 (0) 1, 1, 1, 2
1.50	18 (18) 6, 11, 29, 55	4 (3) 2, 3, 6, 9	3 (2) 2, 2, 4, 5	2 (1) 1, 1, 2, 3	1 (0) 1, 1, 1, 2
2.00	13 (11) 5, 8, 19, 33	3 (3) 2, 2, 5, 8	2 (1) 2, 2, 3, 4	1 (1) 1, 1, 2, 3	1 (0) 1, 1, 1, 2
Shift (γ)			$\lambda = 0.20$		
0.25	760 (1281) 58, 306, 1587, 4020	16 (20) 5, 9, 29, 64	8 (8) 3, 5, 13, 27	5 (6) 1, 3, 9, 20	6 (11) 1, 3, 14, 185
0.50	291 (462) 28, 124, 586, 1322	9 (8) 4, 6, 14, 24	4 (3) 2, 3, 6, 10	3 (3) 1, 1, 4, 6	1 (2) 1, 1, 3, 5
0.75	164 (252) 19, 73, 325, 710	8 (6) 3, 5, 11, 19	4 (3) 2, 3,6, 8	2 (2) 1, 1, 3, 4	1 (0) 1, 1, 1, 3
1.00	98 (145) 15, 46, 191, 415	7 (5) 3, 5, 10, 17	4 (2) 2, 3, 5, 8	2 (2) 1, 1, 3, 4	1 (0) 1, 1, 1, 2
1.50	44 (58) 10, 23, 81, 165	6 (4) 3, 4, 8, 13	3 (1) 2, 3, 4, 6	2 (2) 1, 1, 3, 4	1 (0) 1, 1, 1, 2
2.00	26 (28) 8, 15, 43, 85	5 (3) 3, 4, 7, 10	3 (2) 2, 2, 4, 6	1 (2) 1, 1, 3, 3	1 (0) 1, 1, 1, 2

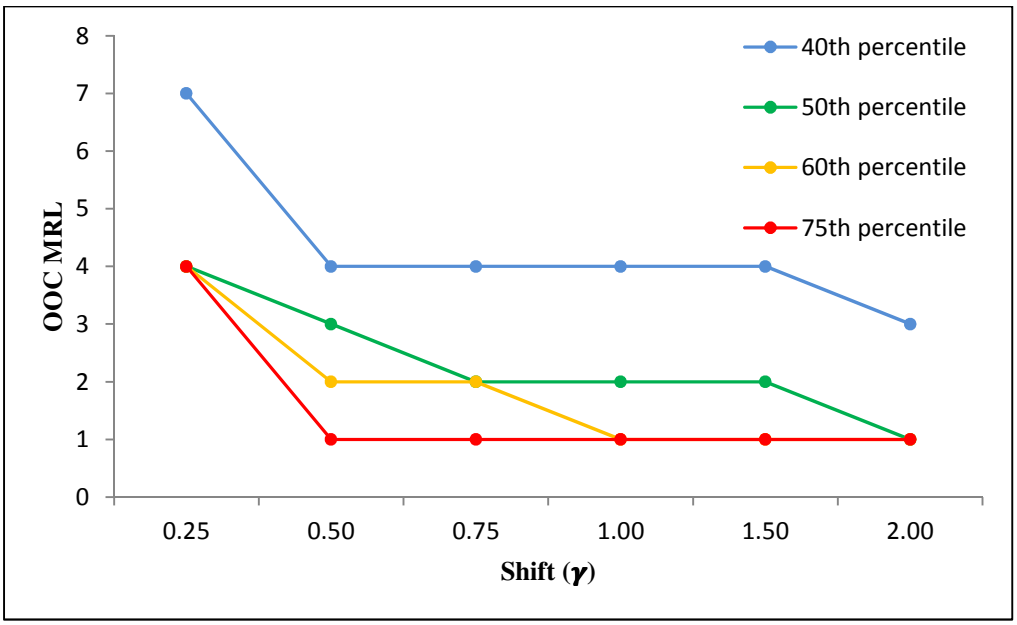

Figure 4.42a. *MRL* performance comparison of the NPEWMA-EX chart based on various percentiles[xxxix] of the reference sample under the *AsymmMixN2* distribution with $m = 100$, $n = 5$ and $\lambda = 0.05$

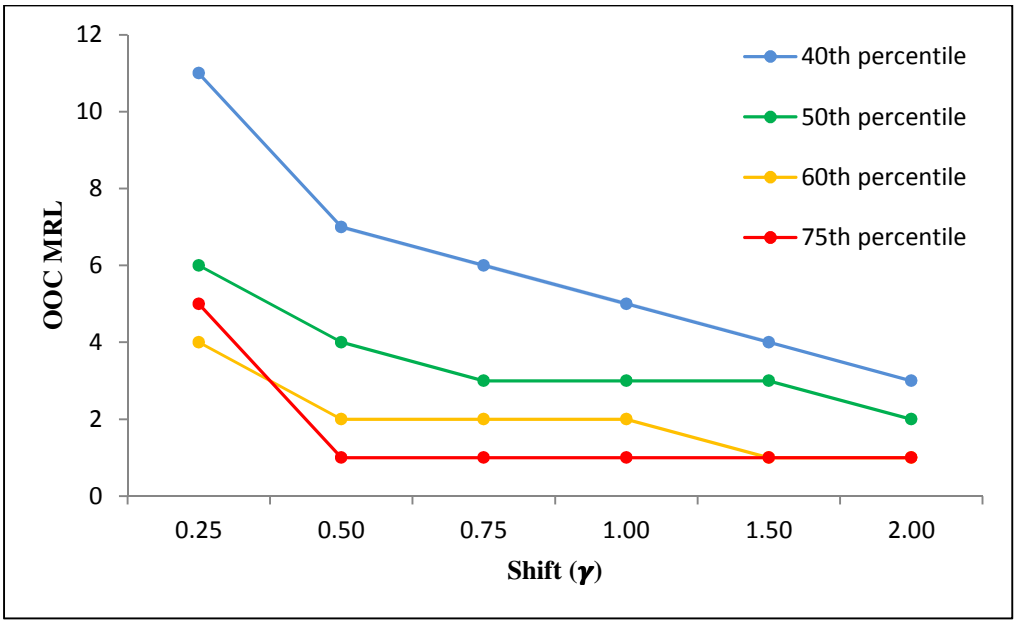

Figure 4.42b. *MRL* performance comparison of the NPEWMA-EX chart based on various percentiles[xxxix] of the reference sample under the *AsymmMixN2* distribution with $m = 100$, $n = 5$ and $\lambda = 0.10$

[xxxix] Note that the line graph of the 25th percentile is omitted, since it is performing the worst, i.e. it has large OOC *MRL* values. Deleting the 25th percentile makes the graph more visually appealing.

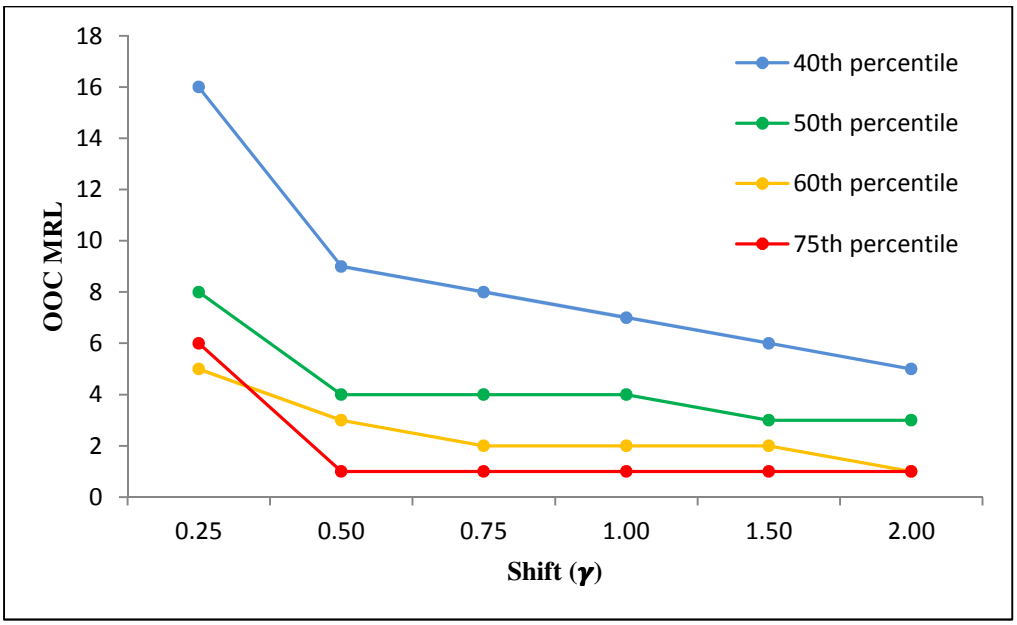

Figure 4.42c. *MRL* performance comparison of the NPEWMA-EX chart based on various percentiles[xl] of the reference sample under the *AsymmMixN2* distribution with $m = 100$, $n = 5$ and $\lambda = 0.20$

From Table 4.37 it can be seen that when the underlying process distribution is *AsymmMixN2*, we have similar results to when the process distribution is *SymmMixN* or *AsymmMixN1*, i.e. for all λ, the NPEWMA-EX chart based on the 60th percentile performs best for $\gamma = 0.25$, whereas the NPEWMA-EX chart based on the 75th percentile performs best for all other shifts under consideration. This is illustrated in Figures 4.42a,b,c for $\lambda = 0.05$, 0.10 and 0.20, respectively, where it can also clearly be seen that the NPEWMA-EX chart based on the 25th percentile is performing the worst.

[xl] Note that the line graph of the 25th percentile is omitted, since it is performing the worst, i.e. it has large OOC *MRL* values. Deleting the 25th percentile makes the graph more visually appealing.

Table 4.38. Control chart performance comparison under *Log-Logistic*($\alpha = 1, \beta = 2.5$) distribution for $m = 100$ and $n = 5$ when target $MRL_0 = 350$

Shift (γ)	25th percentile	40th percentile	50th percentile	60th percentile	75th percentile
	$\lambda = 0.05$				
0.25	12 (23) 3, 6, 29, 187	13 (30) 2, 5, 35, 327	14 (46) 1, 5, 51, 856	19 (81) 2, 6, 87, 1673	37 (270) 2, 8, 278, 4180
0.50	3 (3) 3, 3, 6, 11	4 (3) 2, 3, 6, 13	3 (6) 1, 1, 7, 18	4 (7) 1, 2, 9, 32	7 (20) 1, 3, 23, 304
0.75	3 (0) 3, 3, 3, 5	2 (1) 4, 3, 2, 2	1 (2) 1, 1, 3, 5	2 (3) 1, 1, 4, 7	3 (4) 1, 2, 6, 24
1.00	3 (0) 3, 3, 3, 3	2 (0) 2, 2, 2, 3	1 (0) 1, 1, 1, 3	1 (1) 1, 1, 2, 4	2 (2) 1, 1, 3, 8
1.50	3 (0) 3, 3, 3, 3	2 (0) 2, 2, 2, 2	1 (0) 1, 1, 1, 1	1 (0) 1, 1, 1, 1	1 (0) 1, 1, 1, 2
2.00	3 (0) 3, 3, 3, 3	2 (0) 2, 2, 2, 2	1 (0) 1, 1, 1, 1	1 (0) 1, 1, 1, 1	1 (0) 1, 1, 1, 1
Shift (γ)	**$\lambda = 0.10$**				
0.25	21 (38) 5, 11, 49, 308	20 (48) 2, 8, 56, 433	23 (70) 3, 9, 79, 763	28 (102) 2, 9, 111, 1086	50 (239) 2, 11, 250, 2028
0.50	6 (4) 5, 5, 9, 15	4 (5) 2, 3, 8, 17	5 (6) 2, 3, 9, 24	5 (10) 1, 2, 12, 42	9 (25) 1, 3, 28, 276
0.75	5 (0) 5, 5, 5, 6	2 (1) 2, 2, 3, 6	3 (2) 2, 2, 4, 7	2 (3) 1, 1, 4, 9	3 (5) 1, 2, 7, 30
1.00	5 (0) 5, 5, 5, 5	2 (0) 2, 2, 2, 3	2 (0) 2, 2, 2, 3	1 (1) 1, 1, 2, 4	2 (2) 1, 1, 3, 9
1.50	5 (0) 5, 5, 5, 5	2 (0) 2, 2, 2, 2	2 (0) 2, 2, 2, 2	1 (0) 1, 1, 1, 1	1 (0) 1, 1, 1, 2
2.00	5 (0) 5, 5, 5, 5	2 (0) 2, 2, 2, 2	2 (0) 2, 2, 2, 2	1 (0) 1, 1, 1, 1	1 (0) 1, 1, 1, 1
Shift (γ)	**$\lambda = 0.20$**				
0.25	50 (132) 8, 21, 153, 887	35 (86) 5, 14, 100, 583	37 (105) 4, 14, 119, 688	39 (122) 3, 13, 135, 797	54 (194) 2, 15, 209, 1443
0.50	9 (7) 6, 6, 13, 27	7 (6) 3, 5, 11, 26	7 (8) 2, 4, 12, 35	7 (11) 1, 4, 15, 57	11 (26) 1, 4, 30, 209
0.75	6 (0) 6, 6, 6, 9	4 (2) 3, 3, 5, 7	3 (3) 2, 2, 5, 8	3 (4) 1, 1, 5, 11	4 (7) 1, 2, 9, 33
1.00	6 (0) 6, 6, 6, 6	3 (0) 3, 3, 3, 4	2 (1) 2, 2, 3, 4	1 (2) 1, 1, 3, 5	2 (3) 1, 1, 4, 10
1.50	6 (0) 6, 6, 6, 6	3 (0) 3, 3, 3, 3	2 (0) 2, 2, 2, 2	1 (0) 1, 1, 1, 1	1 (0) 1, 1, 1, 3
2.00	6 (0) 6, 6, 6, 6	3 (0) 3, 3, 3, 3	2 (0) 2, 2, 2, 2	1 (0) 1, 1, 1, 1	1 (0) 1, 1, 1, 1

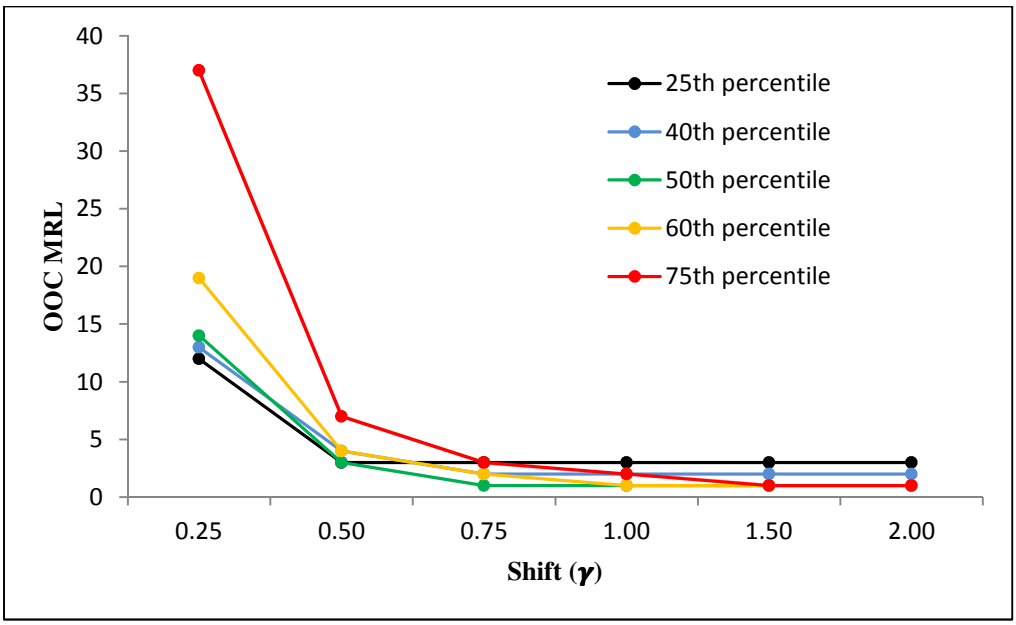

Figure 4.43a. *MRL* performance comparison of the NPEWMA-EX chart based on various percentiles of the reference sample under the *Log-Logistic* distribution with $m = 100$, $n = 5$ and $\lambda = 0.05$

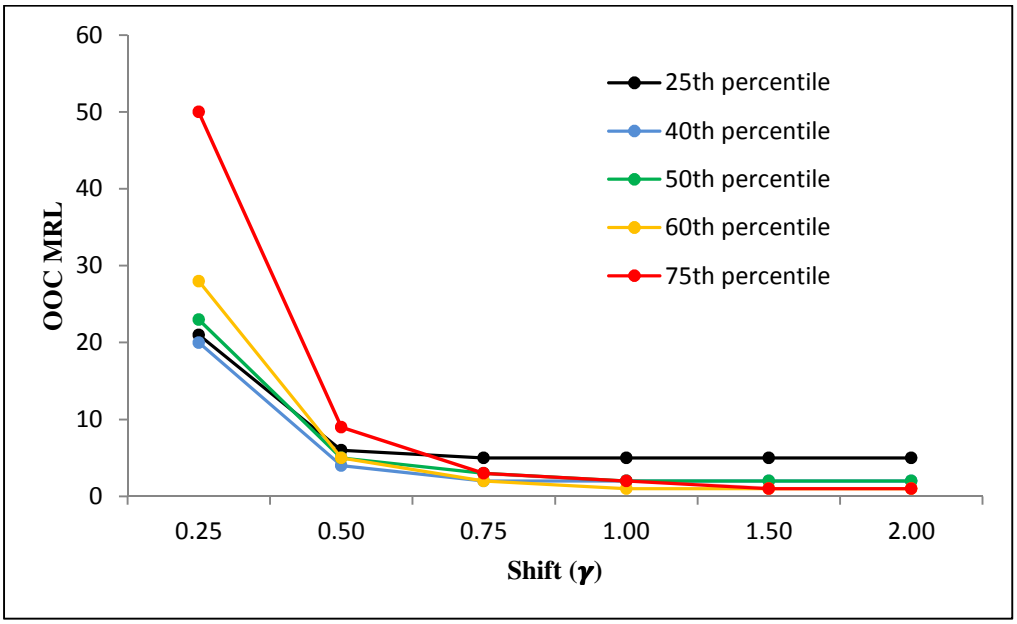

Figure 4.43b. *MRL* performance comparison of the NPEWMA-EX chart based on various percentiles of the reference sample under the *Log-Logistic* distribution with $m = 100$, $n = 5$ and $\lambda = 0.10$

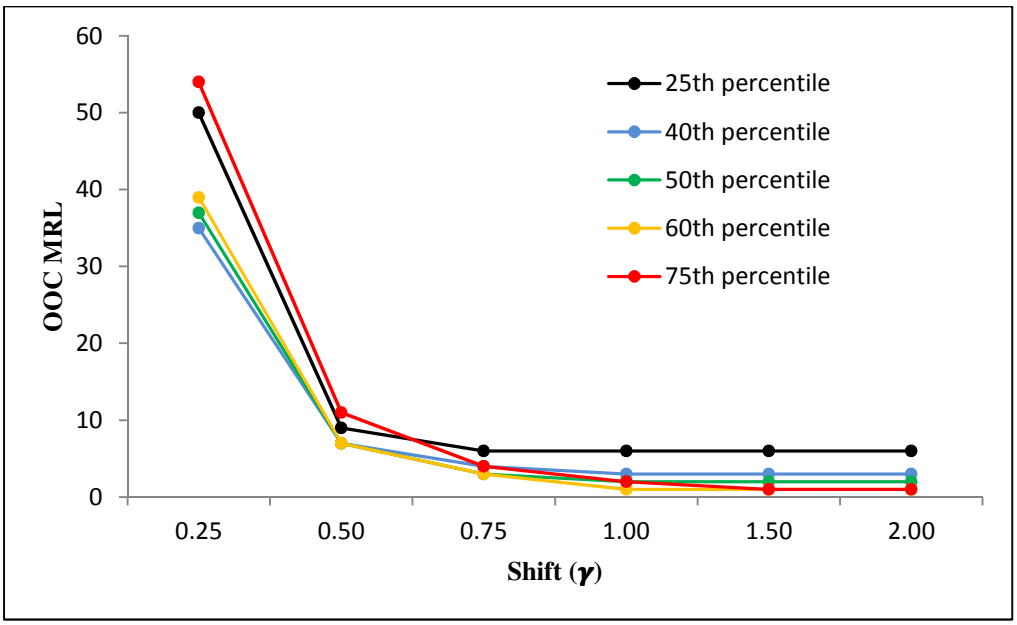

Figure 4.43c. *MRL* performance comparison of the NPEWMA-EX chart based on various percentiles of the reference sample under the *Log-Logistic* distribution with $m = 100$, $n = 5$ and $\lambda = 0.20$

From Table 4.38 it can be seen that for $\gamma = 0.25$ and 0.50 the NPEWMA-EX charts based on lower order percentiles perform best, specifically, for $\lambda = 0.05$ the NPEWMA-EX chart based on the 1st quartile performs best, whereas for $\lambda = 0.10$ and 0.20 the NPEWMA-EX chart based on the 40th percentile performs best. As the magnitude of the shift increases, we find that the NPEWMA-EX charts based on higher order percentiles perform best. For example, for $\gamma = 1.50$ and 2.00 the NPEWMA-EX charts based on the 50th, 60th and 75th percentiles performs best for $\lambda = 0.05$, whereas the latter two charts performs best for $\lambda = 0.10$ and 0.20, respectively. This is illustrated in Figures 4.43a,b,c for $\lambda = 0.05$, 0.10 and 0.20, respectively,

The observations from Tables 4.32 to 4.38 are summarized in Table 4.39 below along with some recommendations. Note that for brevity, a shorthand notation is used to describe the charts. For example, the NPEWMA-EX chart based on the 50th percentile is denoted by EX(50), and if two charts perform similarly, for example, if the NEWMA-EX chart based on the 50th and 60th percentiles perform similarly, the notation EX(50,60) is used.

Table 4.39. Summary of the efficiency of different reference sample percentiles for the NPEWMA-EX chart

<table>
<tr><th></th><th>$\gamma = 0.25$</th><th>$\gamma = 0.50$</th><th>$\gamma = 0.75$</th><th>$\gamma = 1.00$</th><th>$\gamma = 1.50$</th><th>$\gamma = 2.00$</th></tr>
<tr><td colspan="7">Symmetric distributions</td></tr>
<tr><td>N(0,1)</td><td colspan="6">For all λ the EX(75) chart performs best</td></tr>
<tr><td>DE(0,1)</td><td colspan="4">For all λ the EX(60) chart performs best</td><td colspan="2">For all λ the EX(75) chart performs best</td></tr>
<tr><td>SymmMixN</td><td>For all λ the EX(60) chart performs best</td><td colspan="5">For all λ the EX(75) chart performs best</td></tr>
<tr><td colspan="7">Asymmetric distributions</td></tr>
<tr><td>EXP(1)</td><td colspan="3">For all λ the EX(25) chart performs best</td><td>For all λ the EX(40) chart performs best</td><td>For all λ the EX(50) chart performs best</td><td>For all λ the EX(60) chart performs best</td></tr>
<tr><td>AsymmMixN1</td><td>For all λ the EX(60) chart performs best</td><td colspan="5">For all λ the EX(75) chart performs best</td></tr>
<tr><td>AsymmMixN2</td><td>For all λ the EX(60) chart performs best</td><td colspan="5">For all λ the EX(75) chart performs best</td></tr>
<tr><td>Log-Logistic</td><td colspan="2">$\lambda = 0.05$: EX(25)

$\lambda = 0.10$ and $\lambda = 0.20$: EX(40)</td><td>$\lambda = 0.05$ and $\lambda = 0.20$: EX(50)

$\lambda = 0.10$: EX(40)</td><td>$\lambda = 0.05$: EX(50)

$\lambda = 0.10$ and $\lambda = 0.20$: EX(60)</td><td colspan="2">$\lambda = 0.05$: EX(50,60,75)

$\lambda = 0.10$ and $\lambda = 0.20$: EX(60,75)</td></tr>
</table>

Illustrative examples

Example 4.6

First we illustrate the NPEWMA-EX chart using a well-known dataset from Montgomery (2001; Tables 5.1 and 5.2) on the inside diameters of piston rings manufactured by a forging process. The data given in Table 5.1 contains twenty-five retrospective or Phase I samples, each of size five, that were collected when the process was thought to be IC, i.e. $m = 125$. An analysis in Montgomery (2001) showed that these data are from an IC process and thus can be considered to be Phase I reference data. Note also that for these data, a goodness of fit test for normality is not rejected. This does not guarantee that the normality assumption for a traditional or parametric EWMA chart is valid but often the practical implication is as such. We instead apply and contrast the proposed nonparametric exceedance charts based on the 25^{th}, 40^{th}, 50^{th} (median), 60^{th} and the 75^{th} percentile, respectively, of the reference sample. The values of the respective reference sample percentiles are as follows: 25^{th} percentile = 73.995, 40^{th} percentile = 73.998, median = 74.001, 60^{th} percentile = 74.004 and 75^{th} percentile = 74.008. All of the measurements are in mm.

In order to calculate the Phase II exceedance control charts, we use the data in Table 5.2 of Montgomery (2001) that contains fifteen prospective (Phase II) samples each of five observations ($n = 5$). The smoothing constant is taken to be $\lambda = 0.05$ and L is found such that $MRL_0 = 350$.

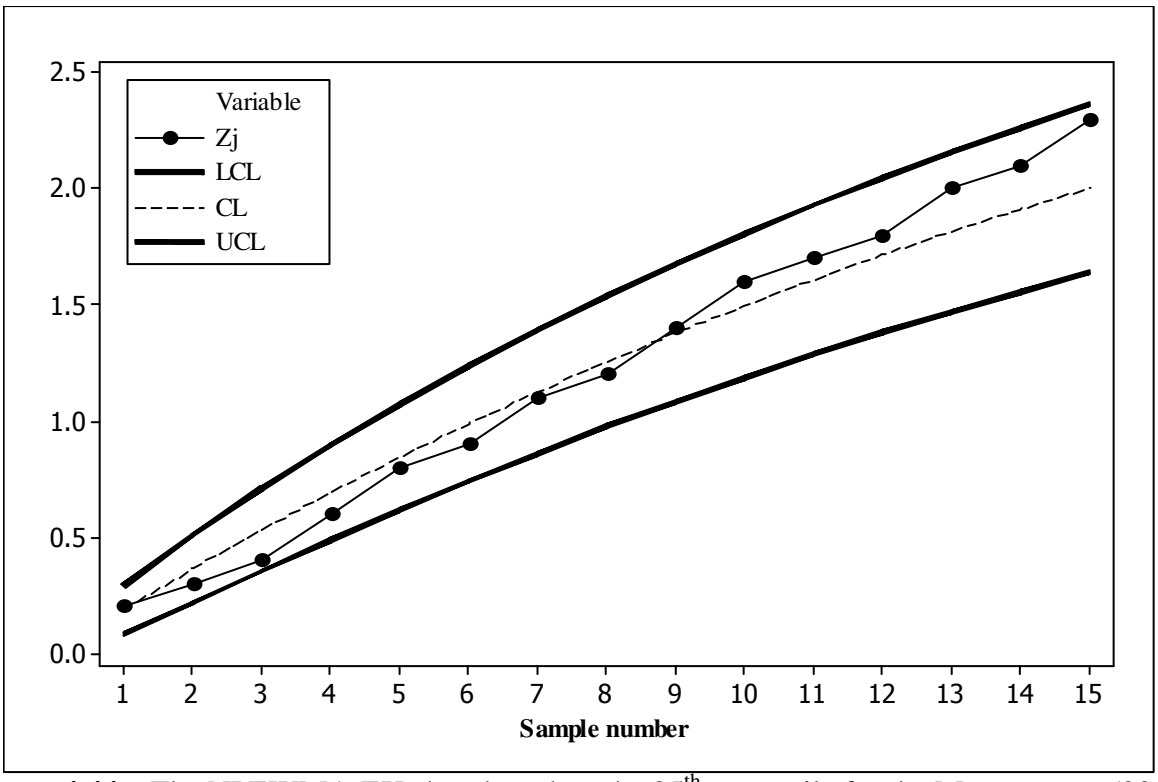

Figure 4.44a. The NPEWMA-EX chart based on the 25th percentile for the Montgomery (2001) piston ring data

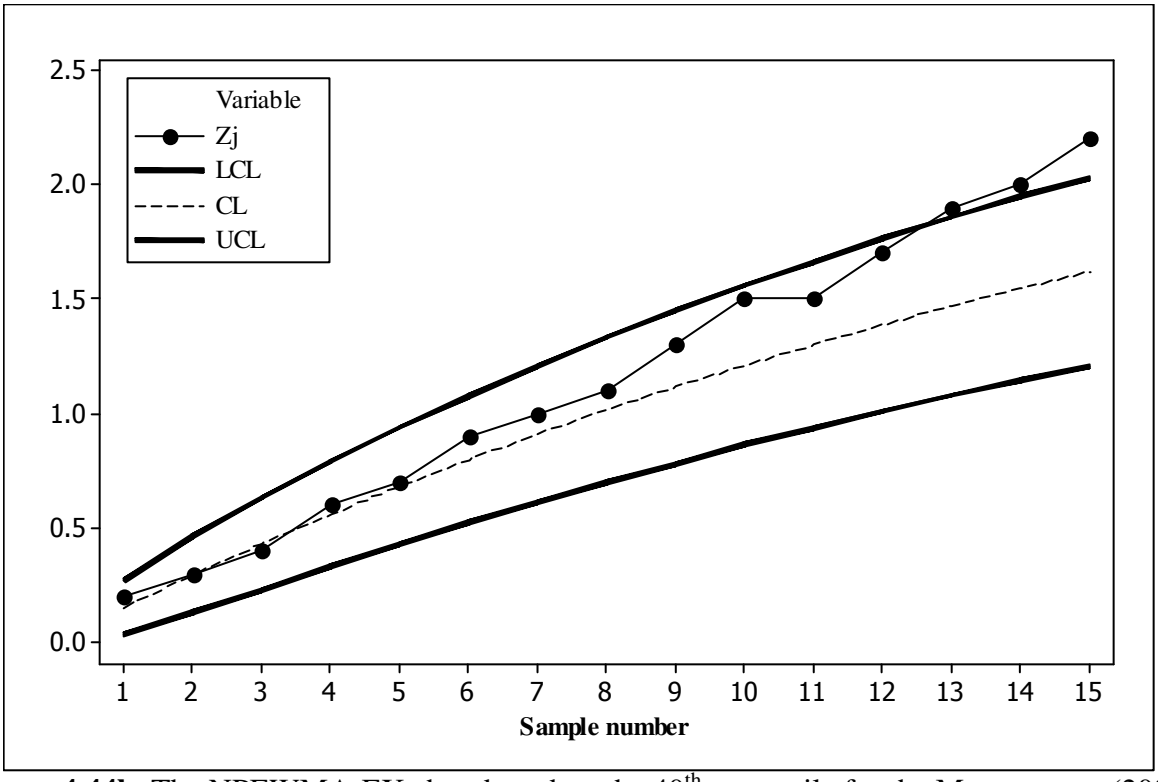

Figure 4.44b. The NPEWMA-EX chart based on the 40th percentile for the Montgomery (2001) piston ring data

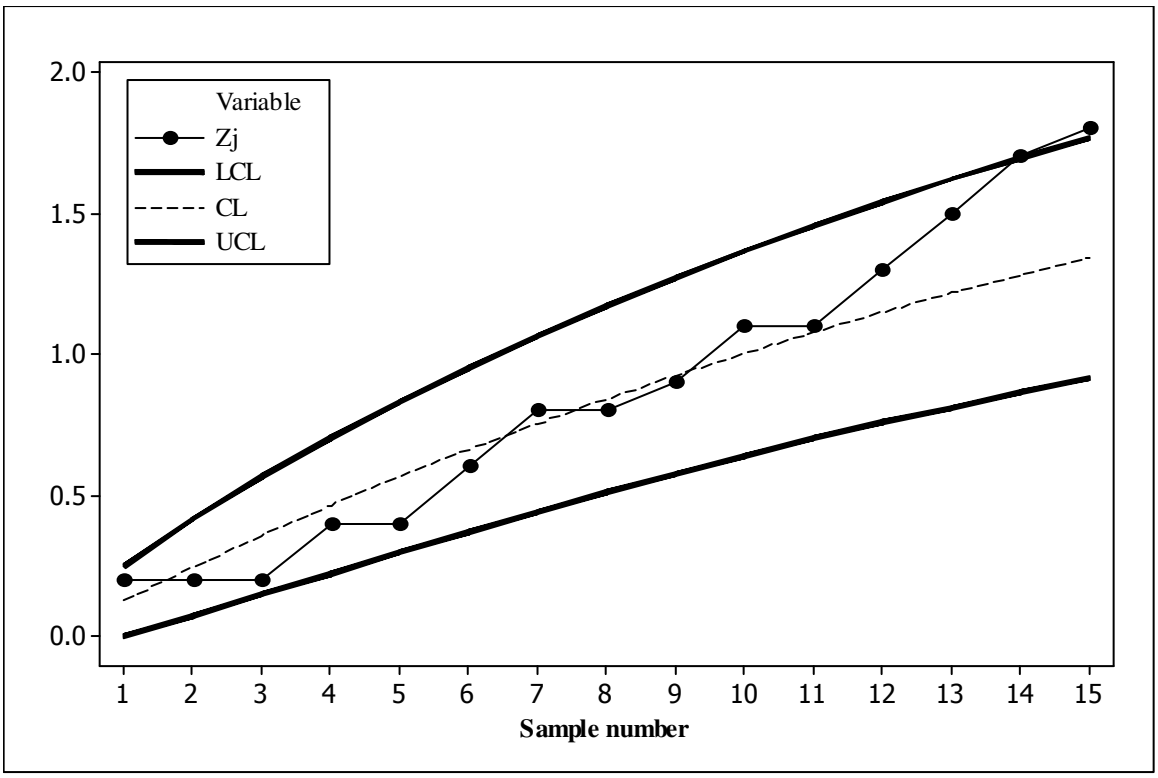

Figure 4.44c. The NPEWMA-EX chart based on the median for the Montgomery (2001) piston ring data

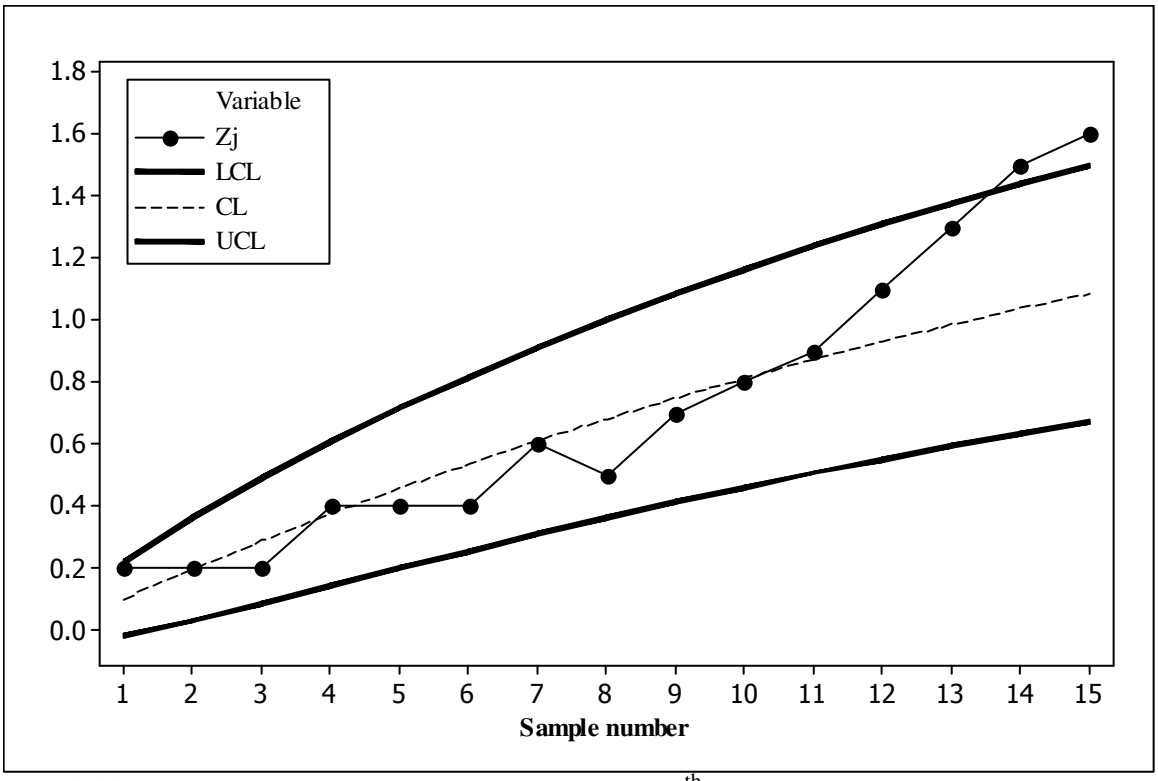

Figure 4.44d. The NPEWMA-EX chart based on the 60th percentile for the Montgomery (2001) piston ring data

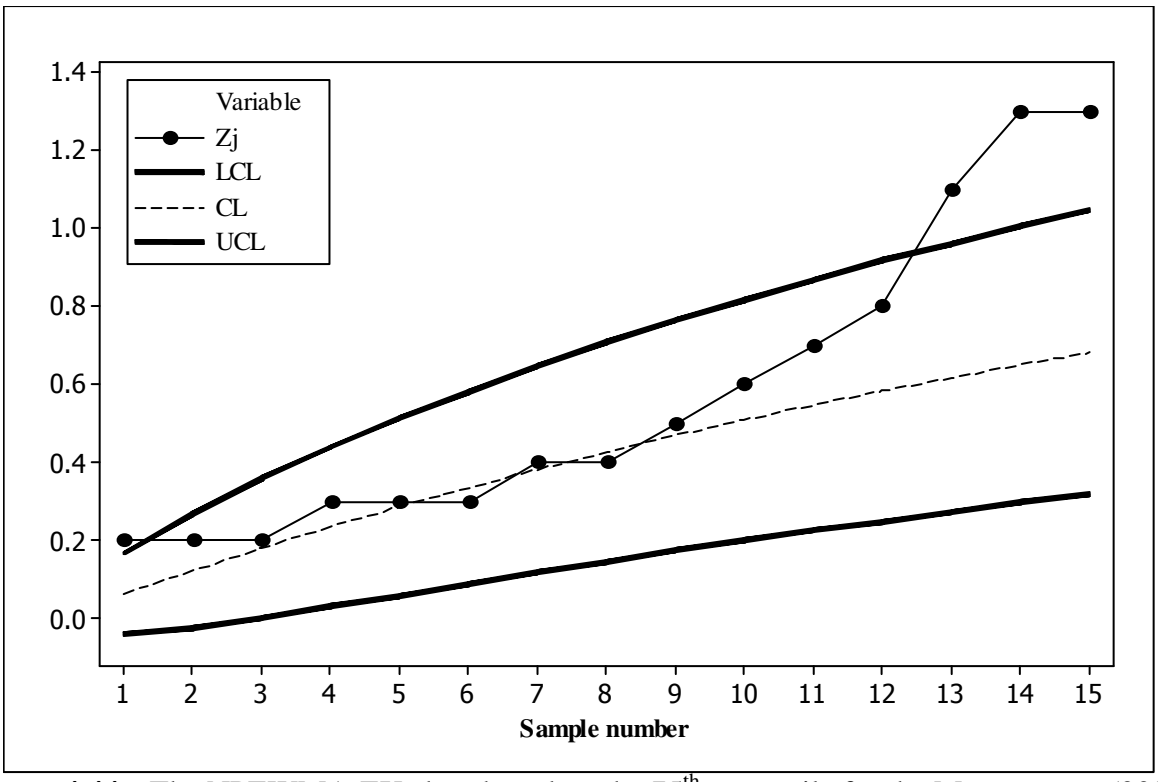

Figure 4.44e. The NPEWMA-EX chart based on the 75th percentile for the Montgomery (2001) piston ring data

From Figures 4.44b,e we see that the NPEWMA-EX chart based on the 40th and 75th percentiles perform the best and similarly, signaling at sample number 13. Table 4.39 suggests that the NPEWMA-EX chart based on 75th percentile performs best when the underlying process distribution is normal which can clearly be seen in Figure 4.44e. The NPEWMA-EX chart based on the 50th and 60th percentiles signal on samples number 15 and 14, respectively, whereas the NPEWMA-EX chart based on the 25th percentile performs worst, since it doesn't signal at all.

For our first example, the data did not reject a goodness of fit test for normality. Nonparametric charts are useful for all continuous distributions and heavier tailed distributions are of particular interest in practice as they can give rise to more outliers which do not necessarily indicate an OOC process. So we illustrate the NEWMA-EX chart when the data follow a symmetric yet heavier tailed distribution (than the normal) with some simulated data from the Double Exponential distribution.

Example 4.7

In practice the underlying process distribution is often unknown or other than the normal and this is where the nonparametric charts can be really useful. To illustrate the application of the NPEWMA-EX chart when the data follow a symmetric yet heavier tailed distribution (than the normal)we use some simulated data from the Laplace (or double exponential) distribution; *DE*(0,1) which is known to have a median of zero and a standard deviation equal to $\sqrt{2}$. An IC reference sample of size 100 (m = 100) was generated from this distribution and each data point was scaled so that the transformed observations have a standard deviation of 1. For the reference data we find the median equal to -0.052. Next the Phase II samples, each of size 5 (n = 5), were independently and sequentially generated by transforming the observations from a *DE*(0,1) distribution so that the resulting observations have a median of $\gamma/\sqrt{n}$ ($= 0.112$ for γ = 0.25 and n = 5) and a standard deviation of 1. Consequently, the Phase II samples can be thought of as having been drawn from a process that is OOC in the median.

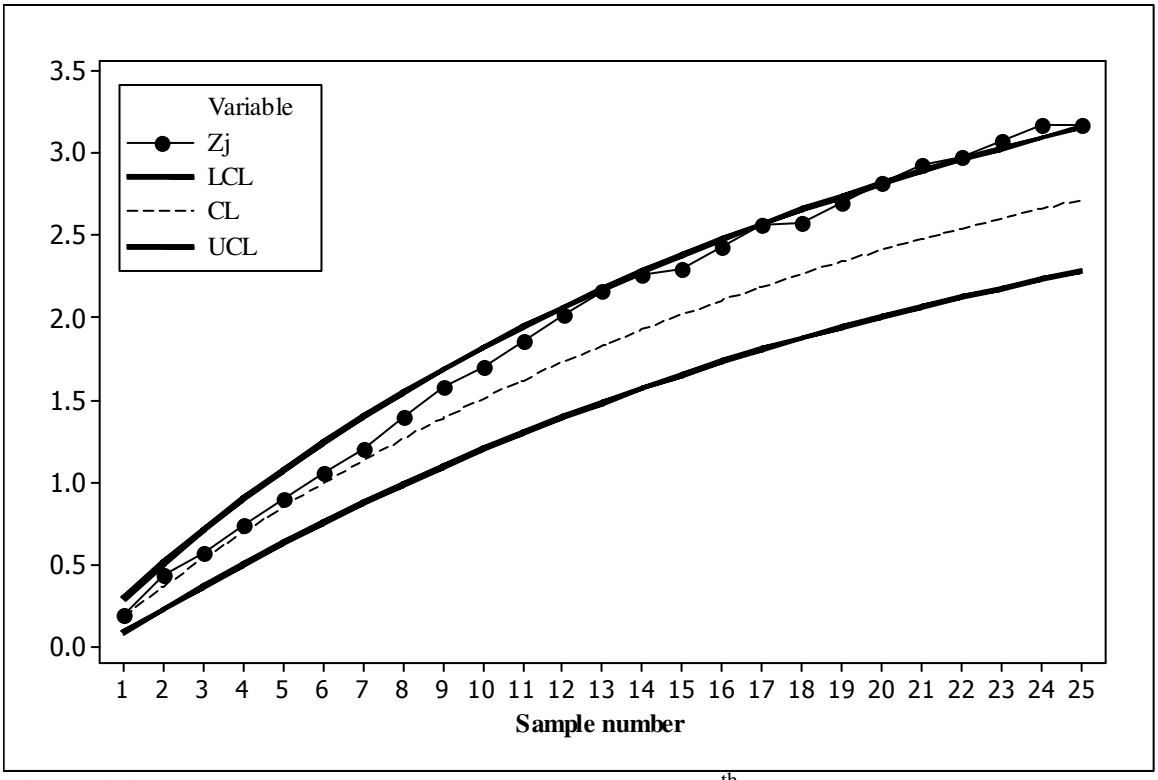

Figure 4.45a. The NPEWMA-EX chart based on the 25th percentile for the simulated data

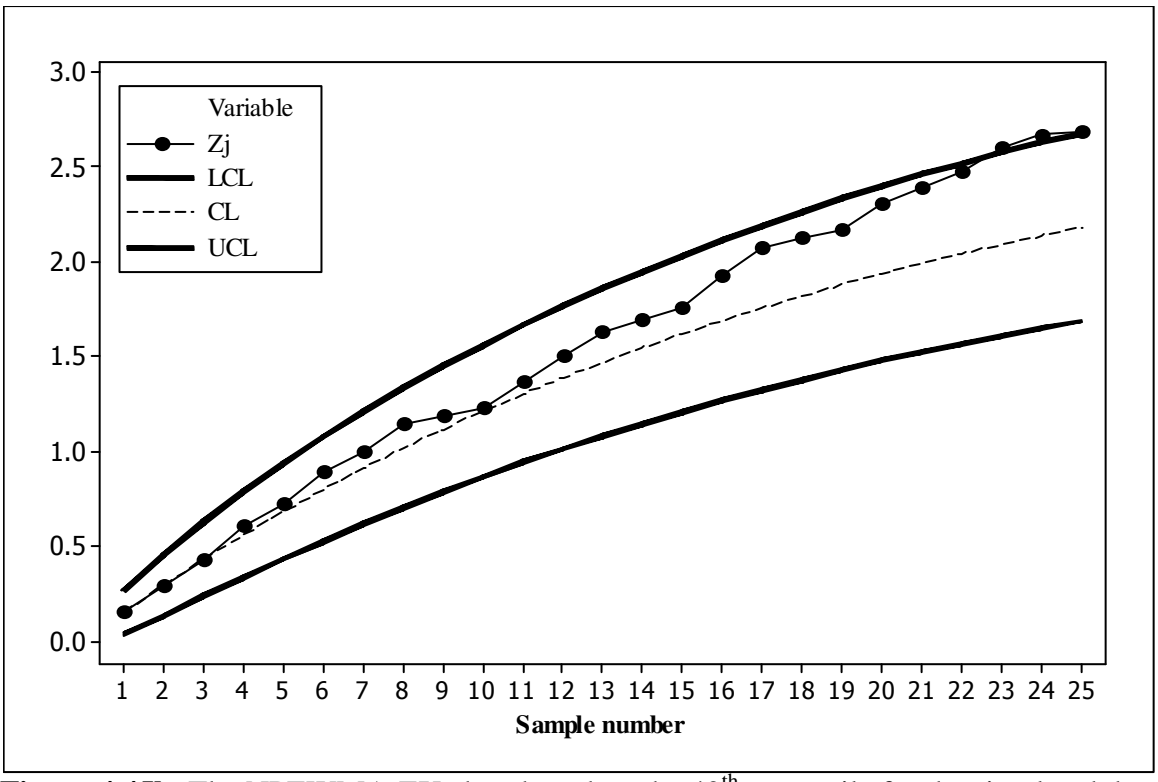

Figure 4.45b. The NPEWMA-EX chart based on the 40th percentile for the simulated data

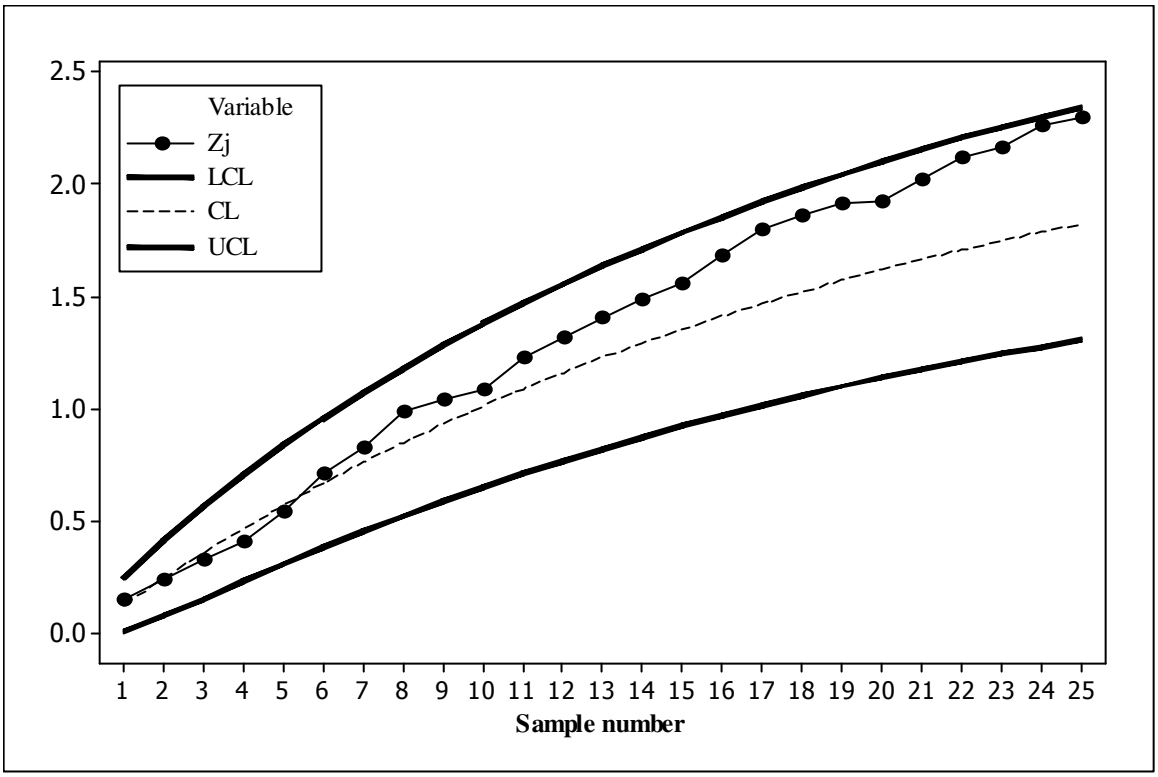

Figure 4.45c. The NPEWMA-EX chart based on the median for the simulated data

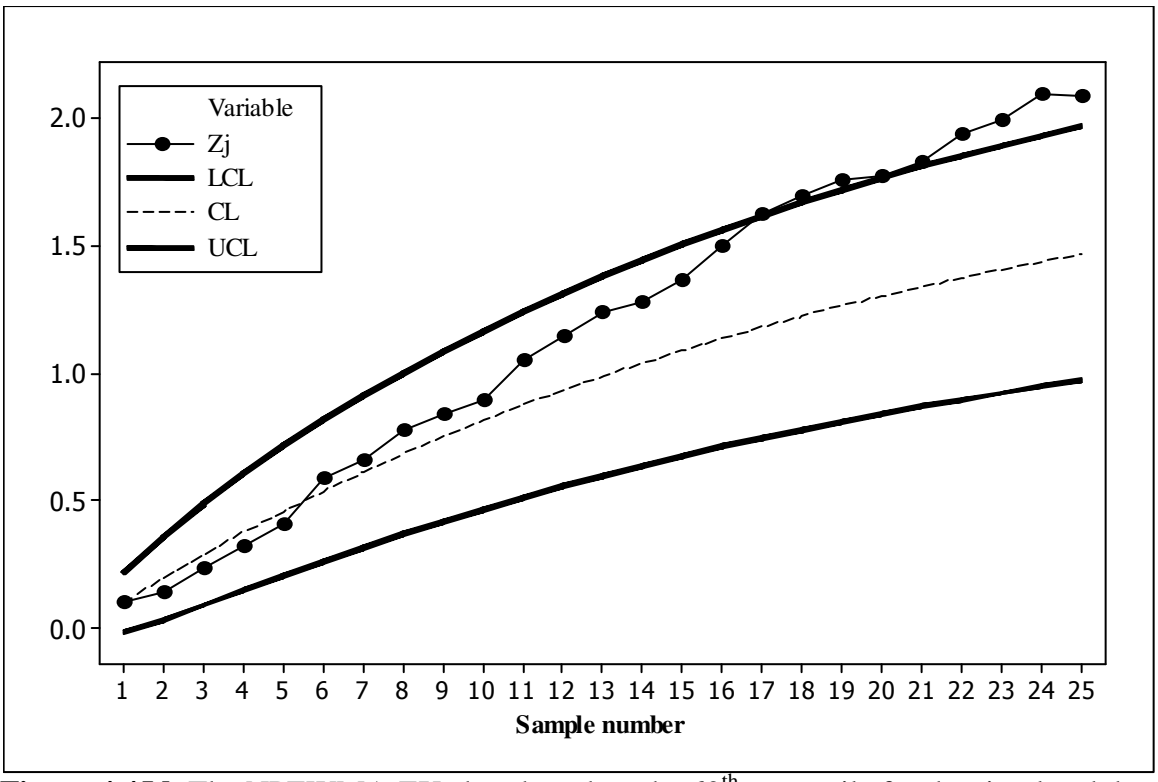

Figure 4.45d. The NPEWMA-EX chart based on the 60th percentile for the simulated data

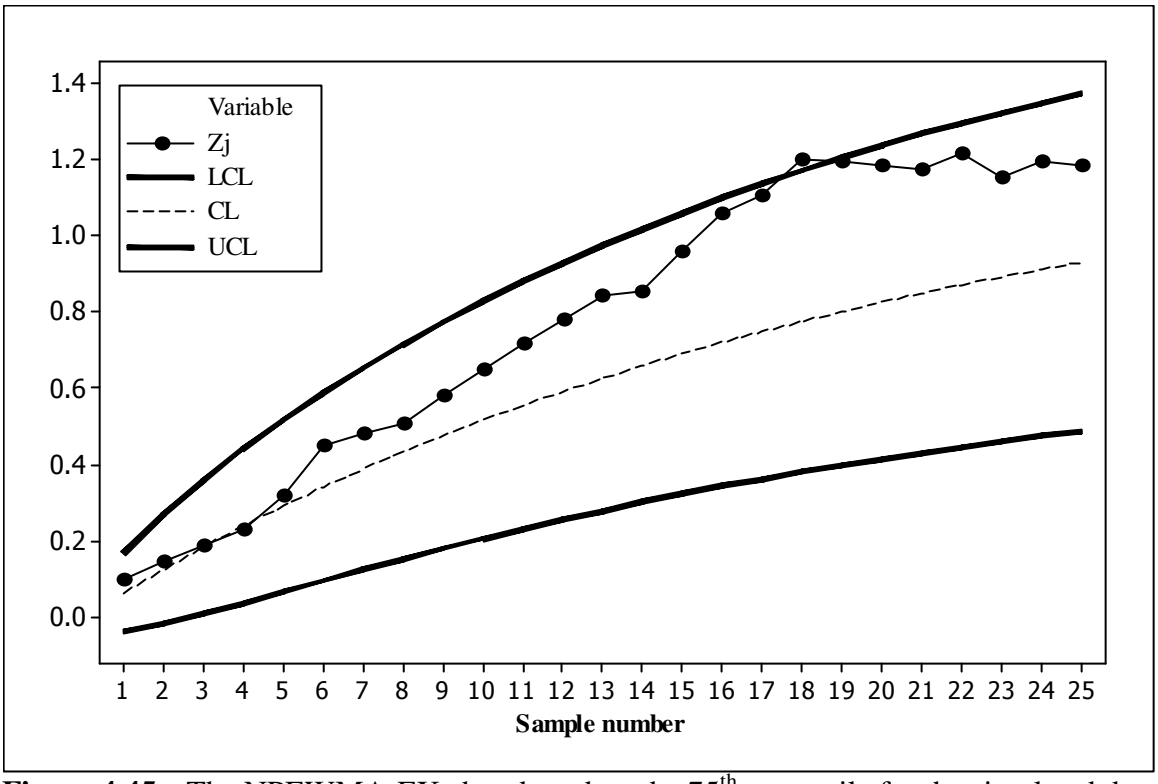

Figure 4.45e. The NPEWMA-EX chart based on the 75th percentile for the simulated data

From Figure 4.45d we can see that the NPEWMA-EX chart based on the 60th percentile is performing best, since it signals the earliest at sample number 17. Performing second best is the NPEWMA-EX chart based on the 75th percentile, signaling on sample number 18. This is consistent

with the conclusions drawn in Table 4.39. The NPEWMA-EX charts based on the 25th and 40th percentiles signal on sample numbers 21 and 23, respectively, and the NPEWMA-EX chart based on the median performs the worst, since it doesn't signal at all.

4.4.6 Summary

NPEWMA charts offer an attractive alternative in practice as they combine the inherent advantages of nonparametric charts with the better small shift detection capability of EWMA-type charts. We examine a class of NPEWMA charts based on the exceedance statistic by investigating which order statistic (percentile), from the reference sample, should be used for good overall performance. We conclude that the NPEWMA -EX chart, based on higher order percentiles, such as the 60th or 75th percentiles, are good overall charts for detecting a larger location shift. Other reference sample percentiles, such as the 25th or the 40th, can also be used when a smaller shift in location is expected. Overall, it is seen that the exceedance EWMA chart based on higher percentiles performs better than its competitors in many cases for a number of distributions. More specifically, for moderate to large shifts there is little doubt that the practitioner should use the exceedance chart based on the 75th percentile which signals quickly for all reference values under consideration. This is an interesting result in the literature on nonparametric exceedance / precedence tests and control charts. Note that our metric of comparison is the *MRL*, which we recommend over the *ARL*.

4.5 Concluding remarks

In this chapter we proposed a NPCUSUM chart and a NPEWMA chart for monitoring the unknown median based on a reference sample. The proposed charts are based on what are known as precedence or exceedance test statistics. CUSUM and EWMA charts take advantage of the sequentially (time ordered) accumulating nature of the data arising in a typical SPC environment and are known to be more efficient in detecting smaller shifts. The traditional parametric CUSUM-$\overline{X}$ and EWMA-$\overline{X}$ charts can lack IC robustness and as such the corresponding false alarm rates can be a practical concern. Nonparametric CUSUM and EWMA charts offer an attractive alternative in such situations as they combine the inherent advantages of nonparametric charts (IC robustness) with the better small shift detection capability of CUSUM-type and EWMA-type charts.

4.6 Appendices

4.6.1 Appendix 4A: Markov chain approach

4.6.1.1 The Markov chain approach for the NPCUSUM-EX control chart

There are two main approaches to studying the run-length distribution of a CUSUM chart. For continuous observations, Page (1954) described an integral equation approach. An alternative method based on Markov chain theory was developed by Brook and Evans (1972). Since the proposed chart is a binomial CUSUM chart conditionally on $X_{(r)}$, we can use the results of Gan (1993) to derive the conditional run-length distribution. Then the unconditional run-length distribution is obtained by simply averaging over the distribution of $X_{(r)}$.

In order to implement the Markov chain approach, we introduce some new notations. Write $k = nk^*$ such that $(nd + k) = n(d + k^*) = nd^*$, say, so that $k = n(d^* - d)$. Note that when $k = 0$, $d^* = d$. Thus the charting statistic in Equation (4.2) can be expressed as

$$C_j = \max[0, C_{j-1} + (U_{j,r} - nd^*)], \text{ for } j = 1,2,3, \ldots$$

with $C_0 = 0$.

Note that the charting statistic above is very similar to the one proposed in Gan (1993); the latter defined the binomial CUSUM statistic as $C_j = \max[0, C_{j-1} + X_j - k]$ for $j = 1,2,3, \ldots$ and $k = a/b$. Thus, in order to use the results in Gan (1993) we need a similar expression and, accordingly, we set $nd^* = a/b$ so that $d^* = a/nb$. Now, as in Gan (1993) suppose that $H = c/nb$ and (already defined) $d^* = a/nb$ where a, b and c are all positive integers. Then, again as in Gan (1993), when the process is declared to be IC the possible values of C_j are given by $\{0, 1/nb, 2/nb, \ldots, c/nb\}$; these are the transient states of the Markov chain. If $C_j > c/nb$, then the process is declared to be OOC and C_j is said to be in the absorbing state. Using the simplified notation structure of Gan (1993) by labeling the transient states as $\{1, 2, \ldots, c + 1\}$ corresponding to $\left\{C_j = \frac{i}{nb};\ i = 0,1,2, \ldots, c\right\}$, respectively, and by denoting the $(c + 2)^{\text{th}}$ state as the absorbing state, we can write the one-step transition probability matrix in a partitioned form

$$M = \begin{pmatrix} Q & \underline{p} \\ \underline{0}' & 1 \end{pmatrix} = \begin{pmatrix} p_{11} & p_{12} & \cdots & \cdots & p_{1,c+1} & p_{1,c+2} \\ p_{21} & p_{22} & \cdots & \cdots & p_{2,c+1} & p_{2,c+2} \\ & \cdots & & & \cdots & \\ & \cdots & & & \cdots & \\ p_{c+1,1} & p_{c+1,0} & & & p_{c+1,c+1} & p_{c+1,c+2} \\ 0 & 0 & \cdots & & 0 & 1 \end{pmatrix}$$

where p_{ij} denotes the one-step transition probability from state i to state j; the essential transition probability sub-matrix Q contains all the probabilities of going from one transient state to another; the column vector $\underline{p}$ contains all the probabilities of going from each transient state to the absorbing state; $\underline{0}'$ a row vector of zeros which contains all the probabilities of going from the absorbing state to each transient state and the scalar value 1 is the probability of going from the absorbing state to the absorbing state. The elements of the essential transition probability sub-matrix Q may be calculated given $X_{(r)} = x_{(r)}$ and it is easy to see that, for $i = 1, 2, \ldots, c+1$,

$$\begin{aligned} p_{i1} &= P\left(C_j = 0 \,\middle|\, C_{j-1} = \tfrac{i-1}{b};\ X_{(r)} = x_{(r)}\right) \\ &= P\left(\max[0, C_{j-1} + (U_{j,r} - nd^*)] = 0 \,\middle|\, C_{j-1} = \tfrac{i-1}{b};\ X_{(r)} = x_{(r)}\right) \end{aligned}$$

Note that in order for $\max[0, C_{j-1} + (U_{j,r} - nd^*)]$ to equal zero, $C_{j-1} + (U_{j,r} - nd^*)$ must be less than or equal to zero. Therefore,

$$\begin{aligned} p_{i1} &= P\left(C_{j-1} + U_{j,r} - nd^* \le 0 \,\middle|\, C_{j-1} = \tfrac{i-1}{b};\ X_{(r)} = x_{(r)}\right) \\ &= P\left(\tfrac{i-1}{b} + U_{j,r} - n\left(\tfrac{a}{nb}\right) \le 0 \,\middle|\, X_{(r)} = x_{(r)}\right) \text{ since } d^* = a/nb \\ &= P\left(U_{j,r} \le \tfrac{a-i+1}{b} \,\middle|\, X_{(r)} = x_{(r)}\right) \text{ with } \tfrac{a-i+1}{b} \ge 0 \text{ since } U_{j,r}|X_{(r)} \sim BIN(n, p_r) \end{aligned}$$

Therefore,

$$p_{i1} = \begin{cases} P\left(U_{j,r} \le \dfrac{a-i+1}{b} \,\middle|\, X_{(r)} = x_{(r)}\right) & \text{if } \dfrac{a-i+1}{b} \ge 0 \\ 0 & \text{otherwise} \end{cases}.$$

Similarly for $i = 1, 2, \ldots, c+1$, and for $j = 2, 3, \ldots, c+1$, we have that

$$p_{ij} = P\left(C_j = \frac{j-1}{b} \,\middle|\, C_{k-1} = \frac{i-1}{b};\ X_{(r)} = x_{(r)}\right)$$

$$= \begin{cases} P\left(U_{j,r} \leq \dfrac{a - i + j}{b} \middle| X_{(r)} = x_{(r)}\right) & \text{if} \quad \dfrac{a - i + j}{b} = 0,1,\ldots,n \\ 0 & \text{otherwise} \end{cases}.$$

Note that the conditional probabilities can be calculated directly using Result 4B.1 in Appendix 4B, that is, given $X_{(r)} = x_{(r)}$, $U_{j,r}$ follows a binomial distribution with parameters (n, p_r) where $p_r = P(Y > X_{(r)} | X_{(r)})$. For the NPCUSUM-EX median chart based on the reference sample median, we may substitute n and 2 for a and b, respectively (so that $d = 0.5$). Note that when the process is IC, $p_r = 1 - V_{(r)}$, where $V_{(r)} = F(X_{(r)})$ follows a beta distribution with parameters r and $m - r + 1$ whatever the continuous F may be. Now defining N_i as the run-length variable with a starting value equal to $(i-1)/b$, i.e. $C_0 = \frac{i-1}{nb}$ and $\mu_i = E(N_i | X_{(r)})$ as the conditional average run-length for $i = 1, 2, \ldots, c+1$, we have, from the properties of Markov chains (see Section 1.10.1),

$$\underline{\mu} = (\mu_1, \mu_2, \ldots, \mu_{c+1})' = (I - Q)^{-1}\underline{1}. \qquad \text{(A1)}$$

the unconditional *ARL* is given by averaging this over the probability distribution of $X_{(r)}$. Thus, the unconditional average run-length is given by

$$\mu_1^* = EE(N_1 | X_{(r)}) = \int E(N_1 | X_{(r)})\, dF(X_{(r)}) = \int \mu_1\, dF(X_{(r)}) = \int \mu_1\, dV_{(r)}. \qquad \text{(A2)}$$

Expressions for the conditional and unconditional run-length distributions can be obtained similarly using properties and results of Markov chains from which other run-length distribution characteristics such as the standard deviation and the percentiles can be found.

Note that using Equation (A2), one can approximate the unconditional ARL_0, replacing the integral in Equation (A2) by a sum, which yields

$$ARL_0 = \mu_1^*(\text{IC}) = \lim_{l \to 0} \sum_{\varsigma} (\mu_1 | p_r = \varsigma, \text{IC}) \int_{\varsigma - \frac{l}{2}}^{\varsigma + \frac{l}{2}} \frac{1}{B(r, m - r + 1)} y^{r-1}(1-y)^{m-r} dy, \qquad \text{(A3)}$$

where ς ranges from $a - l/2$ to $b + l/2$ in steps of l; l is a small positive proper fraction; a and b are such that $0 < a < b < 1$, satisfying

$$\int_0^a \mu_1 \, dV_{(r)} \cong 0 \;\; and \;\; \int_b^1 \mu_1 \, dV_{(r)} \cong 0.$$

The IC conditional mean, $(\mu_1 | p_r = \varsigma, \text{IC})$, can be calculated by using the Markov chain formula in (A1). Let us consider an example. Suppose m = 1000, n = 5, H = 15 and we consider exceedance over the median. For even m, the quantity r is not unique but approximately take r = 500.5. Hence the IC distribution of p_r is (approximately) a *Beta*(500.5, 500.5). Take a value of p_r, say 0.35. In the IC case, $P(p_r < 0.35|\text{IC}) = 3.963355 \times 10^{-22}$. Further, using (A1), we find $(\mu_1 | p_r = 0.35, \text{IC}) = 9.39 \times 10^9$. Since $P(p_r < 0.35|\text{IC}) \approx 0$, the contribution of $(\mu_1 | p_r = 0.35, \text{IC})\, P[p_r \in \Delta_{0.35,\varepsilon}]$ is of the order 10^{-13} and is therefore negligible, where $\Delta_{0.35,\varepsilon}$ is an ε-neighbourhood (ε close to zero) containing 0.35.

Similarly $P(Z > 0.65 \mid Beta(500.5, 500.5)) \approx 0$. The main point is that for calculating the unconditional ARL_0 using (A3), it is sufficient to consider values for ς in the interval (0.3, 0.7) as other values of ς do not contribute any significant amounts in the sum. This interval, however, will vary with m as well as r and has to be determined with care. For example, for m = 1000, n = 5 and H = 15 we may set a = 0.3, l = 0.0001 and b = 0.7. Thus we find from (A3)

$$\mu_1^*(IC) = \sum_{\varsigma=0.29995(0.0001)0.70005} (\mu_1 | \, p_r = \varsigma) \int_{\varsigma-0.00005}^{\varsigma+0.00005} f(t)dt,$$

where $f(t)$ is the pdf of the *Beta*(500.5, 500.5) distribution. This yields μ_1^* = 352.359 (the ARL_0). If on the other hand, we set l = 0.00005, that is, if we use a smaller partition of the interval, we get a slightly better approximation μ_1^* = 352.3584. However, these two results are pretty close for all practical proposes. Therefore, we use l = 0.0001 and calculate the ARL_0 for m = 1000 and n = 5 for H = 15.5 and 16.5, respectively, employing the above technique. The results obtained are 388.7368 and 474.3201, respectively. Note that these findings are very similar to the results in Table 4.2 obtained via Monte Carlo simulation, in course of finding H under a nominal ARL_0 of 370 and 500 for m = 1000 and n = 5. Moreover, matrix inversion is often troublesome when ς is close to 0 or 1 and hence this process is not very efficient if m is small. In addition, for large matrices, matrix inversion, using SAS® v 9.3, can be very time-consuming. Thus in this dissertation we use Monte Carlo simulations (see Section 1.10.2) to evaluate the run-length distribution instead of the above

method, which requires extreme care and large m, to work efficiently. Although the values of the run-length percentiles are found to be very stable under the two methods, slight sampling fluctuations were observed. We used 100 000 Monte Carlo simulations to achieve reasonably small standard error, that is within the 2% error bands satisfying the modified Mundfrom's criteria (see Schaffer and Kim (2007)), of the estimated values.

4.6.1.2 The Markov chain approach for the NPEWMA-EX control chart

The reader is referred to Section 1.10.1 for a detailed discussion of the Markov chain appraoch. Here, only the steps regarding the Markov chain approach for the NPEWMA-EX chart are provided.

Step 1:

Obtain the transition probability matrix M (see Equation (1.11) and Section 1.10.1 for a thorough discussion on setting up the transition probability matrix).

Step 2:

Compute the transition probabilities, p_{ij}'s, where p_{ij} is the conditional probability that the charting statistic at time k, Z_k, lies within state j, given that the charting statistic at time $k-1$, Z_{k-1}, lies within state i (an approximation to the latter probability is obtained by setting Z_{k-1} equal to S_i which denotes the midpoint of state i), that is

$$p_{ij} = P\left(Z_k \text{ lies within state } j \middle| Z_{k-1} \text{ lies within state } i;\ X_{(r)} = x_{(r)}\right)$$

$$= P\left(S_j - \tau < Z_k \leq S_j + \tau | Z_{k-1} = S_i;\ X_{(r)} = x_{(r)}\right)$$

$$= P\left(\frac{(S_j-\tau)-(1-\lambda)S_i}{\lambda} < U_{k,r} \leq \frac{(S_j+\tau)-(1-\lambda)S_i}{\lambda} \middle| X_{(r)} = x_{(r)}\right).$$

Step 3:

Using results from Fu and Lou (2003), calculate the conditional *ARL* the of run-length variable N for a given $X_{(r)}$ given by $E\ (N|\ X_{(r)})$ using Equation (1.13). For the IC case, the p_{ij}'s are calculated assuming the process is IC which yields the conditional IC *ARL*.

Step 4:

The unconditional *ARL* of N is given by averaging the conditional *ARL* over the probability distribution of $X_{(r)}$. Thus, the unconditional *ARL* is given by

$$\mu^* = EE\ (N|\ X_{(r)}) = \int E\ (N|\ X_{(r)})\ dF(X_{(r)}) = \int \mu\, dV_{(r)},\ \text{say.}$$

In the IC case, this may be approximated by applying numerical integration using the relation

$$ARL_0 = \mu^*(\text{IC}) = \lim_{l\to 0} \sum_{\varsigma}(\mu|\ p_r = \varsigma, \text{IC}) \int_{\varsigma-\frac{l}{2}}^{\varsigma+\frac{l}{2}} \frac{1}{B(r,m-r+1)} y^{r-1}(1-y)^{m-r} dy,$$

where ς ranges from $a - l/2$ to $b + l/2$ in steps of l, l is a small positive proper fraction, a and b are such that $0 < a < b < 1$, satisfying

$$\int_0^a \mu\, dV_{(r)} \cong 0 \ \text{ and } \int_b^1 \mu\, dV_{(r)} \cong 0.$$

Expressions for the conditional and unconditional run-length distributions can be obtained quite similarly using properties and results of Markov chains (see Equations (1.12) to (1.15)), from which other run-length distribution characteristics such as the standard deviation and the percentiles can be found.

4.6.2 Appendix 4B: Some mathematical results

Result 4B.1

Given (conditionally on) $X_{(r)}$, the $U_{j,r}$'s are independently binomially distributed with parameters (n, p_r) for any $j = 1,2,3, \dots$, i.e. $U_{j,r}|X_{(r)} \sim BIN(n, p_r)$.

Proof

Since $U_{j,r}$ is the number of Y-observations in the j^{th} Phase II sample that exceeds $X_{(r)}$, given $X_{(r)}$, the random variable $U_{j,r}$ follows a binomial distribution with parameters (n, p_r) where $p_r = P[Y > X_{(r)}| X_{(r)}]$.

Result 4B.2

The (unconditional) IC distribution of $U_{j,r}$ $(\forall j)$, for a fixed j, is distribution-free and is given by the pmf

$$P(U_{j,r} = u) = \frac{\binom{u+m-r}{u}\binom{n-u+r-1}{n-u}}{\binom{m+n}{n}} \text{ with } u = 0,1,2, \dots, n.$$

Proof

If $U_{j,r} = u$, then u of the Y-observations in the j^{th} Phase II sample are greater than $X_{(r)}$ and, consequently, $n - u$ of the Y-observations in the j^{th} Phase II sample are less than or equal to $X_{(r)}$. If we combine the reference sample (containing m X-observations) with the test sample (containing n Y-observations) we obtain a single sample consisting of $N = m + n$ observations. From this combined sample, r X-observations and $n - u$ Y-observations in the j^{th} Phase II sample are less than or equal to $X_{(r)}$. On the other hand, $m - r$ X-observations and u Y-observations in the j^{th} Phase II sample are greater than $X_{(r)}$. There is a total of $n - u + r - 1$ observations that are less than $X_{(r)}$ and $u + m - r$ observations that are greater than $X_{(r)}$. The unconditional IC distribution of $U_{j,r}$ can be obtained by using combinatorics which allows one to count the number of

experimental outcomes when the experiment involves selecting a number of objects, say t, from a larger set of objects, say T. The rule then states that the number of combinations of T objects taken t at a time is given by $\binom{T}{t}$. By using such combinatorial arguments the unconditional IC distribution of $U_{j,r}$ $(\forall j)$ is given by

$$P(U_{j,r} = u) = \frac{\binom{u+m-r}{u}\binom{n-u+r-1}{n-u}}{\binom{m+n}{n}} \text{ with } u = 0,1,2,\dots,n.$$

Thus, the unconditional IC distribution of $U_{j,r}$ $(\forall j)$ is the negative hypergeometric distribution (see Randles and Wolfe (1979) page 373). Note that Result 4B.2 has been obtained by other researchers more directly; see, for example, Chakraborti and Van der Laan (2000) Remark 2.

Next we extend Result 4B.2 and show that the (unconditional) joint distribution of $U_{j,r}$ for $j = 1,2,\dots,v$ is distribution-free when the process is IC. This establishes that the NPEWMA-EX and NPCUSUM-EX charts are distribution-free.

Result 4B.3

The unconditional IC distribution of $U_{j,r}$ for $j = 1,2,\dots,v$ where $v > 1$ is a positive integer, is distribution-free.

Proof

Firstly, the probability integral transformation is considered. If $U = F_X(X)$ then U has a uniform(0,1) distribution and $U_{(r)} = F_X(X_{(r)})$ is the r^{th} order statistic of a random sample from the uniform(0,1) distribution function with density function

$$f_{U_{(r)}}(u) = \frac{1}{B(r, m-r+1)} u^{r-1}(1-u)^{m-r}, \qquad 0 \le u \le 1 \tag{A4.1}$$

which is the $Beta(r, m-r+1)$ distribution. Note that $B(r, m-r+1) = \frac{(r-1)!(m-r)!}{m!}$.

Now, suppose that $u_{j,r}$ assumes the values $0,1,2,\dots,n$ for all $j = 1,2,\dots,v$ then by noting that

i. from Result 4B.1, given $X_{(r)}$, the $U_{j,r}$, $j = 1,2,\dots,v$, are independent $BIN(n, p_r)$ variables,

ii. when averaging over the distribution of $X_{(r)}$, we find the unconditional distribution of $U_{j,r}$, i.e.

$$\begin{aligned} P(U_{j,r} = u) &= E\left[P\left(U_{j,r} = u \middle| X_{(r)}\right)\right] = \binom{n}{u} \int p_r^u (1 - p_r)^{n-u}\, dF\left(X_{(r)}\right) \\ &= \binom{n}{u} \int [1 - G(t)]^u [G(t)]^{n-u}\, dF_{X_{(r)}}(t) \end{aligned} \tag{A4.2}$$

and

iii. when the process is in-control we have $F = G$ in point (ii) or, stated differently, the in-control $p_r = 1 - F\left(x_{(r)}\right)$.

Then, by using all the above information, the joint distribution of $(U_{1,r}, U_{2,r}, \dots, U_{v,r})$, when the process is IC, is given by

$$P\left(U_{1,r} = u_1, U_{2,r} = u_2, \dots, U_{v,r} = u_v\right)$$

$$= E_{X_{(r)}}\left(P\left(U_{1,r} = u_1\,, U_{2,r} = u_2, \dots, U_{v,r} = u_v \mid X_{(r)} = x_{(r)}\right)\right)$$

$$= \binom{n}{u_1}\binom{n}{u_2}\dots\binom{n}{u_v}\int_{-\infty}^{\infty} p_r^{\sum_{j=1}^{v} u_j}(1-p_r)^{nv-\sum_{j=1}^{v} u_j} f_{X_{(r)}}\left(x_{(r)}\right)dx_{(r)}$$ from Equation (A4.2)

$$= \binom{n}{u_1}\binom{n}{u_2}\dots\binom{n}{u_v}\int_{-\infty}^{\infty}\left(1-P\left(Y \le X_{(r)}\right)\right)^{\sum_{j=1}^{v} u_j}\left(P\left(Y \le X_{(r)}\right)\right)^{nv-\sum_{j=1}^{v} u_j} f_{X_{(r)}}\left(x_{(r)}\right)dx_{(r)}$$

$$= \binom{n}{u_1}\binom{n}{u_2}\dots\binom{n}{u_v}\int_{-\infty}^{\infty}\left(1-G\left(X_{(r)}\right)\right)^{\sum_{j=1}^{v} u_j}\left(G\left(X_{(r)}\right)\right)^{nv-\sum_{j=1}^{v} u_j} f_{X_{(r)}}\left(x_{(r)}\right)dx_{(r)}$$ since $Y_{ji} \sim$ iid G $(i = 1,2,\dots,n\,;\; j = 1,2,\dots)$ it follows

$$P\left(Y \le X_{(r)}\right) = G\left(X_{(r)}\right)$$

$$= \binom{n}{u_1}\binom{n}{u_2}\dots\binom{n}{u_v}\int_0^1\left(1-G(F^{-1}(t))\right)^{\sum_{j=1}^{v} u_j}\left(G(F^{-1}(t))\right)^{nv-\sum_{j=1}^{v} u_j} f_{U_{(r)}}(t)dt$$ with the pdf of $U_{(r)} \sim Beta(r, m-r+1)$

If the process is IC if follows that $G = F$ and, consequently, $G(F^{-1}(t)) = t$. Thus,

$$= \binom{n}{u_1}\binom{n}{u_2}\dots\binom{n}{u_v}\int_0^1(1-t)^{\sum_{j=1}^{v} u_j}(t)^{nv-\sum_{j=1}^{v} u_j}\frac{t^{r-1}(1-t)^{m-r}}{B(r,m-r+1)}dt$$ from Equation (A4.1)

$$= \binom{n}{u_1}\binom{n}{u_2}\dots\binom{n}{u_v}\int_0^1\frac{t^{\left(nv+r-\sum_{j=1}^{v} u_j\right)-1}(1-t)^{\left(\sum_{j=1}^{v} u_j+m-r+1\right)-1}}{B(r,m-r+1)}dt$$

$$= \binom{n}{u_1}\binom{n}{u_2}\dots\binom{n}{u_v}\frac{B\left(nv+r-\sum_{j=1}^{v}u_j,\ \sum_{j=1}^{v}u_j+m-r+1\right)}{B(r,\ m-r+1)}$$

$$= \binom{n}{u_1}\binom{n}{u_2}\dots\binom{n}{u_v}\frac{B\left(\sum_{j=1}^{v}u_j+m-r+1,\ nv+r-\sum_{j=1}^{v}u_j\right)}{B(r,\ m-r+1)} \quad \text{since } B(a,b)=B(b,a)$$

Hence the unconditional IC joint distribution of exceedance statistics from any fixed number of independent Phase II samples is distribution-free.

Result 4B.4

For exact time-varying control limits, we have

$$E\left(Z_j|\ \text{IC}\right) = n(1-a)\left(1-(1-\lambda)^j\right)$$

and (4.6)

$$STDEV\left(Z_j|\ \text{IC}\right) = \sqrt{\left(\frac{na(1-a)}{m+2}\right)\left\{n(1-(1-\lambda)^j)^2 + \frac{\lambda(m+1)}{2-\lambda}(1-(1-\lambda)^{2j})\right\}}.$$

Proof

The conditional IC expected value of the charting statistic ($\boldsymbol{Z_j = \left(\lambda U_{j,r} + (1-\lambda)Z_{j-1}\right)}$):

By using properties of expected values, recursive substitution (see Appendix 1A) and a finite geometric series (see Equation (A1.4) in Appendix 1A) together with the fact that $E\left(U_{j,r}|X_{(r)}\right) = np_r\ \forall j\ (j = 1,2,\dots)$ and $Z_0 = 0$ we obtain the following:

$$\begin{aligned}
&E\left(Z_j|X_{(r)}\right)\\
&= E\left(\lambda U_{j,r} + (1-\lambda)Z_{j-1}|X_{(r)}\right)\\
&= E\left(\lambda\textstyle\sum_{k=0}^{j-1}(1-\lambda)^k\, U_{j-k,r} + (1-\lambda)^j Z_0|X_{(r)}\right)\\
&= np_r\left(1-(1-\lambda)^j\right)
\end{aligned}$$

The conditional IC variance and standard deviation of the charting statistic ($\boldsymbol{Z_j = \left(\lambda U_{j,r} + (1-\lambda)Z_{j-1}\right)}$):

By using properties of variance, recursive substitution (see Appendix 1A) and a finite geometric series (see Equation (A1.4) in Appendix 1A) along with the fact that $VAR\left(U_{j,r}|X_{(r)}\right) = np_r(1-p_r)\ \forall j\ (j = 1,2,\dots)$ we obtain the following:

$$VAR\left(Z_j|X_{(r)}\right)$$
$$= VAR\left(\lambda\sum_{k=0}^{j-1}(1-\lambda)^k U_{j-k,r} + (1-\lambda)^j Z_0|X_{(r)}\right)$$
$$= np_r(1-p_r)\lambda^2\left(\frac{1-(1-\lambda)^{2j}}{1-(1-\lambda)^2}\right)$$

The last expression simplifies to $np_r(1-p_r)\lambda\left(\frac{1-(1-\lambda)^{2j}}{2-\lambda}\right)$ so that

$$STDEV\left(Z_j|X_{(r)}\right) = \sqrt{\frac{\lambda}{2-\lambda}(1-(1-\lambda)^{2j})np_r(1-p_r)}.$$

In order to obtain the unconditional properties of the charting statistic, we first have to provide some properties of p_r.

Properties of p_r:

In the IC case $F\left(X_{(r)}\right) = 1-p_r$ follows a Beta distribution with parameters r and $m+1-r$.

Hence,

$E(p_r) = \frac{m+1-r}{m+1}$ and $E(p_r^2) = \frac{m^2+3m+2-2rm-3r+r^2}{(m+1)(m+2)}$ so that $VAR(p_r) = \frac{r(m+1-r)}{(m+1)^2(m+2)}$.

The unconditional IC expected value of the charting statistic ($Z_j = \left(\lambda U_{j,r} + (1-\lambda)Z_{j-1}\right)$):

$$E\left(Z_j\right) = E_{X_{(r)}}E\left(Z_j \mid X_{(r)}\right) = E_{X_{(r)}}\left(np_r\left(1-(1-\lambda)^j\right)\right) = n\left(1-(1-\lambda)^j\right)E_{X_{(r)}}(p_r) =$$
$$n\left(1-(1-\lambda)^j\right)\left(\frac{m+1-r}{m+1}\right) = n\left(1-(1-\lambda)^j\right)(1-a)$$
where $a = r/(m+1)$.

The unconditional IC variance and standard deviation of the charting statistic ($\boldsymbol{Z_j = (\lambda U_{j,r} + (1-\lambda) Z_{j-1})}$:

$$var(Z_j) = var\left[E\left(Z_j \middle| X_{(r)}\right)\right] + E\left[var\left(Z_j \middle| X_{(r)}\right)\right]$$

$$= var\left[np_r\left(1-(1-\lambda)^j\right)\right] + E\left[\frac{\lambda}{2-\lambda}\left(1-(1-\lambda)^{2j}\right)np_r(1-p_r)\right]$$

$$= n^2\left(1-(1-\lambda)^j\right)^2 var(p_r) + \frac{\lambda}{2-\lambda}\left(1-(1-\lambda)^{2j}\right)n(E(p_r) - E(p_r^2))$$

$$= n^2 \frac{r(m-r+1)}{(m+1)^2(m+2)}\left(1-(1-\lambda)^j\right)^2 + \frac{\lambda}{2-\lambda}\left(1-(1-\lambda)^{2j}\right)n\frac{r(m-r+1)}{(m+1)(m+2)}$$

$$= n^2 \frac{r(m-r+1)}{(m+1)(m+1)(m+2)}\left(1-(1-\lambda)^j\right)^2 + \frac{\lambda}{2-\lambda}\left(1-(1-\lambda)^{2j}\right)n\frac{r(m-r+1)}{(m+1)(m+2)}$$

$$= n\frac{a(1-a)}{(m+2)}\left\{n\left(1-(1-\lambda)^j\right)^2 + \frac{\lambda(m+1)}{2-\lambda}\left(1-(1-\lambda)^{2j}\right)\right\}$$

where $a = r/(m+1)$.

Therefore,

$$STDEV\left(Z_j \middle| \text{ IC}\right) = \sqrt{\left(\frac{na(1-a)}{m+2}\right)\left\{n(1-(1-\lambda)^j)^2 + \frac{\lambda(m+1)}{2-\lambda}(1-(1-\lambda)^{2j})\right\}}.$$

For steady-state control limits, we have

$$E(Z_j|\,\mathrm{IC}) = n(1-a)$$

and (4.6)

$$STDEV(Z_j|\,\mathrm{IC}) = \sqrt{\left(\frac{na(1-a)}{m+2}\right)\left\{n + \frac{\lambda(m+1)}{2-\lambda}\right\}}.$$

Proof

The conditional IC expected value of the charting statistic ($\boldsymbol{Z_j = (\lambda U_{j,r} + (1-\lambda)Z_{j-1})}$):

By using properties of expected values, recursive substitution (see Appendix 1A) and a finite geometric series (see Equation (A1.4) in Appendix 1A) together with the fact that $E(U_{j,r}|X_{(r)}) = np_r\ \forall j\ (j = 1,2,\dots)$ and $Z_0 = np_r$ we obtain the following:

$$\begin{aligned}
&E(Z_j|X_{(r)}) \\
&= E(\lambda U_{j,r} + (1-\lambda)Z_{j-1}|X_{(r)}) \\
&= E\left(\lambda \textstyle\sum_{k=0}^{j-1}(1-\lambda)^k U_{j-k,r} + (1-\lambda)^j Z_0|X_{(r)}\right) \\
&= np_r\left(1-(1-\lambda)^j\right) + np_r(1-\lambda)^j \\
&= np_r
\end{aligned}$$

The conditional IC variance and standard deviation of the charting statistic ($\boldsymbol{Z_j = (\lambda U_{j,r} + (1-\lambda)Z_{j-1})}$):

By using properties of variance, recursive substitution (see Appendix 1A) and a finite geometric series (see Equation (A1.4) in Appendix 1A) along with the fact that $VAR(U_{j,r}|X_{(r)}) = np_r(1-p_r)\ \forall j\ (j = 1,2,\dots)$ we obtain the following:

$$VAR\left(Z_j|X_{(r)}\right)$$
$$= VAR\left(\lambda\sum_{k=0}^{j-1}(1-\lambda)^k U_{j-k,r} + (1-\lambda)^j Z_0|X_{(r)}\right)$$
$$= np_r(1-p_r)\lambda^2\left(\frac{1-(1-\lambda)^{2j}}{1-(1-\lambda)^2}\right)$$

The last expression simplifies to $np_r(1-p_r)\lambda\left(\frac{1-(1-\lambda)^{2j}}{2-\lambda}\right)$ so that

$$STDEV\left(Z_j|X_{(r)}\right) = \sqrt{\frac{\lambda}{2-\lambda}(1-(1-\lambda)^{2j})np_r(1-p_r)}.$$

However, the term $\left(1-(1-\lambda)^{2j}\right)$ approach unity as $j \to \infty$, so that the term can be dropped.

$$STDEV\left(Z_j|X_{(r)}\right) = \sqrt{\frac{\lambda}{2-\lambda}np_r(1-p_r)}.$$

In order to obtain the unconditional properties of the charting statistic, we first have to provide some properties of p_r.

Properties of p_r:

In the IC case $F\left(X_{(r)}\right) = 1-p_r$ follows a Beta distribution with parameters r and $m+1-r$.

Hence,

$E(p_r) = \frac{m+1-r}{m+1}$ and $E(p_r^2) = \frac{m^2+3m+2-2rm-3r+r^2}{(m+1)(m+2)}$ so that $VAR(p_r) = \frac{r(m+1-r)}{(m+1)^2(m+2)}$.

The unconditional IC expected value of the charting statistic ($Z_j = \left(\lambda U_{j,r} + (1-\lambda)Z_{j-1}\right)$):

$$E\left(Z_j\right) = E_{X_{(r)}}\left(Z_j \mid X_{(r)}\right) = E_{X_{(r)}}(np_r) = nE_{X_{(r)}}(p_r) = n\left(\frac{m+1-r}{m+1}\right) = n(1-a)$$

where $a = r/(m+1)$.

The unconditional IC variance and standard deviation of the charting statistic ($\boldsymbol{Z_j = \left(\lambda U_{j,r} + (1-\lambda)Z_{j-1}\right)}$):

$$var(Z_j) = var\left[E\left(Z_j \middle| X_{(r)}\right)\right] + E\left[var\left(Z_j \middle| X_{(r)}\right)\right]$$

$$= var[np_r] + E\left[\frac{\lambda}{2-\lambda} np_r(1-p_r)\right]$$

$$= n^2 var(p_r) + \frac{\lambda}{2-\lambda} n(E(p_r) - E(p_r^2))$$

$$= n^2 \frac{r(m-r+1)}{(m+1)^2(m+2)} + \frac{\lambda}{2-\lambda} n \frac{r(m-r+1)}{(m+1)(m+2)}$$

$$= n^2 \frac{r(m-r+1)}{(m+1)(m+1)(m+2)} + \frac{\lambda}{2-\lambda} n \frac{r(m-r+1)}{(m+1)(m+2)}$$

$$= n \frac{a(1-a)}{(m+2)} \left\{n + \frac{\lambda(m+1)}{2-\lambda}\right\}$$

where $a = r/(m+1)$.

Therefore,

$$STDEV\left(Z_j \middle| \text{ IC}\right) = \sqrt{\left(\frac{na(1-a)}{m+2}\right)\left\{n + \frac{\lambda(m+1)}{2-\lambda}\right\}}.$$

4.6.3 Appendix 4C: Winsorization

As is well-known, the *ARL* isn't a robust measure, i.e. it is dramatically impacted by the presence of outliers and, consequently, using winsorization is often necessary for practical applications. This further complicates the interpretation. In this section Monte Carlo simulations using small reference sample sizes are considered for the NPCUSUM-EX control chart. When $m < 200$, we recommend setting a-priori the maximum allowable length (of monitoring) at a certain high level, say, S. This will eliminate the possibility of high extreme runs by induced termination at S, which may be 10 to 15 times the nominal ARL_0. Therefore, in course of estimation of the run-length via Monte Carlo studies, if we don't observe a value of the run-length variable (i.e. if the chart does signal) less than or equal to S, we enforce termination of the monitoring process (simulation of data) and set the run-length value equal to S. As a result, we obtain a winsorized *ARL* with winsorization at the upper tail of the run-length distribution.

While Tables 4.8 to 4.12 are based on Monte Carlo simulations with termination enforced at $S = 5000$ simulations, in Tables 4C.1 and 4C.2, we present a case study when a termination is enforced at $S = 2000$ simulations. In all those tables, we record the percentage of simulation replicates that naturally terminate before S and refer it as winsorization level (WL). Tables 4C.1 and 4C.2 show the effect of the choice of a lower value of S. For brevity, only the normal distribution and target $ARL_0 = 370$ (for Table 4C.1) and target $ARL_0 = 500$ (for Table 4C.2) are considered. We see from Tables 4C.1 and 4C.2 that the control limits are naturally overestimated and as a consequence the OOC run-lengths also increase a little when the shift is small. The following points are essential to note while working with winsorization:

i. The winsorized *ARL* with winsorization at the upper tail of the run-length distribution slightly underestimates the true *ARL*.

ii. Winsorization at the upper tail of the run-length distribution stabilizes the variance and, consequently, increases the efficiency of the estimate of the ARL_0.

iii. H^* determined on the basis of the winsorized ARL_0 overestimates the true H.

Table 4C.1. The IC and OOC characteristics[xli] of the run-length distribution for $m = 100$ and $n = 5$ for the $N(0,1)$ distribution with nominal $ARL_0 = 370$ and winsorization at the 2000th step

	Chart Type					
	Parametric CUSUM-$\overline{X}$ chart with parameters estimated from a Phase I sample		NPCUSUM-Rank chart		NPCUSUM-EX median chart	
Winsorization level (WL)	WL = 90.6	WL = 92.6	WL = 90.6	WL = 92.7	WL = 90.7	WL = 92.9
Control limits	$H = 9.00$	$H = 5.20$	$H = 595.0$	$H = 94.1$	$H = 10.35$	$H = 5.15$
k	0	$0.5\sigma/\sqrt{n}$	0	$0.5\sqrt{mn(m+n+1)/12}$	0	$k = n(d^* - d)$ $= 5 \times 0.07 = 0.35$
d^* / γ	NA	NA	NA	NA	0.50	$0.5\sqrt{\frac{n(m+n+1)}{4(m+2)}} \approx 0.57$
0.00	367.44 (612.93) 15, 34, 78, 303, 2000	365.84 (576.38) 11, 34, 101, 359, 2000	369.49 (612.77) 15, 33, 80, 309, 2000	368.60 (543.36) 7, 39, 129, 412, 2000	366.25 (611.08) 15, 34, 80, 304, 2000	371.06 (568.33) 11, 37, 112, 387, 2000
0.25	81.82 (224.01) 10, 18, 29, 55, 258	98.61 (247.75) 7, 15, 29, 72, 386	84.66 (237.11) 10, 17, 28, 55, 270	109.51 (232.28) 4, 14, 38, 101, 440	110.48 (285.48) 11, 20, 33, 70, 427	133.13 (284.64) 8, 18, 42, 104, 547
0.50	25.60 (50.31) 8, 12, 17, 26, 59	26.99 (62.22) 5, 9, 14, 25, 78	26.19 (58.50) 8, 12, 17, 26, 61	36.57 (81.63) 3, 8, 16, 36, 124	37.97 (102.56) 9, 14, 21, 33, 105	45.90 (114.99) 6, 11, 19, 39, 158
0.75	14.37 (9.07) 7, 9, 12, 17, 29	12.71 (14.03) 4, 6, 9, 15, 31	14.75 (9.76) 6, 9, 12, 17, 30	15.52 (24.71) 2, 5, 9, 17, 46	18.93 (17.13) 8, 11, 15, 21, 41	20.89 (36.14) 5, 8, 13, 22, 58
1.00	10.51 (4.81) 5, 8, 10, 12, 19	8.26 (5.23) 3, 5, 7, 10, 17	10.76 (4.94) 5, 8, 10, 13, 19	8.55 (8.27) 2, 4, 7, 10, 22	13.62 (7.38) 7, 9, 12, 16, 25	12.13 (11.61) 4, 7, 9, 14, 30
1.50	6.98 (2.16) 4, 5, 7, 8, 11	5.07 (2.08) 3, 4, 5, 6, 9	7.31 (2.31) 4, 6, 7, 9, 11	4.63 (2.61) 2, 3, 4, 6, 9	9.19 (2.95) 6, 7, 9, 11, 15	6.97 (3.60) 3, 5, 6, 8, 14
2.00	5.28 (1.35) 3, 4, 5, 6, 8	3.70 (1.23) 2, 3, 3, 4, 6	5.70 (1.43) 4, 5, 5, 6, 8	3.34 (1.45) 2, 2, 3, 4, 6	7.22 (1.83) 5, 6, 7, 8, 11	5.10 (2.04) 3, 4, 5, 6, 8

[xli] Note that, the first row of each of the cells shows the *ARL* and *SDRL* values whereas the second row shows the 5th, 25th, 50th, 75th and 95th percentiles (in this order).

Table 4C.2. The IC and OOC characteristics[xlii] of the run-length distribution for $m = 100$ and $n = 5$ for the $N(0,1)$ distribution with nominal $ARL_0 = 500$ and winsorization at the 2000th step

	Chart Type					
	Parametric CUSUM-$\bar{X}$ chart with parameters estimated from a Phase I sample		NPCUSUM-Rank chart		NPCUSUM-EX median chart	
Winsorization level (WL)	WL = 85.1	WL = 86.7	WL = 84.7	WL = 88.9	WL = 85.2	WL = 89.1
Control limits	$H = 11.05$	$H = 5.95$	$H = 725.0$	$H = 246$	$H = 12.10$	$H = 5.85$
k	0	$0.5\sigma/\sqrt{n}$	0	$0.5\sqrt{mn(m+n+1)/12}$	0	$k = n(d^* - d)$ $= 5 \times 0.07 = 0.35$
d^* / γ	NA	NA	NA	NA	0.50	$0.5\sqrt{\frac{n(m+n+1)}{4(m+2)}} \approx 0.57$
0.00	498.49 (712.37) 20, 45, 111, 586, 2000	505.28 (687.54) 14, 45, 146, 636, 2000	505.34 (715.71) 20, 44, 118, 606, 2000	503.9843 (656.38) 10,57, 189, 660, 2000	489.23 (709.53) 19, 43, 109, 553, 2000	502.26 (676.35) 14, 46, 15, 650, 2000
0.25	125.02 (323.68) 13, 23, 36, 73, 488	134.21 (320.59) 8, 18, 35, 90, 605	123.61 (314.23) 13, 23, 36, 73, 490	168.01 (340.48) 5, 19, 51, 146, 762	141.68 (341.30) 6, 14, 24, 40, 88, 636	178.81 (360.39) 9, 22, 51, 149, 871
0.50	32.09 (69.69) 10, 15, 21, 32, 71	34.71 (88.19) 6, 11, 17, 31, 103	33.01 (80.32) 10, 15, 21, 32, 72	45.76 (108.06) 3, 10, 19, 44, 163	49.18 (130.78) 11, 17, 25, 40, 126	61.53 (152.20) 6, 13, 23, 51, 220
0.75	17.66 (12.21) 8, 11, 15, 20, 35	15.00 (20.13) 5, 7, 11, 17, 36	17.92 (11.75) 8, 12, 15, 21, 35	18.14 (32.02) 3, 6, 11, 20, 54	23.20 (27.99) 9, 14, 18, 25, 47	25.09 (56.04) 6, 9, 14, 24, 70
1.00	12.67 (5.28) 7, 9, 12, 15, 22	9.36 (5.58) 4, 6, 8, 11, 19	12.90 (5.28) 7, 9, 12, 15, 23	9.71 (10.00) 2, 5, 7, 12, 24	16.19 (9.79) 9, 11, 14, 19, 30	13.78 (16.79) 5, 7, 10, 15, 34
1.50	8.38 (2.41) 5, 7, 8, 10, 13	5.65 (2.23) 3, 4, 5, 7, 10	8.79 (2.57) 5, 7, 8, 10, 13	5.18 (2.88) 2, 3, 5, 6, 10	10.92 (3.46) 7, 9, 10, 13, 17	7.58 (3.77) 4, 6, 6, 9, 14
2.00	6.32 (1.50) 4, 5, 6, 7, 9	4.15 (1.28) 3, 3, 4, 5, 6	6.77 (1.57) 5, 6, 7, 8, 10	3.60 (1.55) 2, 2, 3, 4, 6	8.56 (1.96) 6, 7, 8, 9, 12	5.63 (1.81) 3, 4, 5, 6, 9

[xlii] Note that, the first row of each of the cells shows the *ARL* and *SDRL* values whereas the second row shows the 5th, 25th, 50th, 75th and 95th percentiles (in this order).

4.6.4 Appendix 4D: SAS® programs

4.6.4.1 SAS® program to compute the run-length characteristics of the NPCUSUM-EX chart when the underlying process distribution is normal

```
proc iml;
m = 100;                          *Size of the IC Phase I reference sample;
sim = 100000;                     *Number of simulations;
runlength = j(sim,1,.);
n = 5;                            *Size of the Phase II test sample;
percentile_of_interest = 75;      *Percentile of interest;
r = (percentile_of_interest/100)*m;
gamma = 0.5;                      *Shift;
stdev = 1;
mean = gamma/sqrt(n);
d = (m-r+1)/(m+1);
*Stdev of Uj,r;
A = r/(m+1);
var_ujr =n*(n-1)* ((r+1)/(m+2))*A-(n*n)*(A*A)+n*A;
stdev_ujr = sqrt(var_ujr);
* Design parameters;
gamma_for_k = gamma;
k = (0.5*gamma_for_k)*stdev_ujr;
H = 12;
*Obtaining the percentile;
keep = j(2,1,.);
*Generating an IC Phase I sample;
xi = j(m,1,.);
do j = 1 to sim;
* Generating observations from the Normal distribution;
call randgen(xi,'NORMAL',0,1);
xi_rank = xi || rank(xi);
do l = 1 to m;
    if xi_rank[l,2] = r then keep[1,]=xi_rank[l,1];
    if xi_rank[l,2] = (r+1) then keep[2,]=xi_rank[l,1];
    val_of_percentile = sum(keep)/2;
end;
*Calculating the CUSUM;
count = 0;
indicator = 0;
Ci_1_plus = 0;
Ci_1_minus = 0;
do i = 1 to 100000000 until (indicator = 1);
count = count + 1;
*Generating a Phase II sample;
yi = j(n,1,.);
call randgen(yi,'NORMAL',mean,1);
*Calculating the precedence statistic;
precedence = j(n,1,0);
        do i = 1 to n;
            if yi[i,]>val_of_percentile then precedence[i,]=1;
        end;
U = sum(precedence);
*Charting statistics;
Ci_plus = max (0, (Ci_1_plus + (U - n*d) - k));
Ci_minus = max (0, (Ci_1_minus - (U - n*d) - k));
*Comparing the charting statistics to the control limits;
if ((Ci_plus >= H) | (Ci_minus >= H)) then indicator = 1;
```

```
      Ci_1_plus = Ci_plus;
      Ci_1_minus = Ci_minus;
end;
runlength[j,1] = count;
end;
create CUSUM from runlength [colname = {RL}];
append from runlength;
proc univariate data = CUSUM noprint;
var RL;
output out = output_row1 median = median qrange = IQR;
output out = output_row2 p5 = lower_perc q1 = first_quar q3 = third_quar p95 =
upper_perc;
proc print data = output_row1;
proc print data = output_row2;
run;
```

4.6.4.2 SAS® program to compute the run-length characteristics of the NPCUSUM-Rank chart when the underlying process distribution is normal

```
quit;
proc iml;
m = 100;                                *Size of the IC Phase I reference sample;
sim = 100000;                           *Number of simulations;
runl = j(sim,1,.);
n = 5;                                  *Size of the Phase II test sample;
exp_w = (n*(n+m+1))/2;                  *Expected value of W;
stdev_w = sqrt (n*m*(n+m+1)/12);        *Standard deviation of W;
gamma = 0.25;                           *Shift;
stdev = 1;
mean  = gamma/sqrt(n);
gamma_for_k = gamma;                    *Design parameters of CUSUM chart;
k = (gamma_for_k)*stdev_w;
H = 386;
do j = 1 to sim;
count = 0;                              * Initializing values;
indicator = 0;
Ci_1_plus = 0;
Ci_1_minus = 0;
xi = j(m,1,.);
 zeros = j(m,1,0);
call randgen(xi,'NORMAL',0,1);          * Generating an IC Phase I sample;
xii = zeros||xi;
do i = 1 to 10000000 until (indicator = 1);
      count = count + 1;
      yi = j(n,1,.);
      call randgen(yi,'NORMAL',mean,1);    * Generating a Phase II sample;
      *Obtaining the rank-sum statistics;
      ones = j(n,1,1);
      yii = ones||yi;
      comb = xii // yii;
      rank = ranktie(comb[,2]);
      comb_rank = comb || rank;
      call sort (comb_rank, {2 3}, {3});
      W_vec = comb_rank[,1]#comb_rank[,3];
      W = sum(W_vec);
      *Charting statistics;
      Ci_plus = max (0, Ci_1_plus + W - exp_w - k);
      Ci_minus = max (0, Ci_1_minus + exp_w - k - W);
      *Comparing the charting statistics to the control limits;
      if ((Ci_plus >= H) | (Ci_minus >= H)) then indicator = 1;
      Ci_1_plus = Ci_plus;
      Ci_1_minus = Ci_minus;
end;
runl[j,1] = count;
end;
create CUSUM from runl [colname = {RL}];
append from runl;
proc univariate data = CUSUM noprint;
var RL;
output out = output_row1 median = median qrange = IQR;
output out = output_row2 p5 = lower_perc q1 = first_quar q3 = third_quar p95 =
upper_perc;
proc print data = output_row1;
proc print data = output_row2;
run;
```

4.6.4.3 SAS® program to compute the run-length characteristics of the CUSUM-$\overline{X}$ chart when the underlying process distribution is normal

```
quit;
proc iml;
sim = 100000;            * Number of simulations;
m = 100;                 *Size of the IC Phase I reference sample;
n = 5;                   *Size of the Phase II test sample;
stdev = 1;
H = 30.1;                *Decision interval;
k = 0.1*stdev/sqrt(n);   *Reference value;
gamma = 0;               *Shift;
runl = j(sim,1,.);
mean = gamma*stdev/(sqrt(n));
do o = 1 to sim;
      *Generating Phase I observations from the Normal distribution;
      xi = j(m,1,.);
      call randgen(xi,'NORMAL',0,1);
      *Obtaining the average and variance;
      x_bar = sum(xi)/m;
      ave_vec = j(m,1,x_bar);
      diff_vec = xi - ave_vec;
      diff_vec_sq = diff_vec # diff_vec;
      var_x = sum(diff_vec_sq)/(m-1);
      *Initializing values;
      indicator = 0;
      count = 0;
      Ci_1_plus = 0;
      Ci_1_minus = 0;
      do i = 1 to 1000000000 until (indicator = 1);
      count = count + 1;
      *Generating Phase II observations from the Normal distribution;
      yi = j(n,1,.);
      call randgen(yi,'NORMAL',mean,1);
      *Obtaining the average;
      y_bar = sum(yi)/n;
      *Obtaining the var;
      y_ave_vec = j(n,1,y_bar);
      y_diff_vec = yi - y_ave_vec;
      y_diff_vec_sq = y_diff_vec # y_diff_vec;
      var_y = sum(y_diff_vec_sq)/(n - 1);
      fin = sqrt(m*n*(m+n-2)/(m+n))*(y_bar-x_bar)/sqrt((m-1)*var_x+(n-1)*var_y);
      * Charting statistics;
      Ci_plus = max(0, (Ci_1_plus + fin - k));
      Ci_minus = max(0, (Ci_1_minus - fin - k));
      *Comparing the charting statistics to the control limits;
            if ((Ci_plus >= H) | (Ci_minus >= H)) then indicator = 1;
            Ci_1_plus = Ci_plus;
            Ci_1_minus = Ci_minus;
      end;
      runl[o,1] = count;
end;
create CUSUM from runl[colname={RL}];
append from runl;
proc univariate data = CUSUM noprint;
var RL;
output out=Final mean=mean_ std=std_ p5=p5_ q1=q1_ median=median_ q3=q3_
p95=p95_;
proc print data = Final;
run;
```

4.6.4.4 SAS® program to compute the run-length characteristics of the NPEWMA-EX chart when the underlying process distribution is normal

```
proc iml;
m = 100;                          *Size of the IC Phase I reference sample;
r = 25;                           * Percentile of interest;
sim = 100000;                     *Number of simulations;
runlength = j(sim,1,.);
n = 5;                            *Size of the Phase II test sample;
lambda = 0.05;                    *Design parameter of the EWMA control chart;
L = 2.041;                        *Design parameter of the EWMA control chart;
gamma = 0;                        *Shift;
stdev = 1;
mean  = gamma*(stdev/sqrt(n));
*Generating an IC Phase I sample;
xi = j(m,1,.);
do j = 1 to sim;
      * Generating observations from the Normal distribution;
      call randgen(xi,'NORMAL',0,1);
      call SORTNDX(xi_sorted, xi, {1});
      xi=xi[xi_sorted,];
      val_of_percentile = xi[r,1];  *Obtaining the percentile;
      *Calculating the EWMA;
      count = 0;
      indicator = 0;
      z_1=0;
      do i = 1 to 100000000000000000 until (indicator = 1);
      count = count + 1;
      *Generating a Phase II sample;
      y = j(n,1,.);
      *Generating observations from the Normal distribution;
      call randgen(y,'NORMAL',mean,1);
      *Calculating the precedence statistic;
      precedence = j(n,1,0);
        do ll = 1 to n;
            if y[ll,]> val_of_percentile then precedence[ll,]=1;
        end;
      U = sum(precedence);
      *Charting statistic;
      z = lambda*U + (1-lambda)*z_1;
      *Control limits;
      UCL= n*((m - r + 1)/(m + 1 ))*(1-(1-lambda)**(i))+L*sqrt(((n**2)*(r*(m-
      r+1))/(((m+1)**2)*(m+2)))*((1-(1-lambda)**(i))**2)+(1-(1-
      lambda)**(2*(i)))*(lambda/(2-lambda))*n*(r*(m-r+1))/((m+1)*(m+2))) ;
      LCL= n*((m - r + 1)/(m + 1 ))*(1-(1-lambda)**(i))-L*sqrt(((n**2)*(r*(m-
      r+1))/(((m+1)**2)*(m+2)))*((1-(1-lambda)**(i))**2)+(1-(1-
      lambda)**(2*(i)))*(lambda/(2-lambda))*n*(r*(m-r+1))/((m+1)*(m+2))) ;
      if (z < UCL) & (z > LCL) then do; indicator = 0; end;
      if (z > UCL) | (z < LCL) then do; indicator = 1; end;
      z_1=z;
end;
runlength[j,1] = count;
end;
create EWMA from runlength [colname = {RL}];
append from runlength;
proc univariate data = EWMA noprint;
var RL;
output out=Final median=median_ p5=p5_ q1=q1_ q3=q3_  p95=p95_;
proc print data = Final;
run;
```

4.6.4.5 SAS® program to compute the run-length characteristics of the NPEWMA-Rank chart when the underlying process distribution is normal

```
quit;
proc iml;
m = 100;                                *Size of the IC Phase I reference sample;
sim = 10000;                            *Number of simulations;
runl = j(sim,1,.);
n = 5;                                  *Size of the Phase II test sample;
exp_w = (n*(n+m+1))/2;                  *Expected value of W;
stdev_w = sqrt (n*m*(n+m+1)/12);        *Standard deviation of W;
lambda = 0.2;                           *Smoothing parameter of the EWMA chart;
LCL = 219.5;                            *Lower control limit;
UCL = 310.5;                            *Upper control limit;
gamma = 2;                              *Shift;
stdev = 1;
mean  = gamma*(stdev/sqrt(n));
do j = 1 to sim;
*Initializing values;
count = 0;
indicator = 0;
zi_1 = exp_W;
xi = j(m,1,.);
zeros = j(m,1,0);
*Generating an IC Phase I sample;
call randgen(xi,'NORMAL',0,1);
xii = zeros||xi;
do i = 1 to 100000000000000000 until (indicator = 1);
      count = count + 1;
      yi = j(n,1,.);
      *Generating a Phase II sample;
      call randgen(yi,'NORMAL',mean,1);
      *Obtaining the rank-sum statistics;
      ones = j(n,1,1);
      yii = ones||yi;
      comb = xii // yii;
      rank = ranktie(comb[,2]);
      comb_rank = comb || rank;
      call sort (comb_rank, {2 3}, {3});
      W_vec = comb_rank[,1]#comb_rank[,3];
      W = sum(W_vec);
      *Charting statistic;
      zi = lambda*W + (1-lambda)*zi_1;
      *Comparing the charting statistics to the control limits;
      if ((zi >= UCL) | (zi <= LCL)) then indicator = 1;
      zi_1 = zi;
end;
runl[j,1] = count;
end;
create EWMA from runl [colname = {RL}];
append from runl;
proc univariate data = EWMA noprint;
histogram;
inset mean std p5 q1 median q3 p95 / format = 10.2;
run;
```

4.6.4.6 SAS® program to compute the run-length characteristics of the EWMA-$\overline{X}$ chart when the underlying process distribution is normal

```
quit;
data final;
proc iml;
sim = 100000;                    *Number of simulations;
runl = j(sim,1,.);
lambda = 0.2;                    *Design parameter of the EWMA control chart;
L = 3;                           *Design parameter of the EWMA control chart;
n = 5;                           *Phase II test sample size;
m = 100;                         *Phase I reference sample size;
gamma = 2;                       *Shift;
stdev = 1;
mean = gamma*(stdev/sqrt(n));
UCL = 0 + 1.01*L*sqrt((lambda/(2-lambda)));      *Upper control limit;
LCL = 0 - 1.01*L*sqrt((lambda/(2-lambda)));      *Lower control limit;
do k = 1 to sim;
      *Generating an IC Phase I sample;
      xi = j(m,1,.);
      call randgen(xi,'NORMAL',0,1);
      x_bar = sum(xi)/m;
      ave_vec = j(m,1,x_bar);
      diff_vec = xi - ave_vec;
      diff_vec_sq = diff_vec # diff_vec;
      var_x = sum(diff_vec_sq)/(m - 1);
      *Initializing values;
      indicator = 0;
      count = 0;
      zi_1 = 0;
      do i = 1 to 100000 until (indicator = 1);
      count = count + 1;
      *Generating Phase II samples;
      yi = j(n,1,.);
      call randgen(yi,'NORMAL',mean,1);
      y_bar = sum(yi)/n;
      y_ave_vec = j(n,1,y_bar);
      y_diff_vec = yi - y_ave_vec;
      y_diff_vec_sq = y_diff_vec # y_diff_vec;
      var_y = sum(y_diff_vec_sq)/(n - 1);
      fin = sqrt(m*n*(m+n-2)/(m+n))*(y_bar-x_bar)/sqrt((m-1)*var_x+(n-1)*var_y);
      * Charting statistic;
      zi = lambda*fin + (1 - lambda) * zi_1;
      * Comparing charting statistic with the control limits;
      if (zi<UCL) & (zi>LCL) then do; indicator = 0; end;
      if (zi>UCL) | (zi<LCL) then do; indicator = 1; end;
      zi_1 = zi;
end;
      runl[k,1] = count;
end;
create EWMA from runl[colname={RL}];
append from runl;
proc univariate data = EWMA noprint;
var RL;
output out=Final mean=mean_ std=std_ p5=p5_ q1=q1_ median=median_ q3=q3_
p95=p95_;
proc print data = Final;
run;
```

4.6.4.7 SAS® programs to compute the run-length characteristics of the above-mentioned charts when the underlying process distribution is non-normal

Distribution	Necessary amendments to the SAS® programs above

$GAM(\alpha, 1)$	*Shape parameter (α) of the Gamma distribution;
	shape = 1; * α = 1 for GAM(1,1) which is EXP(1);
	* α = 3 for GAM(3,1);
	
	* IC distribution;
	call randgen(xi,'gamma',shape);
	xi = (xi - shape)/sqrt(shape);
	
	* OOC distribution;
	call randgen(yi,'gamma', shape);
	yi=(yi-shape)/sqrt(shape)+gamma*(stdev/sqrt(n));

$t(3)$	*Degrees of freedom for the t-distribution;
	df = 3;
	
	* IC distribution;
	call randgen(xi,'t',df);
	term = sqrt ((df-2)/df);
	xi = xi # term;
	
	* OOC distribution;
	call randgen(yi,'t',df);
	yi = yi # term + gamma/sqrt(n);

$DE(0,1)$	*Computing the stdev;
	stdev = sqrt(2);
	
	* Note that a Probability Integral Transformation was used to obtain the Double Exponential distribution;
	* IC distribution;
	xi = j(m,1,.);
	ui = j(m,1,.);
	call randgen(ui,'UNIFORM');
	xi=quantile('laplace',ui,0,1);
	xi = (1/sqrt(2))*xi;
	
	* OOC distribution;
	yi = j(n,1,.);
	uni = j(n,1,.);
	call randgen(uni,'UNIFORM');
	yi=quantile('laplace',uni,gamma*(stdev/sqrt(n)),1);
	yi = (1/sqrt(2))*yi;

Mixture or Contaminated Normal

```
*Mixture level;
eta = 0.4;
m1 =  (1-eta)*m;
m2 = eta*m;
n1 = (1-eta)*n;
n2 = eta*n;

*Mixture normal distribution;
mu1 = 0;
mu2 = 0;
sigma1 = 0.25;
sigma2 = 4;
overall_mean = (1-eta)*mu1 + eta*mu2;
overall_var  = ( (1-eta)*(mu1*mu1 + sigma1*sigma1) + eta*(mu2*mu2
               + sigma2*sigma2) ) - (overall_mean**2);
overall_stdev = sqrt(overall_var);
*Generating an IC Phase I sample;
xi_1 = j(m1,1,.);
xi_2 = j(m2,1,.);

* Generating observations from the CN distribution;
call randgen(xi_1,'NORMAL',mu1,sigma1);
call randgen(xi_2,'NORMAL',mu2,sigma2);
xi = xi_1//xi_2;
xi = (xi - overall_mean) / overall_stdev;

*Generating a Phase II sample;
yi_1 = j(n1,1,.);
yi_2 = j(n2,1,.);

*Generating observations from the CN distribution;
call randgen(yi_1,'NORMAL',mu1,sigma1);
call randgen(yi_2,'NORMAL',mu2,sigma2);
y = yi_1//yi_2;
y = (y - overall_mean) / overall_stdev + gamma/sqrt(n);
```

Log-Logistic ($\alpha = 1, \beta = 2.5$)

```
*Parameters of the Log-logistic distribution;
alpha = 1;
beta = 2.5;

*Computing the stdev;
pi = constant('PI');
t = pi/beta;
var = (alpha*alpha)*(((2*t)/sin(2*t))-(t*t)/(sin(t)*sin(t)));
stdev = sqrt(var);

* Note that a Probability Integral Transformation was used to
obtain the Log-Logistic distribution;
* IC distribution;
temp_1 = j(m,1,.);
call randgen (temp_1, 'UNIFORM');
xi = log(alpha)+(1/beta)*(log(temp_1/(1-
     temp_1)));
xi = exp(xi);

* OOC distribution;
call randgen (temp_2, 'UNIFORM');
yi = log(alpha)+(1/beta)*(log(temp_2/(1-temp_2)));
yi = exp(yi)+ gamma*(stdev/sqrt(n)) ;
```

Chapter 5

Concluding Remarks: Summary and Recommendations for Future Research

In this final section we give a brief summary of the research conducted in this dissertation and offer concluding remarks concerning unanswered questions and future research opportunities.

Statistical Process Control (SPC) is a collection of statistical procedures and problem solving tools that are used to control, monitor and improve the quality of the output of a process. In this dissertation we focused on a variety of aspects related to a powerful statistical tool often used in quality improvement efforts within the realm of SPC, namely, the control chart. More specifically, we focused on nonparametric control charts since standard control charts are often based on the assumption that the observations follow a specific parametric distribution (such as the normal distribution).

However, in many applications we do not have enough information to make this assumption. In such situations, development and application of control charts that do not depend on a particular distributional assumption is desirable and this is where nonparametric or distribution-free control charts can be useful. A key advantage of nonparametric charts is that its in-control run-length distribution is the same for all continuous process distributions. This means, for example, that the false alarm rate and the in-control average run-length of a nonparametric chart is the same for all continuous distributions. This is not true for parametric control charts in general and consequently their in-control robustness can be a legitimate concern.

In this dissertation we discussed some ideas and recent developments in the area of univariate nonparametric control charts. In the next few paragraphs we point out some of the highlights of the research carried out in this dissertation and state some future research ideas that could be pursued. We also list the research outputs associated with this dissertation; this includes technical reports and peer-reviewed articles that have been published, articles that have been accepted for publication, local and international conferences where papers have been presented and draft articles that have been submitted for publication and are currently under review.

Phase I control charting

Chapter 1 served as an introduction where some important terminology and concepts related to SPC were defined, In Chapter 2 we started off by giving a literature overview of Shewhart-type Phase I control charts followed by the design and implementation of these charts. A nonparametric Shewhart-type Phase I control chart for monitoring the location of a continuous variable was proposed. The chart is based on the pooled median of the available Phase I samples and the charting statistics are the counts (number of observations) in each sample that are less than the pooled median. Although the literature on Phase I control charting has witnessed a tremendous growth (and rightfully so) in the last few years, much more remains to be done. We list a few of these ideas below.

i. From a practical standpoint, control charting procedures must be made more accessible to practitioners and, to this end, the ease of implementation is vital. Computer programs, add-ons to popular software packages such as Minitab® SAS®, and R® and / or websites would greatly help in this effort.

ii. In terms of theoretical (i.e. desk research), more work needs to be done on nonparametric Phase I charts for monitoring scale and joint monitoring of location and scale. Although there are some articles in the literature that address these problems (see e.g. Human et al. (2010b)), these are parametric control charting procedures based on the assumption that the observations follow a specific parametric distribution. As far as we are aware, the only articles considering Phase I control charts for evaluating process scale were published recently, in 2010, by Jones-Farmer and Champ (2010) and Bakir (2010), respectively.

iii. Development of nonparametric Phase I control charts for individual measurements needs to be done. Frequently in practice, situations arise that require a charting procedure for individuals data, for example, when little data are available or where it does not make sense to group measurements. Although there are some articles in the literature that address this problem (see e.g. Nelson (1982), Roes et al. (1993) and Bryce et al. (1997)), these are parametric control charting procedures based on the assumption that the observations follow a specific parametric distribution. It has been pointed out that with individuals data, since the central limit theorem does not apply, the validity of normal theory charts such as the ones mentioned in Montgomery (2009, Chapter 6, page 226) become suspect at best.

Phase II control charting

In Chapters 3 and 4 of this dissertation Phase II control charts were introduced and considered for the case when the underlying parameters of the process distribution are known or specified (see Chapter 3) and for the case when the underlying parameters of the process distribution are unknown and need to be estimated (see Chapter 4). Various nonparametric Phase II control charts were proposed and studied in this body of work; these included two nonparametric EWMA charts based on the sign and signed-rank statistics for the situation when the IC process median is specified or known, a nonparametric EWMA chart based on exceedance statistics for monitoring the unknown median and a nonparametric CUSUM chart based on exceedance statistics for monitoring the unknown median. Although the literature on nonparametric Phase II control charting has witnessed a tremendous growth (and rightfully so) in the last few years, much more remains to be done:

i. From a practical standpoint, nonparametric control charting procedures must be made more accessible to practitioners and, to this end, it would help if software developers were to include nonparametric control charting applications to their computer programs. Consequently, add-ons to popular software packages such as Minitab® SAS®, and R® and / or websites would greatly help in this effort.

ii. There is a major shortcoming regarding the application of nonparametric charts in industry. This could be due to a number of contributing factors, such as the fact that nonparametric methods are not well-known, since they are only typically touched on in undergraduate and / or postgraduate courses in most programs. Also, in a search of standard SPC books on the market, very little on nonparametric control charting was found. For example, in the well-known SPC book by Montgomery (2009), only one page is devoted to nonparametric control charts (see Montgomery (2009) page 487). Thus, in a well-known SPC book of over 700 pages only 1 page is devoted to nonparametric control charting applications.

iii. In terms of research, more work needs to be done on nonparametric Phase II charts for monitoring scale and joint monitoring of location and scale. Recently, in their overview paper, Chakraborti et al. (2011) noted that not much work is currently available on nonparametric Phase II charts for monitoring scale and joint monitoring of location and scale. Although there are some articles in the literature that address the problem of monitoring scale (see e.g. Chang

and Gan (1994), Chen et al. (2001) and Castagliola (2005)), these are parametric control charting procedures based on the assumption that the observations follow a specific parametric distribution. In the literature, only a handful of articles have been published on nonparametric Phase II charts for monitoring scale and joint monitoring of location and scale; these include Amin et al. (1995), Das and Bhattacharya (2008), Murakami and Matsuki (2010), Khilare and Shirke (2012), Ross et al. (2011), Mukherjee and Chakraborti (2012) and Chowdhury et al. (2013).

Research outputs

Next we list the research outputs associated with this dissertation. This includes technical reports and peer-reviewed articles that have been published, articles that have been accepted for publication, local and international conferences where papers have been presented and draft articles that have been submitted and are currently under review.

Published articles

i. Mukherjee, A., Graham, M.A. and Chakraborti, S. (2013). "Distribution-free exceedance CUSUM control charts for location." *Communications in Statistics - Simulation and Computation*, 42 (5), 1153-1187.

ii. Graham, M.A., Mukherjee, A. and Chakraborti, S. (2012). "Distribution-free exponentially weighted moving average control charts for monitoring unknown location." *Computational Statistics and Data Analysis*, 56 (8), 2539–2561.

iii. Graham, M.A., Chakraborti, S. and Human, S.W. (2011). "A nonparametric EWMA sign chart for location based on individual measurements." *Quality Engineering*, 23 (3), 227-241.

iv. Graham, M.A., Chakraborti, S. and Human, S.W. (2011). "A nonparametric exponentially weighted moving average signed-rank chart for monitoring location." *Computational Statistics and Data Analysis*, 55 (8), 2490-2503.

v. Chakraborti, S., Human, S.W. and Graham, M.A. (2011). "Nonparametric (distribution-free) quality control charts." In Handbook of Methods and Applications of Statistics: Engineering, Quality Control, and Physical Sciences. N. Balakrishnan, Ed., 298-329, John Wiley & Sons, New York.

vi. Graham, M.A., Human, S.W. and Chakraborti, S. (2010). "A Phase I nonparametric Shewhart-type control chart based on the median." *Journal of Applied Statistics,* 37 (11), 1795-1813.

vii. Chakraborti, S., Human, S.W. and Graham, M.A. (2009). "Phase I Statistical Process Control charts: An overview and some results." *Quality Engineering*, 21 (1), 52-62.

Articles under review

i. Graham, M.A., Chakraborti, S. and Mukherjee, A. "Design and implementation of CUSUM exceedance control charts for unknown location." Submitted to *Computational Statistics and Data Analysis*.

Technical reports

i. Graham, M.A., Human, S.W. and Chakraborti, S. (2009). "A nonparametric EWMA control chart based on the sign statistic." Technical report, 09/04, Department of Statistics, University of Pretoria, Pretoria, South Africa, ISBN 978-1-86854-777-7.

International conferences (presentations)

i. Graham, M.A., Mukherjee, A. and Chakraborti, S. (2012). "Nonparametric control charts for monitoring location based on the exceedance statistic." Joint Statistical Meetings (JSM), San Diego, California, USA, 28 July – 2 August 2012.

ii. Graham, M.A., Mukherjee, A. and Chakraborti, S. (2012). "Nonparametric control charts based on exceedance statistics." The 22nd Columbian Symposium on Statistics, Bucaramanga, Colombia, 17 – 21 July 2012.

iii. Graham, M.A., Chakraborti, S. and Human, S.W. (2011). "Monitoring location: A nonparametric control chart based on the signed-rank statistic." The 58th Session of the International Statistical Institute (ISI), Dublin, Ireland, 21 – 26 August 2011.

iv. Graham, M.A., Chakraborti, S. and Human, S.W. (2010). "A nonparametric EWMA control chart for location based on the sign statistic." Joint Statistical Meetings (JSM), Vancouver, British Columbia, Canada, 31 July – 5 August 2010.

v. Graham, M.A., Human, S.W. and Chakraborti, S. (2009). "The design and implementation of a Phase I nonparametric control chart based on the median." The 57th Session of the International Statistical Institute (ISI), Durban, South Africa, 16 – 22 August 2009.

International conferences (published proceedings)

i. Graham, M.A., Mukherjee, A. and Chakraborti, S. (2012). "Nonparametric control charts for monitoring location based on the exceedance statistic." *JSM 2012 Proceedings, Section on Quality and Productivity,* 1611 – 1625, San Diego, California, USA.

ii. Graham, M.A., Chakraborti, S. and Human, S.W. (2011). "Monitoring location: A nonparametric control chart based on the signed-rank statistic." *International Statistical Institute (ISI) Proceedings*, Dublin, Ireland.

iii. Graham, M.A., Chakraborti, S. and Human, S.W. (2010). "A nonparametric EWMA control chart for location based on the sign statistic." *JSM 2010 Proceedings, Section on Quality and Productivity*, 1808 – 1816, Vancouver, British Columbia, Canada.

National conferences (presentations)

i. Graham, M.A., Mukherjee, A. and Chakraborti, S. (2012). "Nonparametric CUSUM and EWMA control charts for monitoring unknown location based on the exceedance statistic." The 54th annual conference of the South African Statistical Association (SASA), Nelson Mandela Metropolitan University (NMMU), Port Elizabeth, 5 – 9 November 2012.

ii. Graham, M.A., Mukherjee, A. and Chakraborti, S. (2012). "Monitoring location: Distribution-free exponentially weighted moving average control charts based on the exceedance statistic." 1st ICCSSA (Institute of Certificated and Chartered Statisticians of South Africa) Convention, Lagoon Beach Hotel, Milnerton, Cape Town, 28 – 29 March 2012.

iii. Graham, M.A., Chakraborti, S. and Human, S.W. (2011). "Nonparametric exponentially weighted moving average control charts based on the sign and signed-rank statistics." The 53rd annual conference of the South African Statistical Association (SASA), CSIR, Pretoria, South Africa, 1 – 3 November 2011.

iv. Graham, M.A., Chakraborti, S. and Human, S.W. (2010). "Monitoring location: A nonparametric EWMA control chart based on the sign statistic." The 52nd annual conference of the South African Statistical Association (SASA), North-West University, Potchefstroom Campus, South Africa, 8 – 12 November 2010.

v. Graham, M.A., Human, S.W. and Chakraborti, S. (2008). "A Phase I nonparametric control chart based on the median." The 51st annual conference of the South African Statistical Association (SASA), University of Pretoria, Pretoria, South Africa, 27 – 31 October 2008.

The end.

References

Agresti, A. and Coull, B.A. (1998). "Approximate is better than "exact" for interval estimation of binomial proportions." *The American Statistician*, **52** (2), 119-126.

Amin, R.W. and Searcy, A.J. (1991). "A nonparametric exponentially weighted moving average control scheme." *Communications in Statistics: Simulation and Computation*, **20** (4), 1049-1072.

Amin, R.W. and Widmaier, O. (1999). "Sign control charts with variable sampling intervals." *Communications in Statistics: Theory and Methods,* **28** (8), 1961-1985.

Amin, R.W., Reynolds Jr. M.R. and Bakir, S.T. (1995). "Nonparametric quality control charts based on the sign statistic." *Communications in Statistics: Theory and Methods,* **24** (6), 1597-1623.

Bakir, S.T. (2003). "A quality control chart based on signed-ranks." *Joint Statistical Meetings – Section on Quality and Productivity,* 423-429.

Bakir, S.T. (2004). "A distribution-free Shewhart quality control chart based on signed-ranks." *Quality Engineering,* **16** (4), 613-623.

Bakir, S.T. (2006). "Distribution-free quality control charts based on signed-rank-like statistics." *Communications in Statistics: Theory and Methods*, **35** (4), 743-757.

Bakir, S.T. (2010). "A nonparametric test for homogeneity of variances: Application to GPA's of students across academic majors." *IABR & ITLC Conference Proceedings,* Orlando, Florida, USA.

Bakir, S.T. (2011). *Distribution-Free (Nonparametric) Statistical Quality Control Charts: A Concise Summary Part I (1920's-2000).*

Bakir, S.T. and Reynolds, Jr. M.R. (1979). "A nonparametric procedure for process control based on within-group ranking." *Technometrics*, **21** (2), 175-183.

Balakrishnan, N. and Ng, H.K.T. (2006). *Precedence-type tests and applications*, John Wiley and Sons, Hoboken, New Jersey.

Balakrishnan, N., Triantafyllou, I.S. and Koutras, M.V. (2009). "Nonparametric control charts based on runs and Wilcoxon-type rank-sum statistics." *Journal of Statistical Planning and Inference*, **139** (9), 3177-3192.

Balakrishnan, N., Triantafyllou, I.S. and Koutras, M.V. (2010). "A distribution-free control chart based on order statistics." *Communications in Statistics: Theory and Methods,* **39** (20), 3652-3677.

Barnard, G.A. (1959). "Control charts and stochastic processes." *Journal of the Royal Statistical Society, B,* **21** (2), 239-271.

Blyth, C.R. and Still, H.A. (1983). "Binomial confidence intervals." Journal of the American Statistical Association, **78**, 108-116.

Bodden, K.M. and Ridgon, S.E. (1999). "A program for approximating the in-control ARL for the MEWMA chart." *Journal of Quality Technology*, **31** (1), 120-123.

Borror C.M, Champ, C.W. and Rigdon, S.E. (1998). "Poisson EWMA control charts." *Journal of Quality Technology*, **30** (4), 352-361.

Borror, C.M., Montgomery, D.C. and Runger, G.C. (1999). "Robustness of the EWMA control chart to non-normality." *Journal of Quality Technology,* **31** (3), 309-316.

Brook, D. and Evans, D.A. (1972). "An approach to the probability distribution of CUSUM run length." *Biometrika*, **59** (3), 539-549.

Brown, L.D., Cai, T.T. and DasGupta, A. (2001). "Interval estimation for a binomial proportion." *Statistical Science*, **16** (2), 101-117.

Bryce, G.R., Gaudard, M.A. and Joiner, B.L. (1997). "Estimating the standard deviation for individuals control charts." *Quality Engineering*, **10** (2), 331-341.

Capizzi, G. and Masarotto, G. (2003). "An adaptive exponentially weighted moving average control chart." *Technometrics*, **45** (3), 199-207.

Capizzi, G. and Masarotto, G. (2012). "Adaptive generalized likelihood ratio control charts for detecting unknown patterned mean shifts." *Journal of Quality Technology*, **44** (4), 281-303.

Casella, G. and Berger, R.L. (2002). *Statistical Inference*, 2nd Edition. Duxbury.

Castagliola, P. (2005). "A new S^2-EWMA control chart for monitoring the process variance." *Quality and Reliability Engineering International*, **21** (8), 781-794.

Chakraborti, S. (2007). "Run length distribution and percentiles: The Shewhart $\overline{X}$ chart with unknown parameters." *Quality Engineering,* **19** (2), 119-127.

Chakraborti, S. and Eryilmaz, S. (2007). "A nonparametric Shewhart-type signed-rank control chart based on runs." *Communications in Statistics: Simulation and Computation,* **36** (2), 335-356.

Chakraborti, S. and Graham, M.A. (2007). "Nonparametric control charts." *Encyclopedia of Statistics in Quality and Reliability,* **1**, 415 – 429, John Wiley, New York.

Chakraborti, S. and Van de Wiel, M.A. (2008). "A nonparametric control chart based on the Mann-Whitney statistic." *IMS Collections. Beyond Parametrics in Interdisciplinary Research: Festschrift in Honor of Professor Pranab K. Sen*, **1**, 156-172.

Chakraborti, S. and Van der Laan (2000). "Precedence probability and prediction intervals." *The Statistician,* **49** (2), 219-228.

Chakraborti, S., Eryilmaz, S. and Human, S.W. (2009). "A phase II nonparametric control chart based on precedence statistics with runs-type signaling rules." *Computational Statistics and Data Analysis*, **53** (4), 1054-1065.

Chakraborti, S., Human, S.W. and Graham, M.A. (2009). "Phase I statistical process control charts: An overview and some results." *Quality Engineering*, **21** (1), 52-62.

Chakraborti, S., Human, S.W. and Graham, M.A. (2011). "Nonparametric (distribution-free) quality control charts." In Handbook of Methods and Applications of Statistics: Engineering, Quality Control, and Physical Sciences. N. Balakrishnan, Ed., 298-329, John Wiley & Sons, New York.

Chakraborti, S., Van der Laan, P. and Bakir, S.T. (2001). "Nonparametric control charts: An overview and some results." *Journal of Quality Technology,* **33** (3), 304-315.

Chakraborti, S., Van der Laan, P. and Van de Wiel, M.A. (2004). "A class of distribution-free control charts." *Journal of the Royal Statistical Society. Series C*: *Applied Statistics*, **53** (3), 443-462.

Champ, C.W. and Chou, S.P. (2003). "Comparison of standard and individual limits Phase I Shewhart $\overline{X}$, *R* and *S* charts." *Quality and Reliability Engineering International,* **19**, 161-170.

Champ, C.W. and Jones, L.A. (2004). "Designing Phase I $\overline{X}$ charts with small sample sizes." *Quality and Reliability Engineering International,* **20** (5), 497-510.

Chang, T.C. and Gan, F.F. (1994). "Optimal designs of the one-sided EWMA charts for monitoring a process variance." *J. Statist. Computation and Simulations*, **49**, 33-48.

Chatterjee, S. and Qiu, P. (2009). "Distribution-free cumulative sum control charts using bootstrap-based control limits." *The Annals of Applied Statistics*, **3** (1), 349 – 369.

Chen, G., Cheng, S.W. and Xie, H. (2001). "Monitoring process mean and variability with one EWMA chart." *Journal of Quality Technology*, **33** (2), 223-233.

Chou, S.P. and Champ, C.W. (1995). "A comparison of two Phase I control charts." Proceedings of the Quality and Productivity Section of the American Statistical Association, 31-35.

Chowdhury, S., Mukherjee, A. and Chakraborti, S. (2013). "A new distribution-free control chart for joint monitoring of unknown location and scale parameters of continuous distributions." *Quality and Reliability Engineering International*, DOI: 10.1002/qre.1488.

Coelho, M.L.I., Chakraborti, S. and Graham, M.A. (2013). "A comparison of three Phase I control charts." *Submitted.*

Crosier, R.B. (1986). "A new two-sided cumulative sum quality control scheme." *Technometrics*, **28** (3), 187-194.

Das, N. (2009). "A comparison study of three non-parametric control charts to detect shift in location parameters." *International Journal of Advanced Manufacturing Technology*, **41** (7/8), 799–807.

Das, N. and Bhattacharya, A. (2008). "A new non-parametric control chart for controlling variability." Quality *Technology and Quantitative Management*, **5** (4), 351-361.

Derman, C. and Ross, S.M. (1997). *Statistical Aspects of Quality Control*, San Diego: Academic Press.

Ewan, W.D. (1963). "When and how to use CUSUM charts." *Technometrics*, **5** (1), 1-22.

Ewan, W.D. and Kemp, K.W. (1960). "Sampling inspection of continuous processes with no autocorrelation between successive results." *Biometrika*, **47**, 363-380.

Fligner, M.A. and Wolfe, D.A. (1976). "Some applications of sample analogues to the probability integral transformation and a coverage property." *The American Statistician*, **30**, 78-85.

Fu, J.C. and Lou, W.Y.W. (2003). *Distribution Theory of Runs and Patterns and Its Applications: A Finite Markov Chain Imbedding Approach.* Singapore: World Scientific Publishing.

Gan, F.F. (1993). "An optimal design of CUSUM control charts for binomial counts." *Journal of Applied Statistics,* **20** (4), 445-460.

Gan, F.F. (1994). "An optimal design of cumulative sum control chart based on median run length." *Communications in Statistics: Simulation and Computation*, **23** (2), 485 - 503.

Ghosh, B.K. (1979). "A comparison of some approximate confidence intervals for the binomial parameter." Journal of the American Statistical Association, **74**, 894-900.

Gibbons, J.D. and Chakraborti, S. (2010). *Nonparametric Statistical Inference,* 5th ed., Taylor and Francis, Boca Rator, FL.

Goldsmith, R.L. and Whitfield, H. (1961). "Average run lengths in cumulative chart quality control schemes." *Technometrics,* **3** (1), 11-20.

Graham, M.A., Chakraborti, S. and Human, S.W. (2011). "A nonparametric EWMA sign chart for location based on individual measurements." *Quality Engineering*, 23 (3), 227-241.

Graham, M.A., Chakraborti, S. and Human, S.W. (2011). "A nonparametric exponentially weighted moving average signed-rank chart for monitoring location." *Computational Statistics and Data Analysis*, 55 (8), 2490-2503.

Graham, M.A., Chakraborti, S. and Mukherjee, A. (2013). "Design and implementation of CUSUM exceedance control charts for unknown location." Submitted to *Computational Statistics and Data Analysis.*

Graham, M.A., Human, S.W. and Chakraborti, S. (2009). "A nonparametric EWMA control chart based on the sign statistic." Technical report, 09/04, Department of Statistics, University of Pretoria, Pretoria, South Africa, ISBN 978-1-86854-777-7.

Graham, M.A., Human, S.W. and Chakraborti, S. (2010). "A Phase I nonparametric Shewhart-type control chart based on the median." *Journal of Applied Statistics,* **37** (11), 1795-1813.

Graham, M.A., Mukherjee, A. and Chakraborti, S. (2012). "Distribution-free exponentially weighted moving average control charts for monitoring unknown location." *Computational Statistics and Data Analysis*, 56 (8), 2539–2561.

Hawkins, D.M. (1992). "Evaluation of average run lengths of cumulative sum charts for an arbitrary data distribution." *Communications in Statistics: Simulation and Computation*, **21**, 1001-1020.

Hawkins, D.M. (1993). "Cumulative sum control charting: An underutilized SPC tool." *Quality Engineering*, **5** (3), 463-477.

Hawkins, D.M. and Deng, Q. (2010). "A nonparametric change-point control chart." *Journal of Quality Technology*, **42** (2), 165-173.

Hawkins, D.M. and Olwell, D.H. (1998). *Cumulative sum charts and charting for quality improvement*. Springer-Verlag, New York.

Hawkins, D.M., Qiu, P. and Kang, C.W. (2003). "The changepoint model for statistical process control." *Journal of Quality Technology*, **35** (4), 355-366.

Hillier, F.S. (1969). "$\overline{X}$ and R chart control limits based on a small number of subgroups." *Journal of Quality Technology,* **1** (1), 17-26.

Human, S.W. (2009). "Univariate parametric and nonparametric statistical quality control techniques with estimated process parameters." Published PhD dissertation, Department of Statistics, University of Pretoria.

Human, S.W. and Graham, M.A. (2007). "Average run lengths and operating characteristic curves." *Encyclopedia of Statistics in Quality and Reliability,* 1, 159-168, John Wiley, New York.

Human, S.W., Chakraborti, S. and Smit, C.F. (2009). "Shewhart-type S^2, S and R control charts for Phase I applications." Technical Report, 2009/01, Department of Statistics, University of Pretoria.

Human, S.W., Chakraborti, S. and Smit, C.F. (2010a). "Nonparametric Shewhart-type sign control charts based on runs." *Communications in Statistics: Theory and Methods*, **39** (11), 2046 – 2062.

Human, S.W., Chakraborti, S. and Smit, C.F. (2010b). "Shewhart-type control charts for variation in phase I data analysis." *Computational Statistics and Data Analysis*, **54** (4), 863-874.

Human, S.W., Kritzinger, P. and Chakraborti, S. (2011). "Robustness of the EWMA control chart for individual observations". *Journal of Applied Statistics*, **38** (10), 2071-2087.

Janacek, G.J. and Meikle, S.E. (1997). "Control charts based on medians." *The Statistician*, **46** (1), 19-31.

Jensen, W.A., Jones-Farmer, L.A., Champ, C.W. and Woodall, W.H. (2006). "Effects of parameter estimation on control chart properties: A literature review." *Journal of Quality Technology,* **38** (4), 349-364.

Johnson, N.L. (1961). "Simple theoretical approach to cumulative sum control charts." *Journal of the American Statistical Association,* **56**, 835-840.

Jones, L.A. and Champ, C.W. (2002). "Phase I control charts for times between events." *Quality and Reliability Engineering International,* **18**, 479-488.

Jones, L. A., Champ, C. W. and Rigdon, S.E. (2004). "The run length distribution of the CUSUM with estimated parameters". *Journal of Quality Technology*, **36** (1), 95-108.

Jones-Farmer, L.A. and Champ, C.W. (2010). "A distribution-free Phase I control chart for subgroup scale." *Journal of Quality Technology*, **42** (4), 373-387.

Jones-Farmer, L.A., Jordan, V. and Champ, C.W. (2009). "Distribution-free Phase I control charts for subgroup location." *Journal of Quality Technology*, **41** (3), 304-316.

Kantam, R.R.L. and Rao, G.S. (2005). "Cumulative sum control chart for log-logistic distribution." *InterStat: Statistics on the Internet*, **7**, 1-9.

Khilare, S.K. and Shirke, D.T. (2012). "Nonparametric synthetic control charts for process variation." *Quality and Reliability Engineering International*, **28** (2), 193-202.

Khoo, M.B.C. (2003). "Design of runs rules schemes." *Quality Engineering* **16** (1), 27-43.

Khoo, M.B.C. and Ariffin, K.N. (2006). "Two improved runs rules for the Shewhart $\overline{X}$ control chart." *Quality Engineering* **18**, 173-178.

Khoo, M.B.C., Wong, V.H., Wu, Z. and Castagliola, P. (2011). "Optimal designs of the multivariate synthetic chart for monitoring the process mean vector based on median run length." *Quality and Reliability Engineering International*, **27** (8), 981-997.

Kim, S.H., Alexopoulos, C., Tsui, K.L. and Wilson, J.R. (2007). "A distribution-free tabular CUSUM chart for autocorrelated data." *IIE Transactions*, **39** (3), 317-330.

King, E.P. (1954). "Probability limits for the average chart when process standards are unspecified." *Industrial Quality Control,* **10**, 62-64.

Klein, M. (2000). "Two alternatives to the Shewhart $\overline{X}$ control chart." *Journal of Quality Technology*, **32** (4), 427-431.

Koning, A.J. (2006). "Model-based control charts in phase 1 statistical process control." *Statistica Neerlandica,* **60** (3), 327-338.

Lehmann, E.L. (1975). *Nonparametrics: Statistical Methods Based on Ranks*. Holden-Day, Inc. San Francisco, CA.

Li, S.Y., Tang, L.C. and Ng, S.H. (2010). "Nonparametric CUSUM and EWMA control charts for detecting mean shifts." *Journal of Quality Technology*, **42** (2), 209-226.

Lucas, J.M. (1985). "Cumulative sum (CUSUM) control schemes." *Communications in Statistics: Theory and Methods,* **14**, 2689-2704.

Lucas, J.M. and Saccucci, M.S. (1990). "Exponentially weighted moving average control schemes: Properties and enhancements." *Technometrics,* **32** (1), 1-12.

McDonald, D. (1990). "A CUSUM procedure based on sequential ranks." *Naval Research Logistics*, **37** (5), 627-646.

McGilchrist, C.A. and Woodyer, K.D. (1975). "Note on a distribution-free CUSUM technique." *Technometrics,* **17** (3), 321-325.

Meeker, W.Q. and Escobar, L.A. (1998). *Statistical Methods for Reliability Data*, John Wiley, New York, NY.

Molnau, W.E., Runger, G.C., Montgomery, D.C., Skinner, K.R., Loredo, E.N. and Prabhu, S.S. (2001). "A program for ARL calculation of multivariate EWMA charts." *Journal of Quality Technology*, **33** (4), 515-521.

Montgomery, D.C. (2001). *Introduction to Statistical Quality Control,* 4th Edition, John Wiley, New York, NY.

Montgomery, D.C. (2005). *Introduction to Statistical Quality Control,* 5th Edition, John Wiley, New York, NY.

Montgomery, D.C. (2009). *Statistical Quality Control: A Modern Introduction*, 6th ed., John Wiley, New York, NY.

Mukherjee, A. and Chakraborti, S. (2012). "A distribution-free control chart for the joint monitoring of location and scale." *Quality and Reliability Engineering International*, **28** (3), 335-352.

Mukherjee, A., Graham, M.A. and Chakraborti, S. (2013). "Distribution-free exceedance CUSUM control charts for location." *Communications in Statistics - Simulation and Computation*, 42 (5), 1153-1187.

Murakami, H. and Matsuki, T. (2010). "A nonparametric control chart based on the Mood statistic for dispersion." *International Journal of Advanced Manufacturing Technology*, **49**, 757-763.

Nelson, L.S. (1982). "Control charts for individual measurements." *Journal of Quality Technology*, **14** (3), 172-173.

Nelson, P.R., Wludyka, P.S. and Copeland, K.A.F. (2005). *The Analysis of Means: A graphical method for comparing means, rates and proportions*. ASA-SIAM Series on Statistics and Applied Probability, Philadelphia, PA.

Page, E.S. (1954). "Continuous inspection schemes." *Biometrika*, **41** (1), 100-115.

Page, E. S. (1961). "Cumulative sum charts." *Technometrics*, **3** (1), 1-9.

Radson, D. and Boyd, A.H. (2005). "Graphical representation of run length distributions." *Quality Engineering*, **17** (2), 301-308.

Randles, R.H. and Wolfe, D.A. (1979). *Introduction to the Theory of Nonparametric Statistics,* John Wiley and Sons, New York.

Reynolds, M.R. Jr. (1996). "Variable-sampling-interval control charts with sampling at fixed times." *IIE Transactions*, **28** (6), 497-510.

Reynolds, M.R. Jr. (2012). "The Bernoulli CUSUM chart for detecting decreases in a proportion." *Quality and Reliability Engineering International*, Online Version.

Reynolds, M.R. Jr. and Arnold, J.C. (2001). "EWMA control charts with variable sample sizes and variable sampling intervals." *IIE Transactions*, **33** (6), 511-530.

Reynolds, M.R. Jr., Amin, R.W. and Arnold, J.C. (1990). "CUSUM charts with Variable Sampling Intervals." *Technometrics*, **32** (4), 371-384.

Roberts, S.W. (1959). "Control chart tests based on geometric moving averages." *Technometrics,* **1** (3), 239-250.

Rocke, D.M. (1989). "Robust control charts." *Technometrics*, **31** (2), 173-184.

Rocke, D.M., Downs, G.W. and Rocke, A.J. (1982). "Are robust estimators really necessary?" *Technometrics*, **24** (2), 95-101.

Roes, K.C.B., Does, R.J.M.M. and Schurink, Y. (1993). "Shewhart-type control charts for individual observations." *Journal of Quality Technology*, **25** (3), 188-198.

Ross, G.J. and Adams, N.M. (2012). "Two nonparametric control charts for detecting arbitrary distribution changes." *Journal of Quality Technology*, **44** (2), 1-15.

Ross, G.J., Adams, N.M., Tasoulis, D.K. and Hand, D.J. (2012). "Exponentially weighted moving average charts for detecting concept drift." http://arxiv.org/pdf/1212.6018v1.pdf

Ross, G.J., Tasoulis, D.K. and Adams, N.M. (2011). "Nonparametric monitoring of data streams for changes in location and scale." *Technometrics*, **53** (4), 379-389.

Ruggeri, F., Kenett, R.S. and Faltin, F.W. (2007). "Exponentially weighted moving average (EWMA) control chart." *Encyclopedia of Statistics in Quality and Reliability,* **2**, 633-639, John Wiley, New York.

Ryan, T.P. (2000). *Statistical Methods for Quality Improvement*, 2nd ed., John Wiley & Sons, Inc.

Saccucci, M.S. and Lucas, J.M. (1990). "Average run lengths for exponentially weighted moving average control schemes using the Markov chain approach." *Journal of Quality Technology*, **22** (2), 154-157.

Saccucci, M.S., Amin, R.W. and Lucas, J.M. (1992). "Exponentially weighted moving average control schemes with variable sampling intervals." *Communications in Statistics: Simulation and Computation*, **21** (3), 627-657.

SAS Version 9.2. SAS Institute Inc., Cary, NC.

Schaffer, J.R. and Kim, M.J. (2007). "Number of replicates required in control chart Monte Carlo simulation studies. *Communications in Statistics: Simulation and Computation*, **36** (5), 1075-1087.

Shewhart, W.A. (1924). "Some applications of statistical methods to the analysis of physical and engineering data." *Bell Technical Journal*, **3**, 43-87.

Spliid, H. (2010). "An exponentially weighted moving average control chart for Bernoulli data." *Quality and Reliability Engineering International*, **26** (1), 97-113.

Steiner, S.H. (1999). "EWMA control charts with time-varying control limits and fast initial response." *Journal of Quality Technology,* **31** (1), 75-86.

Steiner, S.H. and Jones, M. (2010). "Risk-adjusted survival time monitoring with an updating exponentially weighted moving average (EWMA) control chart." *Statistics in Medicine*, **29**, 444-454.

Sullivan, J.H. and Woodall, W. H. (1996). "A control chart for preliminary analysis of individual observations." *Journal of Quality Technology,* **28** (3), 265-278.

Vollset, S.E. (1993). "Confidence intervals for a binomial proportion." Statistics in Medicine, **12**, 809-824.

Western Electronic Company. (1956). *Statistical Quality Control Handbook,* Western Electric Corporation, Indianapolis, IN.

Woodall, W.H. (1984). "On the Markov chain approach to the two-sided CUSUM procedure." *Technometrics*, **26**, 41-46.

Woodall, W.H. (2000). "Controversies and contradictions in Statistical Process Control." *Journal of Quality Technology,* **32** (4), 341-350.

Woodall, W.H. and Adams, B. (1993). "The statistical design of CUSUM charts." *Quality Engineering*, **5**, 559-570.

Woodall, W.H. and Mahmoud, M.A. (2005). "The inertial properties of quality control charts." *Technometrics*, **47** (4), 425 – 436.

Woodall, W.H. and Montgomery, D.C. (1999). "Research issues and ideas in statistical process control." *Journal of Quality Technology*, **31** (4), 376-386.

Yang, C.H. and Hillier, F.S. (1970). "Mean and variance control chart limits based on a small number of subgroups." *Journal of Quality Technology,* **2** (1), 9-16.

Yang, S. and Cheng, S.W. (2011). "A new non-parametric CUSUM mean chart." *Quality and Reliability Engineering International*, **27** (7), 867-875.

Yashchin, E. (1993). "Statistical control schemes: Methods, applications and generalizations." *International Statistical Review*, **61** (1), 41-66.

Yu, Y. (2007). "Some contributions to Statistical Process Control." MSc dissertation, McMaster University, Hamilton, Ontario.

Zhou, C., Zou, C., Zhang, Y. and Wang, Z. (2009). "Nonparametric control chart based on change-point model." *Statistical Papers*, **50** (1), 13-28.